



Weakly-supervised learning for emboli characterization with Transcranial Doppler (TCD) monitoring

PhD Student: Yamil Vindas-Yassine¹

Supervisors: Philippe Delachartre¹, Emmanuel Roux¹, Blaise Kévin Guépié²

Collaborators: Marilys Almar³

Doctoral School: EEA

Funding: Regional Project CAREMB

¹Univ.Lyon, INSA-Lyon, Université Claude Bernard Lyon 1, UJM-Saint Etienne, CNRS, Inserm, CREATIS UMR 5220, U1206, F-69100, LYON, France

²Université de Technologie de Troyes, Laboratoire Informatique et Société Numérique, Troyes, France

³Atys Medical, Soucieu-en-Jarrest, France

Outline

I. Context

- a) Medical and scientific context
- b) Emboli classification methods
- c) Challenges and objectives

II. Contribution 1 : Semi-automatic data annotation

- a) State-of-the-art
- b) Proposed method
- c) Results

III. Contribution 2 : Multi-feature medical signal classification

- a) State-of-the-art
- b) Proposed method
- c) Results

IV. Contribution 3 : Model compression based on extreme quantization

- a) State-of-the-art
- b) Proposed method
- c) Results

V. Conclusion and perspectives

Outline

I. Context

- a) **Medical and scientific context**
- b) **Emboli classification methods**
- c) **Challenges and objectives**

II. Contribution 1 : Semi-automatic data annotation

- a) **State-of-the-art**
- b) **Proposed method**
- c) **Results**

III. Contribution 2 : Multi-feature medical signal classification

- a) **State-of-the-art**
- b) **Proposed method**
- c) **Results**

IV. Contribution 3 : Model compression based on extreme quantization

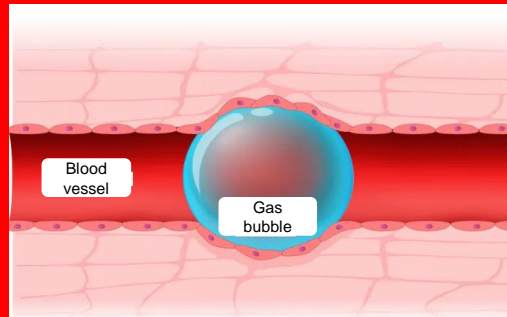
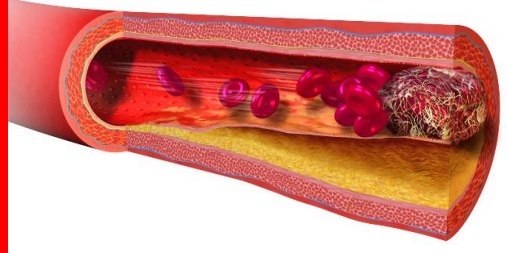
- a) **State-of-the-art**
- b) **Proposed method**
- c) **Results**

V. Conclusion and perspectives

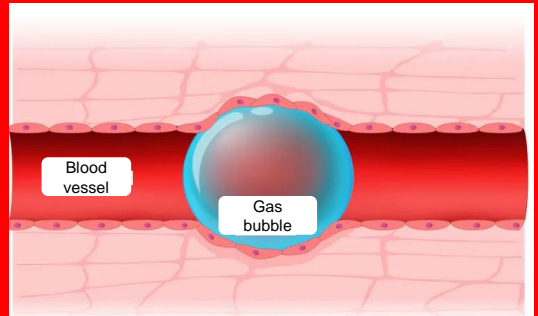
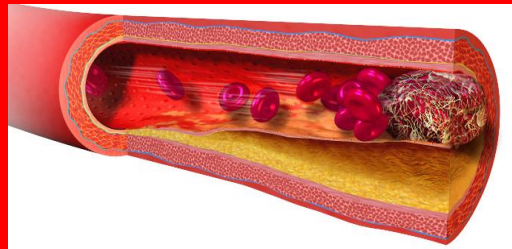
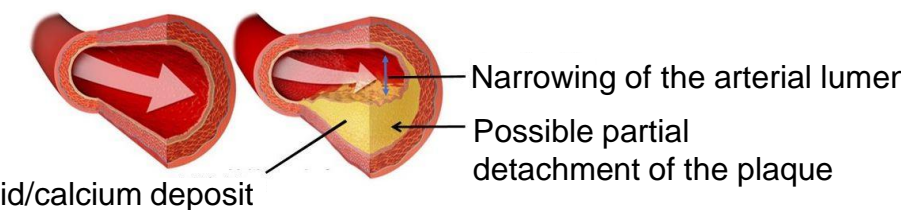
WHAT ?

WHAT ?

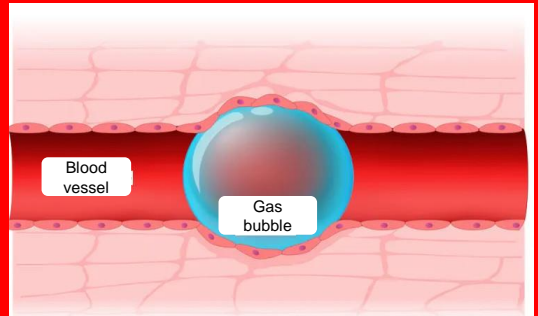
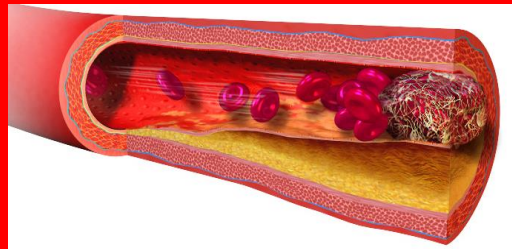
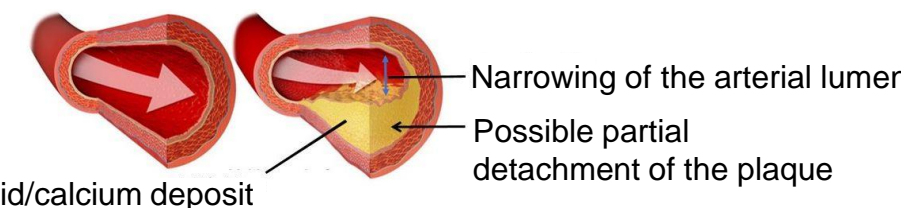
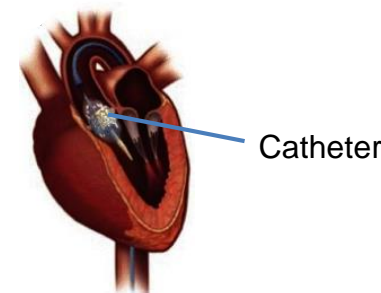
Emboli



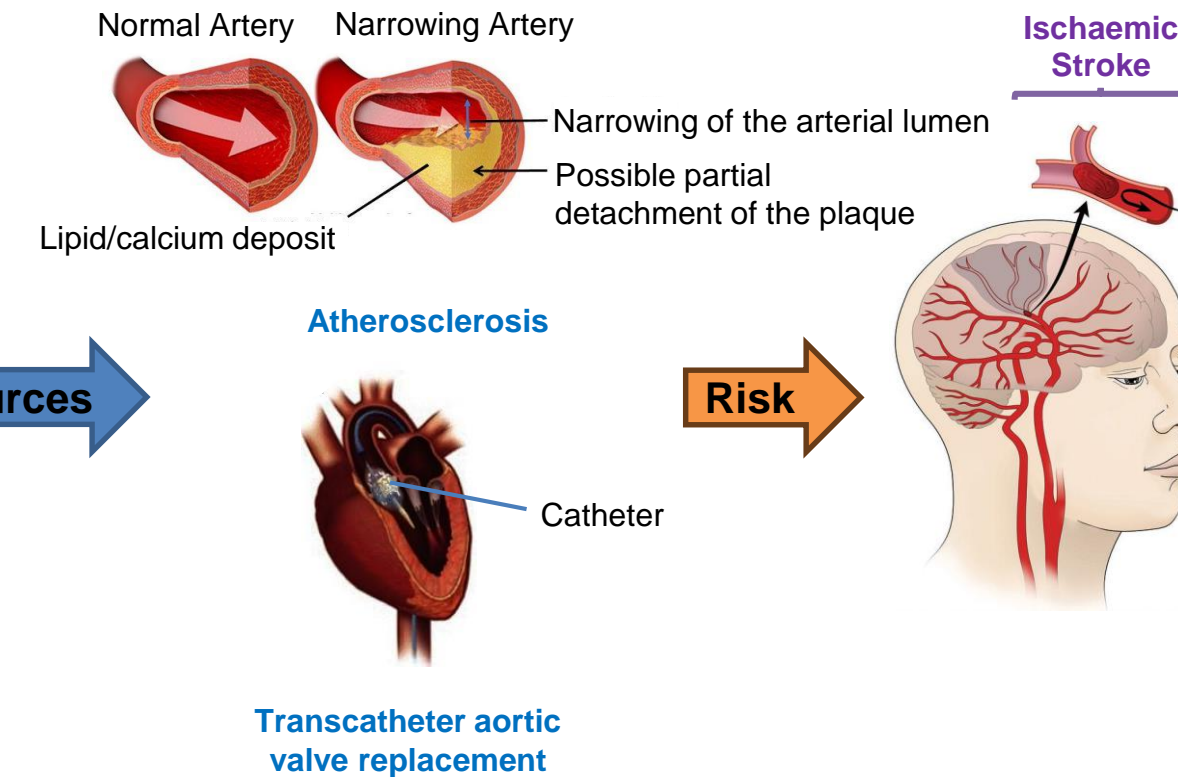
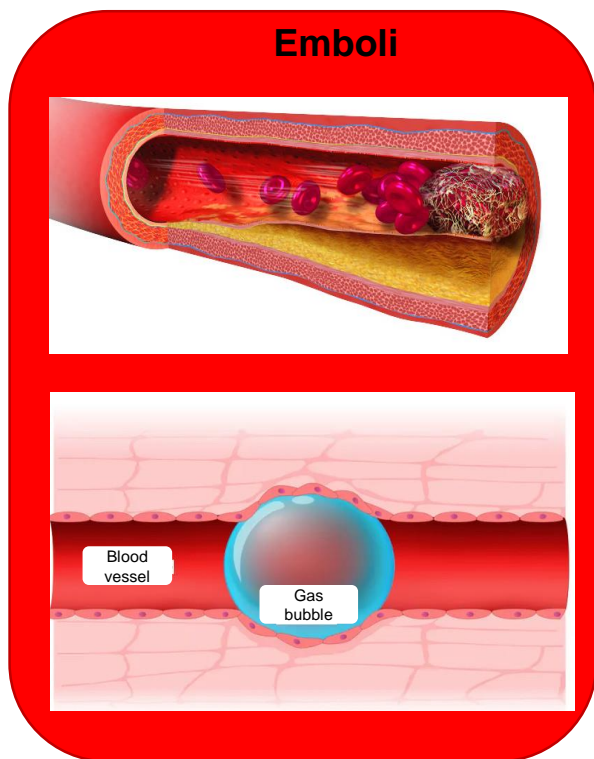
WHAT ?

Emboli**Sources** →**Normal Artery** **Narrowing Artery****Atherosclerosis**

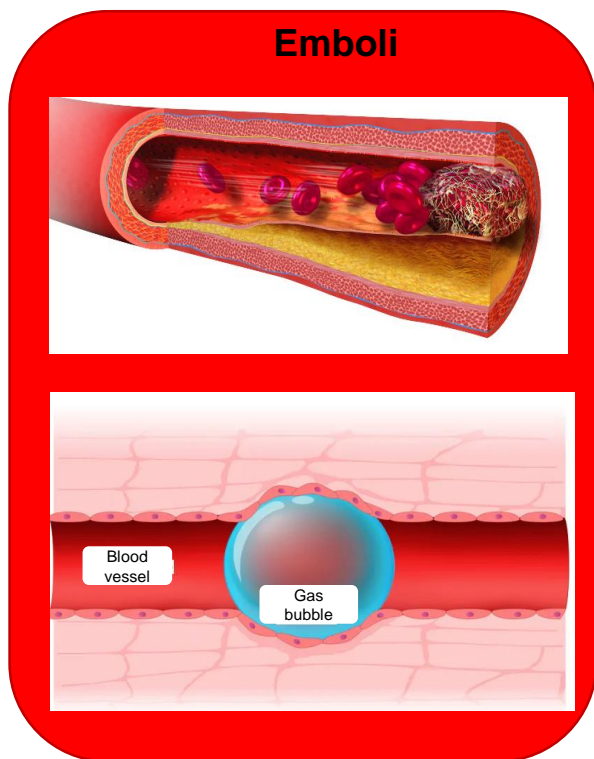
WHAT ?

Emboli**Sources** →**Normal Artery** **Narrowing Artery****Atherosclerosis****Transcatheter aortic valve replacement**

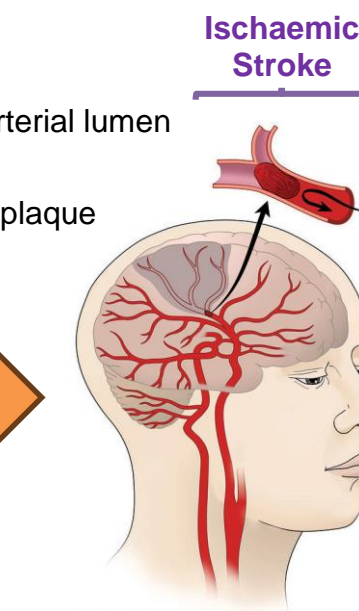
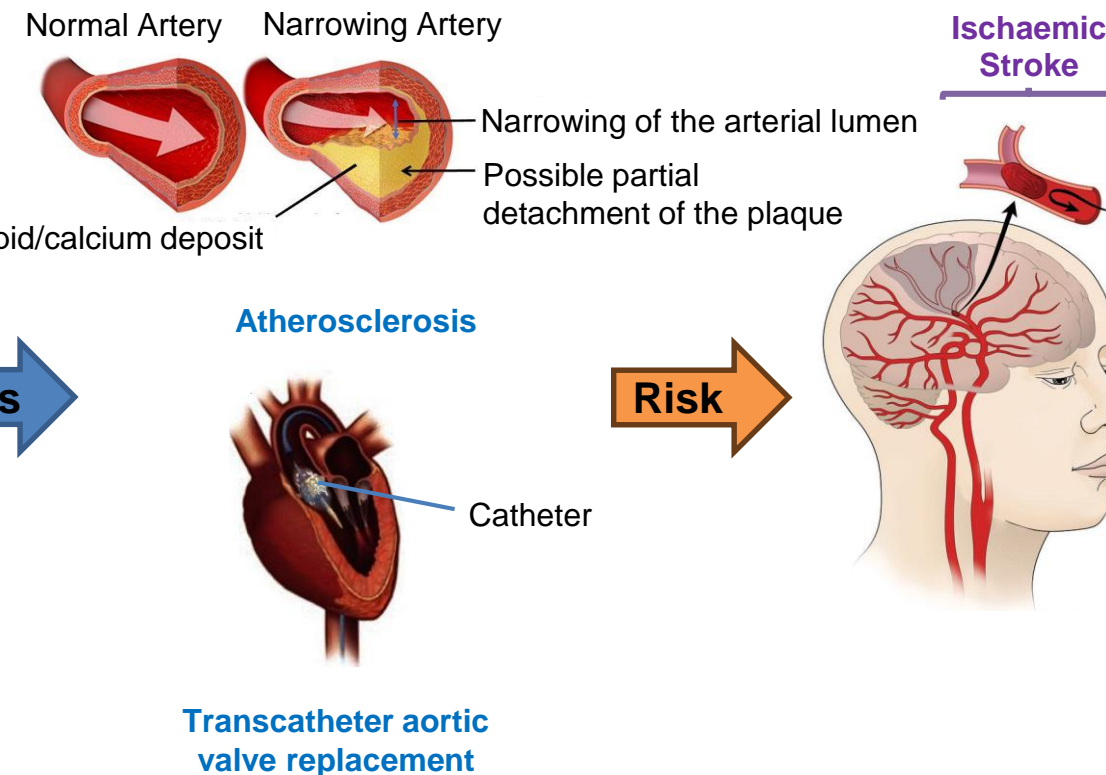
WHAT ?



WHAT ?



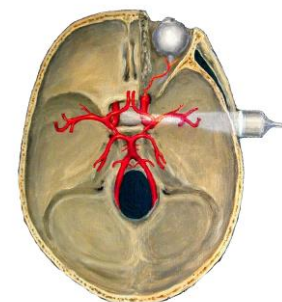
Sources



Transcranial Doppler (TCD)
TCD-X from Atys Medical

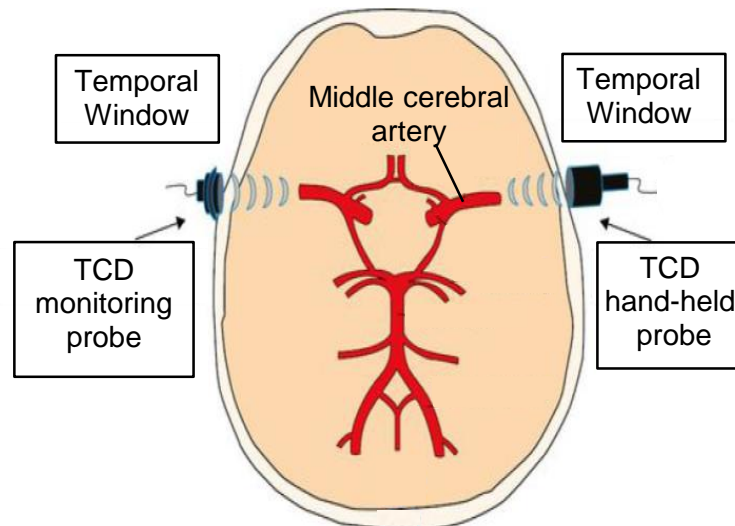


Detection

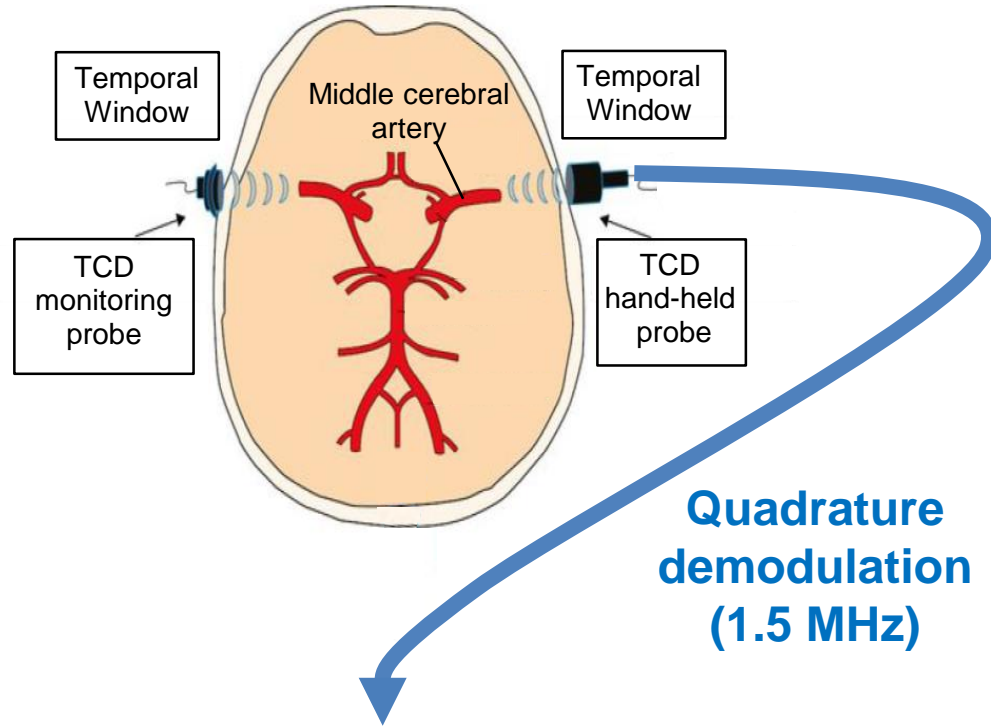


How ?

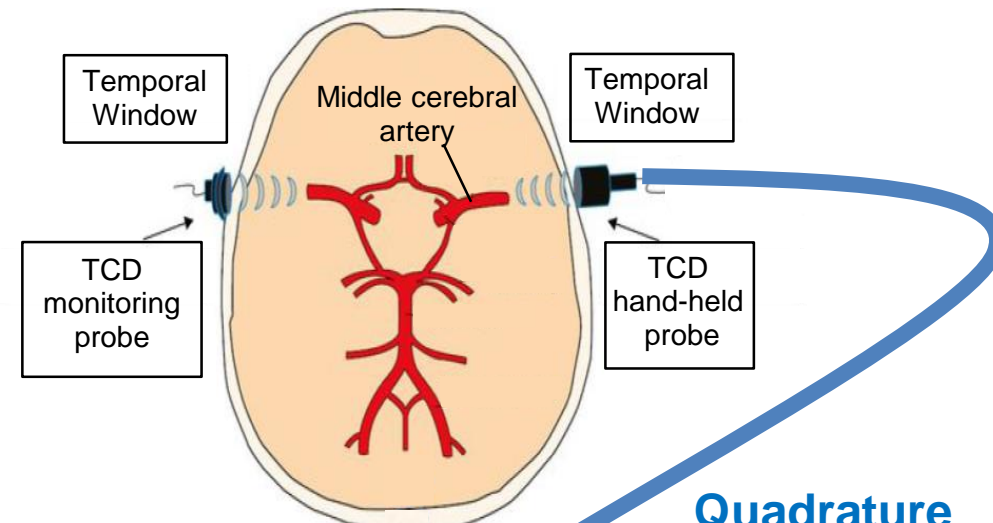
How ?



How ?



How ?



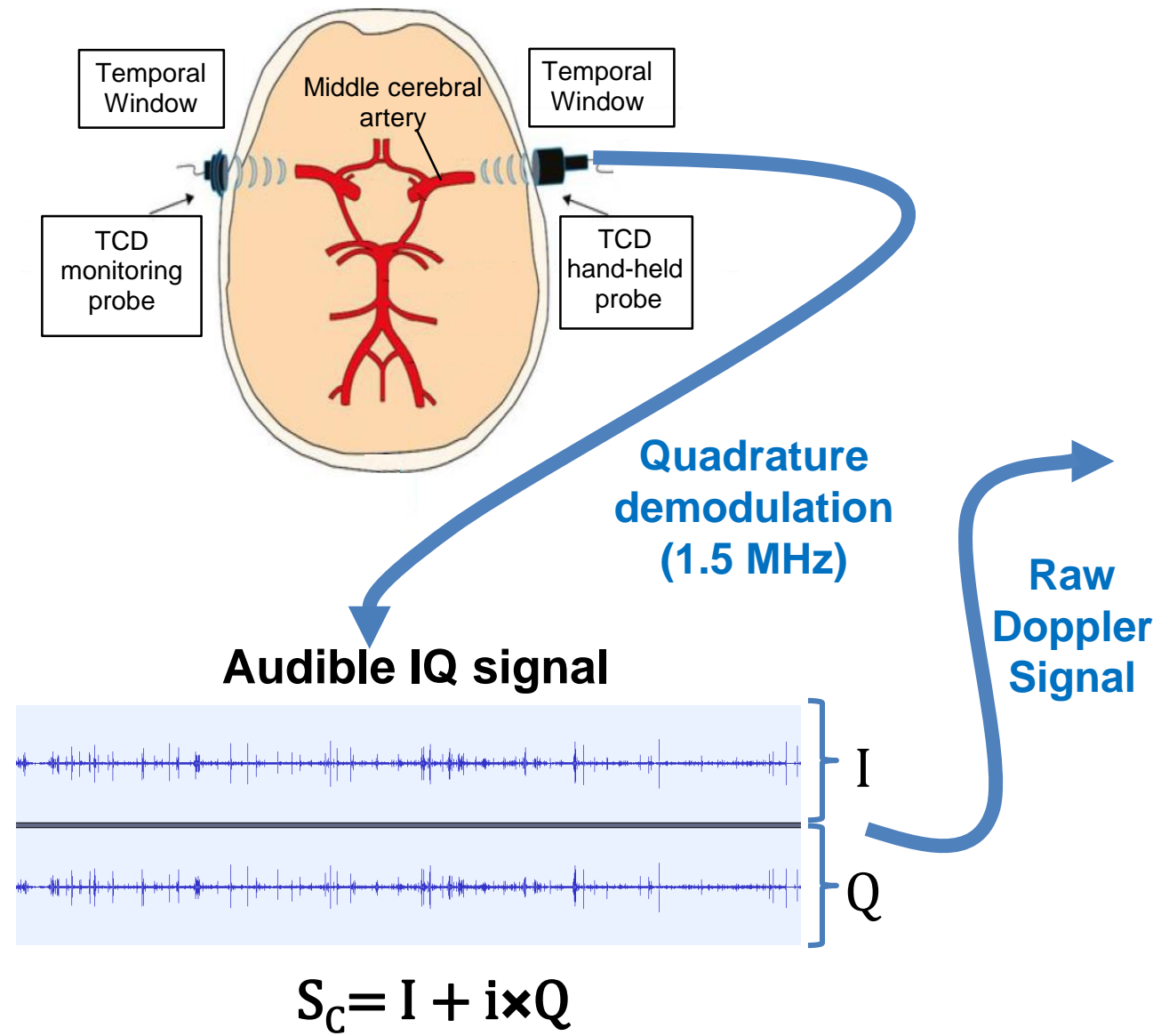
Quadrature
demodulation
(1.5 MHz)

Audible IQ signal

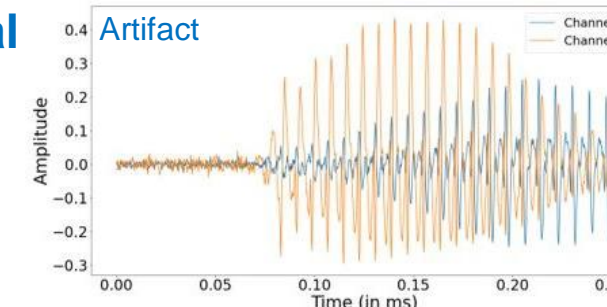
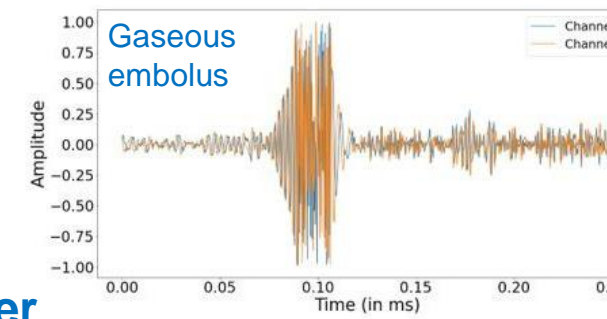
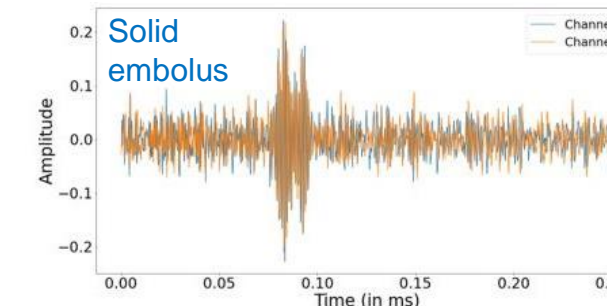
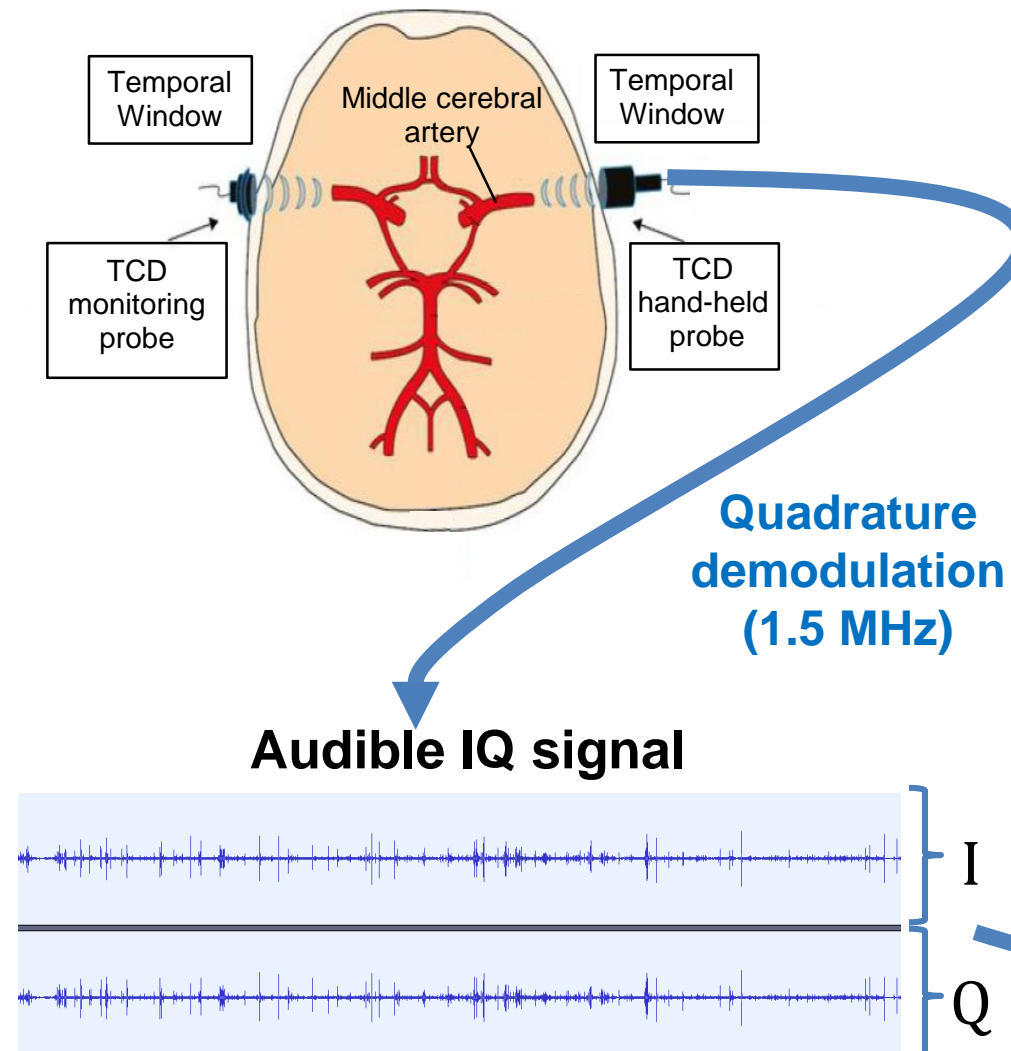


$$S_c = I + i \times Q$$

How ?

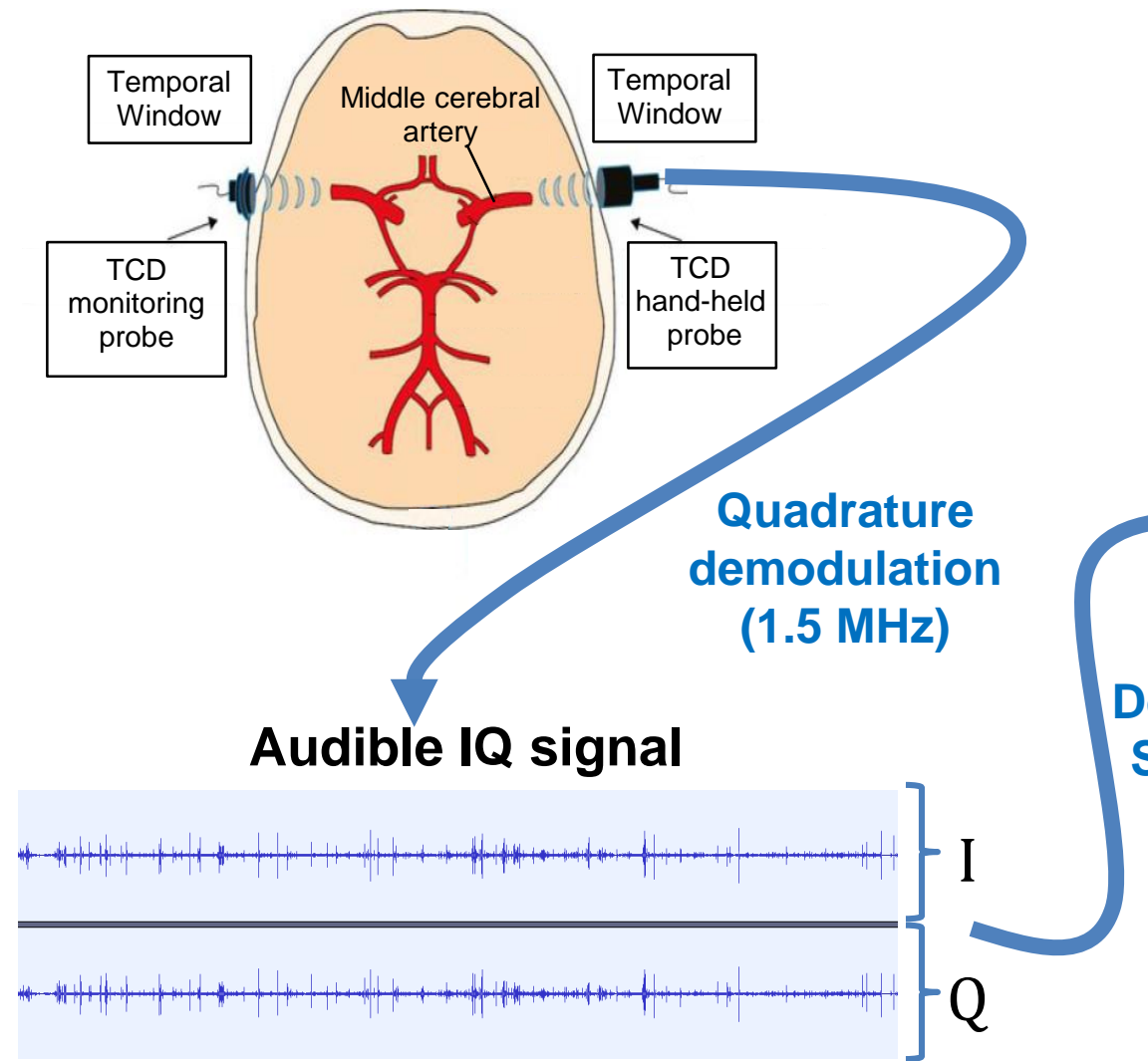


How ?

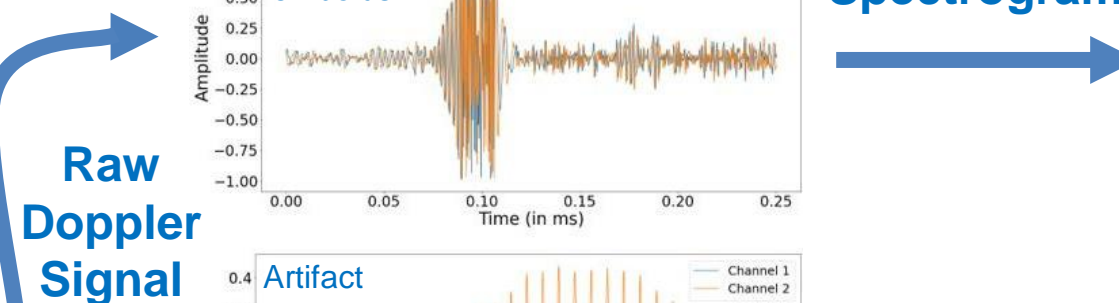
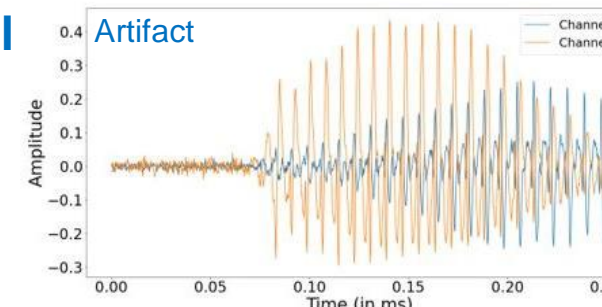
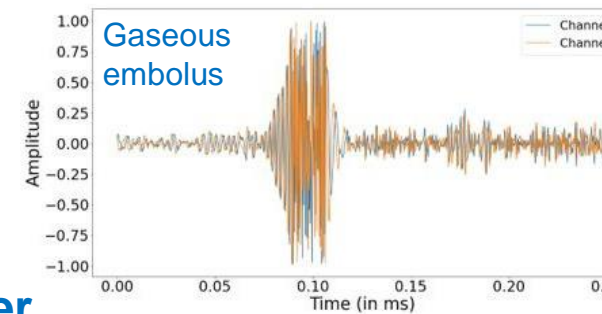
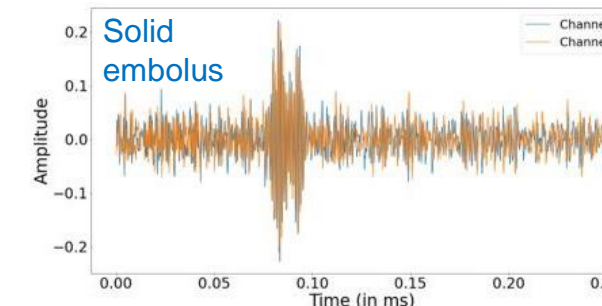


$$S_c = I + i \times Q$$

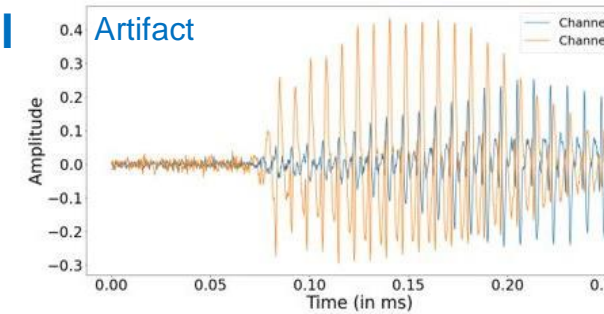
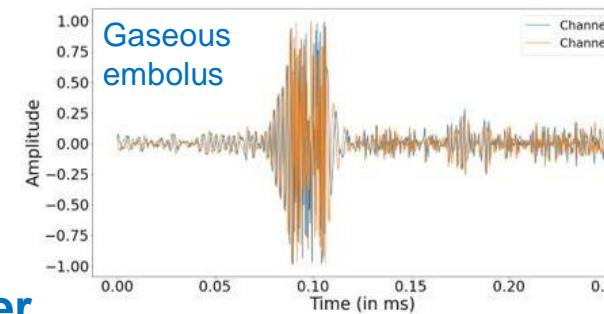
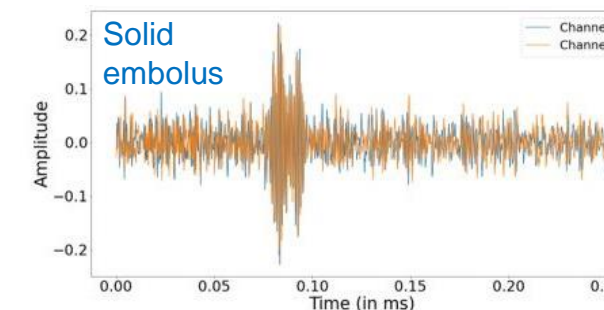
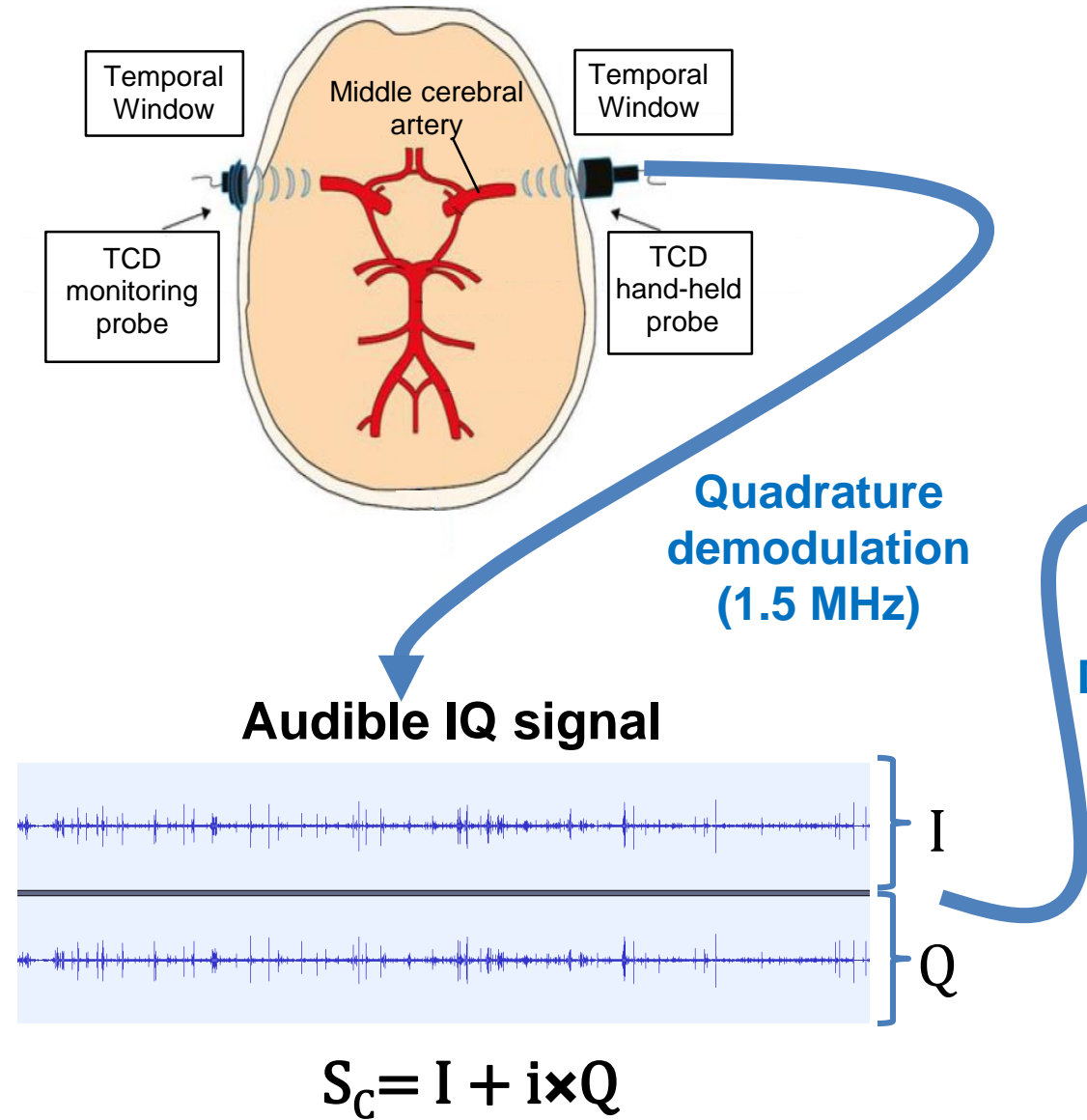
How ?



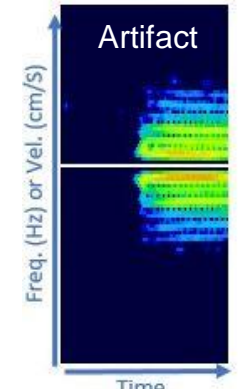
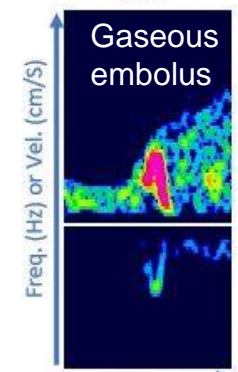
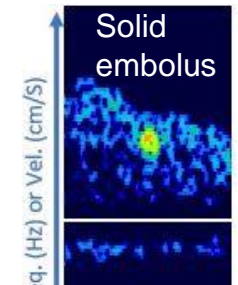
$$S_c = I + i \times Q$$



How ?

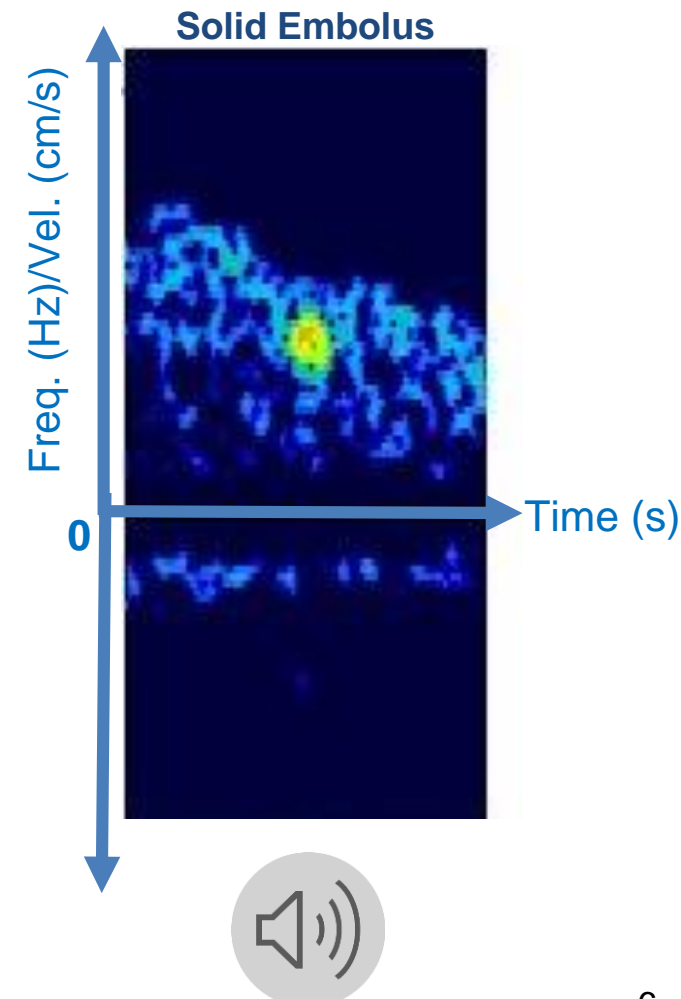


Spectrogram



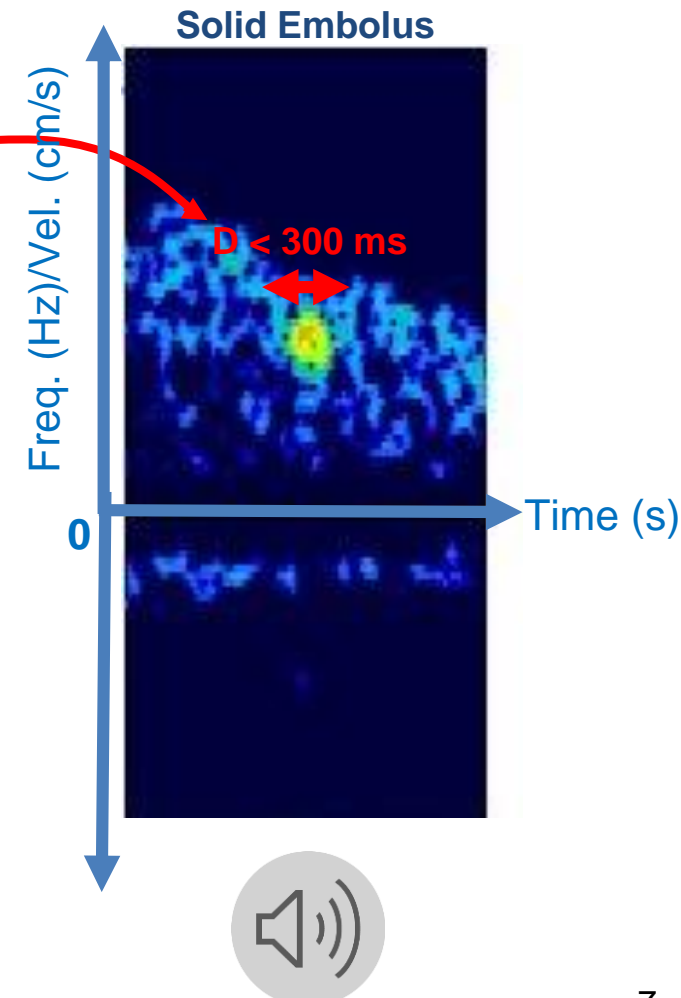
Emboli detection criteria

- **Basic identification criteria of Doppler microembolic signals***
 - Duration < 300 ms → High intensity transient signals (**HITS**)
 - Unidirectional in the time-frequency domain.
 - → No symmetry with respect to the zero-frequency baseline.
 - Musical "chirp" or "snap" sound.
 - Intensity increase of at least 3dB with respect to the blood flow signal.
 - → Defined through the hits-to-blood ratio (**HBR**)



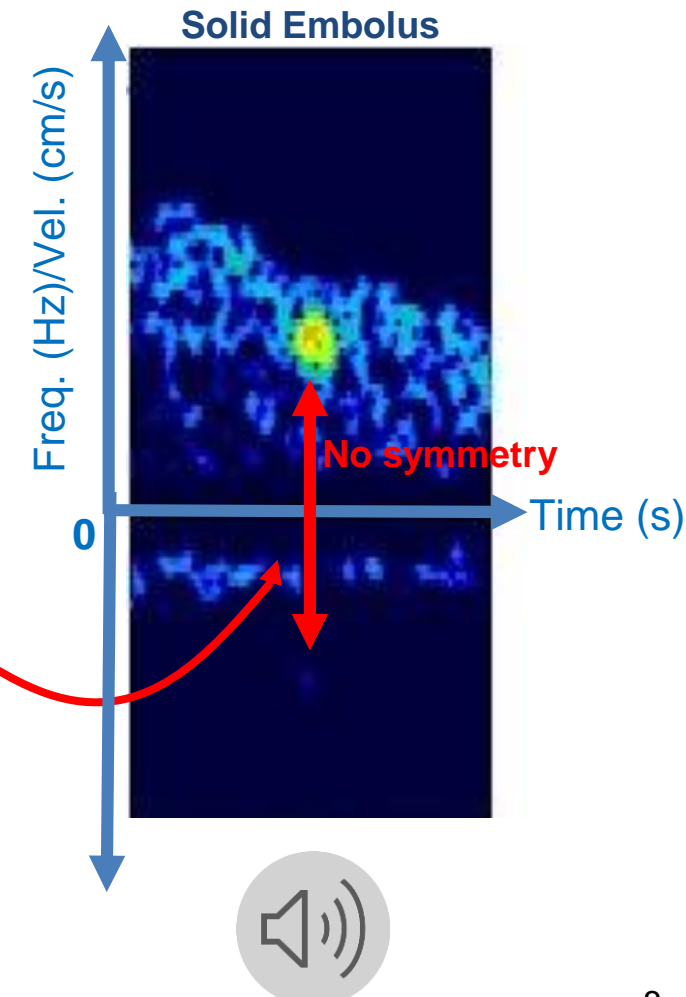
Emboli detection criteria

- **Basic identification criteria of Doppler microembolic signals***
 - **Duration < 300 ms** → High intensity transient signals (**HITS**)
 - **Unidirectional** in the time-frequency domain.
 - → **No symmetry** with respect to the zero-frequency baseline.
 - **Musical "chirp" or "snap" sound.**
 - **Intensity increase** of at least **3dB** with respect to the blood flow signal.
 - → Defined through the hits-to-blood ratio (**HBR**)



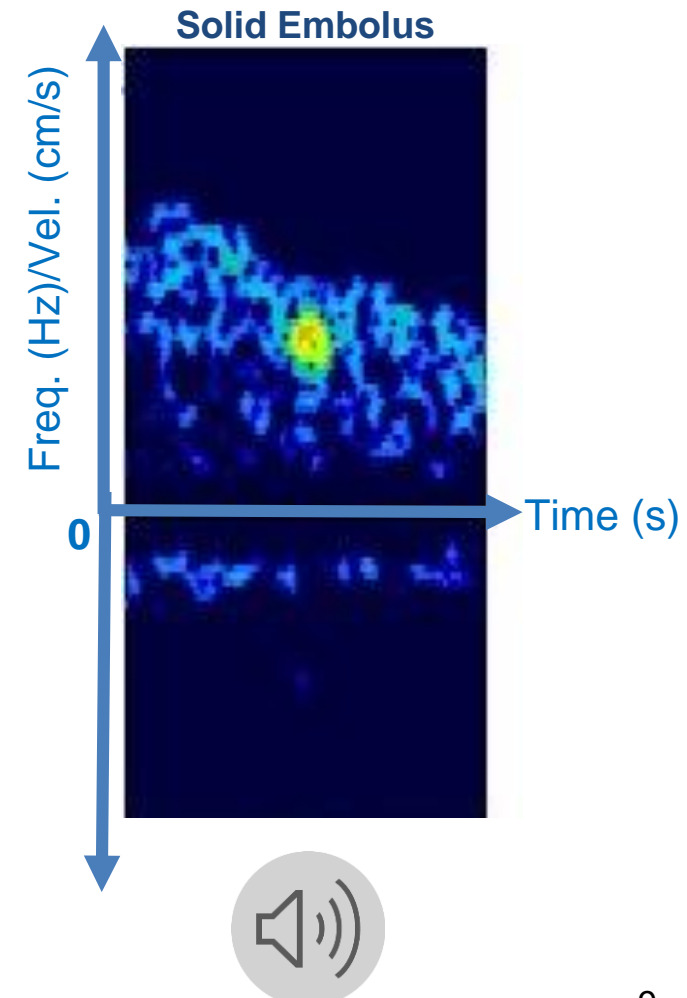
Emboli detection criteria

- **Basic identification criteria of Doppler microembolic signals***
 - Duration < 300 ms → High intensity transient signals (**HITS**)
 - **Unidirectional** in the time-frequency domain.
 - → **No symmetry** with respect to the zero-frequency baseline.
 - **Musical "chirp" or "snap" sound.**
 - **Intensity increase** of at least **3dB** with respect to the blood flow signal.
 - → Defined through the hits-to-blood ratio (**HBR**)



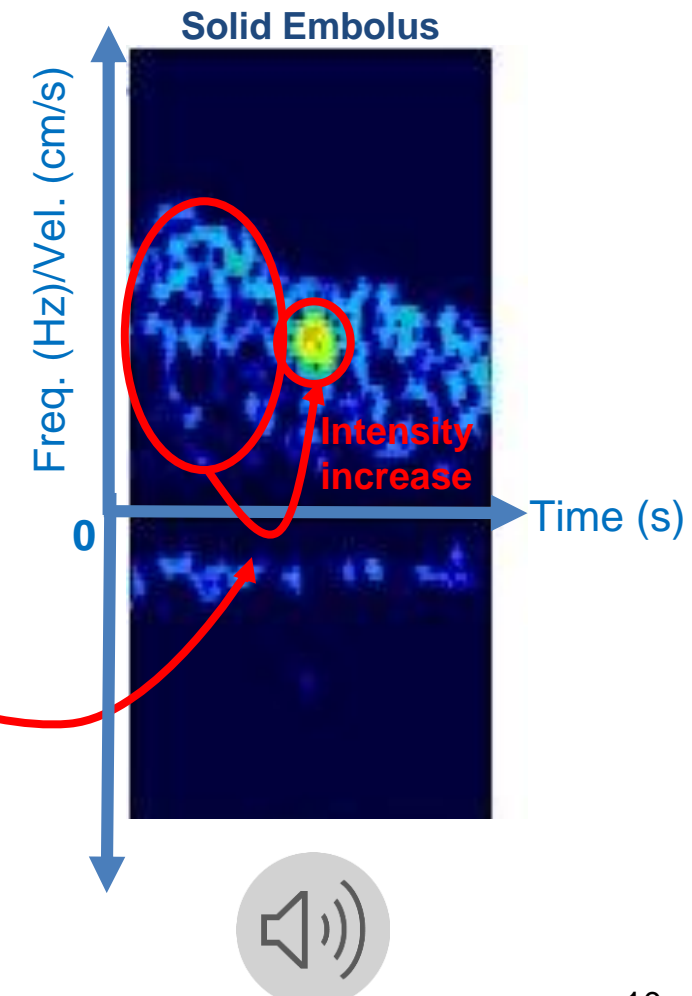
Emboli detection criteria

- **Basic identification criteria of Doppler microembolic signals***
 - Duration < 300 ms → High intensity transient signals (**HITS**)
 - Unidirectional in the time-frequency domain.
 - → No symmetry with respect to the zero-frequency baseline.
 - Musical "chirp" or "snap" sound.
 - Intensity increase of at least 3dB with respect to the blood flow signal.
 - → Defined through the hits-to-blood ratio (**HBR**)



Emboli detection criteria

- **Basic identification criteria of Doppler microembolic signals***
 - Duration < 300 ms → High intensity transient signals (**HITS**)
 - **Unidirectional** in the time-frequency domain.
 - → **No symmetry** with respect to the zero-frequency baseline.
 - **Musical "chirp" or "snap" sound.**
 - **Intensity increase** of at least **3dB** with respect to the blood flow signal.
 - → Defined through the hits-to-blood ratio (**HBR**)



Outline

I. Context

- a) Medical and scientific context
- b) **Embolus classification methods**
- c) Challenges and objectives

II. Contribution 1 : Semi-automatic data annotation

- a) State-of-the-art
- b) Proposed method
- c) Results

III. Contribution 2 : Multi-feature medical signal classification

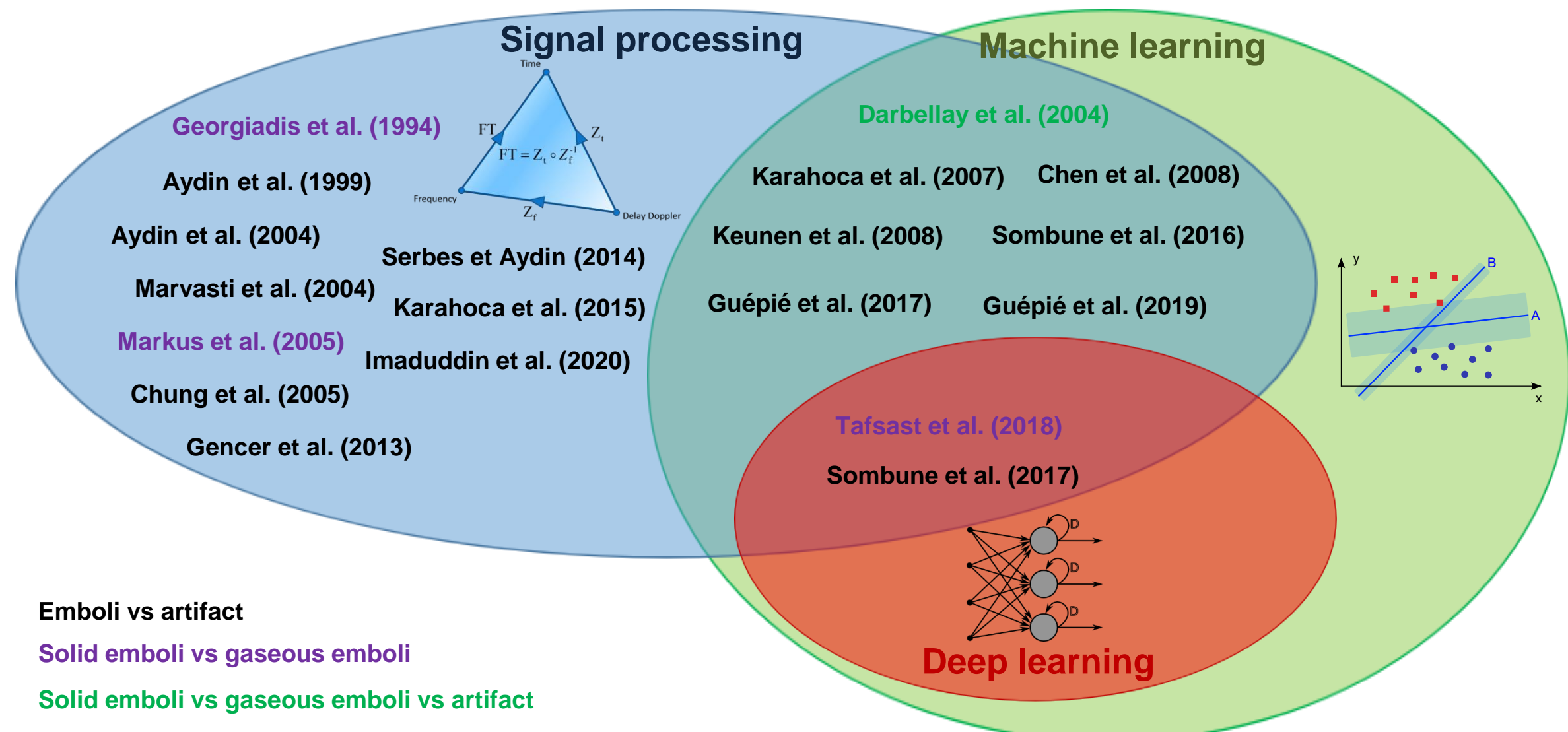
- a) State-of-the-art
- b) Proposed method
- c) Results

IV. Contribution 3 : Model compression based on extreme quantization

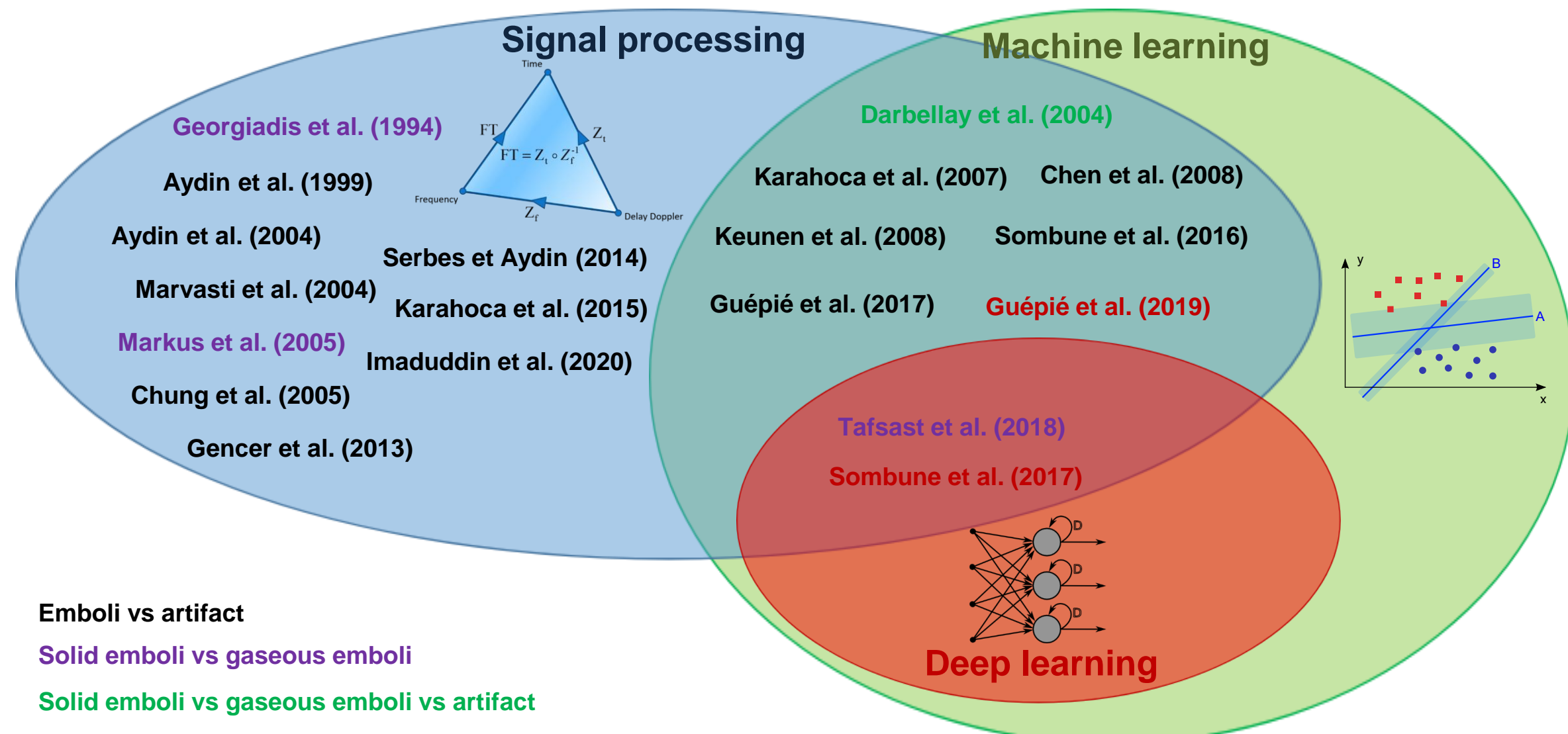
- a) State-of-the-art
- b) Proposed method
- c) Results

V. Conclusion and perspectives

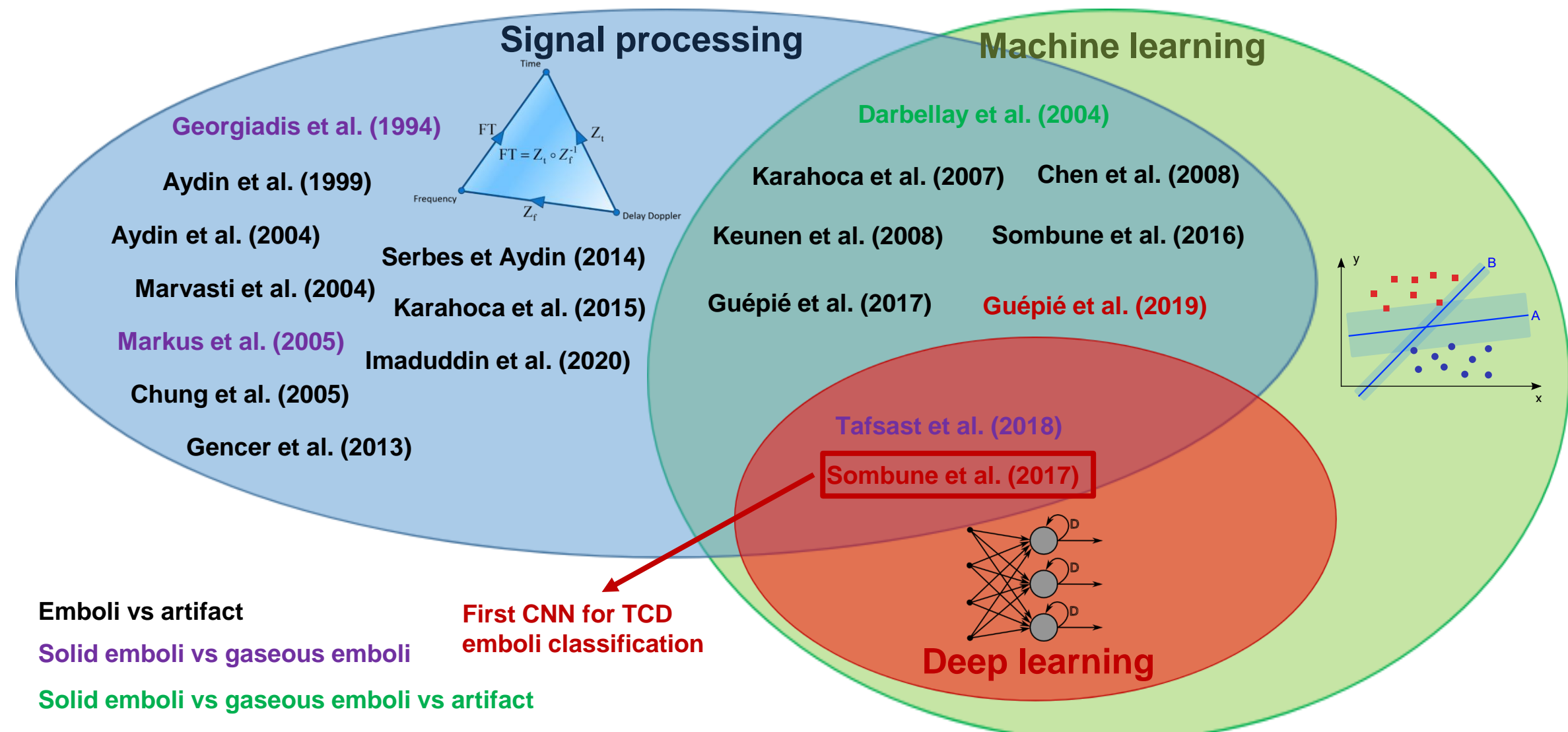
Emboli classification



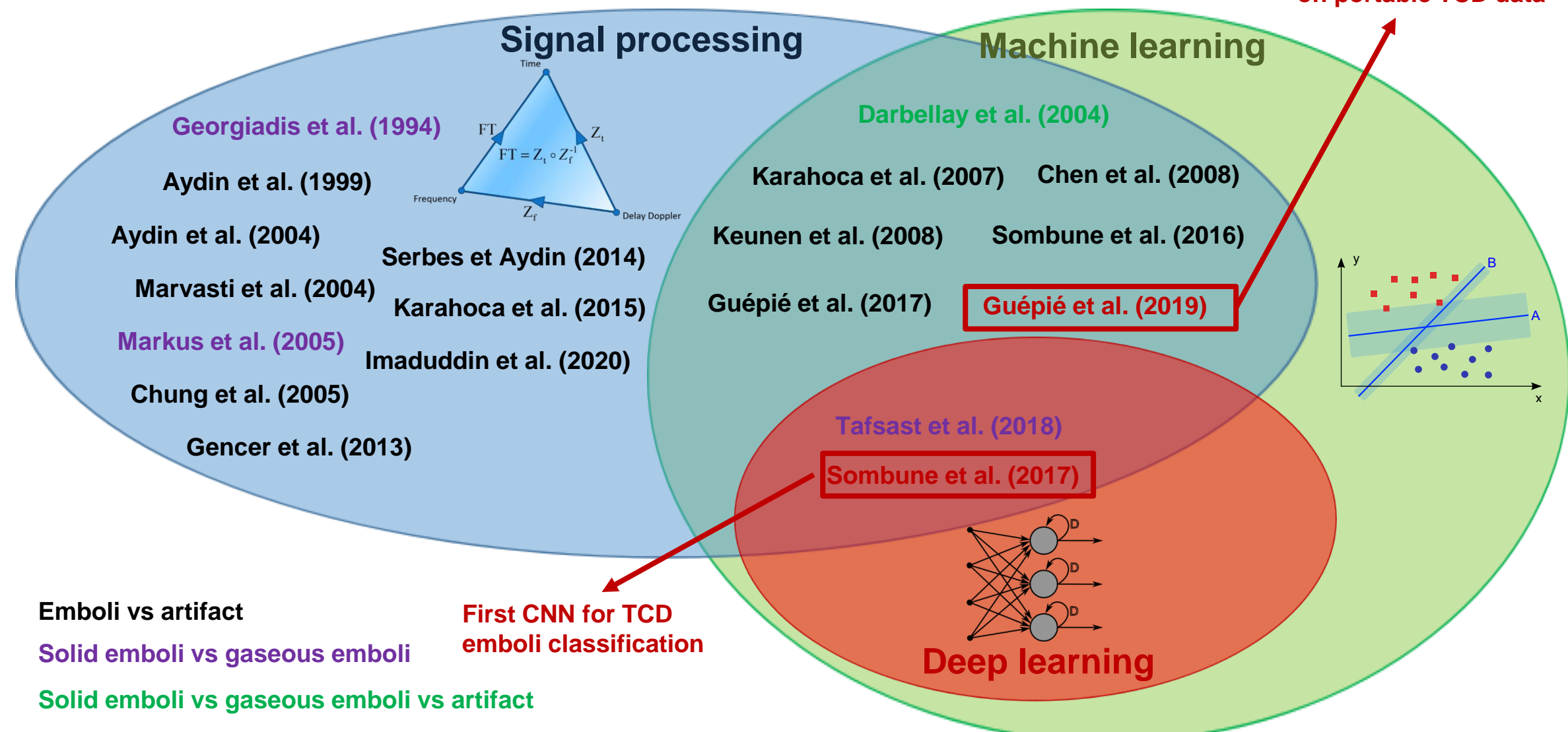
Emboli classification



Emboli classification



Emboli classification

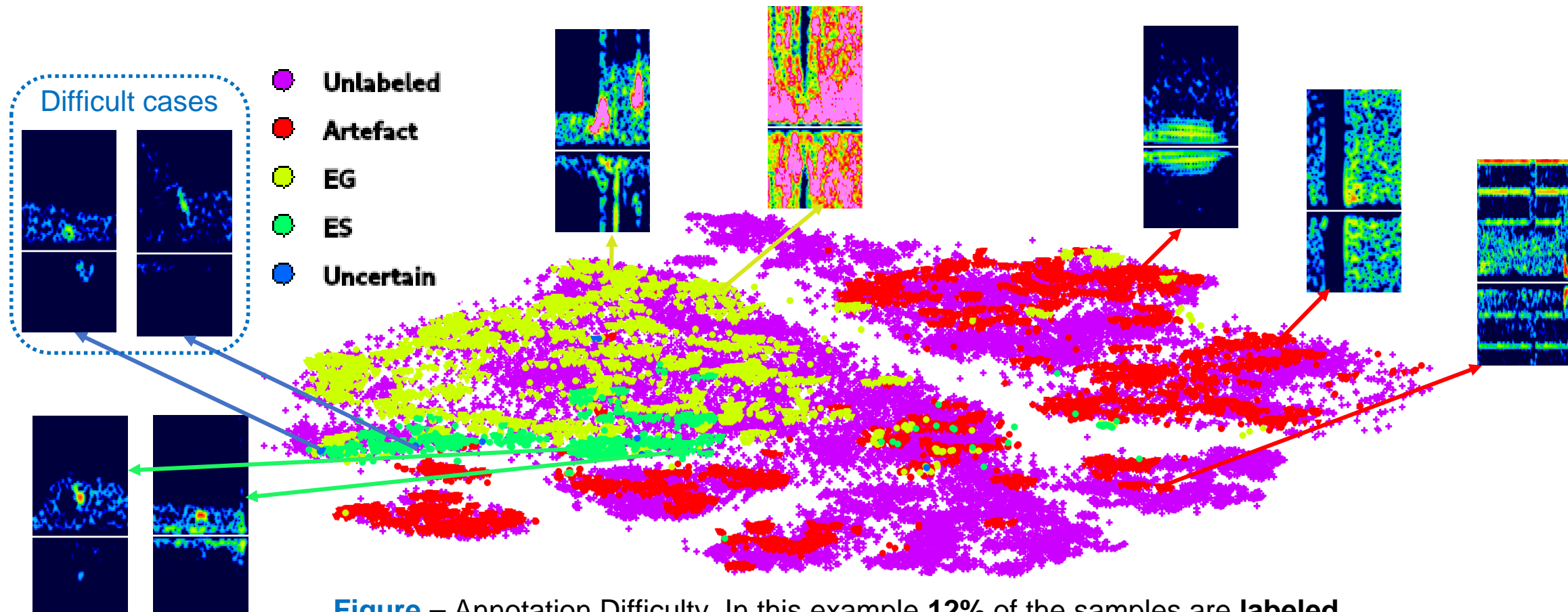


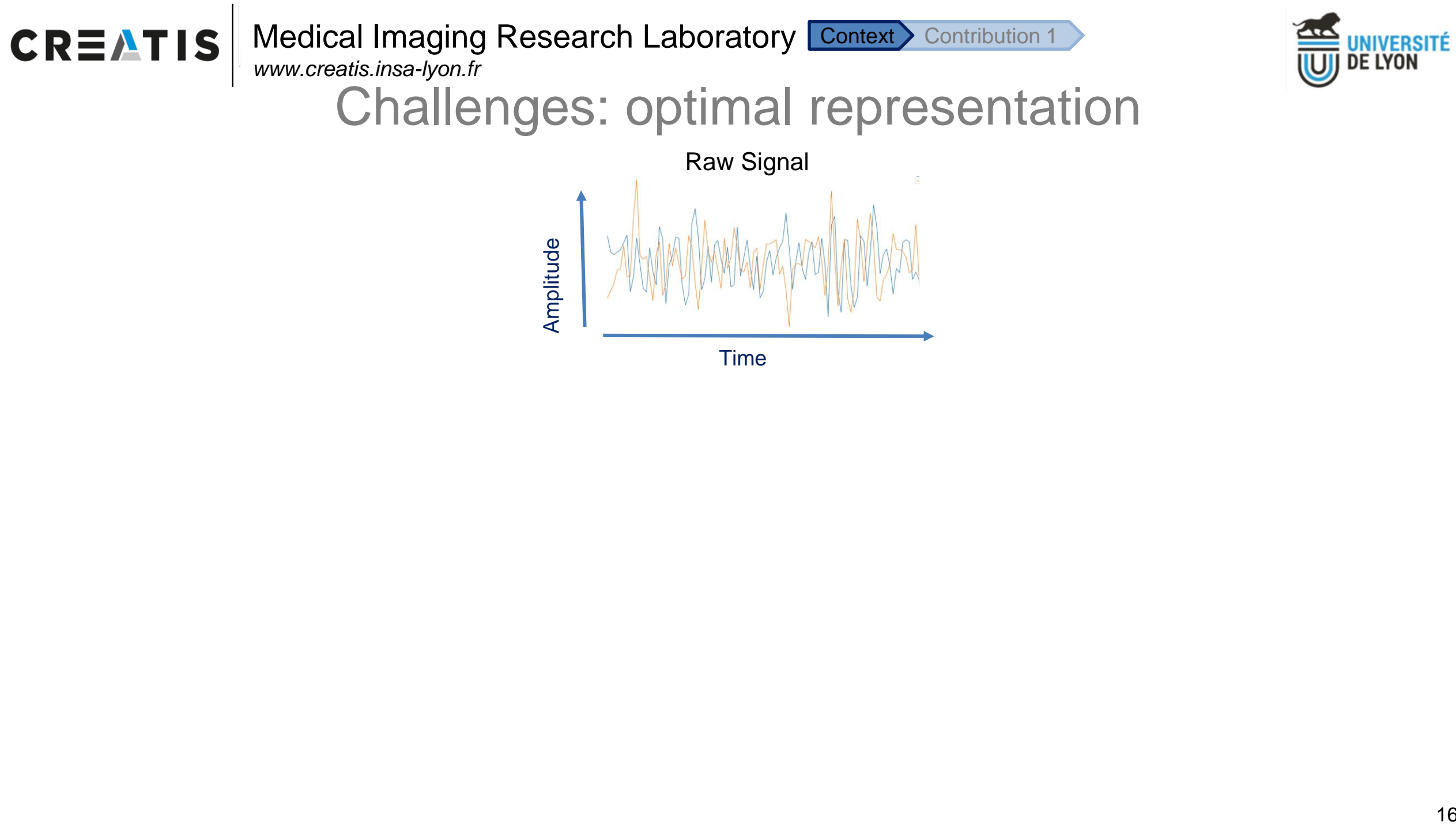
Outline

- I. **Context**
 - a) Medical and scientific context
 - b) Emboli classification methods
 - c) **Challenges and objectives**
- II. **Contribution 1 : Semi-automatic data annotation**
 - a) State-of-the-art
 - b) Proposed method
 - c) Results
- III. **Contribution 2 : Multi-feature medical signal classification**
 - a) State-of-the-art
 - b) Proposed method
 - c) Results
- IV. **Contribution 3 : Model compression based on extreme quantization**
 - a) State-of-the-art
 - b) Proposed method
 - c) Results
- V. **Conclusion and perspectives**

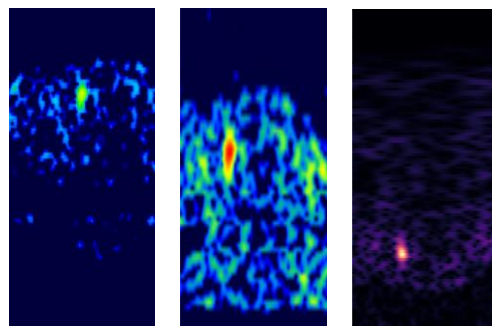
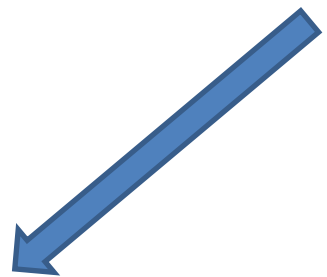
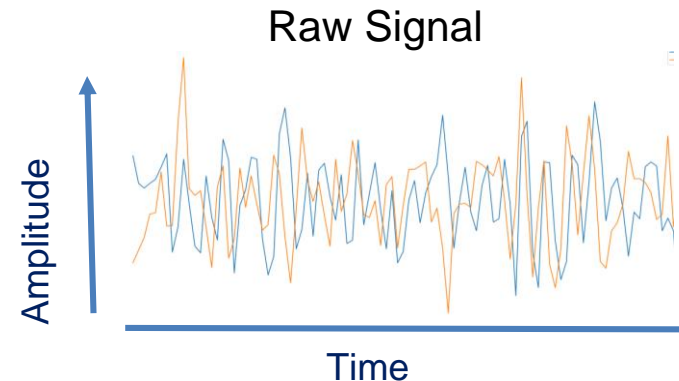
Challenges: data annotation

- No public TCD emboli dataset.
- Expensive annotation (8685/68491 labeled samples).
- Annotation difficulty → Noisy labels.
- Imbalanced classes (solid emboli < 10% HITS).



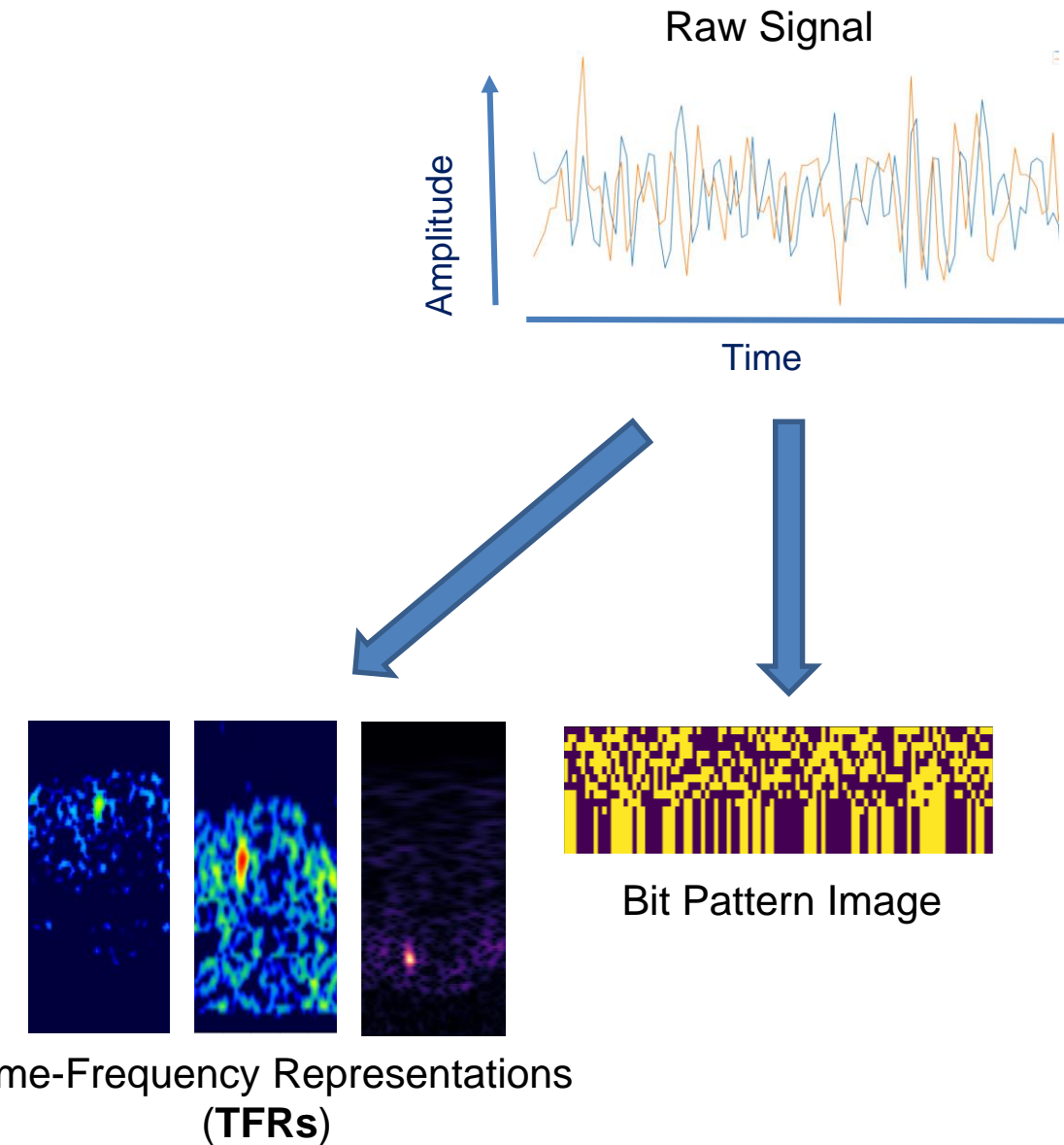


Challenges: optimal representation

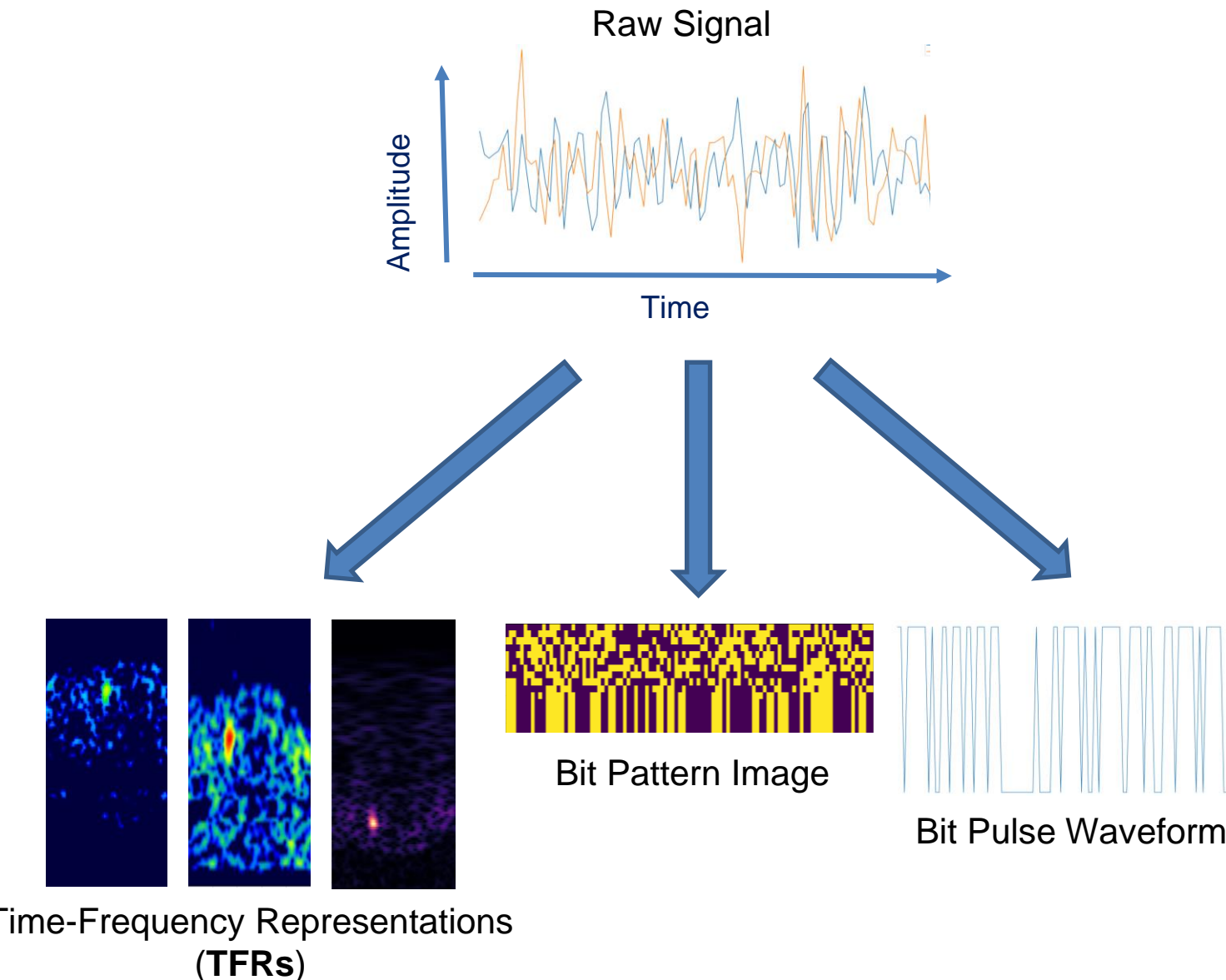


Time-Frequency Representations
(TFRs)

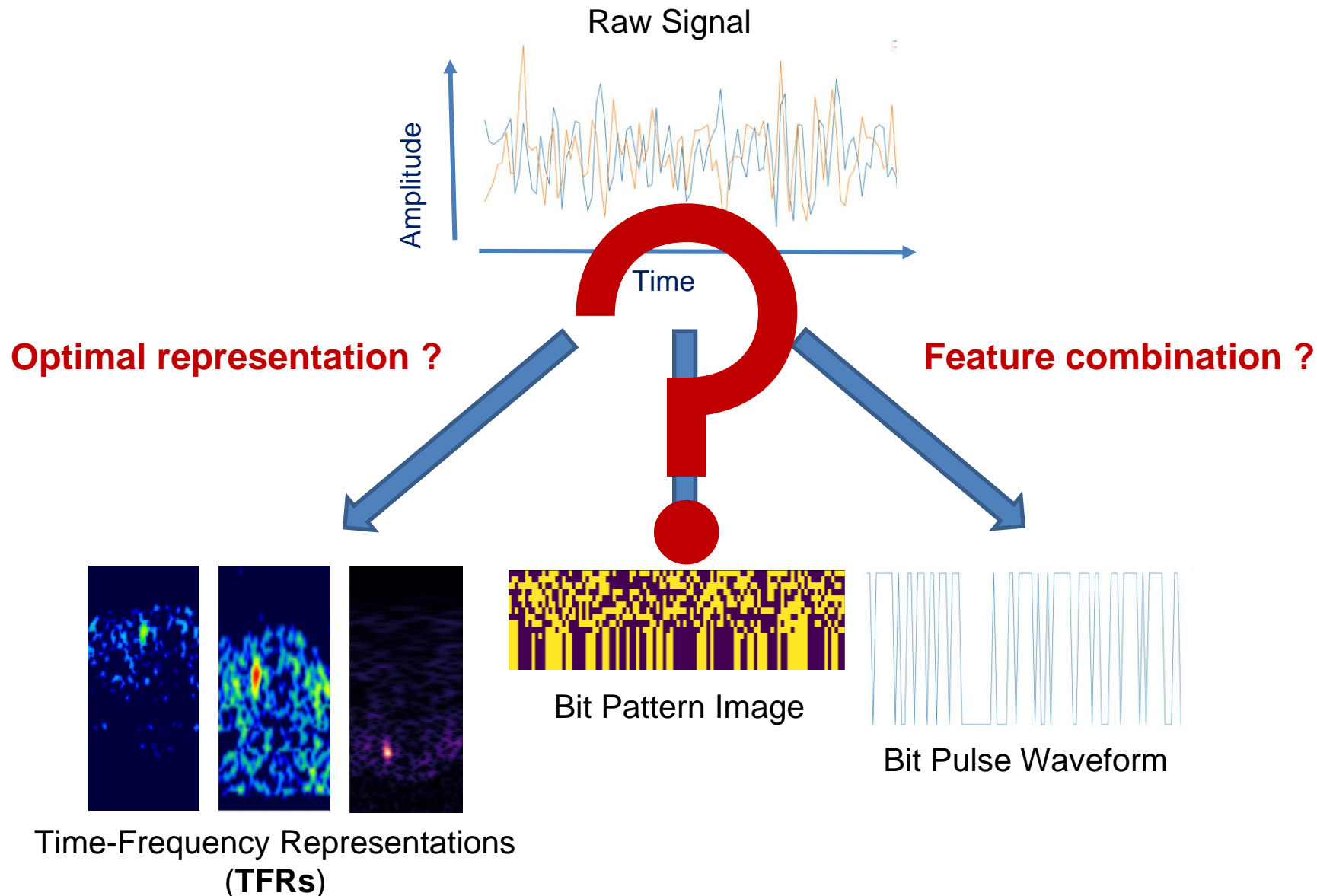
Challenges: optimal representation



Challenges: optimal representation



Challenges: optimal representation



Challenges: model compression



Figure – Portable transcranial Doppler (TCD) from Atys Medical.

Challenges: model compression



Figure – Portable transcranial Doppler (TCD) from Atys Medical.



Limited memory resources.

Challenges: model compression



Figure – Portable transcranial Doppler (TCD) from Atys Medical.

- Limited memory resources.
- Limited computation resources.

Challenges: model compression



Figure – Portable transcranial Doppler (TCD) from Atys Medical.

- Limited memory resources.
- Limited computation resources.
- Energy constraints.

Challenges: model compression



Figure – Portable transcranial Doppler (TCD) from Atys Medical.

- Limited memory resources.
- Limited computation resources.
- Energy constraints.

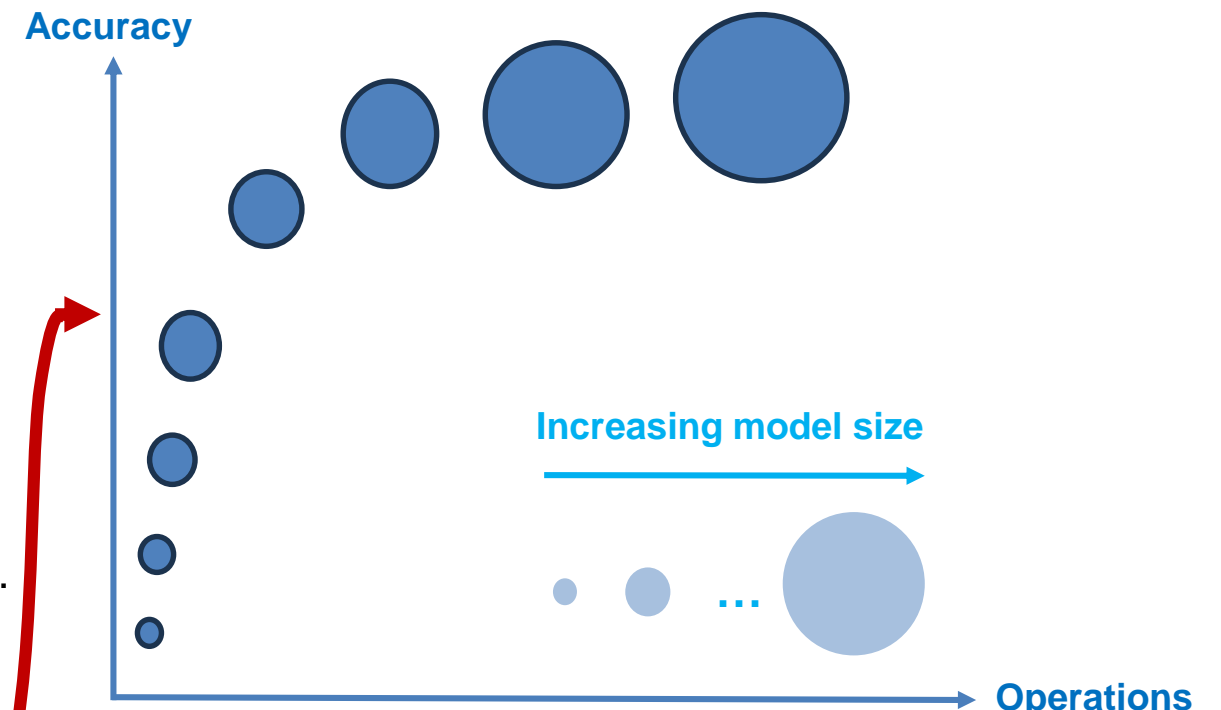
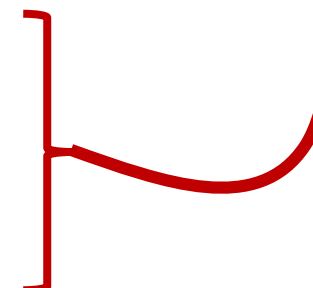


Figure – Classification accuracy based on the size and number of floating-point operations of different deep learning models (inspired from Abbas et al. 2021)

Objectives and Contributions

Objectives and Contributions

Dataset creation and annotation

* Vindas et al. (IUS 2021), Vindas et al. (MEDIA 2022), Vindas et al. (IUS 2023)

** Vindas et al. (MLHC 2022), Vindas et al. (IABM 2023), Vindas et al. (EUSIPCO 2023), and Vindas et al. (Pattern Recognition 2023)

Objectives and Contributions

Dataset creation and annotation



- Semi-supervised data annotation*
- Soft labelling (annotation)*

* Vindas et al. (IUS 2021), Vindas et al. (MEDIA 2022), Vindas et al. (IUS 2023)

** Vindas et al. (MLHC 2022), Vindas et al. (IABM 2023), Vindas et al. (EUSIPCO 2023), and Vindas et al. (Pattern Recognition 2023)

Objectives and Contributions

Dataset creation and annotation



- Semi-supervised data annotation*
- Soft labelling (annotation)*

Multiple representations

Objectives and Contributions

Dataset creation and annotation



- Semi-supervised data annotation*
- Soft labelling (annotation)*

Multiple representations



- Different models with different inputs**
- Multi-feature models

* Vindas et al. (IUS 2021), Vindas et al. (MEDIA 2022), Vindas et al. (IUS 2023)

** Vindas et al. (MLHC 2022), Vindas et al. (IABM 2023), Vindas et al. (EUSIPCO 2023), and Vindas et al. (Pattern Recognition 2023)

Objectives and Contributions

Dataset creation and annotation



- Semi-supervised data annotation*
- Soft labelling (annotation)*

Multiple representations



- Different models with different inputs**
- Multi-feature models

Resource hungry models

* Vindas et al. (IUS 2021), Vindas et al. (MEDIA 2022), Vindas et al. (IUS 2023)

** Vindas et al. (MLHC 2022), Vindas et al. (IABM 2023), Vindas et al. (EUSIPCO 2023), and Vindas et al. (Pattern Recognition 2023)

Objectives and Contributions

Dataset creation and annotation



- Semi-supervised data annotation*
- Soft labelling (annotation)*

Multiple representations



- Different models with different inputs**
- Multi-feature models

Resource hungry models



- Lite models
- Model compression
- (Soft labelling training)

* Vindas et al. (IUS 2021), Vindas et al. (MEDIA 2022), Vindas et al. (IUS 2023)

** Vindas et al. (MLHC 2022), Vindas et al. (IABM 2023), Vindas et al. (EUSIPCO 2023), and Vindas et al. (Pattern Recognition 2023)

Objectives and Contributions

Dataset creation and annotation 

- Semi-supervised data annotation*
- Soft labelling (annotation)*

Multiple representations 

- Different models with different inputs**
- Multi-feature models

Resource hungry models 

- Lite models
- Model compression
- (Soft labelling training)

* Vindas et al. (IUS 2021), Vindas et al. (MEDIA 2022), Vindas et al. (IUS 2023)

** Vindas et al. (MLHC 2022), Vindas et al. (IABM 2023), Vindas et al. (EUSIPCO 2023), and Vindas et al. (Pattern Recognition 2023)

Outline

I. Context

- a) Medical and scientific context
- b) Emboli classification methods
- c) Challenges and objectives

II. Contribution 1 : Semi-automatic data annotation

- a) State-of-the-art
- b) Proposed method
- c) Results

III. Contribution 2 : Multi-feature medical signal classification

- a) State-of-the-art
- b) Proposed method
- c) Results

IV. Contribution 3 : Model compression based on extreme quantization

- a) State-of-the-art
- b) Proposed method
- c) Results

V. Conclusion and perspectives

Semi-automatic data annotation based on feature space projection

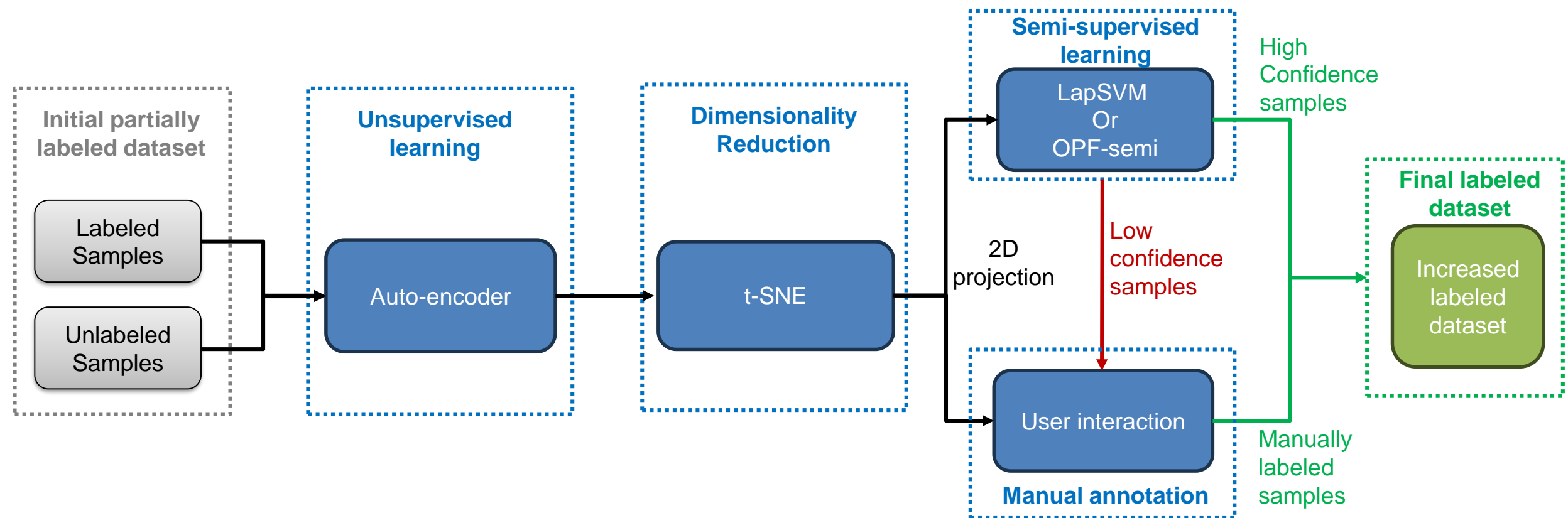


Figure – Semi-automatic data annotation based on feature space projection (Benato et al., 2021)

Semi-automatic data annotation based on feature space projection

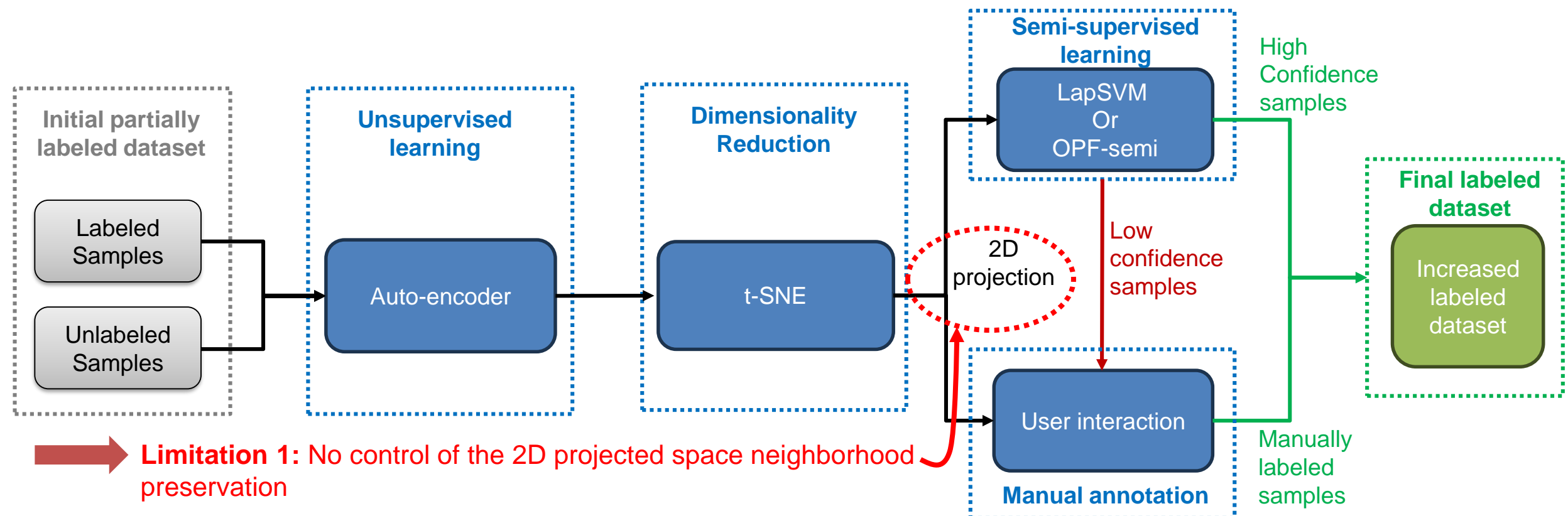


Figure – Semi-automatic data annotation based on feature space projection (Benato et al., 2021)

Semi-automatic data annotation based on feature space projection

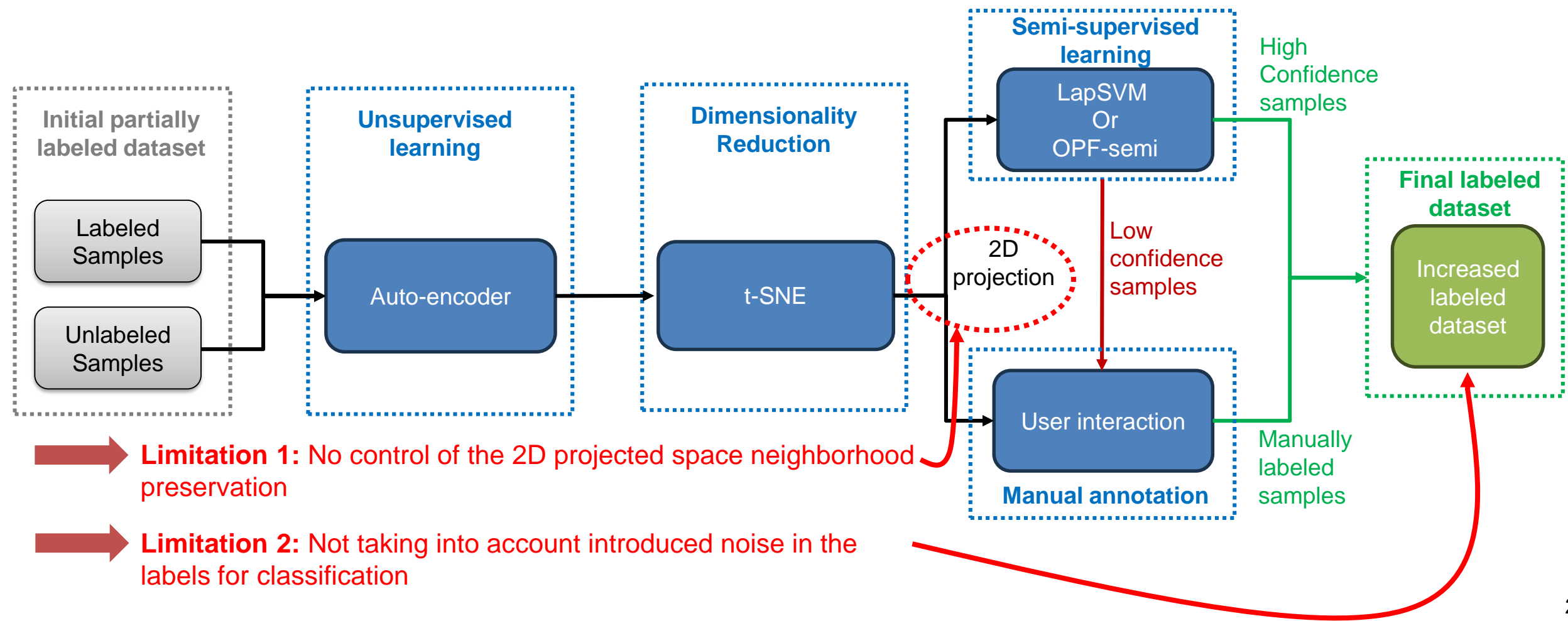


Figure – Semi-automatic data annotation based on feature space projection (Benato et al., 2021)

Possible solution 2D projection quality

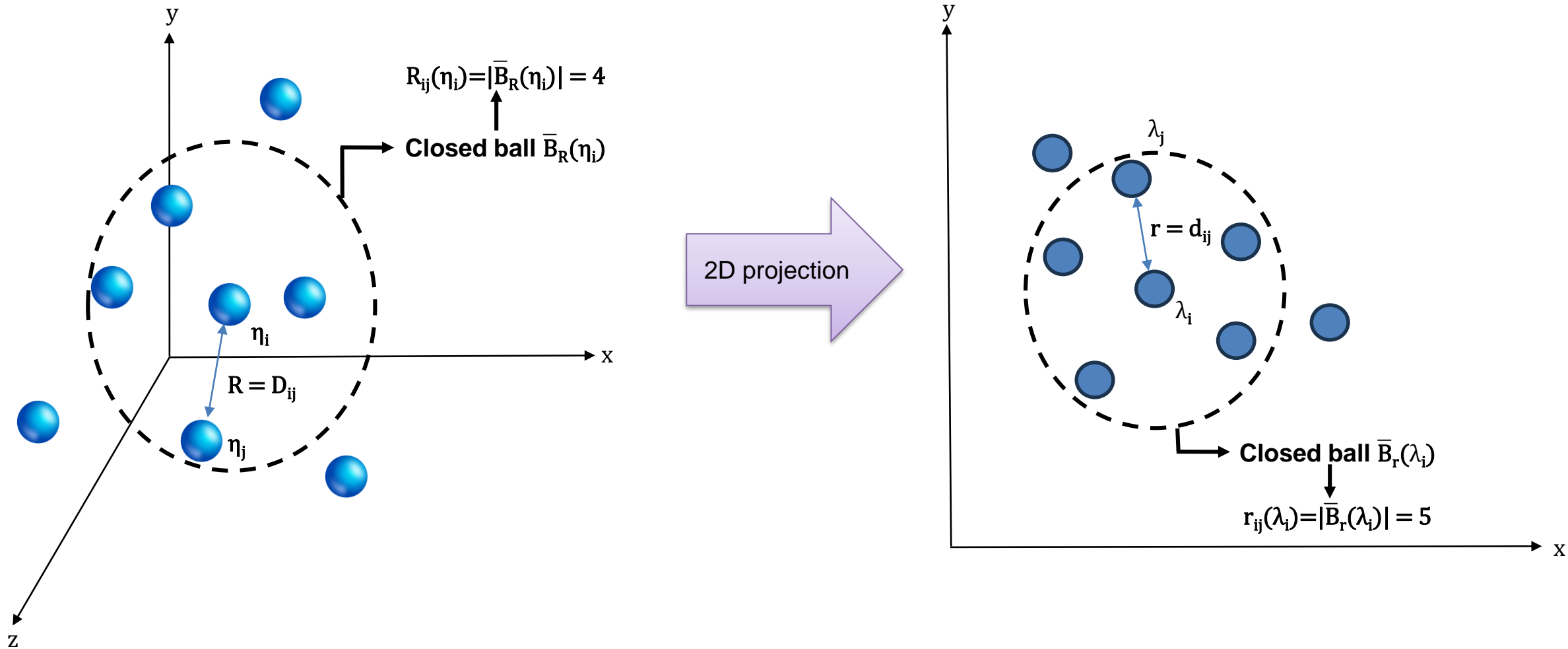


Figure – Ranks definitions during space projection (Lueks et al., 2011).

Possible solution to noisy-labels

Robust loss functions

Possible solution to noisy-labels

Robust loss functions

Flexible

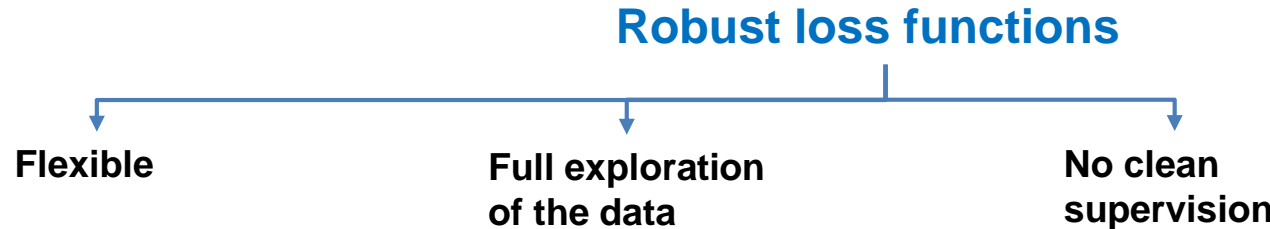
Possible solution to noisy-labels

Robust loss functions

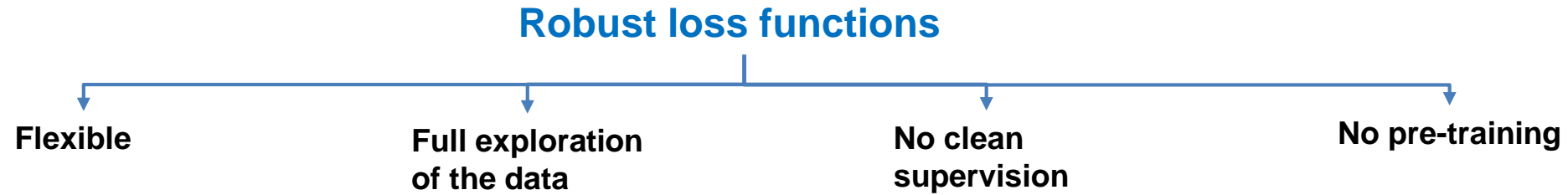
Flexible

Full exploration
of the data

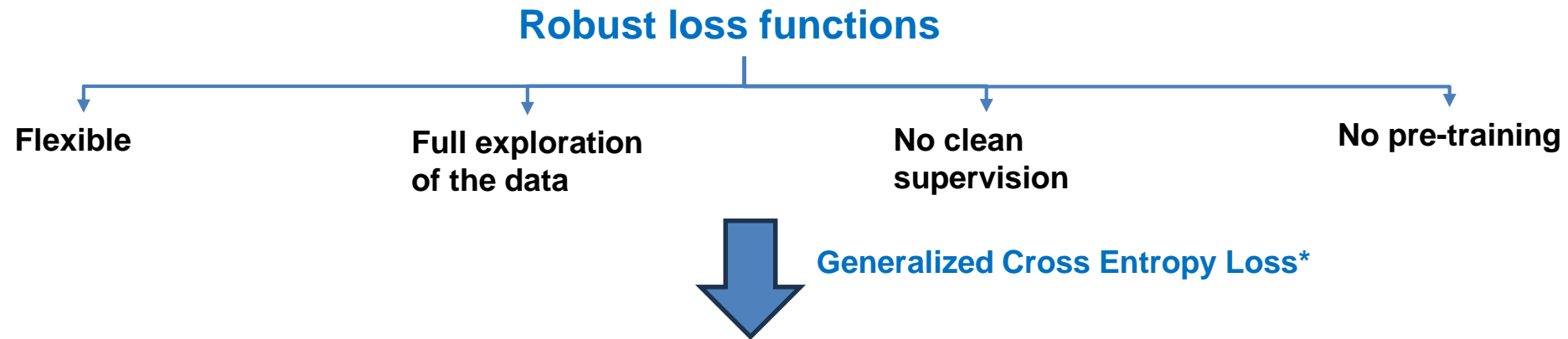
Possible solution to noisy-labels



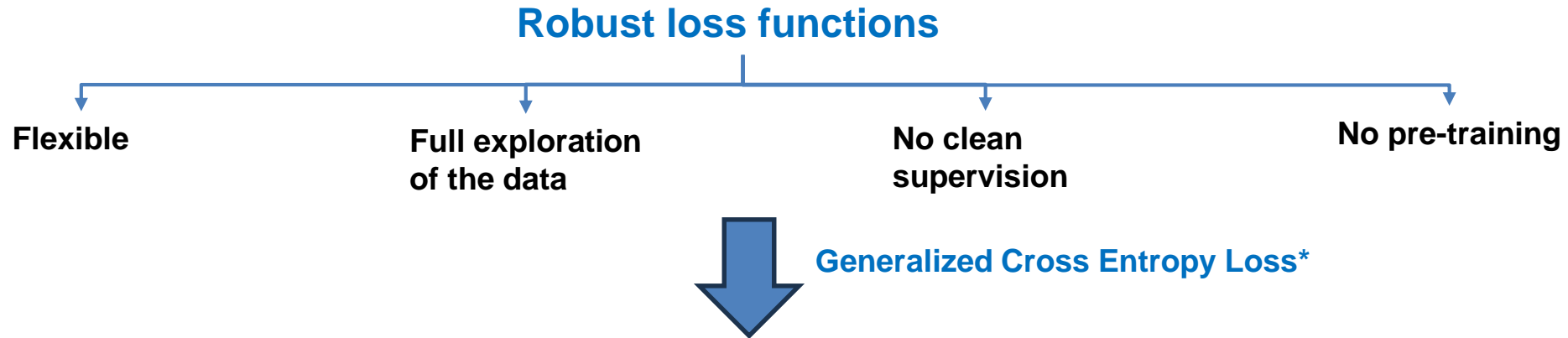
Possible solution to noisy-labels



Possible solution to noisy-labels



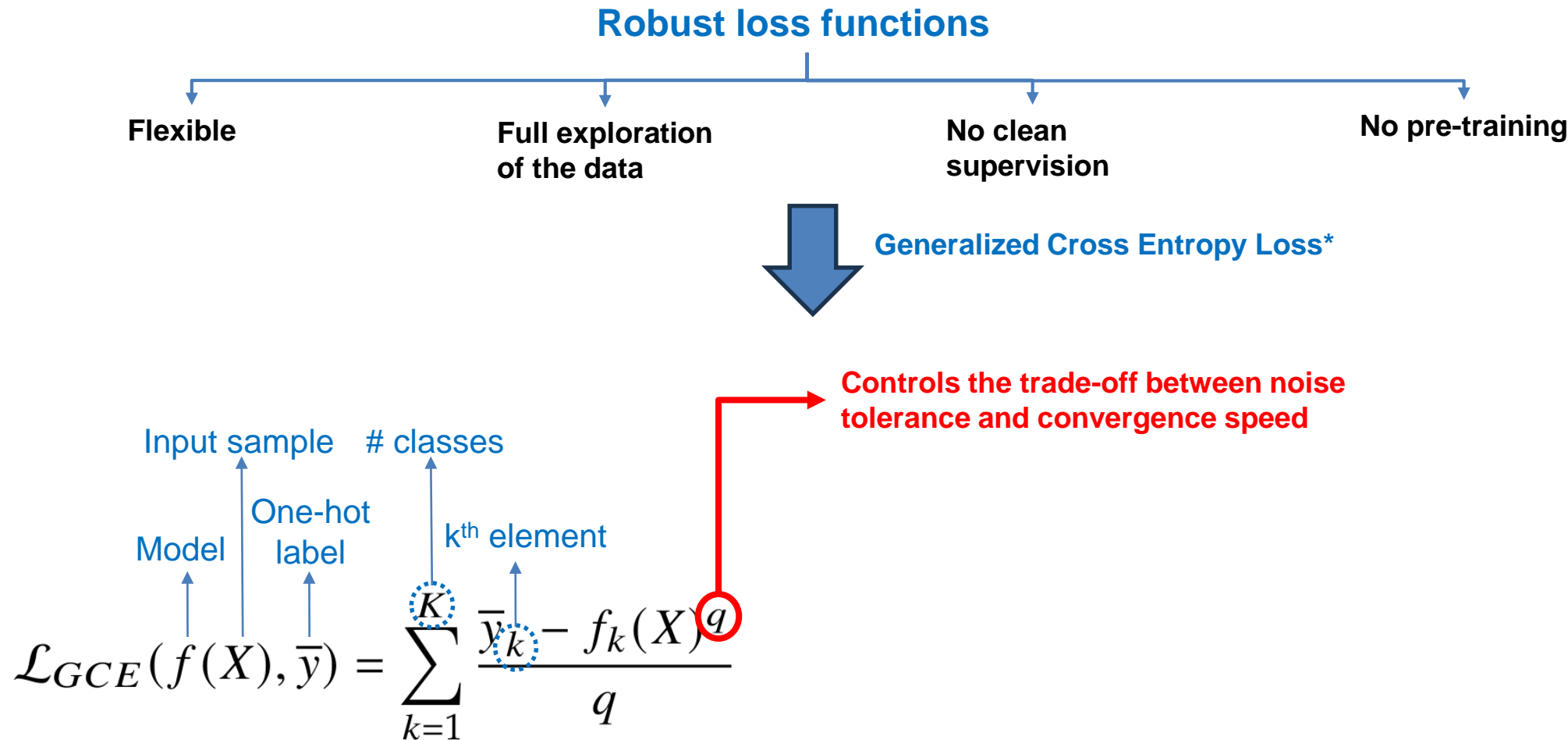
Possible solution to noisy-labels



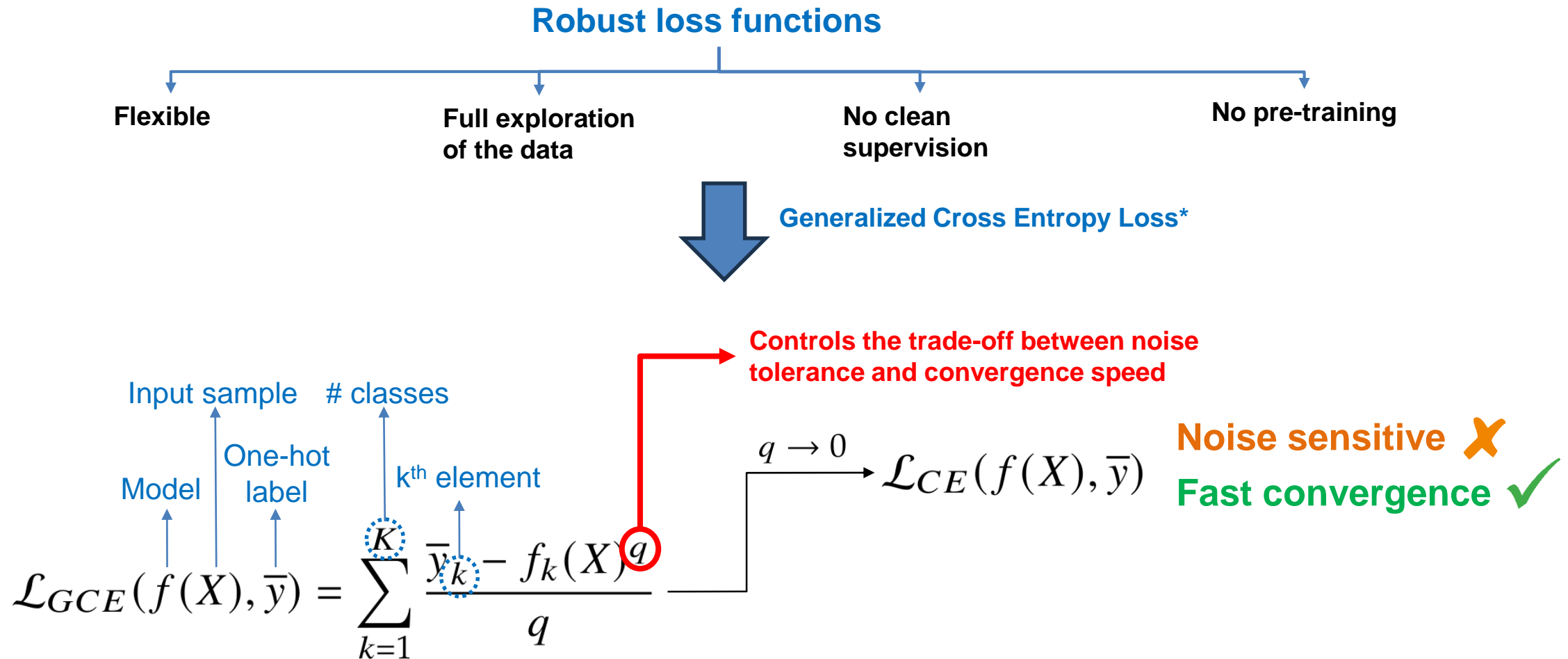
$$\mathcal{L}_{GCE}(f(X), \bar{y}) = \sum_{k=1}^K \frac{\bar{y}_k - f_k(X)^q}{q}$$

Input sample # classes
 One-hot label kth element
 Model

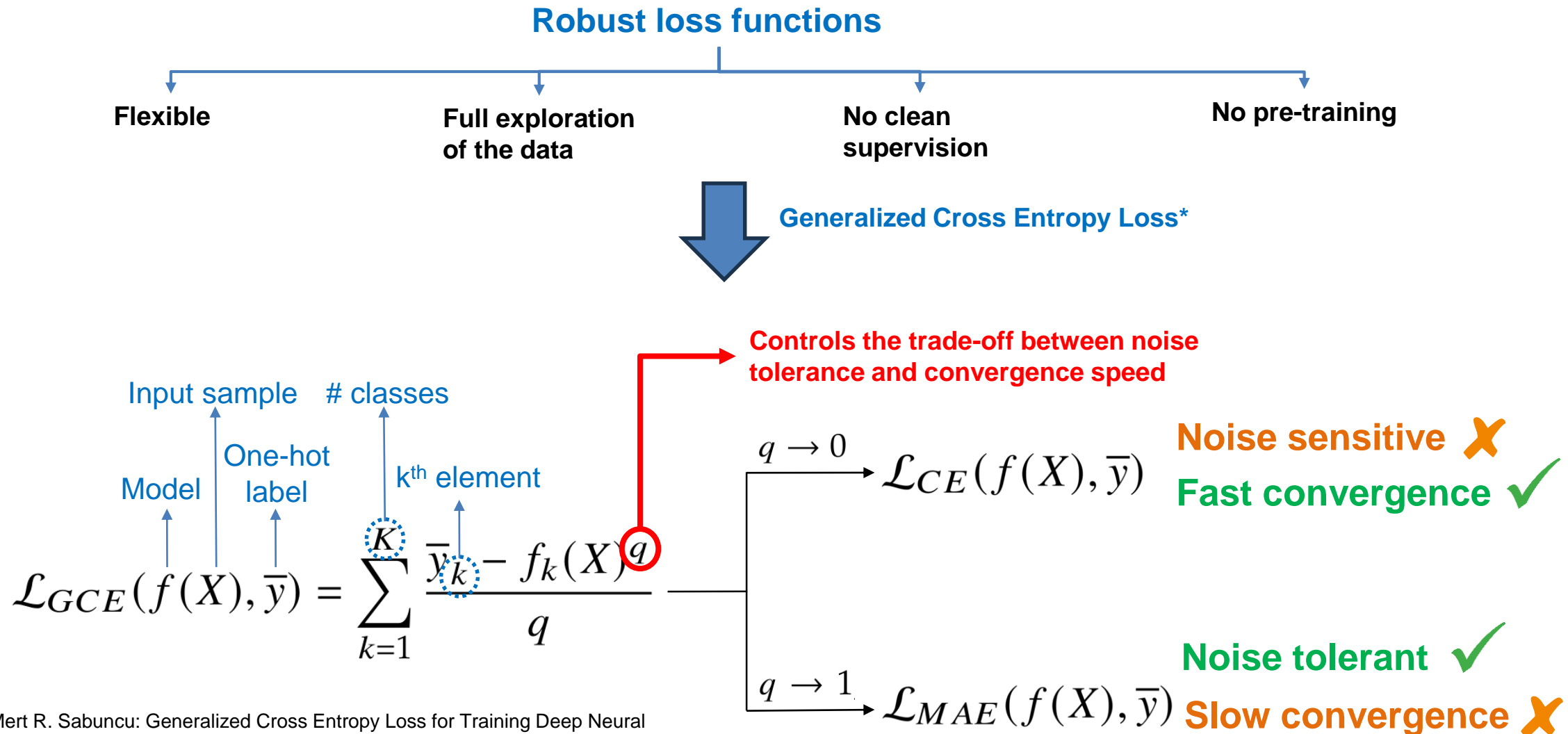
Possible solution to noisy-labels



Possible solution to noisy-labels



Possible solution to noisy-labels



Outline

- I. **Context**
 - a) **Medical and scientific context**
 - b) **Emboli classification methods**
 - c) **Challenges and objectives**
- II. **Contribution 1 : Semi-automatic data annotation**
 - a) **State-of-the-art**
 - b) **Proposed method**
 - c) **Results**
- III. **Contribution 2 : Multi-feature medical signal classification**
 - a) **State-of-the-art**
 - b) **Proposed method**
 - c) **Results**
- IV. **Contribution 3 : Model compression based on extreme quantization**
 - a) **State-of-the-art**
 - b) **Proposed method**
 - c) **Results**
- V. **Conclusion and perspectives**

Claims of contribution 1

- a. **Novel methodology** for **semi-automatic data annotation** based on local-quality (LQ) metrics, called **LQ-KNN**.
- b. **Selection strategy** of the best **projection** obtained by a dimensionality reduction technique.
- c. **Use robust loss** functions to improve the classification performances of a **classifier trained** on a **noisy** semi-automatic labeled **dataset**.

Proposed pipeline

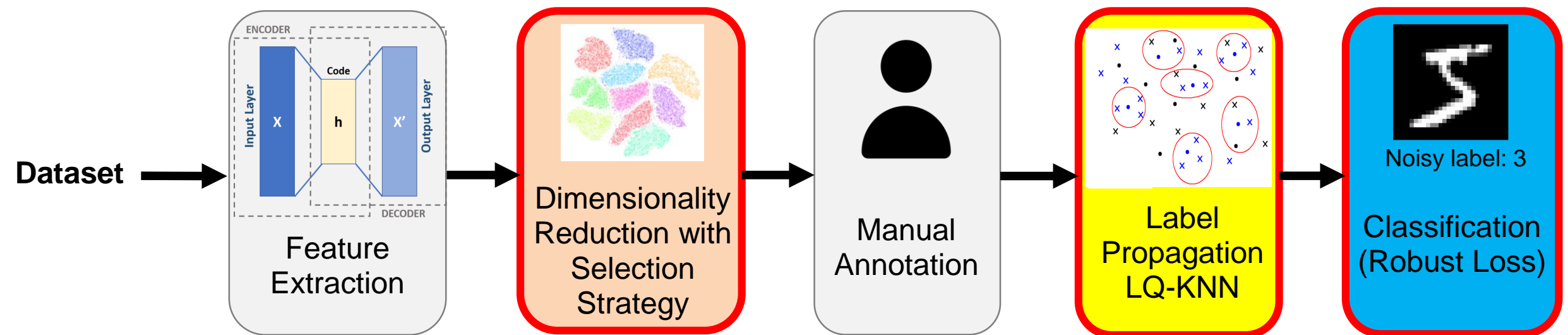
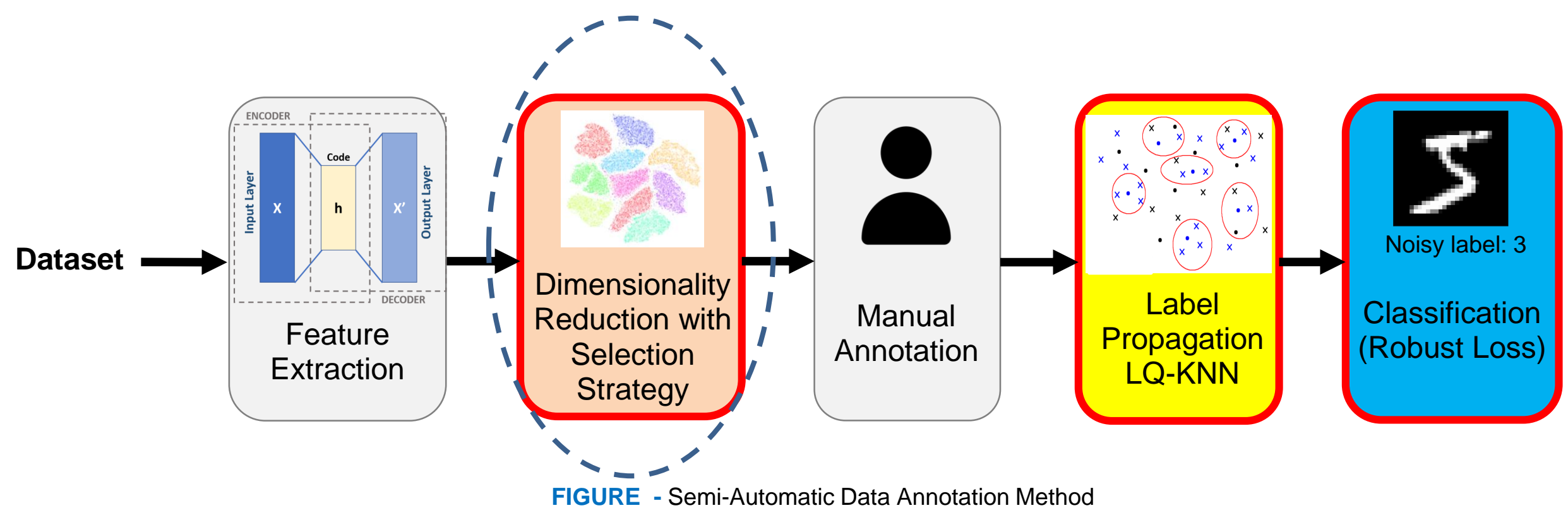
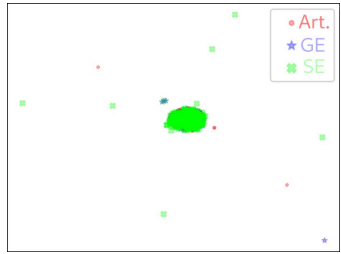


FIGURE - Semi-Automatic Data Annotation Method

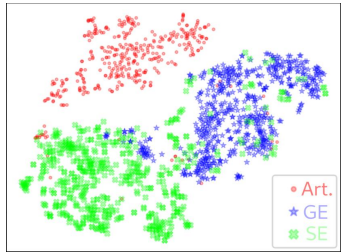
Proposed pipeline



Dimensionality Reduction

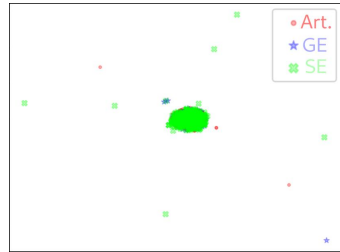
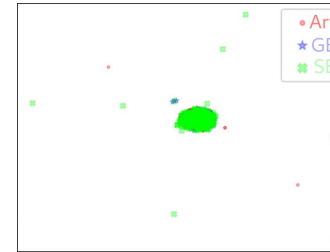


-
-
-



Different computed
2D projections

Dimensionality Reduction

 $S = -0.56$ 

Silhouette Score
 S computation

⋮

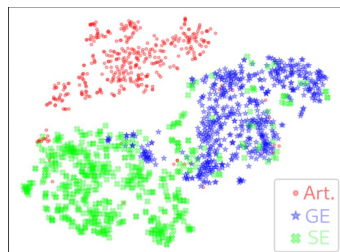
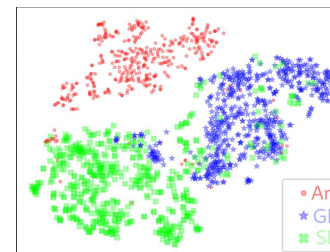
⋮

⋮



⋮

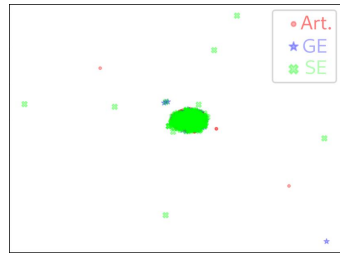
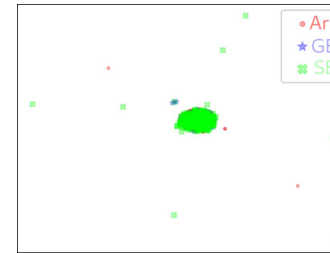
⋮

 $S = 0.49$ 

Silhouette score
 $S \in [-1,1]$

Different computed
2D projections

Dimensionality Reduction

 $S = -0.56$ 

Silhouette Score
 S computation

⋮

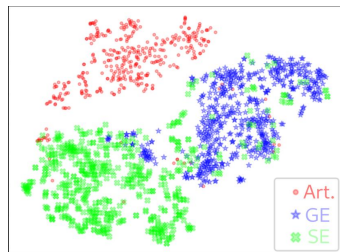
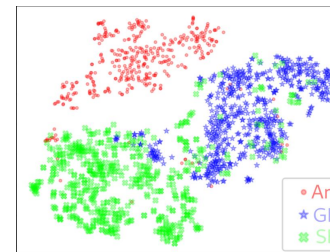
⋮

⋮



⋮

⋮

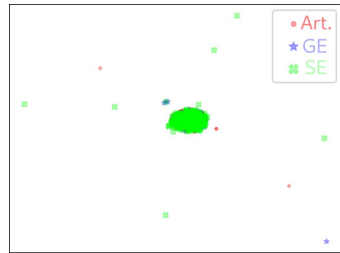
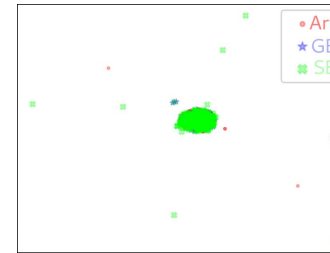
 $S = 0.49$ 

Different computed
2D projections

Silhouette score
 $S \in [-1,1]$

Distant and compact clusters

Dimensionality Reduction

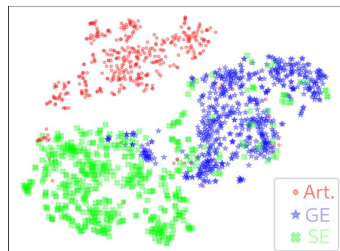
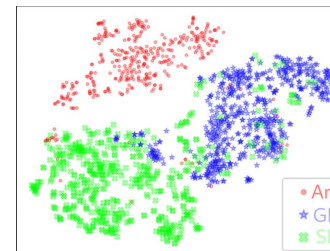
 $S = -0.56$ 

Silhouette Score
 S computation

⋮

⋮

⋮

 $S = 0.49$ 

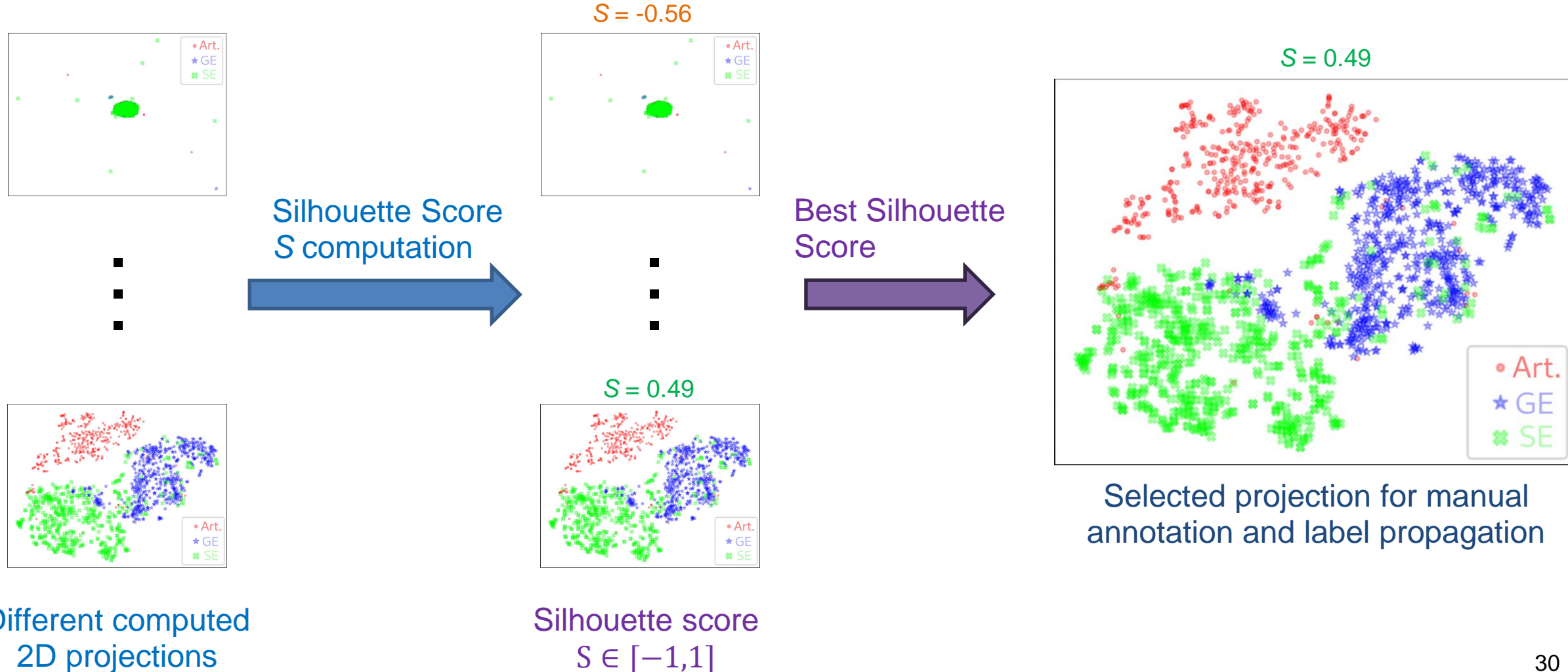
Silhouette score
 $S \in [-1,1]$



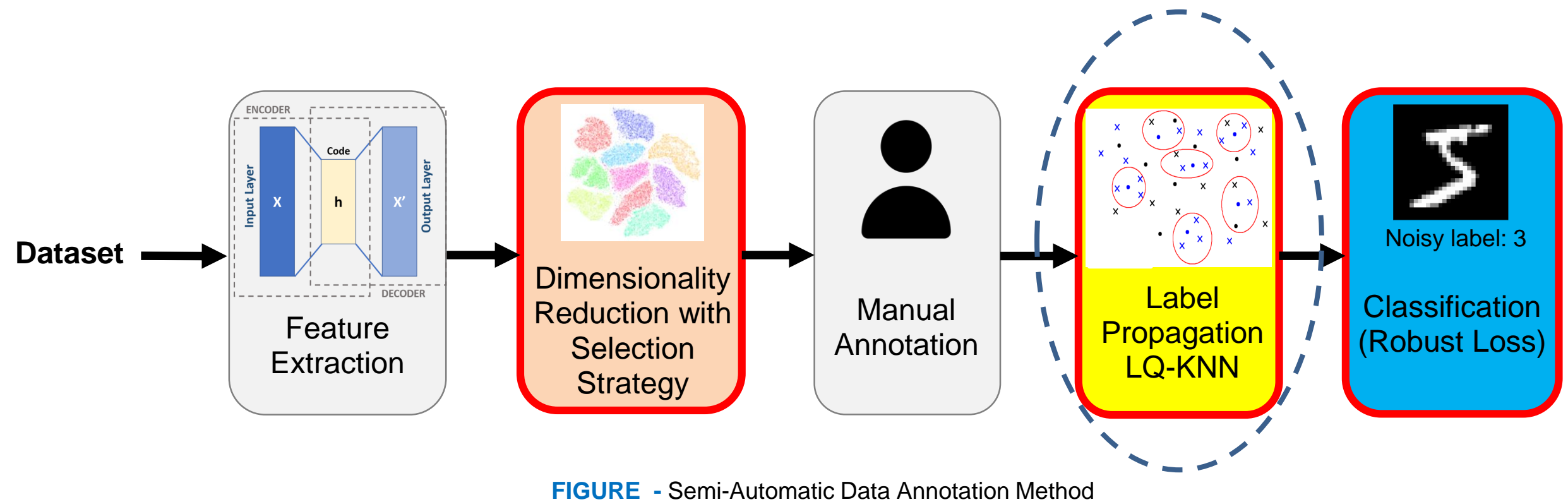
Different computed
2D projections

Overlapping clusters

Dimensionality Reduction



Proposed pipeline



Semi-automatic label propagation: Assumptions

- Based on a **K-nearest neighbors (KNN)** approach.
- **Three assumptions:**
 - Structure/cluster assumption¹.
 - Local structure preservation.
 - Annotation space coverage.

¹ Olivier Chapelle, Bernhard Schölkopf, and Alexander Zien, eds. Semi-supervised learning. Adaptive computation and machine learning. OCLC: ocm64898359. Cambridge, Mass: MIT Press, 2006. 508 pp. isbn: 978-0-262-03358-9

Semi-automatic label propagation: Assumptions

- Based on a **K-nearest neighbors (KNN)** approach.
- **Three assumptions:**
 - Structure/cluster assumption¹.
 - Local structure preservation.
 - Annotation space coverage.

 Local quality (**LQ**) K-nearest neighbor (**KNN**) label propagation : **LQ-KNN**

¹ Olivier Chapelle, Bernhard Schölkopf, and Alexander Zien, eds. Semi-supervised learning. Adaptive computation and machine learning. OCLC: ocm64898359. Cambridge, Mass: MIT Press, 2006. 508 pp. isbn: 978-0-262-03358-9

Semi-automatic label propagation LQ-KNN

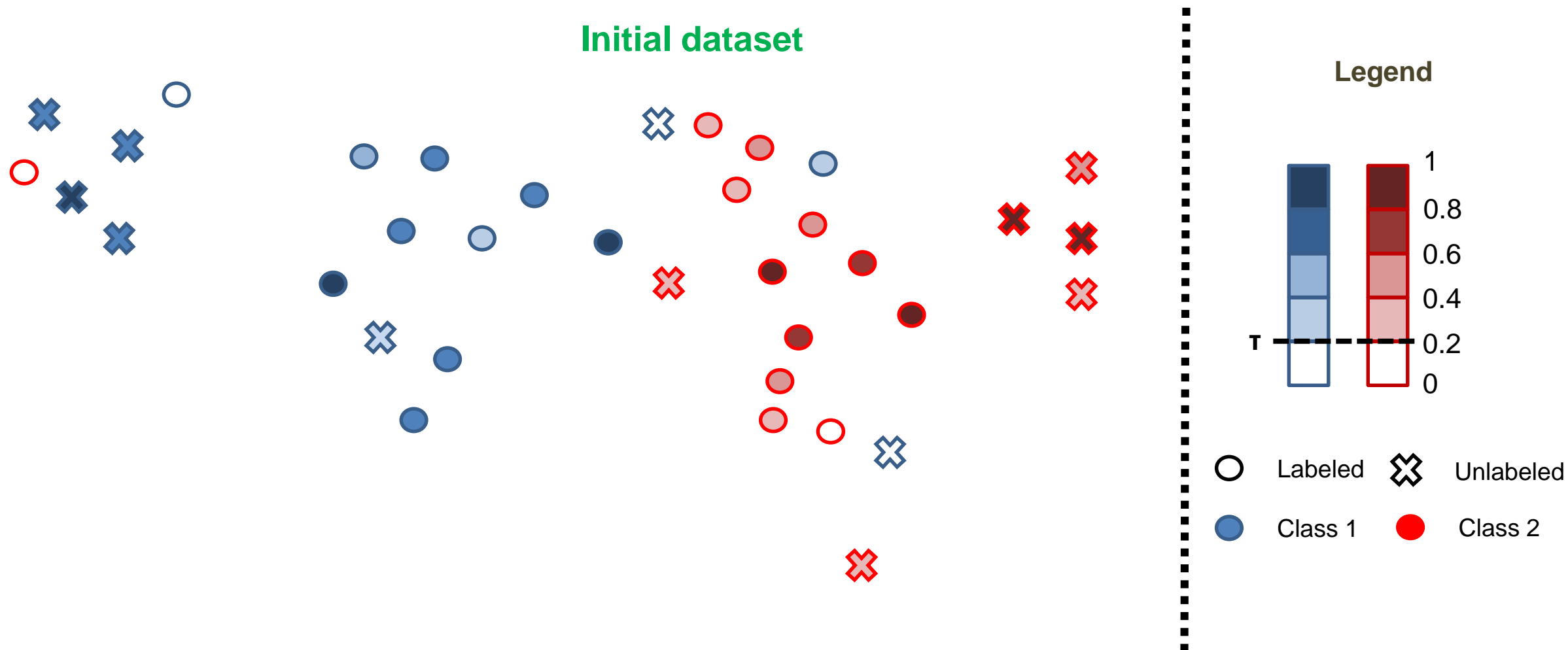


Figure – Example with two neighbors (i.e. $K = 2$ and $\tau = 0.2$).

Semi-automatic label propagation LQ-KNN

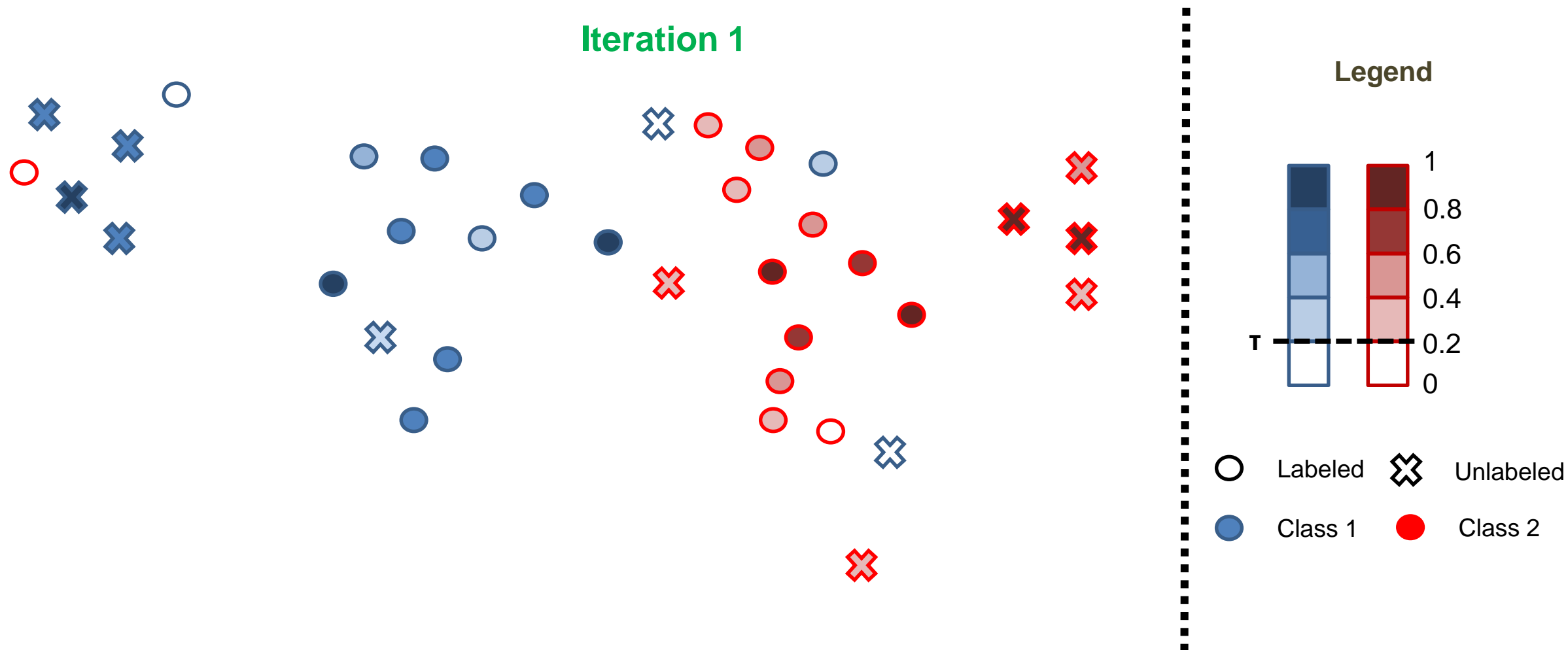


Figure – Example with two neighbors (i.e. $K = 2$ and $\tau = 0.2$).

Semi-automatic label propagation LQ-KNN

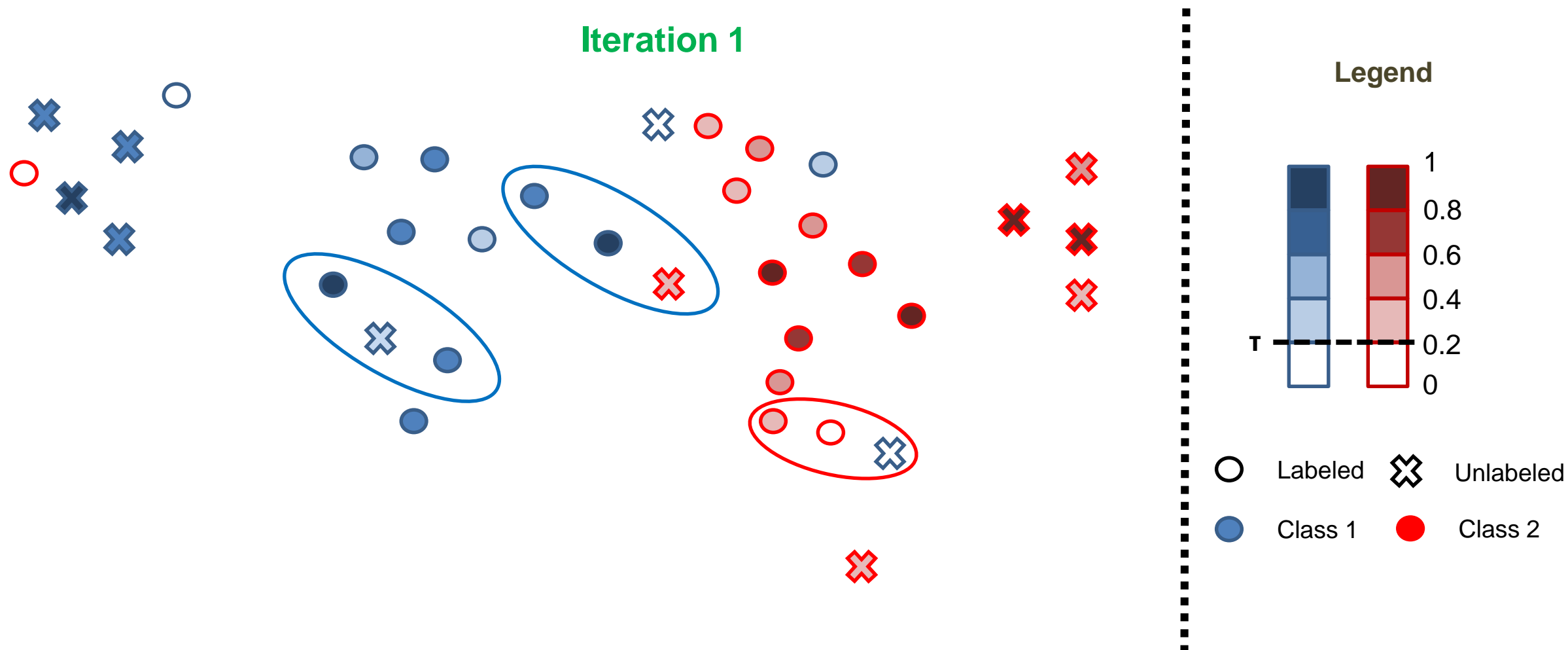


Figure – Example with two neighbors (i.e. $K = 2$ and $\tau = 0.2$).

Semi-automatic label propagation LQ-KNN

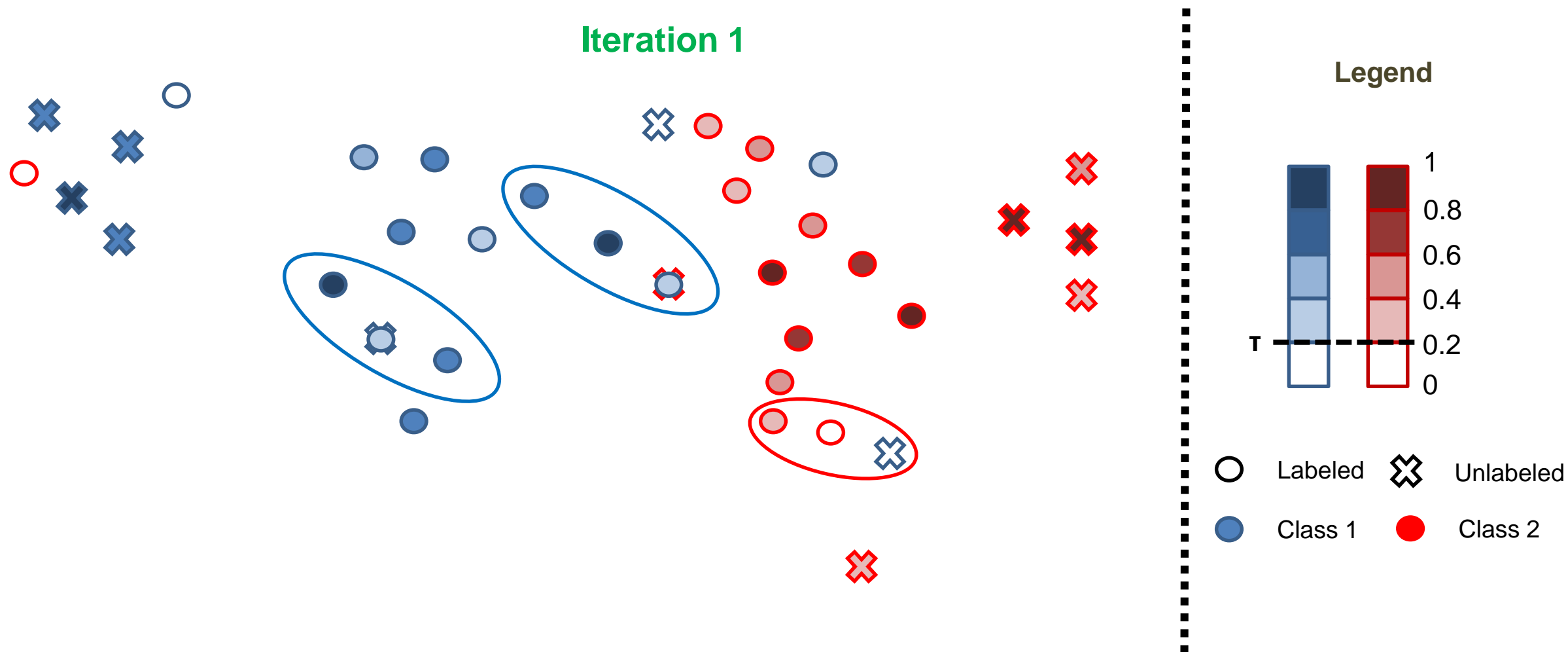


Figure – Example with two neighbors (i.e. $K = 2$ and $\tau = 0.2$).

Semi-automatic label propagation LQ-KNN

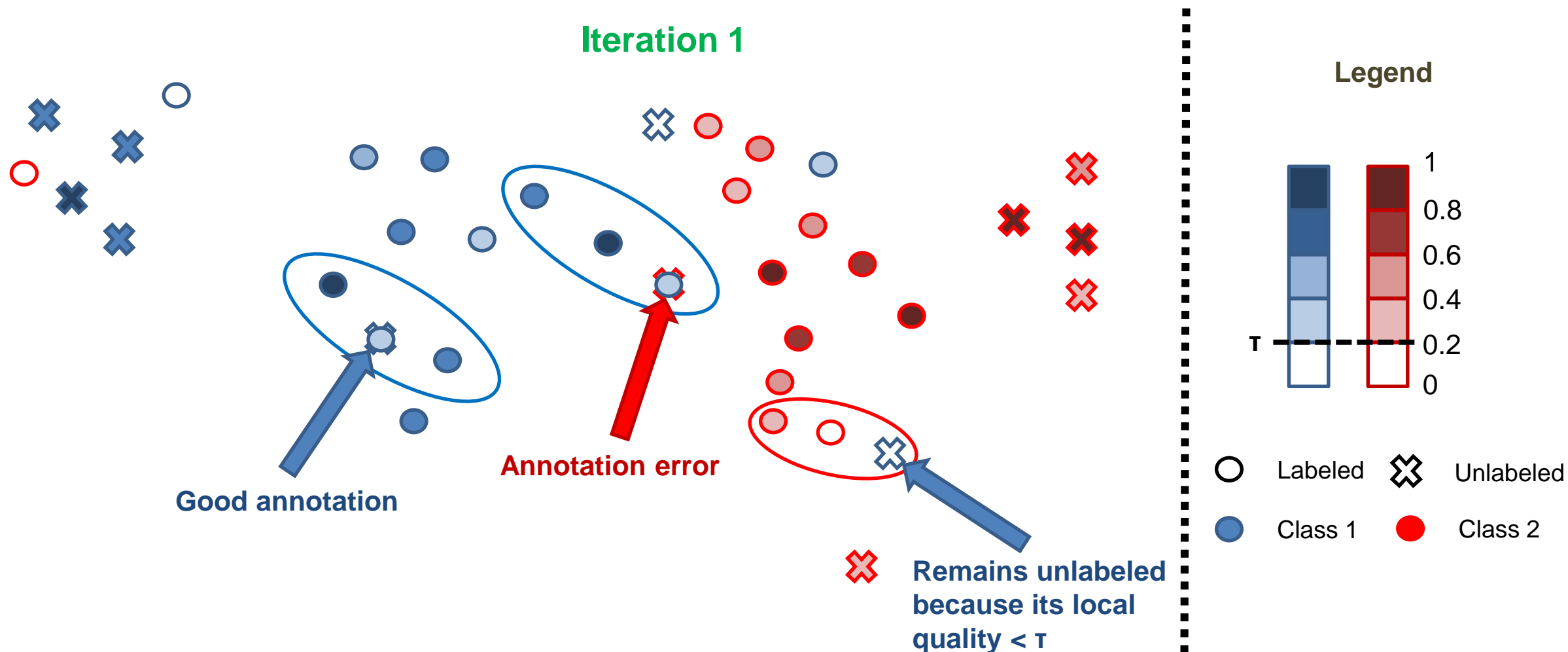


Figure – Example with two neighbors (i.e. $K = 2$ and $\tau = 0.2$).

Semi-automatic label propagation LQ-KNN

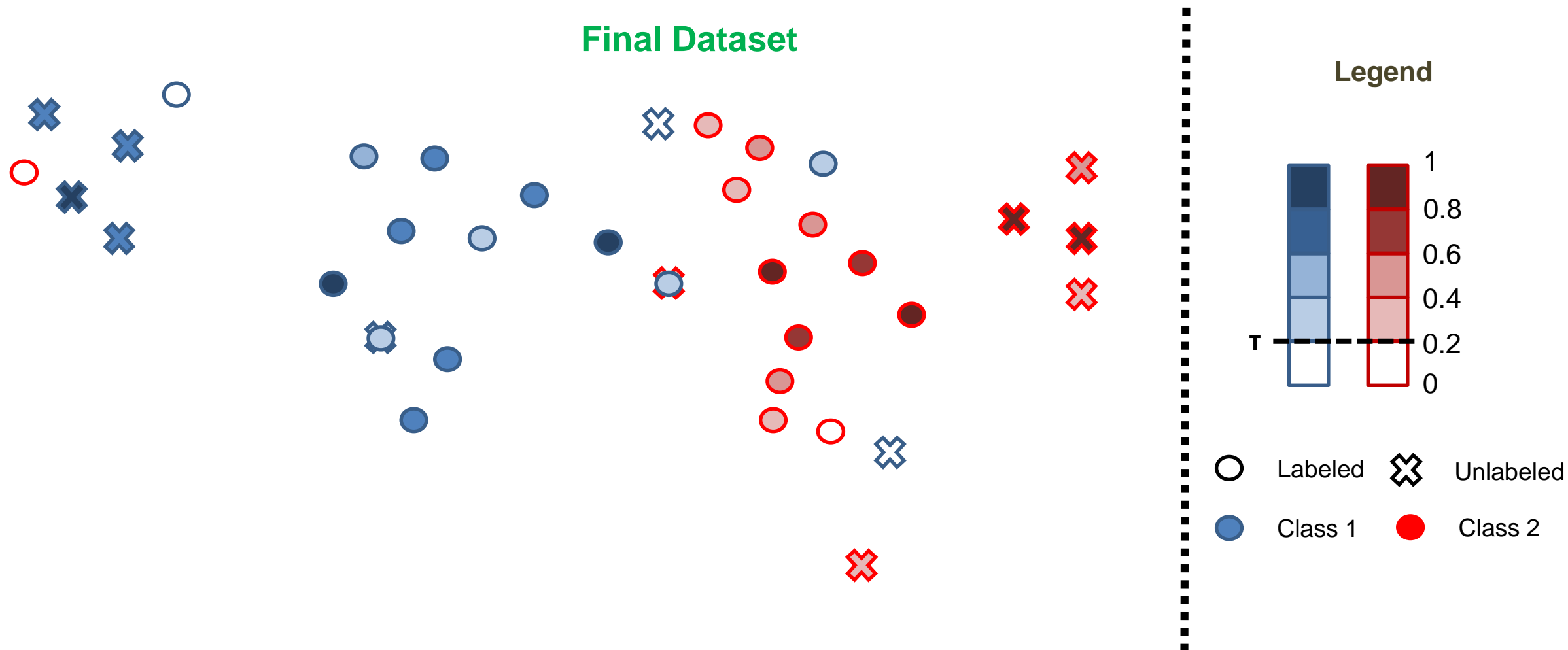


Figure – Example with two neighbors (i.e. $K = 2$ and $\tau = 0.2$).

Semi-automatic label propagation LQ-KNN

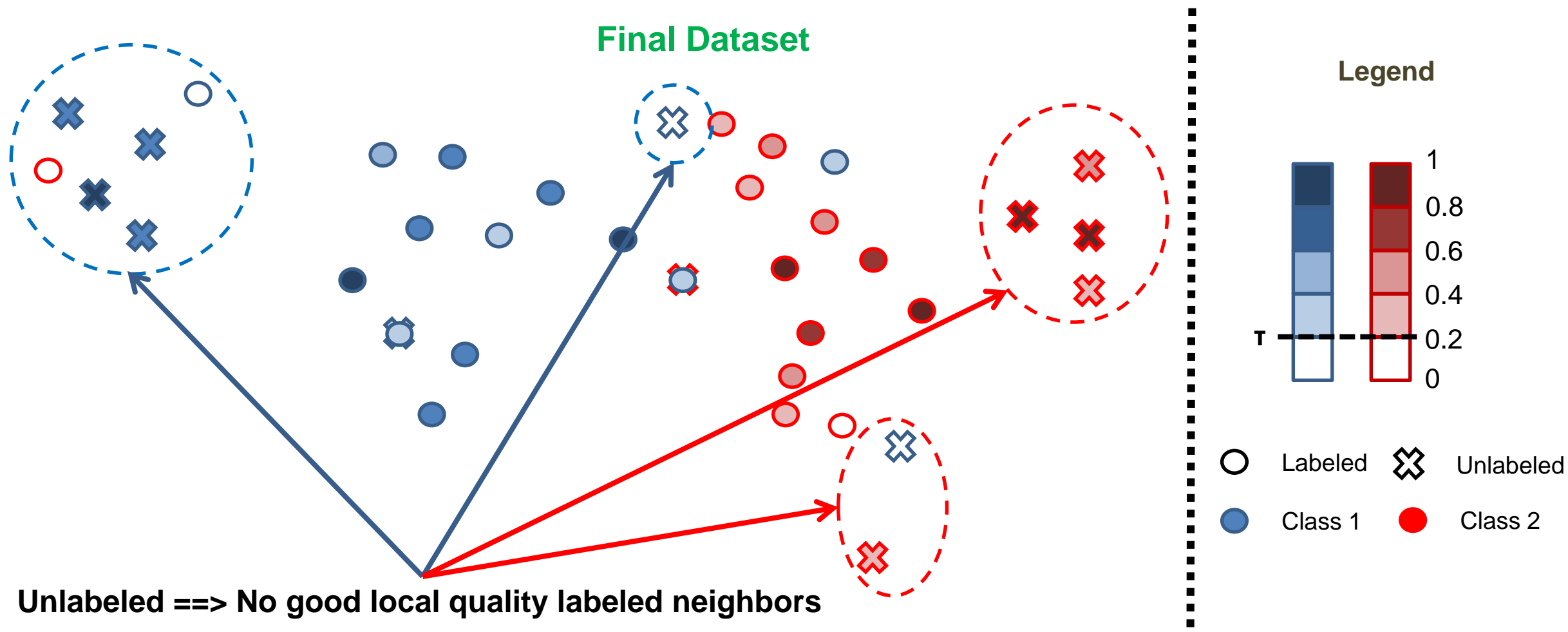


Figure – Example with two neighbors (i.e. $K = 2$ and $\tau = 0.2$).

Outline

- I. **Context**
 - a) **Medical and scientific context**
 - b) **Emboli classification methods**
 - c) **Challenges and objectives**
- II. **Contribution 1 : Semi-automatic data annotation**
 - a) **State-of-the-art**
 - b) **Proposed method**
 - c) **Results**
- III. **Contribution 2 : Multi-feature medical signal classification**
 - a) **State-of-the-art**
 - b) **Proposed method**
 - c) **Results**
- IV. **Contribution 3 : Model compression based on extreme quantization**
 - a) **State-of-the-art**
 - b) **Proposed method**
 - c) **Results**
- V. **Conclusion and perspectives**

Proposed pipeline

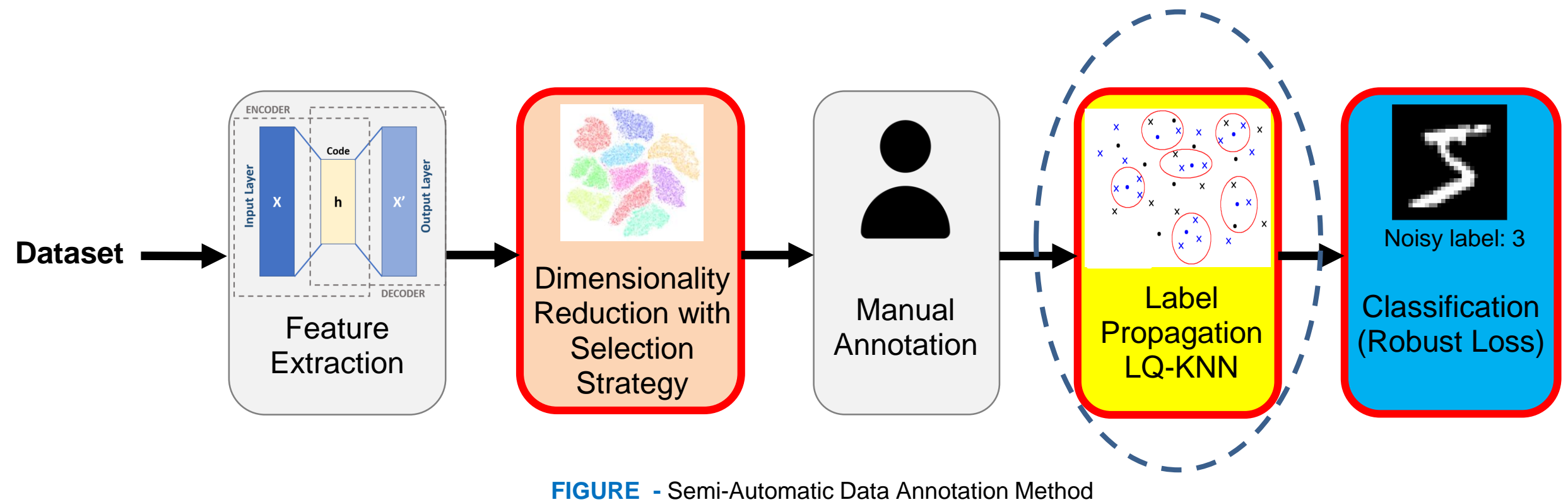


FIGURE - Semi-Automatic Data Annotation Method

Contribution 1.a.: Semi-automatic data annotation method **state-of-the-art comparison**

Dataset	Prop. Method	$ \mathcal{L} $	$ \mathcal{U} $	T	K	Annot. acc.	Final % of labeled samples	Annotation time in ms (/sample)
OrganCMNIST	OPF-Semi			-		75.22 ± 4.48	100 ± 0	86.52 ± 0.51
	Std-KNN	1534	13858	0.1	10	79.86 ± 0.67	99.00 ± 0.20	$(23.41 \pm 1.98) \times 10^{-3}$
	LQ-KNN			-	-	82.73 ± 0.44	96.24 ± 1.09	$(44.36 \pm 5.69) \times 10^{-3}$
HITS	OPF-Semi			-		78.40 ± 13.44	100 ± 0	9.48 ± 1.10
	Std-KNN	152	1393	0.1	10	81.36 ± 1.81	99.58 ± 0.63	$(10.04 \pm 0.18) \times 10^{-3}$
	LQ-KNN			-		82.67 ± 2.02	98.50 ± 0.80	$(16.13 \pm 0.35) \times 10^{-3}$

Table – Label propagation methods comparison on different medical datasets

Contribution 1.a.: Semi-automatic data annotation method **state-of-the-art comparison**

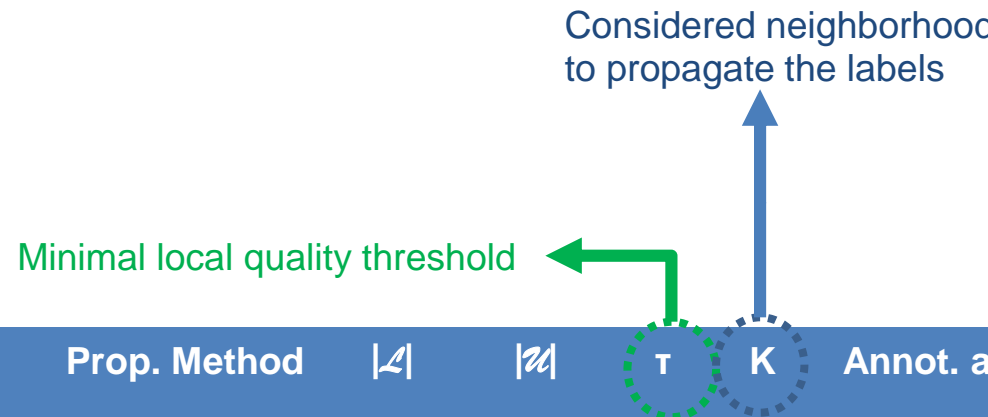
Minimal local quality threshold 



Dataset	Prop. Method	$ \mathcal{L} $	$ \mathcal{U} $	T	K	Annot. acc.	Final % of labeled samples	Annotation time in ms (/sample)
OrganCMNIST	OPF-Semi			-		75.22 ± 4.48	100 ± 0	86.52 ± 0.51
	Std-KNN	1534	13858	0.1	10	79.86 ± 0.67	99.00 ± 0.20	$(23.41 \pm 1.98) \times 10^{-3}$
	LQ-KNN			-	-	82.73 ± 0.44	96.24 ± 1.09	$(44.36 \pm 5.69) \times 10^{-3}$
HITS	OPF-Semi			-		78.40 ± 13.44	100 ± 0	9.48 ± 1.10
	Std-KNN	152	1393	0.1	10	81.36 ± 1.81	99.58 ± 0.63	$(10.04 \pm 0.18) \times 10^{-3}$
	LQ-KNN			-	-	82.67 ± 2.02	98.50 ± 0.80	$(16.13 \pm 0.35) \times 10^{-3}$

Table – Label propagation methods comparison on different medical datasets

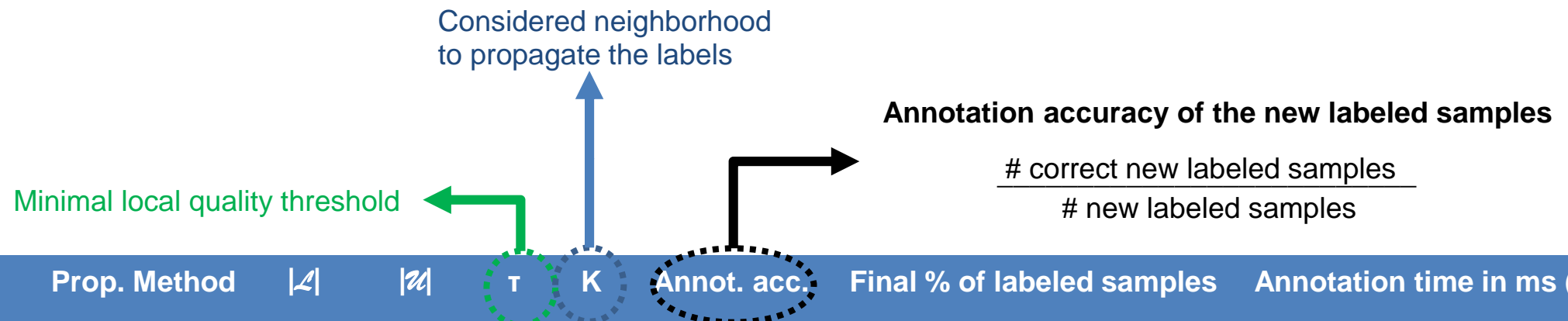
Contribution 1.a.: Semi-automatic data annotation method **state-of-the-art comparison**



Dataset	Prop. Method	$ L $	$ U $	T	K	Annot. acc.	Final % of labeled samples	Annotation time in ms (/sample)
OrganCMNIST	OPF-Semi			-		75.22 ± 4.48	100 ± 0	86.52 ± 0.51
	Std-KNN	1534	13858	0.1	10	79.86 ± 0.67	99.00 ± 0.20	$(23.41 \pm 1.98) \times 10^{-3}$
	LQ-KNN			-	-	82.73 ± 0.44	96.24 ± 1.09	$(44.36 \pm 5.69) \times 10^{-3}$
HITS	OPF-Semi			-		78.40 ± 13.44	100 ± 0	9.48 ± 1.10
	Std-KNN	152	1393	0.1	10	81.36 ± 1.81	99.58 ± 0.63	$(10.04 \pm 0.18) \times 10^{-3}$
	LQ-KNN			-	-	82.67 ± 2.02	98.50 ± 0.80	$(16.13 \pm 0.35) \times 10^{-3}$

Table – Label propagation methods comparison on different medical datasets

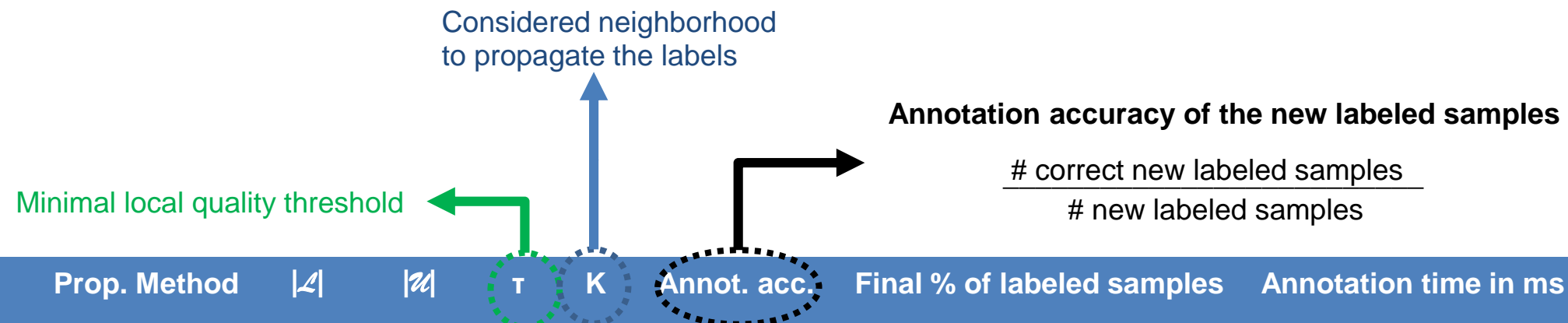
Contribution 1.a.: Semi-automatic data annotation method **state-of-the-art comparison**



Dataset	Prop. Method	$ A $	$ U $	T	K	Final % of labeled samples	Annotation time in ms (/sample)
OrganCMNIST	OPF-Semi			-		75.22 ± 4.48	100 ± 0
	Std-KNN	1534	13858	0.1	10	79.86 ± 0.67	$(23.41 \pm 1.98) \times 10^{-3}$
	LQ-KNN			-	-	82.73 ± 0.44	$(44.36 \pm 5.69) \times 10^{-3}$
HITS	OPF-Semi			-		78.40 ± 13.44	100 ± 0
	Std-KNN	152	1393	0.1	10	81.36 ± 1.81	$(10.04 \pm 0.18) \times 10^{-3}$
	LQ-KNN			-	-	82.67 ± 2.02	$(16.13 \pm 0.35) \times 10^{-3}$

Table – Label propagation methods comparison on different medical datasets

Contribution 1.a.: Semi-automatic data annotation method **state-of-the-art comparison**



Dataset	Prop. Method	$ A $	$ \mathcal{U} $	T	K	Annot. acc.	Final % of labeled samples	Annotation time in ms (/sample)
OrganCMNIST	OPF-Semi			-			75.22 ± 4.48	100 ± 0
	Std-KNN	1534	13858	0.1	10		79.86 ± 0.67	99.00 ± 0.20
	LQ-KNN			-	-		82.73 ± 0.44	$(44.36 \pm 5.69) \times 10^{-3}$
HITS	OPF-Semi			-			78.40 ± 13.44	100 ± 0
	Std-KNN	152	1393	0.1	10		81.36 ± 1.81	99.58 ± 0.63
	LQ-KNN			-	-		82.67 ± 2.02	$(16.13 \pm 0.35) \times 10^{-3}$

Table – Label propagation methods comparison on different medical datasets

Contribution 1.a.: Semi-automatic data annotation method **state-of-the-art comparison**

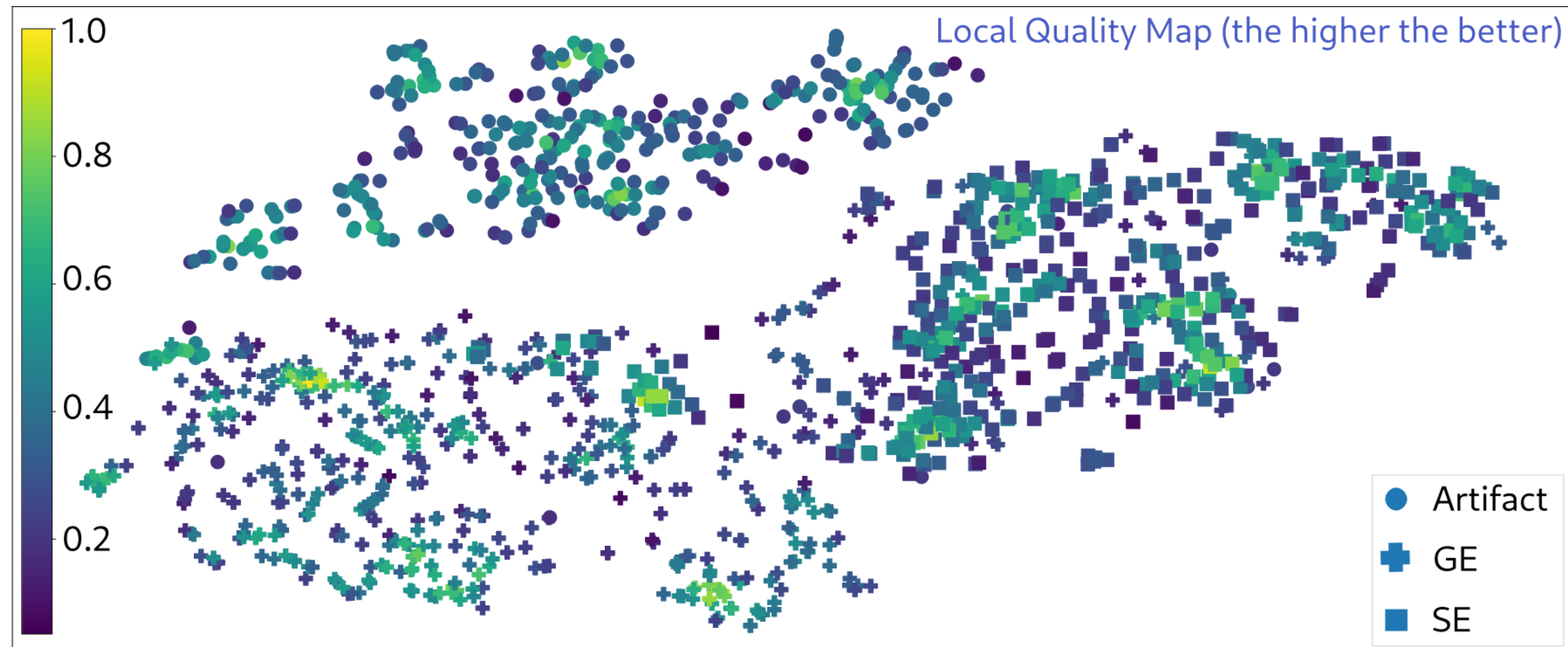


Figure - Local Quality Map of the unlabeled samples

Contribution 1.a.: Semi-automatic data annotation method **state-of-the-art comparison**

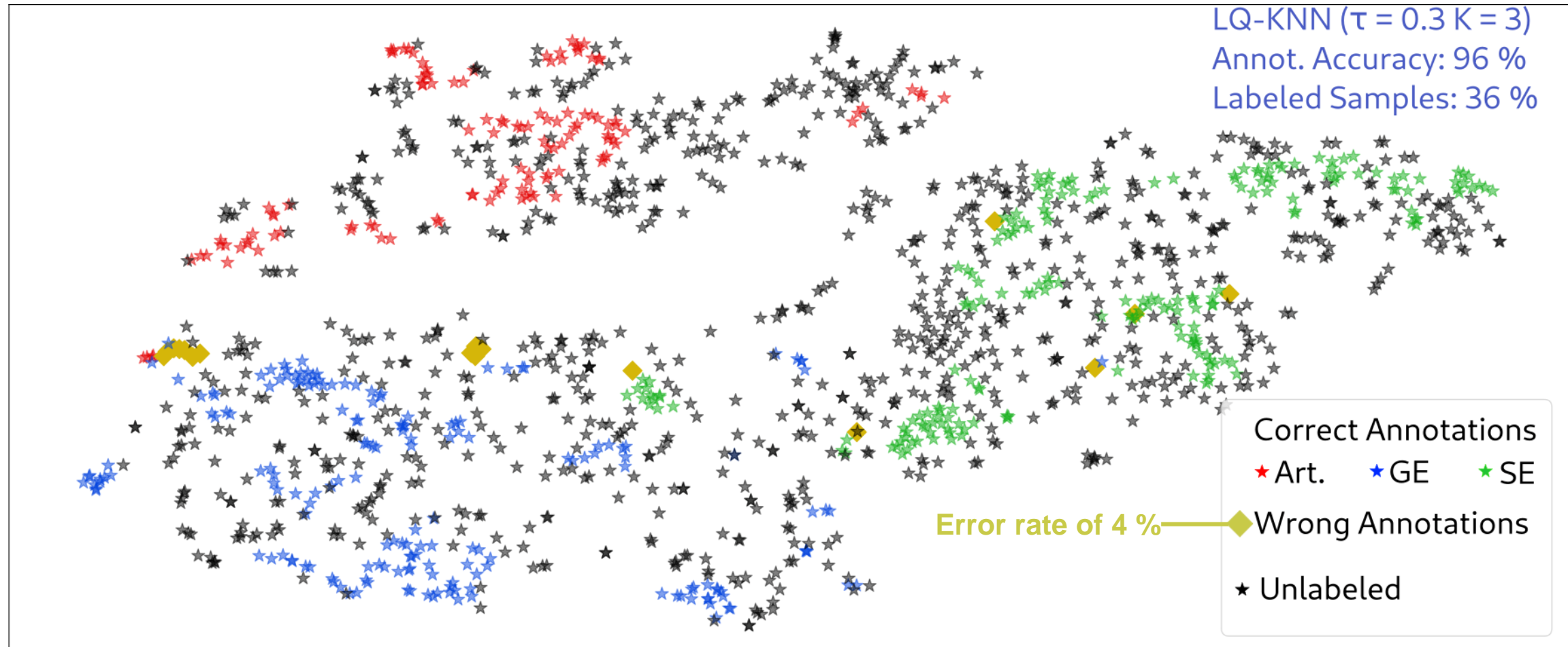


Figure - LQ-KNN label propagation with $K = 3$ and $\tau = 0.3$

Contribution 1.a.: Semi-automatic data annotation method **state-of-the-art comparison**

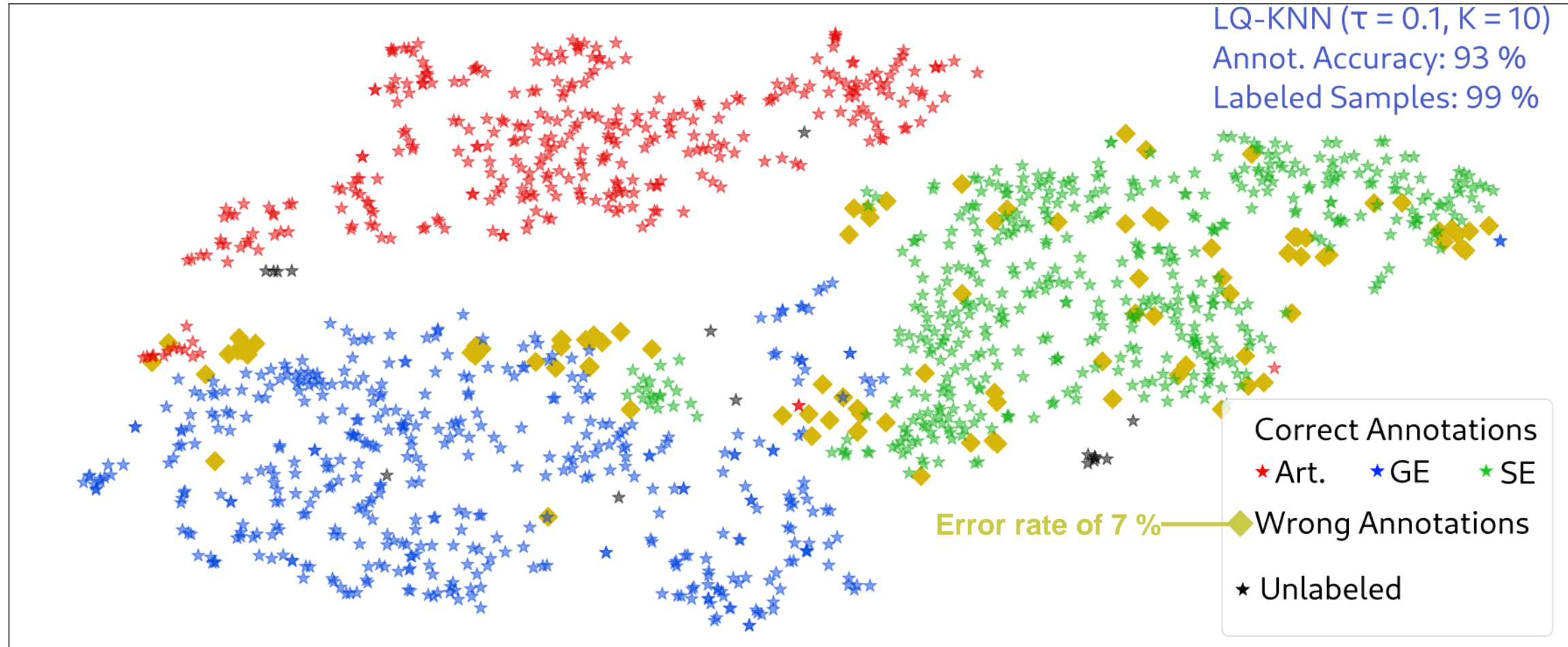


Figure - LQ-KNN label propagation with $K = 10$ and $\tau = 0.1$

Contribution 1.a.: Semi-automatic data annotation method **state-of-the-art comparison**

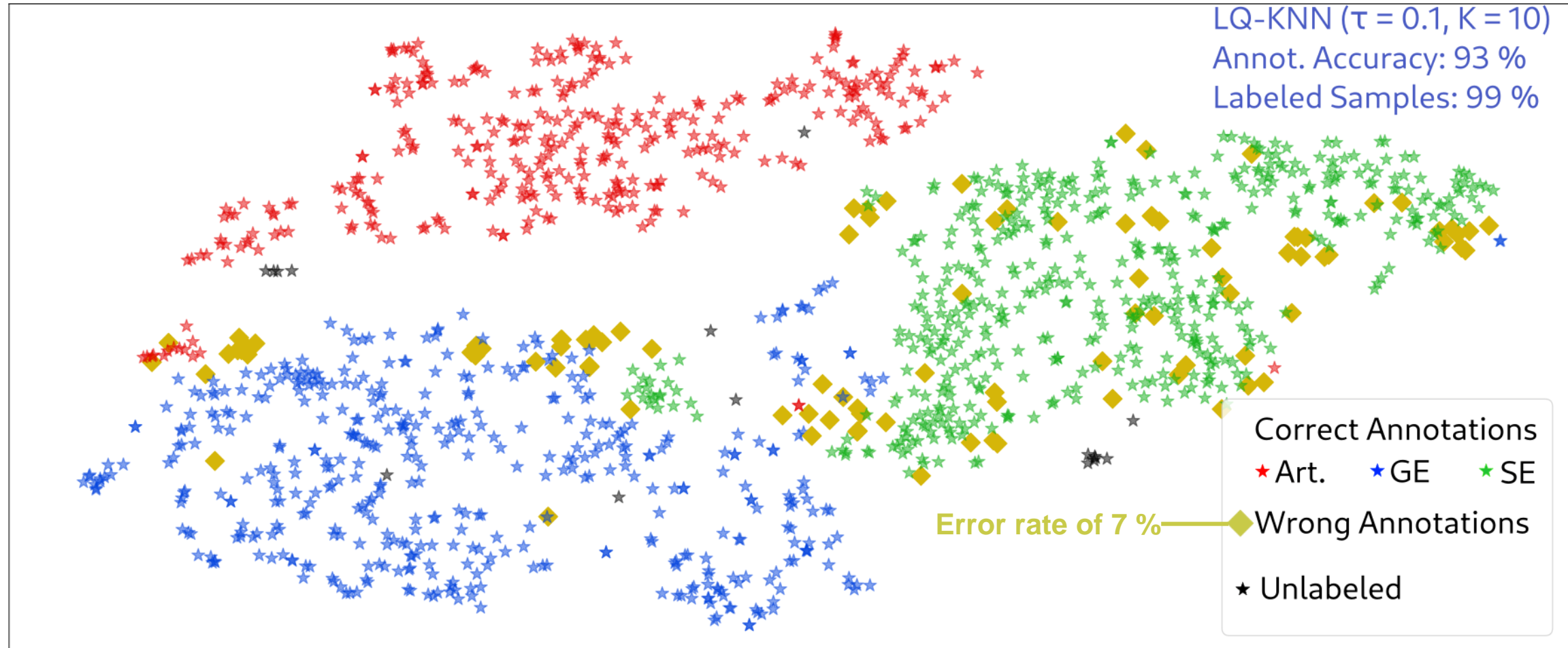


Figure - LQ-KNN label propagation with $K = 10$ and $\tau = 0.1$

→ **K** and **τ** control the **trade-off** between **annotation errors** and **quantity of labeled samples**.

Proposed pipeline

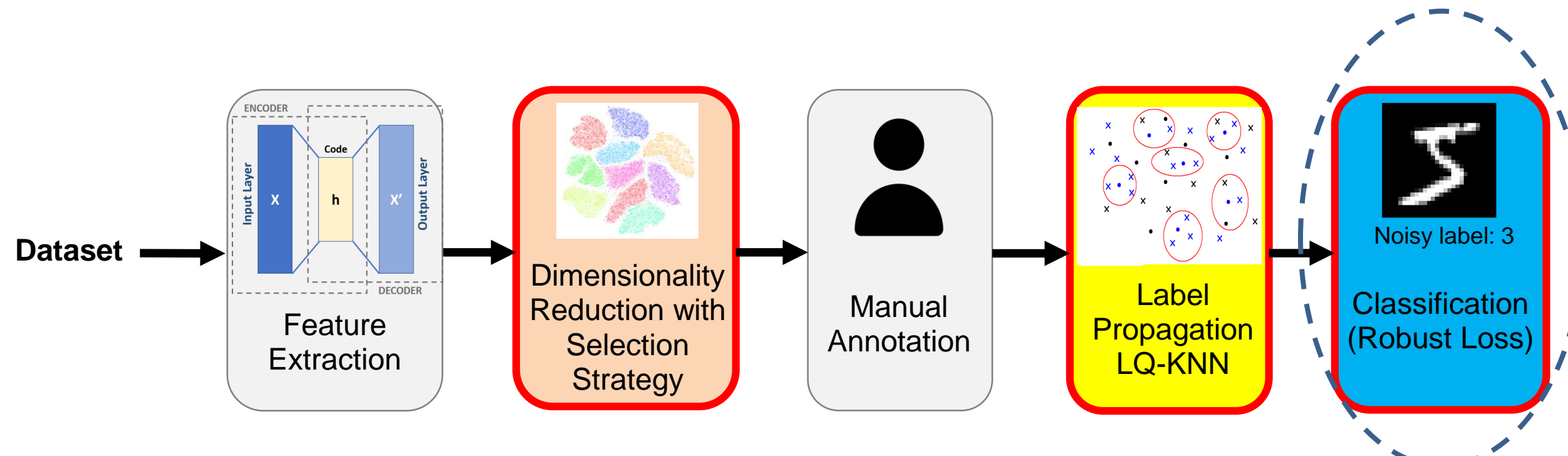
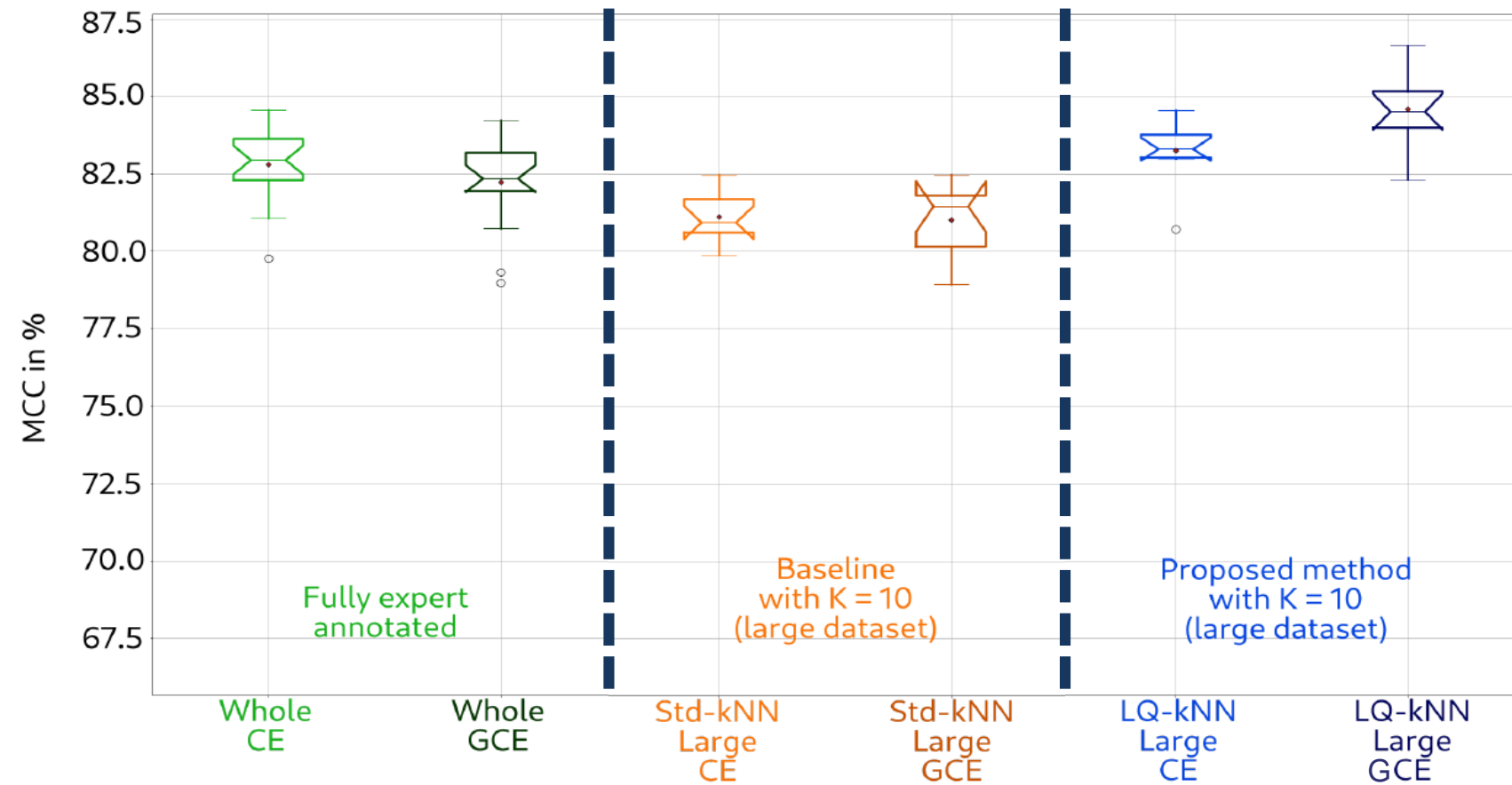
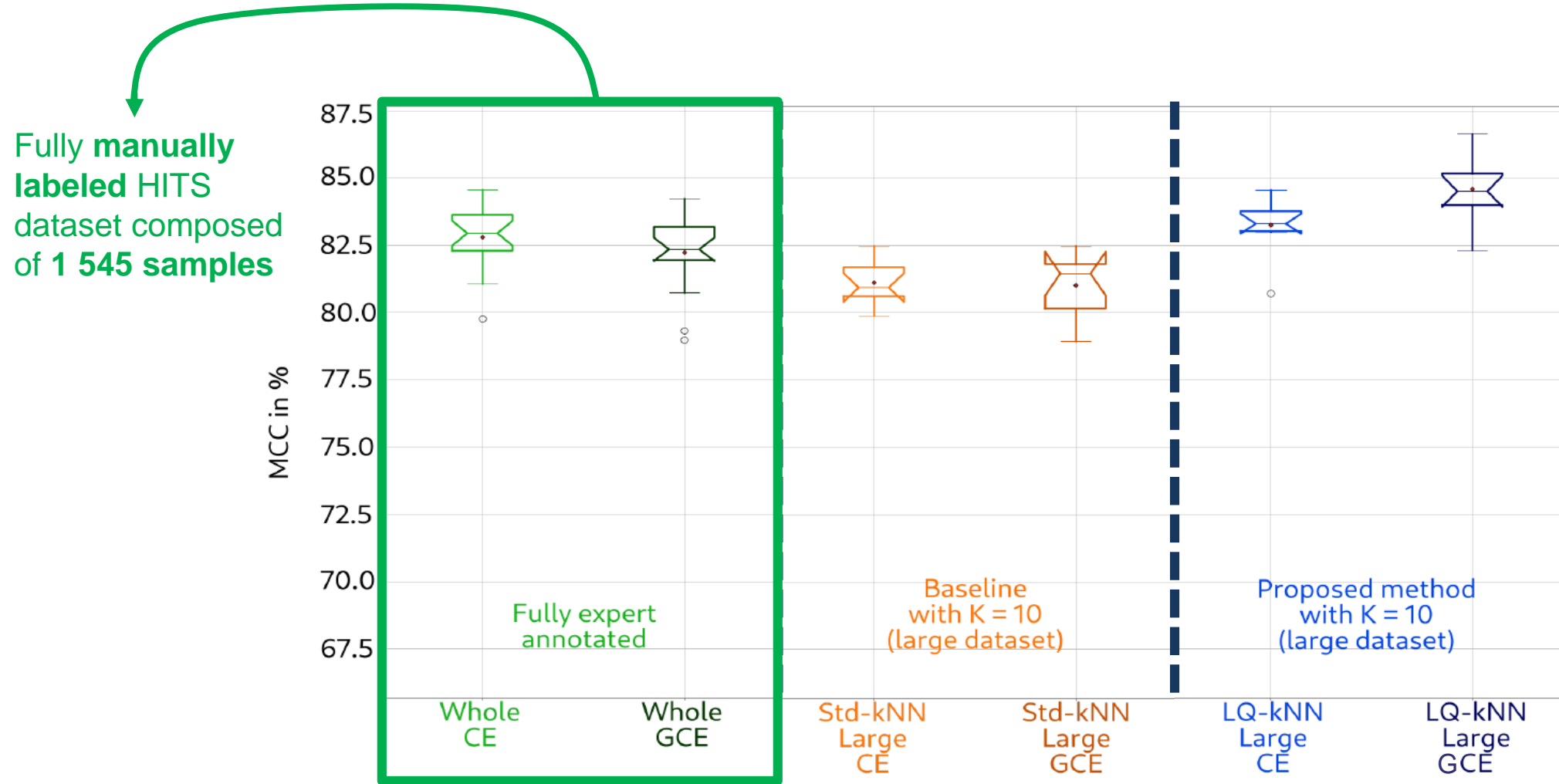


FIGURE - Semi-Automatic Data Annotation Method

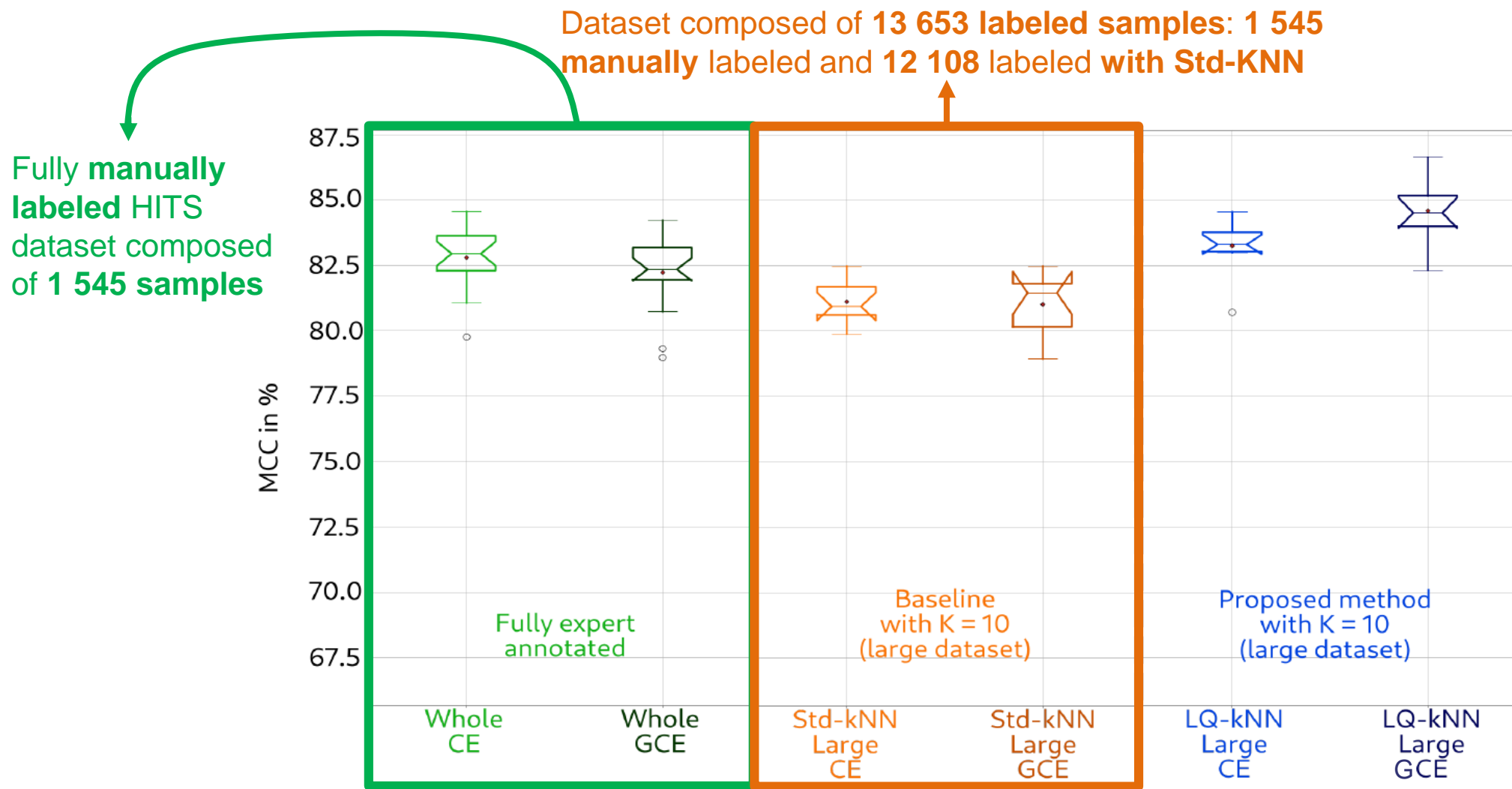
Contribution 1.c: Classification with **robust loss** functions on a **2D CNN** model to **compensate** the **noisy-labels**.



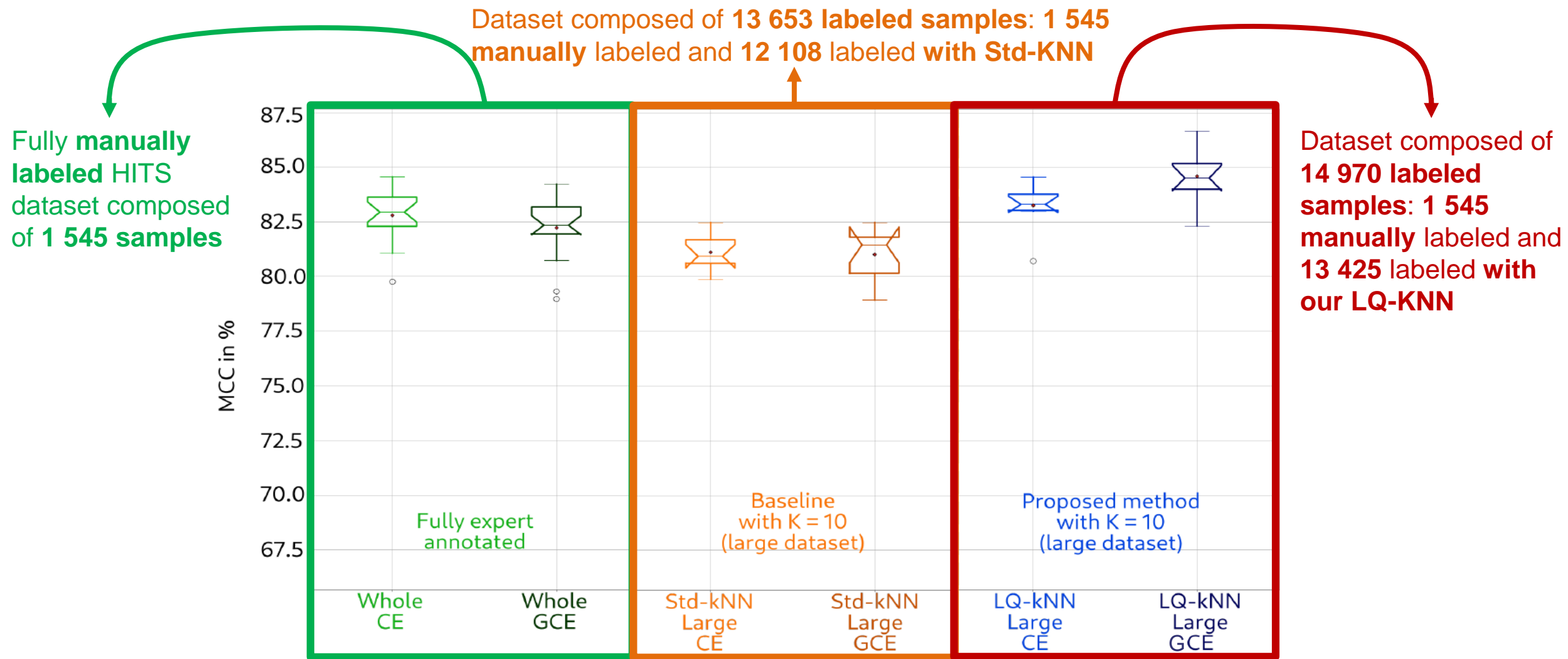
Contribution 1.c: Classification with **robust loss** functions on a **2D CNN** model to **compensate** the **noisy-labels**.



Contribution 1.c: Classification with **robust loss** functions on a **2D CNN** model to **compensate** the **noisy-labels**.



Contribution 1.c: Classification with **robust loss functions** on a **2D CNN** model to **compensate** the **noisy-labels**.



Contribution 1.c: Classification using robust loss functions to compensate the noise in the labels.



Intermediate conclusion

- **Proposed method** outperforms:
 - Baseline (*Std-kNN*).
 - OPF-Semi.

==> **State-of-the-art performances.**
- Proposed method allows to **control** the **annotation error**.
- Optimal projection **selection strategy**:

==> **Improves** the **automatic annotation** process.
- **Classification**:
 - Performances **improved** thanks to semi-automatic data annotation.
 - **Robust loss** functions **compensate** label-**noise**.

==> **Up to 6 %** accuracy improvement.

Objectives and Contributions

Dataset creation and annotation



- Semi-supervised data annotation*
- Soft labelling (annotation)*

Multiple representations



- Different models with different inputs**
- Multi-feature models

Resource hungry models



- Lite models
- Model compression
- (Soft labelling training)

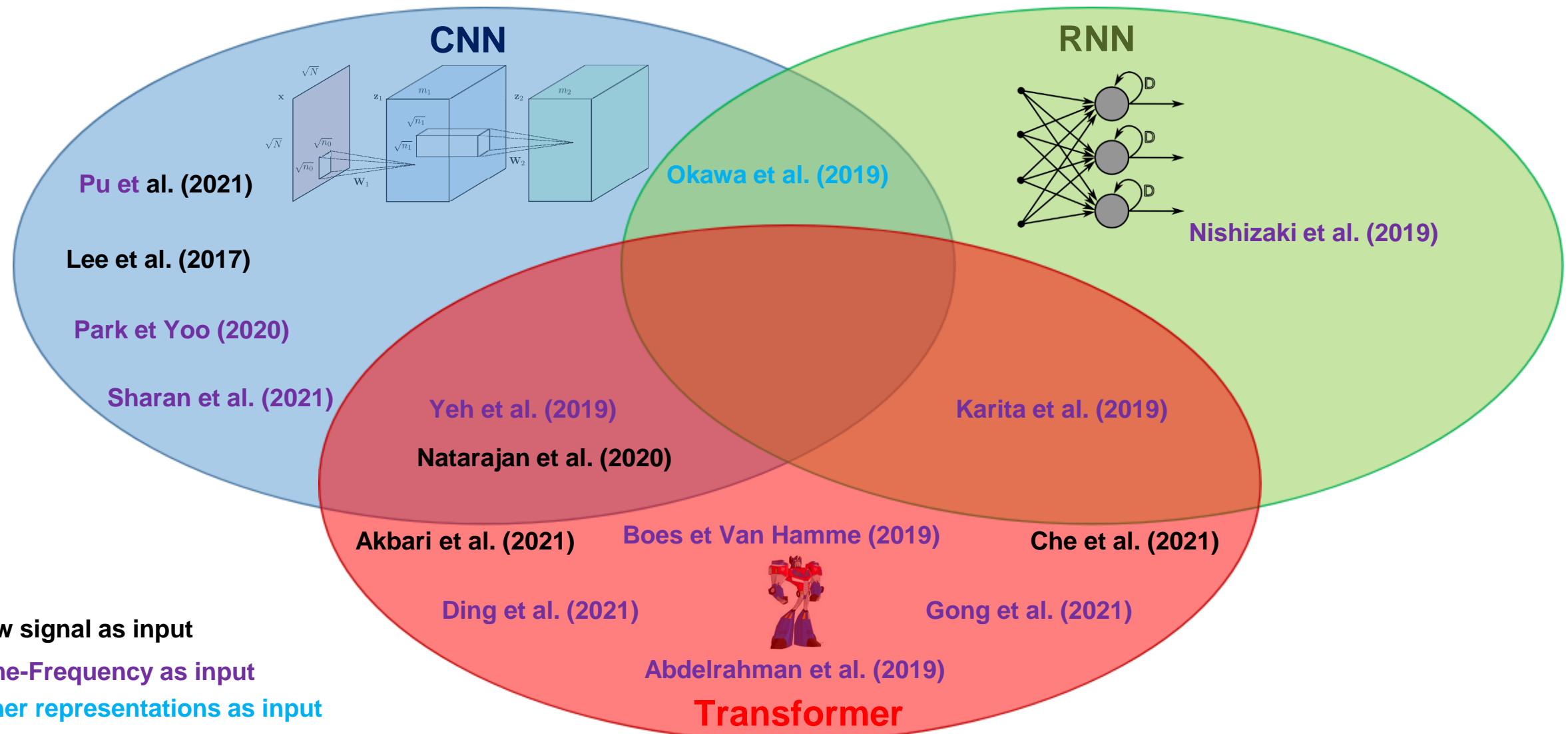
* Vindas et al. (IUS 2021), Vindas et al. (MEDIA 2022), Vindas et al. (IUS 2023)

** Vindas et al. (MLHC 2022), Vindas et al. (IABM 2023), Vindas et al. (EUSIPCO 2023), and Vindas et al. (Pattern Recognition 2023)

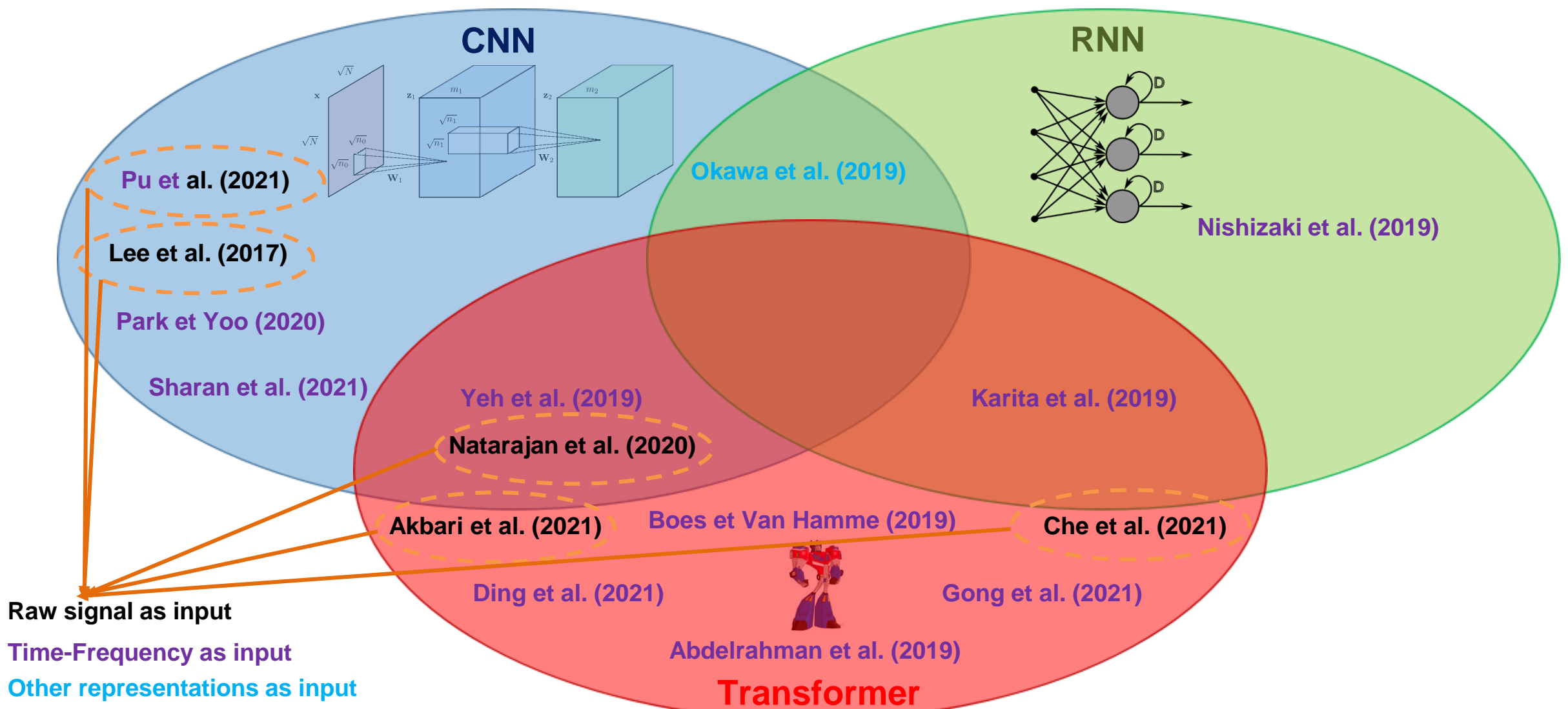
Outline

- I. **Context**
 - a) **Medical and scientific context**
 - b) **Emboli classification methods**
 - c) **Challenges and objectives**
- II. **Contribution 1 : Semi-automatic data annotation**
 - a) **State-of-the-art**
 - b) **Proposed method**
 - c) **Results**
- III. **Contribution 2 : Multi-feature medical signal classification**
 - a) **State-of-the-art**
 - b) **Proposed method**
 - c) **Results**
- IV. **Contribution 3 : Model compression based on extreme quantization**
 - a) **State-of-the-art**
 - b) **Proposed method**
 - c) **Results**
- V. **Conclusion and perspectives**

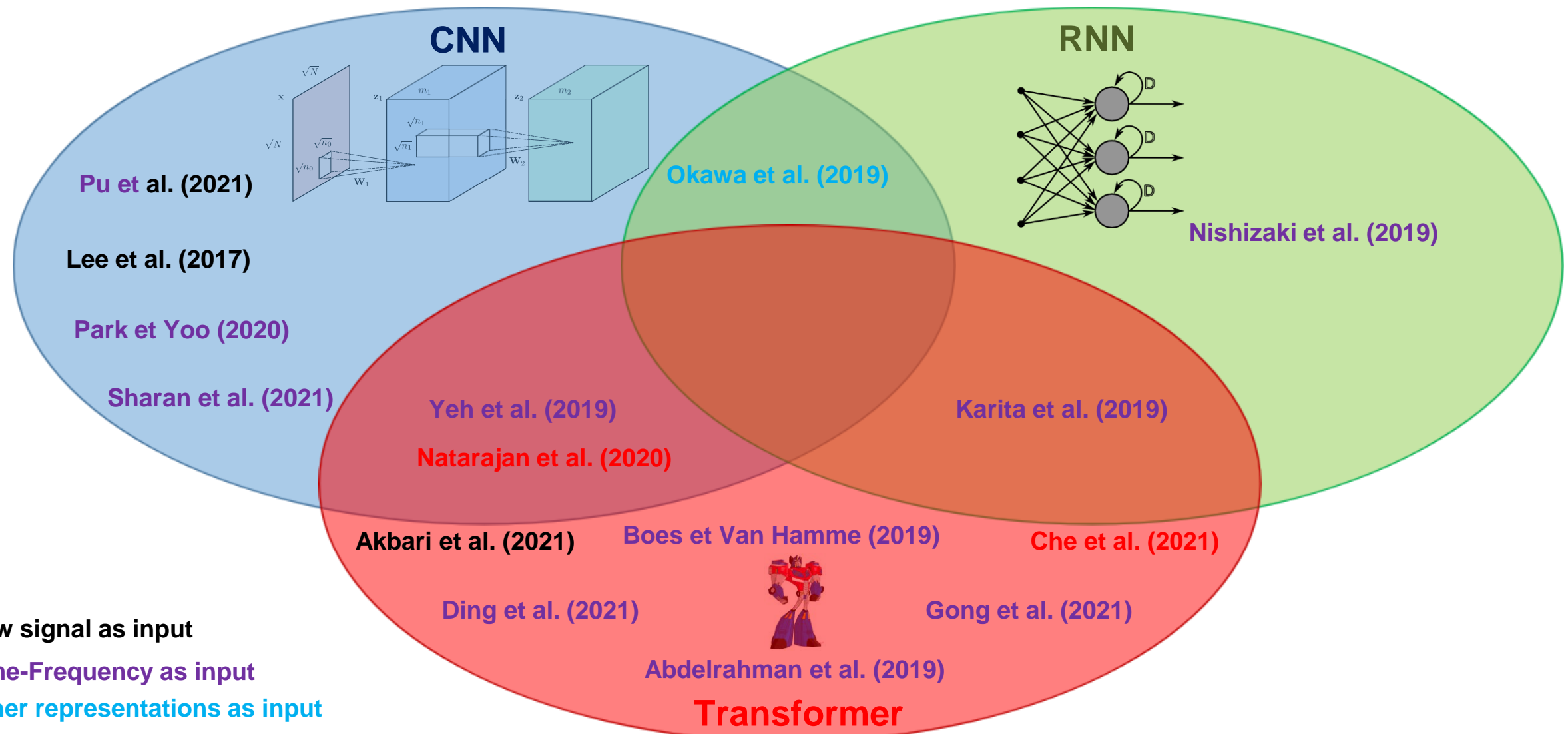
State-of-the-art deep learning signal classification



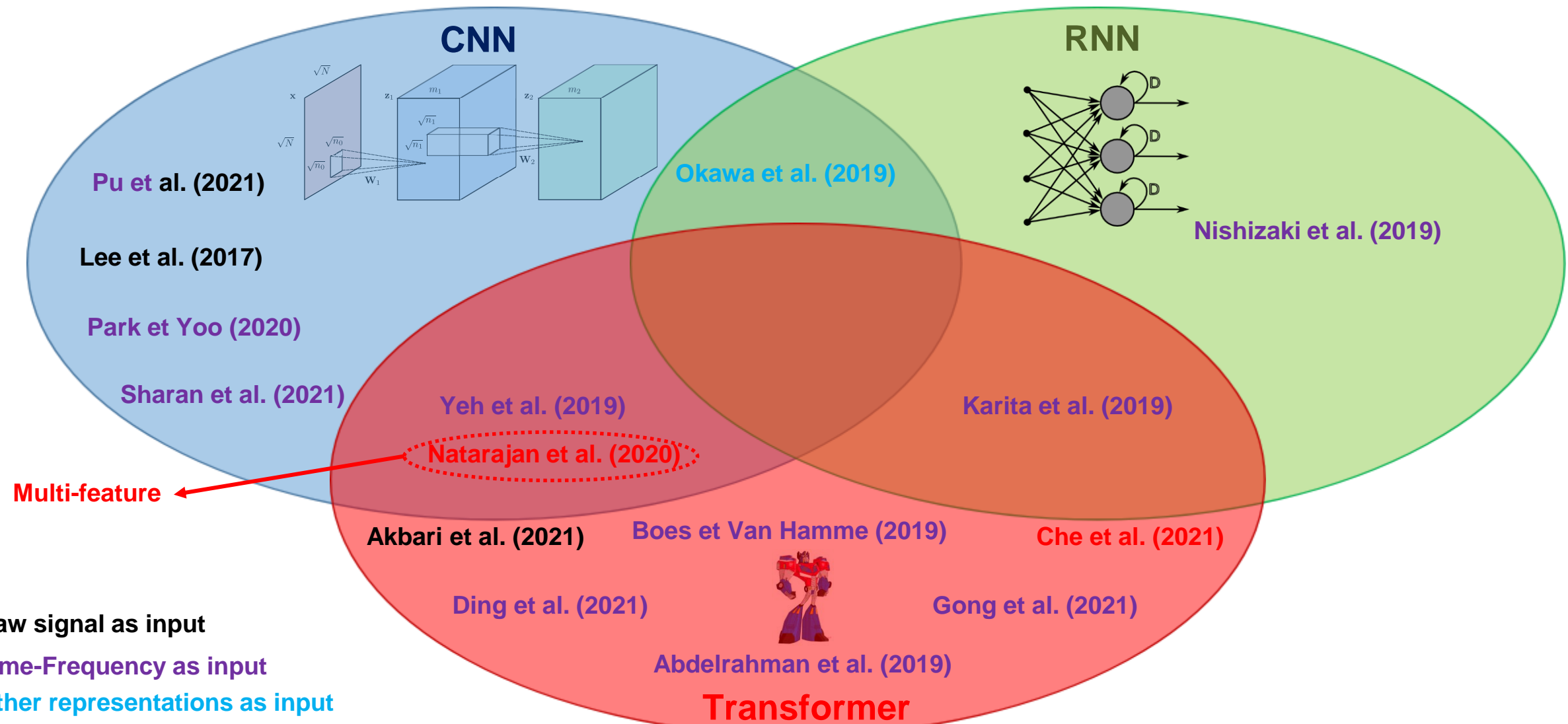
State-of-the-art deep learning signal classification



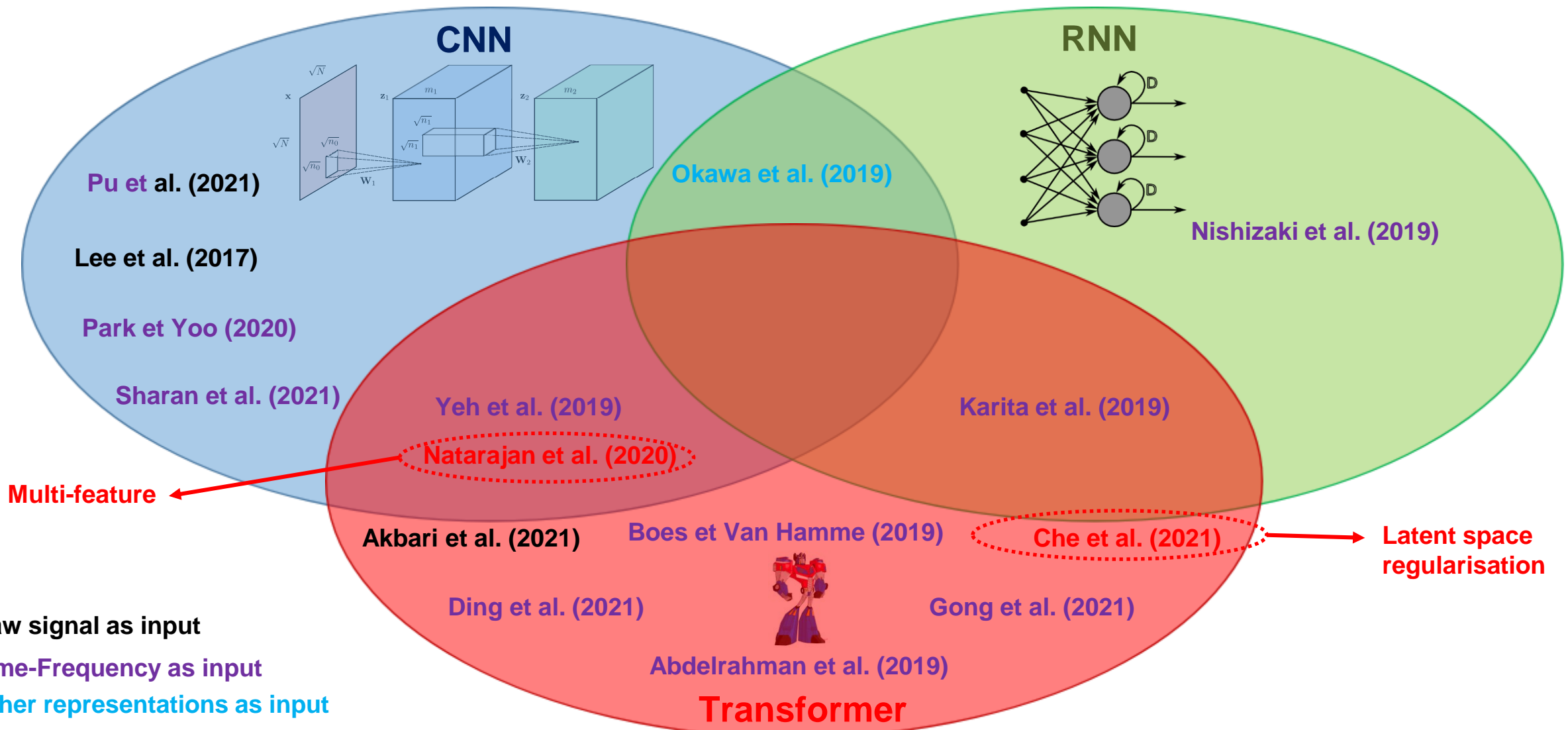
State-of-the-art deep learning signal classification



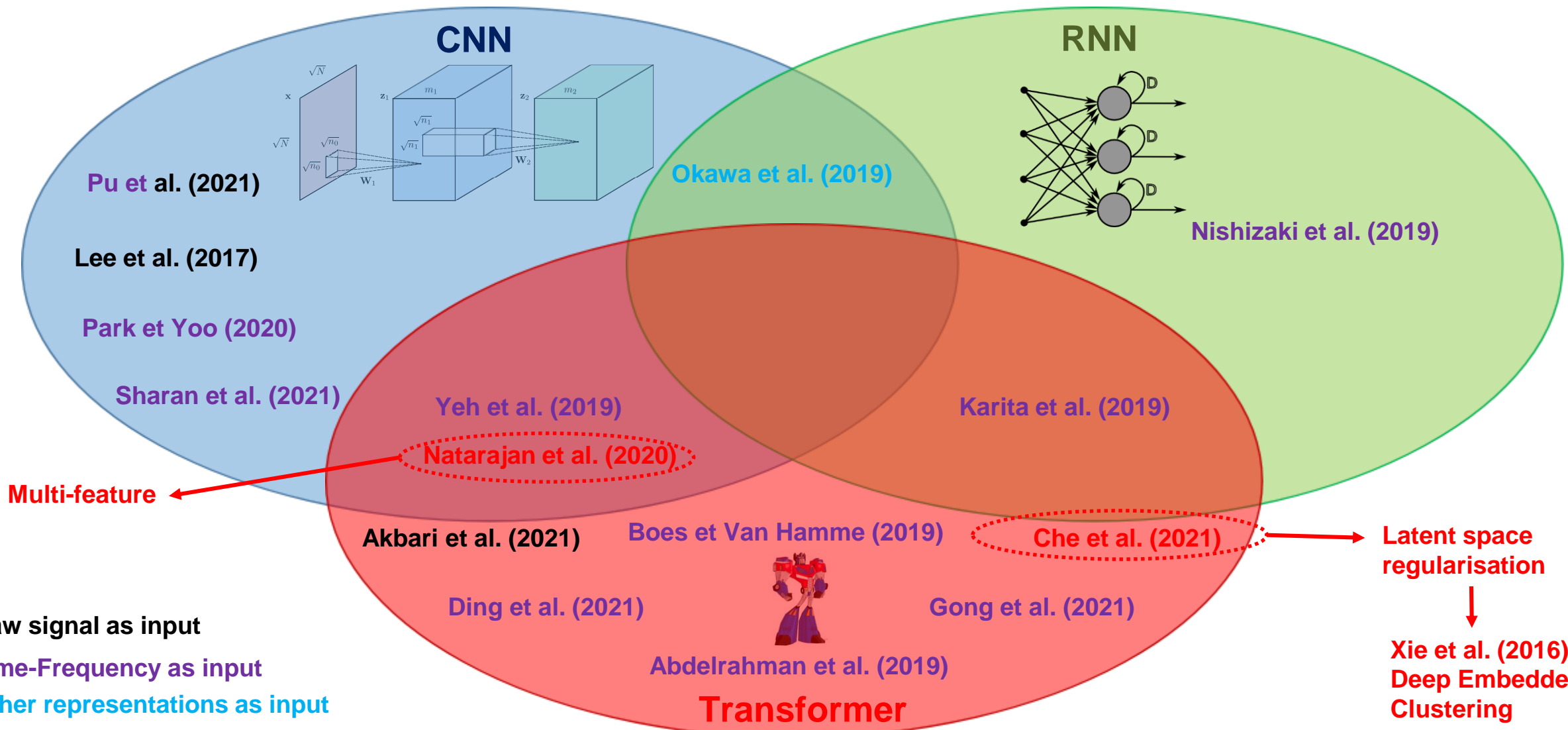
State-of-the-art deep learning signal classification



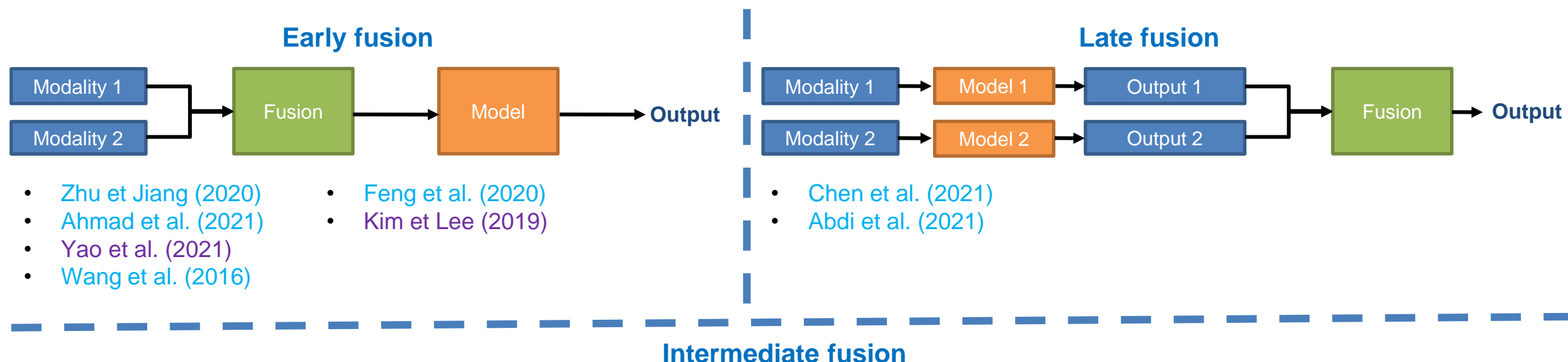
State-of-the-art deep learning signal classification



State-of-the-art deep learning signal classification



State-of-the-art multi-feature learning



Raw signal as input

Time-Frequency as input

Other representations as input

- Mao et al. (2020)
- Tiong et al. (2021)
- Abdi et al. (2021)
- Zhou et al. (2020)
- Zhou et al. (2022)
- Liu (2021)
- Jin et al. (2020)

Deep embedded clustering

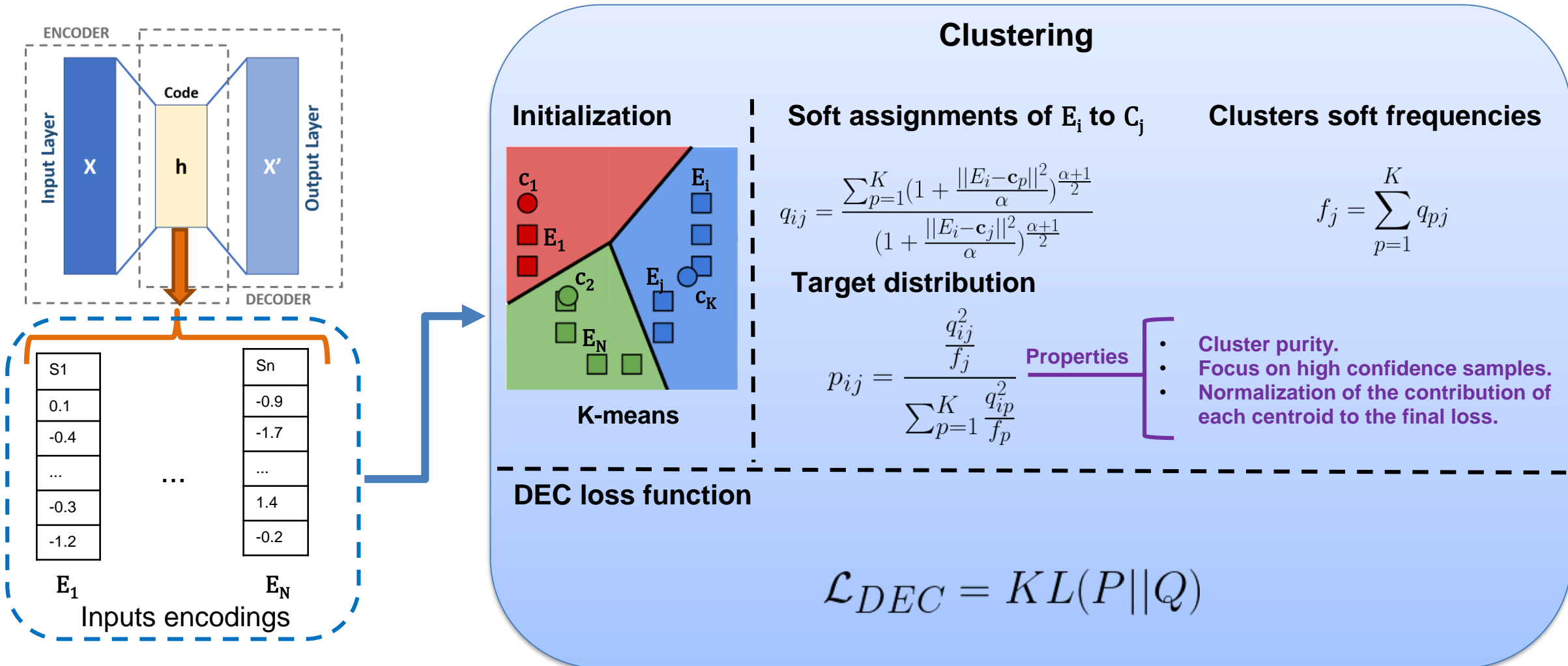


Figure – Deep embedded clustering for unsupervised learning (Xie et al., 2016)

Outline

- I. **Context**
 - a) **Medical and scientific context**
 - b) **Emboli classification methods**
 - c) **Challenges and objectives**
- II. **Contribution 1 : Semi-automatic data annotation**
 - a) **State-of-the-art**
 - b) **Proposed method**
 - c) **Results**
- III. **Contribution 2 : Multi-feature medical signal classification**
 - a) **State-of-the-art**
 - b) **Proposed method**
 - c) **Results**
- IV. **Contribution 3 : Model compression based on extreme quantization**
 - a) **State-of-the-art**
 - b) **Proposed method**
 - c) **Results**
- V. **Conclusion and perspectives**

Claims of contribution 2

- a. Novel **hybrid CNN-transformer** models, **exploiting** the **complementarity** between the **temporal** and **spectral characteristics** of a medical signal.
- b. **Guided** and **regularized intermediate fusion** approach, improving generalization while handling **imbalanced** datasets and **label-noise**.
- c. **Late-fusion** mechanisms, based on **learnable** and **interpretable attention weights**.

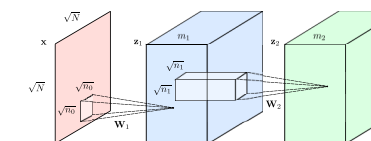
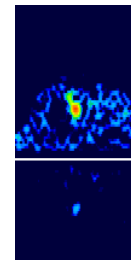
Proposed approach

Objectives:

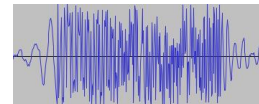
- Improve the classification of TCD signals.
- Exploit the complementarity of different representations.

Models:

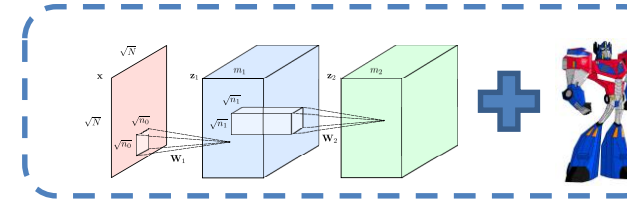
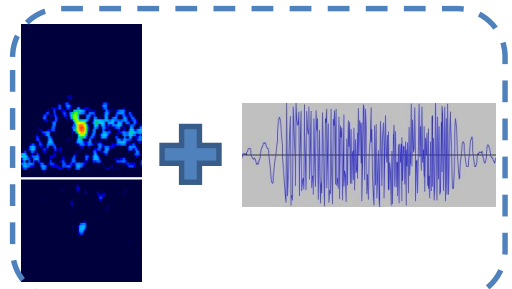
- 2D CNN model for TFRs.



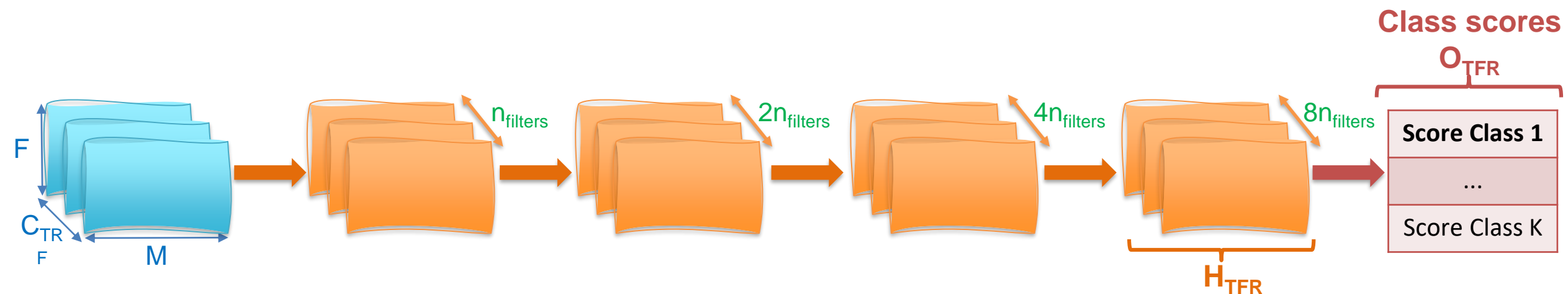
- 1D CNN-Transformer for raw signals.



- Hybrid models for both representations.



Single feature TFR 2D CNN



- 2D Conv. with kernel size (3, 3), padding 1, stride 1 + Batch Norm. + Leaky ReLU + 2D MaxPool with kernel size (2, 2), padding 0 and stride 2
- Fully Connected layer + Dropout

Figure - Proposed 2D CNN

Single feature raw signal 1D CNN-transformer

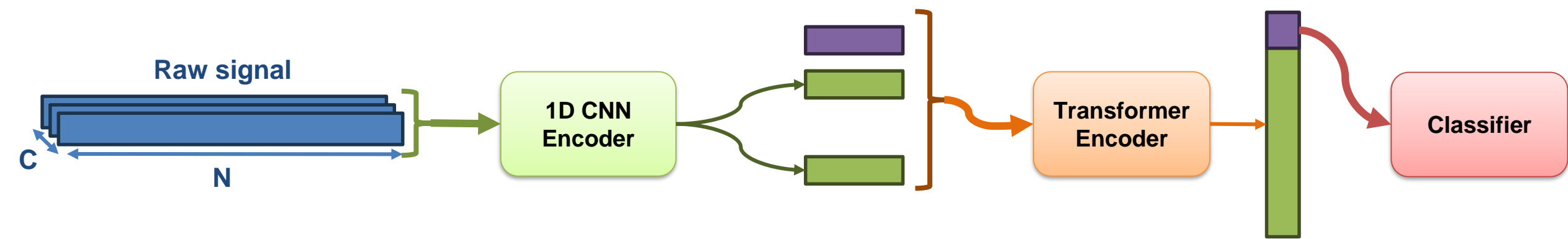


Figure - Proposed 1D CNN Transformer architecture (inspired from [Natarajan et al. 2020](#)).

Single feature raw signal 1D CNN-transformer

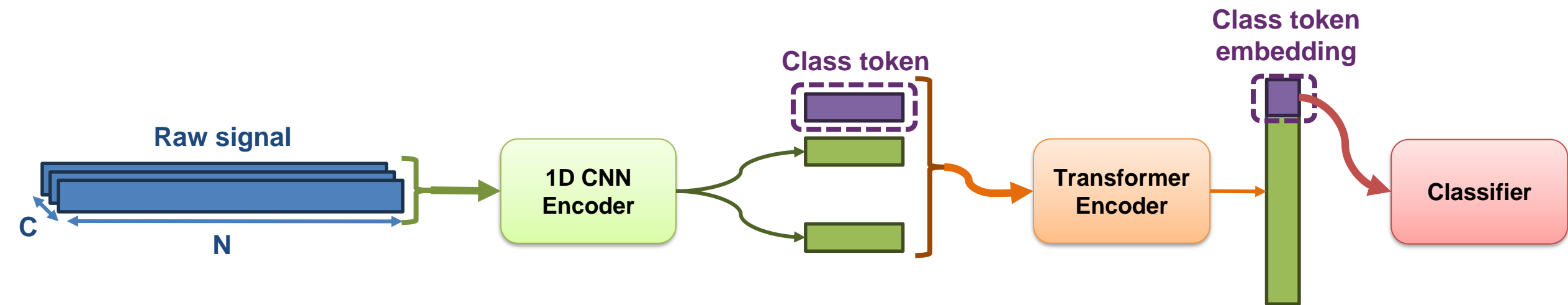


Figure - Proposed 1D CNN Transformer architecture (inspired from [Natarajan et al. 2020](#)).

Guided and regularized intermediate fusion

Guided and regularized intermediate fusion

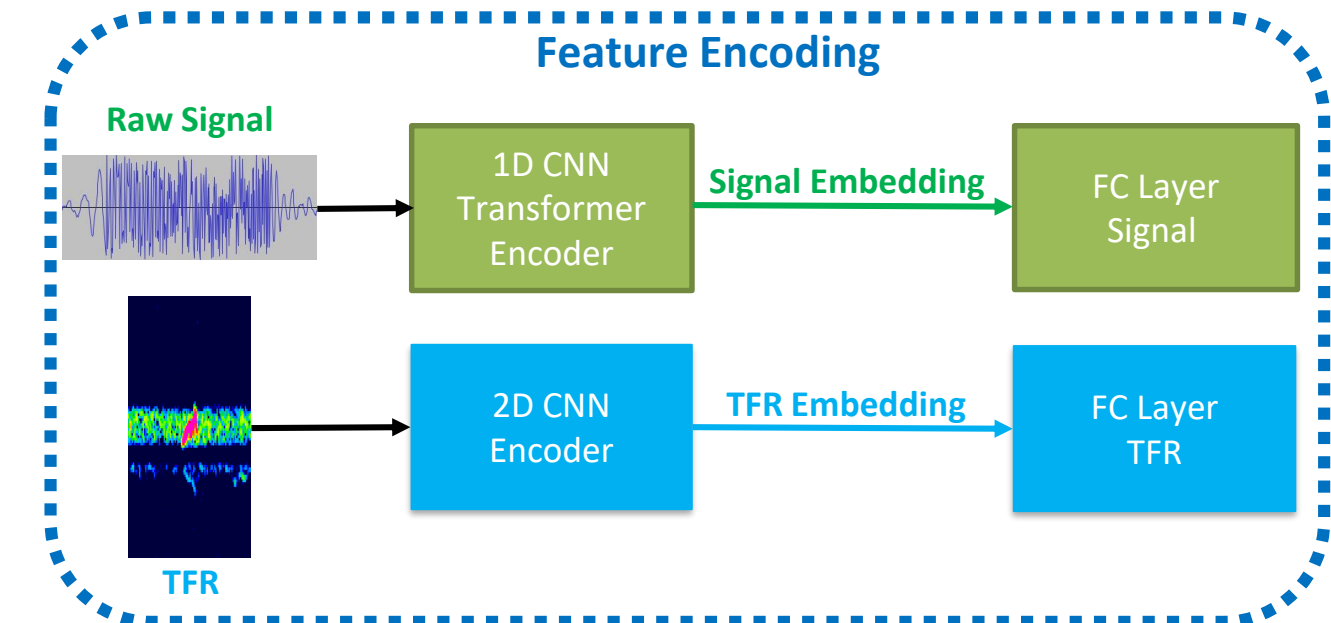


Figure - Proposed **intermediate fusion** hybrid CNN Transformer model.

Guided and regularized intermediate fusion

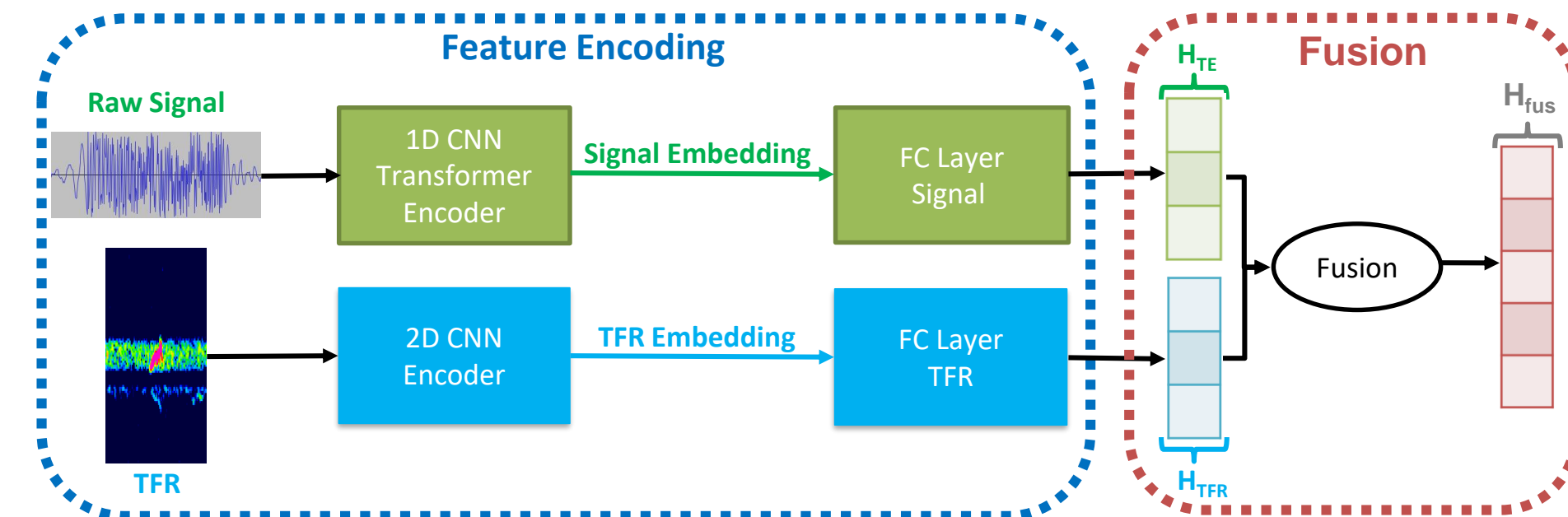


Figure - Proposed **intermediate fusion** hybrid CNN Transformer model.

Guided and regularized intermediate fusion

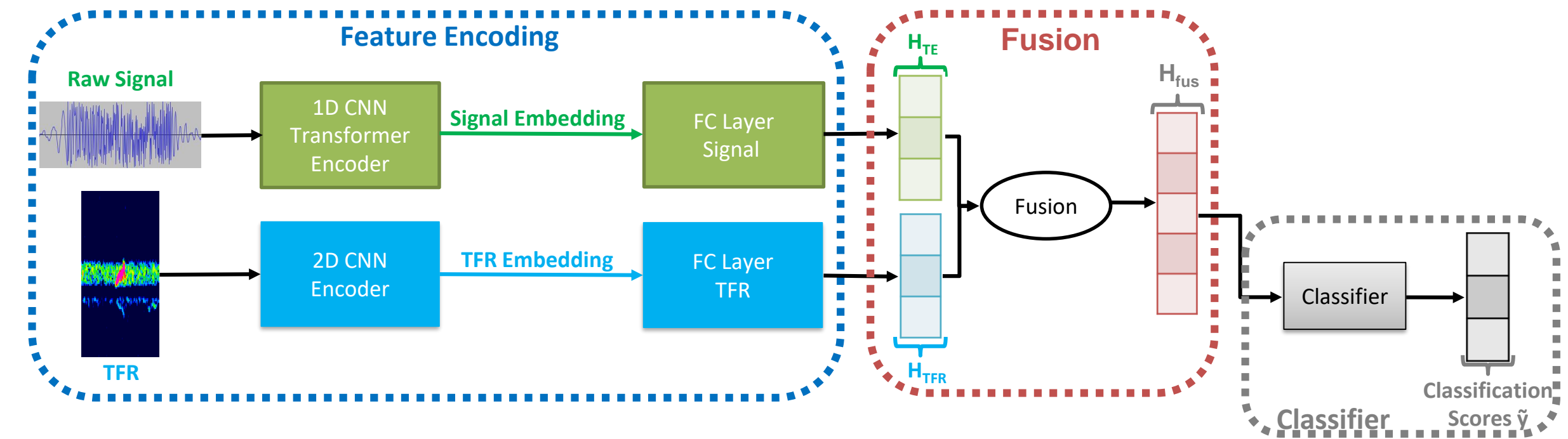


Figure - Proposed **intermediate fusion** hybrid CNN Transformer model.

Guided and regularized intermediate fusion

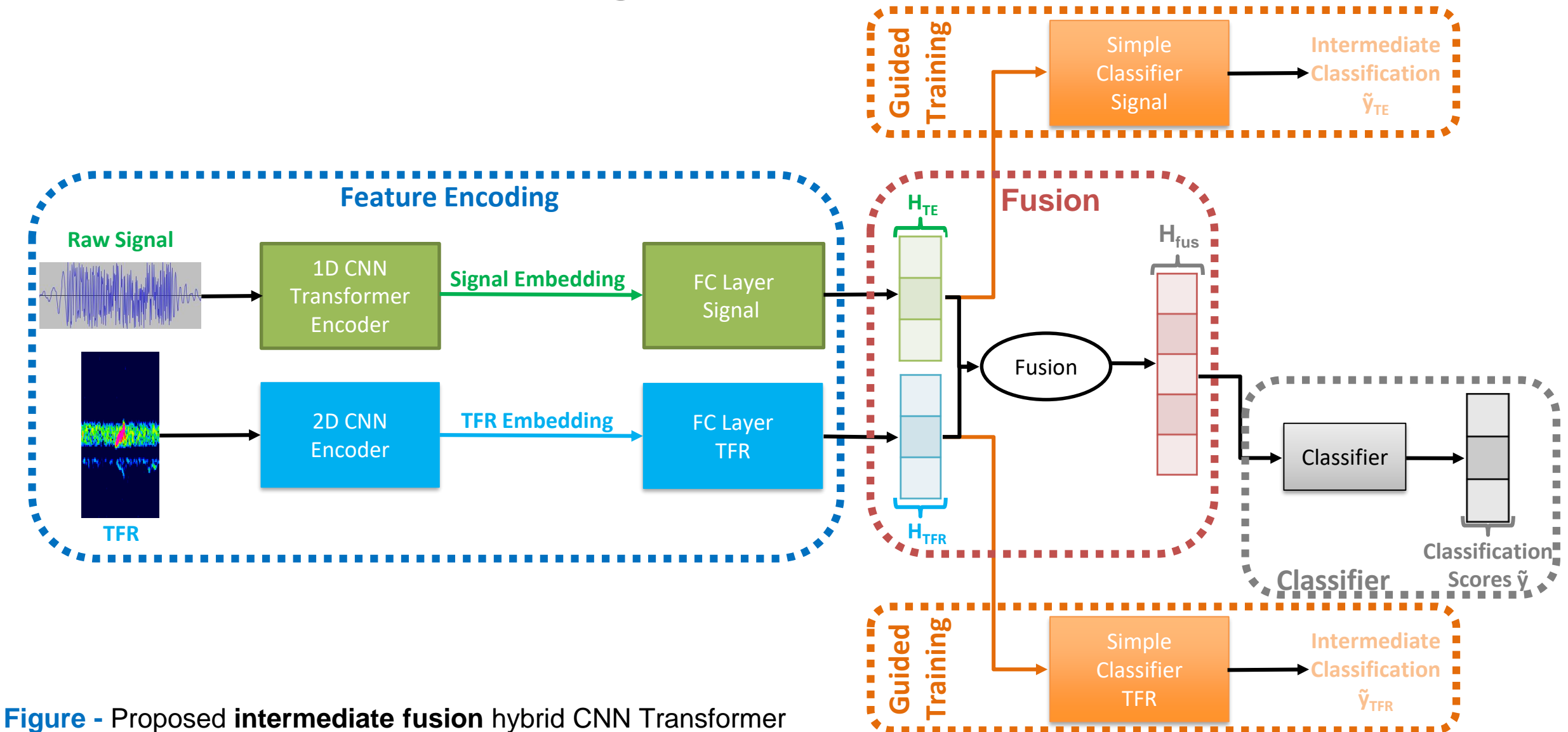


Figure - Proposed **intermediate fusion** hybrid CNN Transformer model.

Guided and regularized intermediate fusion

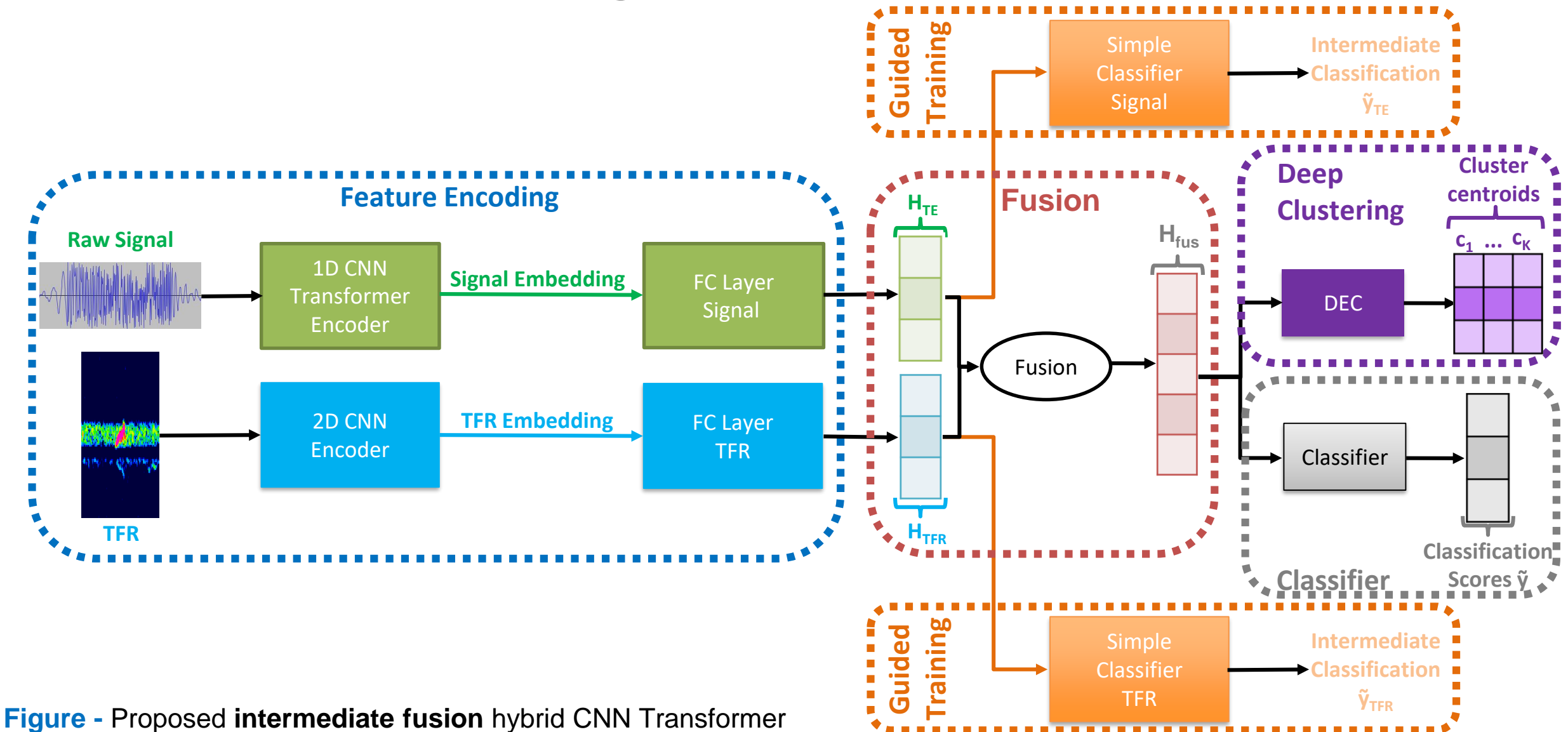


Figure - Proposed **intermediate fusion** hybrid CNN Transformer model.

Intermediate fusion

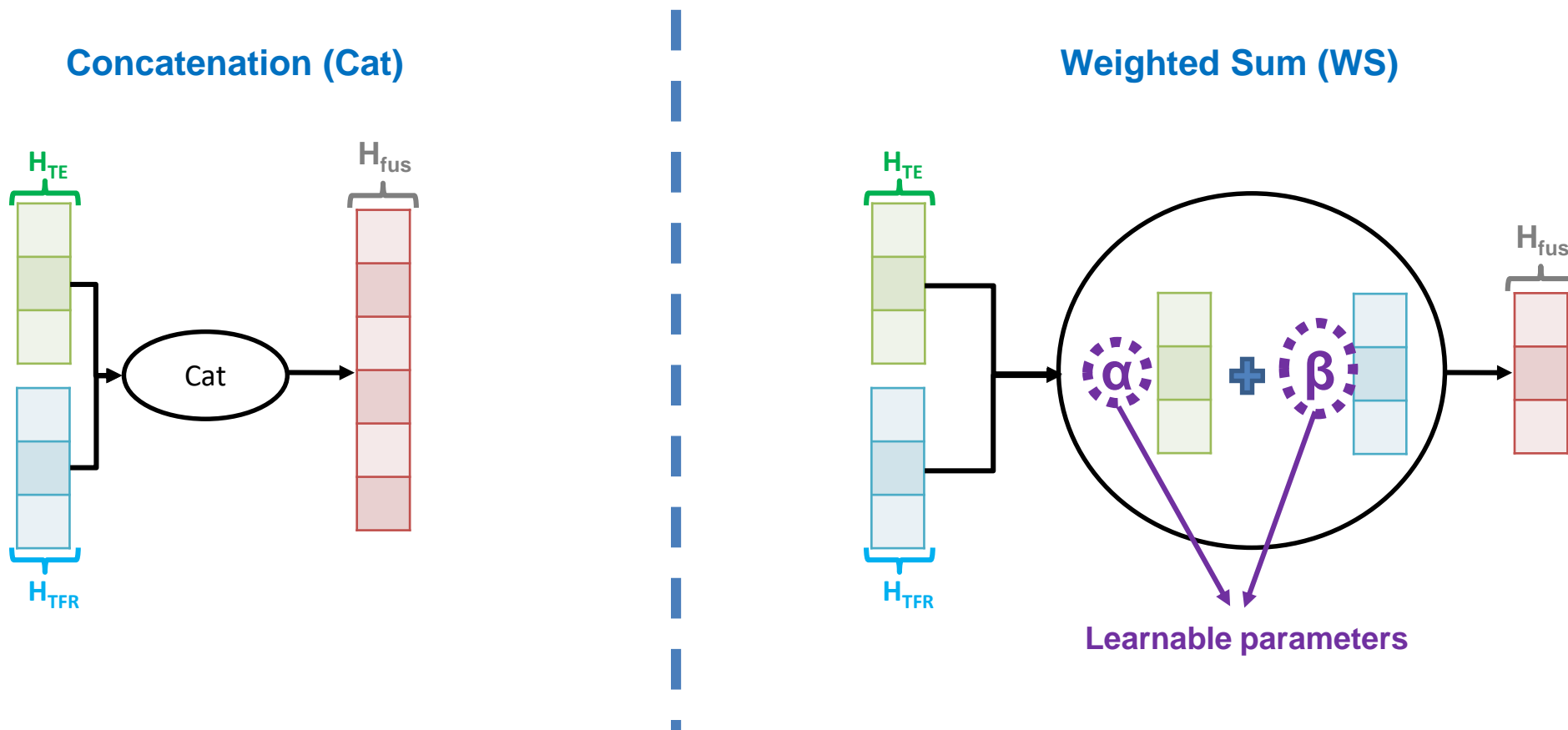


Figure - Proposed intermediate fusion strategies: concatenation and weighted sum

Outline

- I. **Context**
 - a) **Medical and scientific context**
 - b) **Emboli classification methods**
 - c) **Challenges and objectives**
- II. **Contribution 1 : Semi-automatic data annotation**
 - a) **State-of-the-art**
 - b) **Proposed method**
 - c) **Results**
- III. **Contribution 2 : Multi-feature medical signal classification**
 - a) **State-of-the-art**
 - b) **Proposed method**
 - c) **Results**
- IV. **Contribution 3 : Model compression based on extreme quantization**
 - a) **State-of-the-art**
 - b) **Proposed method**
 - c) **Results**
- V. **Conclusion and perspectives**

Experiment: SOTA comparison

Objective:

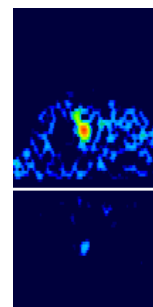
- Highlight the advantage of multi-feature classification.
- Comparison with multi-feature SOTA methods.

Datasets:



HITS:

- TCD Data.
- 1545 samples.
- Three classes.
- Sampling frequency: 4385 Hz.



Metrics:

- Mathews Correlation Coefficient (MCC).

Loss function:

- Cross entropy (CE)

Class	Number of samples
Artifact	403
Gaseous Emboli	569
Solid Emboli	569
Unknown	4

Results

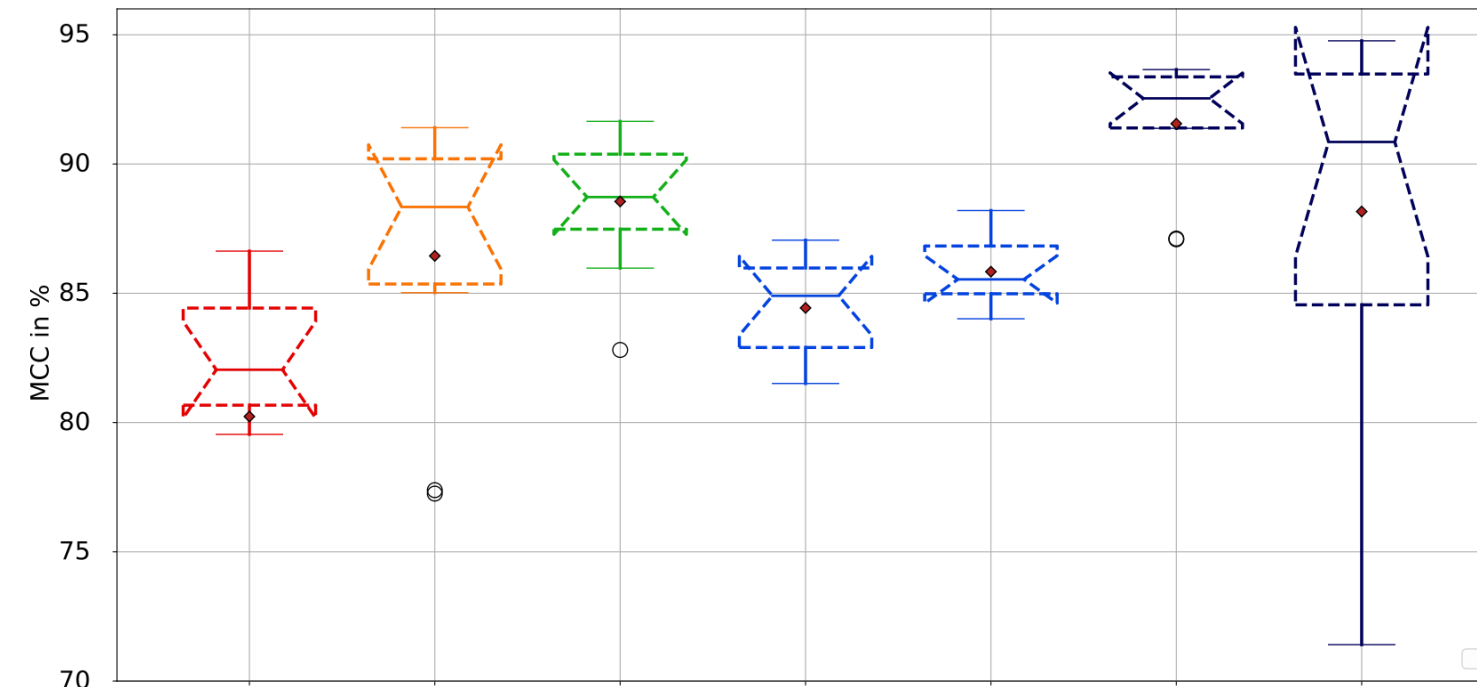


Figure - Comparison of the classification performances of different single and multi-feature models on the HITS dataset

Results

Single feature models

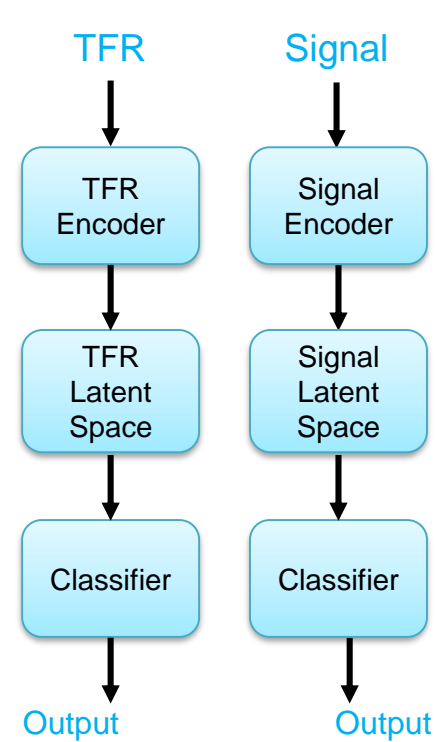
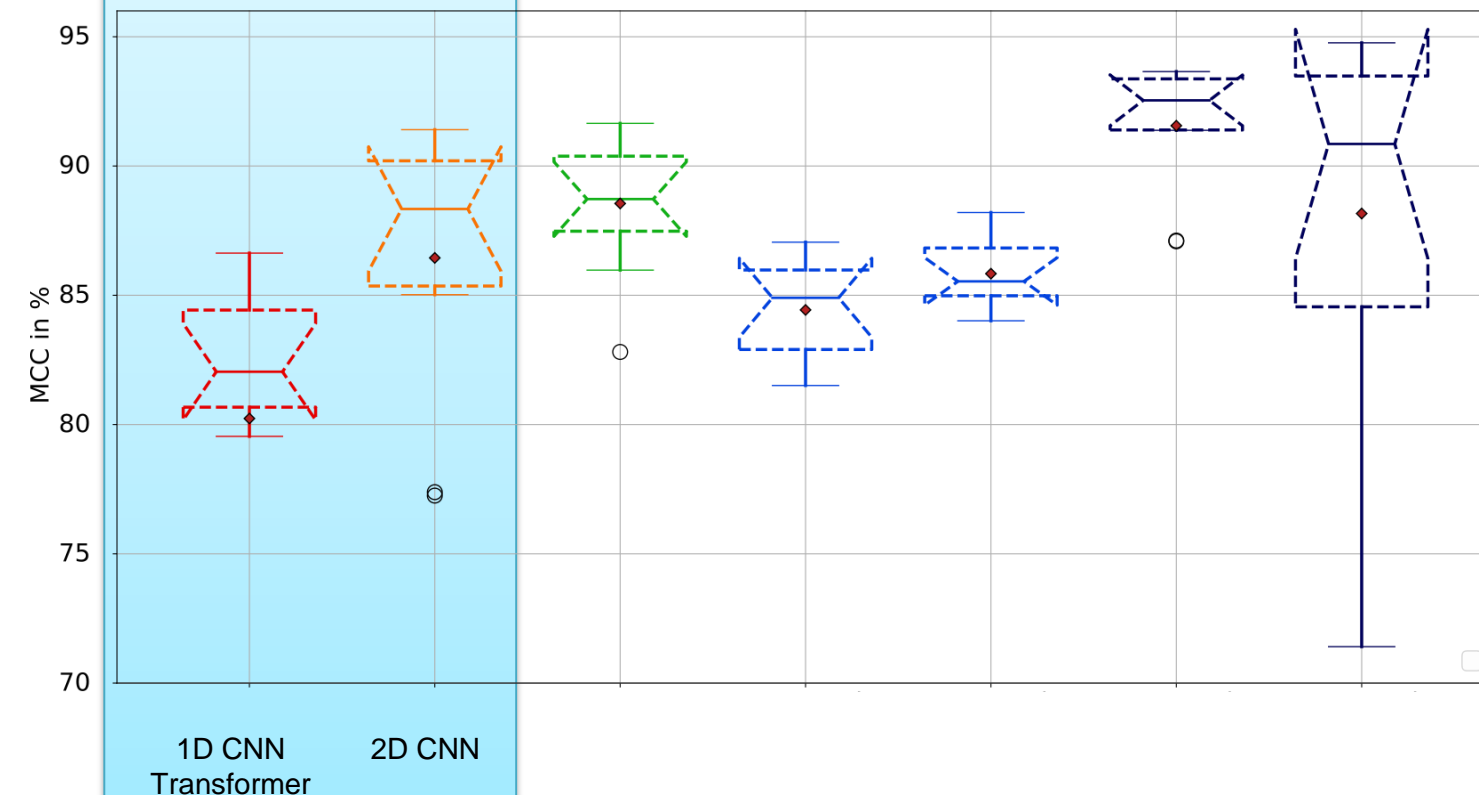


Figure - Comparison of the classification performances of different single and multi-feature models on the HITS dataset

Results

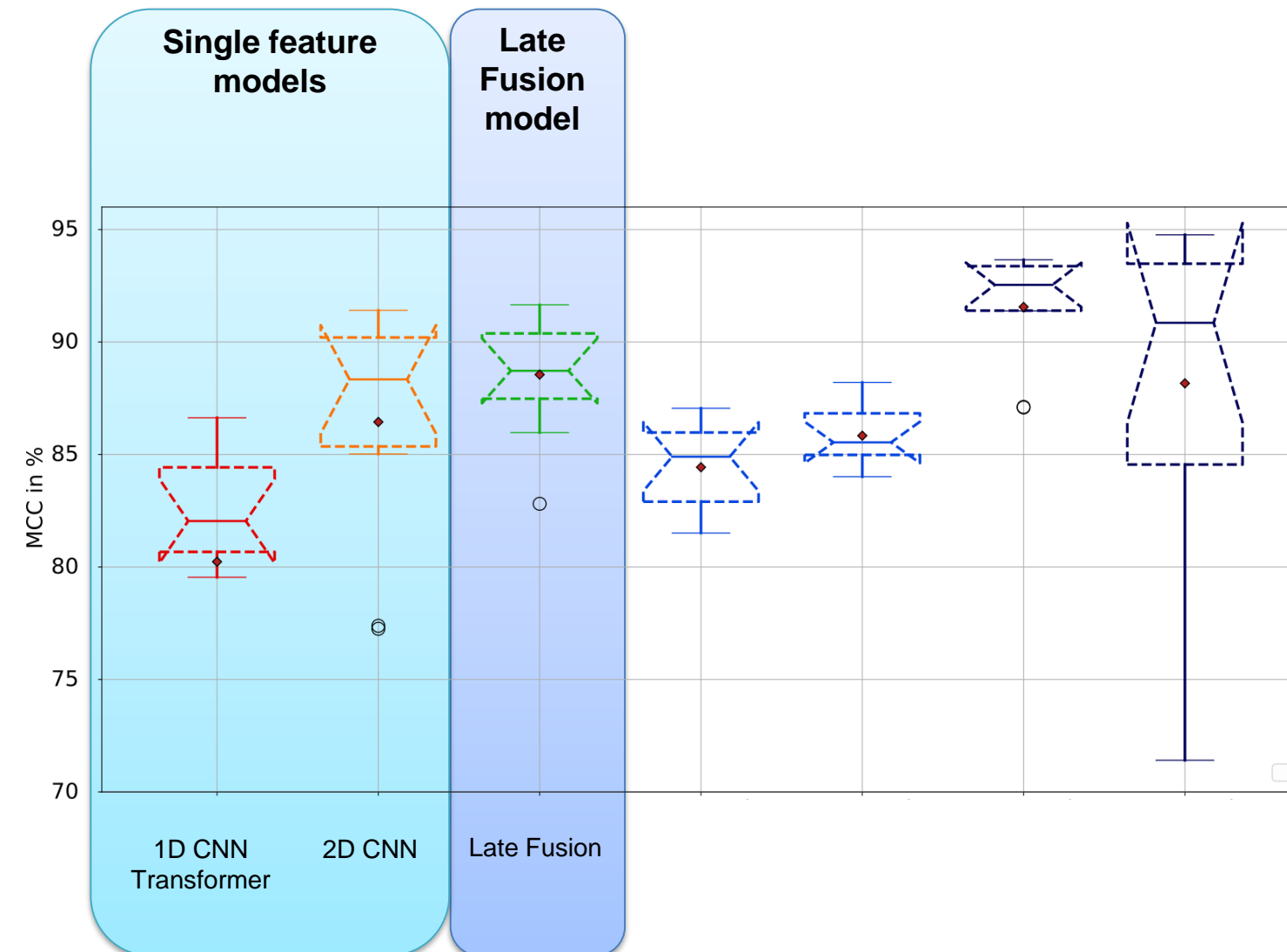


Figure - Comparison of the classification performances of different single and multi-feature models on the HITS dataset

Results

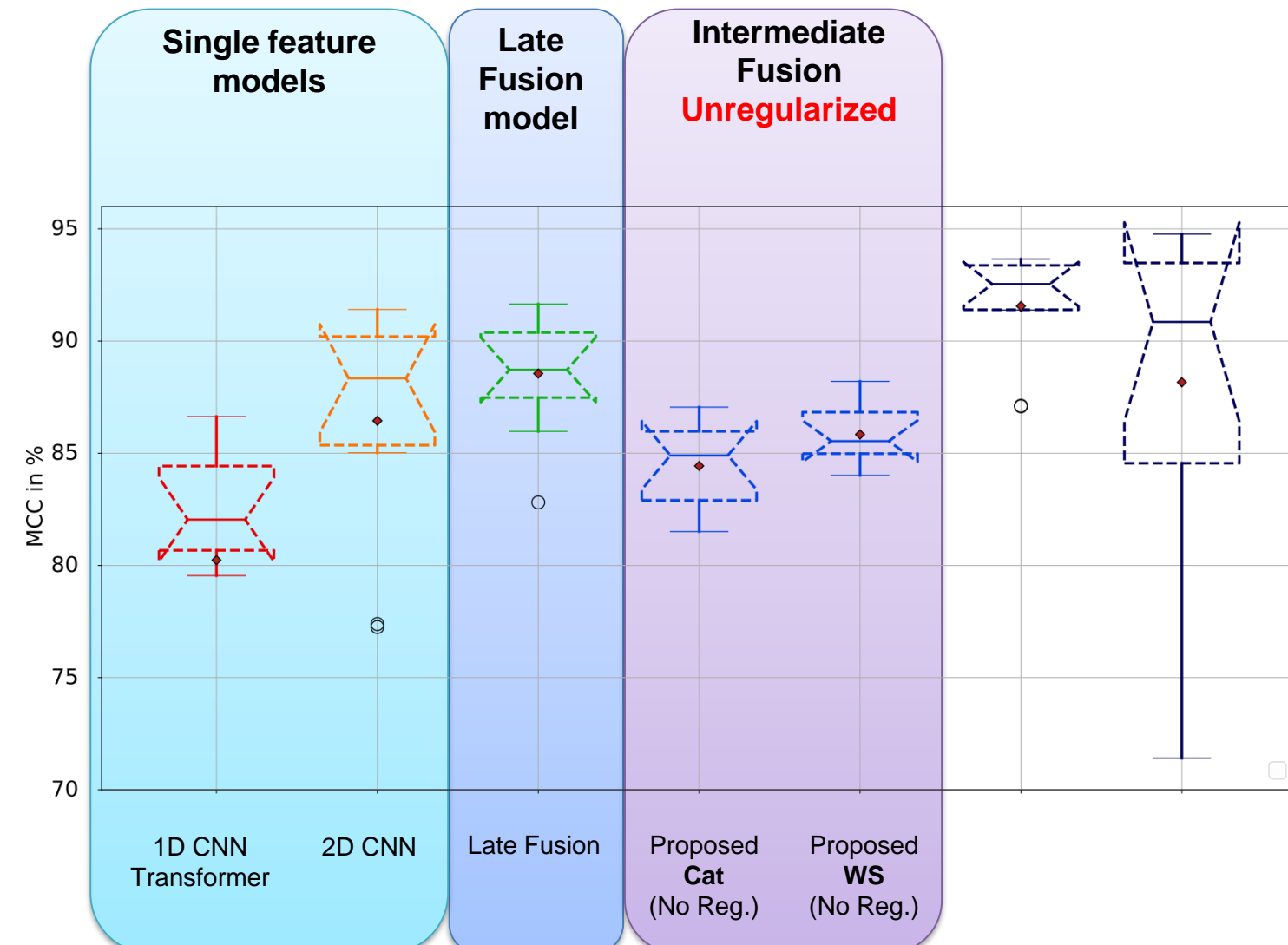
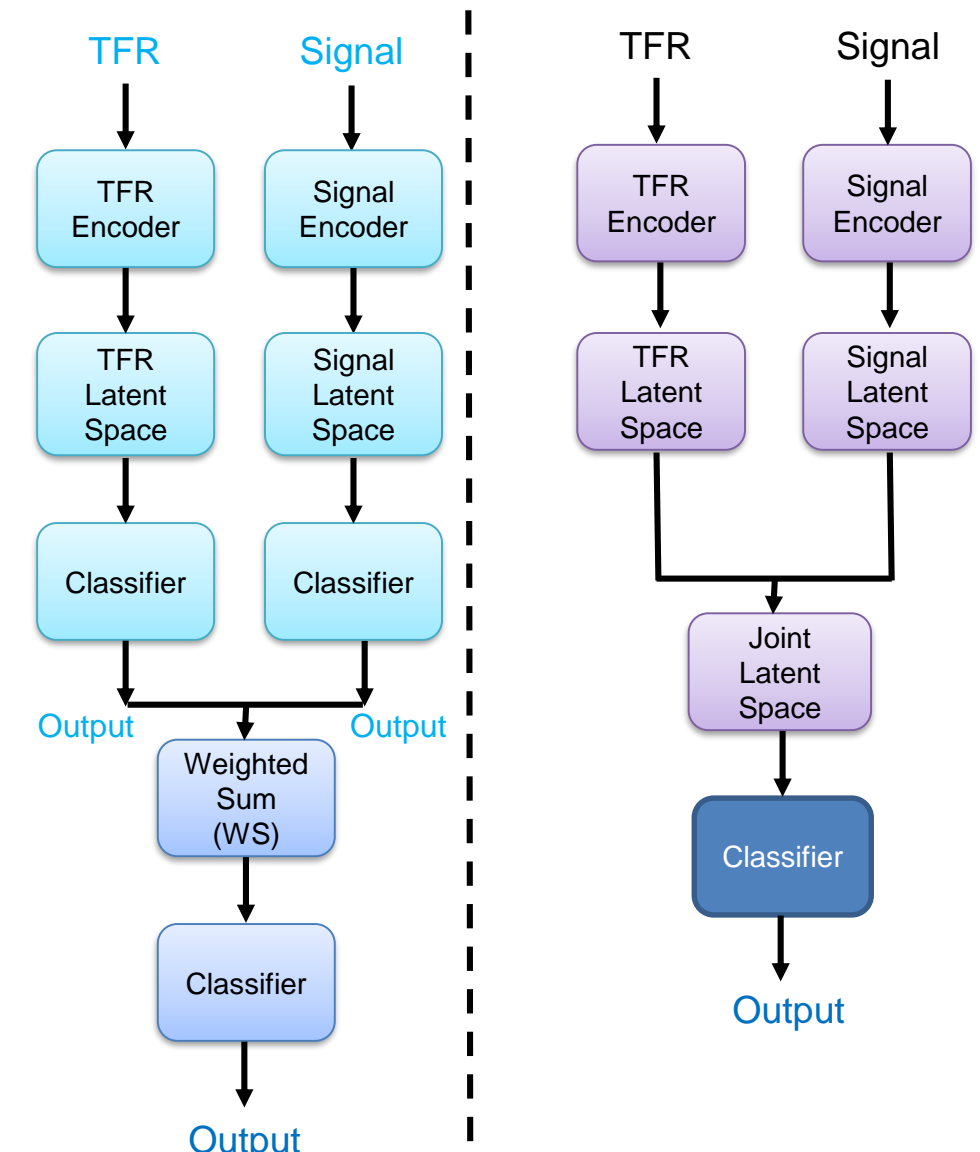


Figure - Comparison of the classification performances of different single and multi-feature models on the HITS dataset



Results

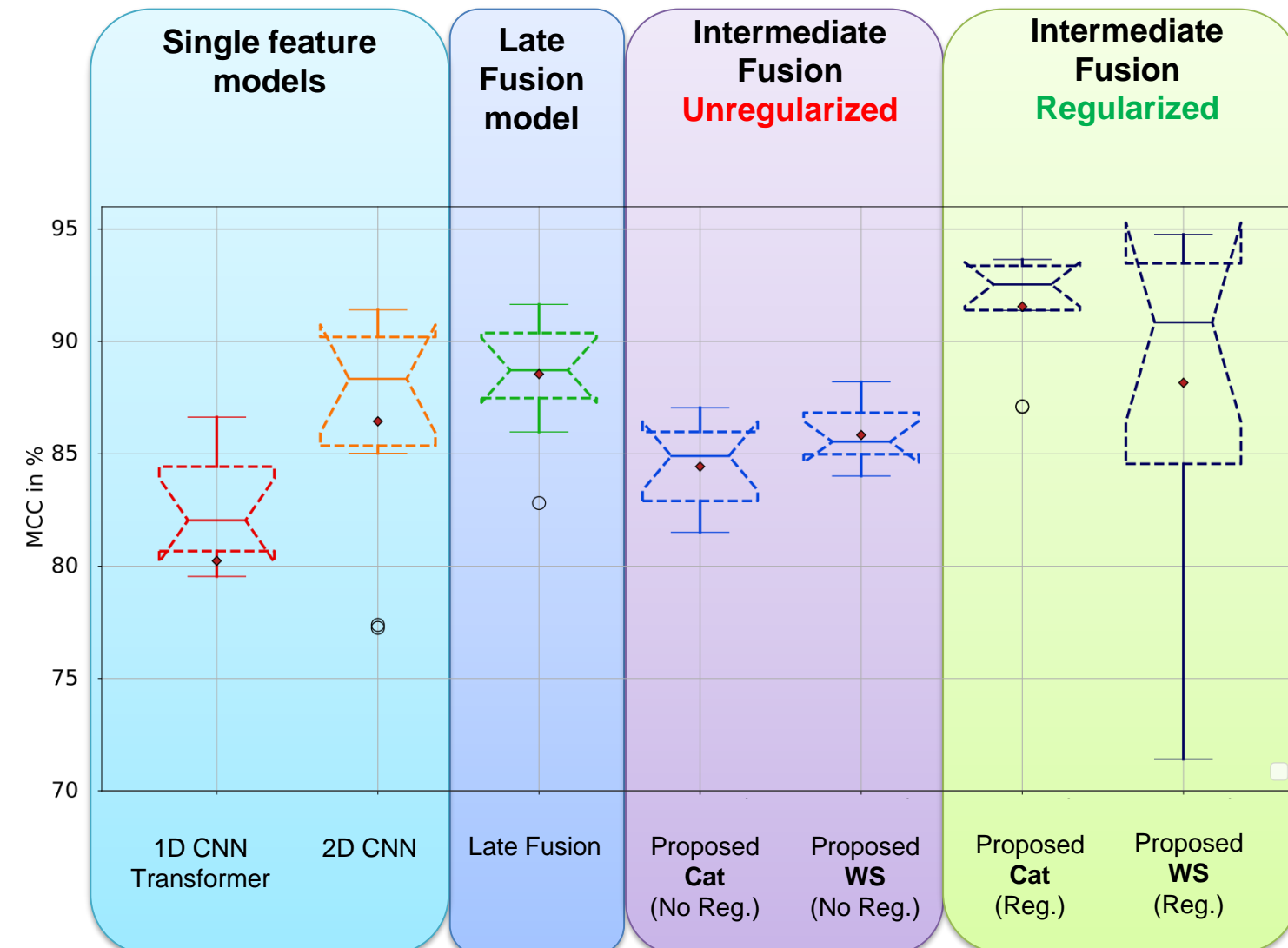
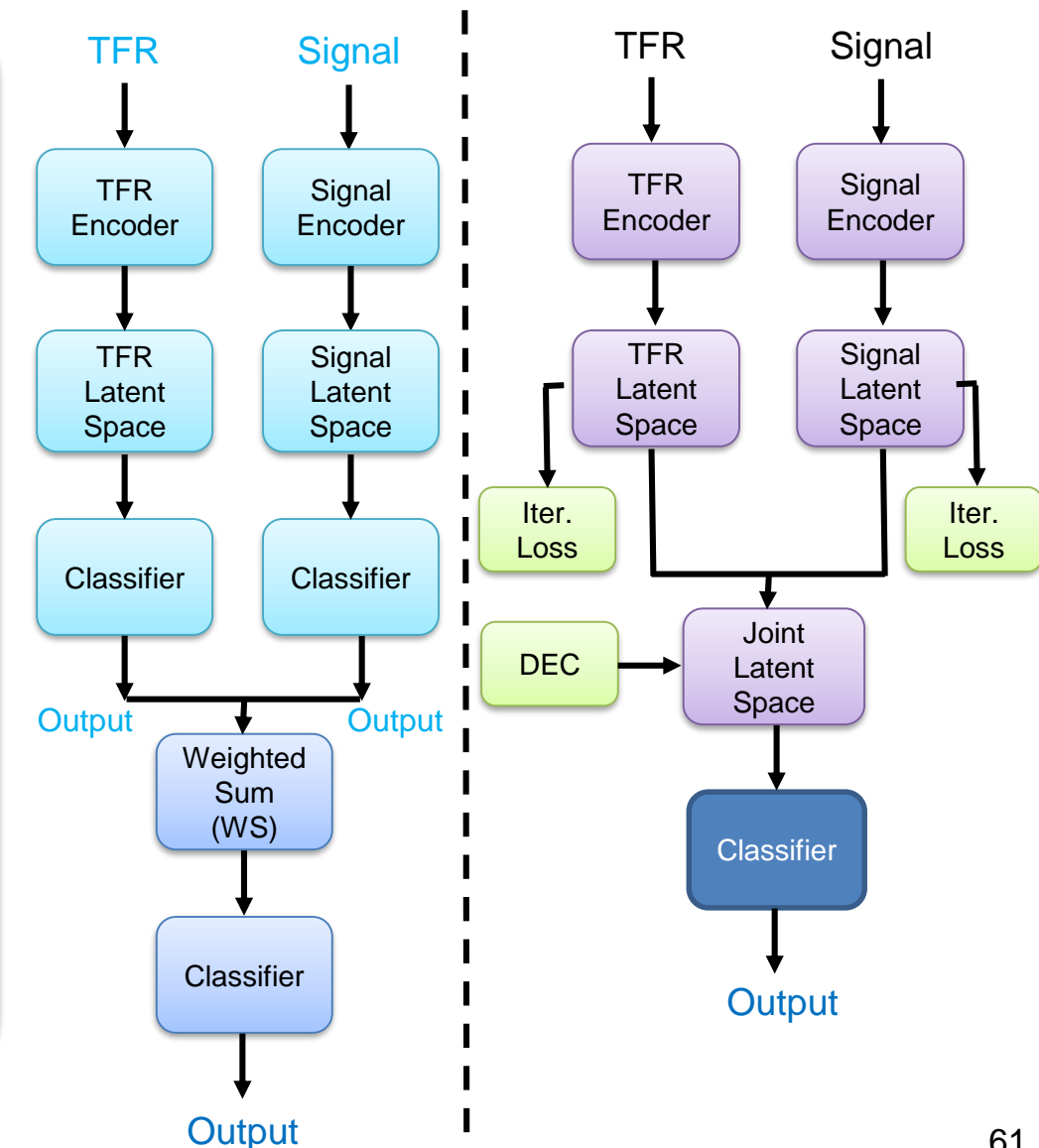
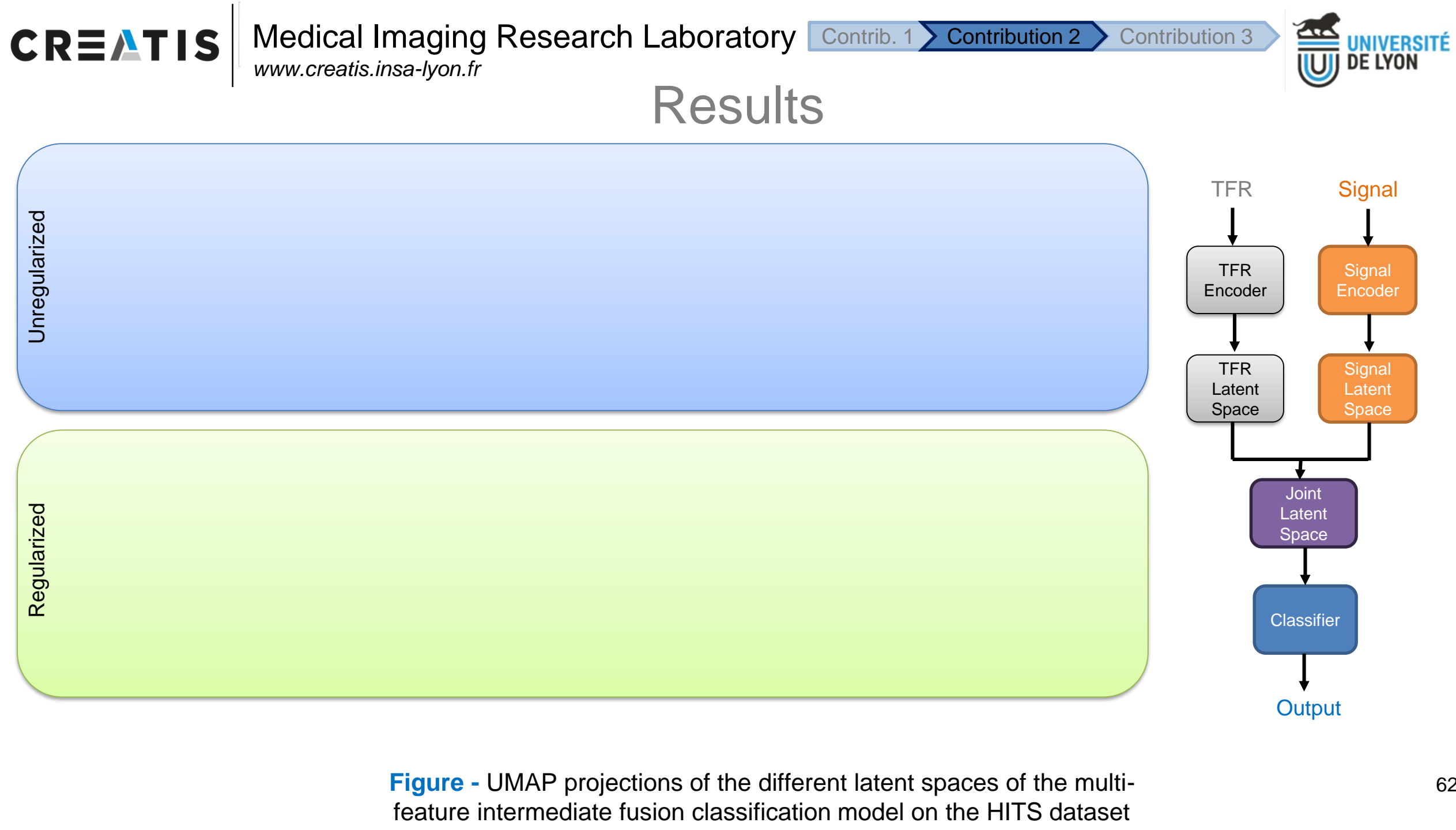


Figure - Comparison of the classification performances of different single and multi-feature models on the HITS dataset





Results

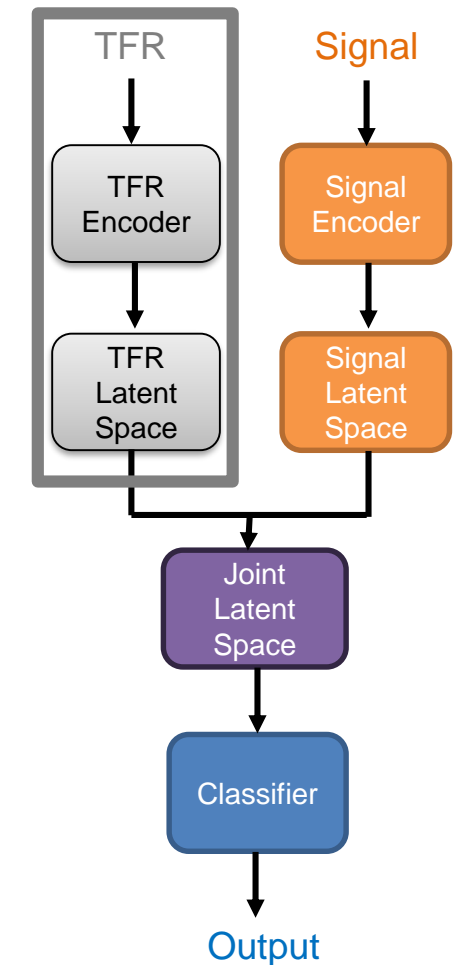
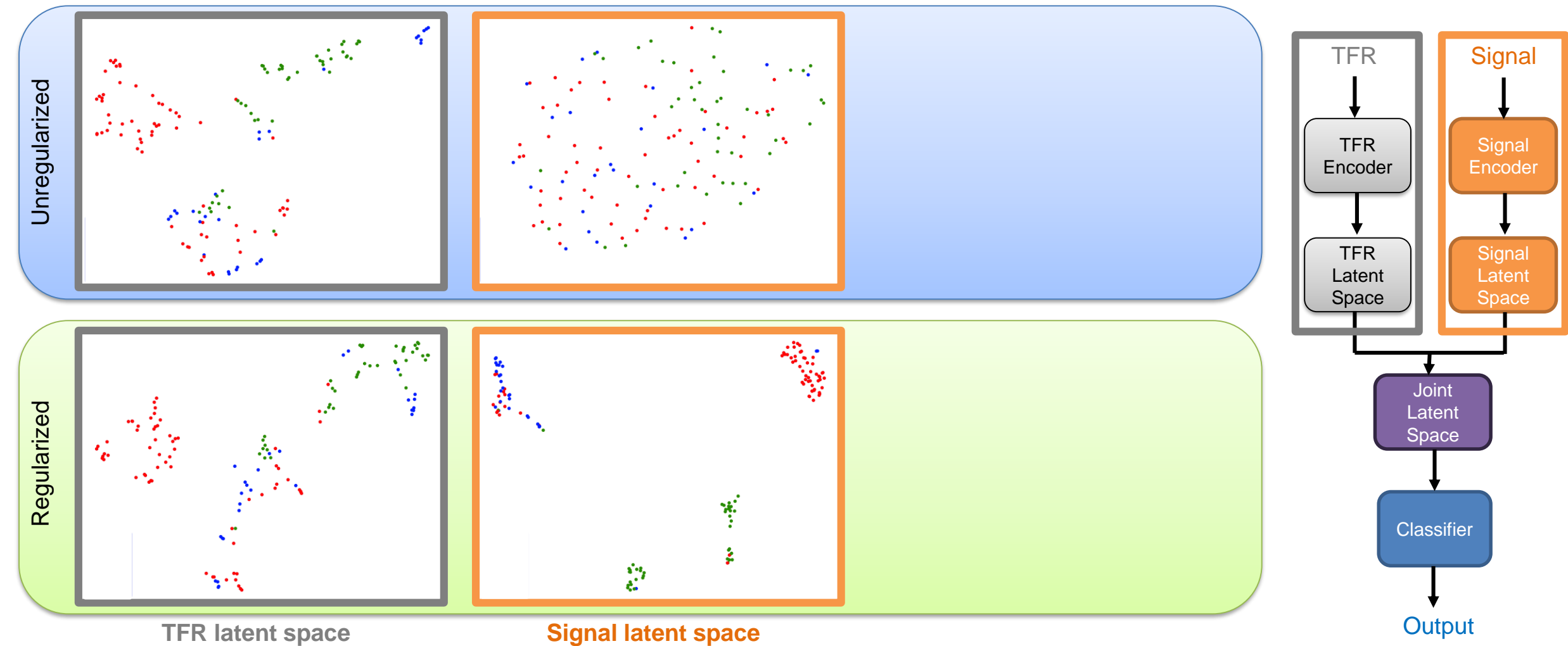


Figure - UMAP projections of the different latent spaces of the multi-feature intermediate fusion classification model on the HITS dataset

Results



- Artifact
- Gaseous embolus
- Solid embolus

Figure - UMAP projections of the different latent spaces of the multi-feature intermediate fusion classification model on the HITS dataset

Results

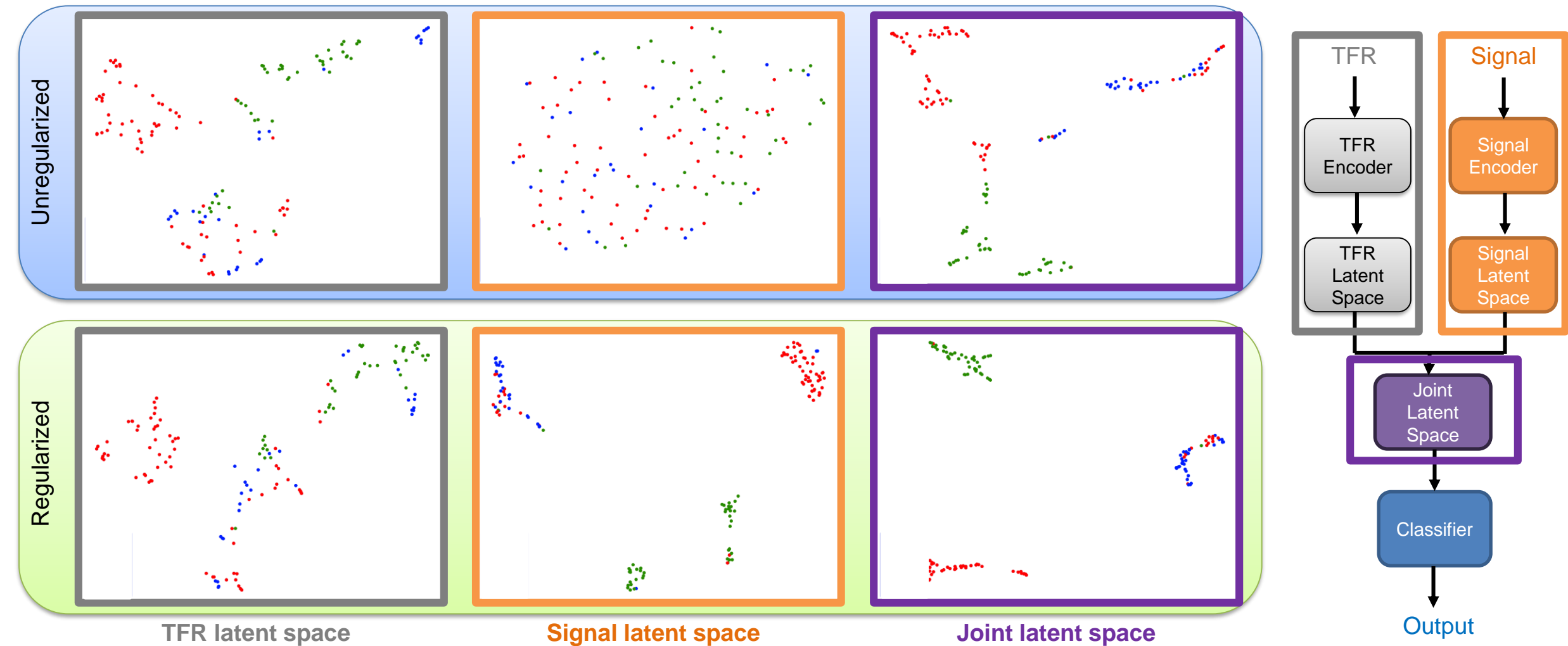


Figure - UMAP projections of the different latent spaces of the multi-feature intermediate fusion classification model on the HITS dataset

Intermediate conclusion

Use of multiple representations of a signal

- TFR and raw signal.
- Two approaches:
 - Late fusion.
 - **Intermediate fusion.**

Intermediate fusion models

- Regularized:
 - **Guided training.**
 - Deep Embedded Clustering (**DEC**).
- End-to-end training.

Results

- **Improvement of HITS classification** performances with **up to +10% MCC**.
- **State-of-the-art results** on other medical signal datasets (EEG and ECG) with up to +4% MCC.



Objectives and Contributions

Dataset creation and annotation 

- Semi-supervised data annotation*
- Soft labelling (annotation)*

Multiple representations 

- Different models with different inputs**
- Multi-feature models

Resource hungry models 

- Lite models
- Model compression
- (Soft labelling training)

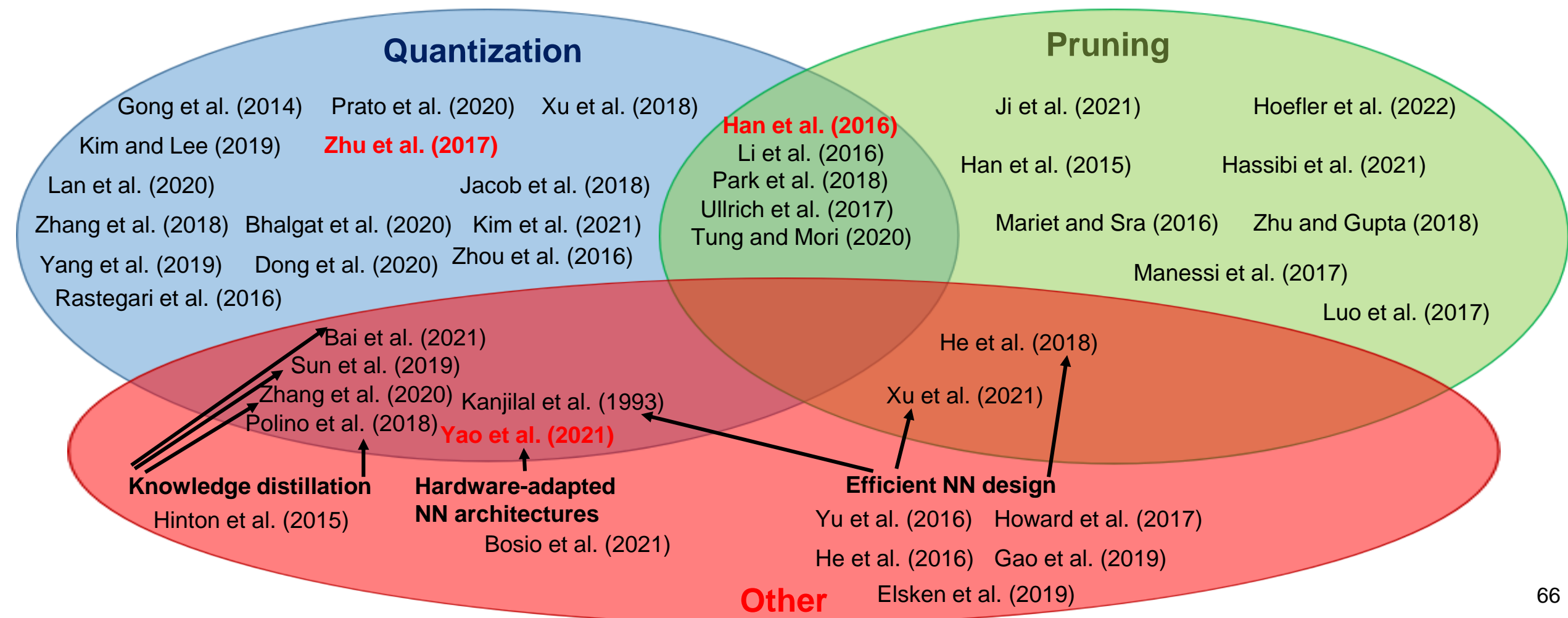
* Vindas et al. (IUS 2021), Vindas et al. (MEDIA 2022), Vindas et al. (IUS 2023)

** Vindas et al. (MLHC 2022), Vindas et al. (IABM 2023), Vindas et al. (EUSIPCO 2023), and Vindas et al. (Pattern Recognition 2023)

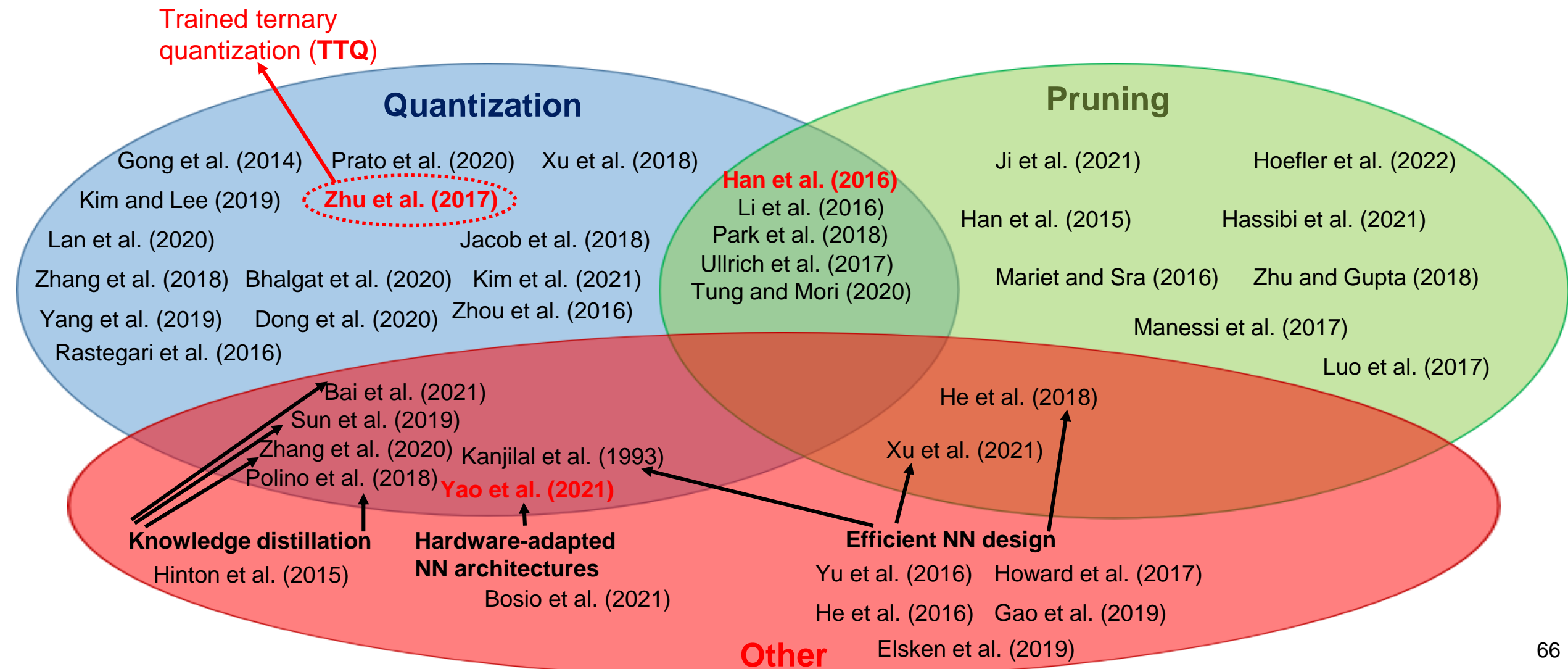
Outline

- I. **Context**
 - a) **Medical and scientific context**
 - b) **Emboli classification methods**
 - c) **Challenges and objectives**
- II. **Contribution 1 : Semi-automatic data annotation**
 - a) **State-of-the-art**
 - b) **Proposed method**
 - c) **Results**
- III. **Contribution 2 : Multi-feature medical signal classification**
 - a) **State-of-the-art**
 - b) **Proposed method**
 - c) **Results**
- IV. **Contribution 3 : Model compression based on extreme quantization**
 - a) **State-of-the-art**
 - b) **Proposed method**
 - c) **Results**
- V. **Conclusion and perspectives**

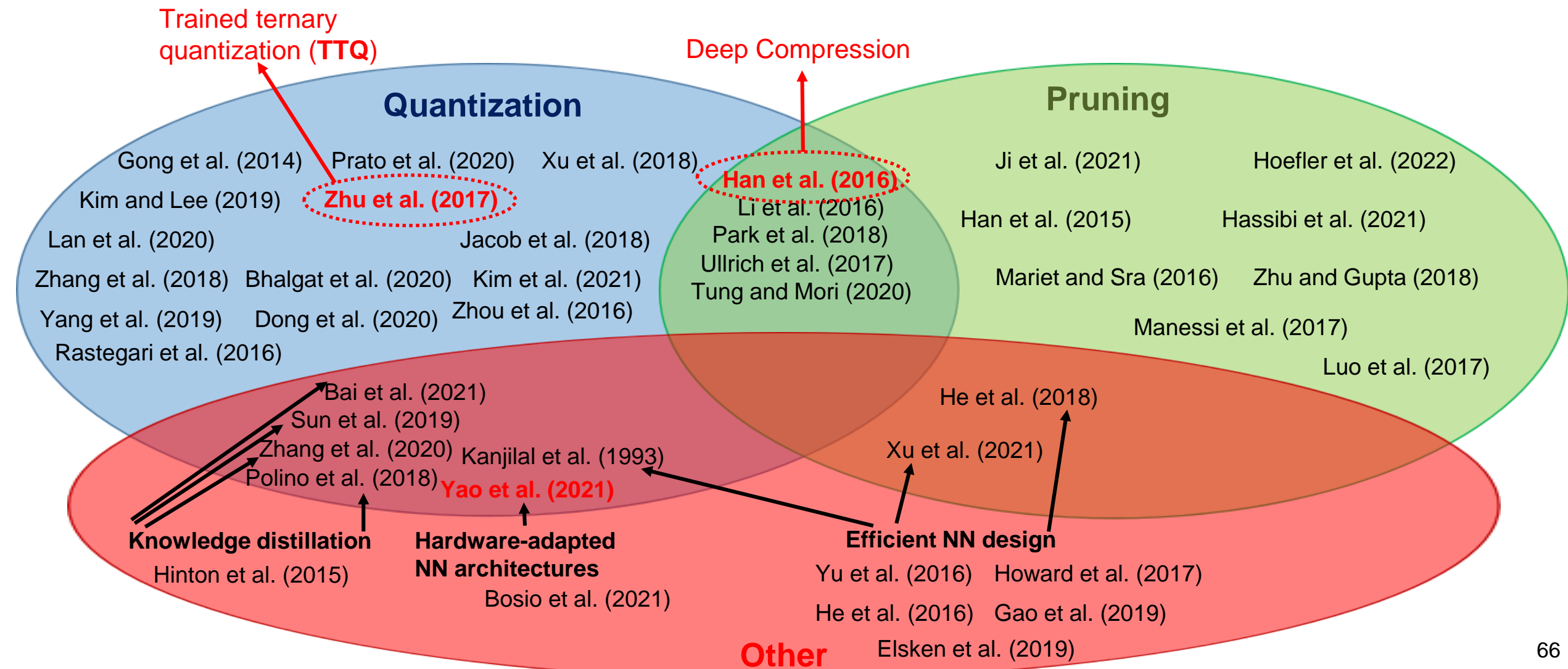
General Overview



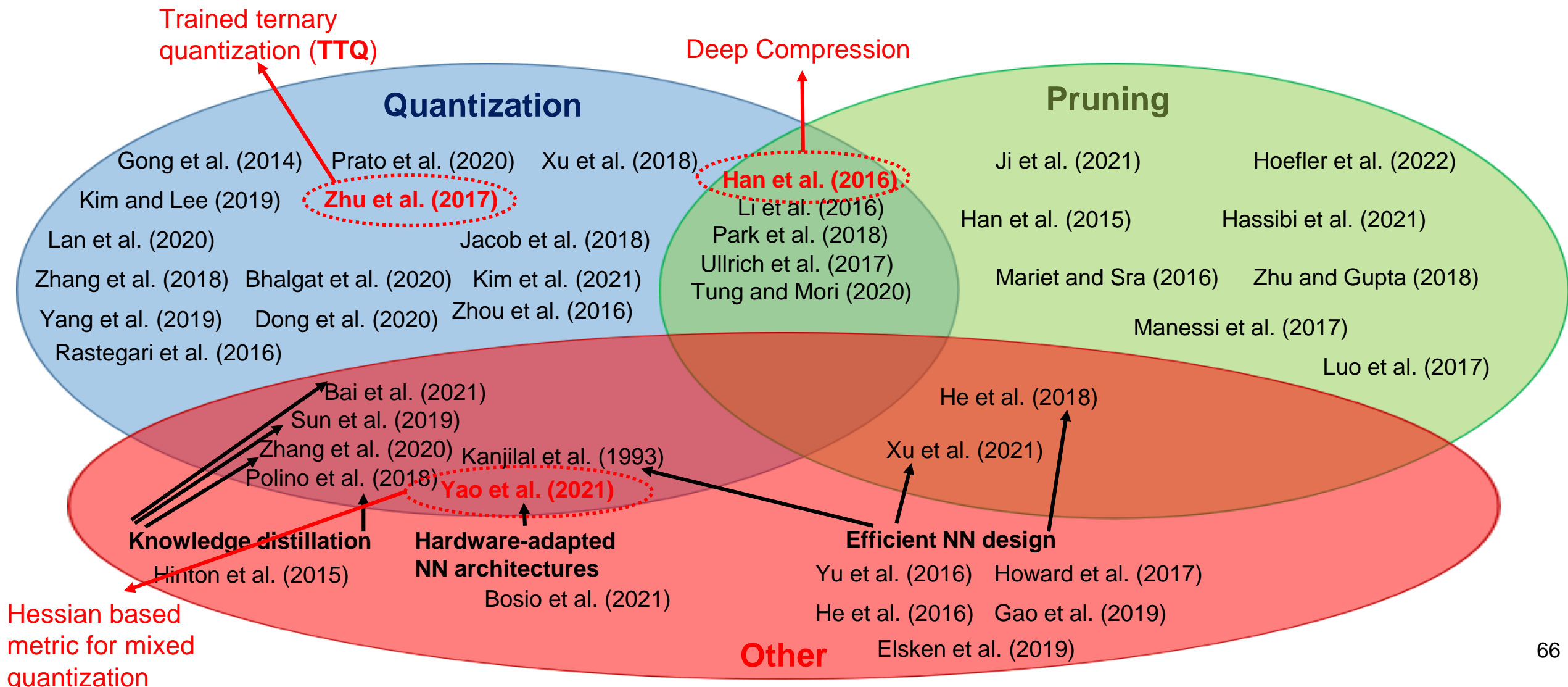
General Overview



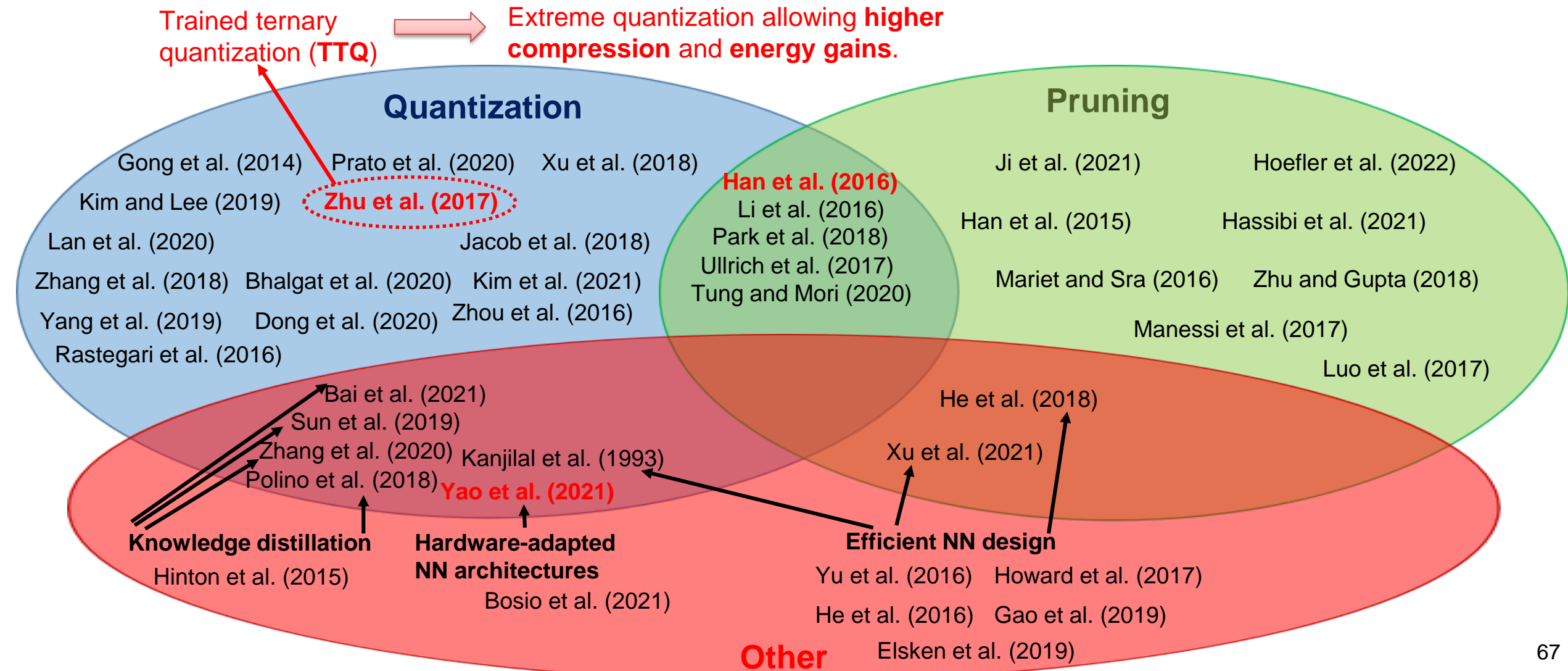
General Overview



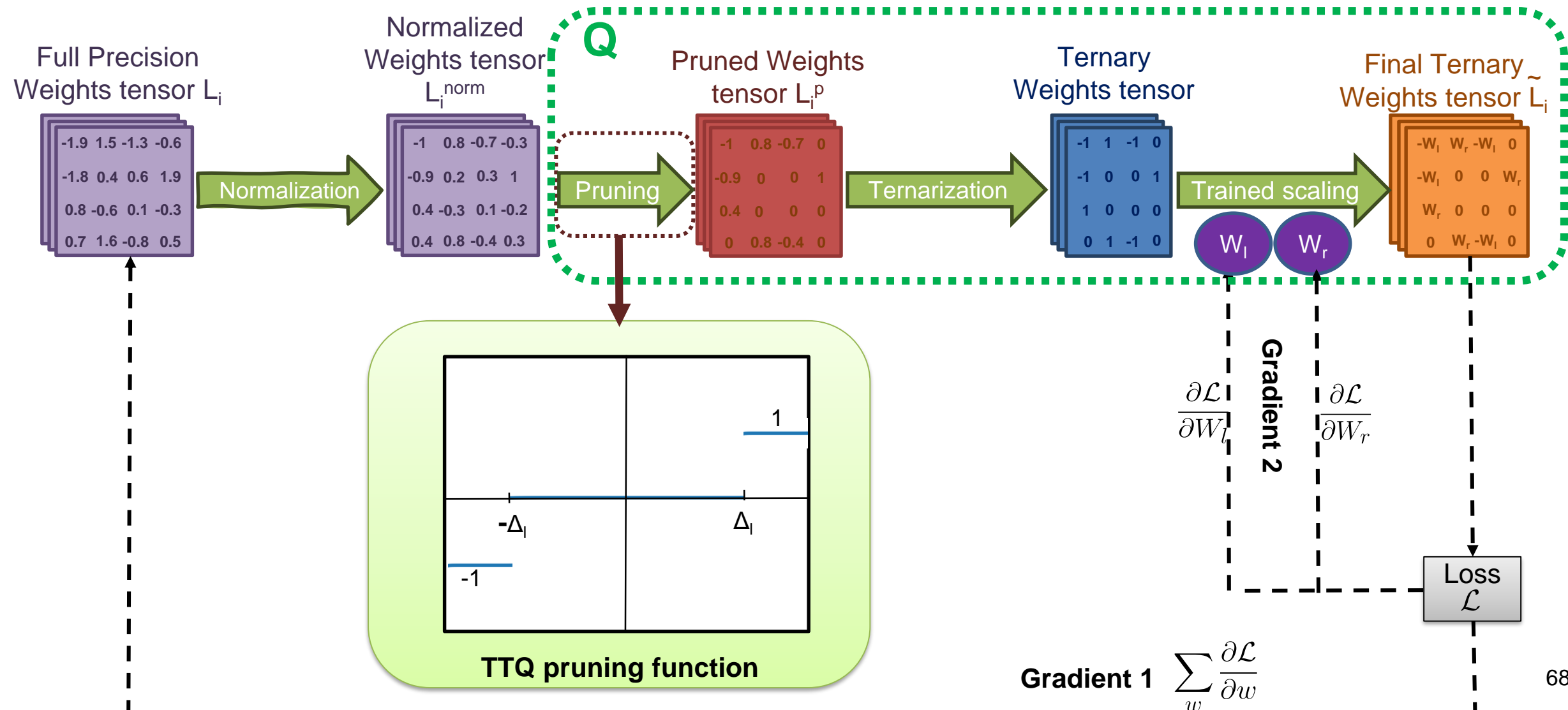
General Overview



General Overview



Trained ternary quantization (TTQ) – Zhu et al., 2017



Outline

- I. **Context**
 - a) **Medical and scientific context**
 - b) **Emboli classification methods**
 - c) **Challenges and objectives**
- II. **Contribution 1 : Semi-automatic data annotation**
 - a) **State-of-the-art**
 - b) **Proposed method**
 - c) **Results**
- III. **Contribution 2 : Multi-feature medical signal classification**
 - a) **State-of-the-art**
 - b) **Proposed method**
 - c) **Results**
- IV. **Contribution 3 : Model compression based on extreme quantization**
 - a) **State-of-the-art**
 - b) **Proposed method**
 - c) **Results**
- V. **Conclusion and perspectives**

Claims of contribution 3

- a. **Novel ternarization heuristic**, based on the weights' statistics.
- b. **Direct asymmetric pruning** before ternarization, allowing a **better trade-off** between compression, energy, and classification.
- c. **Asymmetric parametrization** of the sparsity rate, **controlling** the abovementioned **trade-off**.

Global pipeline

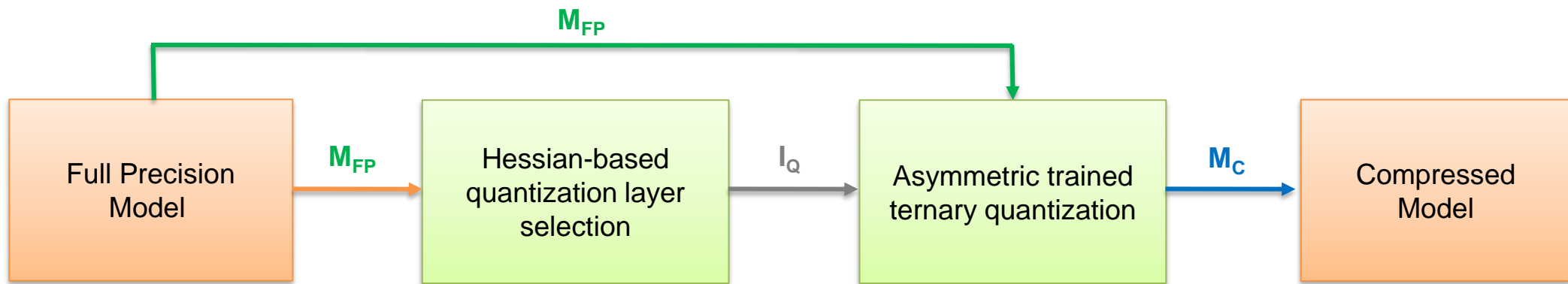
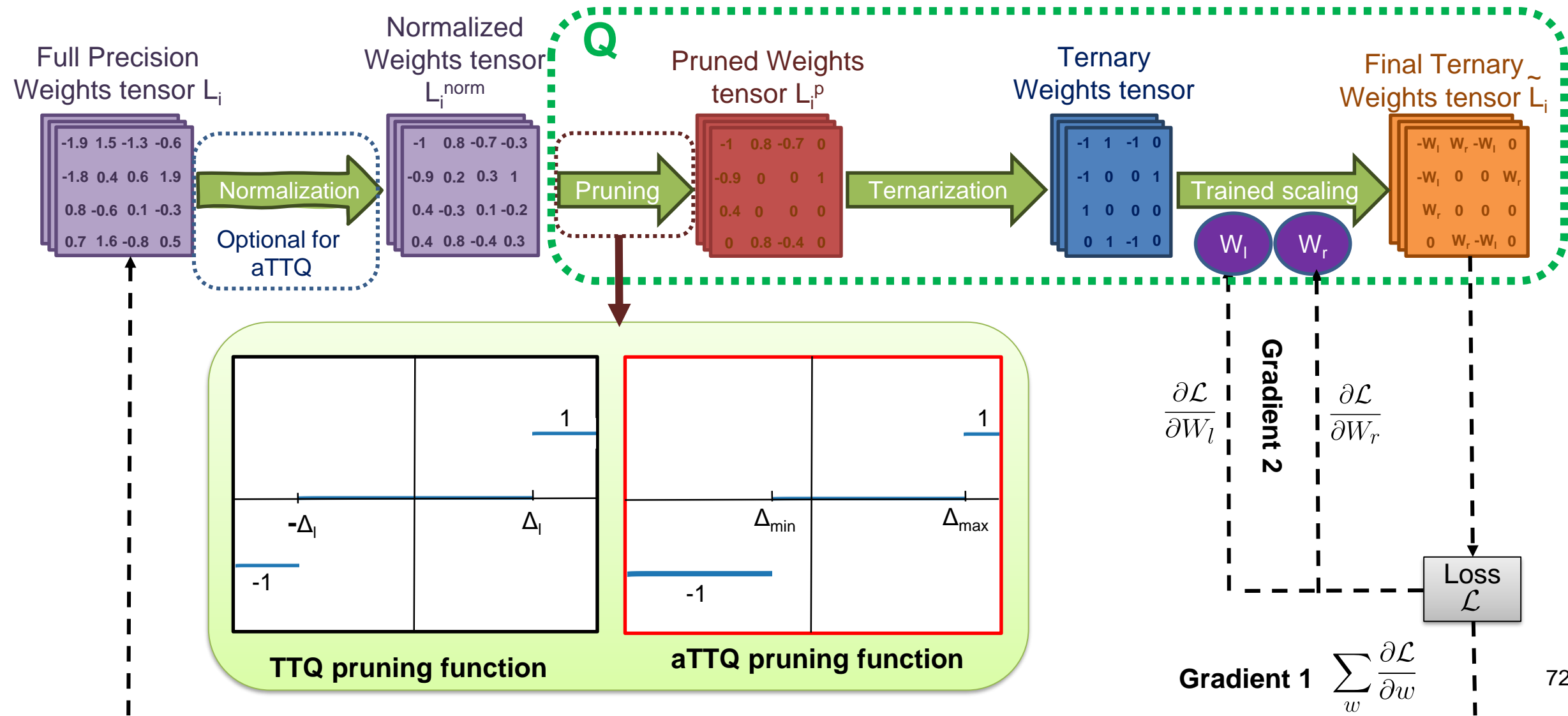
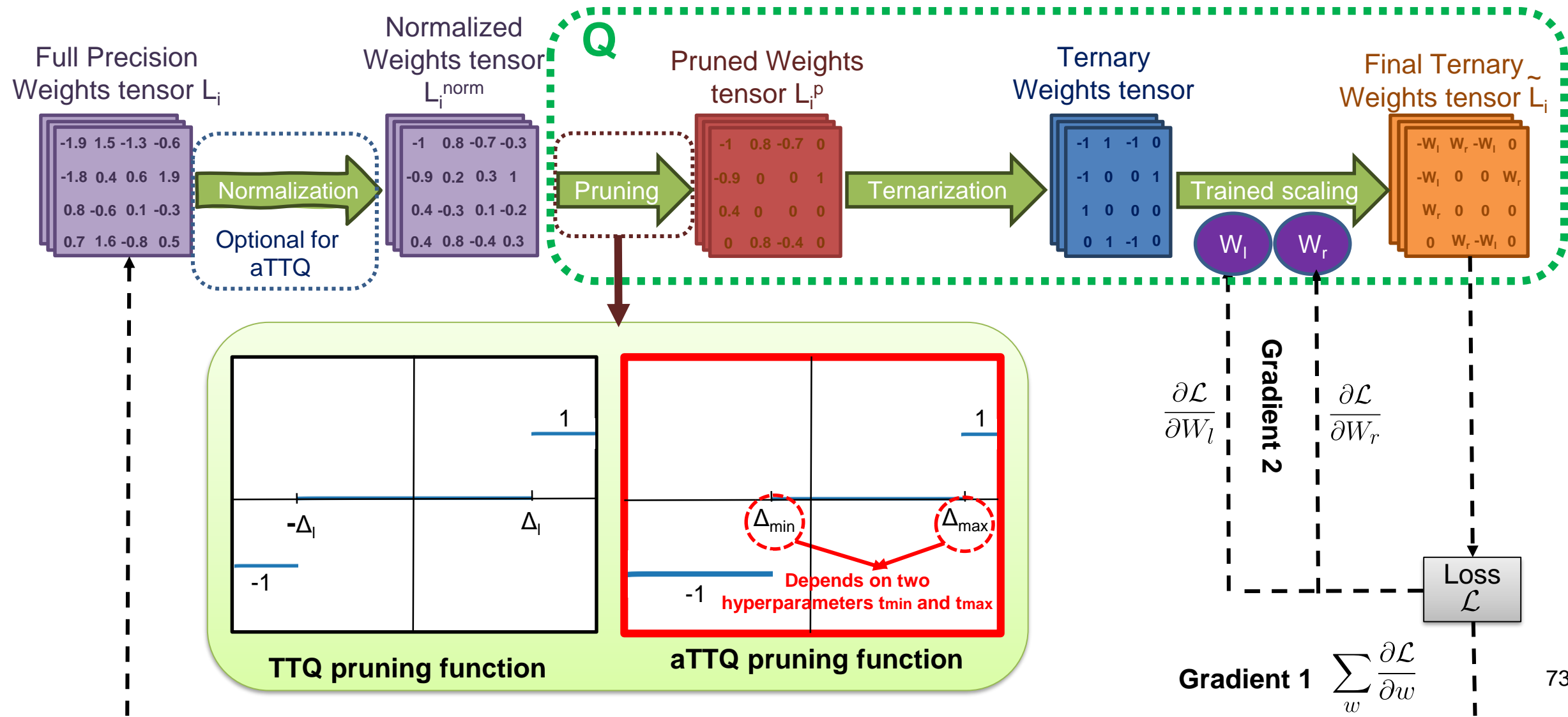


Figure – Global pipeline of our extreme quantization approach.

Asymmetric trained ternary quantization (aTTQ)



Asymmetric trained ternary quantization (aTTQ)



Compression evaluation metrics

Compression-based metrics

$$CR(\mathcal{M}_{FP}, \mathcal{M}_Q) = \frac{nbits(\mathcal{M}_Q)}{nbits(\mathcal{M}_{FP})}$$

$$CR_G(\mathcal{M}_{FP}, \mathcal{M}_Q) = 1 - CR(\mathcal{M}_{FP}, \mathcal{M}_Q)$$

Compression evaluation metrics

Compression-based metrics

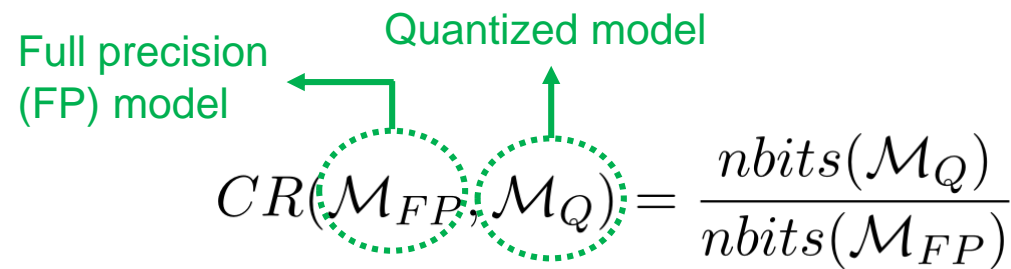
Full precision
(FP) model


$$CR(\mathcal{M}_{FP}, \mathcal{M}_Q) = \frac{nbits(\mathcal{M}_Q)}{nbits(\mathcal{M}_{FP})}$$

$$CR_G(\mathcal{M}_{FP}, \mathcal{M}_Q) = 1 - CR(\mathcal{M}_{FP}, \mathcal{M}_Q)$$

Compression evaluation metrics

Compression-based metrics


$$CR(\mathcal{M}_{FP}, \mathcal{M}_Q) = \frac{nbits(\mathcal{M}_Q)}{nbits(\mathcal{M}_{FP})}$$

$$CR_G(\mathcal{M}_{FP}, \mathcal{M}_Q) = 1 - CR(\mathcal{M}_{FP}, \mathcal{M}_Q)$$

Compression evaluation metrics

Compression-based metrics

$$CR(\mathcal{M}_{FP}, \mathcal{M}_Q) = \frac{nbits(\mathcal{M}_Q)}{nbits(\mathcal{M}_{FP})}$$

Full precision (FP) model Quantized model Function counting the number of bits necessary to store the weights (using COO sparse storage format)

$$CR_G(\mathcal{M}_{FP}, \mathcal{M}_Q) = 1 - CR(\mathcal{M}_{FP}, \mathcal{M}_Q)$$

Compression evaluation metrics

Compression-based metrics

$$CR(\mathcal{M}_{FP}, \mathcal{M}_Q) = \frac{nbits(\mathcal{M}_Q)}{nbits(\mathcal{M}_{FP})}$$

Full precision (FP) model Quantized model Function counting the number of bits necessary to store the weights (using COO sparse storage format)

$$CR_G(\mathcal{M}_{FP}, \mathcal{M}_Q) = 1 - CR(\mathcal{M}_{FP}, \mathcal{M}_Q)$$

The higher the better

Energy evaluation metrics

Energy consumption

$$EC_{Total}(\mathcal{M}) = EC_{MA}(\mathcal{M}) + EC_{DT}(\mathcal{M}) \text{ in Joules}$$

$$EC_S^{Total}(\mathcal{M}_{FP}, \mathcal{M}_Q) = \frac{|EC_{Total}(\mathcal{M}_{FP}) - EC_{Total}(\mathcal{M}_Q)|}{EC_{Total}(\mathcal{M}_{FP})}$$

Energy evaluation metrics

Energy consumption

- Energy consumption due to **Multiplications and Additions (MA)**.
- Takes into account **sparsity**

$$EC_{Total}(\mathcal{M}) = EC_{MA}(\mathcal{M}) + EC_{DT}(\mathcal{M}) \text{ in Joules}$$

$$EC_S^{Total}(\mathcal{M}_{FP}, \mathcal{M}_Q) = \frac{|EC_{Total}(\mathcal{M}_{FP}) - EC_{Total}(\mathcal{M}_Q)|}{EC_{Total}(\mathcal{M}_{FP})}$$

Energy evaluation metrics

Energy consumption

- Energy consumption due to **Multiplications and Additions (MA)**.
- Takes into account **sparsity**

$$EC_{Total}(\mathcal{M}) = EC_{MA}(\mathcal{M}) + EC_{DT}(\mathcal{M}) \text{ in Joules}$$

- Energy consumption due to **Data Transfers (DT)**
- Takes into account **sparsity AND reduced precision**

$$EC_S^{Total}(\mathcal{M}_{FP}, \mathcal{M}_Q) = \frac{|EC_{Total}(\mathcal{M}_{FP}) - EC_{Total}(\mathcal{M}_Q)|}{EC_{Total}(\mathcal{M}_{FP})}$$

Energy evaluation metrics

Energy consumption

- Energy consumption due to **Multiplications and Additions (MA)**.
- Takes into account **sparsity**

$$EC_{Total}(\mathcal{M}) = EC_{MA}(\mathcal{M}) + EC_{DT}(\mathcal{M}) \text{ in Joules}$$

- Energy consumption due to **Data Transfers (DT)**
- Takes into account **sparsity AND reduced precision**

$$EC_S^{Total}(\mathcal{M}_{FP}, \mathcal{M}_Q) = \frac{|EC_{Total}(\mathcal{M}_{FP}) - EC_{Total}(\mathcal{M}_Q)|}{EC_{Total}(\mathcal{M}_{FP})}$$

The higher the better

Outline

I. Context

- a) Medical and scientific context
- b) Emboli classification methods
- c) Challenges and objectives

II. Contribution 1 : Semi-automatic data annotation

- a) State-of-the-art
- b) Proposed method
- c) Results

III. Contribution 2 : Multi-feature medical signal classification

- a) State-of-the-art
- b) Proposed method
- c) Results

IV. Contribution 3 : Model compression based on extreme quantization

- a) State-of-the-art
- b) Proposed method
- c) Results

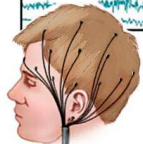
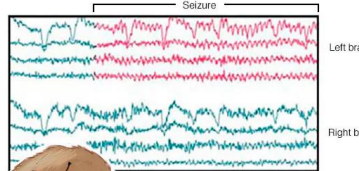
V. Conclusion and perspectives

Experiment: SOTA comparison

Objective:

- Compare **aTTQ** with other extreme quantization methods: **TTQ**.

Datasets:



HITS:

- TCD Data.
- 1 545 samples.
- Three classes.
- Sampling frequency: 4385 Hz.

ESR:

- EEG Data.
- 11 500 samples.
- Two classes.
- Sampling frequency: 174 Hz.

Metrics:

- ΔMCC , MCC drop with respect to the full precision model.
- Energy consumption gain (EC_G).
- Compression rate gain (CR_G).

Models:

- 2D CNN.
- 1D CNN-transformer.

Loss function:

- Cross entropy (CE)

Experiment: SOTA comparison

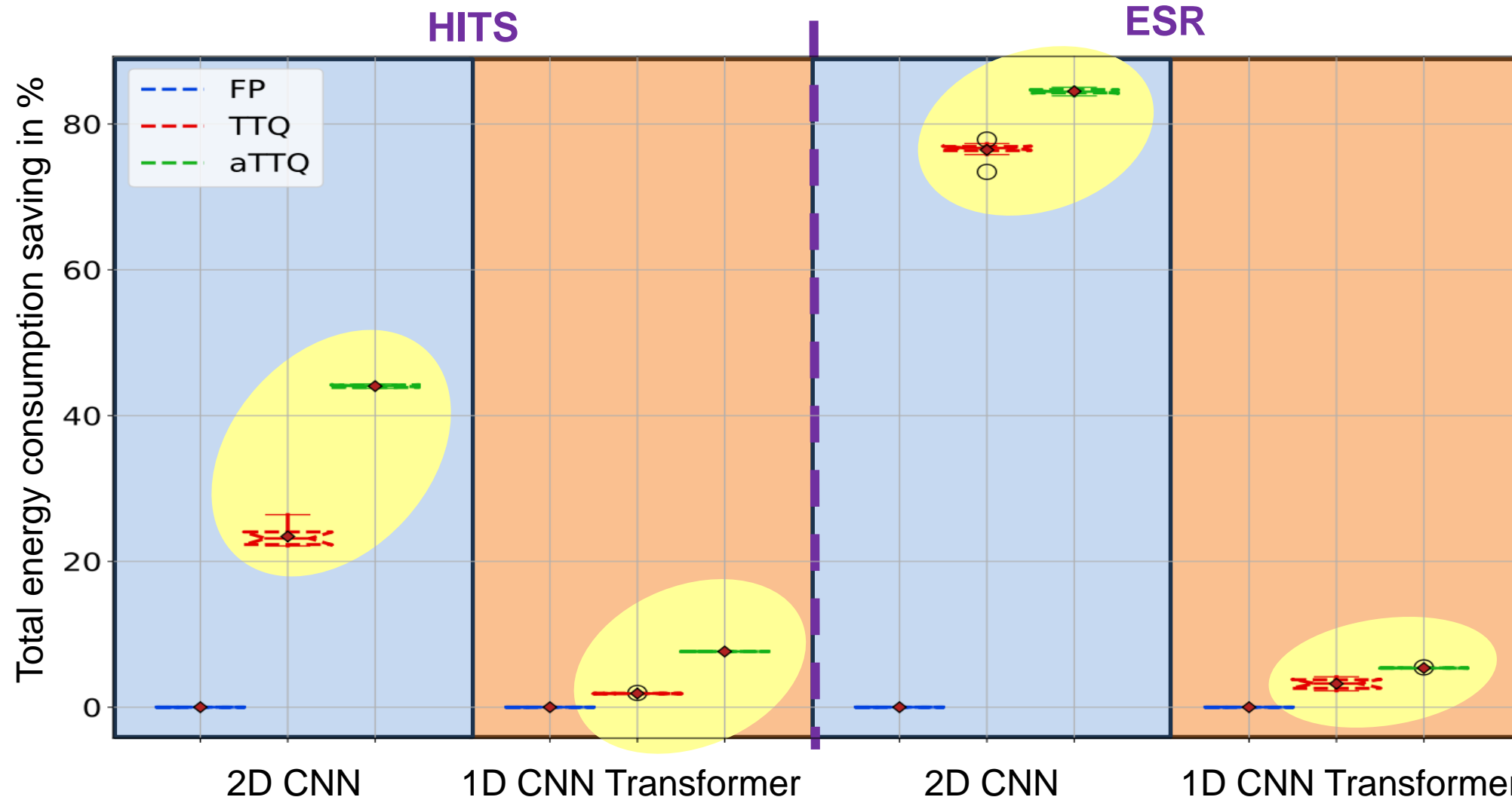


Figure – Comparison of aTTQ with FP and TTQ from the **energy** perspective

Experiment: SOTA comparison

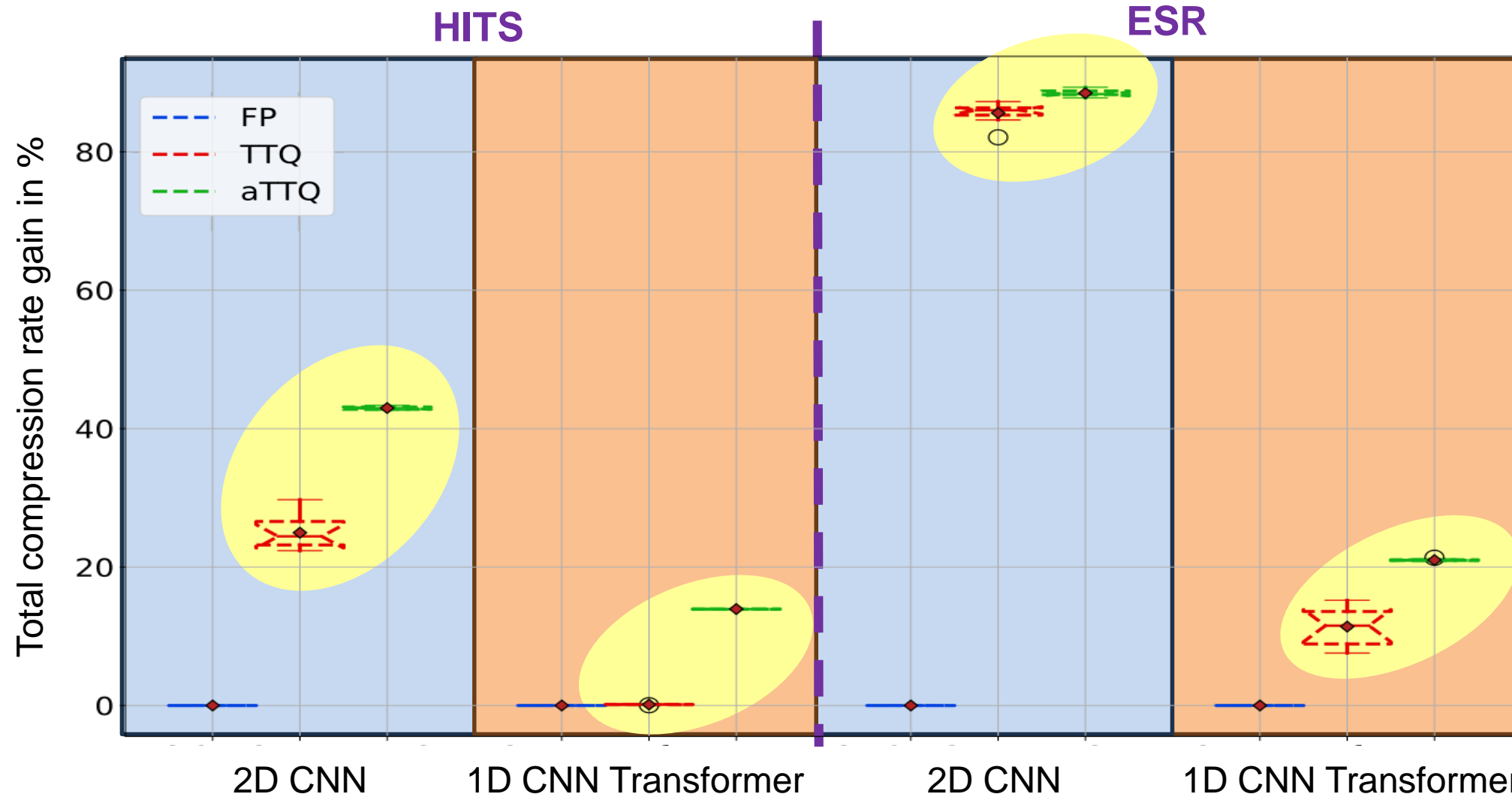


Figure – Comparison of aTTQ with FP and TTQ from the **sparsity/compression** perspective

Experiment: SOTA comparison

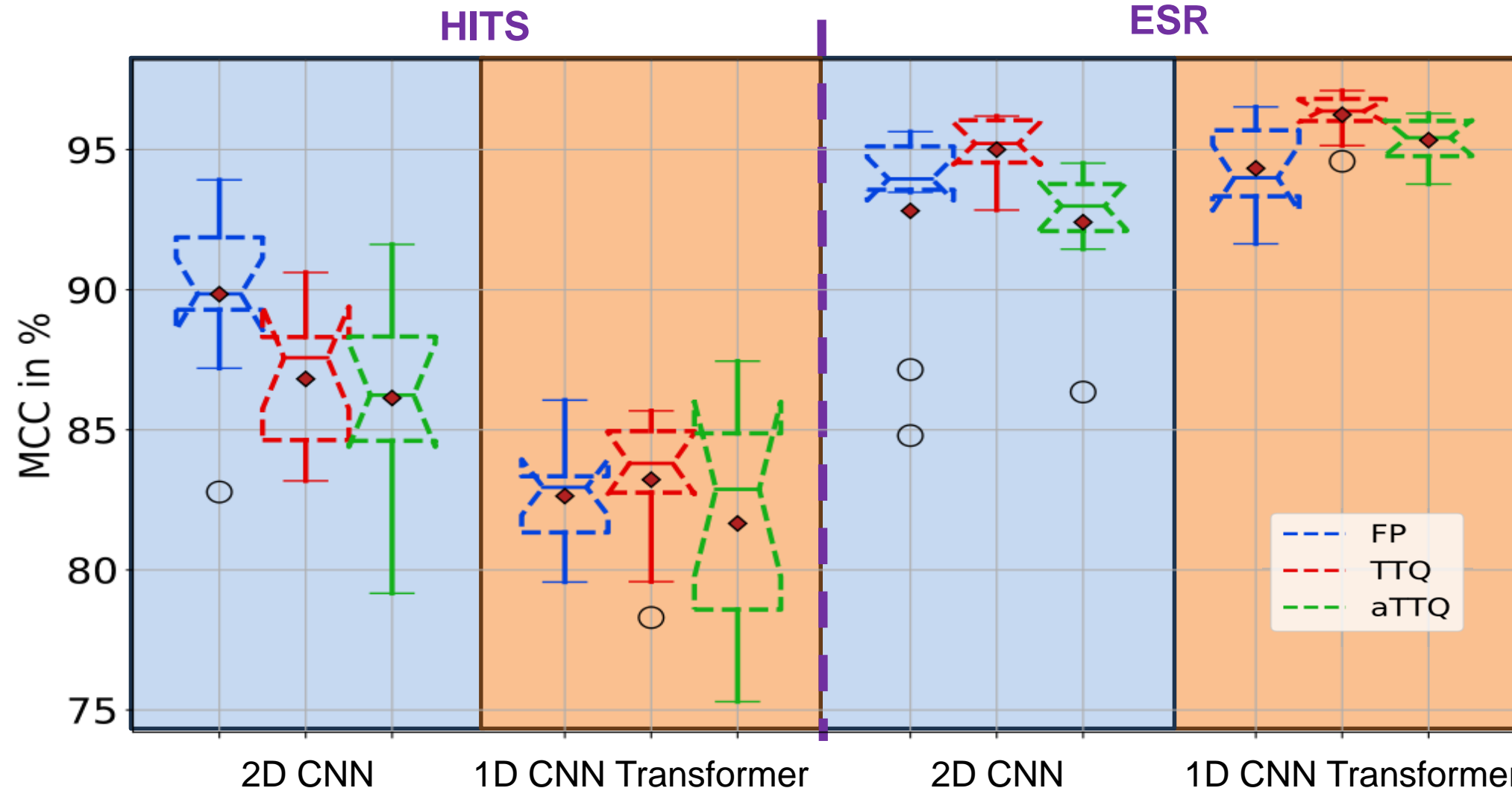


Figure – Comparison of aTTQ with FP and TTQ from the **classification** perspective

Experiment: SOTA comparison

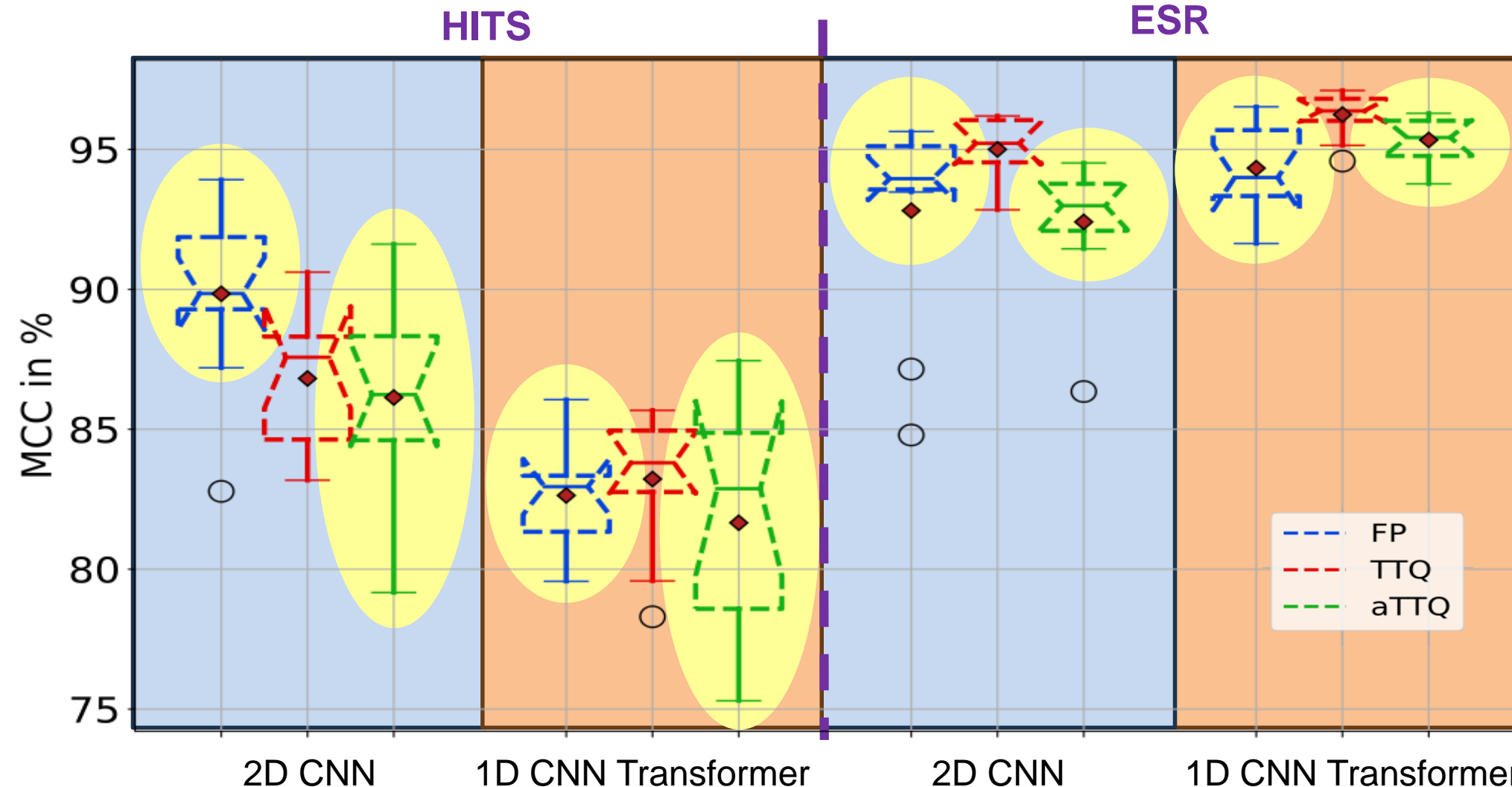


Figure – Comparison of aTTQ with FP and TTQ from the **classification** perspective

Experiment: SOTA comparison

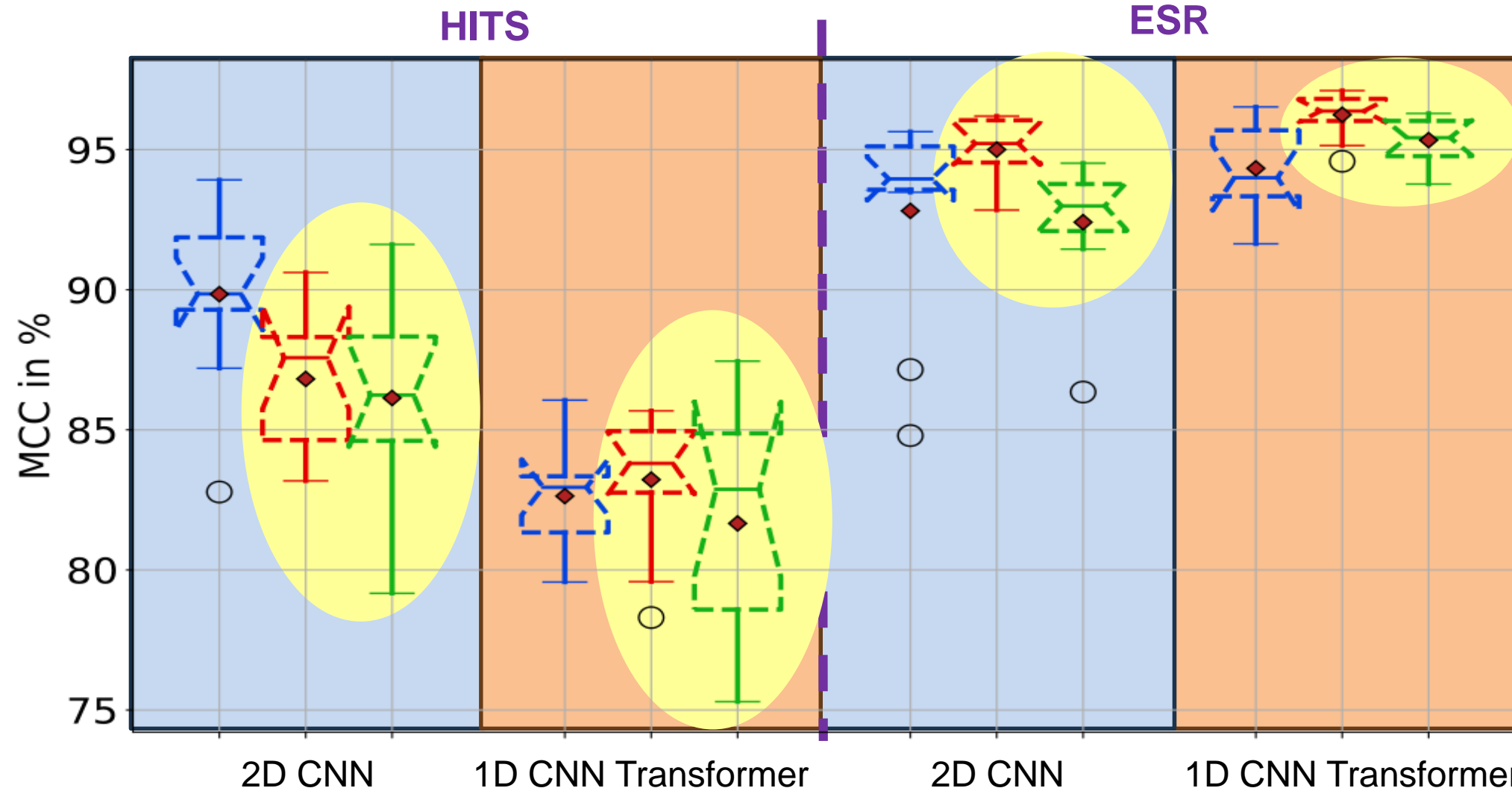


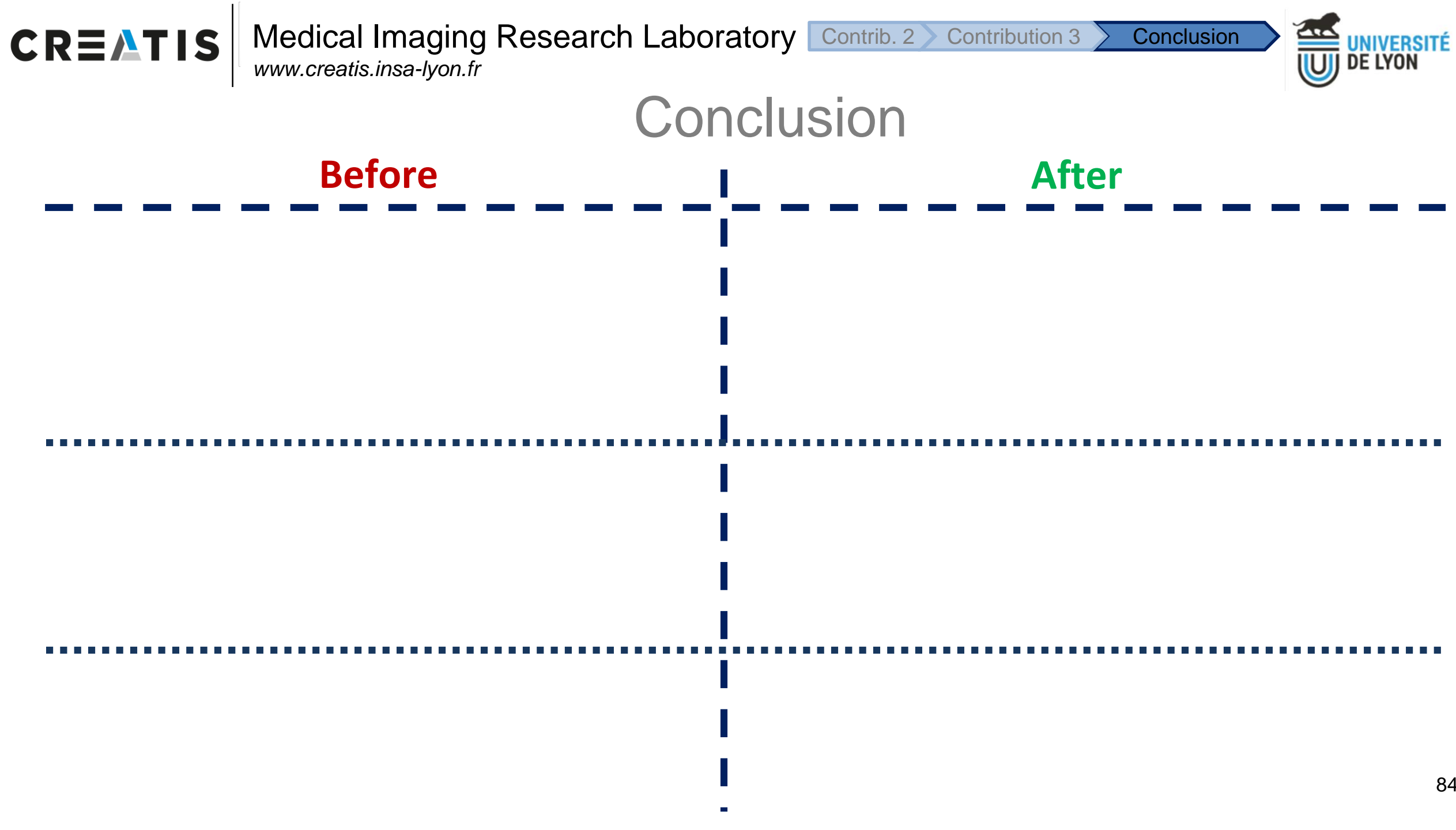
Figure – Comparison of aTTQ with FP and TTQ from the **classification** perspective

Intermediate conclusion

- **Novel ternarization method:**
 - Pruning based on the weights' statistics.
 - Parametrization to control the compression/energy/classification trade-off
- **Better compression/classification trade-off:**
 - Improvement up to 14% CR_G in terms of compression and 6% EC_G^T in terms of energy w.r.t TTQ.
 - For a degradation of only 1.6% in terms of **MCC** on the **HITS** dataset.
- **Two hyperparameters controlling this trade-off:**
 - The larger the gap:
 - The higher the compression performance.
 - The smaller the classification performance.

Outline

- I. **Context**
 - a) **Medical and scientific context**
 - b) **Emboli classification methods**
 - c) **Challenges and objectives**
- II. **Contribution 1 : Semi-automatic data annotation**
 - a) **State-of-the-art**
 - b) **Proposed method**
 - c) **Results**
- III. **Contribution 2 : Multi-feature medical signal classification**
 - a) **State-of-the-art**
 - b) **Proposed method**
 - c) **Results**
- IV. **Contribution 3 : Model compression based on extreme quantization**
 - a) **State-of-the-art**
 - b) **Proposed method**
 - c) **Results**
- V. **Conclusion and perspectives**



Conclusion

Before

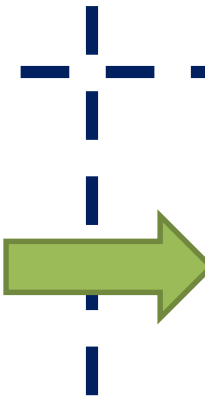
Portable TCD dataset with **2%** of
hard-labeled samples

After

Conclusion

Before

Portable TCD dataset with **2%** of
hard-labeled samples



After

- **12 % of soft-labeled samples**
- **App prototype** for semi-automatic data annotation.

Conclusion

Before

Portable TCD dataset with **2%** of
hard-labeled samples

After

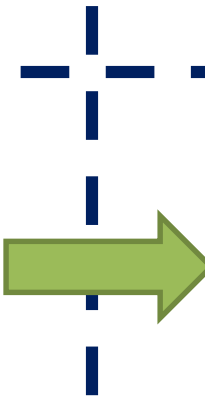
- **12 % of soft-labeled samples**
- **App prototype** for semi-automatic data annotation.

Emboli vs artifact classification
using **time-frequency**
representations

Conclusion

Before

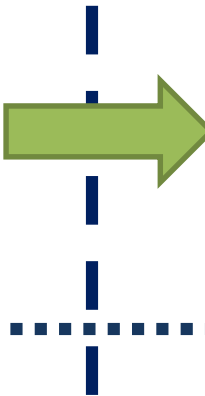
Portable TCD dataset with **2%** of
hard-labeled samples



After

- **12 % of soft-labeled samples**
- **App prototype** for semi-automatic data annotation.

Emboli vs artifact classification
using **time-frequency**
representations



- **Solid embolus vs gaseous embolus vs artifact** classification.
- Single and **multi-feature models** transferred to Atys Medical.

Conclusion

Before

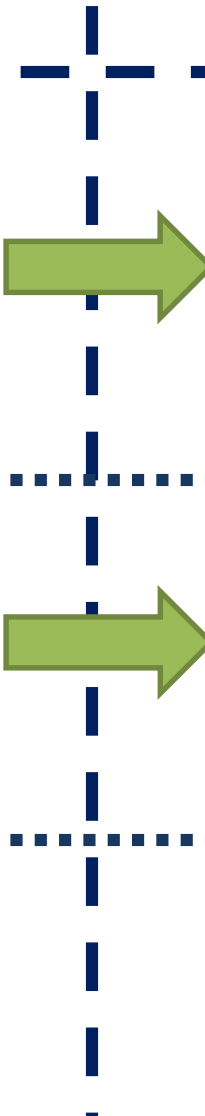
Portable TCD dataset with **2%** of
hard-labeled samples

After

- **12 % of soft-labeled samples**
- **App prototype** for semi-automatic data annotation.

Emboli vs artifact classification
using **time-frequency**
representations

Resource and energy hungry
models



- **Solid embolus vs gaseous embolus vs artifact** classification.
Single and **multi-feature models** transferred to Atys Medical.

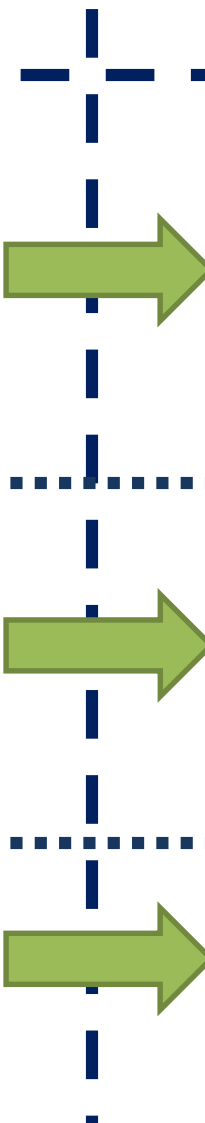
Conclusion

Before

Portable TCD dataset with **2%** of
hard-labeled samples

Emboli vs artifact classification
using **time-frequency**
representations

Resource and energy hungry
models



After

- **12 % of soft-labeled samples**
- **App prototype** for semi-automatic data annotation.

- **Solid embolus vs gaseous embolus vs artifact** classification.
Single and **multi-feature models** transferred to Atys Medical.

- **Compressed sparse and ternary single feature models.**

Perspectives

Perspectives

Dataset creation and annotation

Perspectives

Dataset creation and annotation



Active learning by proposing to human experts the most difficult samples.
Use **soft annotations** through **soft-labels loss functions*** to capture the human expert uncertainty.

Perspectives

Dataset creation and annotation



Active learning by proposing to human experts the most difficult samples.
Use **soft annotations** through **soft-labels loss functions*** to capture the human expert uncertainty.

Multiple representations

Perspectives

Dataset creation and annotation



Active learning by proposing to human experts the most difficult samples.
Use **soft annotations** through **soft-labels loss functions*** to capture the human expert uncertainty.

Multiple representations



Use **other** types of **regularization** (contrastive learning with weak supervision, link constraints, ...).

Perspectives

Dataset creation and annotation



Active learning by proposing to human experts the most difficult samples.

Use **soft annotations** through **soft-labels loss functions*** to capture the human expert uncertainty.

Multiple representations



Use **other** types of **regularization** (contrastive learning with weak supervision, link constraints, ...).

Resource hungry models

Perspectives

Dataset creation and annotation



Active learning by proposing to human experts the most difficult samples.
Use **soft annotations** through **soft-labels loss functions*** to capture the human expert uncertainty.

Multiple representations



Use **other** types of **regularization** (contrastive learning with weak supervision, link constraints, ...).

Resource hungry models



Differentiable pruning function, with asymmetric learnable parameters.

Publications

Journals:

- **Vindas, Y.**, Guépié, B.K., Almar, M., Roux, E., and Delachartre, P., 2022. Semi-automatic data annotation based on feature-space projection and local quality metrics: an application to cerebral emboli characterization, in **Medical Image Analysis**, page 102437, 2022. ISSN 1361-8415. doi: <https://doi.org/10.1016/j.media.2022.102437>.
- **Vindas, Y.**, Roux, E., Guépié, B.K., Almar, M., Delachartre, P., 2023 Guided Deep Embedded Clustering regularization for multi-feature medical signal classification, **Pattern Recognition**, page 109812, 2023. ISSN 0031-3203. <https://doi.org/10.1016/j.patcog.2023.109812>.

Conferences with proceeding:

- **Vindas, Y.**, Roux, E., Guépié, B.K., Almar, M., Delachartre, P., 2021. Semi-supervised annotation of transcranial Doppler ultrasound micro-embolic data, in: 2021 IEEE International Ultrasonics Symposium (**IUS**), pp. 1–4. doi:10.1109/IUS52206.2021.9593847.
- **Vindas, Y.**, Guépié, B.K., Almar, M., Roux, E., and Delachartre, P., 2022. An hybrid CNN-Transformer model based on multi-feature extraction and attention fusion mechanism for cerebral emboli classification, in: **MLHC**. 05–06 Aug 2022, PMLR.
- **Vindas, Y.**, Roux, E., Guépié, B.K., Almar, M., Delachartre, P., 2023 Deep Embedded Clustering regularization for imbalanced cerebral emboli classification using transcranial Doppler ultrasound, in: European Signal Processing Conference (**EUSIPCO**) 04-08 Sep 2023
- **Vindas, Y.**, Roux, E., Guépié, B.K., Almar, M., Delachartre, P., 2023. Soft-labels noise tolerant loss functions for transcranial Doppler ultrasound signal classification, in: 2023 IEEE International Ultrasonics Symposium (**IUS**)

Conferences without proceeding:

- **Vindas, Y.**, Guépié, B.K., Almar, M., Roux, E., and Delachartre, P., 2023. Classification multi-représentation d'emboles cérébraux à partir d'un dispositif de Doppler transcrânien. in:2023 Intelligence Artificielle en Imagerie Biomédicale (**IABM**).

Submitted/In Progress works:

- **Vindas, Y.**, Roux, E., Guépié, B.K., Almar, M., Delachartre, P., 2023. An asymmetric heuristic for trained ternary quantization based on the weights' statistics: an application to medical signal classification. **Submitted to Pattern Recognition Letters**.
- **Vindas, Y.**, Guépié, B.K., Almar, M., Roux, E., and Delachartre, P., 2023. Pruned trained ternary quantization. **In Progress to Information Sciences**.

Thank you for your attention

References (1/3)

- Basic identification criteria of Doppler microembolic signals. Consensus Committee of the Ninth International Cerebral Hemodynamic Symposium. *Stroke*. 1995 Jun;26(6):1123. PMID: 7762033.
- Sombune, P., Phienphanich, P., Phuechpanpaisal, S., Muengtaweepongsa, S., Ruamthanthong, A. and Tantibundhit, C. (2017). Automated embolic signal detection using deep convolutional neural network, 2017 39th Annual International Conference of the IEEE Engineering in Medicine and Biology Society (EMBC), IEEE, pp. 3365–3368.
- Guepie, B., Martin, M., Lacrozaz, V., Almar, M., Guibert, B. and Delachartre, P. (2018). Sequential emboli detection from ultrasound outpatient data, *IEEE Journal of Biomedical and Health Informatics*.
- Georgiadis, D., Grosset, D. G., Kelman, A., Faichney, A. and Lees, K. R. (1994). Prevalence and characteristics of intracranial microemboli signals in patients with different types of prosthetic cardiac valves., *Stroke* 25(3): 587–592.
- Aydin, N., & Markus, H. S. (2000). Optimization of processing parameters for the analysis and detection of embolic signals. *European journal of ultrasound : official journal of the European Federation of Societies for Ultrasound in Medicine and Biology*, 12(1), 69–79.
- N. Aydin, F. Marvasti and H. S. Markus, "Embolic Doppler ultrasound signal detection using discrete wavelet transform," in *IEEE Transactions on Information Technology in Biomedicine*, vol. 8, no. 2, pp. 182-190, June 2004.
- Marvasti, S., Gillies, D., Marvasti, F., & Markus, H. S. (2004). Online automated detection of cerebral embolic signals using a wavelet-based system. *Ultrasound in medicine & biology*, 30(5), 647–653.
- Markus, H. S. and Punter, M. (2005). Can Transcranial Doppler Discriminate Between Solid and Gaseous Microemboli?: Assessment of a Dual-Frequency Transducer System, *Stroke* 36(8): 1731–1734.
- Chung, E., Fan, L., Degg, C., & Evans, D. H. (2005). Detection of Doppler embolic signals: psychoacoustic considerations. *Ultrasound in medicine & biology*, 31(9), 1177–1184.
- Gencer, M., Bilgin, G., & Aydin, N. (2013). Embolic Doppler ultrasound signal detection via fractional Fourier transform. *Annual International Conference of the IEEE Engineering in Medicine and Biology Society. IEEE Engineering in Medicine and Biology Society. Annual International Conference*, 2013, 3050–3053.
- Serbes, G. and Aydin, N. (2014). Denoising performance of modified dual-tree complex wavelet transform for processing quadrature embolic doppler signals, *Medical & Biological Engineering & Computing* 52(1): 29–43.
- Karahoca, A. and Tunga, M. A. (2015). A polynomial based algorithm for detection of embolism, 19(1): 167–177.
- Imdaduddin, S. M., LaRovere, K. L., Kussman, B. D. and Heldt, T. (2019). A time-frequency approach for cerebral embolic load monitoring, *IEEE Transactions on Biomedical Engineering* 67(4): 1007–1018.
- Darbellay GA, Duff R, Vesin J-M, et al. Solid or Gaseous Circulating Brain Emboli: Are They Separable by Transcranial Ultrasound? *Journal of Cerebral Blood Flow & Metabolism*. 2004;24(8):860-868.
- Keunen, R. W. M., Hoogenboezem, R., Wijnands, R., Van den Hengel, A. C. M. and Ackerstaff, R. G. A. (2008). Introduction of an embolus detection system based on analysis of the transcranial Doppler audio-signal, *Journal of Medical Engineering & Technology* 32(4): 296–304.
- A. Karahoca, T. Kucur and N. Aydin, "Data Mining Usage in Emboli Detection," 2007 ECSIS Symposium on Bio-inspired, Learning, and Intelligent Systems for Security (BLISS 2007), Edinburgh, UK, 2007, pp. 159-162.
- Guépié, B. K., Sciolla, B., Millioz, F., Almar, M. and Delachartre, P. (2017). Discrimination between emboli and artifacts for outpatient transcranial doppler ultrasound data, *Medical & Biological Engineering & Computing* 55(10): 1787–1797. Number: 10.
- Chen, Yijiao & Yuanyuan, Wang. (2008). Doppler embolic signal detection using the adaptive wavelet packet basis and neurofuzzy classification. *Pattern Recognition Letters*.
- Sombune, P., Phienphanich, P., Muengtaweepongsa, S., Ruamthanthong, A. and Tantibundhit, C. (2016). Automated embolic signal detection using adaptive gain control and classification using anfis, 2016 38th Annual International Conference of the IEEE Engineering in Medicine and Biology Society (EMBC), pp. 3825–3828.
- Tafasast, A., Ferroudji, K., Hadjili, M. L., Bouakaz, A. and Benoudjit, N. (2018). Automatic microemboli characterization using convolutional neural networks and radio frequency signals, 2018 International Conference on Communications and Electrical Engineering (ICCEE), IEEE, pp. 1–4.
- Benato, B. C., Gomes, J. F., Telea, A. C. and Falcão, A. X. (2021). Semi-automatic data annotation guided by feature space projection, *Pattern Recognition* 109: 107612.
- Lueks, W., Mokbel, B., Biehl, M. and Hammer, B. (2011). How to evaluate dimensionality reduction? - improving the co-ranking matrix, arXiv:1110.3917 [cs].
- Zhilu Zhang, Mert R. Sabuncu: Generalized Cross Entropy Loss for Training Deep Neural Networks with Noisy Labels. *NeurIPS* 2018: 8792-8802.
- Olivier Chapelle, Bernhard Schölkopf, and Alexander Zien, eds. *Semi-supervised learning*. Adaptive computation and machine learning. OCLC: ocm64898359. Cambridge, Mass: MIT Press, 2006. 508 pp. isbn: 978-0-262-03358-9.
- Amorim, W. P., Falcão, A. and Carvalho, M. H. (2014). Semi-supervised pattern classification using optimum-path forest, 2014 27th SIBGRAPI Conference on Graphics, Patterns and Images pp. 111–118.
- Melacci, Stefano & Belkin, Mikhail. (2009). Laplacian Support Vector Machines Trained in the Primal. *Journal of Machine Learning Research*.
- Pu, J., Panagakis, Y. and Pantic, M. (2021). Learning separable time-frequency filterbanks for audio classification, *ICASSP 2021 - 2021 IEEE International Conference on Acoustics, Speech and Signal Processing (ICASSP)*, pp. 3000–3004.
- Lee, J., Park, J., Kim, K. and Nam, J. (2017). Sample-level deep convolutional neural networks for music auto-tagging using raw waveforms, 14th Sound Music Computing Conference.
- Park, H. and Yoo, C. D. (2020). Cnn-based learnable gammatone filterbank and equal-loudness normalization for environmental sound classification, *IEEE Signal Processing Letters* 27: 411– 415.
- Sharan, R., Xiong, H. and Berkovsky, S. (2021). Benchmarking audio signal representation techniques for classification with convolutional neural networks, *Sensors* 21: 3434.
- Yeh, C.-F., Mahadeokar, J., Kalgaonkar, K., Wang, Y., Le, D., Jain, M., Schubert, K., Fuegen, C. and Seltzer, M. L. (2019). Transformer-transducer: End-to-end speech recognition with self-attention, ArXiv abs/1910.12977.
- Natarajan, A., Chang, Y., Mariani, S., Rahman, A., Boerman, G., Vij, S. and Rubin, J. (2020). A wide and deep transformer neural network for 12-lead ecg classification, 2020 Computing in Cardiology, pp. 1–4. xiii.
- Okawa, M., Saito, T., Sawada, N. and Nishizaki, H. (2019). Audio classification of bit- representation waveform, *INTERSPEECH*, pp. 2553–2557.
- Nishizaki, H. and Makino, K. (2019). Signal classification using deep learning, pp. 1–4.
- Karita, S., Wang, X., Watanabe, S., Yoshimura, T., Zhang, W., Chen, N., Hayashi, T., Hori, T., Inaguma, H., Jiang, Z., Someki, M., Soplin, N. and Yamamoto, R. (2019). A comparative study on transformer vs RNN in speech applications, 2019 IEEE Automatic Speech Recognition and Understanding Workshop.
- Boes, W. and Van hamme, H. (2019). Audiovisual transformer architectures for large-scale classification and synchronization of weakly labeled audio events, *Proceedings of the 27th ACM International Conference on Multimedia, MM '19*, Association for Computing Machinery, New York, NY, USA, p. 1961–1969.
- Mohamed, Abdelrahman & Okhonko, Dmytro & Zettlemoyer, Luke. (2019). Transformers with convolutional context for ASR.
- kbari, H., Yuan, L., Qian, R., Chuang, W.-H., Chang, S.-F., Cui, Y. and Gong, B. (2021). Vatt: Transformers for multimodal self-supervised learning from raw video, audio and text, *Advances in Neural Information Processing Systems* 34. 50, 54.
- Ding, Y., Jia, M., Miao, Q. and Cao, Y. (2022). A novel time–frequency transformer based on self–attention mechanism and its application in fault diagnosis of rolling bearings, *Mechanical Systems and Signal Processing* 168: 108616.

References (1/3)

- Che, C., Zhang, P., Zhu, M., Qu, Y. and Jin, B. (2021). Constrained transformer network for ecg signal processing and arrhythmia classification, *BMC Medical Informatics and Decision Making* 21.
- Gong, Y., Chung, Y.-A. and Glass, J. (2021). AST: Audio Spectrogram Transformer, *Proc. Interspeech 2021*, pp. 571–575.
- Xie, J., Girshick, R. and Farhadi, A. (2016). Unsupervised deep embedding for clustering analysis, *Proceedings of the 33rd International Conference on International Conference on Machine Learning - Volume 48*, ICML'16, JMLR.org, p. 478–487.
- Zhu, Y. and Jiang, Y. (2020). Optimization of face recognition algorithm based on deep learning multi feature fusion driven by big data, *Image and Vision Computing* 104: 104023.
- Ahmad, Z., Tabassum, A., Guan, L. and Khan, N. M. (2021). Ecg heartbeat classification using multimodal fusion, *IEEE Access*.
- Yao, T., Gao, F., Zhang, Q. and Ma, Y. (2021). Multi-feature gait recognition with dnn based on semg signals, *Mathematical Biosciences and Engineering* 18: 3521–3542.
- Wang, L., Zhang, J., Liu, P., Choo, K.-K. R. and Huang, F. (2017). Spectral–spatial multi-feature- based deep learning for hyperspectral remote sensing image classification, *Soft Computing* 21.
- Feng, X., Feng, Q., Li, S., Hou, X. and Liu, S. (2020). A deep-learning-based oil-well-testing stage interpretation model integrating multi-feature extraction methods, *Energies* 13(8).
- Kim, J.-G. and Lee, B. (2019). Appliance classification by power signal analysis based on multi- feature combination multi-layer lstm, *Energies* 12(14).
- Chen, X., Cheng, Z., Wang, S., Lu, G., Xv, G., Liu, Q. and Zhu, X. (2021). Atrial fibrillation detection based on multi- feature extraction and convolutional neural network for processing ecg signals, *Computer Methods and Programs in Biomedicine* 202: 106009.
- Abdi, Asad & Shamsuddin, Siti Mariyam & Piran, Jalil. (2019). Deep learning-based sentiment classification of evaluative text based on Multi-feature fusion. *Information Processing & Management*. 56. 1245-1259.
- Tongxue Zhou, Su Ruan, Pierre Vera, Stéphane Canu, “A Tri-attention Fusion Guided Multi-modal Segmentation Network Pattern Recognition”, Elsevier, *Pattern Recognition*, Volume 124, 108417, April 2022.
- Tongxue Zhou, Stéphane Canu, Su Ruan, “Fusion based on attention mechanism and context constrain for multi-modal brain tumor segmentation”, Elsevier, *Computerized Medical Imaging and Graphics*, Volume 86, 101811. December 2020.
- Mao, S., Li, Y., Ma, Y., Zhang, B., Zhou, J. and Wang, K. (2020). Automatic cucumber recognition algorithm for harvesting robots in the natural environment using deep learning and multi- feature fusion, *Computers and Electronics in Agriculture* 170.
- Tiong, L., Kim, S. T. and Ro, Y. (2019). Implementation of multimodal biometric recognition via multi-feature deep learning networks and feature fusion, *Multimedia Tools and Applications* 78.
- Liu, Z.-M. (2021). Multi-feature fusion for specific emitter identification via deep ensemble learning, *Digital Signal Processing* 110: 102939.
- Jin, J., Yang, S., Zhao, B., Luo, L. and Woo, W. L. (2020). Attention-block deep learning based features fusion in wearable social sensor for mental wellbeing evaluations, *IEEE Access* 8: 1–1.
- Horowitz, M. (2014). 1.1 computing's energy problem (and what we can do about it), 2014 IEEE International Solid-State Circuits Conference Digest of Technical Papers (ISSCC), pp. 10–14.
- Molka, D., Hackenberg, D., Schöne, R. and Müller, M. S. (2010). Characterizing the energy consumption of data transfers and arithmetic operations on x8664 processors, *International Conference on Green Computing*, pp. 123–133.
- Gong, Y., Liu, L., Yang, M. and Bourdev, L. D. (2014). Compressing deep convolutional networks using vector quantization.
- Kim, Hyeji & Khan, Muhammad Umar Karim & Kyung, Chong-Min. (2019). Efficient Neural Network Compression.
- Lan, Z., Chen, M., Goodman, S., Gimpel, K., Sharma, P. and Soricut, R. (2020). ALBERT: A lite BERT for self-supervised learning of language representations, 8th International Conference on Learning Representations, ICLR 2020, Addis Ababa, Ethiopia, April 26-30, 2020.
- Zhang, D., Yang, J., Ye, D. and Hua, G. (2018). Lq-nets: Learned quantization for highly accurate and compact deep neural networks, *Computer Vision – ECCV 2018: 15th European Conference*, Munich, Germany, September 8-14, 2018, *Proceedings, Part VIII*, Springer-Verlag, Berlin, Heidelberg, p. 373–390.
- Yang, J., Shen, X., Xing, J., Tian, X., Li, H., Deng, B., Huang, J. and Hua, X.-s. (2019). Quantization networks, *Proceedings of the IEEE/CVF Conference on Computer Vision and Pattern Recognition*.
- Rastegari, M., Ordonez, V., Redmon, J. and Farhadi, A. (2016). Xnor-net: Imagenet classification using binary convolutional neural networks, in B. Leibe, J. Matas, N. Sebe and M. Welling (eds), *Computer Vision – ECCV 2016*, Springer International Publishing, Cham, pp. 525–542.
- Prato, G., Charlaix, E. and Rezagholizadeh, M. (2020). Fully quantized transformer for machine translation, *Findings of the Association for Computational Linguistics: EMNLP 2020*, Association for Computational Linguistics, Online, pp. 1–14.
- Zhu, C., Han, S., Mao, H. and Dally, W. J. (2017). Trained ternary quantization, *International Conference on Learning Representations*.
- Bhagat, Y., Lee, J., Nagel, M., Blankevoort, T. and Kwak, N. (2020). Lsq+: Improving low-bit quantization through learnable offsets and better initialization, *Proceedings of the IEEE/CVF Conference on Computer Vision and Pattern Recognition (CVPR) Workshops*.
- Dong, Z., Yao, Z., Arfeen, D., Gholami, A., Mahoney, M. W. and Keutzer, K. (2020). Hawq-v2: Hessian aware trace-weighted quantization of neural networks, in H. Larochelle, M. Ranzato, R. Hadsell, M. Balcan and H. Lin (eds), *Advances in Neural Information Processing Systems*, Vol. 33, Curran Associates, Inc., pp. 18518–18529.
- Xu, Y., Wang, Y., Zhou, A., Lin, W. and Xiong, H. (2018). Deep neural network compression with single and multiple level quantization, *Proceedings of the AAAI Symposium on Educational Advances in Artificial Intelligence, AAAI'18*, AAAI Press.
- Jacob, B., Kligys, S., Chen, B., Zhu, M., Tang, M., Howard, A., Adam, H. and Kalenichenko, D. (2018). Quantization and training of neural networks for efficient integer-arithmetic-only inference, *Proceedings of the IEEE Conference on Computer Vision and Pattern Recognition (CVPR)*.
- Kim, S., Gholami, A., Yao, Z., Mahoney, M. W. and Keutzer, K. (2021). I-bert: Integer-only bert quantization, *International Conference on Machine Learning*.
- Zhou, S., Ni, Z., Zhou, X., Wen, H., Wu, Y. and Zou, Y. (2016). Dorefa-net: Training low bitwidth convolutional neural networks with low bitwidth gradients, *CoRR abs/1606.06160*.
- Han, S., Mao, H. and Dally, W. J. (2016). Deep compression: Compressing deep neural network with pruning, trained quantization and huffman coding, in Y. Bengio and Y. LeCun (eds), *4th International Conference on Learning Representations*, ICLR 2016, San Juan, Puerto Rico.
- Li, F. and Liu, B. (2016). Ternary weight networks, *ArXiv abs/1605.04711*.
- Park, M. S., Xu, X. and Brick, C. (2018). Squantizer: Simultaneous learning for both sparse and low-precision neural networks, *CoRR abs/1812.08301*.
- Ullrich, K., Meeds, E. and Welling, M. (2017). Soft weight-sharing for neural network compression, *International Conference on Learning Representations*.
- Tung, F. and Mori, G. (2020). Deep neural network compression by in-parallel pruning- quantization, *IEEE Transactions on Pattern Analysis and Machine Intelligence* 42(3): 568–579.
- Ji, T., Jain, S., Ferdman, M., Milder, P., Schwartz, H. A. and Balasubramanian, N. (2021). On the distribution, sparsity, and inference-time quantization of attention values in transformers, *ArXiv abs/2106.01335*.

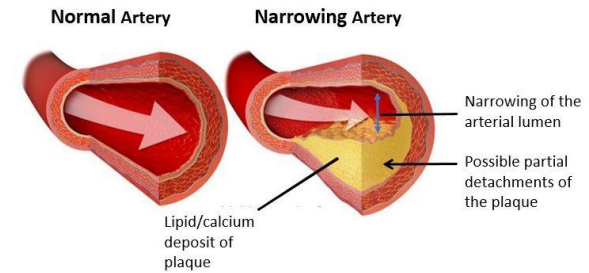
References (1/3)

- Hoefer, T., Alistarh, D., Ben-Nun, T., Dryden, N. and Peste, A. (2022). Sparsity in deep learning: Pruning and growth for efficient inference and training in neural networks, *J. Mach. Learn.*
- Han, S., Pool, J., Tran, J. and Dally, W. (2015). Learning both weights and connections for efficient neural network, *Advances in neural information processing systems* 28.
- Hassibi, B., Stork, D. and Wolff, G. (1993). Optimal brain surgeon and general network pruning, *IEEE International Conference on Neural Networks*, pp. 293–299 vol.1.
- Mariet, Z. and Sra, S. (2016). Diversity networks: Neural network compression using determinantal point processes, *International Conference on Learning Representations (ICLR)*.
- Zhu, M. and Gupta, S. (2018). To prune, or not to prune: Exploring the efficacy of pruning for model compression, *6th International Conference on Learning Representations, ICLR 2018*.
- Manessi, F., Rozza, A., Bianco, S., Napoletano, P. and Schettini, R. (2017). Automated pruning for deep neural network compression.
- Luo, J.-H., Wu, J. and Lin, W. (2017). Thinet: A filter level pruning method for deep neural network compression, pp. 5068–5076.
- He, Y., Lin, J., Liu, Z., Wang, H., Li, L.-J. and Han, S. (2018). Amc: Automl for model compression and acceleration on mobile devices, in V. Ferrari, M. Hebert, C. Sminchisescu and Y. Weiss (eds), *Computer Vision – ECCV 2018*, Springer International Publishing, Cham, pp. 815–832.
- Xu, K., Zhang, D., An, J., Liu, L., Liu, L. and Wang, D. (2021). Genexp: Multi-objective pruning for deep neural network based on genetic algorithm, *Neurocomputing* 451: 81–94.
- Bai, H., Zhang, W., Hou, L., Shang, L., Jin, J., Jiang, X., Liu, Q., Lyu, M. and King, I. (2021). BinaryBERT: Pushing the limit of BERT quantization, *Proceedings of the 59th Annual Meeting of the Association for Computational Linguistics and the 11th International Joint Conference on Natural Language Processing (Volume 1: Long Papers)*, Association for Computational Linguistics, Online, pp. 4334–4348.
- Sun, S., Cheng, Y., Gan, Z. and Liu, J. (2019). Patient knowledge distillation for bert model compression, *Conference on Empirical Methods in Natural Language Processing*.
- Zhang, W., Hou, L., Yin, Y., Shang, L., Chen, X., Jiang, X. and Liu, Q. (2020). Ternarybert: Distillation-aware ultra-low bit bert, *Conference on Empirical Methods in Natural Language Processing*.
- Polino, A., Pascanu, R. and Alistarh, D. (2018). Model compression via distillation and quantization, *ArXiv e-prints* .
- Kanjilal, P., Dey, P. and Banerjee, D. (1993). Reduced-size neural networks through singular value decomposition and subset selection, *Electronics Letters* 29: 1516–1518.
- Yao, Z., Dong, Z., Zheng, Z., Gholami, A., Yu, J., Tan, E., Wang, L., Huang, Q., Wang, Y., Mahoney, M. and Keutzer, K. (2021). Hawq-v3: Dyadic neural network quantization, in M. Meila and T. Zhang (eds), *Proceedings of the 38th International Conference on Machine Learning, Vol. 139 of Proceedings of Machine Learning Research*, PMLR, pp. 11875–11886.
- Hinton, G. E., Vinyals, O. and Dean, J. (2015). Distilling the knowledge in a neural network, *ArXiv abs/1503.02531*.
- Bosio, A., O'Connor, I., Traiola, M., Echavarria, J., Teich, J., Hanif, M. A., Shafique, M., Hamdioui, S., Deveautour, B., Girard, P., Virazel, A. and Bertels, K. (2021). Emerging computing devices: Challenges and opportunities for test and reliability , *26th IEEE European Test Symposium, ETS 2021, Bruges, Belgium, May 24-28, 2021*, IEEE, pp. 1–10.
- Yu, F. and Koltun, V. (2016). Multi-scale context aggregation by dilated convolutions, in Y. Bengio and Y. LeCun (eds), *4th International Conference on Learning Representations, ICLR*.
- Howard, A., Zhu, M., Chen, B., Kalenichenko, D., Wang, W., Weyand, T., Andreetto, M. and Adam, H. (2017). Mobilenets: Efficient convolutional neural networks for mobile vision applications.
- He, K., Zhang, X., Ren, S. and Sun, J. (2016). Deep residual learning for image recognition, *2016 IEEE Conference on Computer Vision and Pattern Recognition (CVPR)*, pp. 770–778.
- Gao, K., Zhang, Q. and Wang, H. (2019). A lightweight residual-inception convolutional neural network, *Journal of Physics: Conference Series* 1237: 032058.
- Elsken, T., Metzen, J. H. and Hutter, F. (2019). Neural architecture search: A survey, *J. Mach. Learn. Res.* 20(1): 1997–2017.

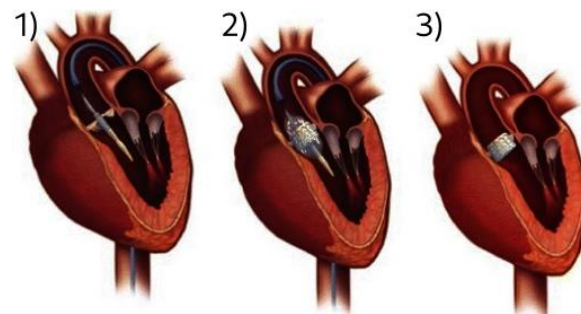
Backslides

Context

WHY ?

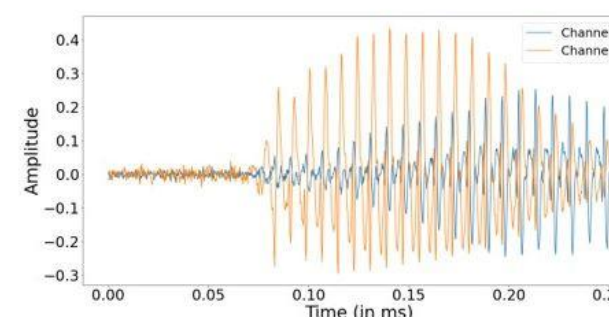
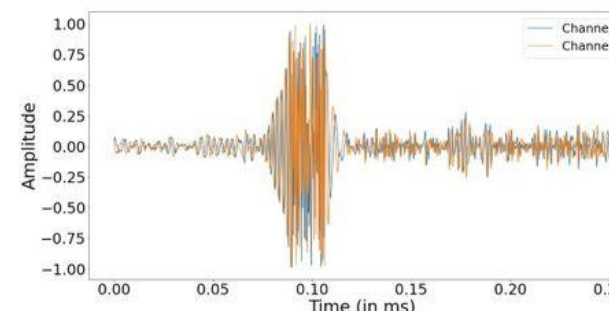
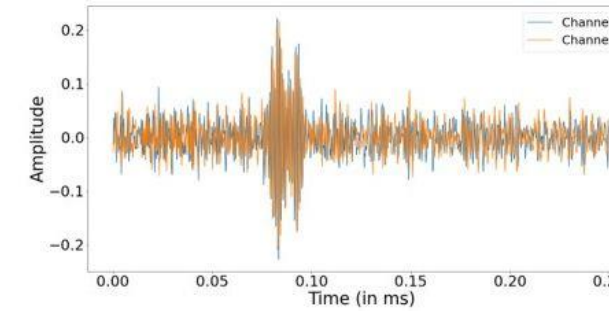
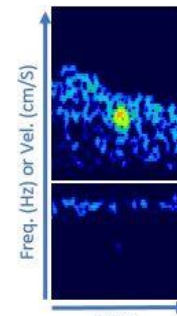


Atherosclerosis

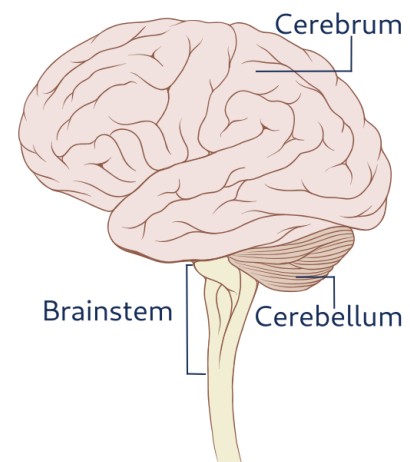


Transcatheter aortic valve replacement

Different Sources

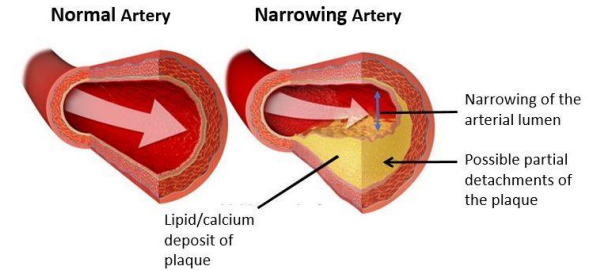


Different Types

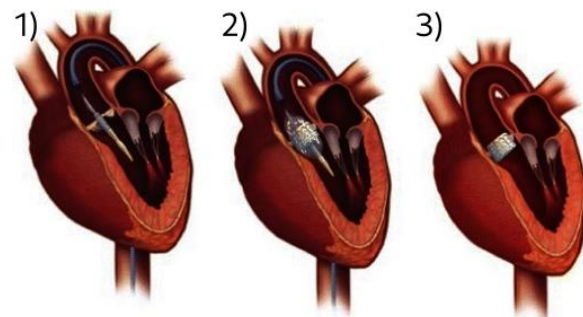


Different Consequences

WHY ?

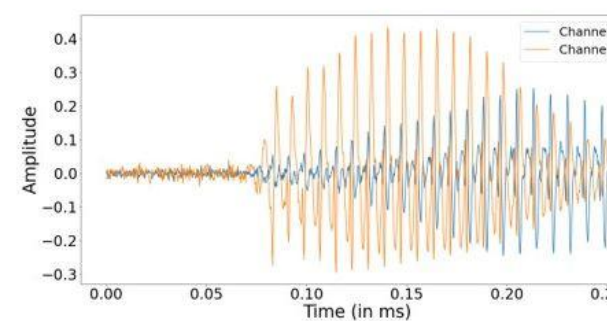
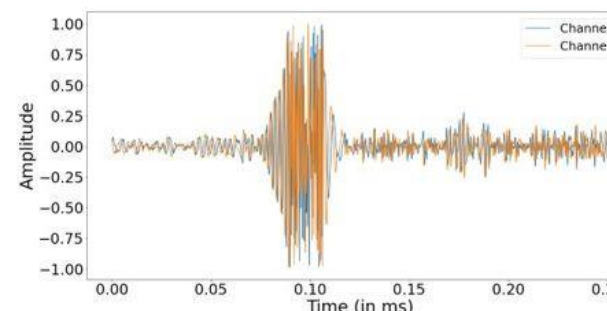
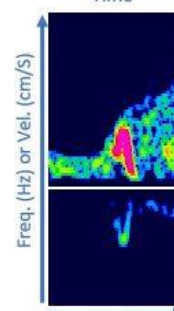
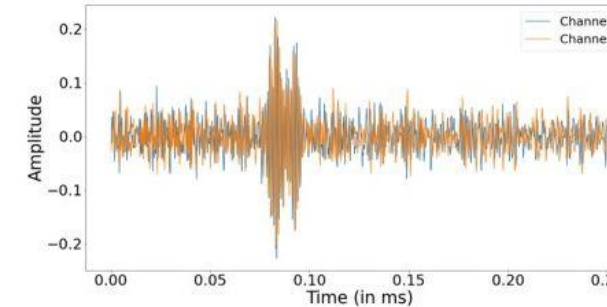
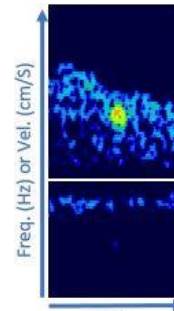


Atherosclerosis

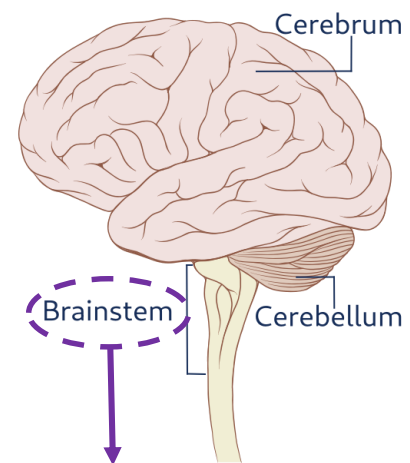


Transcatheter aortic valve replacement

Different Sources



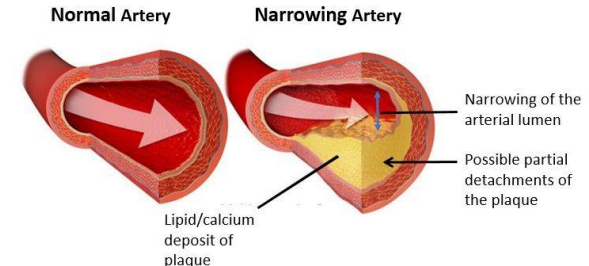
Different Types



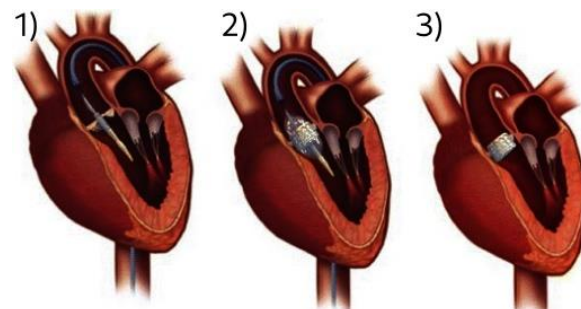
- Temperature regulation.
- Heart rate and blood pressure.
- Vision.
- Balance and coordination.
- Swallowing.
- Coma or death.

Different Consequences

WHY ?

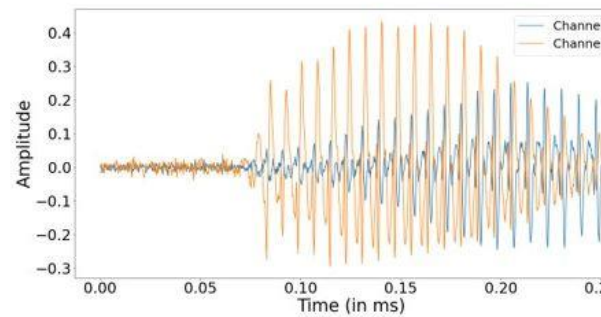
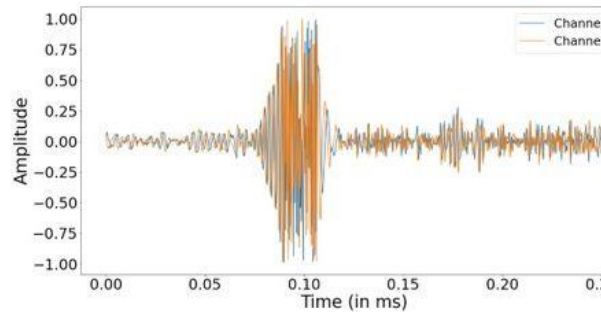
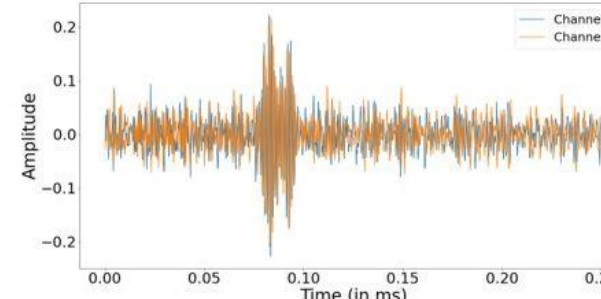
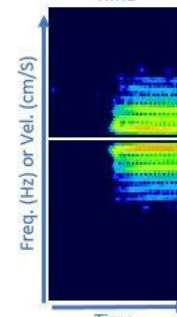
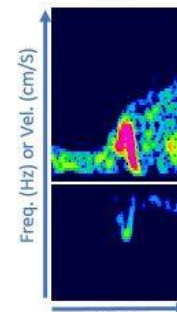
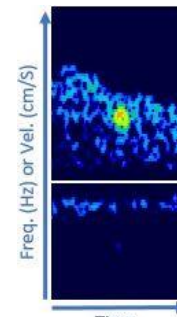


Atherosclerosis

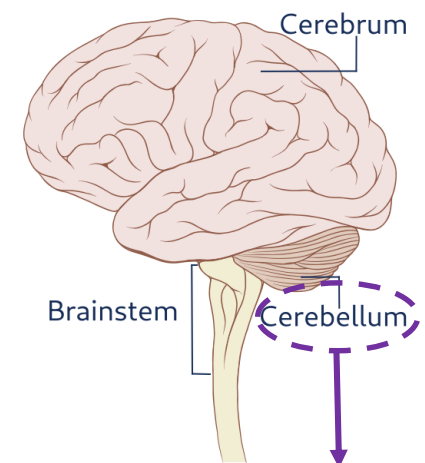


Transcatheter aortic valve replacement

Different Sources



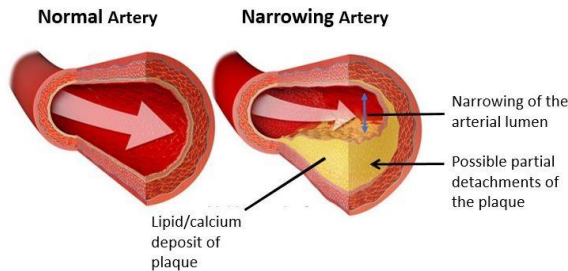
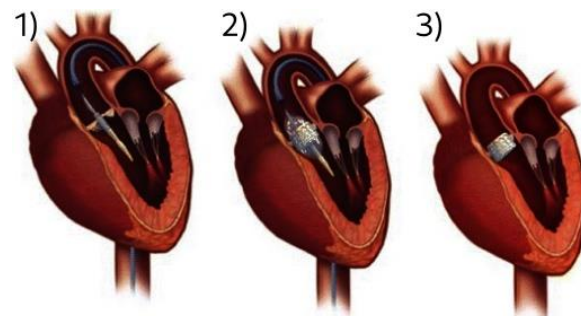
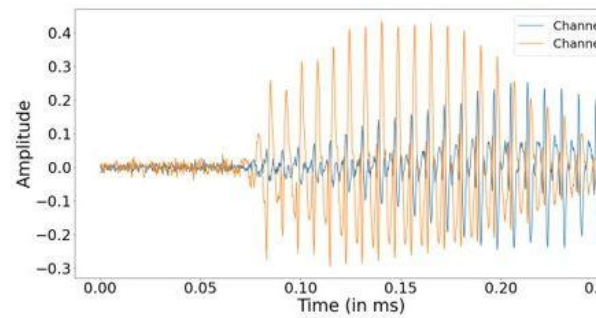
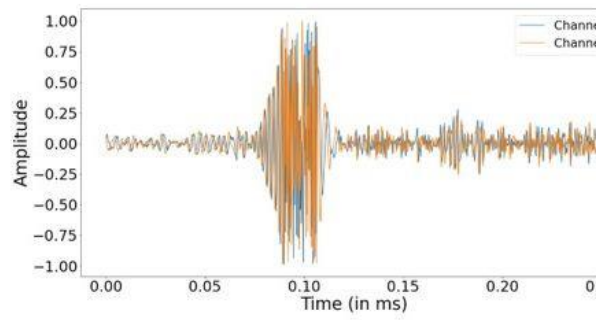
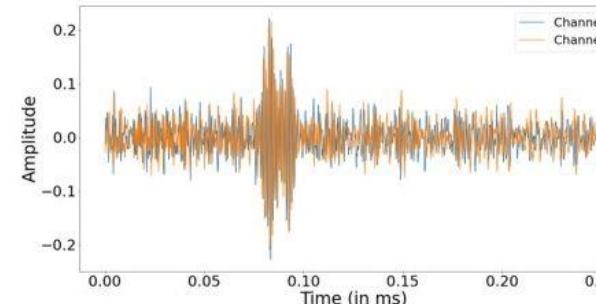
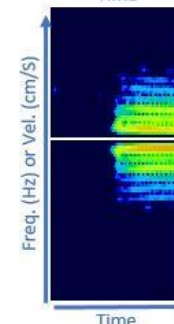
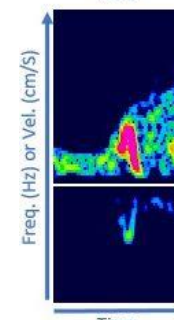
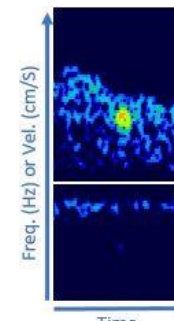
Different Types



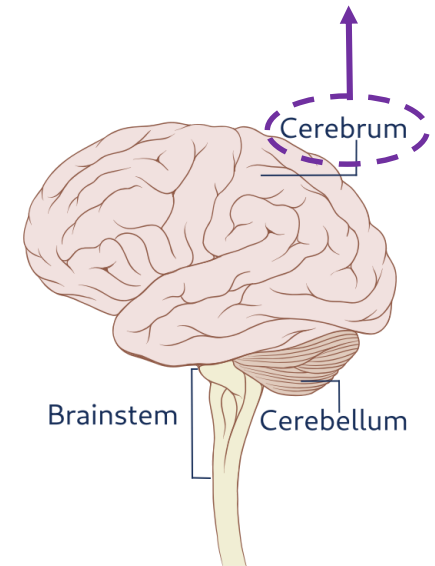
- Balance and posture.
- Muscle movements.
- Headache.
- Nausea.

Different Consequences

WHY ?

**Atherosclerosis****Transcatheter aortic valve replacement****Different Sources****Different Types**

- Memory.
- Reasoning.
- Paralysis.
- Vision and speech.
- Behavior.

**Different Consequences**

Time-frequency representations

Signal $S_c = I + i \times Q$



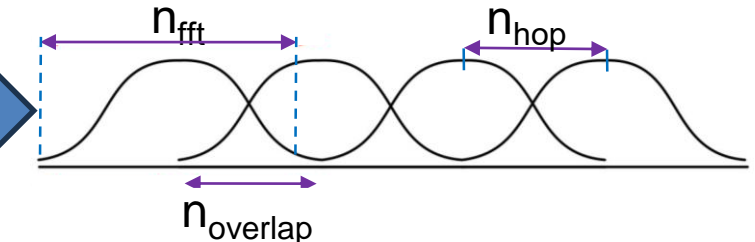
High pass filtering

Signal S_c^F



Windowing

Windows



...

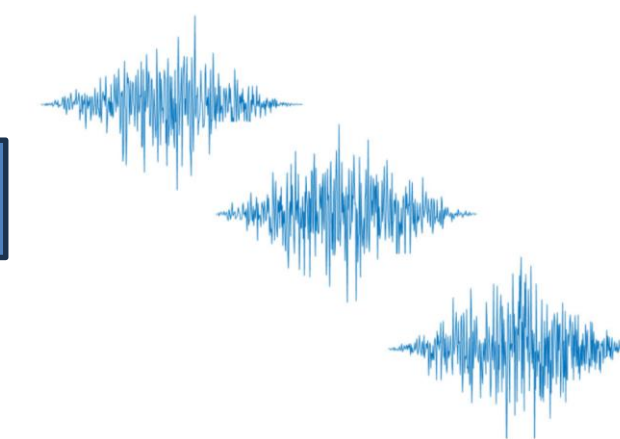
A FFT Output1

A FFT Output2

A FFT Output3

...

FFT



FFT Shift

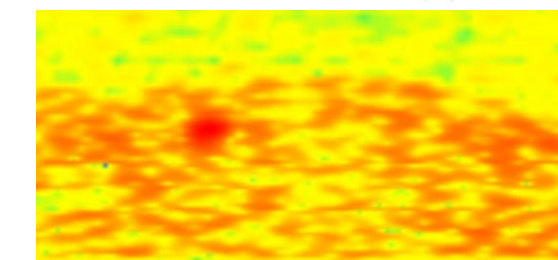
FFT Output1

FFT Output2

FFT Output3

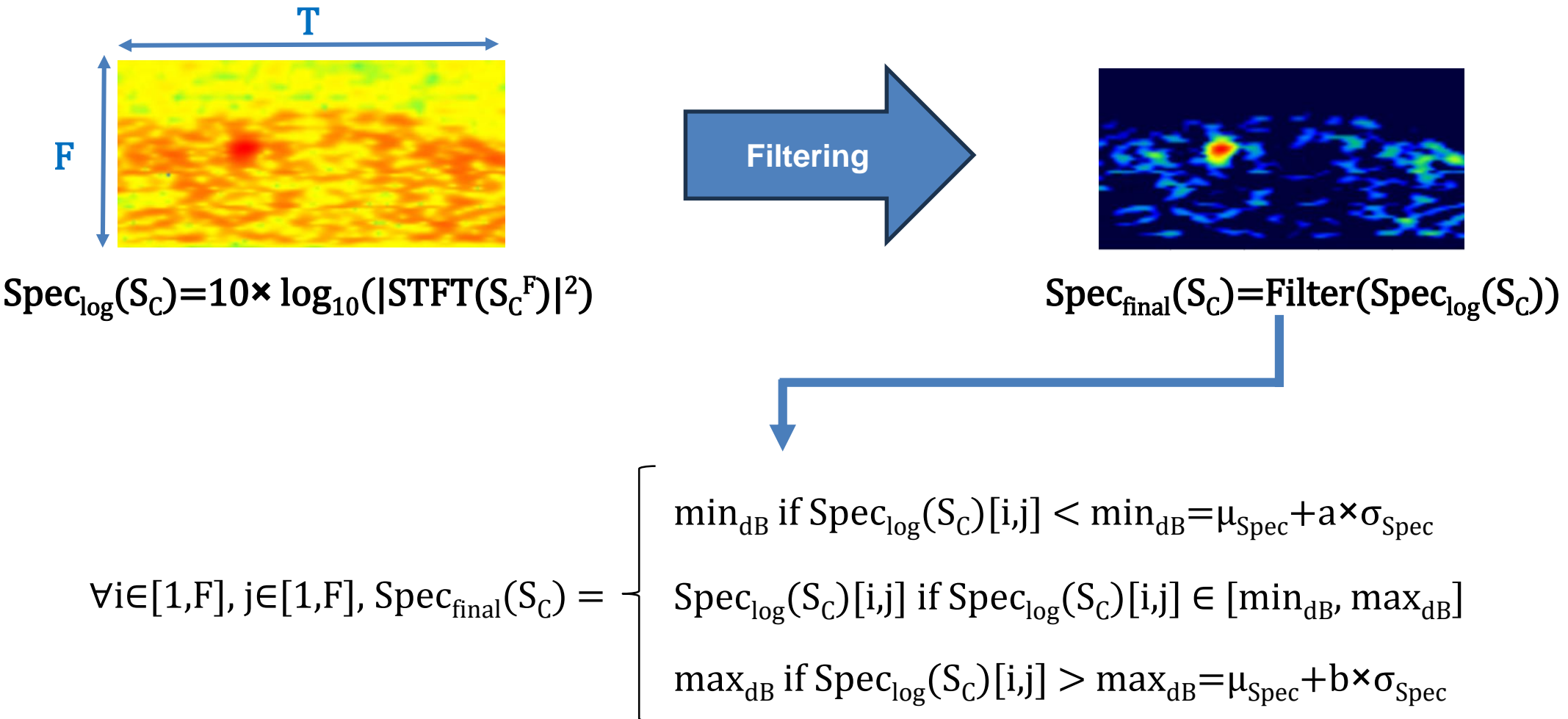
...

Logarithmic spectrogram



$$\text{Spec}_{\log}(S_c) = 10 \times \log_{10}(|\text{STFT}(S_c^F)|^2)$$

Time-frequency representations



Emboli detection

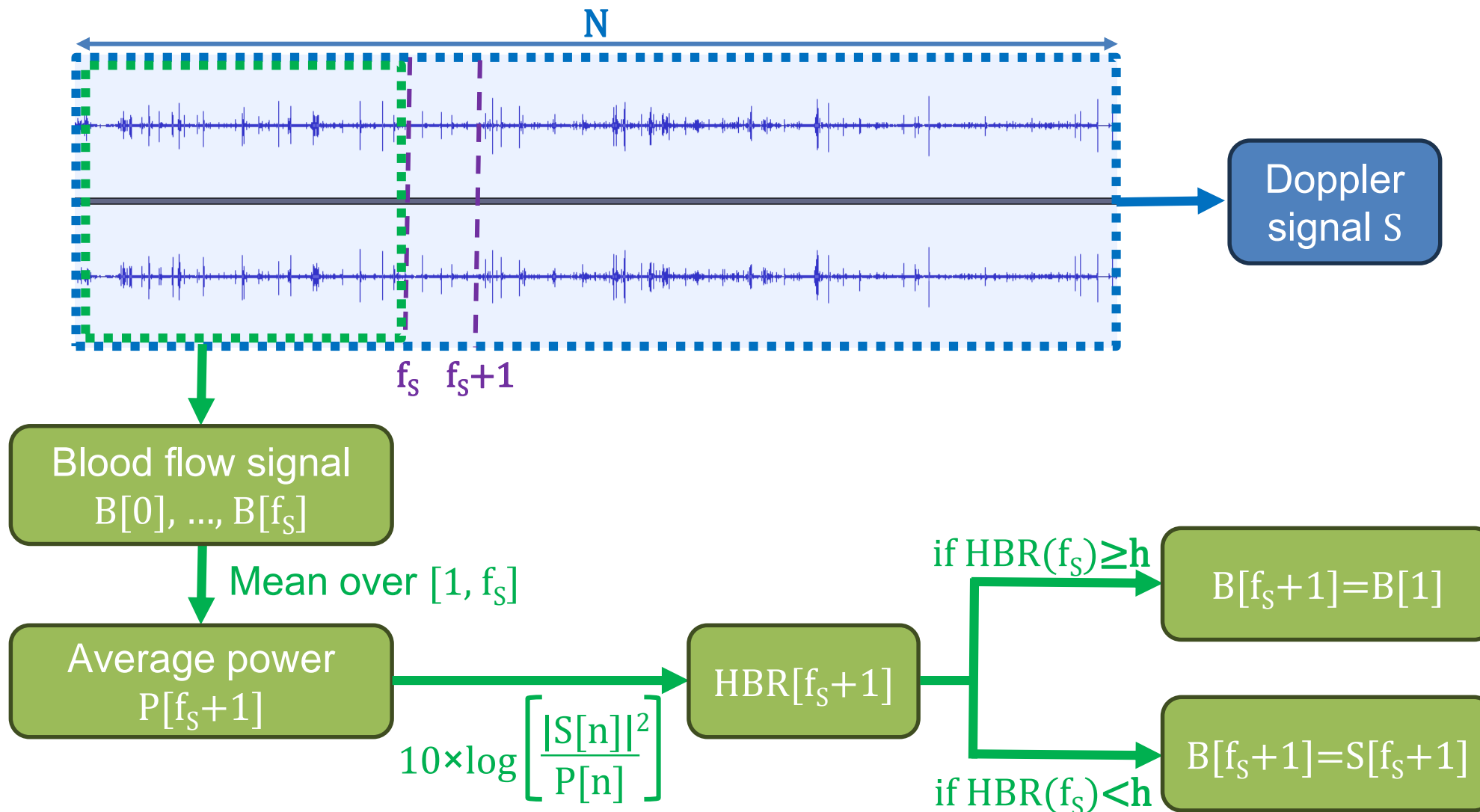
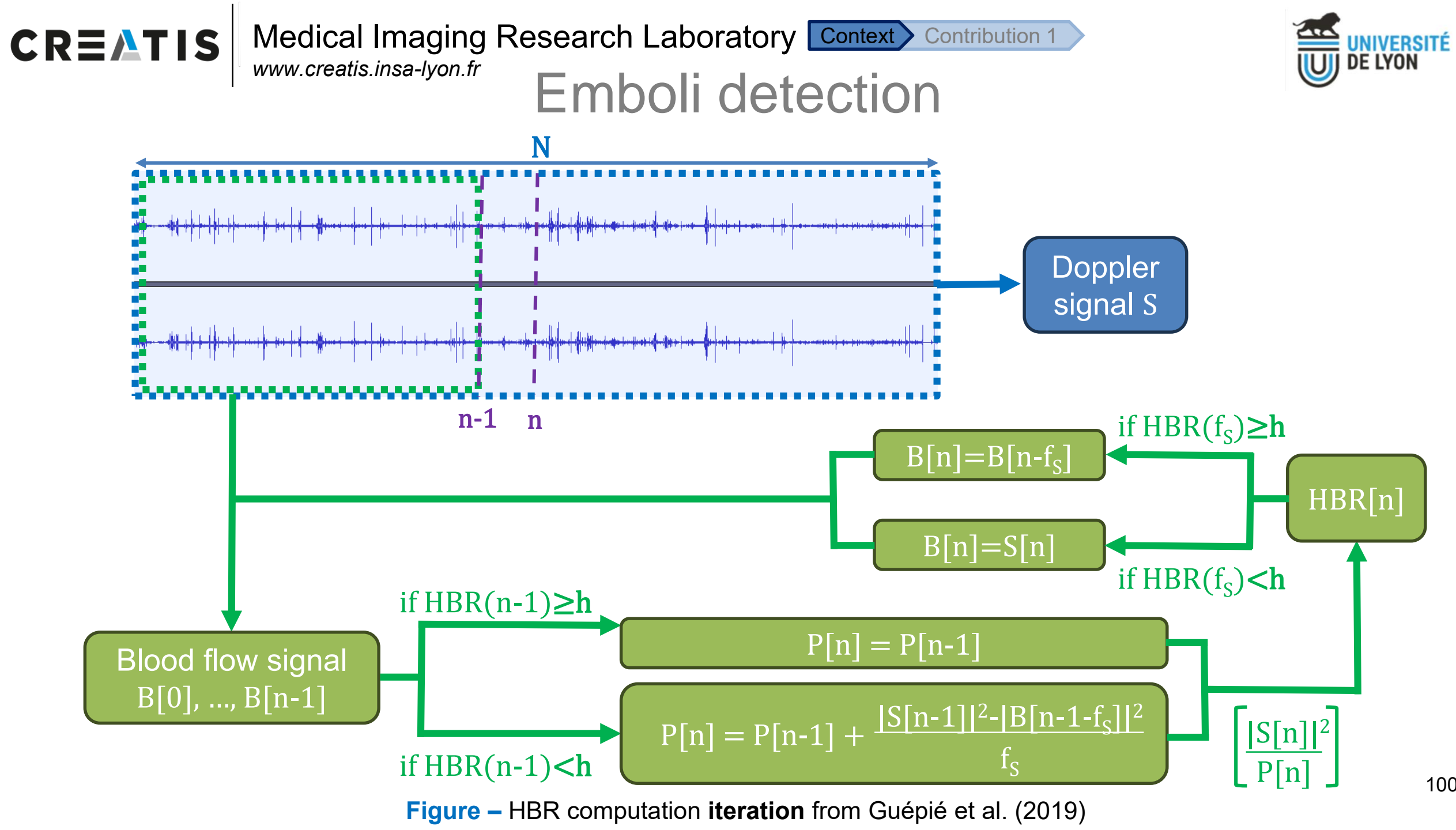
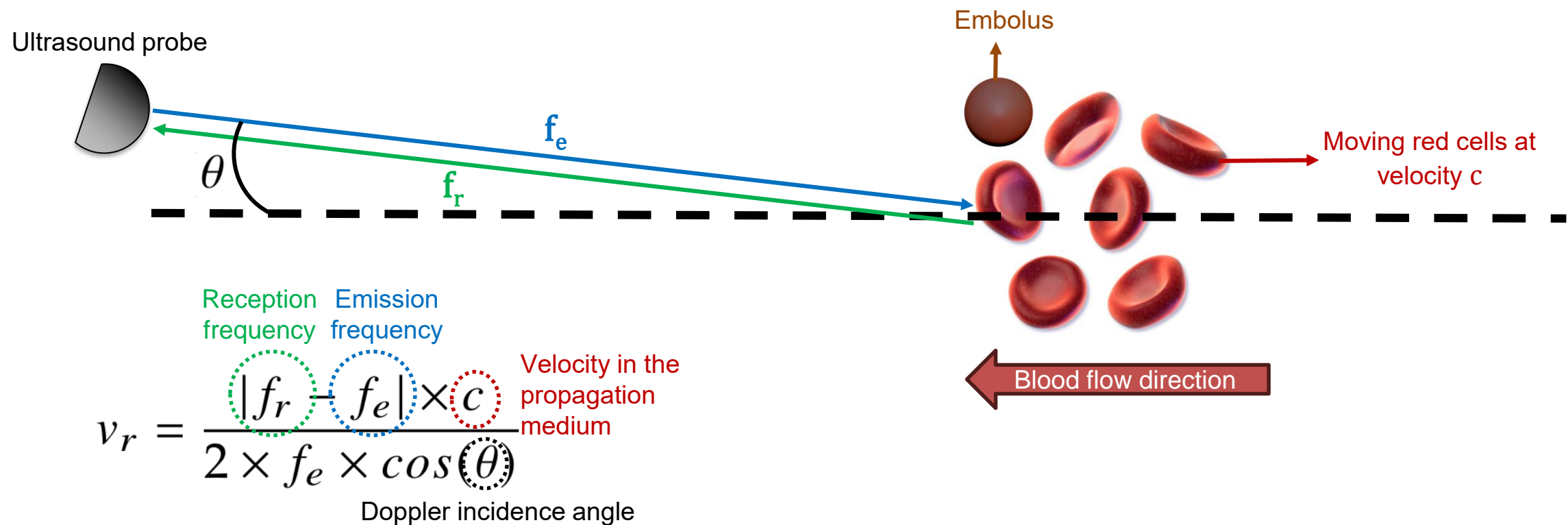


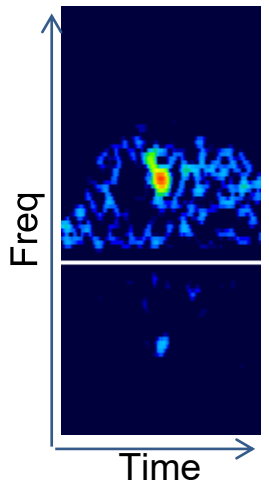
Figure – HBR computation **initialization** from Guépié et al. (2019)



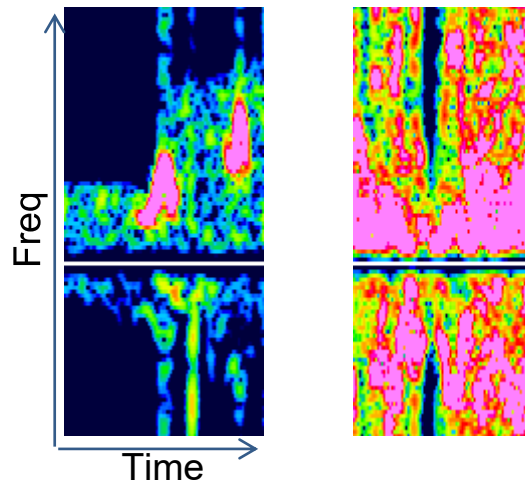
Transcranial Doppler ultrasonography



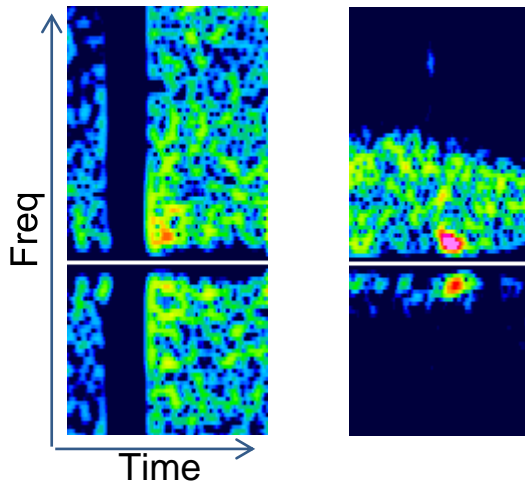
Challenges: data annotation

Solid Emboli

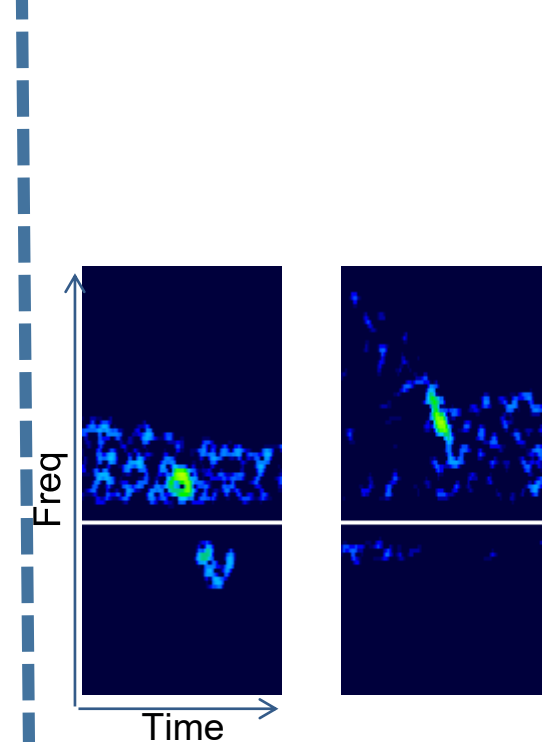
Time →

Gaseous Emboli

Time →

Artifact

Time →

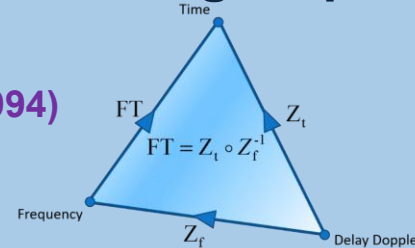
Difficult

Time →

Emboli classification

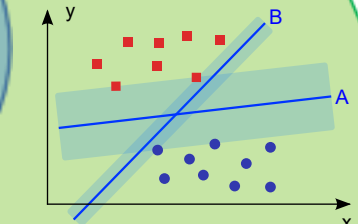
Signal processing

- Georgiadis et al. (1994)
- Aydin et al. (1999)
- Aydin et al. (2004)
- Marvasti et al. (2004)
- Markus et al. (2005)
- Chung et al. (2005)
- Gencer et al. (2013)

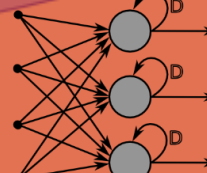


Machine learning

- Darbellay et al. (2004)
- Karahoca et al. (2007)
- Keunen et al. (2008)
- Guépié et al. (2017)
- Tafsast et al. (2018)
- Sombune et al. (2017)
- Chen et al. (2008)
- Sombune et al. (2016)
- Guépié et al. (2019)



Deep learning

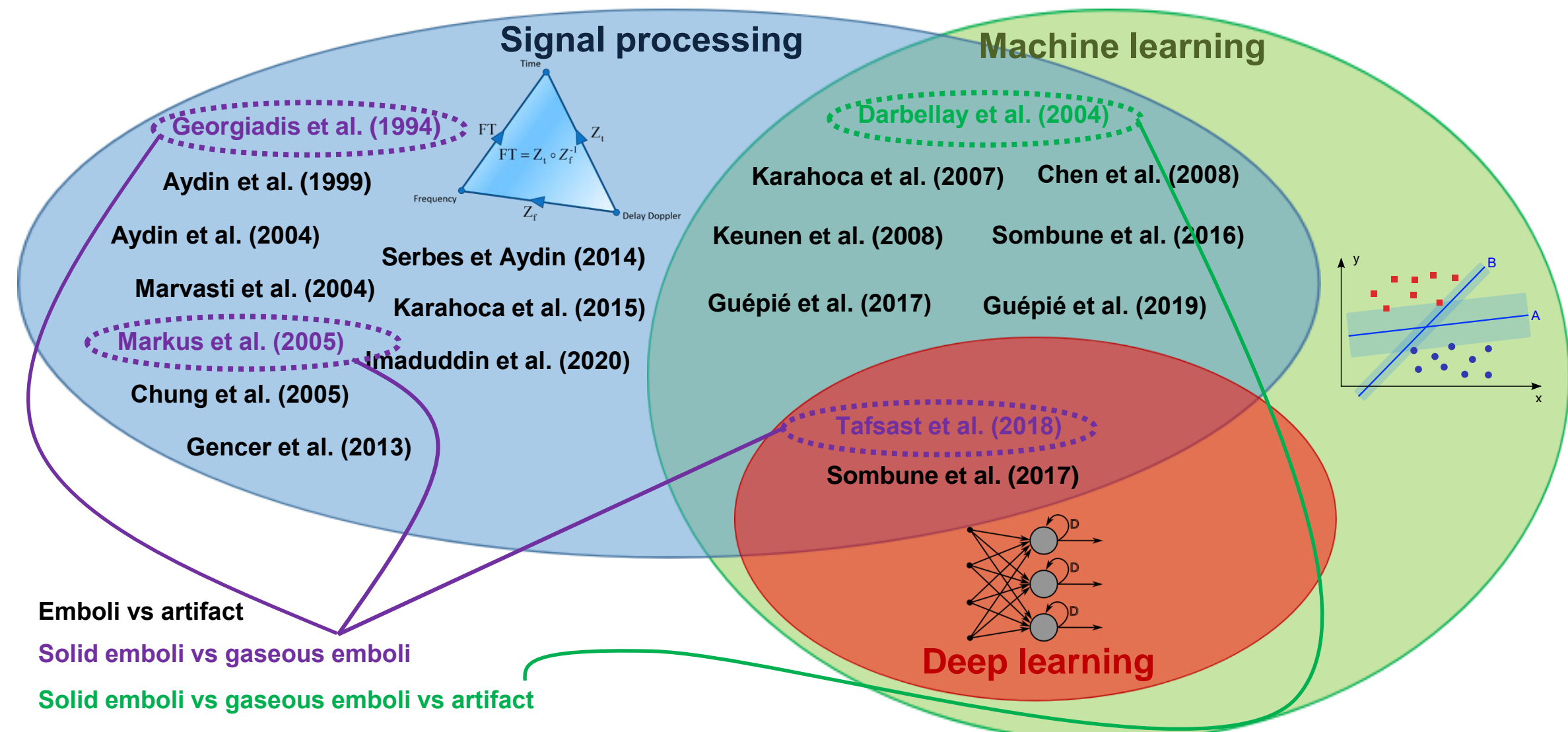


Emboli vs artifact

Solid emboli vs gaseous emboli

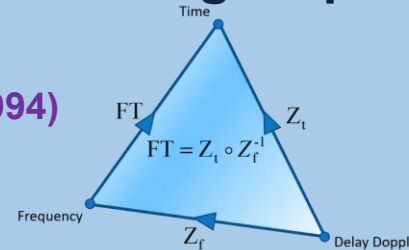
Solid emboli vs gaseous emboli vs artifact

Emboli classification



Emboli classification

Signal processing



- Georgiadis et al. (1994)
- Aydin et al. (1999)
- Aydin et al. (2004)
- Marvasti et al. (2004)
- Markus et al. (2005)
- Chung et al. (2005)
- Gencer et al. (2013)

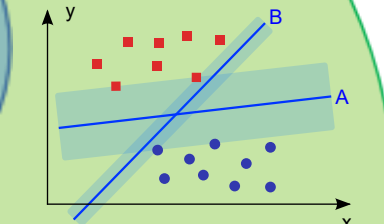
Machine learning

Darbellay et al. (2004)

Karahoca et al. (2007) Chen et al. (2008)

Keunen et al. (2008) Sombune et al. (2016)

Guépié et al. (2017) Guépié et al. (2019)



Emboli vs artifact

Solid emboli vs gaseous emboli

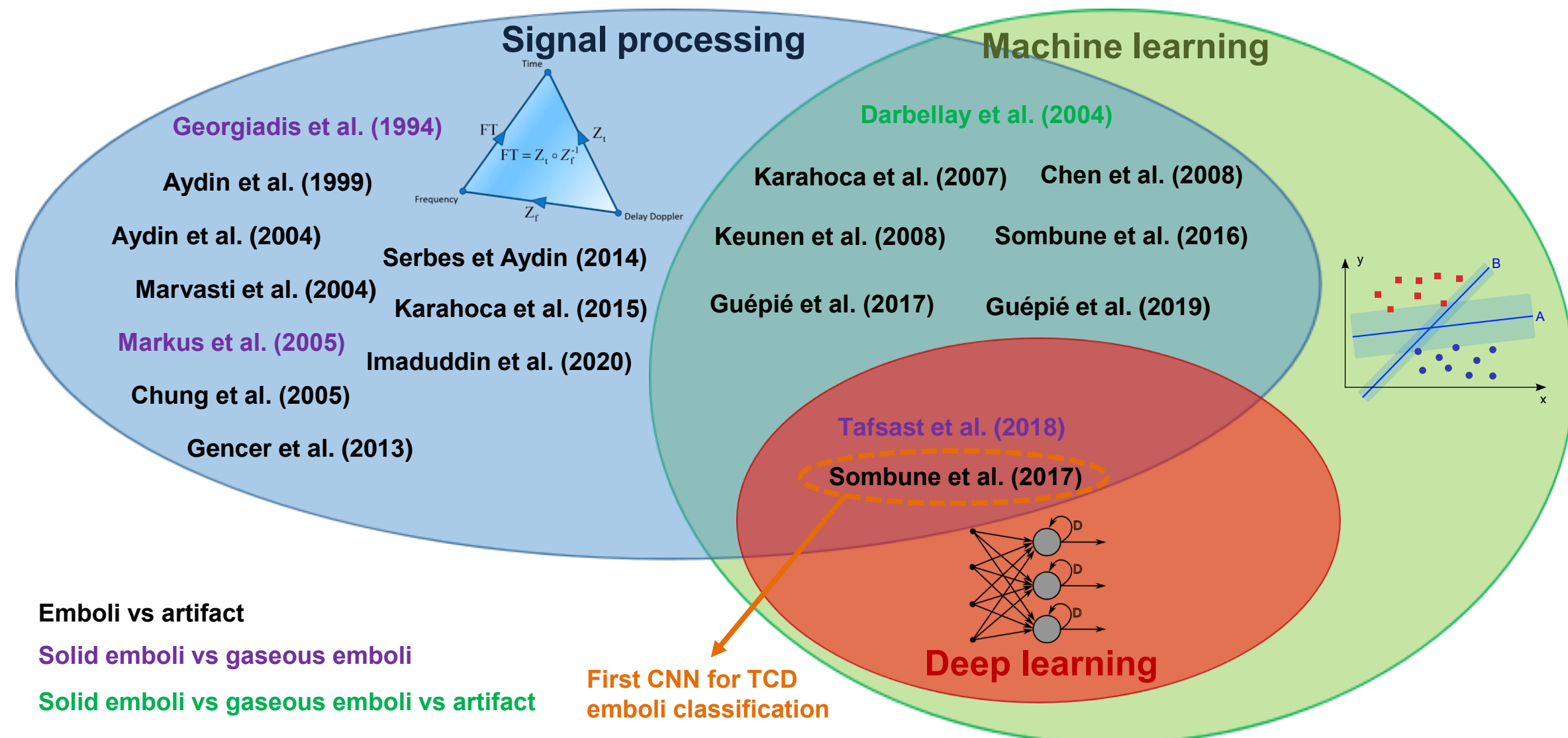
Solid emboli vs gaseous emboli vs artifact

Portable TCD data

Deep learning



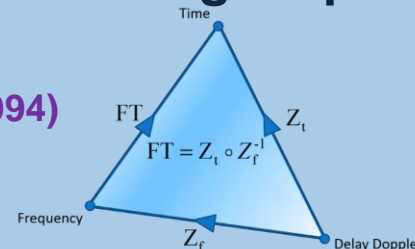
Emboli classification



Emboli classification

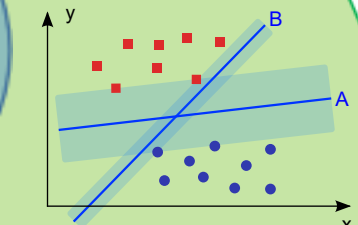
Signal processing

- Georgiadis et al. (1994)
- Aydin et al. (1999)
- Aydin et al. (2004)
- Marvasti et al. (2004)
- Markus et al. (2005)
- Chung et al. (2005)
- Gencer et al. (2013)



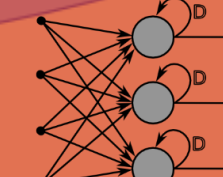
Machine learning

- Darbellay et al. (2004)
- Karahoca et al. (2007) Chen et al. (2008)
- Keunen et al. (2008)
- Sombune et al. (2016)
- Guépié et al. (2017)
- Guépié et al. (2019)**



Tafsast et al. (2018)

Sombune et al. (2017)



Deep learning

Emboli vs artifact

Solid emboli vs gaseous emboli

Solid emboli vs gaseous emboli vs artifact

Emboli classification

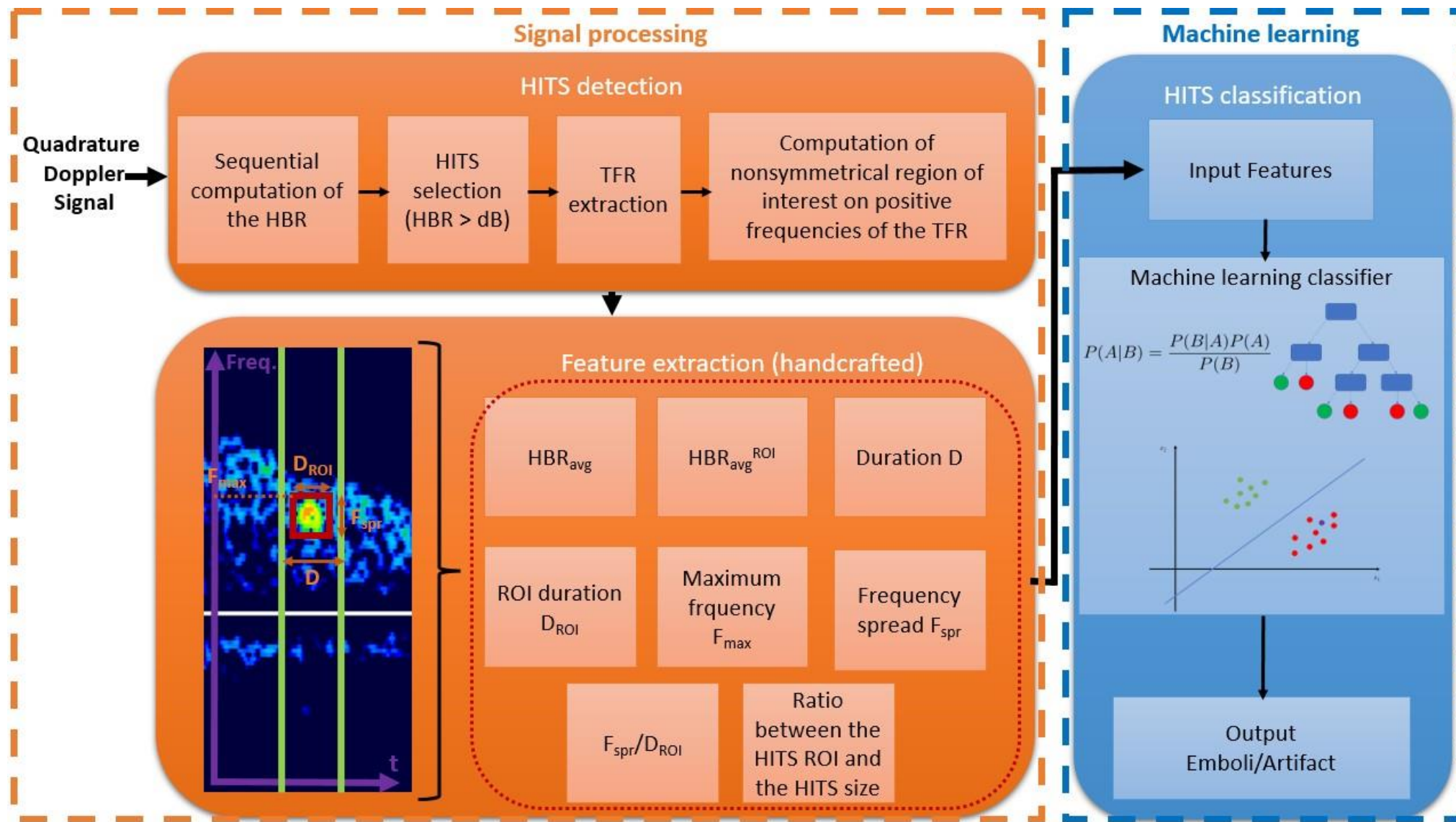
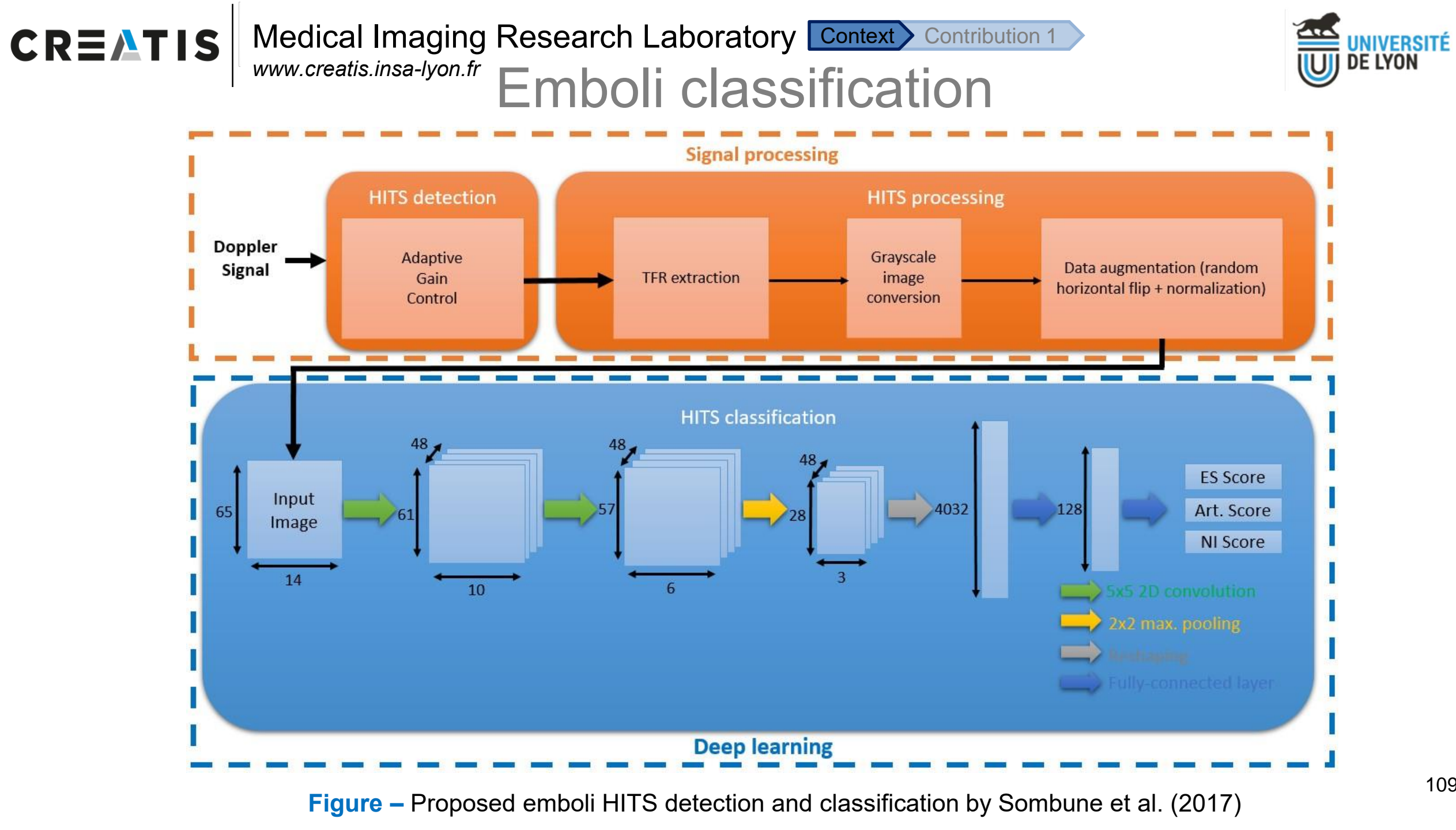
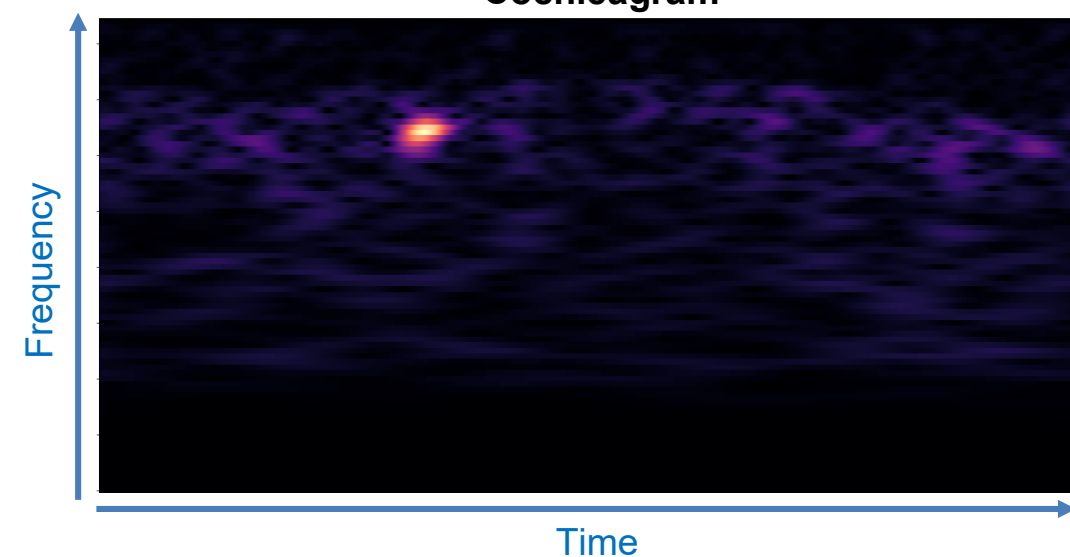
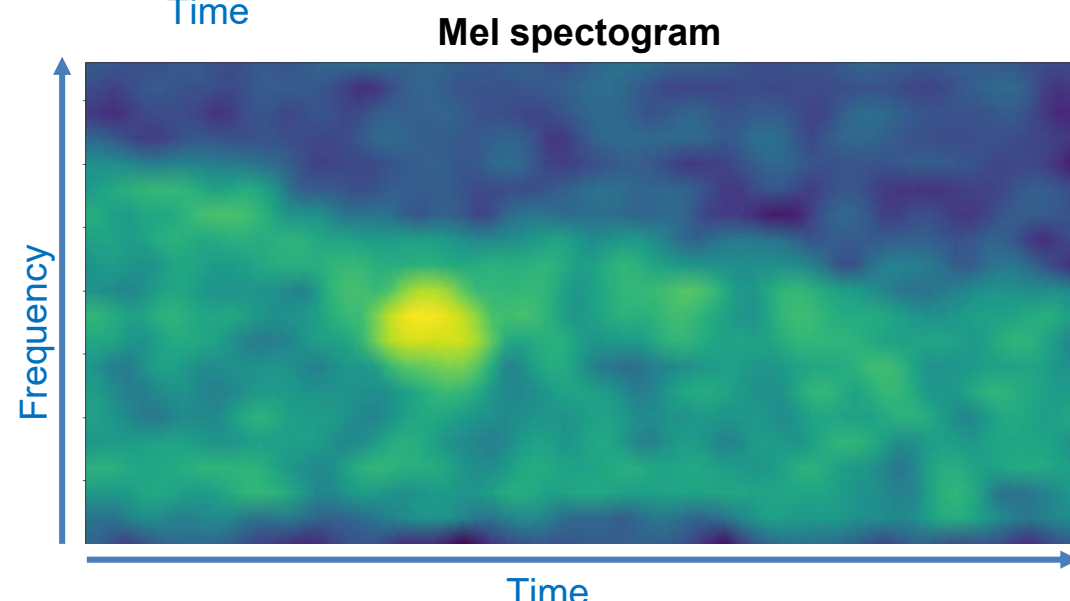
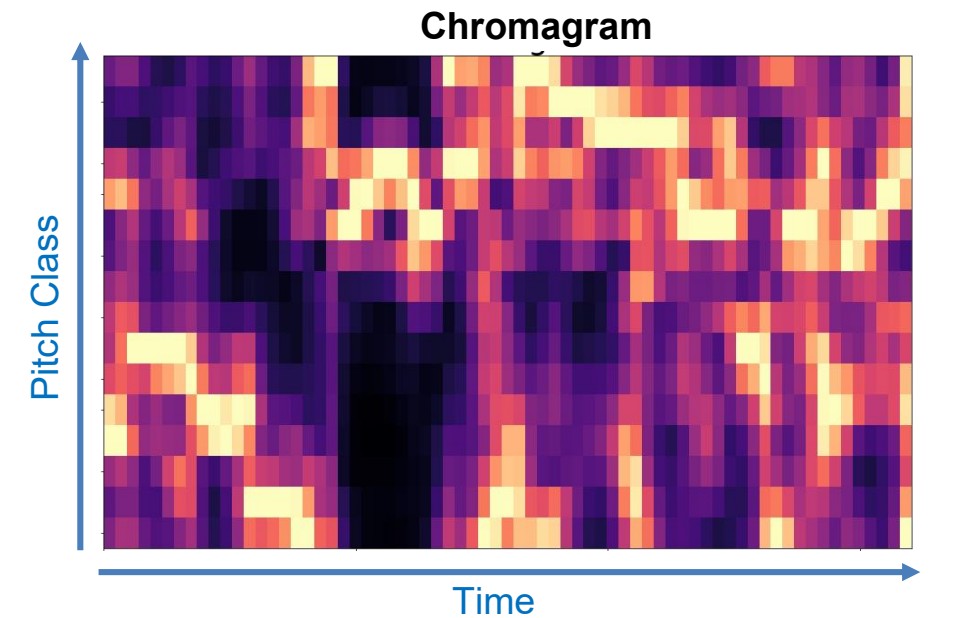
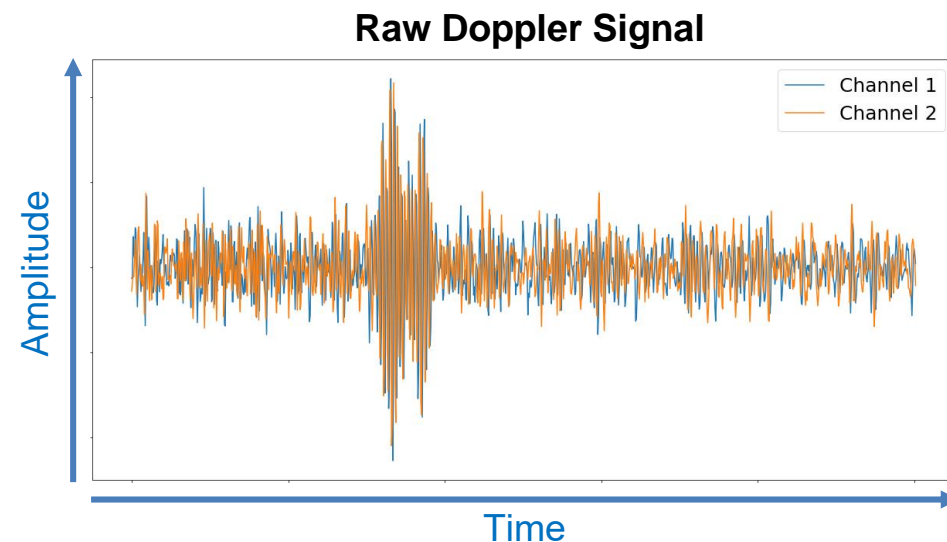
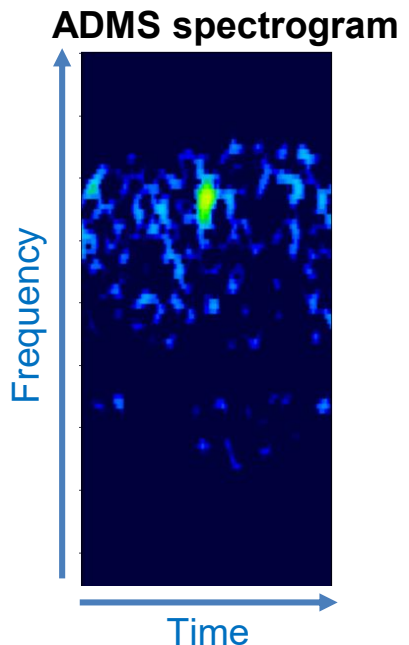


Figure – Proposed emboli detection and classification method of Guépié et al. (2019)

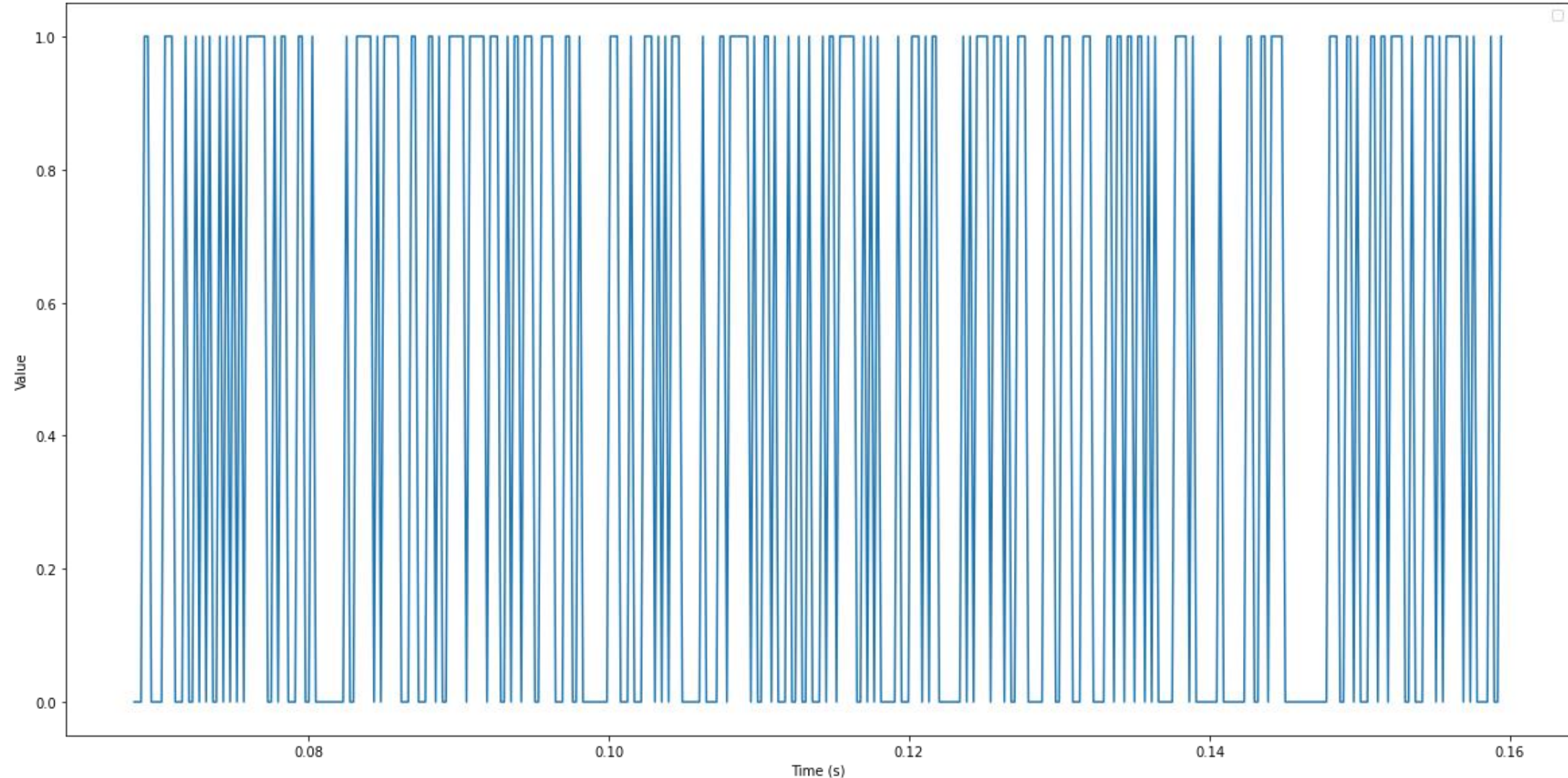


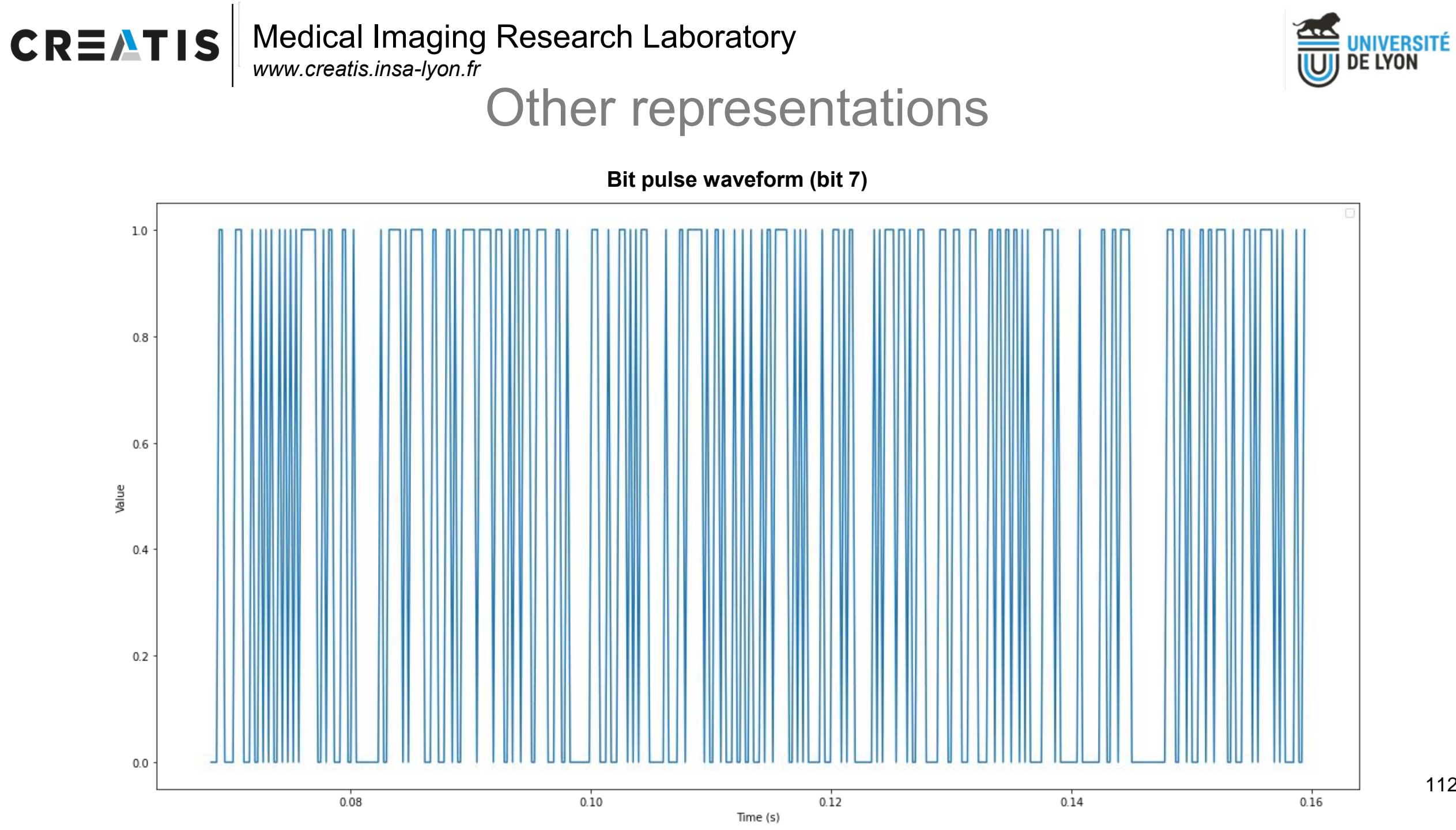
Other representations



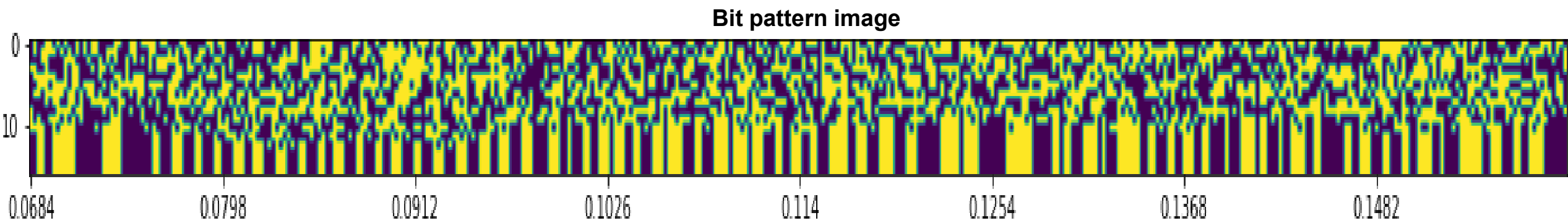
Other representations

Bit pulse waveform (bit 0)





Other representations



Emboli classification

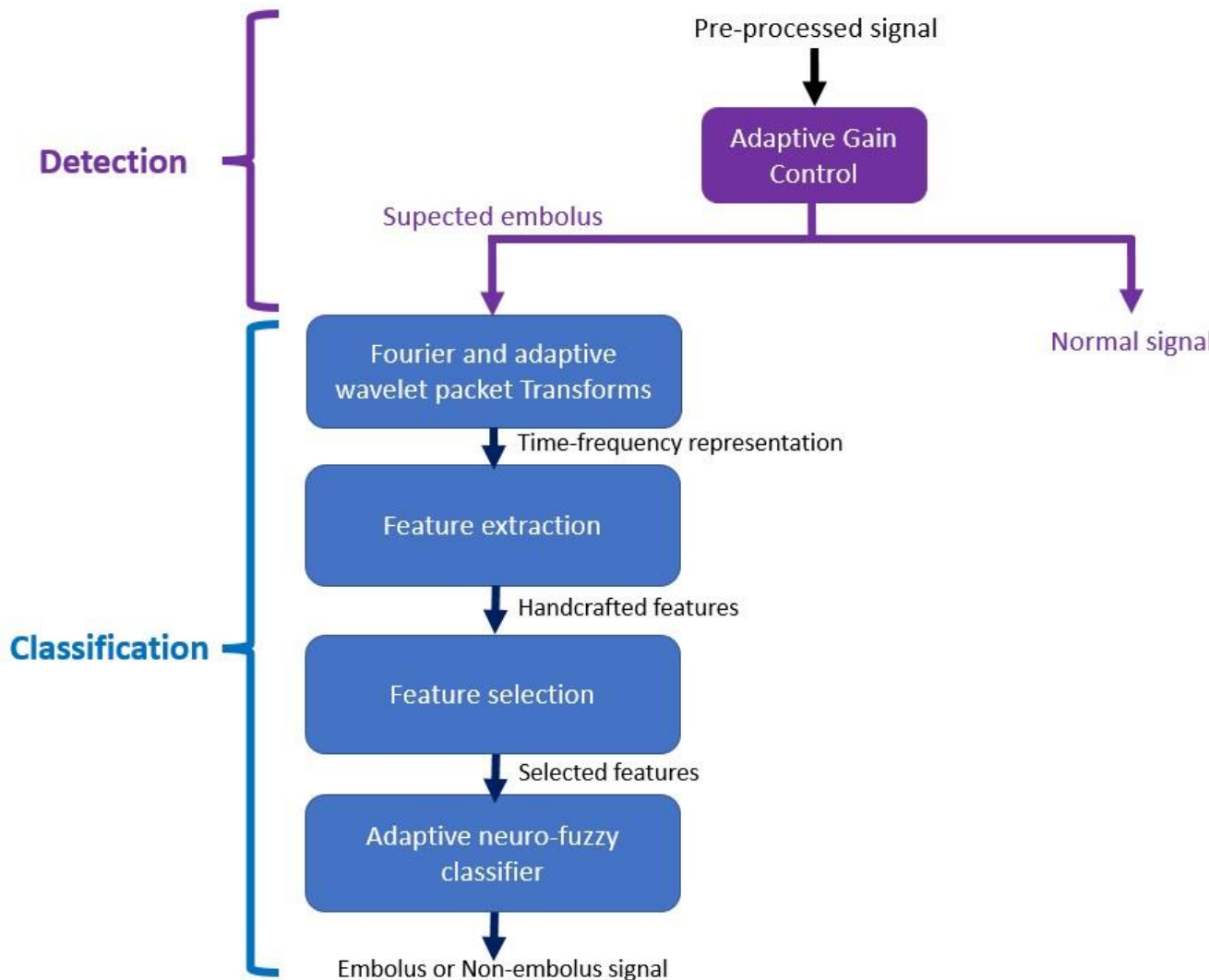


Figure – Proposed emboli ANFIS method by Sombune et al. (2016)

Embolii classification

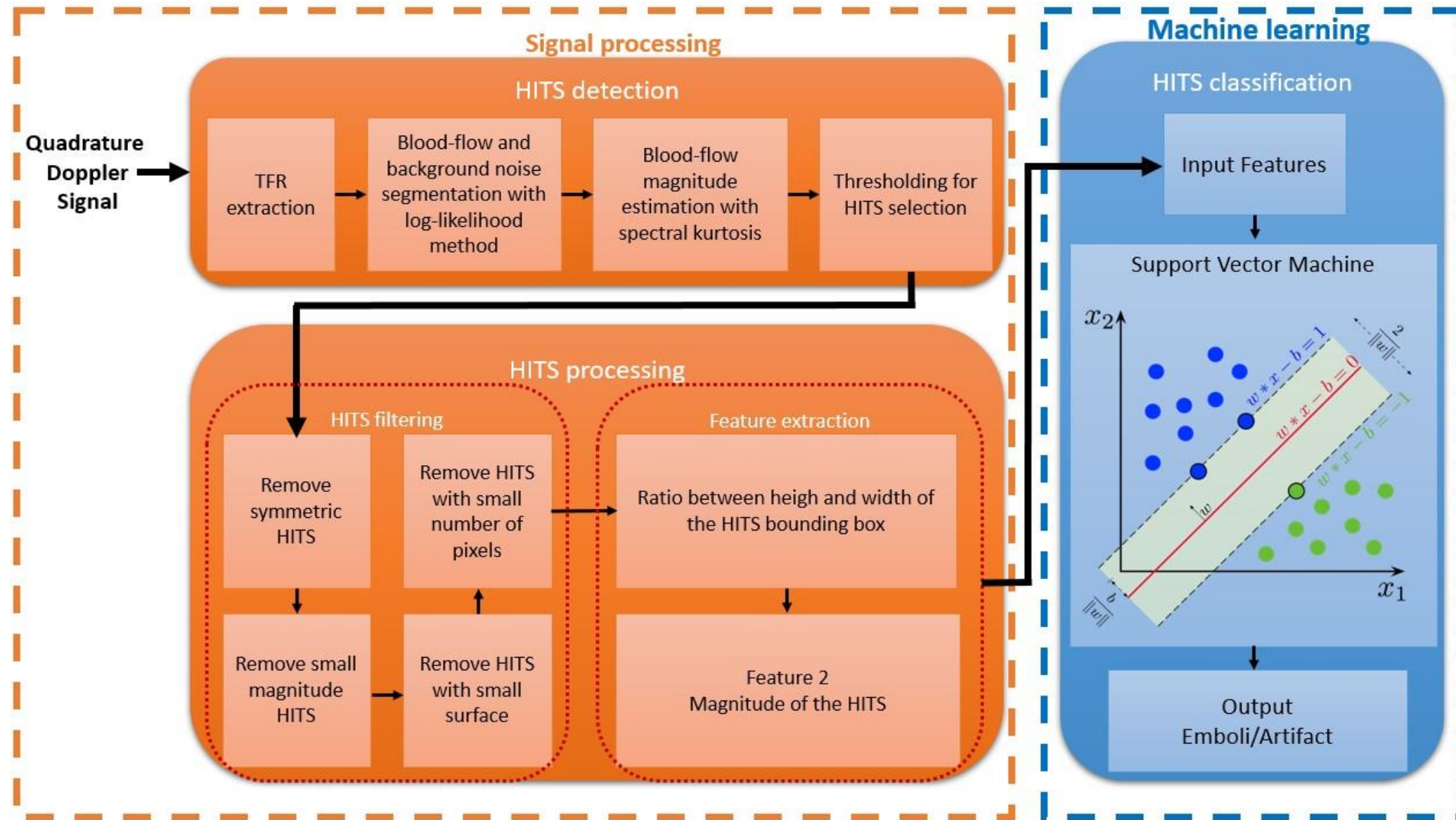


Figure – Proposed emboli detection and classification method of Guépié et al. (2017)

Emboli classification

Authors	Year	Fields	Methods	Classification	Advantages	Limitations
Markus et al.	2005	Signal Processing	-	SE vs GE	- Slightly better results than classical methods	- Use of a dual-frequency TCD - Non portable TCD
Sombune et al.	2017	Deep Learning	CNN	Artifact vs Embolus vs Normal	- No handcrafted features	- Non portable TCD - Not state-of-the-art performances
Guépié et al.	2017	Signal Processing Machine Learning	Likelihood segmentation Spectral Kurtosis, SVM	Artifact vs Embolus	- Good classification performance - Adapt to patients - Operator independent - Portable TCD	- Handcrafted features - No distinction between emboli
Tafsast et al.	2018	Deep Learning	CNN	SE vs GE	Good classification results	- In-vitro study
Guépié et al.	2019	Signal Processing Machine Learning	SVM, Naïve Bayes, Decision Tree	Artifact vs Embolus	- State-of-the-art results - Adapt to patients - Operator independent - Sequential Method - Portable TCD	- Handcrafted features - No distinction between emboli

CREATIS | Medical Imaging Research Laboratory www.creatis.insa-lyon.fr Context Contribution 1

UNIVERSITÉ DE LYON

Challenges: optimal representation

- Temporal dependence.
- One modality, different representations
- Optimal representation ?
- Feature combination ?

The diagram illustrates the challenges of signal representation. At the top, a graph titled "Raw Signal" shows amplitude over time with two colored oscillating lines (orange and blue). Below it, a large red question mark is positioned above a "Bit Pattern Image" (a binary matrix) and a "Bit Pulse Waveform" (a sequence of vertical bars). Four blue arrows point from the text challenges down to these three representations. At the bottom, three smaller images are labeled "Time-Frequency Representations".

Raw Signal

Amplitude

Time

Bit Pattern Image

Bit Pulse Waveform

Time-Frequency Representations

Challenges: model compression

- Limited memory resources.
- Limited computation resources.
- Energy constraints.

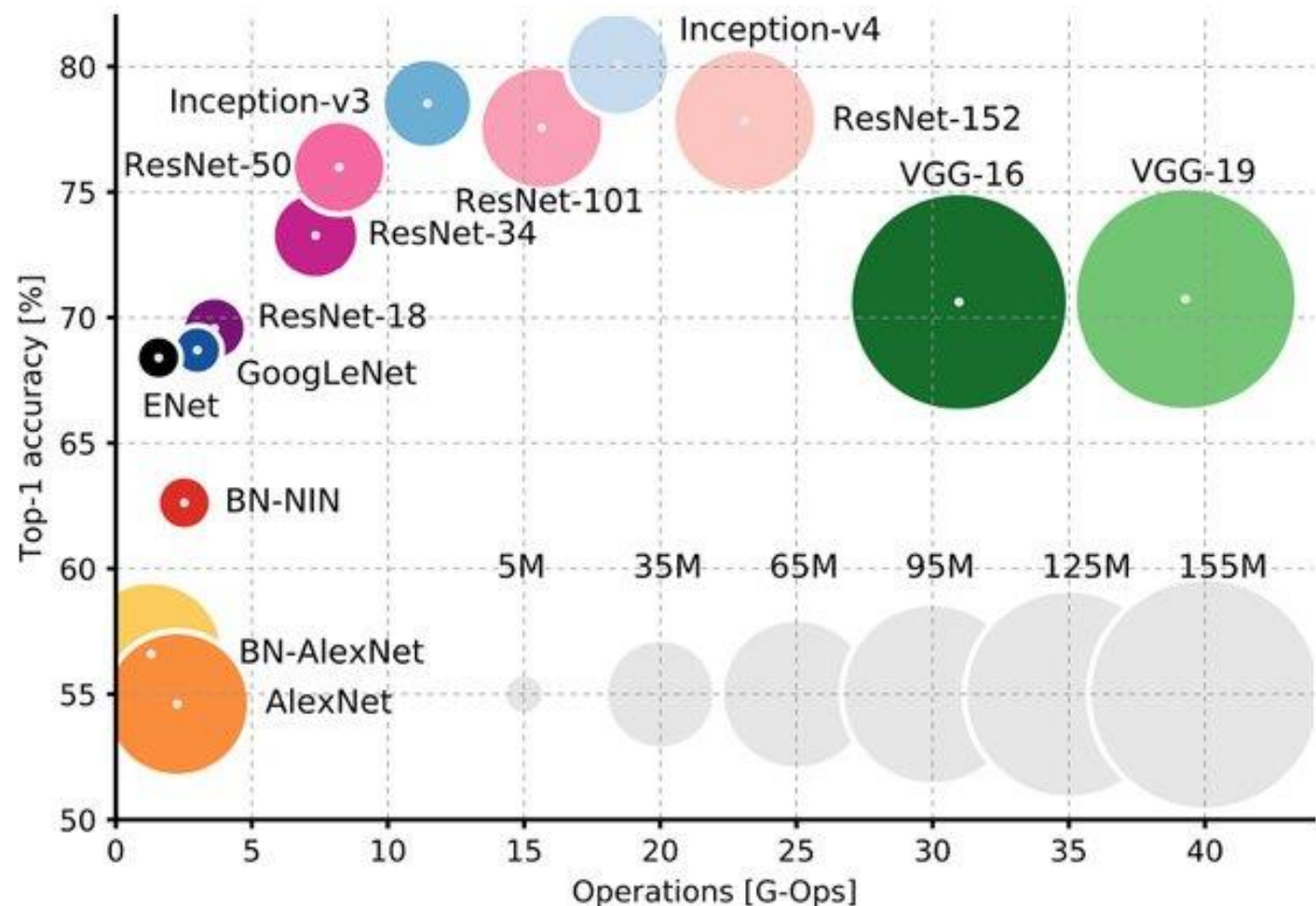


Figure – Classification accuracy based on the size and number of floating-point operations of different deep learning models (Abbas et al. 2021)

Challenges: limited resources

- Limited memory.
- Inference time.

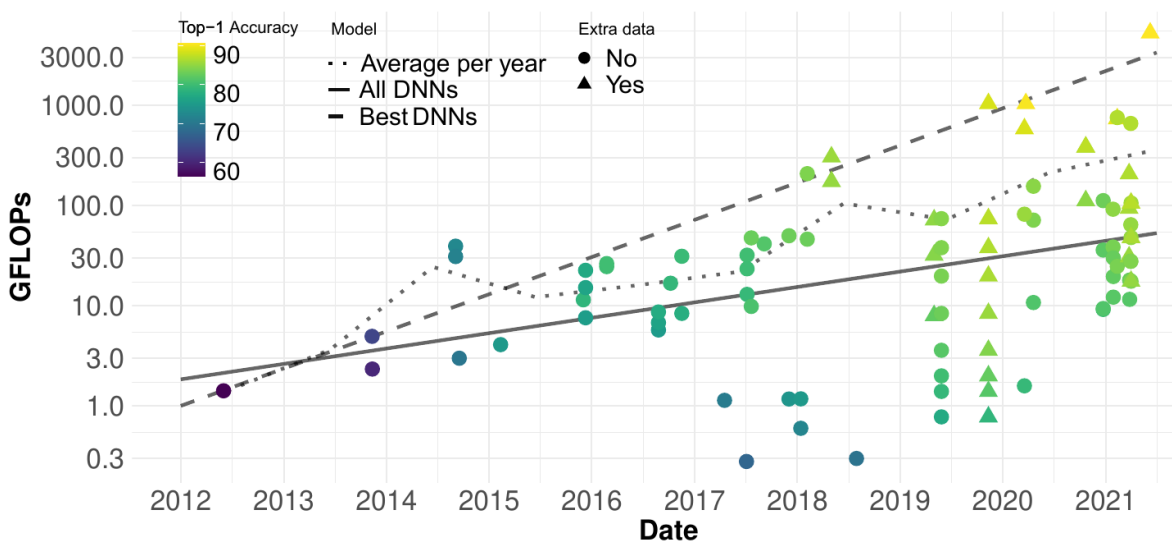


Figure – GFLOPs over the years. The dashed line is a linear fit (logarithmic y-axis) for the models with highest accuracy per year. Desislavov et Martinez-Plumed (2021).

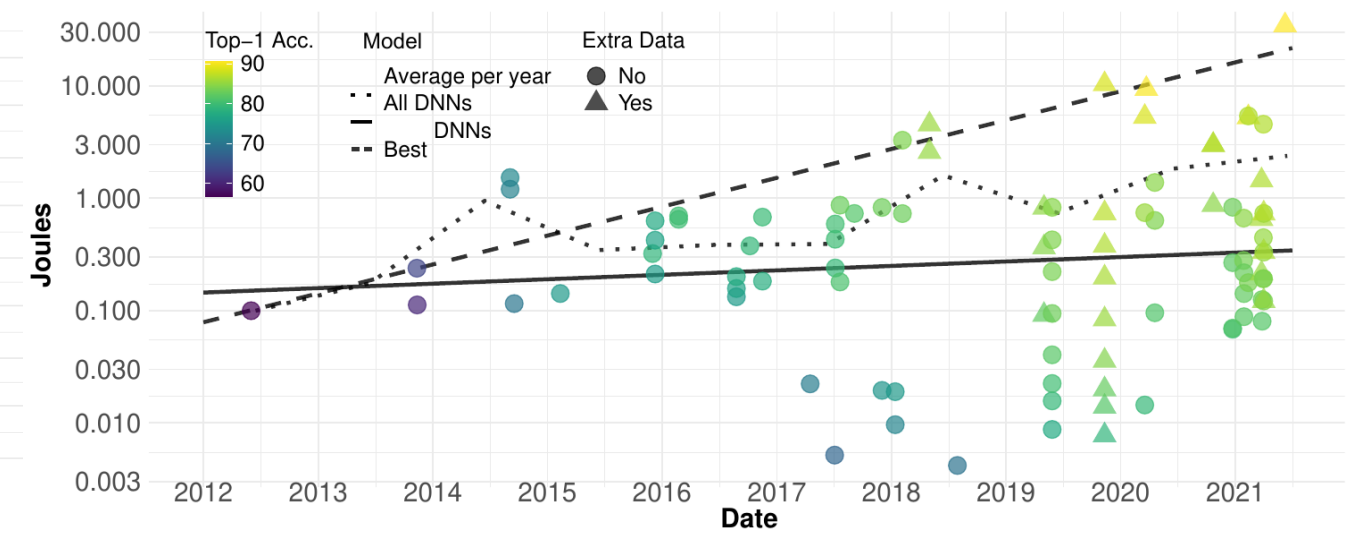


Figure – Estimated Joules of a forward pass (CV). The dashed line is a linear fit (logarithmic y-axis) for the models with highest accuracy per year. Desislavov et Martinez-Plumed (2021).

Challenges: limited resources

- Limited memory.
- Inference time.
- Energy consumption.

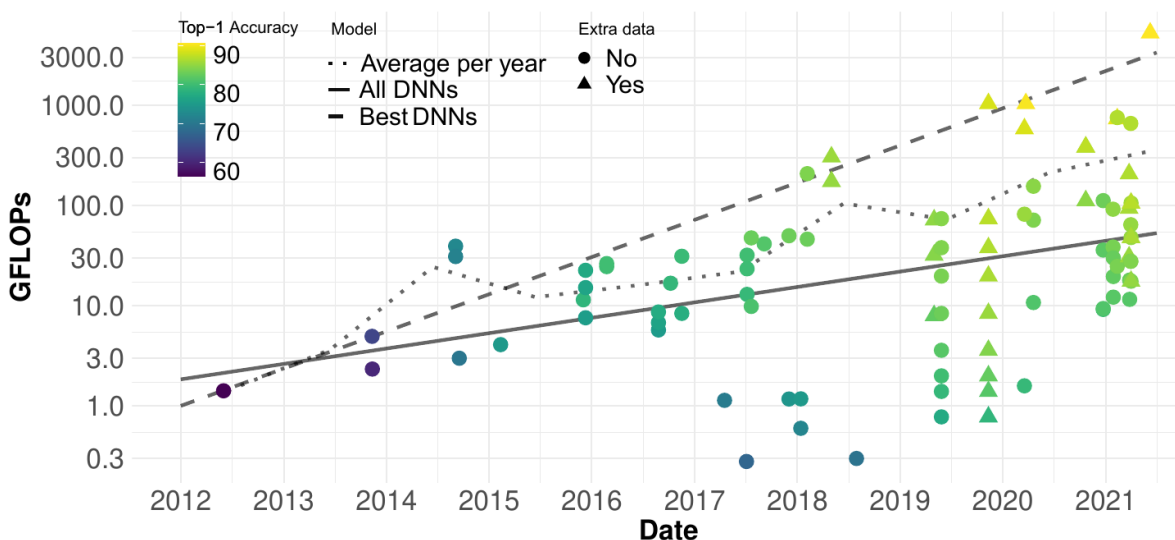


Figure – GFLOPs over the years. The dashed line is a linear fit (logarithmic y-axis) for the models with highest accuracy per year. Desislavov et Martinez-Plumed (2021).

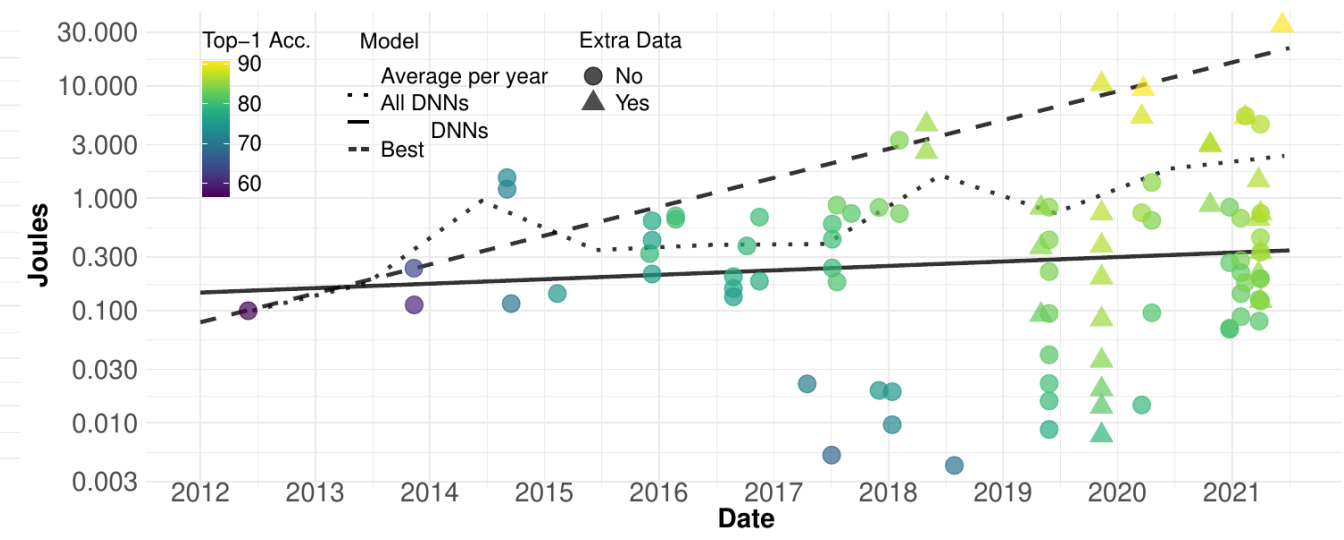


Figure – Estimated Joules of a forward pass (CV). The dashed line is a linear fit (logarithmic y-axis) for the models with highest accuracy per year. Desislavov et Martinez-Plumed (2021).

Contribution 1 : Semi-automatic data annotation

Possible solution to noisy-labels

Category	P1 Flexibility	P2 No Pre-train	P3 Full Exploration	P4 No Supervision	P5 Heavy Noise	P6 Complex Noise
Robust Loss Function	○	○	○	○	✗	✗
Robust Architecture	△	○	○	○	✗	✗
Dedicated Architecture	✗	○	○	✗	△	○
Robust Regularization	○	○	○	○	△	△
Loss Adjustment	○	○	○	✗	✗	✗
Loss Correction	○	○	○	○	✗	✗
Loss Reweighting	○	○	○	○	✗	△
Label Refurbishment	○	○	○	△	✗	△
Sample Selection	○	○	✗	✗	○	△
Meta Learning	○	○	○	△	△	○
Fast Adaption	○	○	○	○	△	○
Learning to Update	○	○	○	✗	△	○
Semi-supervised Learning	○	△	○	○	○	△

Figure – Table from Song et al. 2020. ○ means completely supported, △ means partially supported and ✗ means not supported.

$$\mathcal{L}_{GCE}(f(X), \bar{y}) = \sum_{k=1}^K \frac{\bar{y}_k - f_k(X)^q}{q}$$

Input sample # classes
 Model One-hot label
 kth element

$q \rightarrow 0 \rightarrow \mathcal{L}_{CE}(f(X), \bar{y})$ **Noise sensitive**
 $q \rightarrow 1 \rightarrow \mathcal{L}_{MAE}(f(X), \bar{y})$ **Noise tolerant**

Noisy-labels

Category	Method	P1	P2	P3	P4	P5	P6
Robust Loss Function	<i>Robust MAE</i>	○	○	○	○	✗	✗
	<i>Generalized Cross Entropy</i>	○	○	○	○	✗	✗
	<i>Symmetric Cross Entropy</i>	○	○	○	○	✗	✗
	<i>Curriculum Learning</i>	○	○	○	✗	○	△
Robust Architecture	<i>Weibly Learning</i>	△	✗	○	○	✗	✗
	<i>Noise Model</i>	△	○	○	○	✗	✗
	<i>Dropout Noise Model</i>	△	○	○	○	✗	✗
	<i>S-model</i>	△	○	○	○	✗	✗
	<i>C-model</i>	△	○	○	○	✗	○
	<i>NLNN</i>	△	○	○	○	✗	✗
	<i>Probabilistic Noise Model</i>	✗	✗	○	✗	△	○
	<i>Masking</i>	✗	○	○	✗	△	○
	<i>Contrastive-Additive Noise Network</i>	✗	○	○	○	△	○
	<i>Adversarial Training</i>	○	○	○	○	△	△
	<i>Label Smoothing</i>	○	○	○	○	△	△
	<i>Mixup</i>	○	○	○	○	△	△
Robust Regularization	<i>Bilevel Learning</i>	○	○	○	✗	△	△
	<i>Annotator Confusion</i>	○	✗	○	○	△	△
	<i>Pre-training</i>	○	✗	○	○	△	△
	<i>Backward Correction</i>	○	○	○	✗	✗	✗
	<i>Forward Correction</i>	○	○	○	✗	✗	✗
	<i>Gold Loss Correction</i>	○	✗	○	✗	✗	✗
Loss Adjustment	<i>Importance Reweighting</i>	○	○	○	○	✗	△
	<i>Active Bias</i>	○	○	○	○	✗	△
	<i>Bootstrapping</i>	○	○	○	✗	✗	△
	<i>Dynamic Bootstrapping</i>	○	○	○	○	✗	△
Label Refurbishment	<i>D2L</i>	○	○	○	○	✗	△
	<i>SELFIE</i>	○	○	○	✗	○	△

Category	Method	P1	P2	P3	P4	P5	P6
Sample Selection	<i>Decouple</i>	○	○	✗	○	✗	△
	<i>MentorNet</i>	✗	✗	✗	✗	○	△
	<i>Co-teaching</i>	○	○	✗	✗	○	△
	<i>Co-teaching+</i>	○	○	✗	✗	○	△
	<i>Iterative Detection</i>	○	○	✗	○	○	△
	<i>ITLM</i>	○	○	✗	✗	○	△
	<i>INCV</i>	○	○	✗	○	○	△
Meta Learning	<i>Meta-Regressor</i>	○	○	○	✗	○	○
	<i>MLNT</i>	○	○	○	○	✗	○
	<i>Knowledge Distillation</i>	○	✗	○	✗	△	○
	<i>L2LWS</i>	✗	○	○	○	✗	△
Learning to Update	<i>CWS</i>	✗	○	○	○	✗	△
	<i>Automatic Reweighting</i>	○	○	○	○	✗	△
	<i>Meta-Weight-Net</i>	△	○	○	✗	△	○
	<i>Data Coefficients</i>	○	○	○	✗	○	○
	<i>Label Aggregation</i>	○	✗	○	✗	✗	△
	<i>Two-Stage Framework</i>	○	✗	○	○	○	△
Semi-supervised Learning	<i>SELF</i>	○	○	○	○	○	△
	<i>DivideMix</i>	○	○	○	○	○	△

Figure – Table from Song et al. 2020. ○ means completely supported, △ means partially supported and ✗ means not supported.

OPF-semi

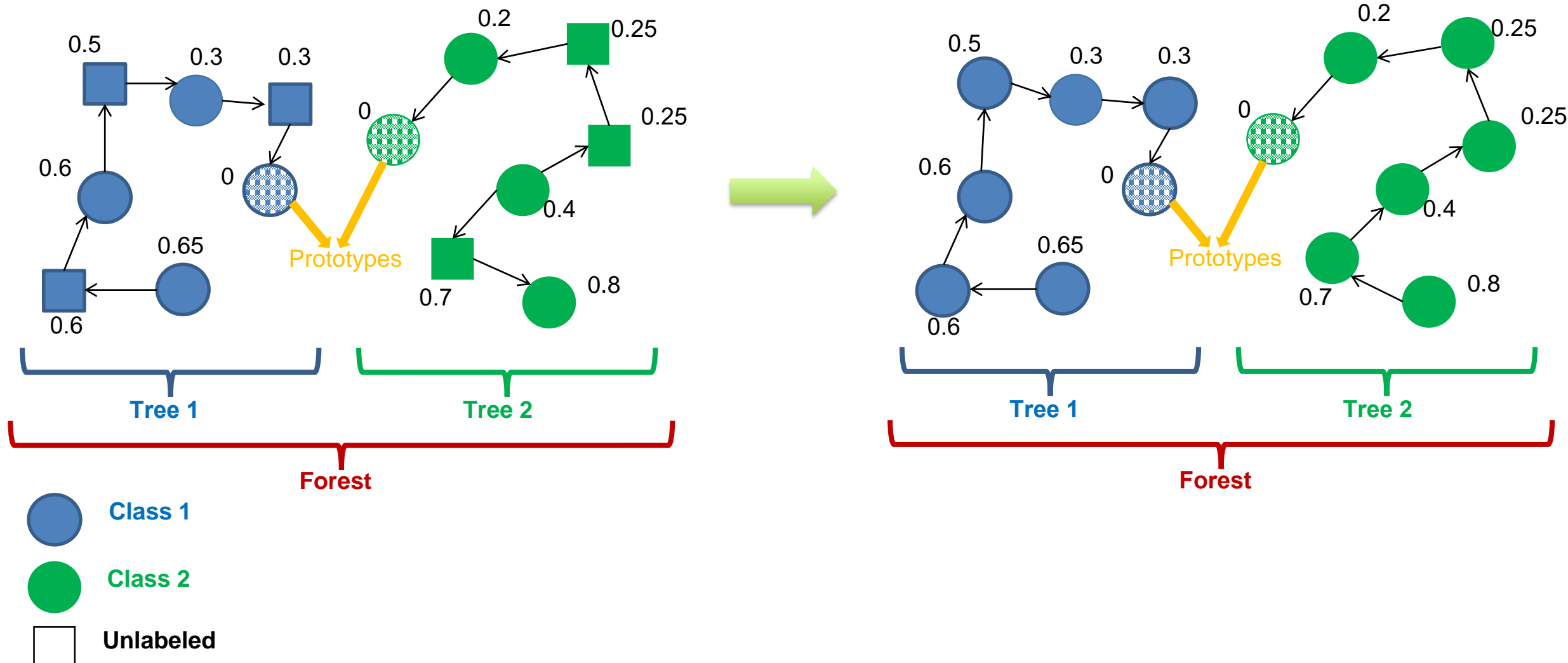


Figure – Semi-supervised optimum path forest (OPF-semi) (Amorim et al., 2014)

Co-ranking framework: local quality

$$Q_L^i(k_s, k_t) = \frac{1}{2 \times k_s \times N} \times \sum_{j=1}^N (\underbrace{\mu_t(R_{ij}, r_{ij}, k_t) \times \mu_s(R_{ij}, r_{ij}, k_s)}_{\text{Rank significance}} + \underbrace{\mu_t(R_{ji}, r_{ji}, k_t) \times \mu_s(R_{ji}, r_{ji}, k_s)}_{\text{Rank error tolerance}})$$

Size of the neighborhood to consider

Rank significance $\mu_s(R_{ij}, r_{ij}, k_s) = \begin{cases} 1 \text{ if } R_{ij} \leq k_s \text{ or } r_{ij} \leq k_s \\ 0 \text{ else} \end{cases}$

Rank error tolerance $\mu_t(R_{ij}, r_{ij}, k_t) = \begin{cases} 1 \text{ if } |R_{ij} - r_{ij}| \leq k_t \\ 0 \text{ else} \end{cases}$

Size of the tolerated ranks errors

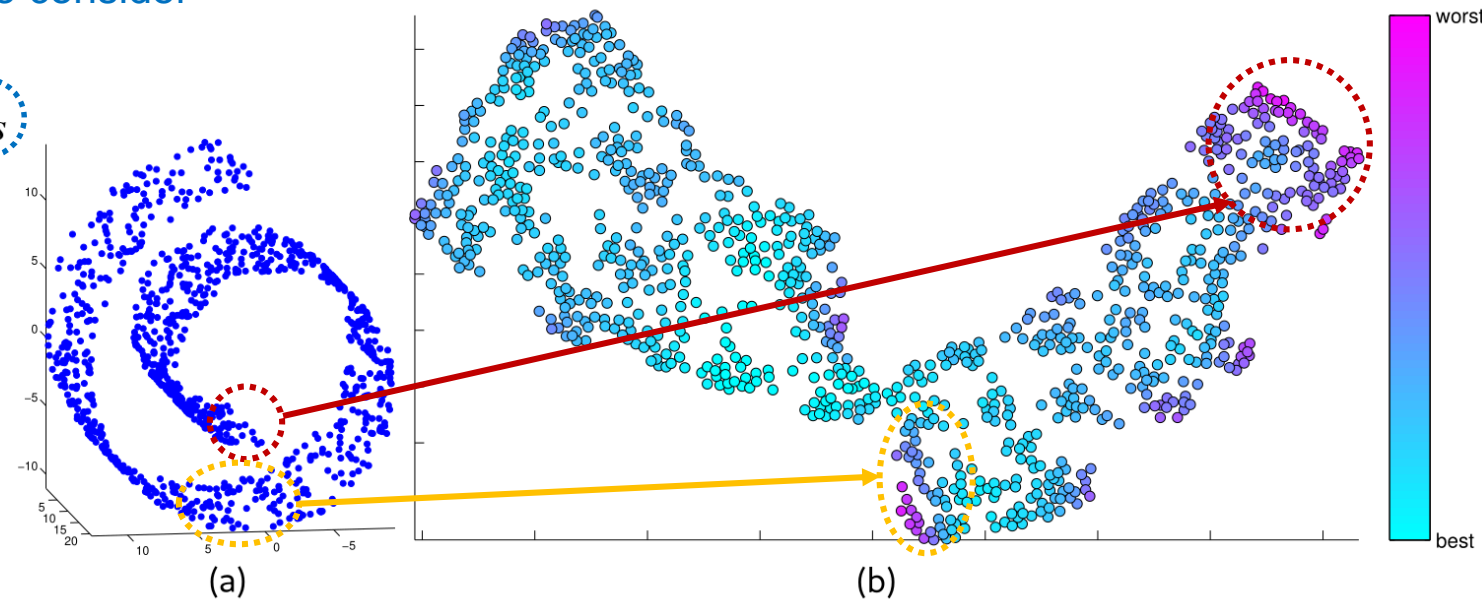


Figure – Illustration of the local quality metric on the Swiss roll benchmark dataset (Lueks et al., 2011).

Global pipeline

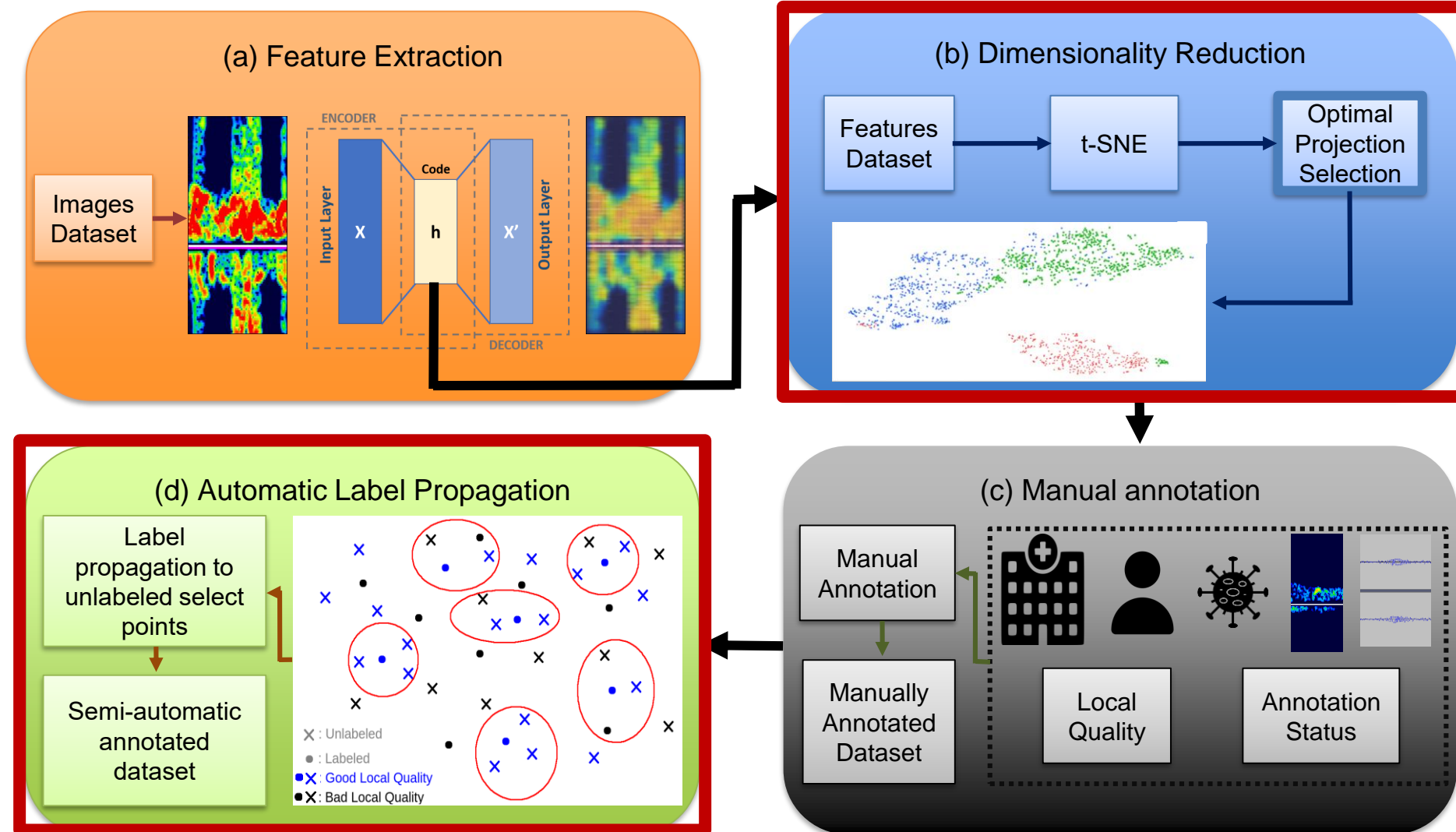
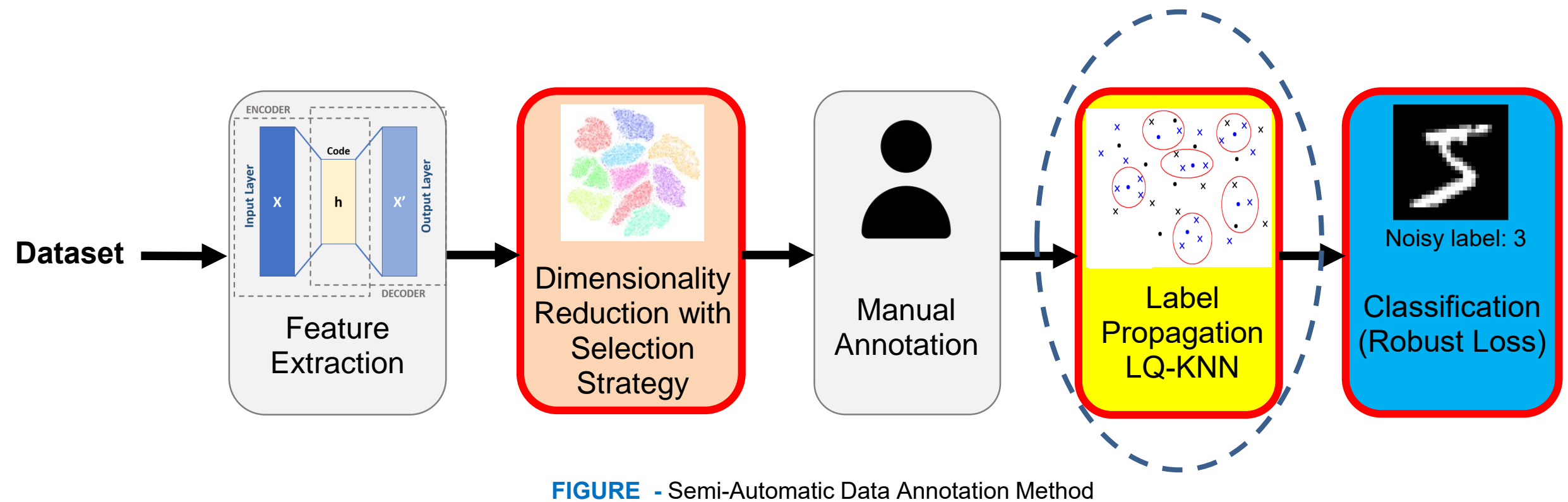


Figure – Global pipeline of our proposed semi-automatic data annotation approach.

Proposed pipeline



Contribution 1.a.: Semi-automatic data annotation method **state-of-the-art comparison**

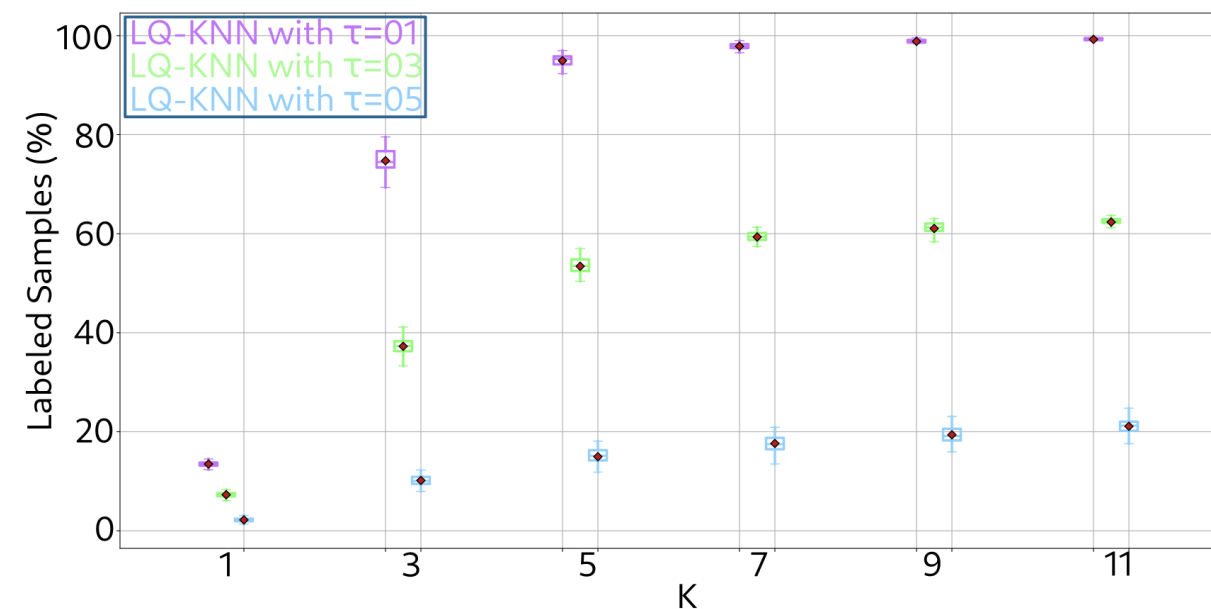
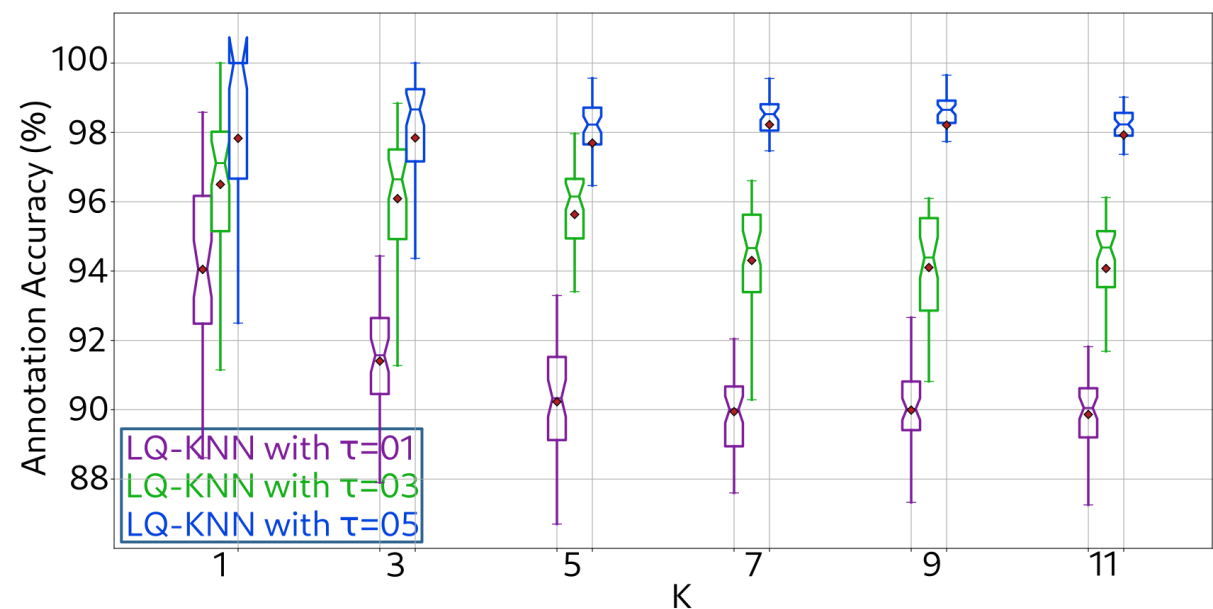
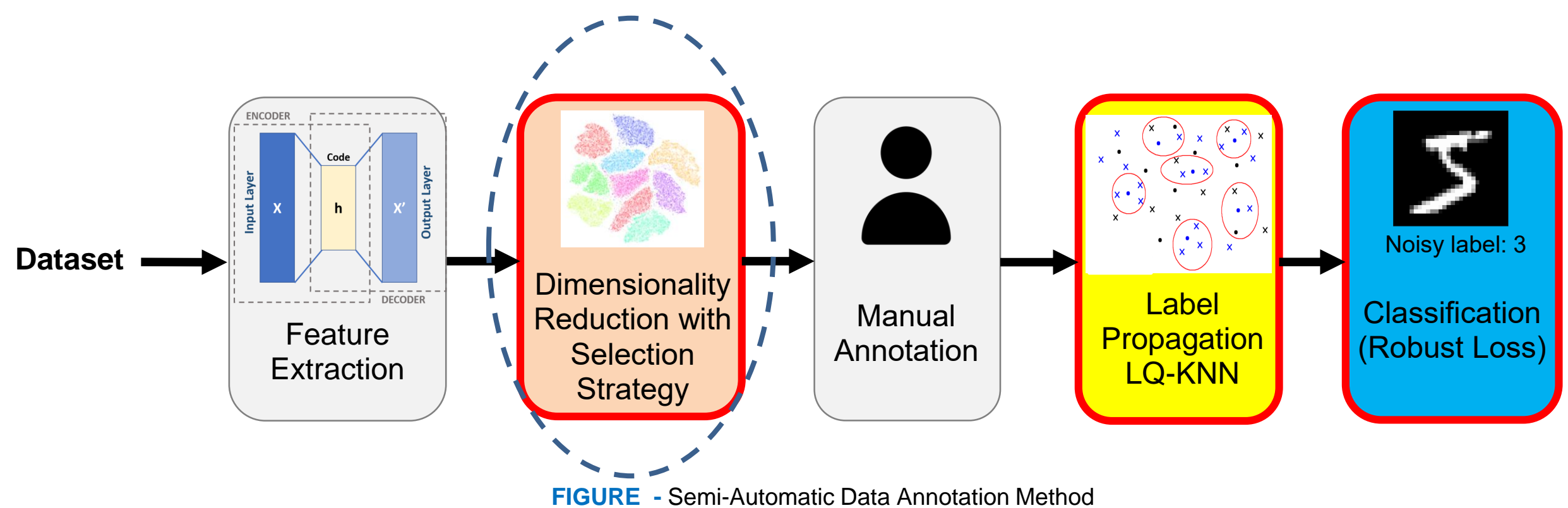


Figure - Comparison of LQ-KNN label propagation with different hyper-parameters using a HITS dataset

Proposed pipeline



Dimensionality Reduction

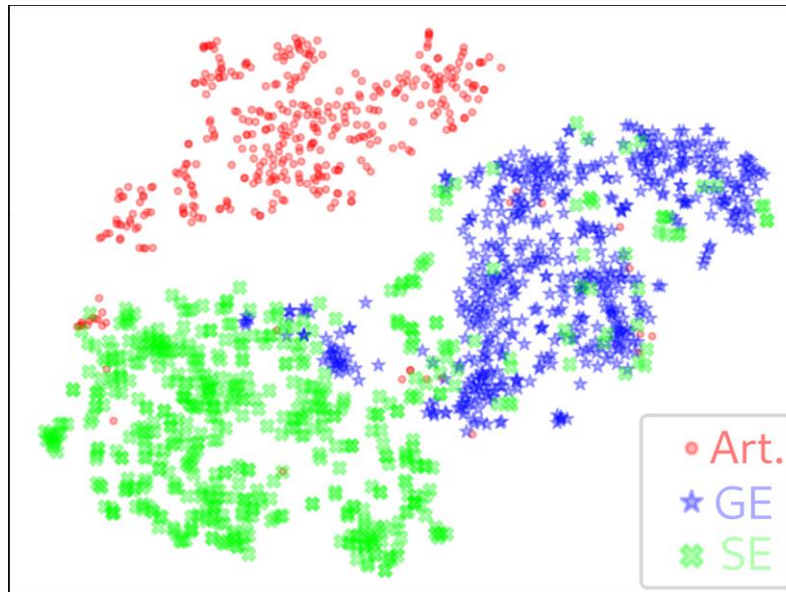
Silhouette Score¹

Compares the **similarity** of a sample k **between** :

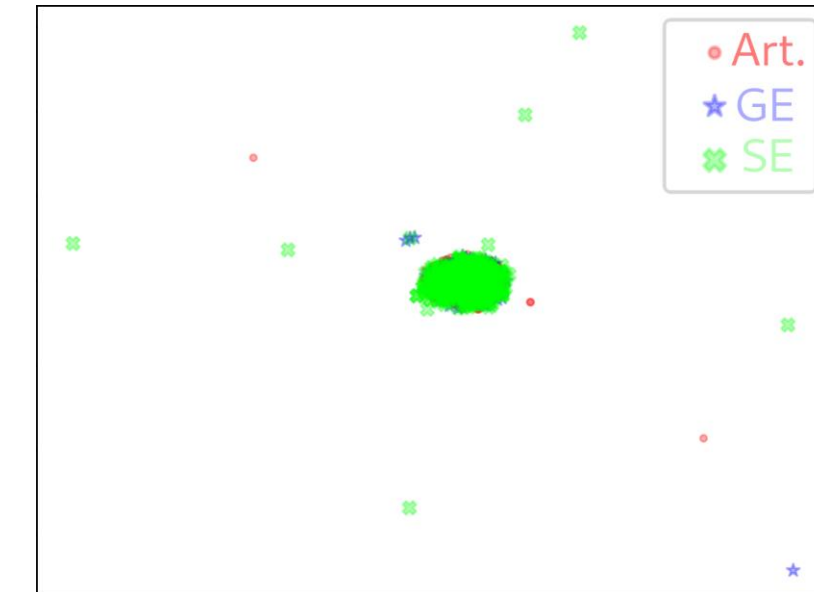
- The **samples** of its **own class**.
 - The samples of **other classes**.
- ==> The higher the better

$$\forall k \in [1, L], s(k) = \begin{cases} \frac{\mu_{\text{inter}}(k) - \mu_{\text{intra}}(k)}{\max(\mu_{\text{inter}}(k), \mu_{\text{intra}}(k))} & \text{if } |C_p| \geq 2 \\ 0 & \text{else} \end{cases}$$

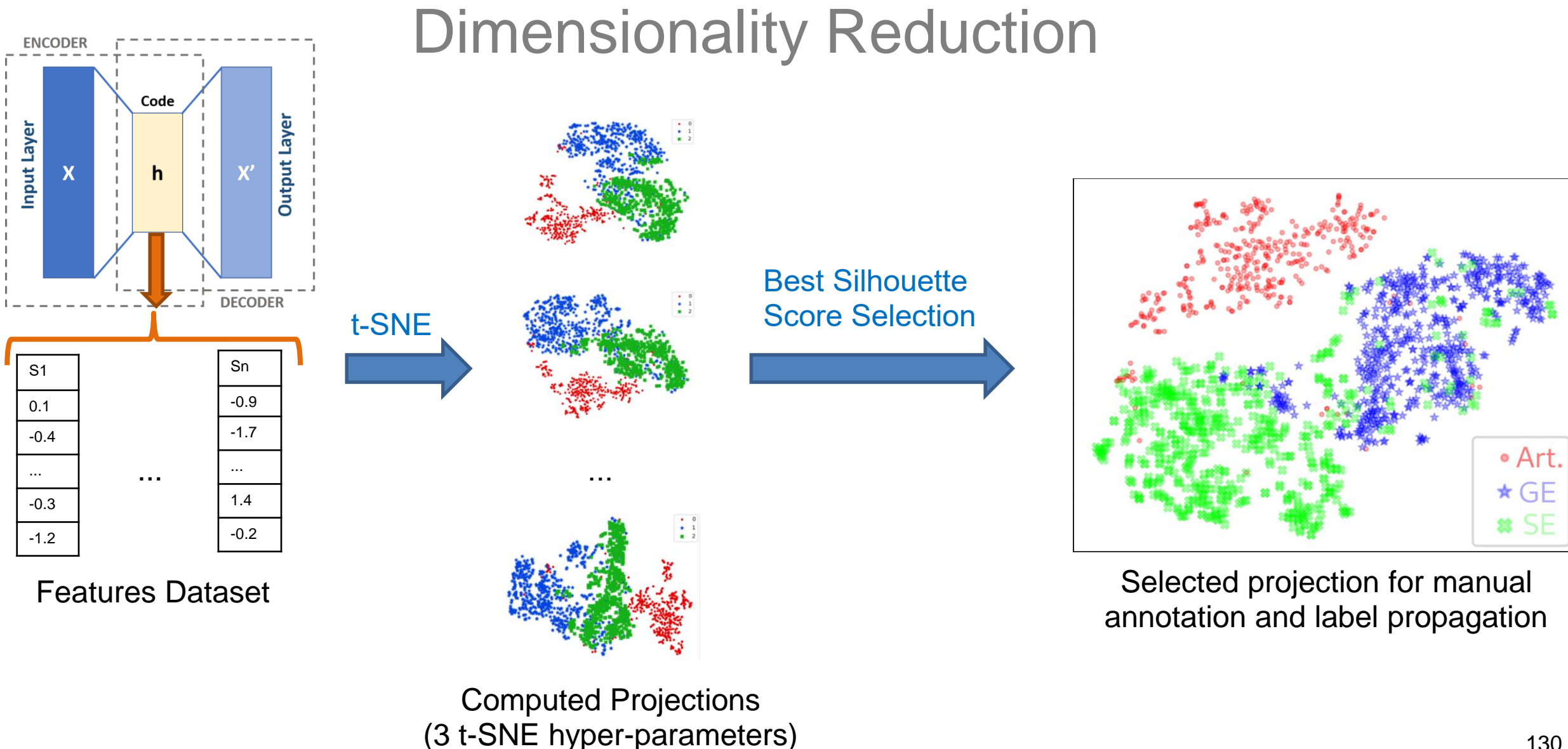
Projection with a Silhouette Score of 0.49



Projection with a Silhouette Score of -0.56



¹Rousseeuw - 1987 - Silhouettes: A graphical aid to the interpretation and validation of cluster analysis



Contribution 1.a.: Semi-automatic data annotation method **state-of-the-art comparison**

Considered neighborhood to propagate the labels



Dataset	Propagation method	$ L $	$ \mathcal{U} $	τ	K	Annotation accuracy	Final % of labeled samples (%)	Annotation time (ms/sample)
MNIST	Std-KNN	1496	13504	-	5	91.83 ± 1.47	95.39 ± 1.05	$(30.98 \pm 5.84) \times 10^{-3}$
	Std-KNN	1496	13504	-	10	90.74 ± 1.45	99.43 ± 0.23	$(28.78 \pm 5.13) \times 10^{-3}$
	LQ-KNN	1496	13504	0.1	5	93.12 ± 1.36	93.88 ± 0.66	$(59.10 \pm 12.35) \times 10^{-3}$
	LQ-KNN	1496	13504	0.1	10	92.66 ± 1.30	98.16 ± 0.42	$(50.48 \pm 11.32) \times 10^{-3}$
OrganCMNIST	OPF-semi	1496	13504	-	-	82.32 ± 6.17	100.0 ± 0.0	102.71 ± 17.52
	Std-KNN	1534	13858	-	5	81.87 ± 0.76	90.26 ± 2.64	$(26.33 \pm 2.65) \times 10^{-3}$
	Std-KNN	1534	13858	-	10	79.86 ± 0.67	99.00 ± 0.20	$(23.41 \pm 1.98) \times 10^{-3}$
	LQ-KNN	1534	13858	0.1	5	84.46 ± 0.57	85.62 ± 1.99	$(53.00 \pm 7.47) \times 10^{-3}$
	LQ-KNN	1534	13858	0.1	10	82.73 ± 0.44	96.24 ± 1.09	$(44.36 \pm 5.69) \times 10^{-3}$
	OPF-semi	1534	13858	-	-	75.22 ± 4.48	100.0 ± 0.0	86.52 ± 0.51
HITS	Std-KNN	152	1393	-	5	82.12 ± 2.37	95.99 ± 1.70	$(10.39 \pm 0.20) \times 10^{-2}$
	Std-KNN	152	1393	-	10	81.36 ± 1.81	99.58 ± 0.63	$(10.04 \pm 0.18) \times 10^{-2}$
	LQ-KNN	152	1393	0.1	5	82.84 ± 2.12	94.48 ± 1.72	$(16.87 \pm 0.48) \times 10^{-3}$
	LQ-KNN	152	1393	0.1	10	82.67 ± 2.02	98.50 ± 0.80	$(16.13 \pm 0.35) \times 10^{-2}$
	OPF-semi	152	1393	-	-	78.40 ± 13.44	100.0 ± 0.0	9.48 ± 1.1

Table – Label propagation methods comparison on different datasets

Metrics:

Annotation accuracy:

$$\frac{\text{\# correct new labeled samples}}{\text{\# new labeled samples}}$$

Percentage of new labeled samples:

$$\frac{\text{\# new labeled samples}}{\text{\# originally unlabeled samples}}$$

Contribution 1.b: Optimal 2D projection selection.

Dataset: HITS Dataset.

Evaluation: Label Propagation on 2 different projections.

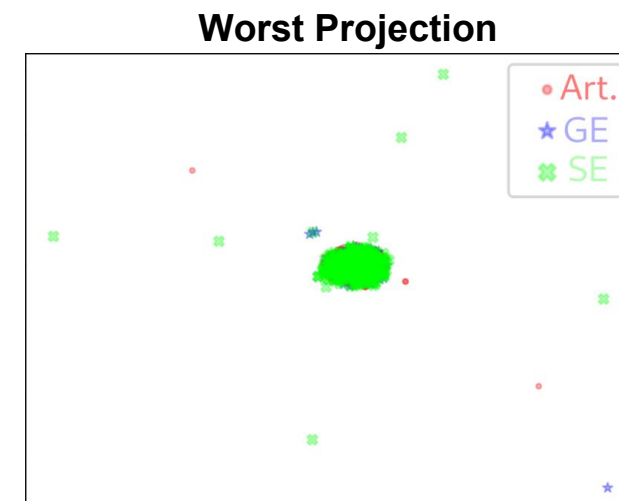
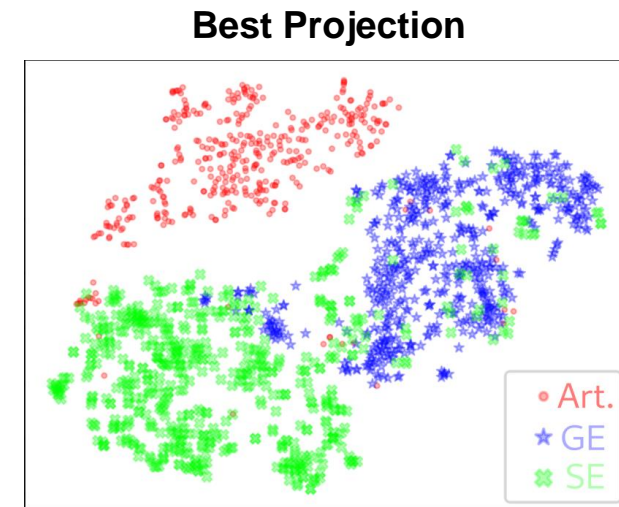
Metrics: Annotation accuracy and percentage of new labeled samples.

Results:

K	Propagation method	Projection	$ \mathcal{L} $	$ \mathcal{U} $	τ	Annotation accuracy	Final % of labeled samples
5	Std-KNN	Best	152	1393	-	89.8 ± 1.63	95.52 ± 1.23
	Std-KNN	Worst	152	1393	-	52.2 ± 2.53	98.78 ± 0.42
5	LQ-KNN	Best	152	1393	0.1	90.23 ± 1.46	94.93 ± 1.32
	LQ-KNN	Worst	152	1393	0.1	70.69 ± 2.64	57.4 ± 2.01

Conclusion:

- Projection selection improves annotation accuracy.
- Our proposed method is more robust against bad projections.



Contribution 1.b: Optimal 2D projection selection.

Dataset: HITS Dataset.

Evaluation: Label Propagation on 2 different projections.

Metrics: Annotation accuracy and percentage of new labeled samples.

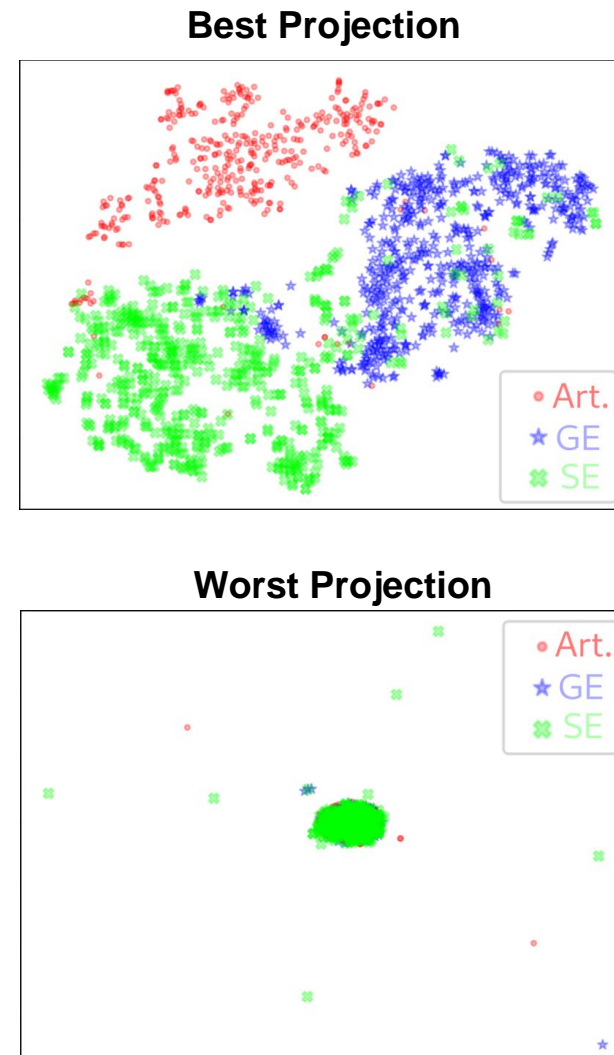
Results:




K	Propagation method	Projection	$ \mathcal{L} $	$ \mathcal{U} $	τ	Annotation accuracy	Final % of labeled samples
5	Std-KNN	Best	152	1393	-	89.8 ± 1.63	95.52 ± 1.23
		Worst	152	1393	-	52.2 ± 2.53	98.78 ± 0.42
5	LQ-KNN	Best	152	1393	0.1	90.23 ± 1.46	94.93 ± 1.32
		Worst	152	1393	0.1	70.69 ± 2.64	57.4 ± 2.01

Conclusion:

- Projection selection improves annotation accuracy.
- Our proposed method is more robust against bad projections.



Contribution 1.b: Optimal 2D projection selection.

Dataset: HITS Dataset.

Evaluation: Label Propagation on 2 different projections.

Metrics: Annotation accuracy and percentage of new labeled samples.

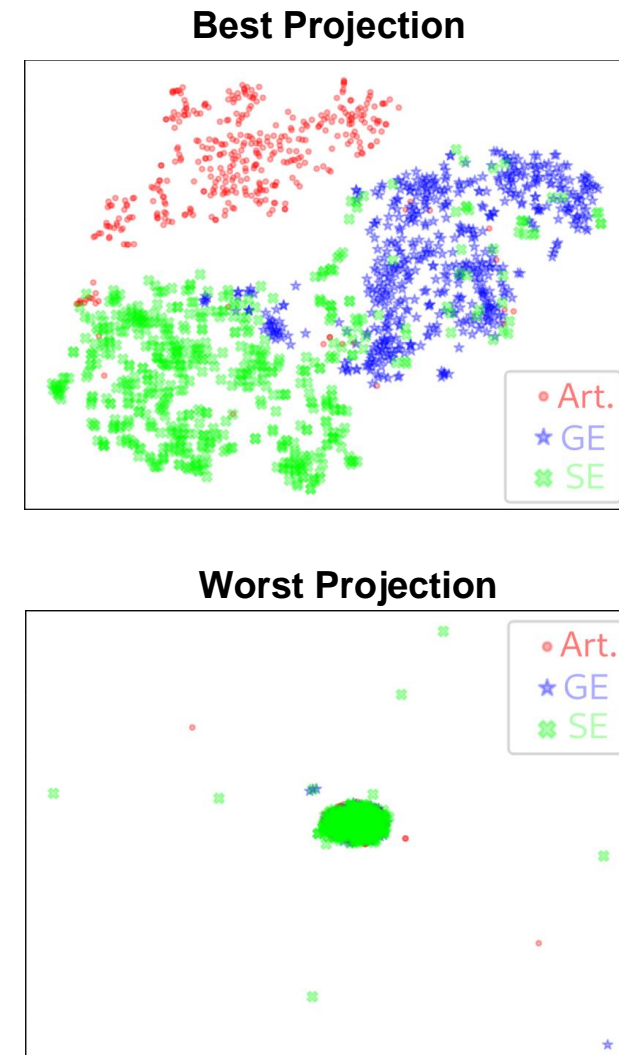
Results:

K	Propagation method	Projection	$ \mathcal{L} $	$ \mathcal{U} $	τ	Annotation accuracy	Final % of labeled samples
5	Std-KNN	Best	152	1393	-	89.8 ± 1.63	95.52 ± 1.23
		Worst	152	1393	-	52.2 ± 2.53	98.78 ± 0.42
5	LQ-KNN	Best	152	1393	0.1	90.23 ± 1.46	94.93 ± 1.32
		Worst	152	1393	0.1	70.69 ± 2.64	57.4 ± 2.01



Conclusion:

- Projection selection improves annotation accuracy.
- Our proposed method is more robust against bad projections.



Contribution 1.c: Classification using robust loss functions to compensate the noise in the labels.

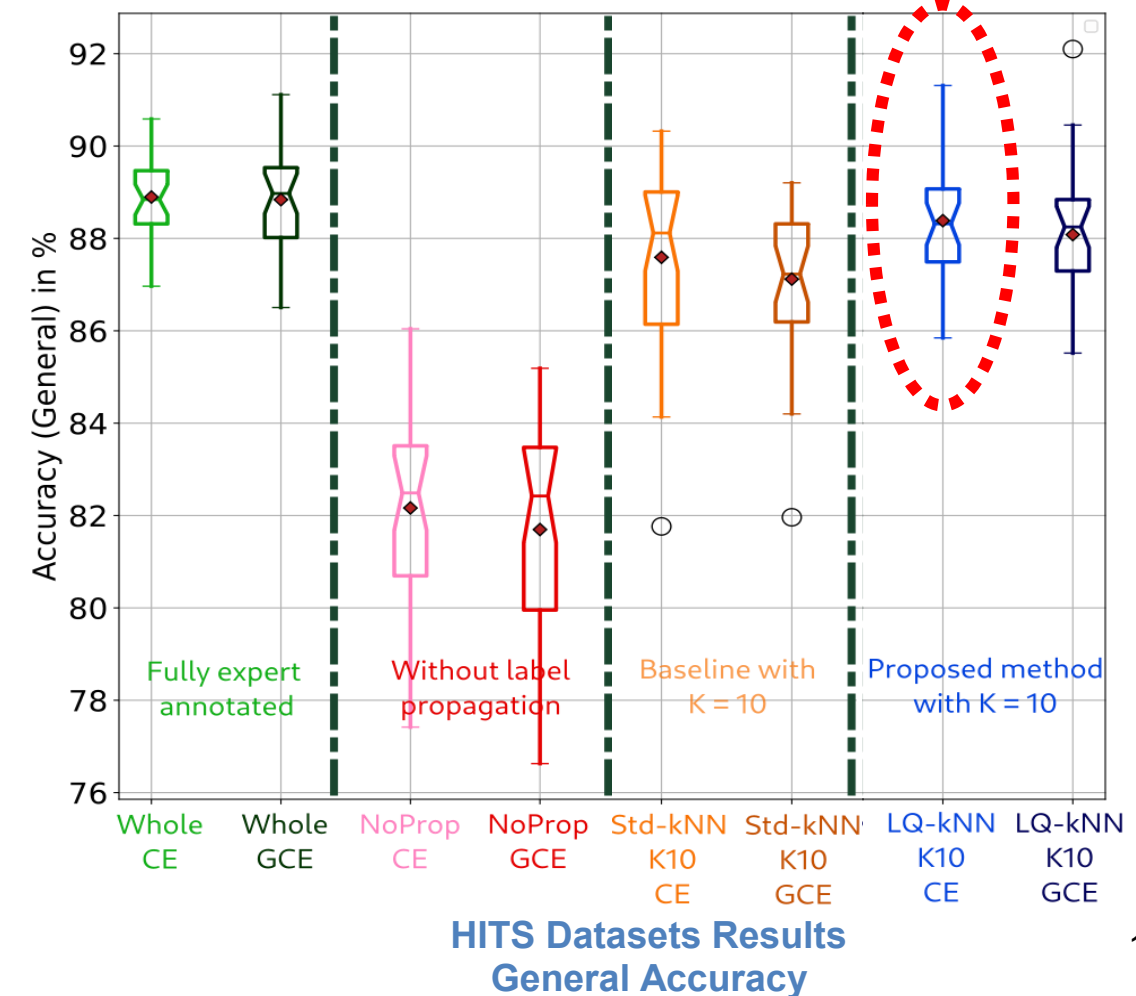
Datasets

Dataset	Core Dataset	Prop. method	$ \mathcal{L} $	$ \mathcal{U} $	# of automatically labeled samples	Mean annot. accuracy	K	τ
HITS No Prop.	HITS	No Prop.	152	1393	-	-	-	-
HITS Whole		No Prop.	1545	0	-	-	-	-
HITS Std-KNN-K10		Std-KNN			1390 ± 2	88.72 ± 2.33	10	-
HITS LQ-KNN-K10		LQ-KNN			1382 ± 3	89.92 ± 1.42	10	0.1

Metrics:

Classification accuracy.
Classification class accuracy.

==> Our method allows to increase the classification accuracy by 6 % with respect to using a reduced dataset (no propagation)



Database Creation

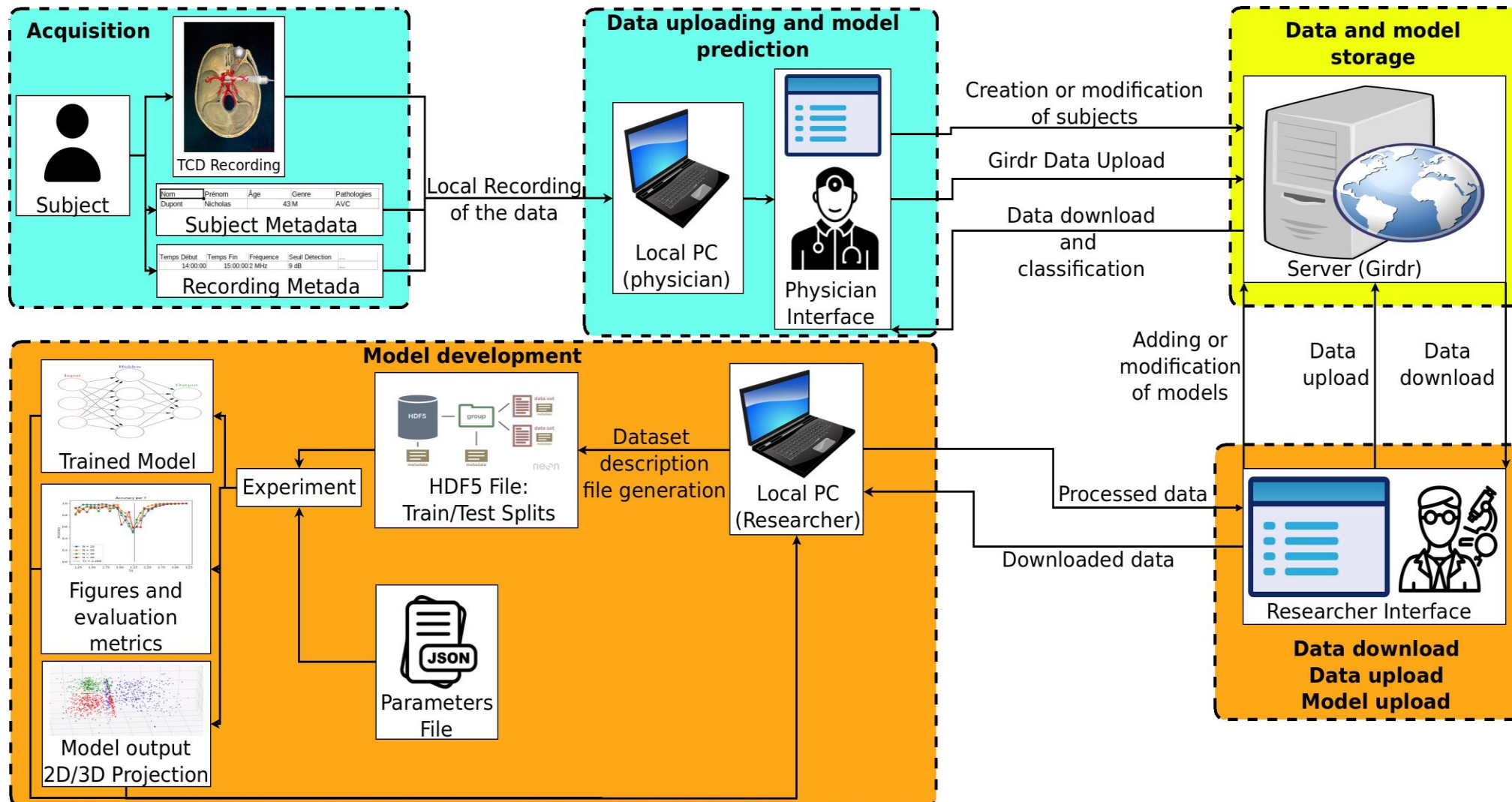


Figure – Data pipeline. Two types of data : raw and derivative.

Database Structure

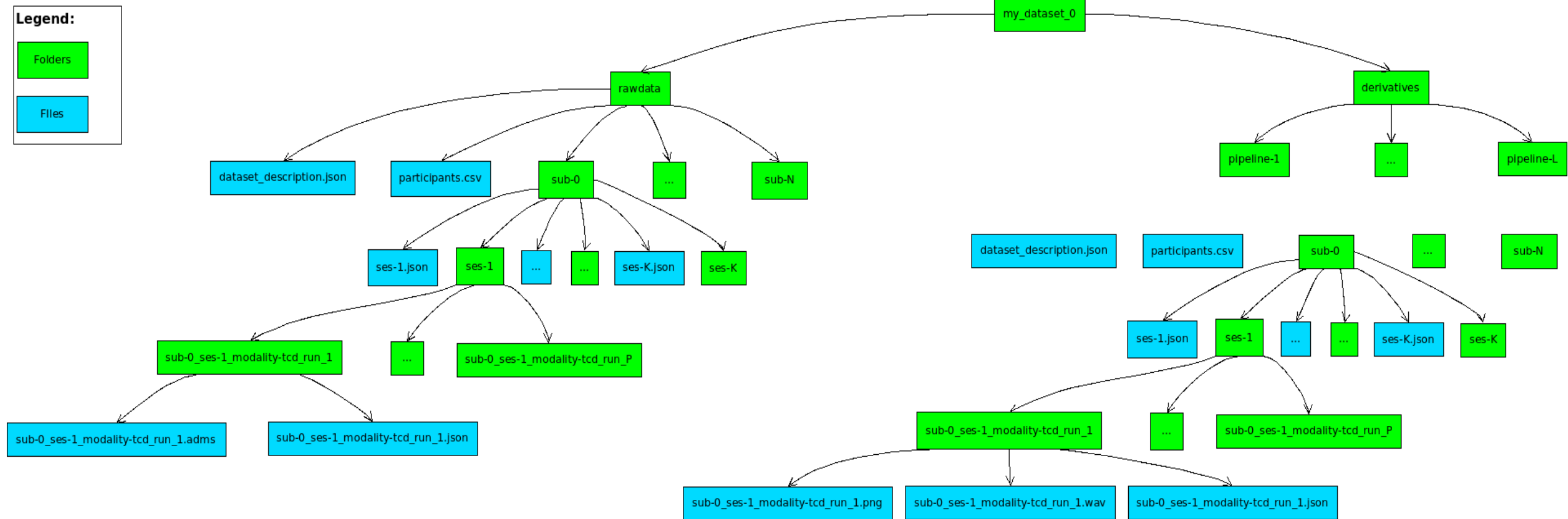


Figure – Database structure on Gridr

Auto-encoders architectures

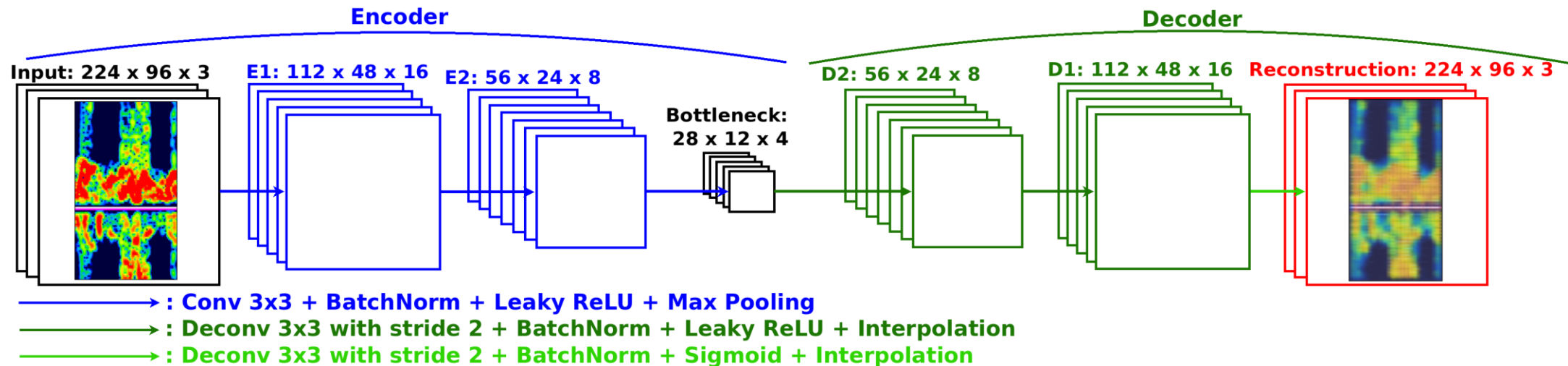


Figure – Convolutional auto-encoder for the HITS dataset.

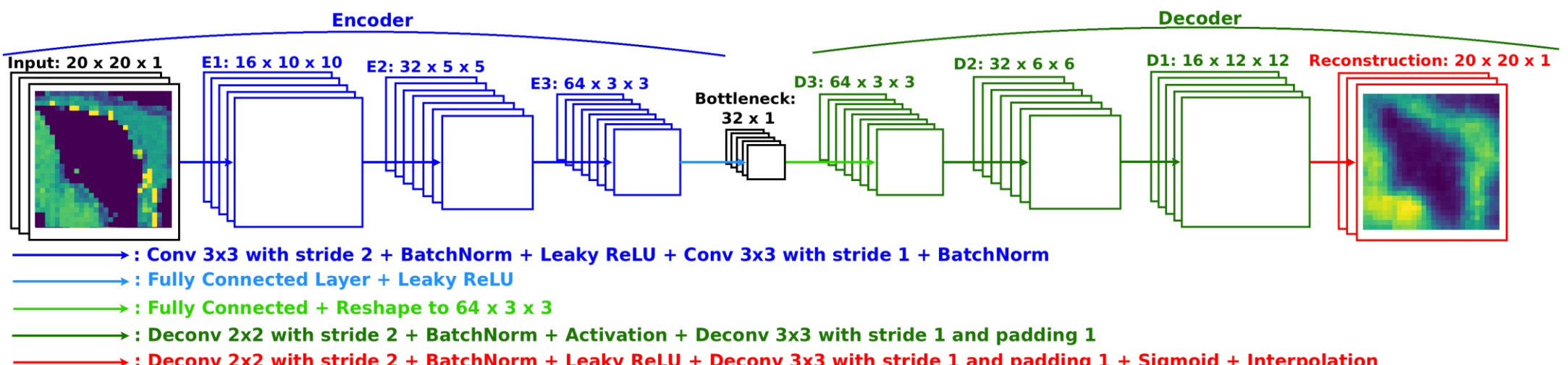


Figure – Convolutional auto-encoder for the OrganCMNIST and MNIST datasets.

Classifiers architectures

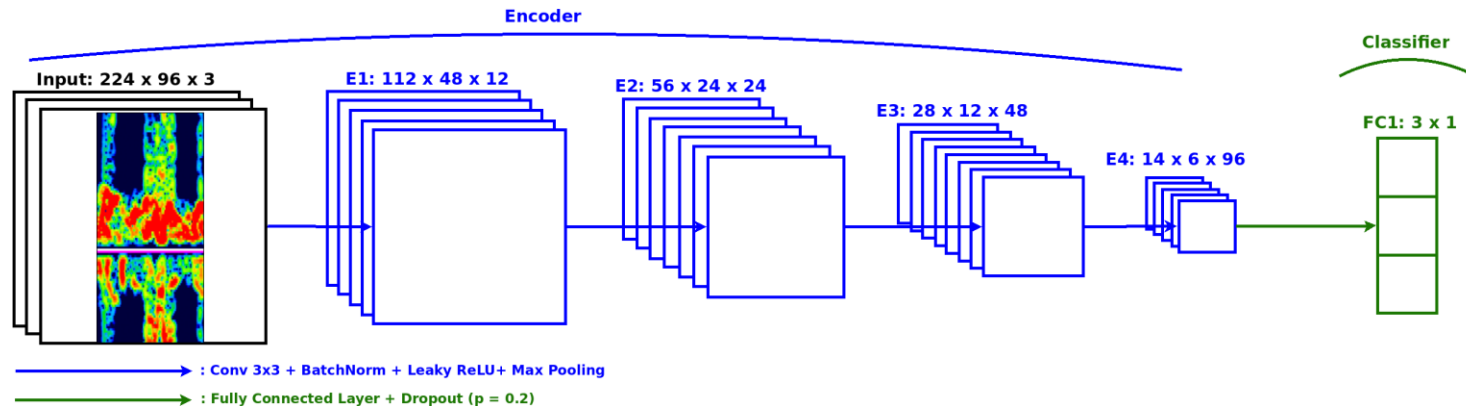


Figure – Convolutional classifier for the HITS dataset.

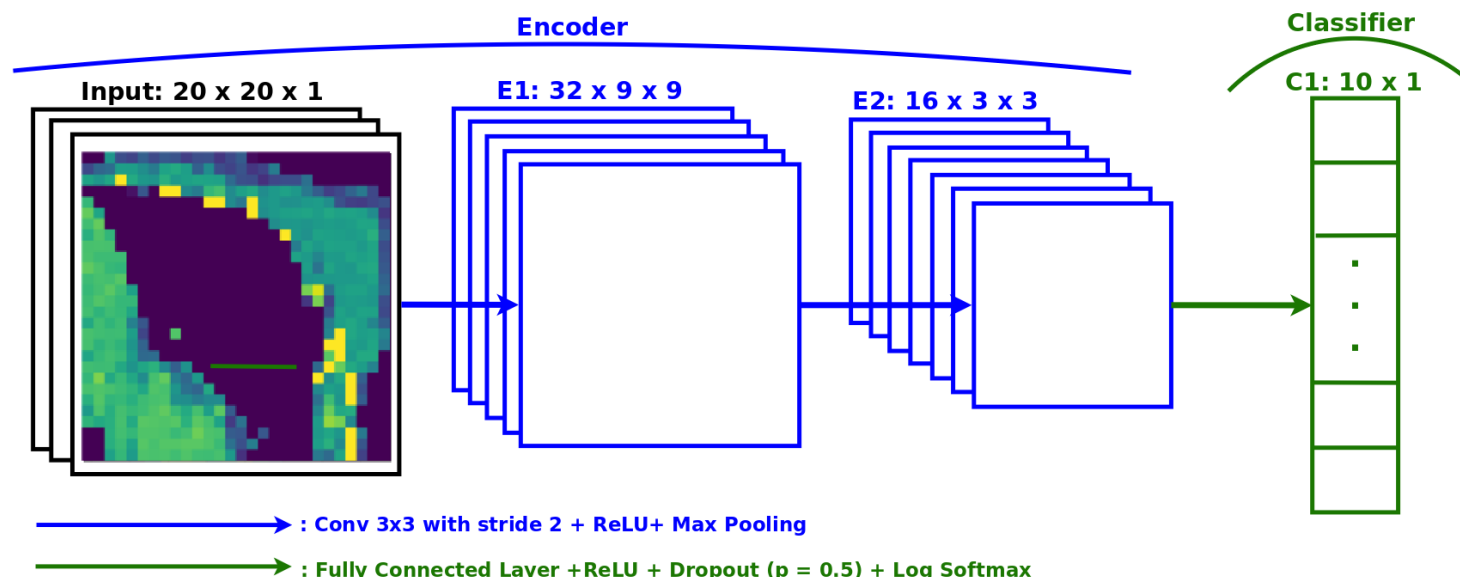


Figure – Convolutional classifier for the OrganCMNIST and MNIST

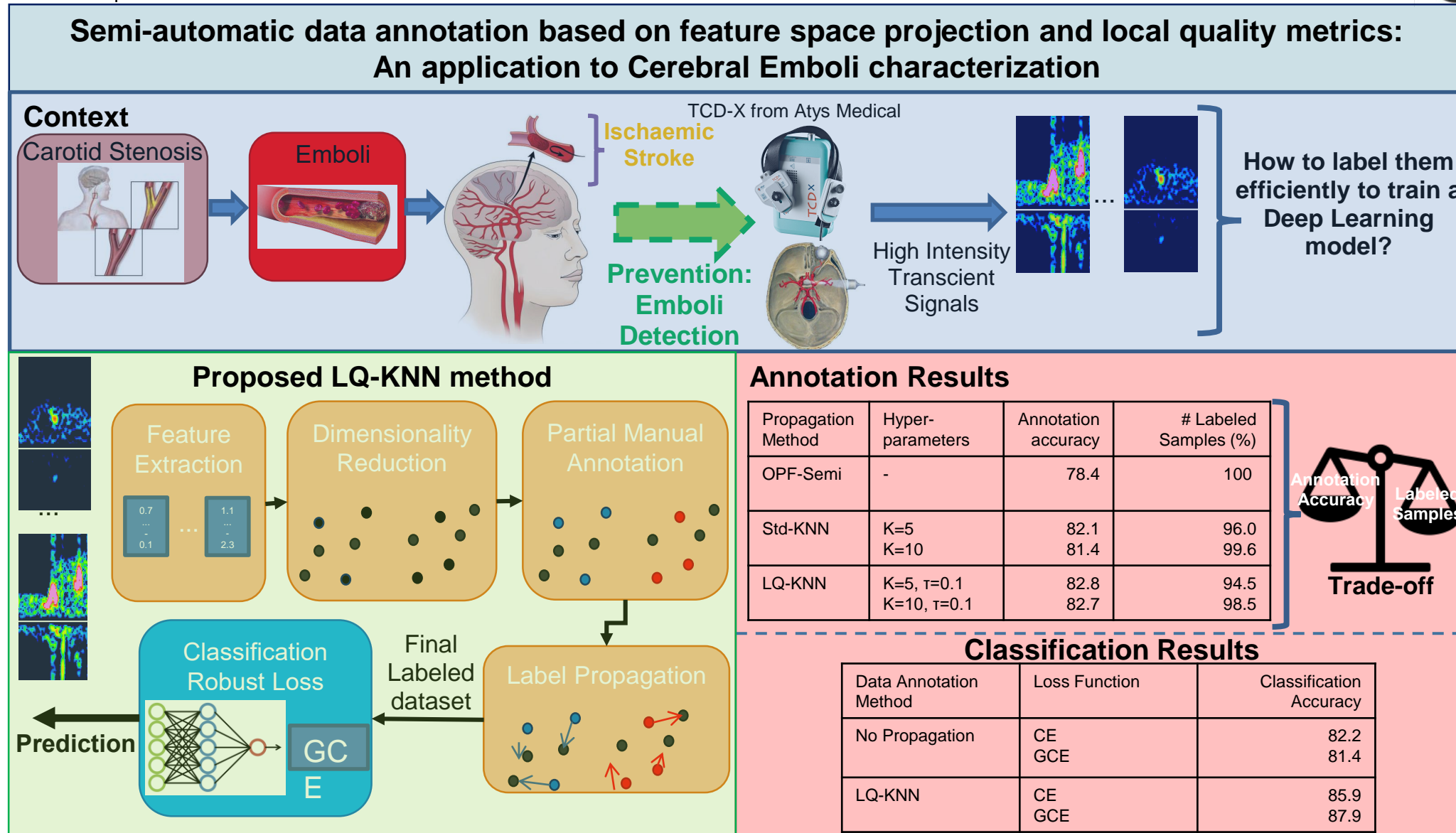


FIGURE - Graphical abstract of Vindas et al. (2022) in Medical Image Analysis

Contribution 2 : Multi-feature medical signal classification

ECG 1D CNN-transformer

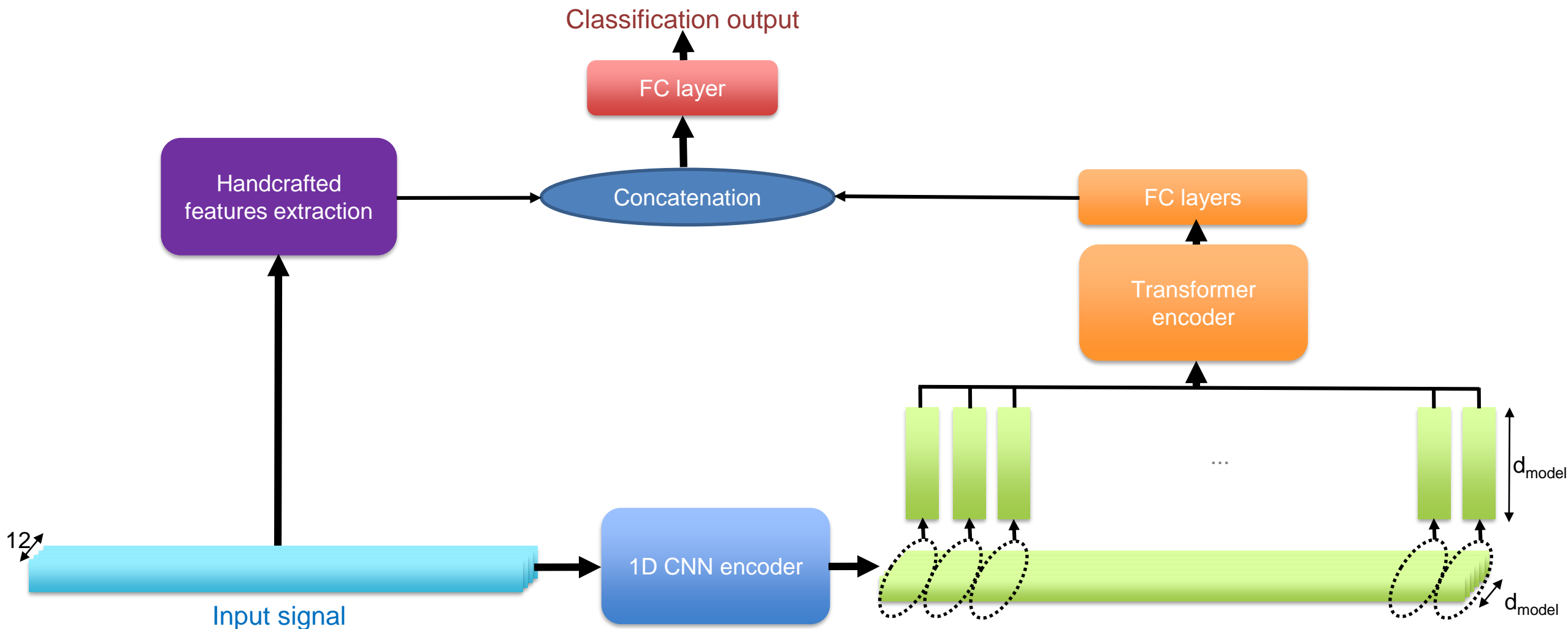
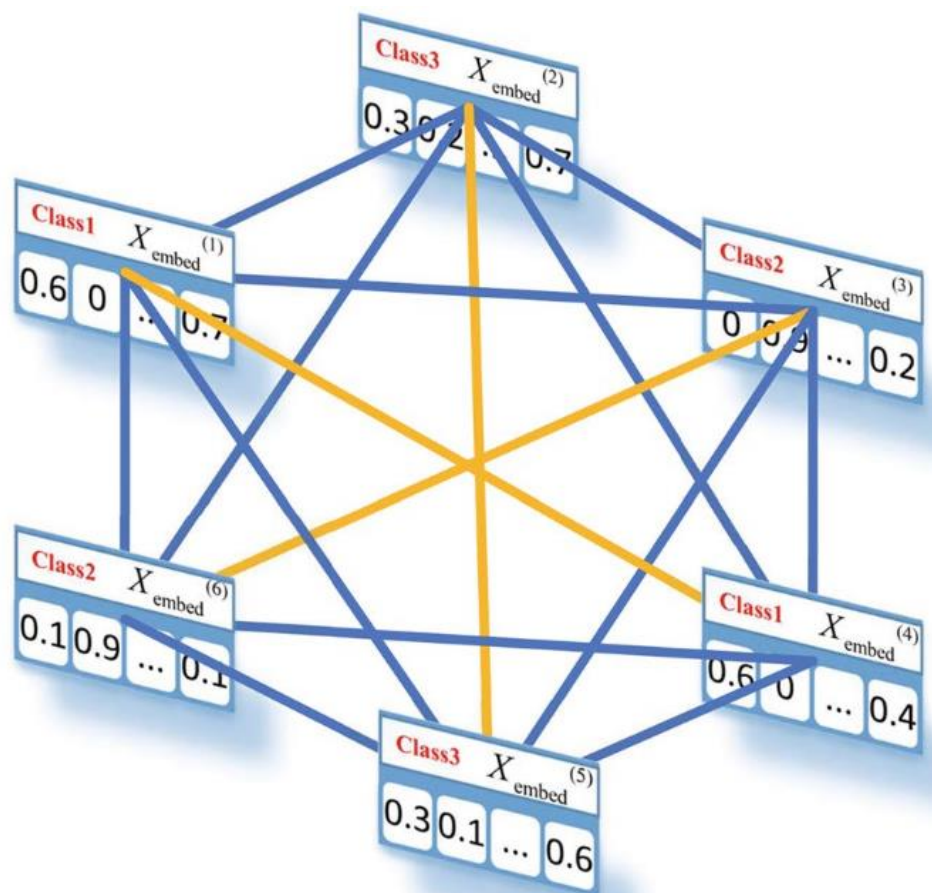
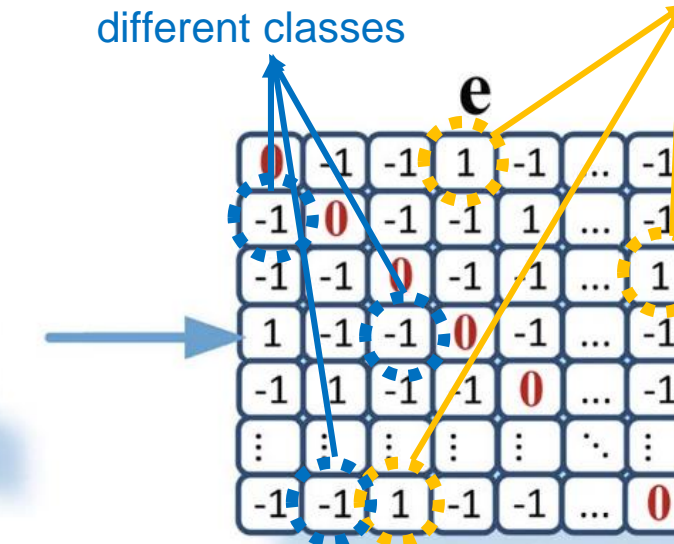


Figure - Proposed 1D CNN-transformer model for ECG signal classification (**Natarajan et al., 2020.**)

Link constraints regularization



-1 → samples of the different classes
1 → samples of the same class



The Link Constraints



Figure – Links constraints regularization illustration for transformer models (Che et al., 2021)

Deep embedded clustering (DEC)

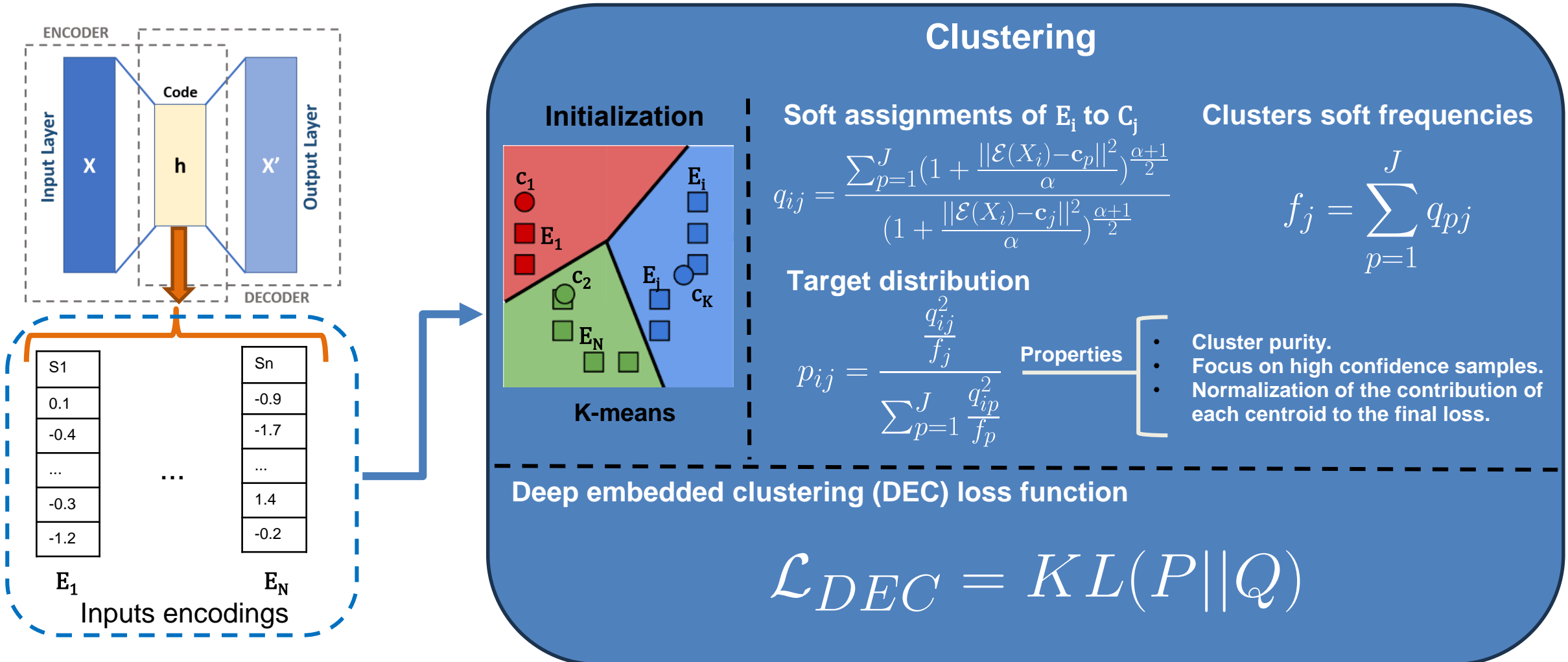


Figure – Deep embedded clustering (DEC) for unsupervised learning (Xie et al., 2016)

Single feature raw signal 1D CNN-transformer

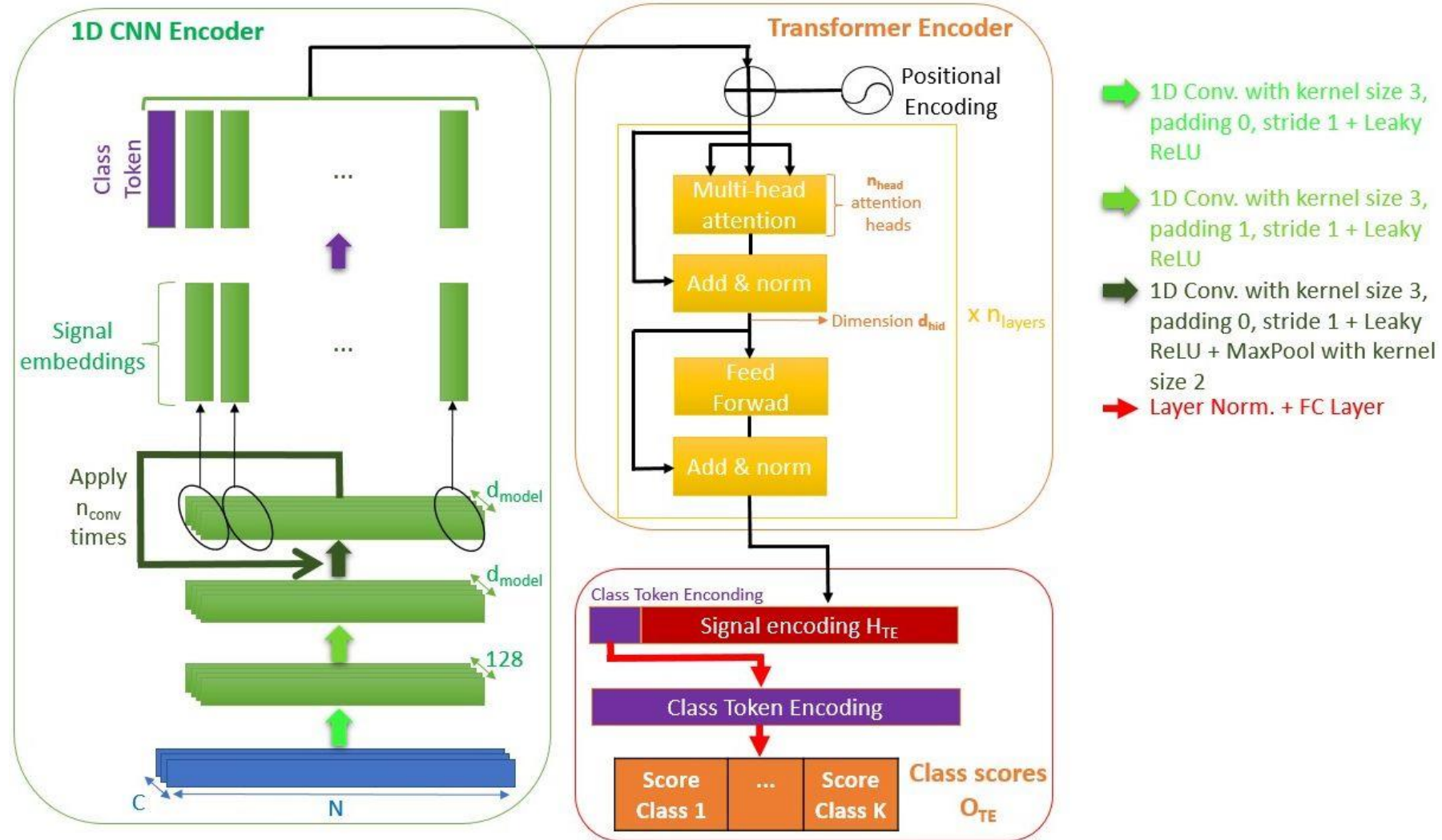


Figure - Proposed 1D CNN Transformer architecture (inspired from [Natarajan et al. 2020](#)).

Single feature raw signal 1D CNN-transformer

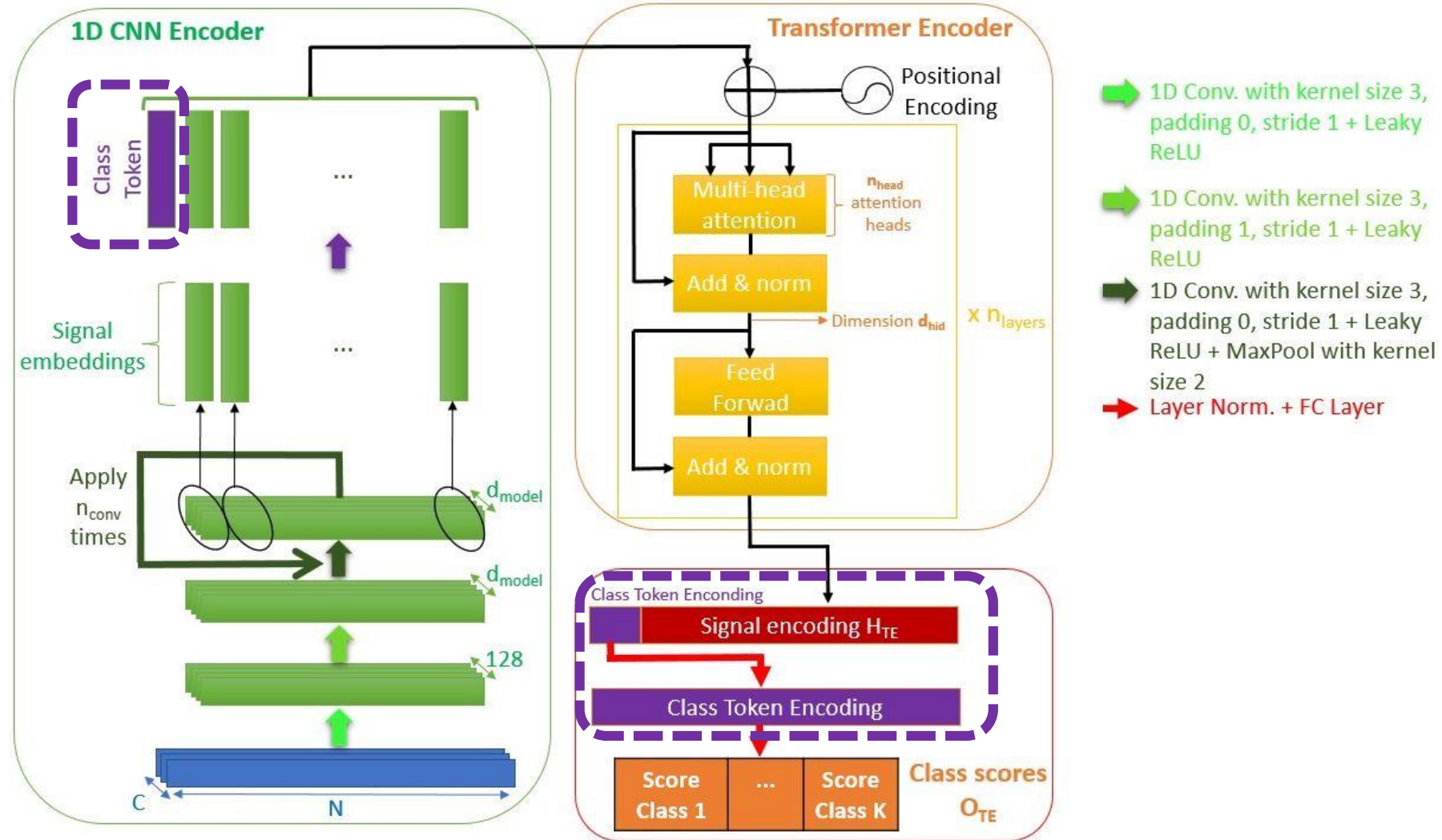
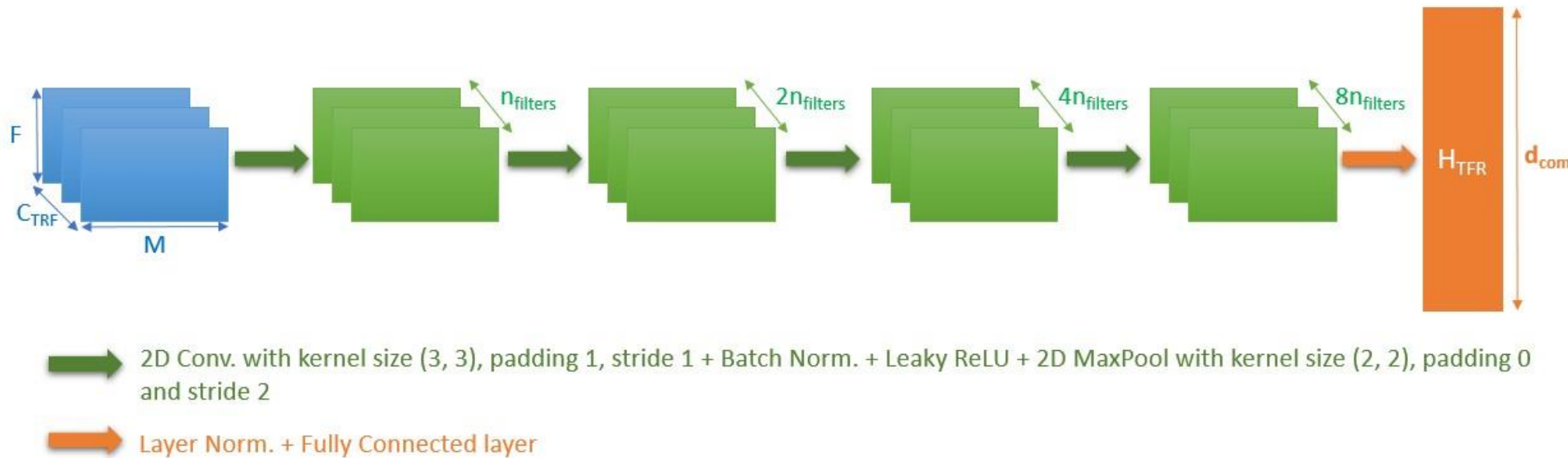
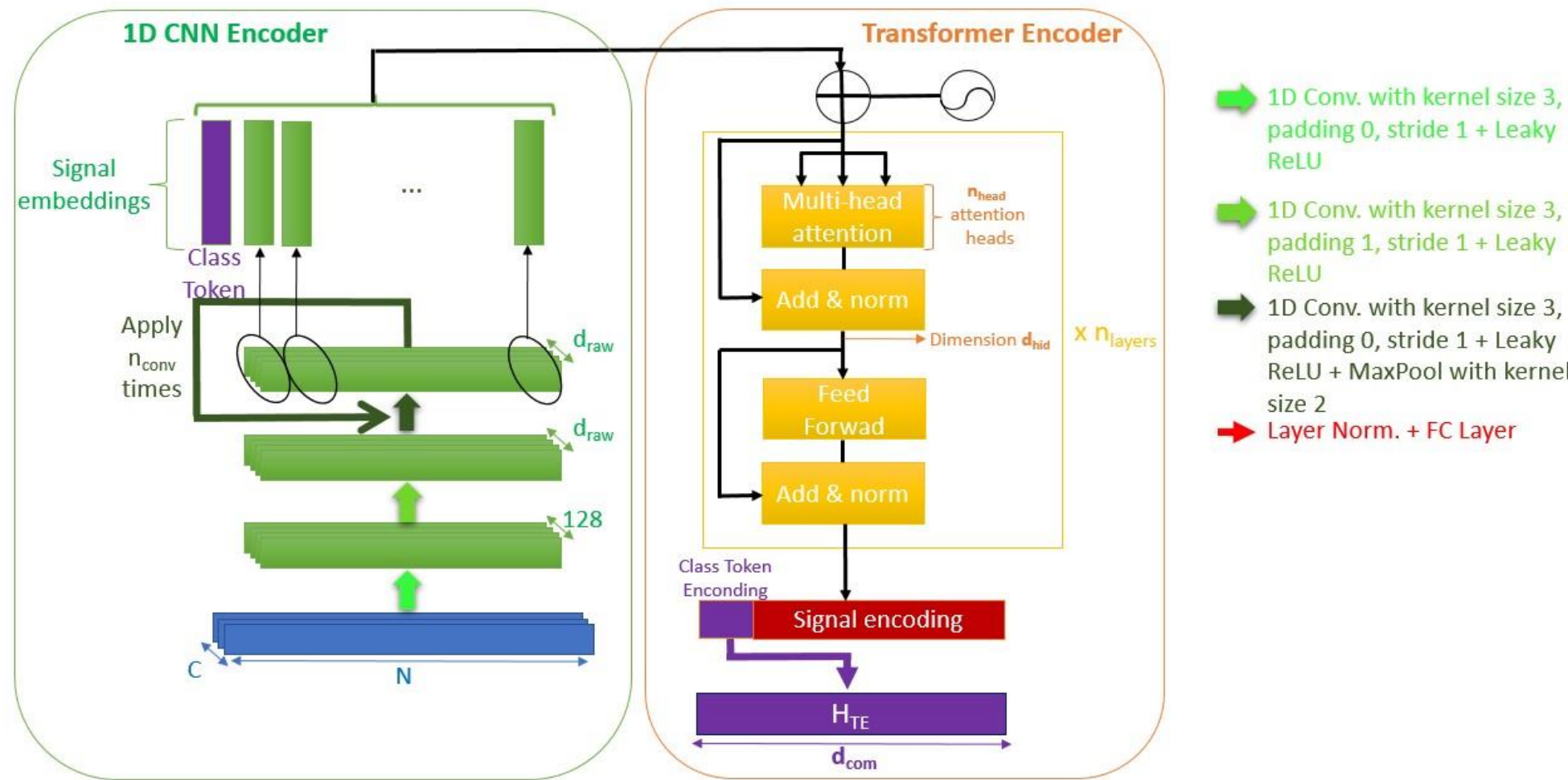


Figure - Proposed 1D CNN Transformer architecture (inspired from [Natarajan et al. 2020](#)).

CNN model late fusion approach

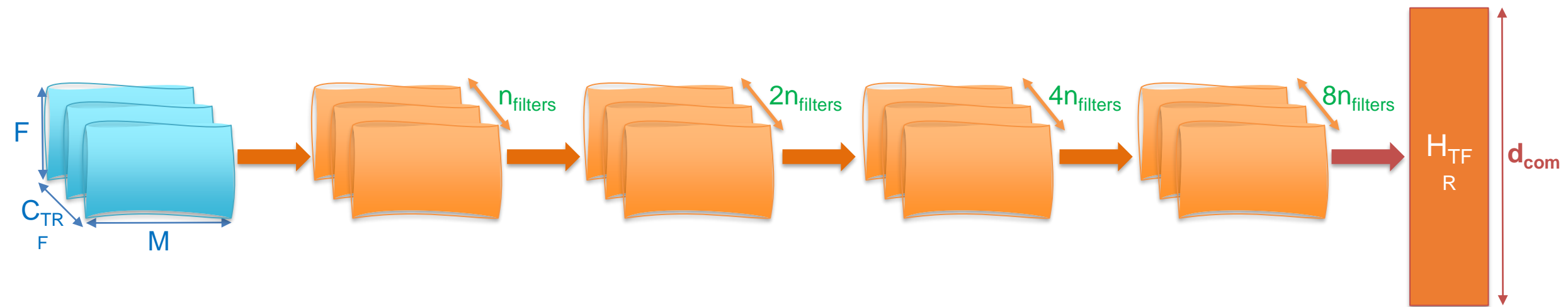


Transformer model intermediate fusion approach



Inspired from Natarajan et al. (2020), A wide and deep transformer neural network for 12-lead ecg classification.

CNN model intermediate fusion approach



- 2D Conv. with kernel size (3, 3), padding 1, stride 1 + Batch Norm. + Leaky ReLU + 2D MaxPool with kernel size (2, 2), padding 0 and stride 2
- Layer Norm. + Fully Connected layer

Late fusion attention weights

Figure - Proposed hybrid CNN Transformer global model

Late fusion attention weights

Raw
Signal

TFR
(Spectrogram)

Figure - Proposed hybrid CNN Transformer global model

Late fusion attention weights

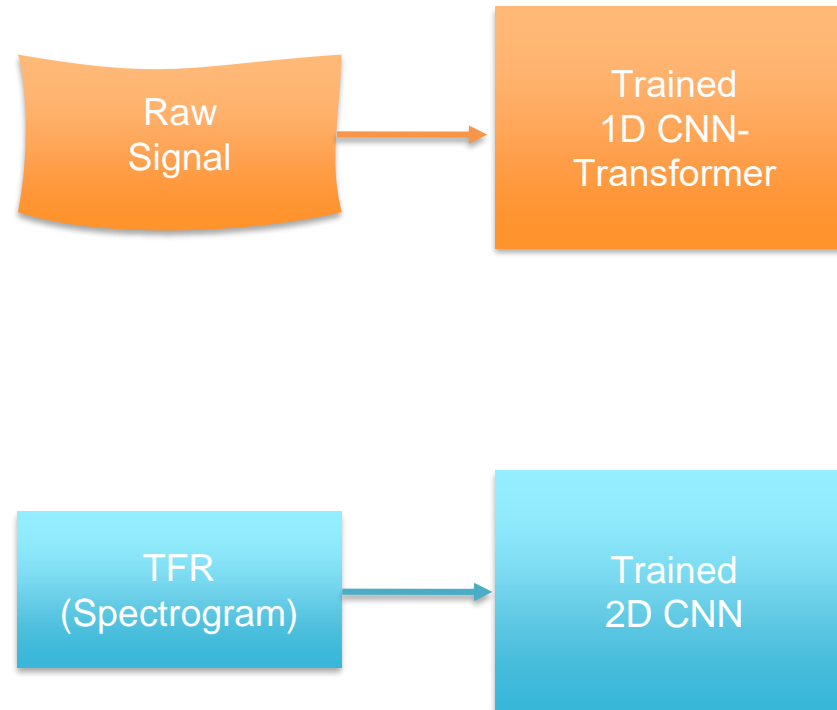


Figure - Proposed hybrid CNN Transformer global model

Late fusion attention weights

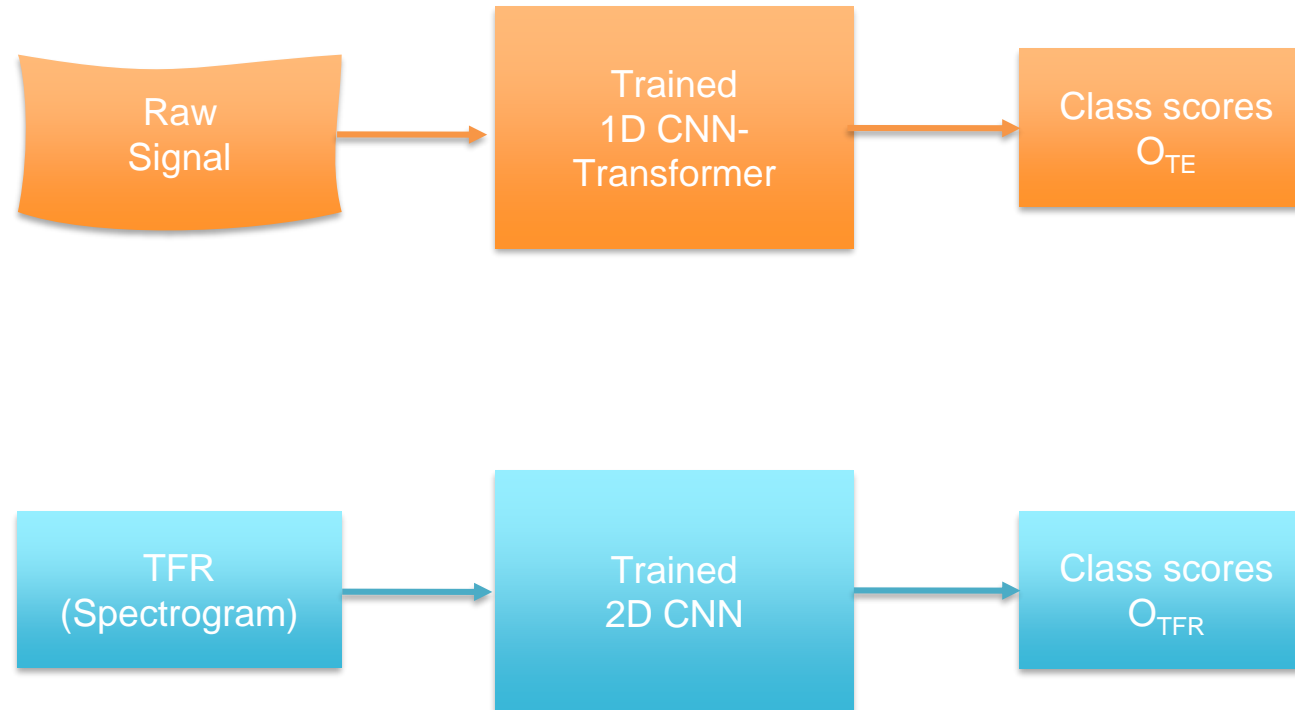


Figure - Proposed hybrid CNN Transformer global model

Late fusion attention weights

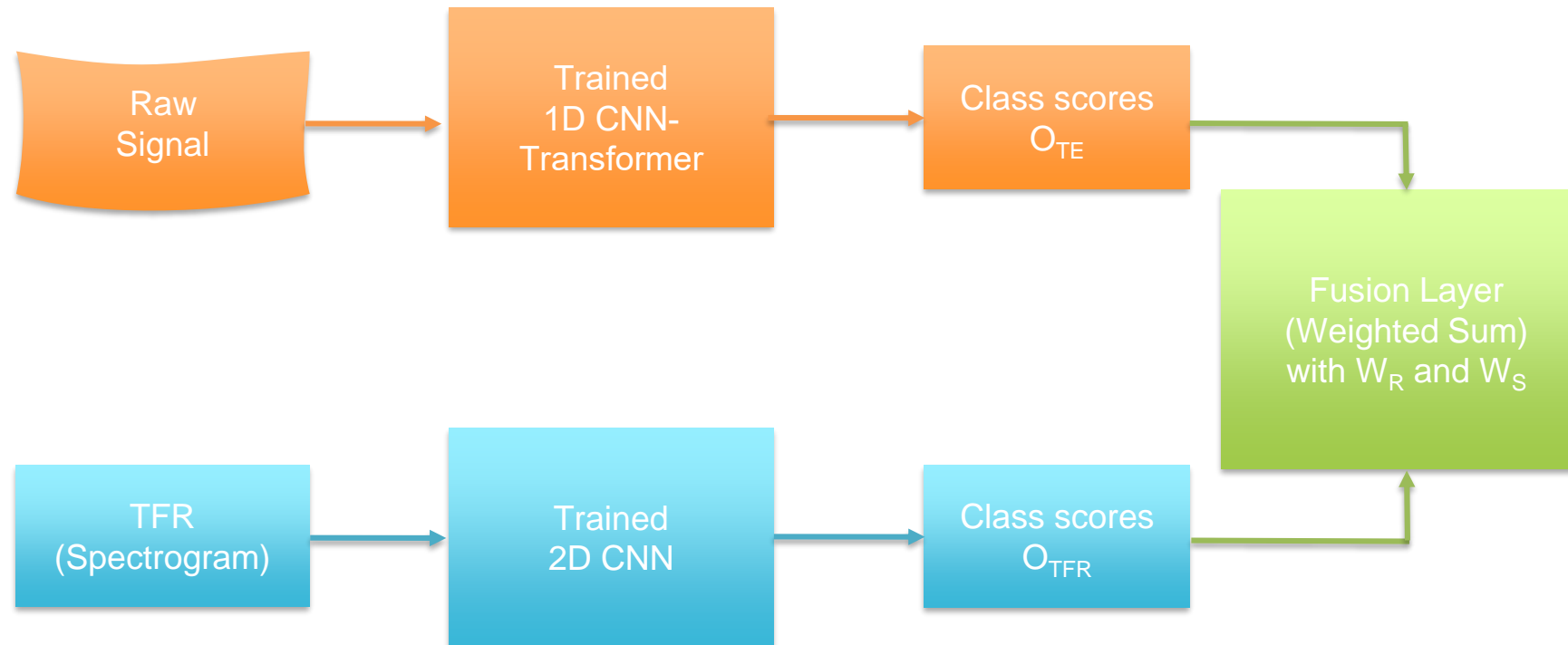


Figure - Proposed hybrid CNN Transformer global model

Late fusion attention weights

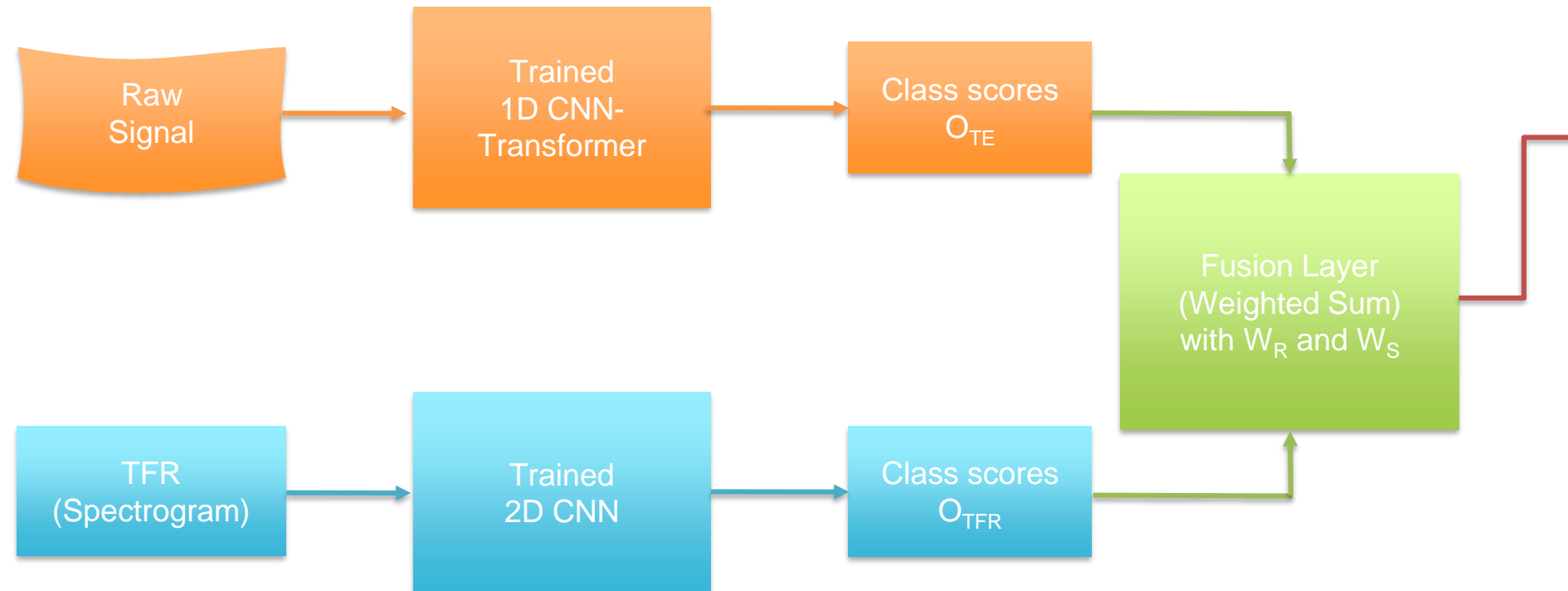


Figure - Proposed hybrid CNN Transformer global model

Late fusion attention weights

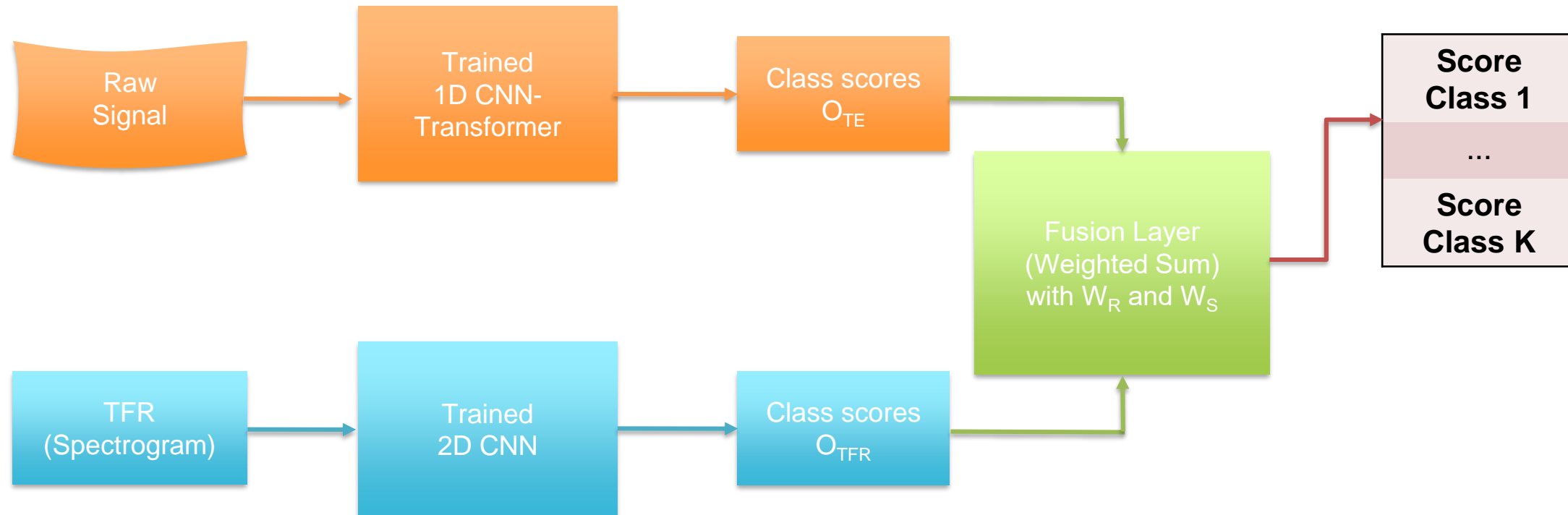


Figure - Proposed hybrid CNN Transformer global model

Late fusion attention weights

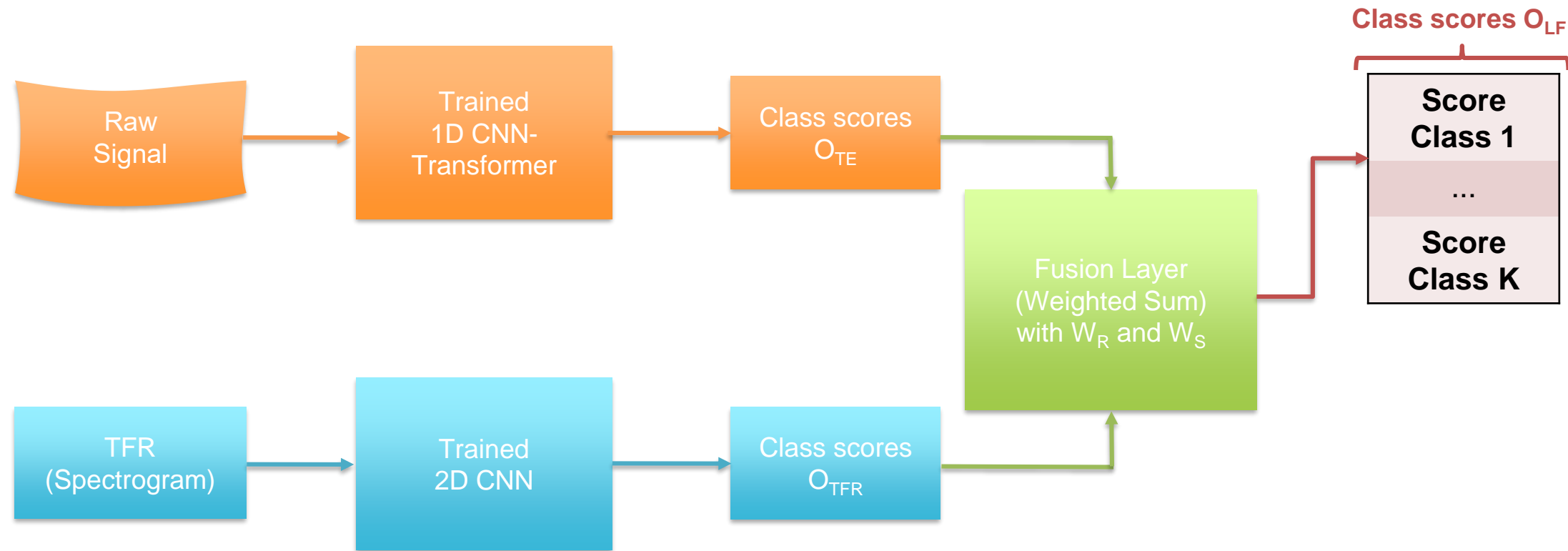


Figure - Proposed hybrid CNN Transformer global model

Late fusion attention weights

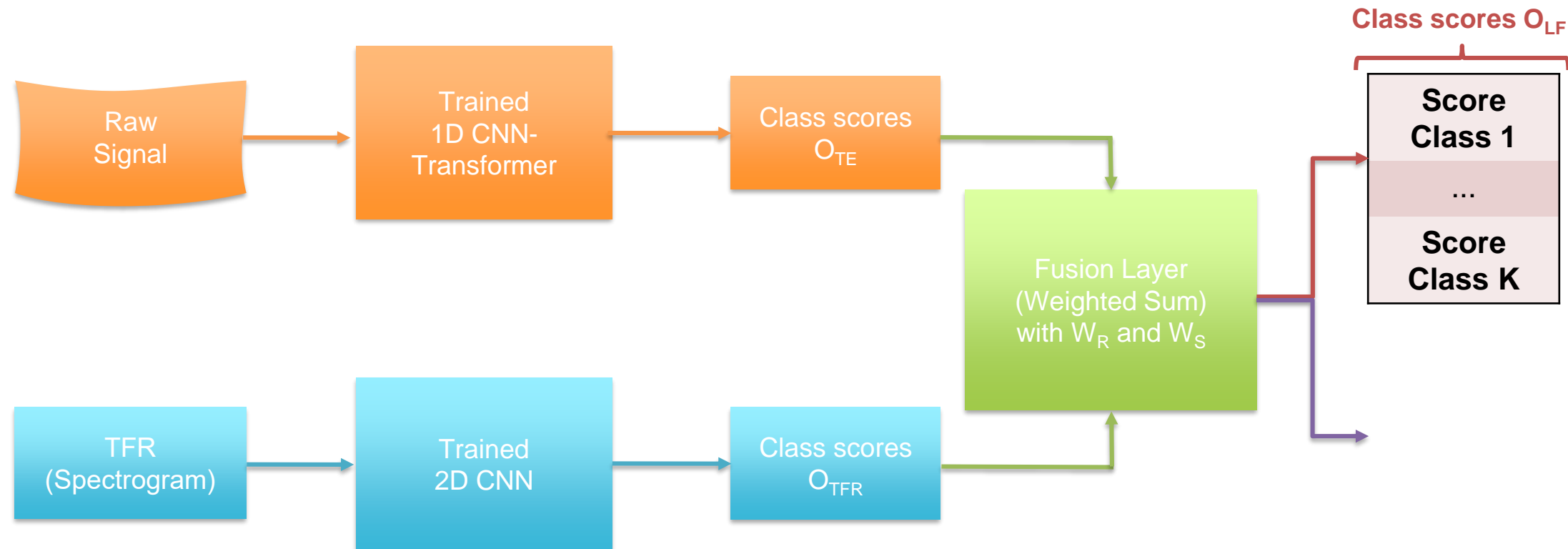


Figure - Proposed hybrid CNN Transformer global model

Late fusion attention weights

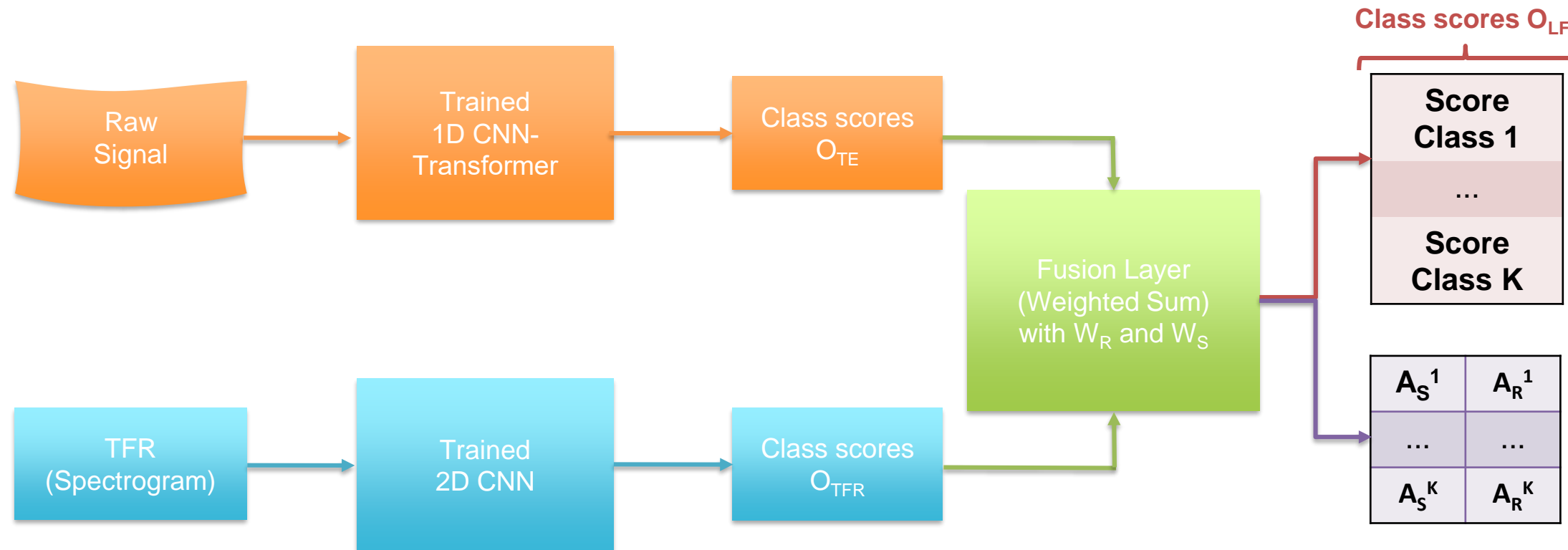


Figure - Proposed hybrid CNN Transformer global model

Late fusion attention weights

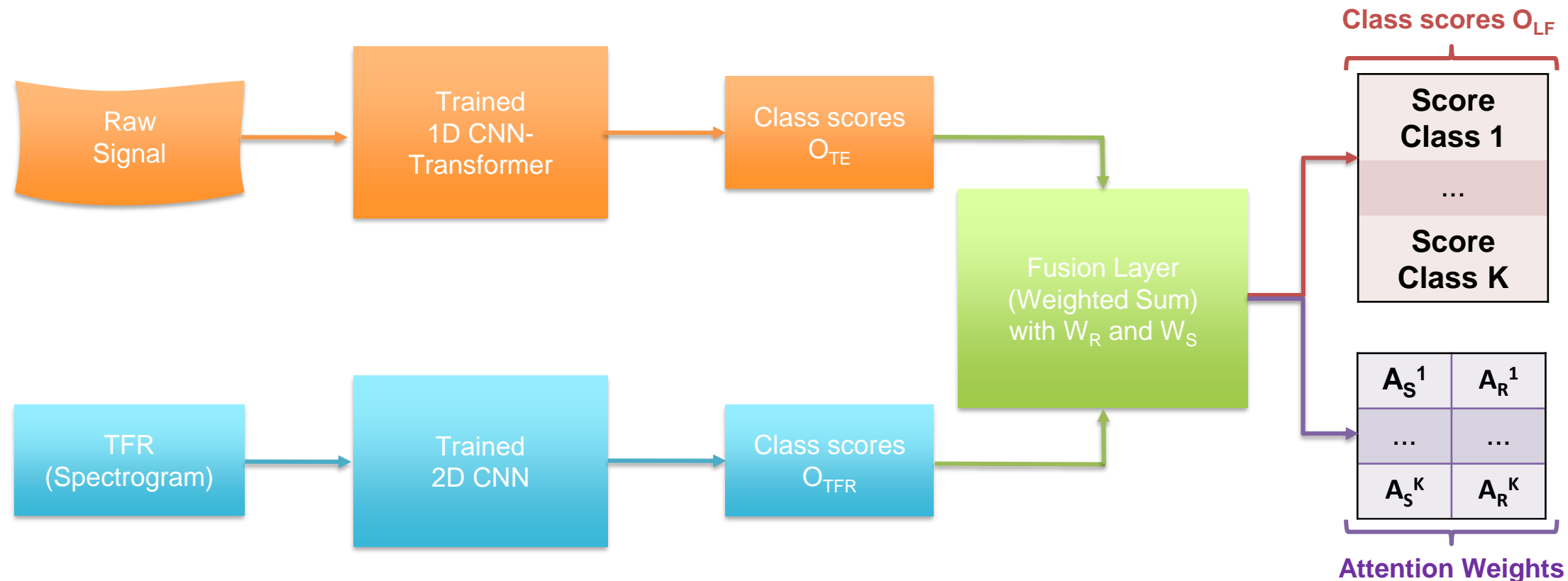


Figure - Proposed hybrid CNN Transformer global model

Late fusion attention weights

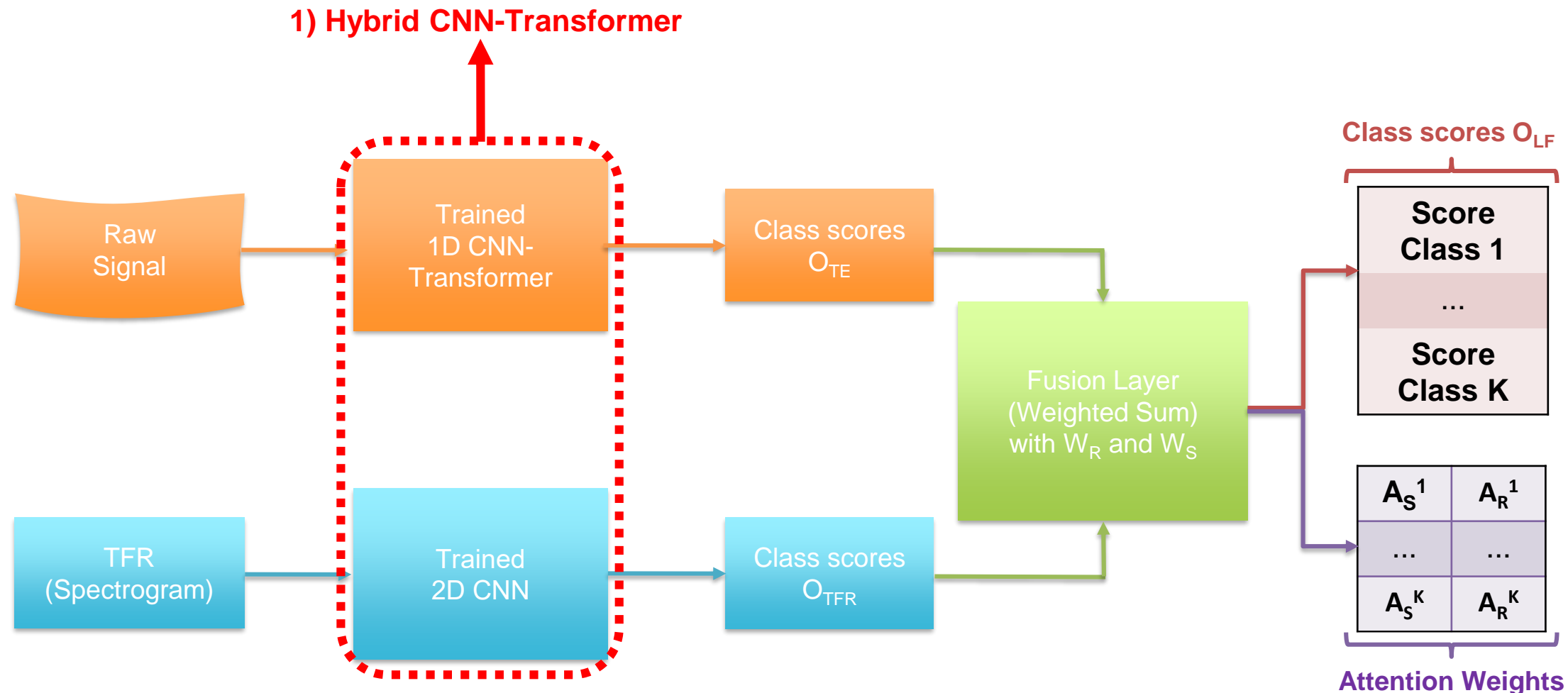


Figure - Proposed hybrid CNN Transformer global model

Late fusion attention weights

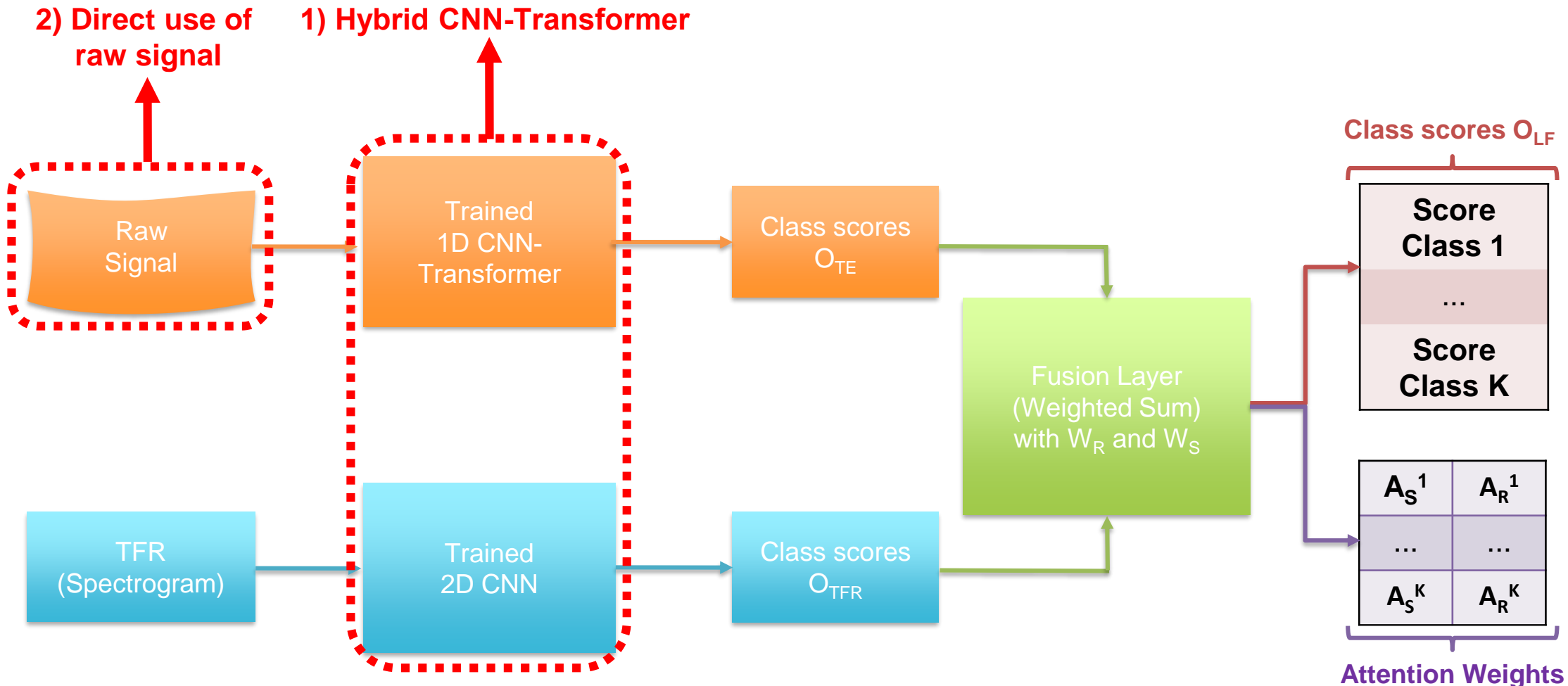


Figure - Proposed hybrid CNN Transformer global model

Late fusion attention weights

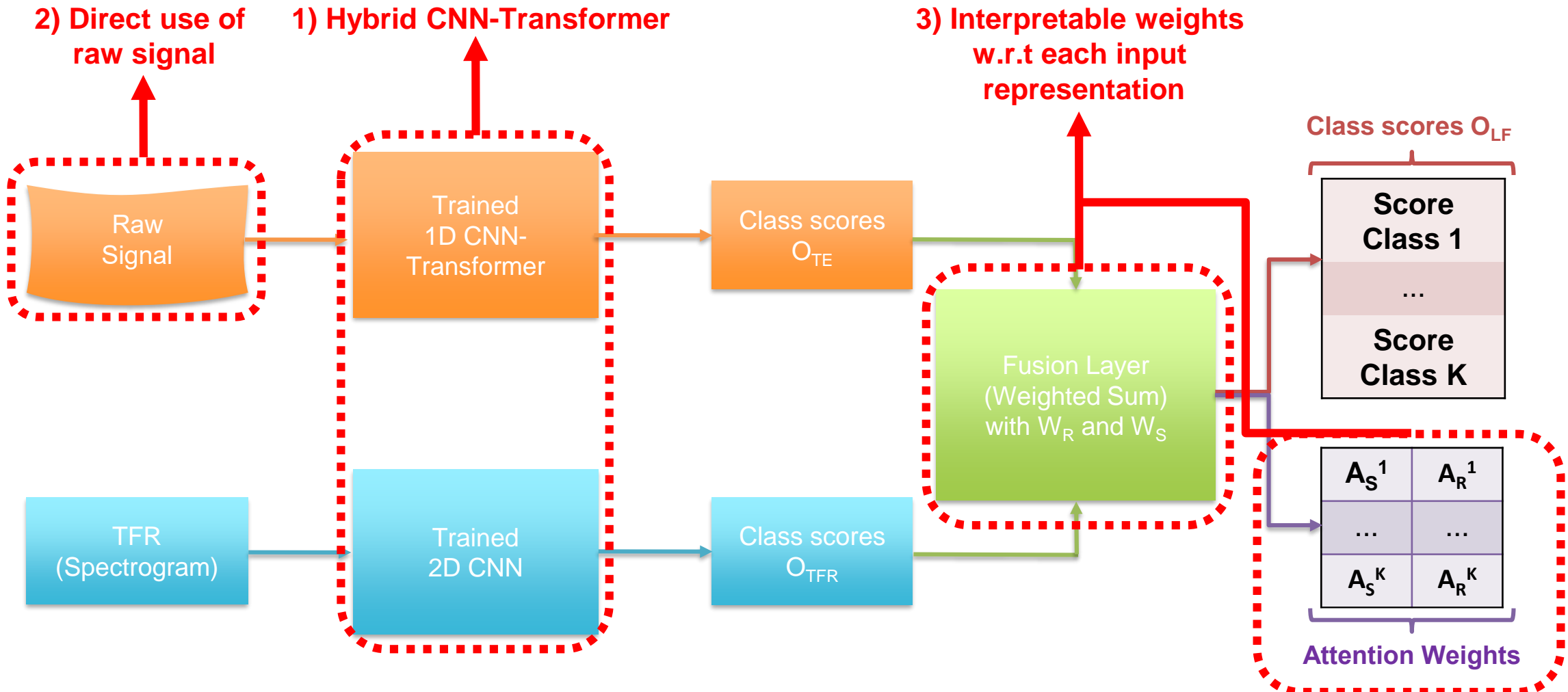


Figure - Proposed hybrid CNN Transformer global model

Guided and regularized intermediate fusion

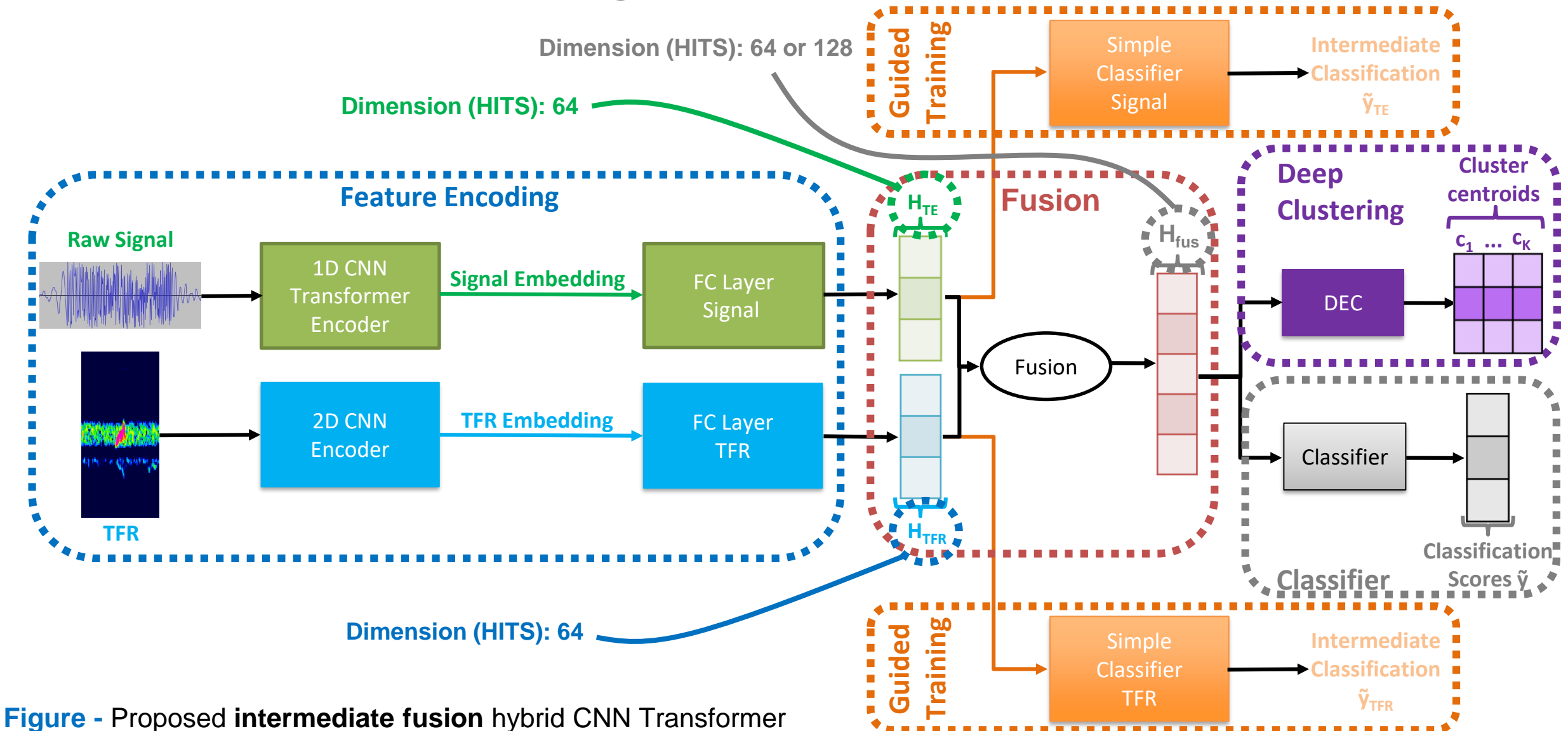


Figure - Proposed **intermediate fusion** hybrid CNN Transformer model.

Results: SOTA comparison HITS validation

Single feature
models

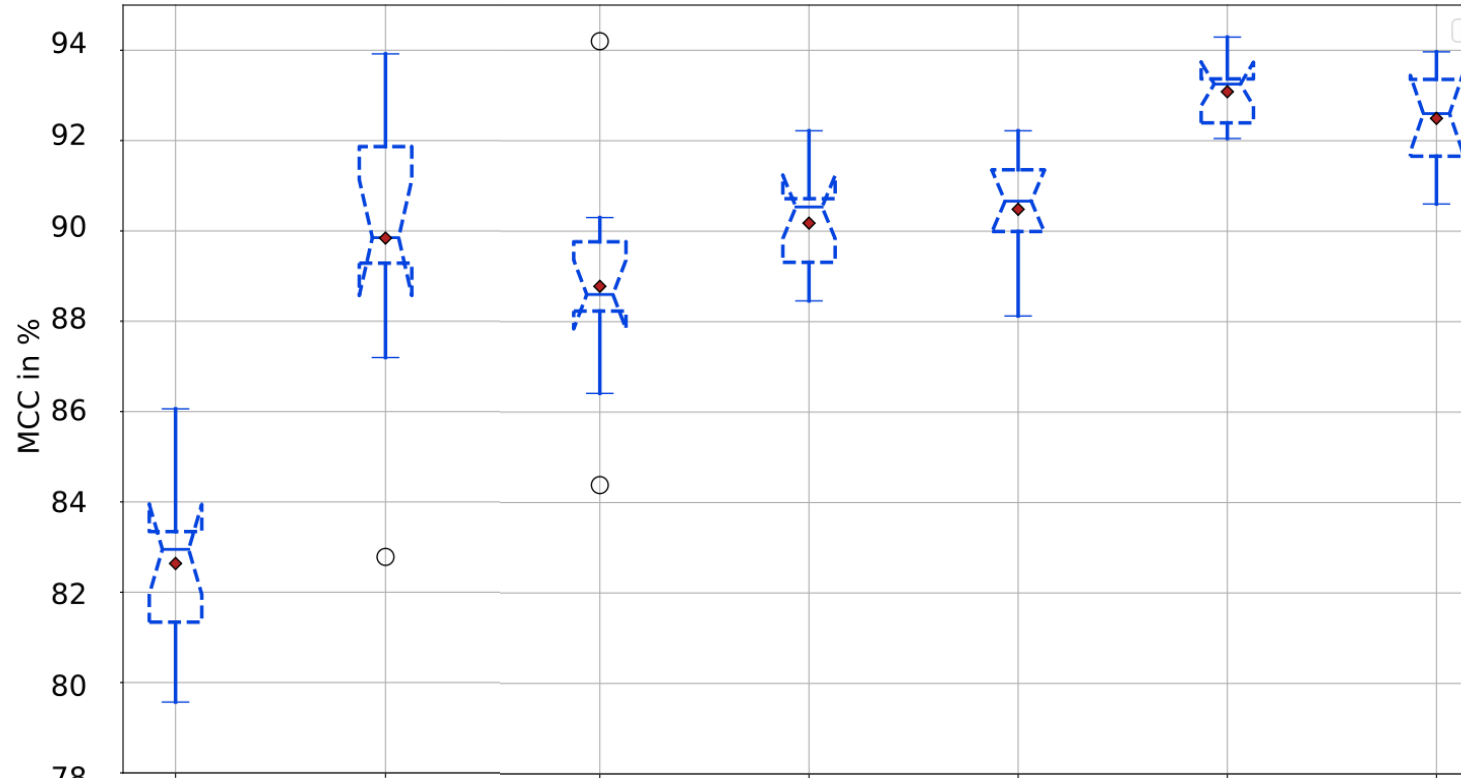


Figure - Comparison of the classification performances of different single and multi-feature models on the HITS dataset

Results: SOTA comparison HITS validation

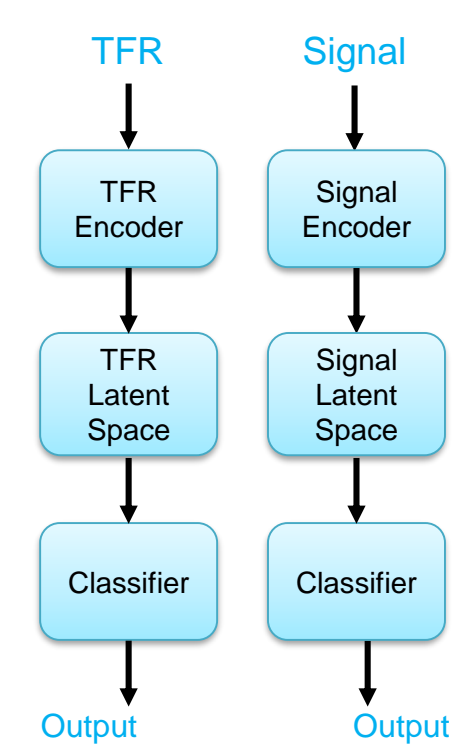
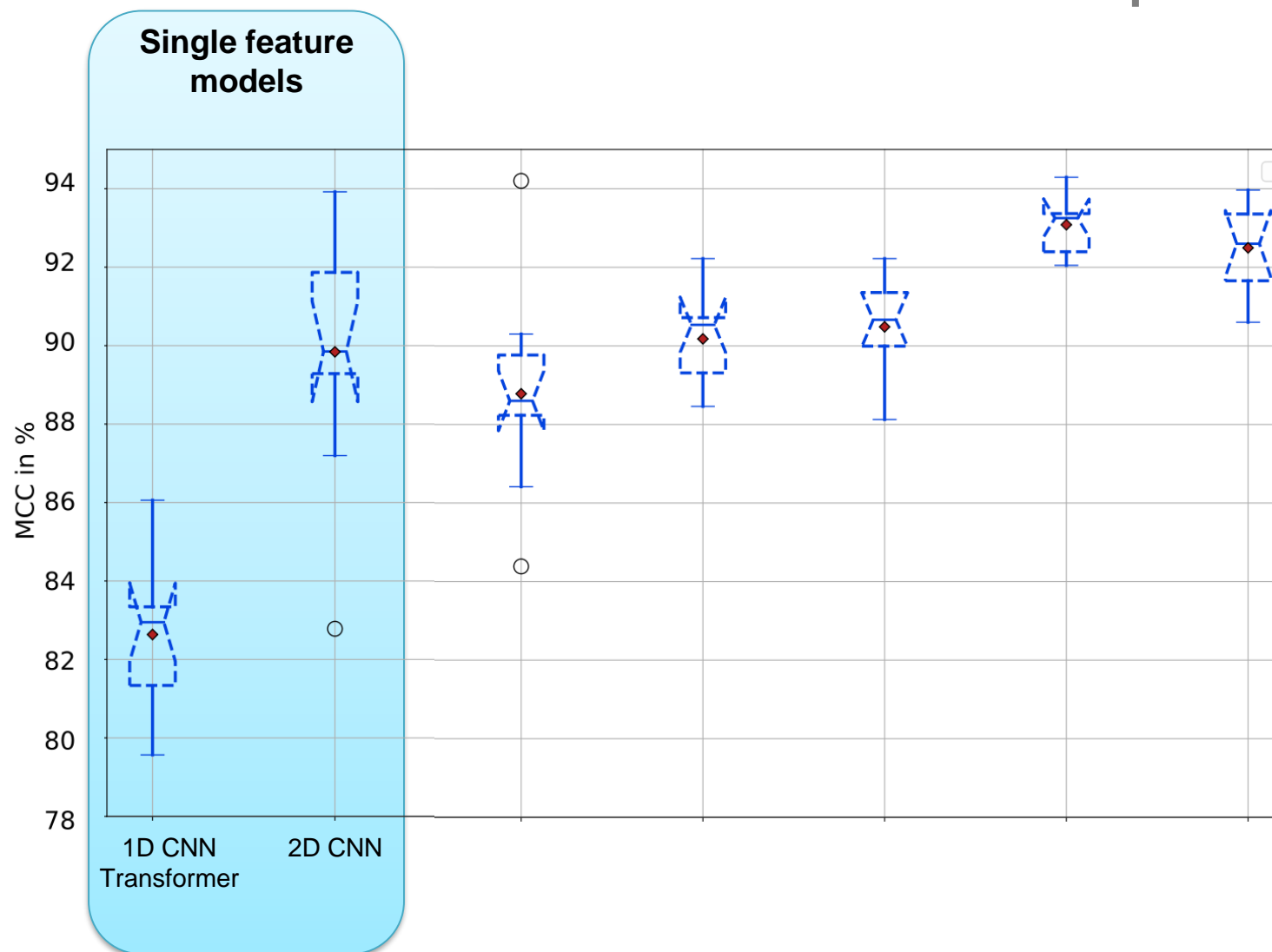


Figure - Comparison of the classification performances of different single and multi-feature models on the HITS dataset

Results: SOTA comparison HITS validation

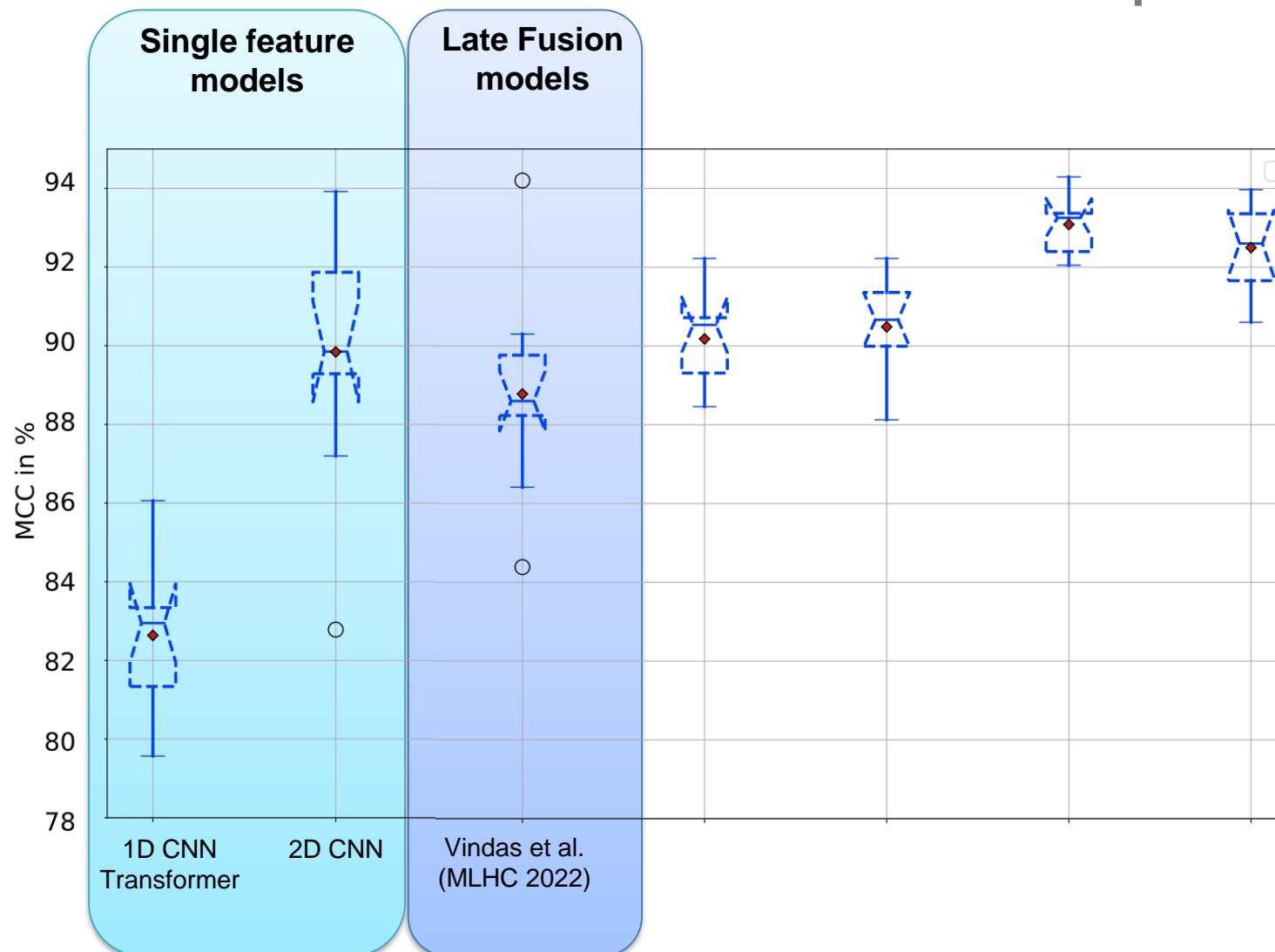
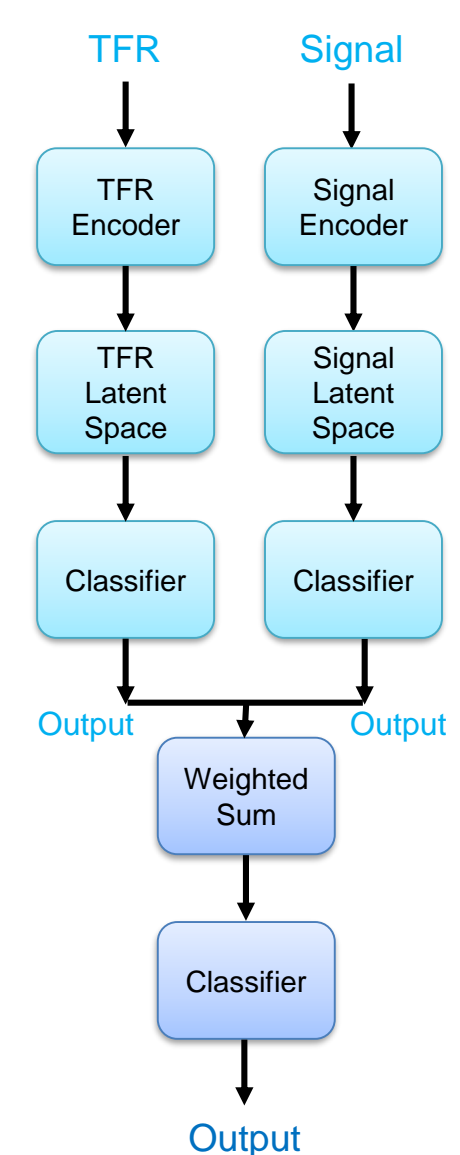


Figure - Comparison of the classification performances of different single and multi-feature models on the HITS dataset



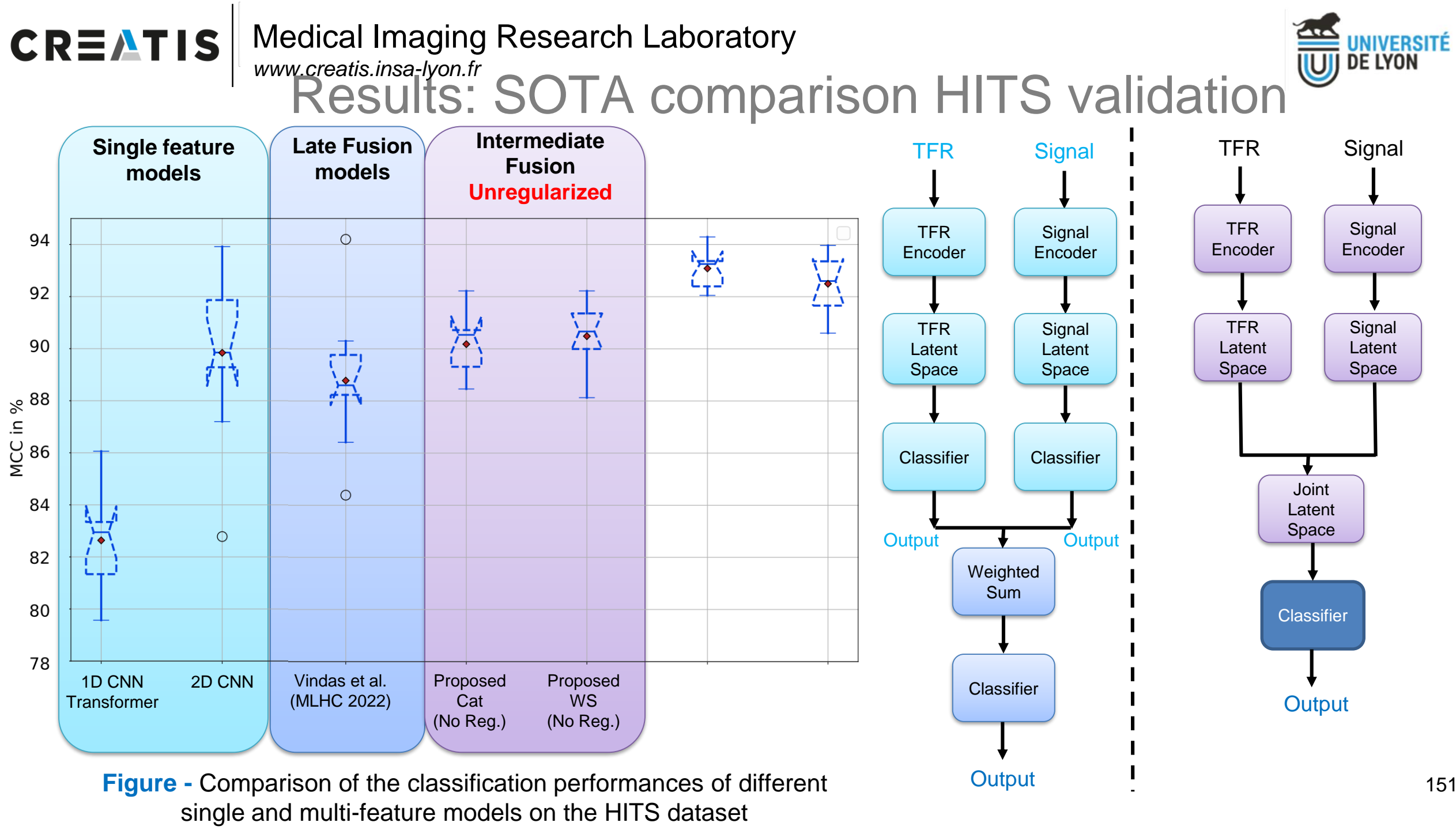


Figure - Comparison of the classification performances of different single and multi-feature models on the HITS dataset

Results: SOTA comparison HITS validation

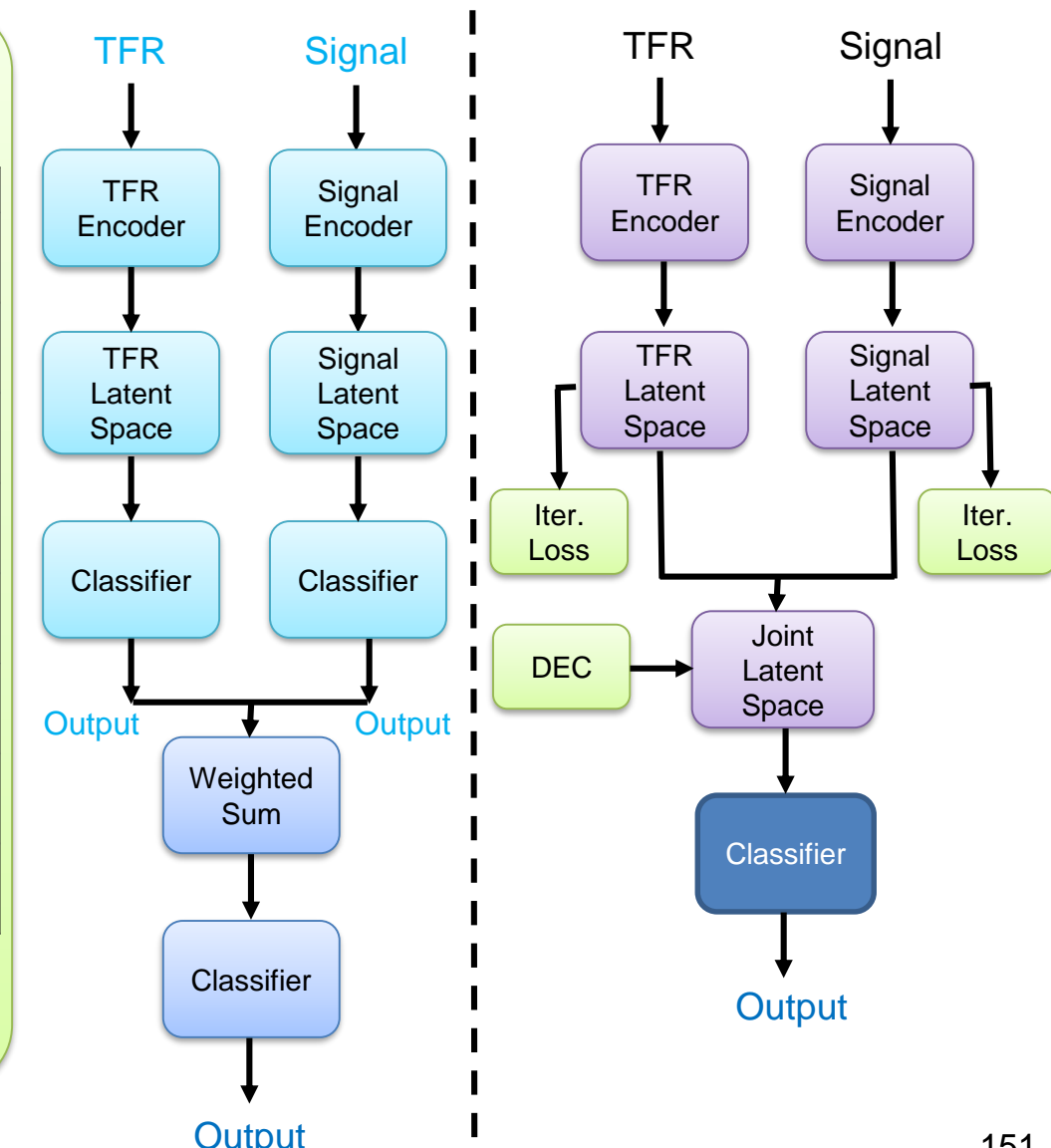
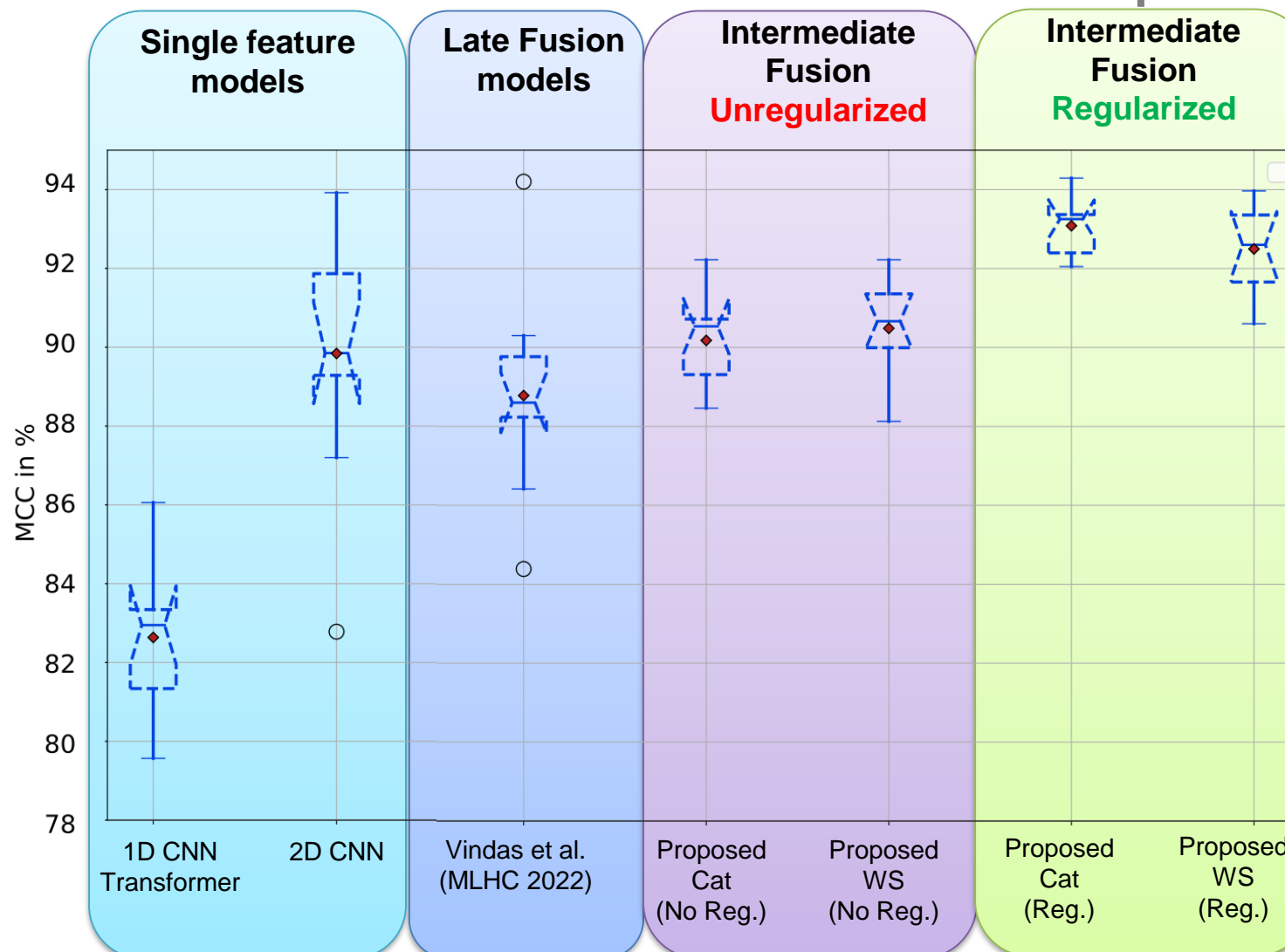


Figure - Comparison of the classification performances of different single and multi-feature models on the HITS dataset

Results Multi-feature classification

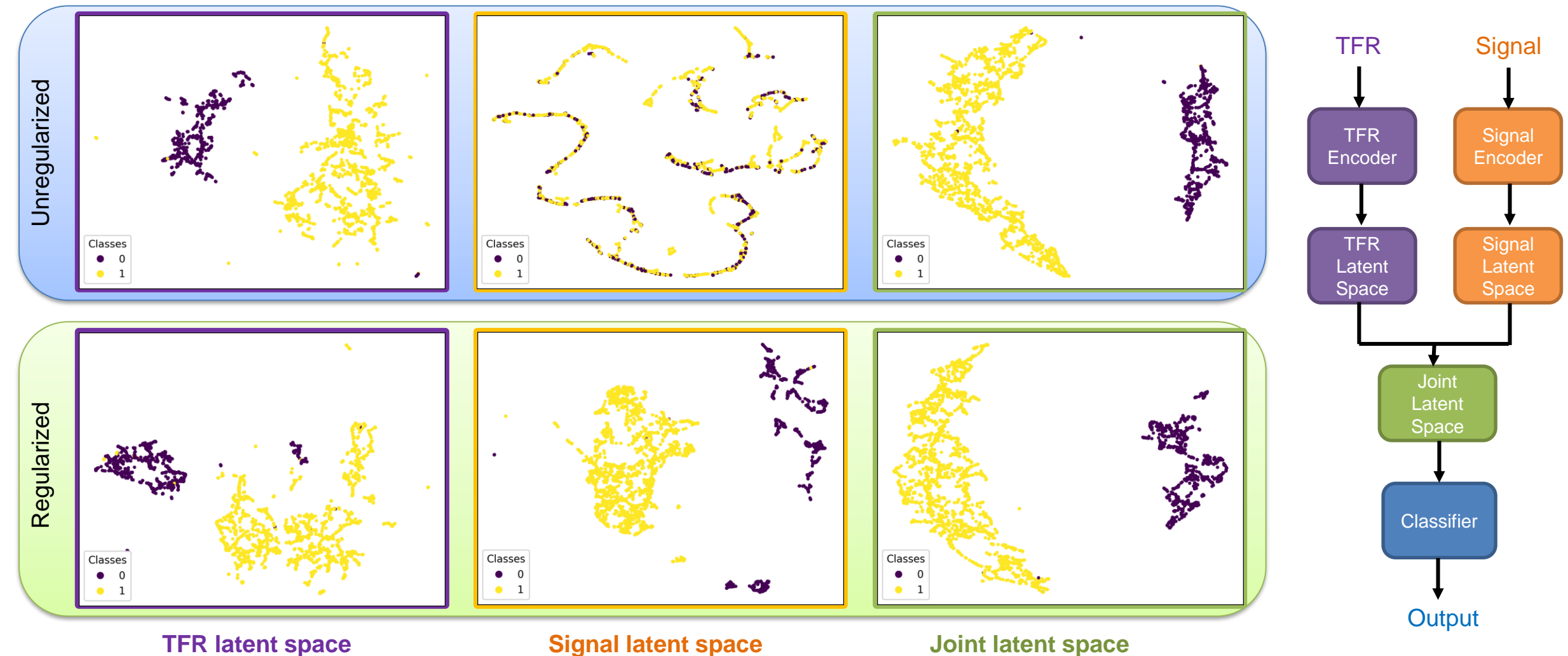
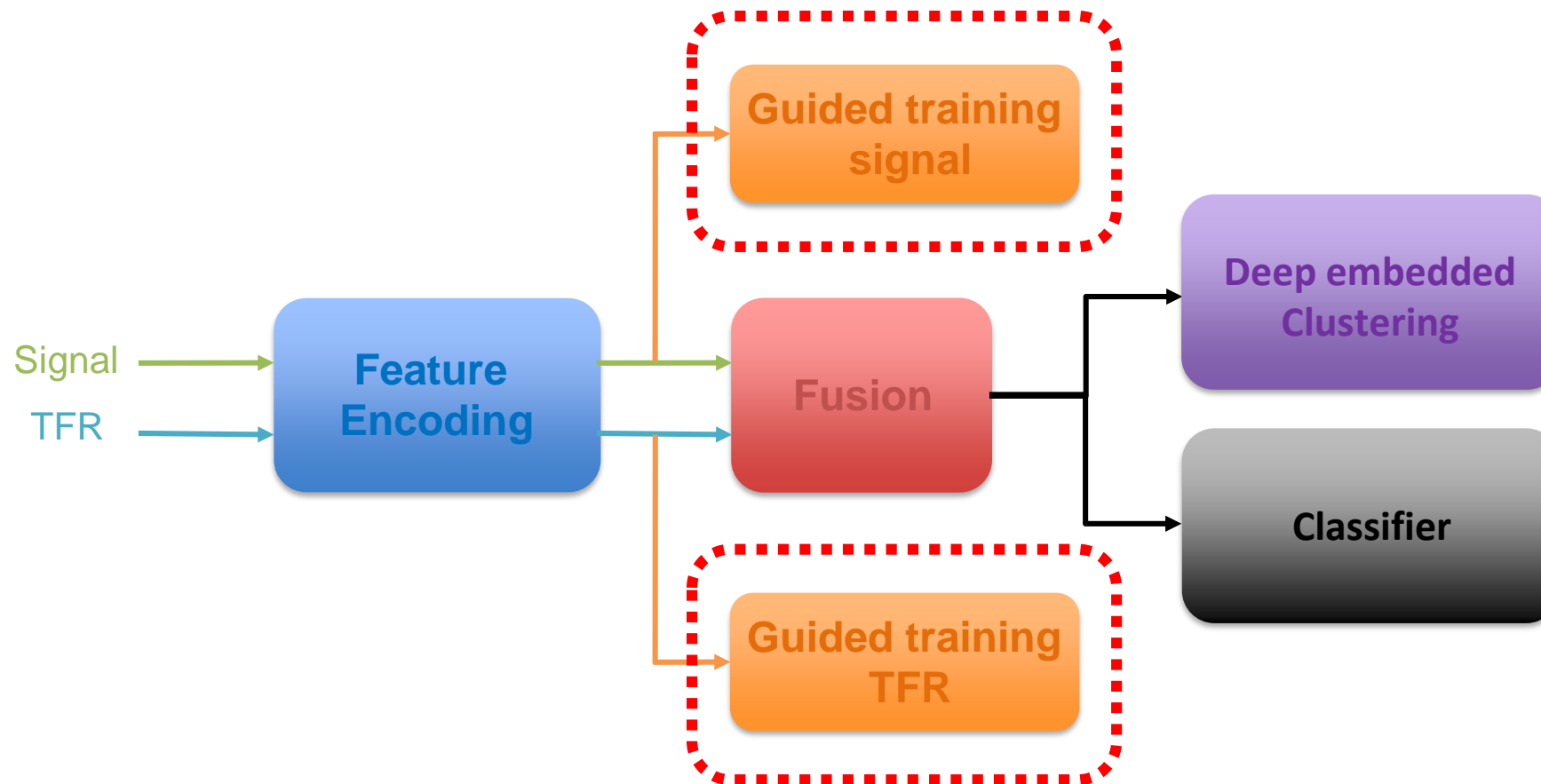


FIGURE - UMAP projections of the different latent spaces of the multi-feature intermediate fusion classification model on the PTB dataset

GDEC



Experiment: influence guided training

Objective:

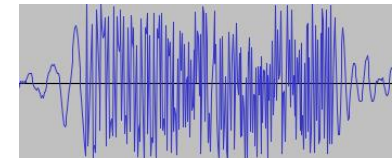
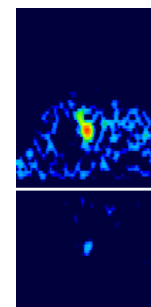
- Influence signal guided training.
- Influence TFR guided training.

Datasets:



HITS:

- TCD Data.
- 1545 samples.
- Three classes.
- Sampling frequency: 4385 Hz.



Metrics:

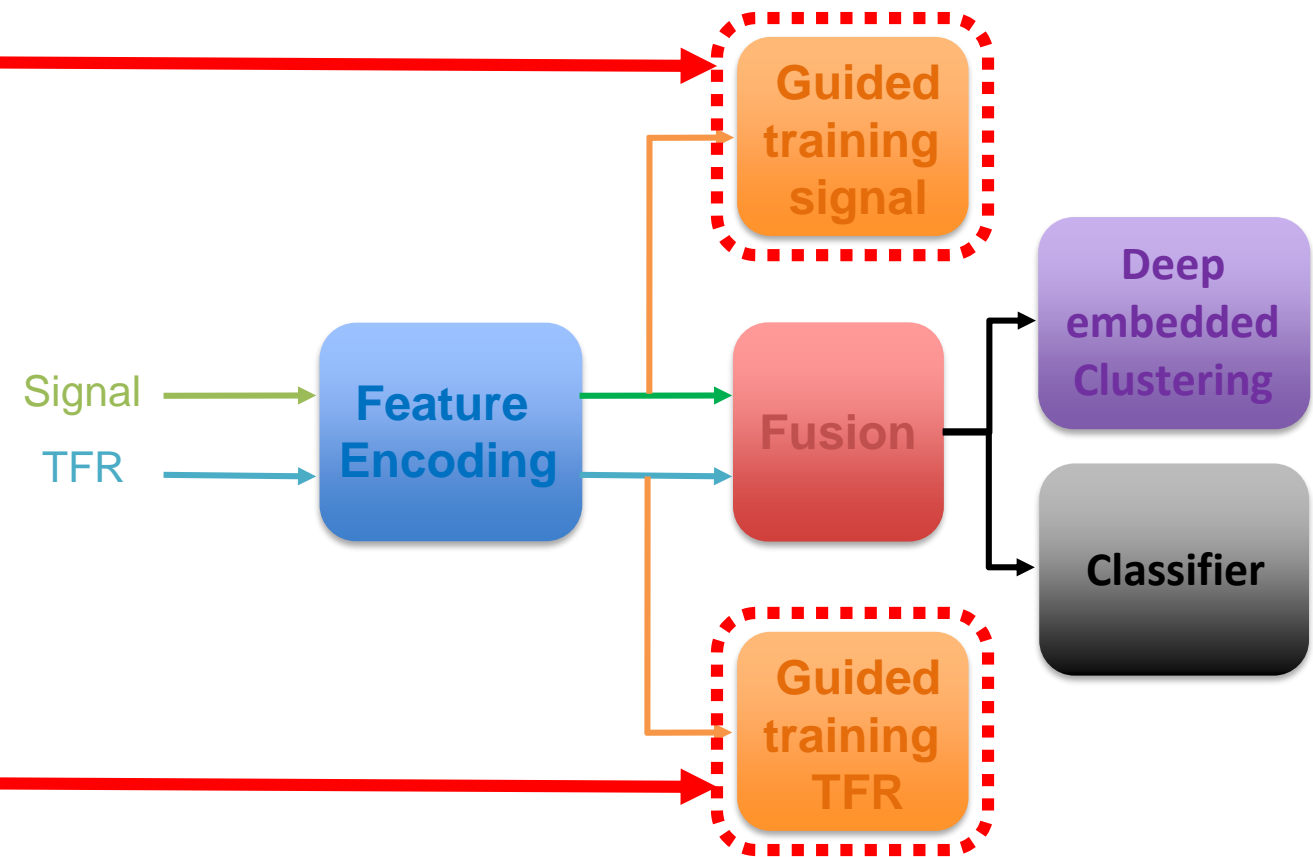
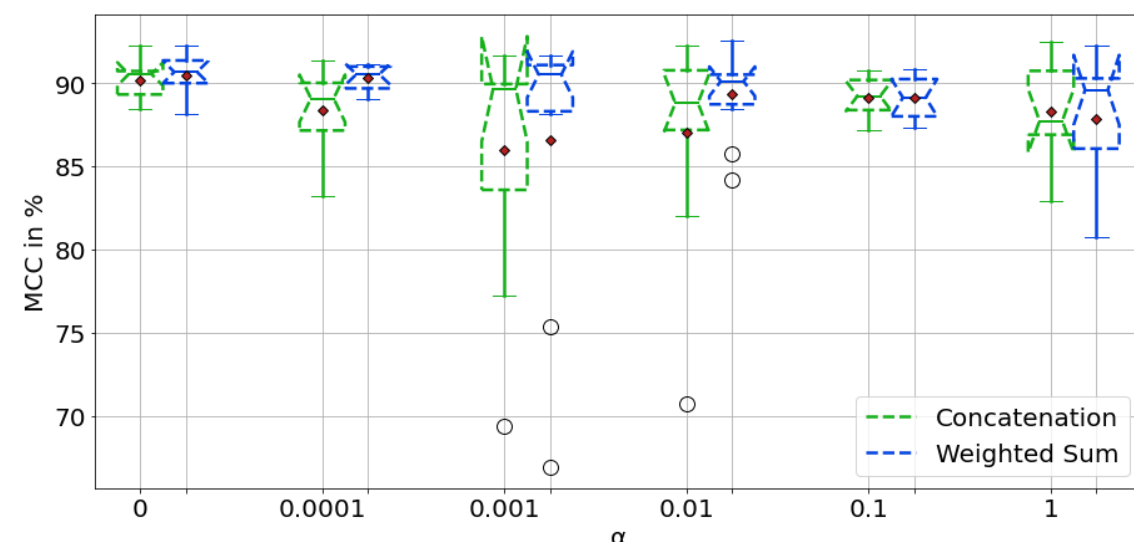
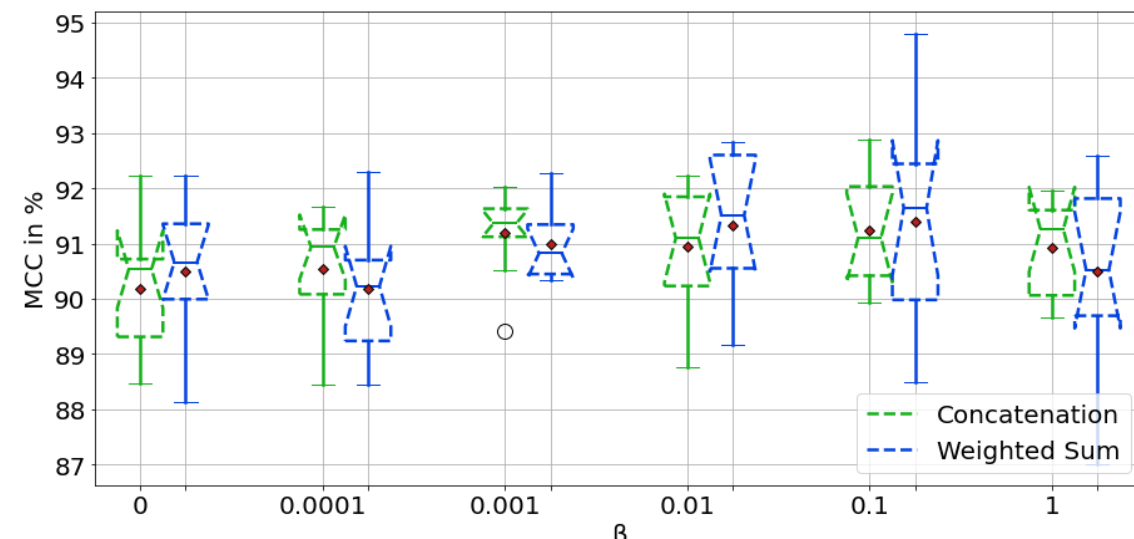
- Mathews Correlation Coefficient (MCC).

Loss function:

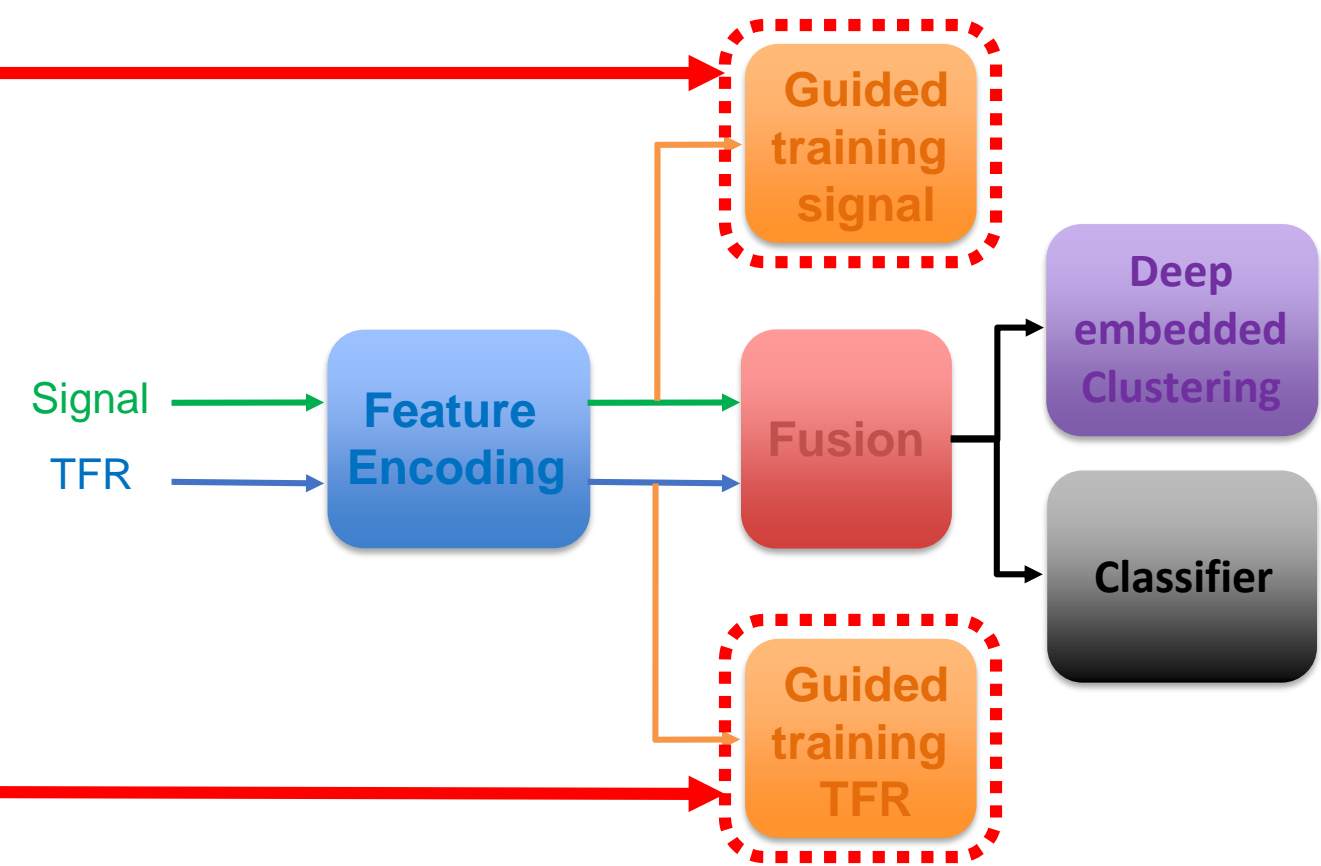
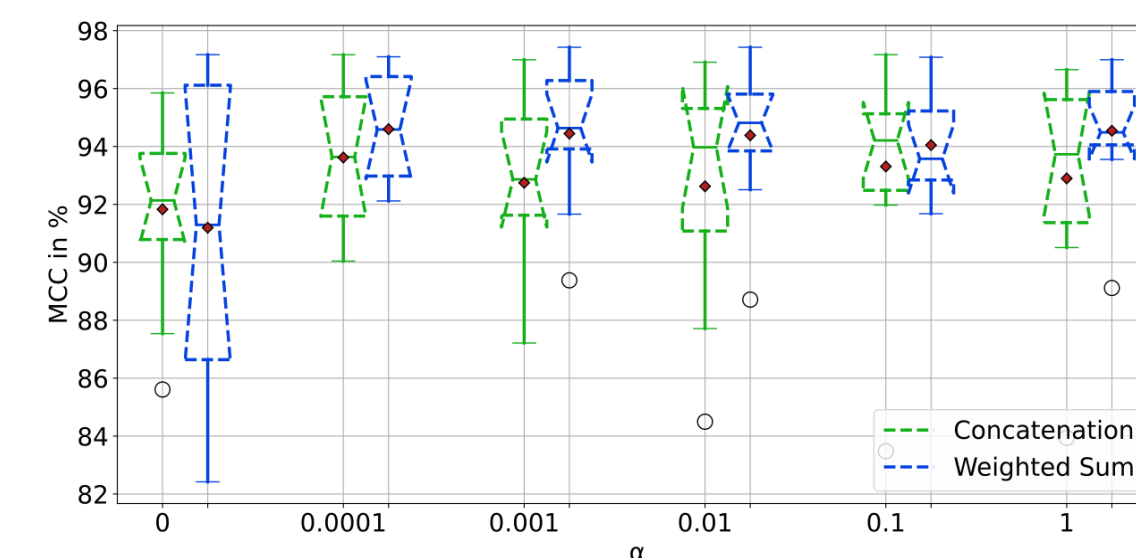
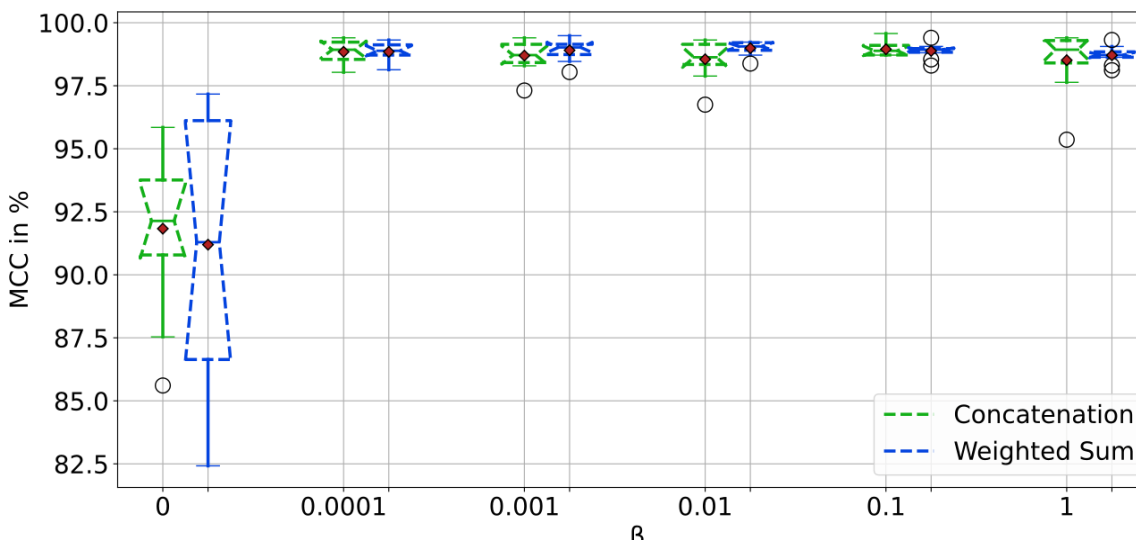
- Cross entropy (CE)

Class	Number of samples
Artifact	403
Gaseous Emboli	569
Solid Emboli	569
Unknown	4

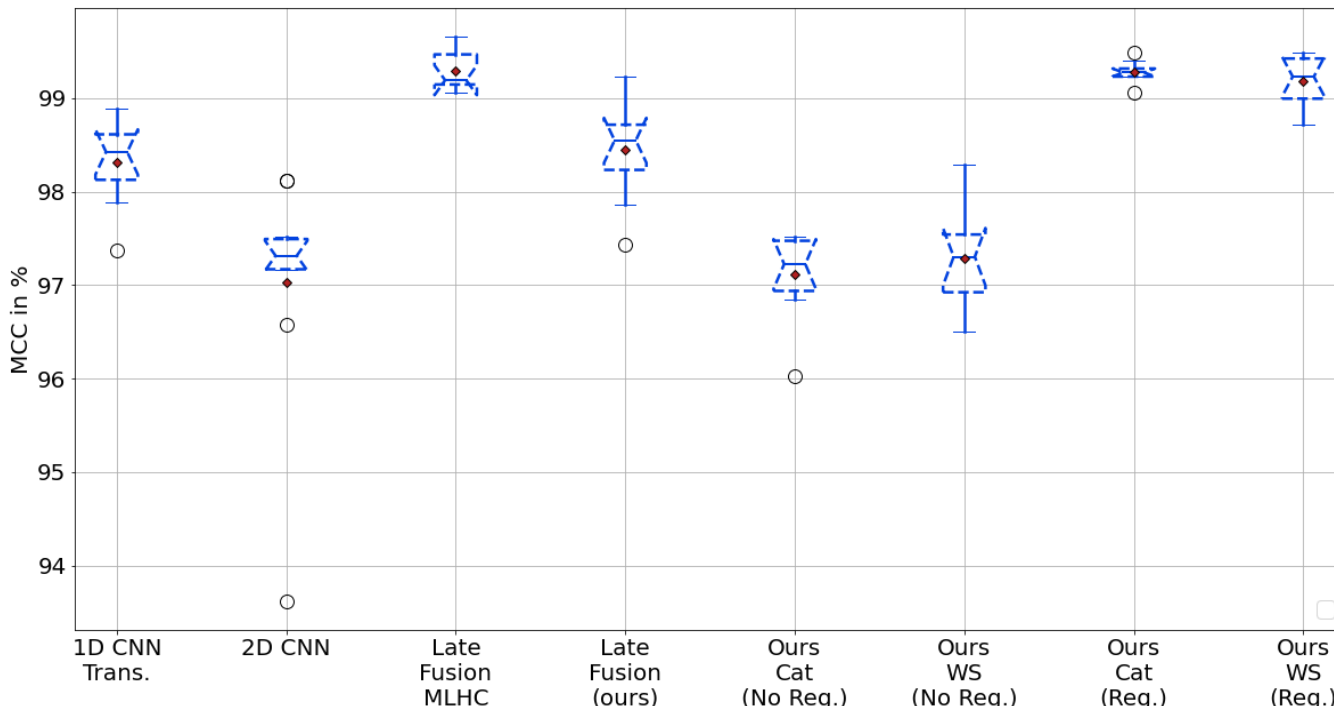
Results



Results: influence guiding PTB



Results Multi-feature classification in PTB



Model	Features	Fusion	F1 Score
1D CNN-Trans.	Raw Signal	-	99.16 ± 0.22
2D CNN	TFR	-	98.51 ± 0.61
Ahmad et al. (2021)	GAF MTF RP	-	98
Late Fusion (MLHC)		Weight. Sum	99.65 ± 0.10
Late Fusion (ours)			99.22 ± 0.25
Ours (No Reg.)		Cat.	98.60 ± 0.22
Ours (No Reg.)		Weight. Sum	98.64 ± 0.25
Ours (Reg.)		Cat.	99.64 ± 0.05
Ours (Reg.)		Weight. Sum	99.59 ± 0.13

FIGURE - Comparison of the classification performances of different single and multi-feature models on the PTB dataset

Late fusion weights interpretability

Late fusion weights interpretability

Attention weights for the HITS dataset

Late fusion weights interpretability

Class	Spectrogram	Raw Signal
Artifacts	0.46 ± 0.29	0.54 ± 0.29
Gaseous Emboli	0.65 ± 0.17	0.35 ± 0.17
Solid Emboli	0.71 ± 0.15	0.29 ± 0.15

Attention weights for the HITS dataset

Late fusion weights interpretability

Class	Spectrogram	Raw Signal
Artifacts	0.46 ± 0.29	0.54 ± 0.29
Gaseous Emboli	0.65 ± 0.17	0.35 ± 0.17
Solid Emboli	0.71 ± 0.15	0.29 ± 0.15

Attention weights for the HITS dataset

Attention weights for the PTB dataset

Late fusion weights interpretability

Class	Spectrogram	Raw Signal
Artifacts	0.46 ± 0.29	0.54 ± 0.29
Gaseous Emboli	0.65 ± 0.17	0.35 ± 0.17
Solid Emboli	0.71 ± 0.15	0.29 ± 0.15

Attention weights for the HITS dataset

Class	Spectrogram	Raw Signal
Normal	0.49 ± 0.12	0.51 ± 0.12
Abnormal	0.18 ± 0.10	0.82 ± 0.10

Attention weights for the PTB dataset

Late fusion weights interpretability

Class	Spectrogram	Raw Signal
Artifacts	0.46 ± 0.29	0.54 ± 0.29
Gaseous Emboli	0.65 ± 0.17	0.35 ± 0.17
Solid Emboli	0.71 ± 0.15	0.29 ± 0.15

Attention weights for the HITS dataset

Class	Spectrogram	Raw Signal
Normal	0.49 ± 0.12	0.51 ± 0.12
Abnormal	0.18 ± 0.10	0.82 ± 0.10

Attention weights for the PTB dataset

Attention weights for the MIT-BIH dataset

Late fusion weights interpretability

Class	Spectrogram	Raw Signal
Artifacts	0.46 ± 0.29	0.54 ± 0.29
Gaseous Emboli	0.65 ± 0.17	0.35 ± 0.17
Solid Emboli	0.71 ± 0.15	0.29 ± 0.15

Attention weights for the HITS dataset

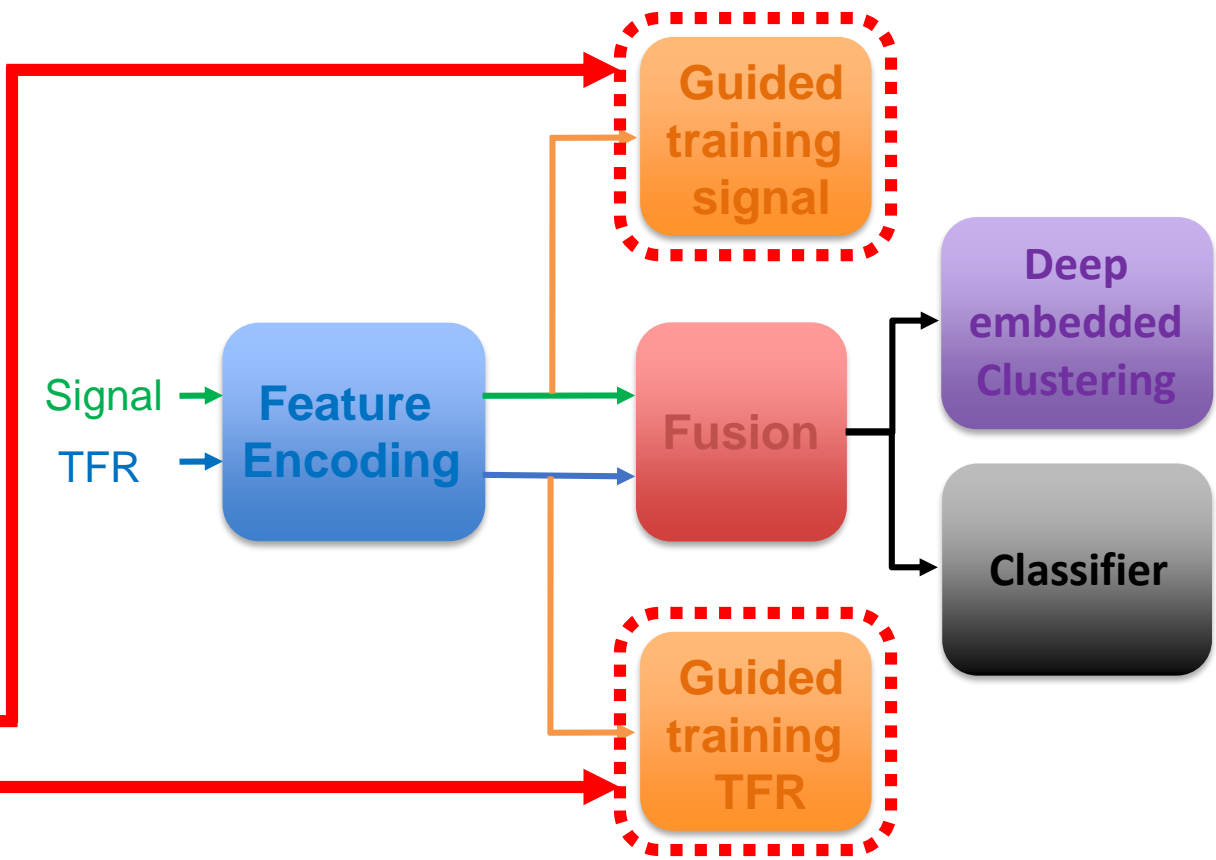
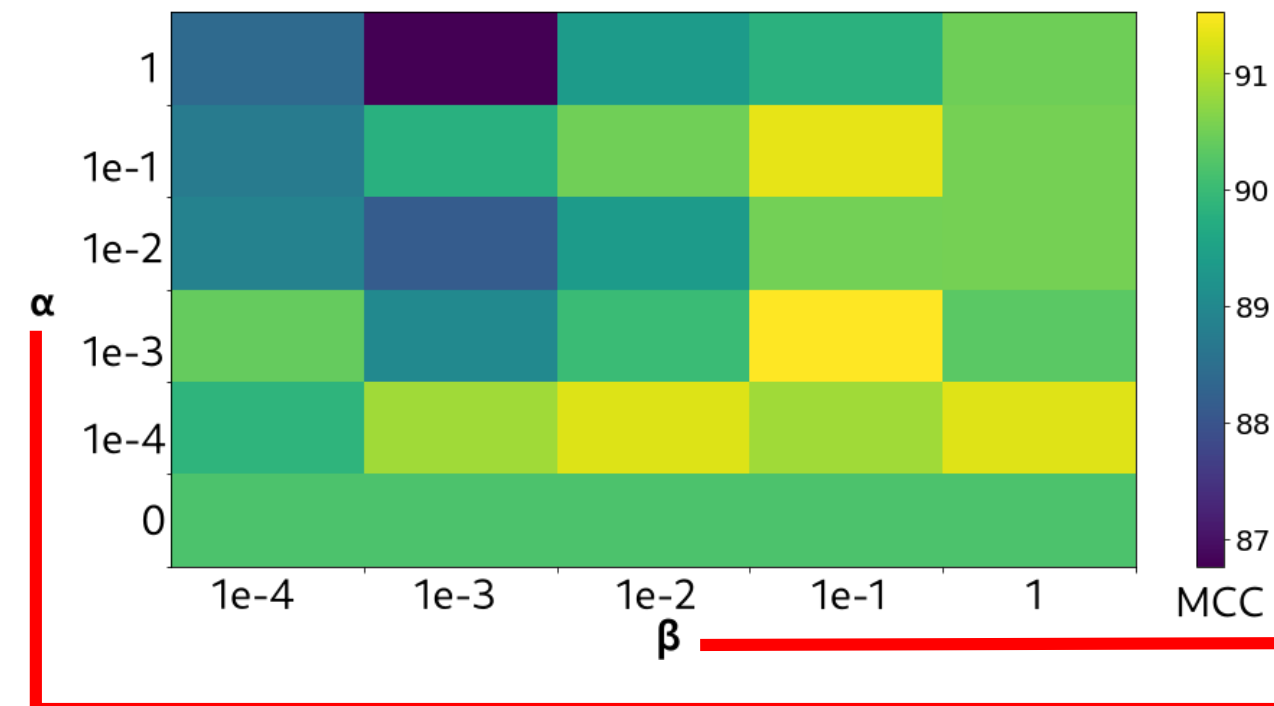
Class	Spectrogram	Raw Signal
Normal	0.49 ± 0.12	0.51 ± 0.12
Abnormal	0.18 ± 0.10	0.82 ± 0.10

Attention weights for the PTB dataset

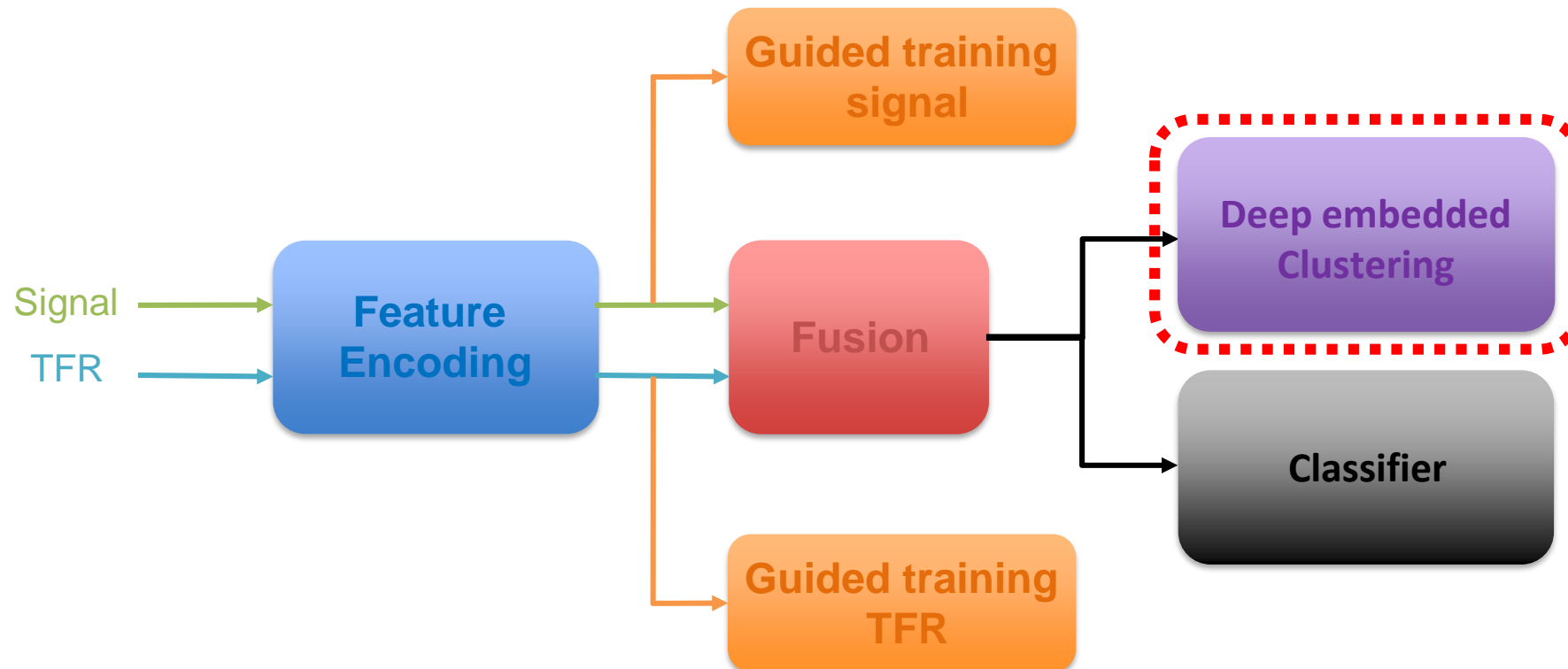
Class	Spectrogram	Raw Signal
N	0.48 ± 0.01	0.52 ± 0.01
S	0.50 ± 0.01	0.50 ± 0.01
V	0.50 ± 0.01	0.50 ± 0.01
F	0.49 ± 0.02	0.51 ± 0.02
Q	0.50 ± 0.003	0.50 ± 0.003

Attention weights for the MIT-BIH dataset

Results: influence guiding HITS bot



GDEC



Experiment: influence DEC

Objective:

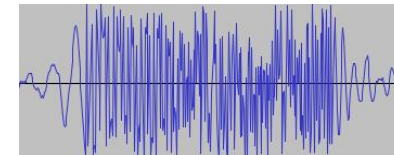
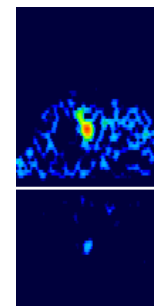
- Influence DEC on the classification performance.

Datasets:



HITS:

- TCD Data.
- 1545 samples.
- Three classes.
- Sampling frequency: 4385 Hz.



Metrics:

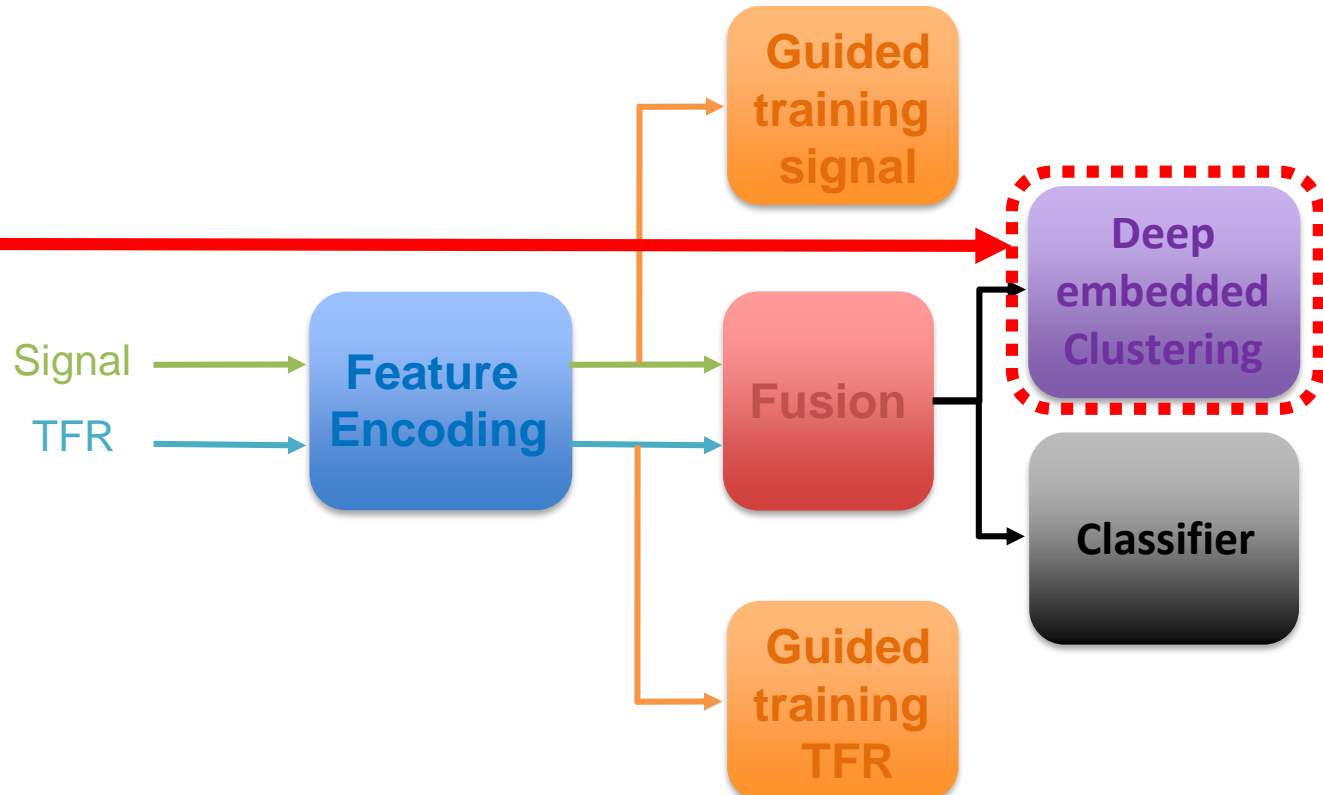
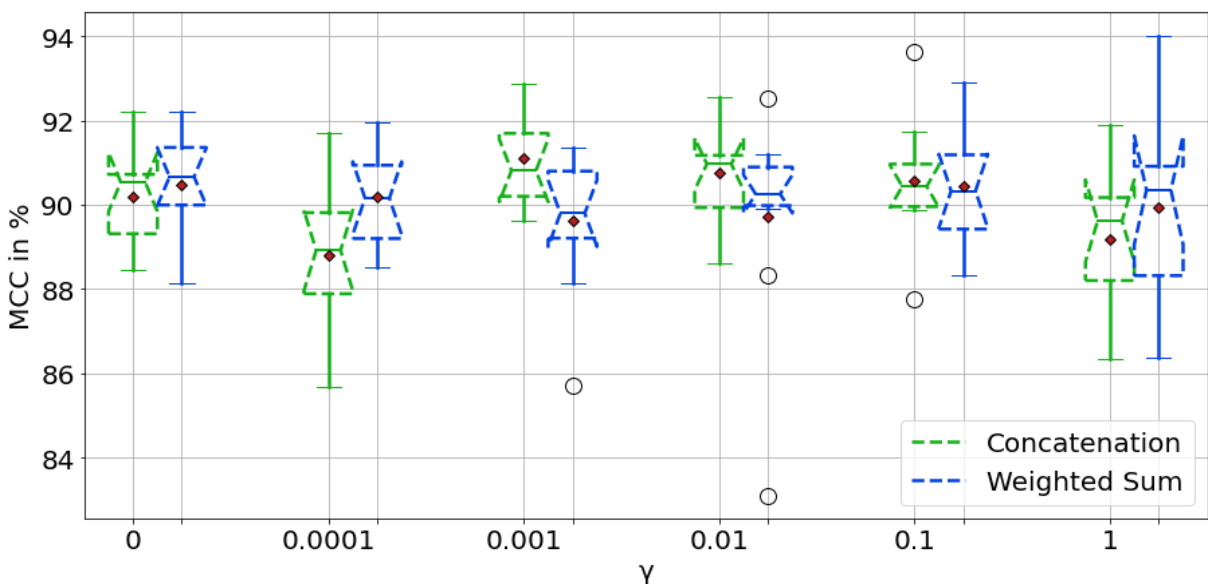
- Mathews Correlation Coefficient (MCC).

Loss function:

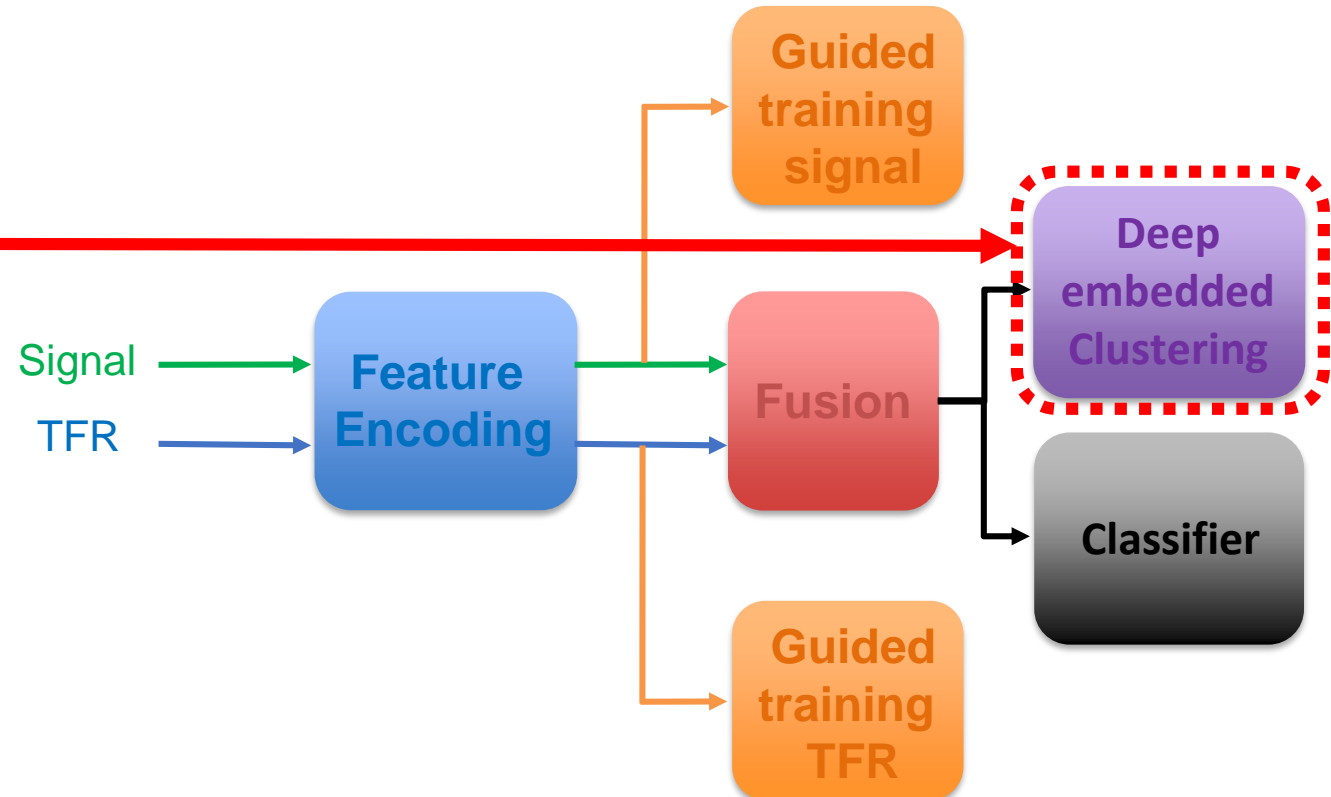
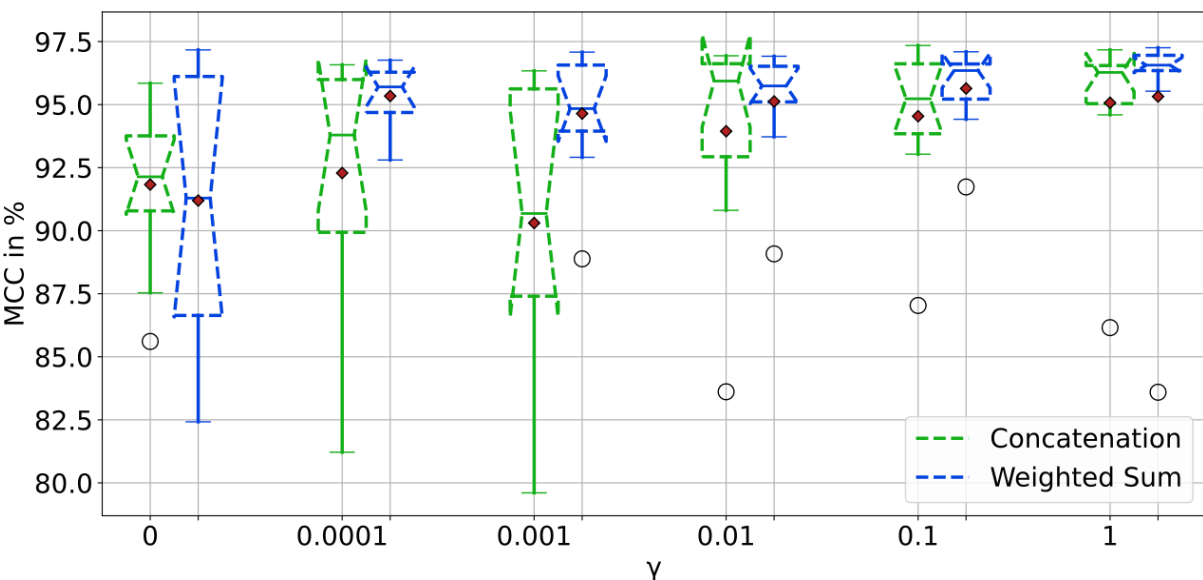
- Cross entropy (CE)

Class	Number of samples
Artifact	403
Gaseous Emboli	569
Solid Emboli	569
Unknown	4

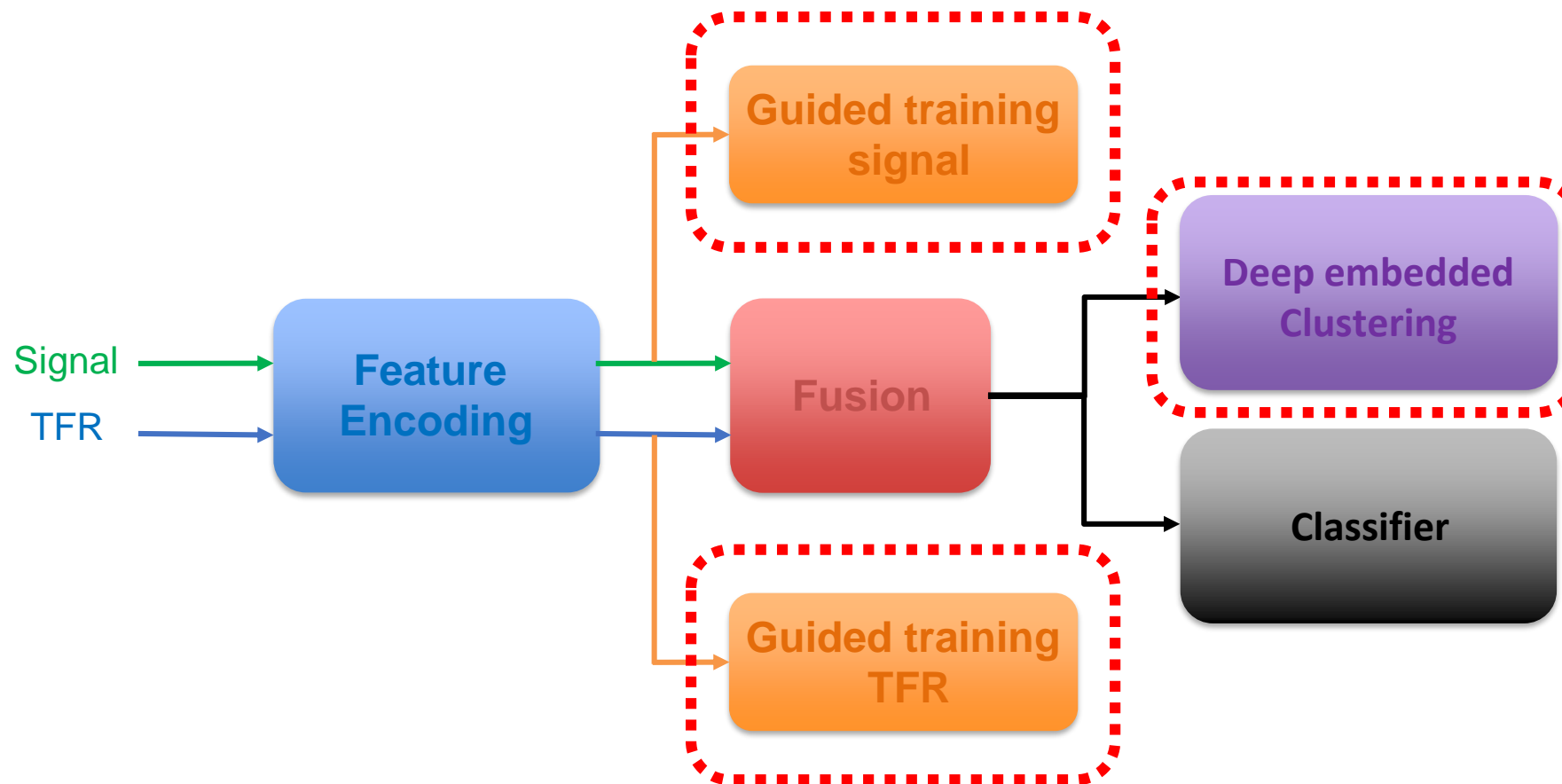
Results



Results: influence DEC PTB



GDEC



Experiment: noise tolerance on HITS-sada

Objective:

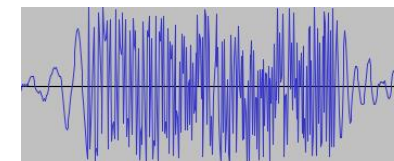
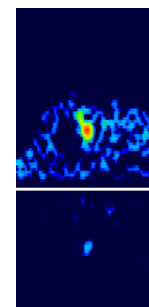
- Study the robustness of GDEC to noisy labeled datasets.

Datasets:



HITS-sada:

- TCD **semi-automatically labeled** data.
- 8 685 samples.
- Three classes.
- Sampling frequency: 4385 Hz.



Metrics:

- Mathews Correlation Coefficient (MCC).
- F1-Score.
- Number of parameters.
- Number of mult-adds.

Loss function:

- **Generalized Cross entropy (GCE).**

Class	Number of samples
Artifact	6 987
Gaseous Emboli	1 002
Solid Emboli	696

Results

Model	MCC	F1-Score	Accuracy	No. Parameters	No. mult-adds (G)
2D CNN	84.03 ± 1.20	86.81 ± 1.50	90.68 ± 1.12	1 681 923	1.23
1D CNN-trans.	85.74 ± 1.16	88.96 ± 0.78	91.35 ± 0.77	766 271	0.173
MIF-GR	87.35 ± 0.85	89.41 ± 0.64	92.59 ± 0.50	4 833 727	1.40

Table – Multi-feature GDCE compared to single feature models on a noisy semi-automatically labeled dataset HITS-sada.

Robustness DEC Imbalanced Datasets

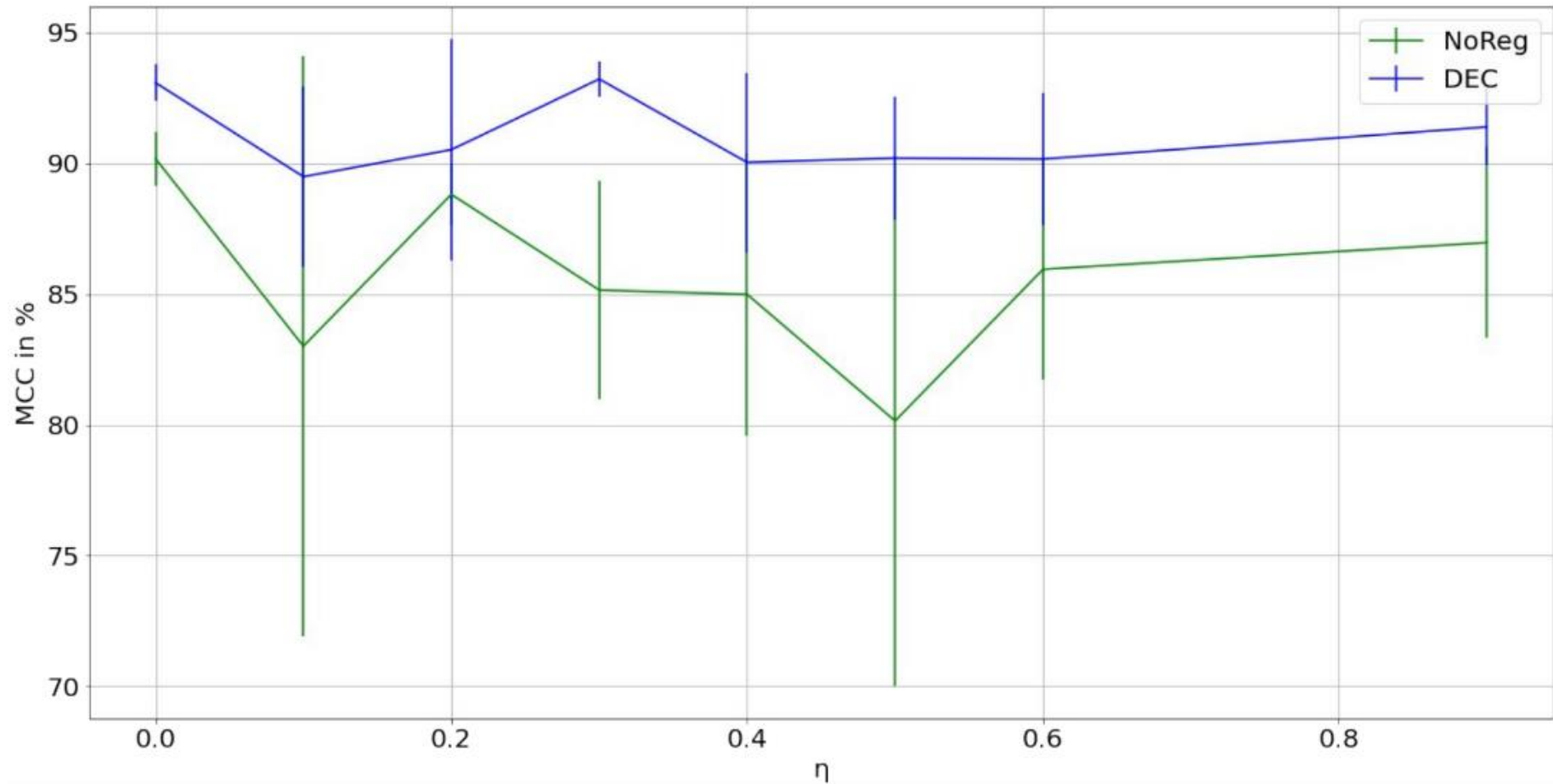


FIGURE - MCC of the multi-feature classification model on the HITS dataset for different levels of label noise.

Robustness DEC Imbalanced Datasets

Noise Rate	Clean Samples	GDEC	Loss	MCC
5	Yes	No	CE	97.08 ± 0.53
		Yes		99.32 ± 0.17
	No	No	CE	88.61 ± 0.74
		Yes		93.13 ± 0.31
	Yes	No	GCE	96.58 ± 0.49
		Yes		98.37 ± 0.27
No	No	No	GCE	94.10 ± 1.09
		Yes		96.70 ± 0.54

Noise rate of 5 %

Noise Rate	Clean Samples	GDEC	Loss	MCC
10	Yes	No	CE	96.98 ± 0.35
		Yes		99.30 ± 0.19
	No	No	CE	78.55 ± 1.45
		Yes		82.30 ± 1.15
	Yes	No	GCE	96.27 ± 0.59
		Yes		98.57 ± 0.36
No	No	No	GCE	90.22 ± 1.30
		Yes		91.90 ± 1.18

Noise rate of 10 %

Noise Rate	Clean Samples	GDEC	Loss	MCC
20	Yes	No	CE	96.96 ± 0.54
		Yes		98.99 ± 0.27
	No	No	CE	59.98 ± 1.98
		Yes		63.77 ± 2.08
	Yes	No	GCE	95.66 ± 0.70
		Yes		97.84 ± 0.52
No	No	No	GCE	71.63 ± 2.52
		Yes		71.66 ± 3.48

Noise rate of 20 %

Table - MCC of the multi-feature classification model on the PTB dataset for different levels of label noise.

Model compression

Model	SA Finished	MCC	Drop MCC	Sparsity rate (%)	Tuning duration
Full precision	-	95.85 ± 0.69	-	0 ± 0	-
TTQ	-	93.86 ± 0.92		29.98 ± 1.42	200
Proposed	-	93.80 ± 0.26		77.41 ± 2.09	200
Proposed SA (x in [-1, 0], y in [0, 1])	No	94.51 ± 0.77		60.96 ± 8.98	200
Proposed Pruning Learned	-	92.50 ± 0.44		77.28 ± 0.22	100
Proposed Pruning Learned alpha too	-	93.85 ± 0.50		85.53 ± 6.53	100

Table - MCC of a (compressed) simple CNN model on a subset of the MNIST dataset

Soft labelling

Model	Dataset	Soft Labels	Mean MCC	Median MCC
2D CNN		No	86.13 ± 3.80	87.76 ± 1.85
		Yes	87.03 ± 3.55	87.47 ± 1.75
CNN-Transformer	HITS Small	No	85.92 ± 1.79	86.01 ± 0.82
		Yes	86.52 ± 3.73	87.63 ± 0.86
Hybrid	HITS Large	No	92.50 ± 1.36	92.74 ± 0.95
		Yes	93.12 ± 1.00	92.59 ± 0.11
		No	85.49 ± 0.77	85.49 ± 0.77
		Yes	86.77 ± 0.96	86.35 ± 0.49

Datasets MLHC 2022

Datasets MLHC 2022



HITS:

- TCD Data.
- 1545 samples.
- Three classes.
- Sampling frequency: 4385 Hz.

Datasets MLHC 2022



HITS:

- TCD Data.
- 1545 samples.
- Three classes.
- Sampling frequency: 4385 Hz.

Class	Number of samples
Artifact	403
Gaseous Emboli	569
Solid Emboli	569
Unknown	4

Datasets MLHC 2022

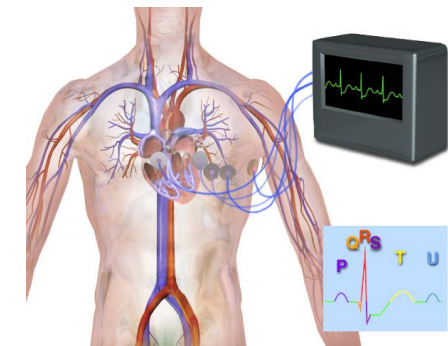


HITS:

- TCD Data.
- 1545 samples.
- Three classes.
- Sampling frequency: 4385 Hz.

Class	Number of samples
Artifact	403
Gaseous Emboli	569
Solid Emboli	569
Unknown	4

PTB:



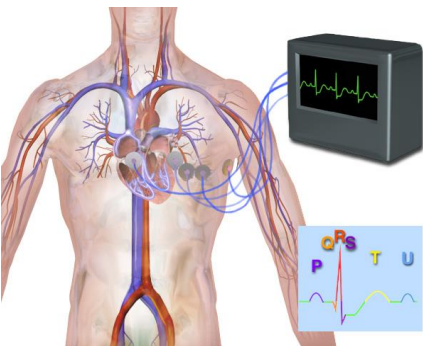
Datasets MLHC 2022



HITS:

- TCD Data.
- 1545 samples.
- Three classes.
- Sampling frequency: 4385 Hz.

Class	Number of samples
Artifact	403
Gaseous Emboli	569
Solid Emboli	569
Unknown	4



PTB:

- ECG Data.
- 14 552 samples.
- Two classes.
- Sampling frequency: 125 Hz.

Class	Number of samples
Normal	10 506
Abnormal	4 046

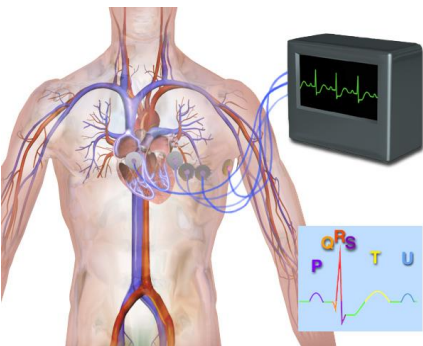
Datasets MLHC 2022



HITS:

- TCD Data.
- 1545 samples.
- Three classes.
- Sampling frequency: 4385 Hz.

Class	Number of samples
Artifact	403
Gaseous Emboli	569
Solid Emboli	569
Unknown	4



PTB:

- ECG Data.
- 14 552 samples.
- Two classes.
- Sampling frequency: 125 Hz.

Class	Number of samples
Normal	10 506
Abnormal	4 046

MIT-BIH:

- ECG Data.
- 109 436 samples.
- Five classes.
- Sampling frequency: 125 Hz.

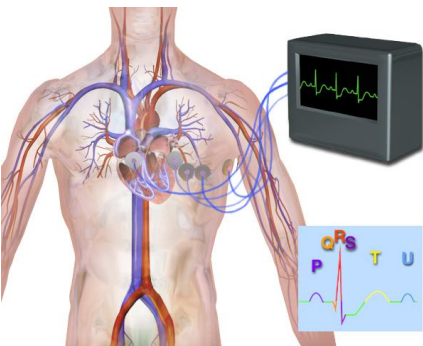
Datasets MLHC 2022



HITS:

- TCD Data.
- 1545 samples.
- Three classes.
- Sampling frequency: 4385 Hz.

Class	Number of samples
Artifact	403
Gaseous Emboli	569
Solid Emboli	569
Unknown	4



PTB:

- ECG Data.
- 14 552 samples.
- Two classes.
- Sampling frequency: 125 Hz.

Class	Number of samples
Normal	10 506
Abnormal	4 046

MIT-BIH:

- ECG Data.
- 109 436 samples.
- Five classes.
- Sampling frequency: 125 Hz.

Class	Number of samples
N	90 589
S	2 779
V	7 226
F	803
Q	8 039

Experiment 1: Advantage of using multiple features MLHC 2022

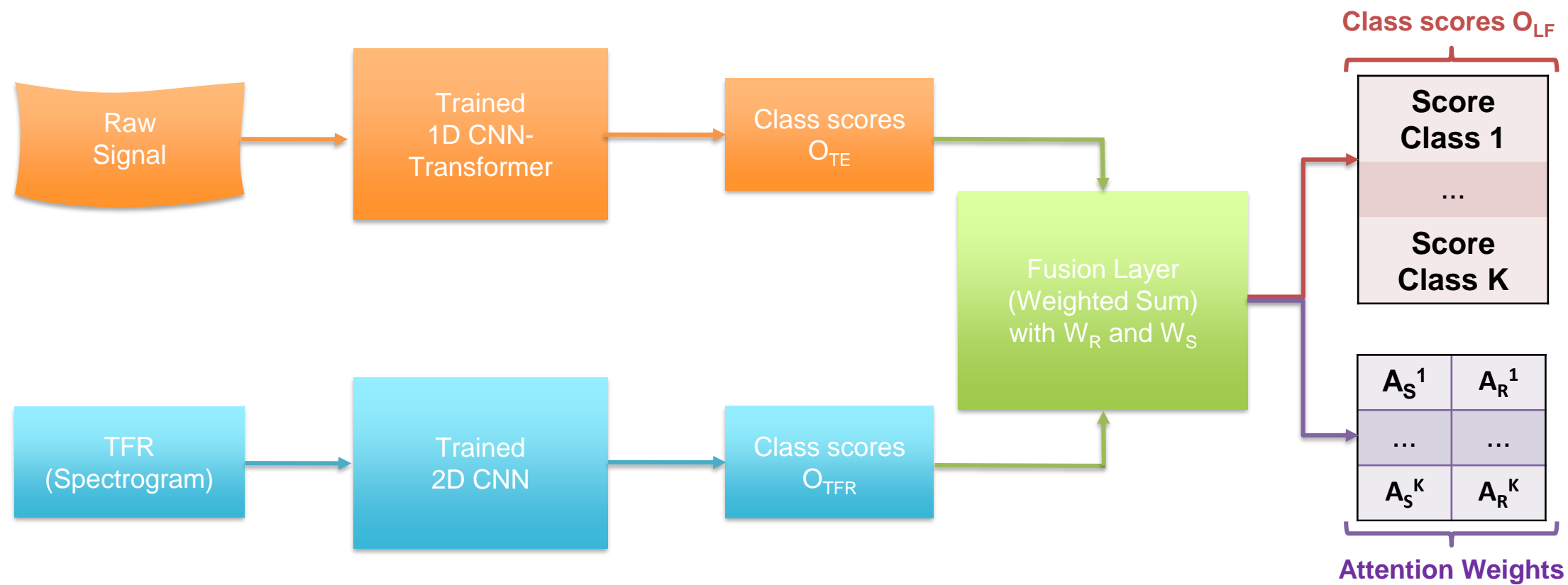


FIGURE - Proposed hybrid CNN Transformer global model

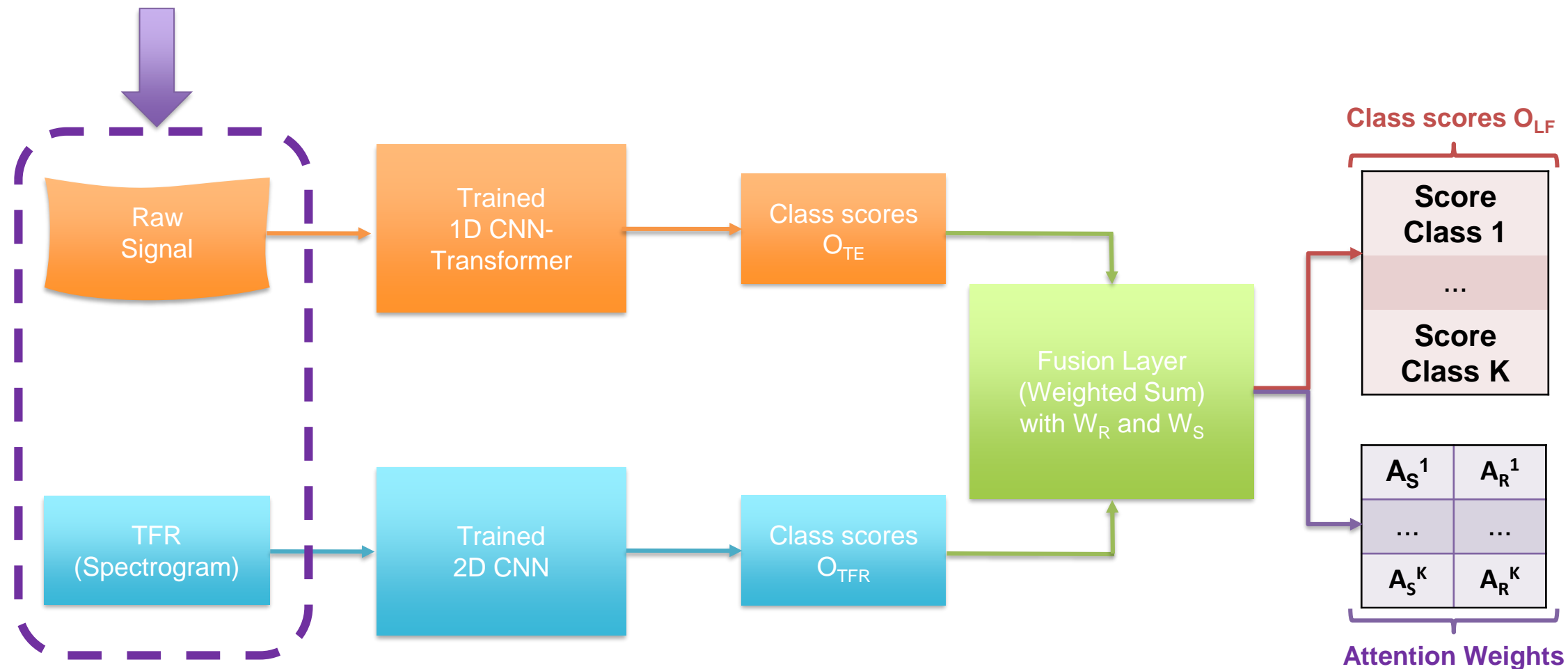


FIGURE - Proposed hybrid CNN Transformer global model

Experimental Setup MLHC 2022

Objective:

- Comparison to **single feature** models.
- Comparison to **SOTA** models.

Models:

- **Single feature models** : 1D CNN-Transformer and 2D CNN.
- **SOTA** : Vindas et al., 2022 (HITS) and Ahmad et al., 2021 (ECG).

Loss function:

- **Cross Entropy Loss**.

Optimizers:

- **ADAM**.
- **NOAM**.

Metrics:

- Matthews Correlation Coefficient (**MCC**).
- **F1-Score**.
- **Accuracy**.

Experimental Setup MLHC 2022

Objective:

- Comparison to **single feature** models.
- Comparison to **SOTA** models.

Models:

- **Single feature models** : 1D CNN-Transformer and 2D CNN.
- **SOTA** : Vindas et al., 2022 (HITS) and Ahmad et al., 2021 (ECG).

Loss function:

- **Cross Entropy Loss**.

Optimizers:

- **ADAM**.
- **NOAM**.

Metrics:

- Matthews Correlation Coefficient (**MCC**). 
 - **F1-Score**. 
 - **Accuracy**. 
- For imbalanced datasets

Results MLHC 2022

Dataset	Model	MCC	F1-Score	Accuracy
HITS	2D CNN (previous work)	85.53 ± 2.98	85.68 ± 2.31	89.48 ± 2.06
	1DCNN-Transformer	80.29 ± 1.83	85.36 ± 1.09	87.37 ± 1.23
	2D CNN	85.03 ± 3.06	86.88 ± 2.38	90.55 ± 2.12
	Hybrid	89.33 ± 2.77	91.15 ± 1.97	93.39 ± 1.74
PTB	MIF (Ahmad et al., 2021)	-	-	98.4
	MFF (Ahmad et al., 2021)	-	-	99.2
	1DCNN-Transformer	97.92 ± 0.28	98.96 ± 0.14	99.16 ± 0.11
	2D CNN	93.42 ± 2.27	96.66 ± 1.20	97.32 ± 0.91
MIT-BIH	Hybrid	99.29 ± 0.21	99.65 ± 0.10	99.71 ± 0.08
	MIF (Ahmad et al., 2021)	-	-	98.6
	MFF (Ahmad et al., 2021)	-	-	99.7
	1DCNN-Transformer	93.17 ± 0.70	89.44 ± 0.99	97.87 ± 0.24
	2D CNN	91.26 ± 0.76	86.40 ± 1.39	97.34 ± 0.26
	Hybrid	94.63 ± 0.29	91.28 ± 0.54	98.37 ± 0.09

Results MLHC 2022

Dataset	Model	MCC	F1-Score	Accuracy
HITS	2D CNN (previous work)	85.53 ± 2.98	85.68 ± 2.31	89.48 ± 2.06
	1DCNN-Transformer	80.29 ± 1.83	85.36 ± 1.09	87.37 ± 1.23
	2D CNN	85.03 ± 3.06	86.88 ± 2.38	90.55 ± 2.12
	Hybrid	89.33 ± 2.77	91.15 ± 1.97	93.39 ± 1.74
	MIF (Ahmad et al., 2021)	-	-	98.4
PTB	MFF (Ahmad et al., 2021)	-	-	99.2
	1DCNN-Transformer	97.92 ± 0.28	98.96 ± 0.14	99.16 ± 0.11
	2D CNN	93.42 ± 2.27	96.66 ± 1.20	97.32 ± 0.91
MIT-BIH	Hybrid	99.29 ± 0.21	99.65 ± 0.10	99.71 ± 0.08
	MIF (Ahmad et al., 2021)	-	-	98.6
	MFF (Ahmad et al., 2021)	-	-	99.7
	1DCNN-Transformer	93.17 ± 0.70	89.44 ± 0.99	97.87 ± 0.24
	2D CNN	91.26 ± 0.76	86.40 ± 1.39	97.34 ± 0.26
	Hybrid	94.63 ± 0.29	91.28 ± 0.54	98.37 ± 0.09

Using both representations increase the classification performances of the model in the three datasets

Results MLHC 2022

Dataset	Model	MCC	F1-Score	Accuracy
HITS	2D CNN (previous work)	85.53 ± 2.98	85.68 ± 2.31	89.48 ± 2.06
	1DCNN-Transformer	80.29 ± 1.83	85.36 ± 1.09	87.37 ± 1.23
	2D CNN	85.03 ± 3.06	86.88 ± 2.38	90.55 ± 2.12
	Hybrid	89.33 ± 2.77	91.15 ± 1.97	93.39 ± 1.74
PTB	MIF (Ahmad et al., 2021)	-	-	98.4
	MFF (Ahmad et al., 2021)	-	-	99.2
	1DCNN-Transformer	97.92 ± 0.28	98.96 ± 0.14	99.16 ± 0.11
	2D CNN	93.42 ± 2.27	96.66 ± 1.20	97.32 ± 0.91
MIT-BIH	Hybrid	99.29 ± 0.21	99.65 ± 0.10	99.71 ± 0.08
	MIF (Ahmad et al., 2021)	-	-	98.6
	MFF (Ahmad et al., 2021)	-	-	99.7
	1DCNN-Transformer	93.17 ± 0.70	89.44 ± 0.99	97.87 ± 0.24
	2D CNN	91.26 ± 0.76	86.40 ± 1.39	97.34 ± 0.26
	Hybrid	94.63 ± 0.29	91.28 ± 0.54	98.37 ± 0.09

More stable models (reduced variability), except for the HITS dataset.

Results MLHC 2022

Dataset	Model	MCC	F1-Score	Accuracy
HITS	2D CNN (previous work)	85.53 ± 2.98	85.68 ± 2.31	89.48 ± 2.06
	1DCNN-Transformer	80.29 ± 1.83	85.36 ± 1.09	87.37 ± 1.23
	2D CNN	85.03 ± 3.06	86.88 ± 2.38	90.55 ± 2.12
	Hybrid	89.33 ± 2.77	91.15 ± 1.97	93.39 ± 1.74
PTB	MIF (Ahmad et al., 2021)	-	-	98.4
	MFF (Ahmad et al., 2021)	-	-	99.2
	1DCNN-Transformer	97.92 ± 0.28	98.96 ± 0.14	99.16 ± 0.11
	2D CNN	93.42 ± 2.27	96.66 ± 1.20	97.32 ± 0.91
MIT-BIH	Hybrid	99.29 ± 0.21	99.65 ± 0.10	99.71 ± 0.08
	MIF (Ahmad et al., 2021)	-	-	98.6
	MFF (Ahmad et al., 2021)	-	-	99.7
	1DCNN-Transformer	93.17 ± 0.70	89.44 ± 0.99	97.87 ± 0.24
	2D CNN	91.26 ± 0.76	86.40 ± 1.39	97.34 ± 0.26
	Hybrid	94.63 ± 0.29	91.28 ± 0.54	98.37 ± 0.09

State-of-the-art results on two datasets.

Experiment 2: Influence of the fusion layer MLHC 2022

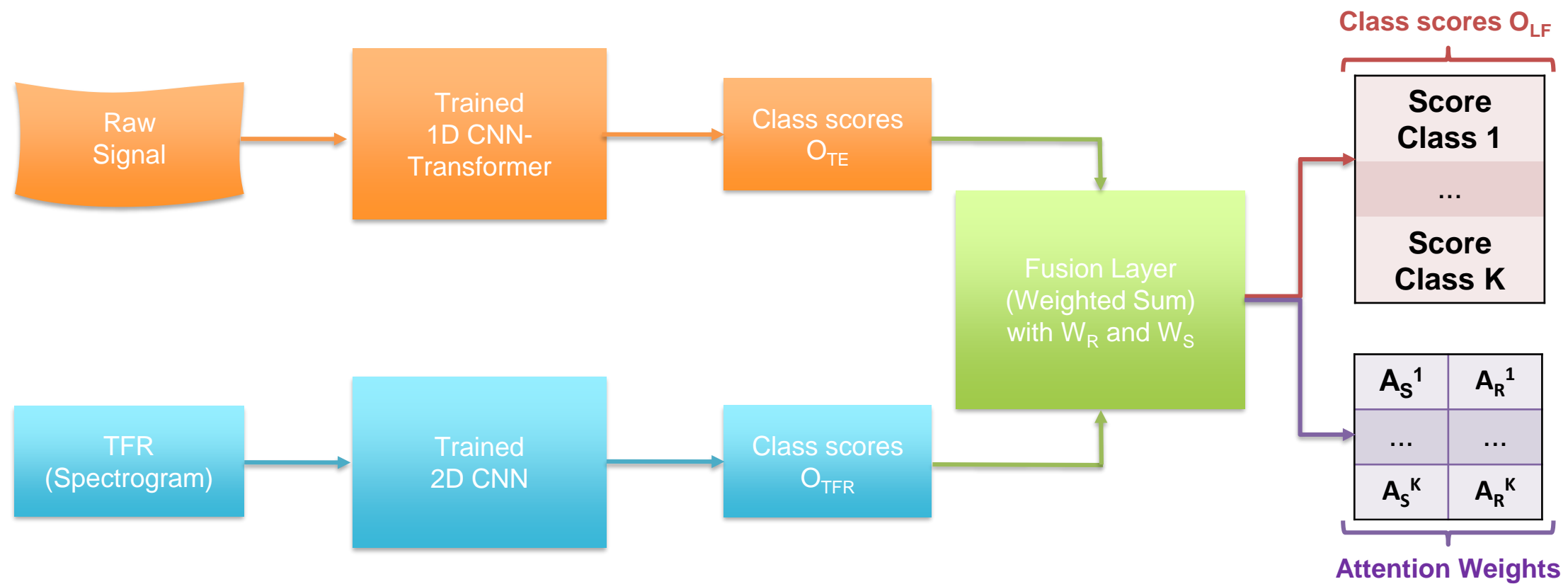


FIGURE - Proposed hybrid CNN Transformer global model

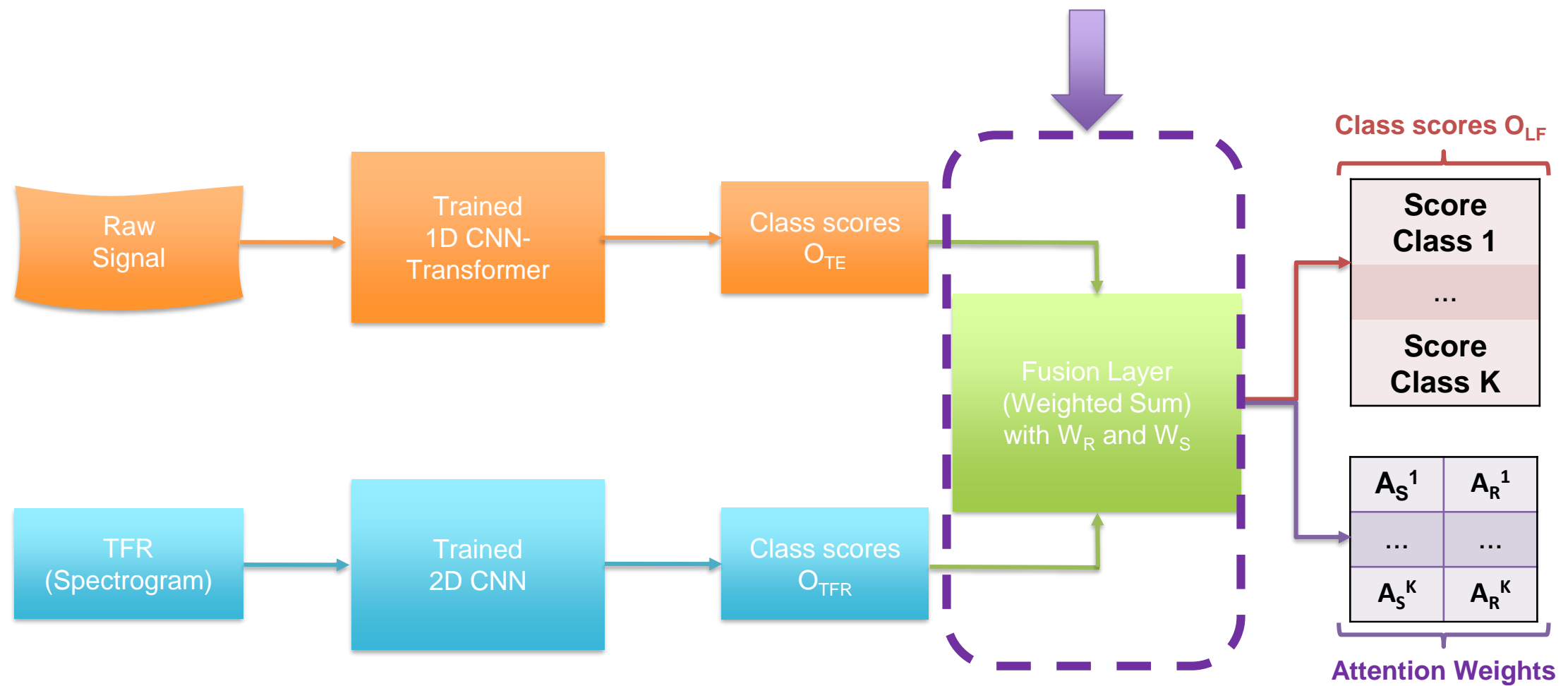


FIGURE - Proposed hybrid CNN Transformer global model

Experimental Setup MLHC 2022

Objective:

- Comparison to **intermediate fusion** models.

Models:

- Concatenation.
- Sum.
- Weighted sum.

Loss function:

- Cross Entropy Loss.

Optimizers:

- NOAM.

Metrics:

- Matthews Correlation Coefficient (**MCC**).
- **F1-Score**.
- Accuracy.

Experimental Setup MLHC 2022

Objective:

- Comparison to **intermediate fusion** models.

Models:

- Concatenation.
- Sum.
- Weighted sum.

Loss function:

- Cross Entropy Loss.

Optimizers:

- NOAM.

Metrics:

- Matthews Correlation Coefficient (**MCC**). 
 - **F1-Score**.
 - **Accuracy**.
- For imbalanced datasets

Results MLHC 2022

Dataset	Fusion Type	MCC	F1-Score	Accuracy
HITS	Concatenation	84.96 ± 2.54	86.37 ± 2.11	90.62 ± 1.65
	Sum	89.04 ± 1.98	90.23 ± 1.71	93.16 ± 1.29
	Weighted Sum	86.31 ± 2.80	87.73 ± 2.32	91.31 ± 1.92
	Hybrid	89.33 ± 2.77	91.15 ± 1.97	93.39 ± 1.74
PTB	Concatenation	92.91 ± 2.61	96.42 ± 1.33	97.11 ± 1.05
	Sum	92.12 ± 2.33	96.02 ± 1.19	96.78 ± 0.99
	Weighted Sum	92.74 ± 2.01	96.35 ± 1.00	97.06 ± 0.81
	Hybrid	99.29 ± 0.21	99.65 ± 0.10	99.71 ± 0.08
MIT-BIH	Concatenation	91.51 ± 0.79	86.93 ± 1.10	97.42 ± 0.27
	Sum	91.89 ± 0.47	87.50 ± 0.87	97.55 ± 0.15
	Weighted Sum	91.56 ± 0.72	86.70 ± 1.13	97.44 ± 0.24
	Hybrid	94.63 ± 0.29	91.28 ± 0.54	98.37 ± 0.09

Results MLHC 2022

Dataset	Fusion Type	MCC	F1-Score	Accuracy
HITS	Concatenation	84.96 ± 2.54	86.37 ± 2.11	90.62 ± 1.65
	Sum	89.04 ± 1.98	90.23 ± 1.71	93.16 ± 1.29
	Weighted Sum	86.31 ± 2.80	87.73 ± 2.32	91.31 ± 1.92
	Hybrid	89.33 ± 2.77	91.15 ± 1.97	93.39 ± 1.74
PTB	Concatenation	92.91 ± 2.61	96.42 ± 1.33	97.11 ± 1.05
	Sum	92.12 ± 2.33	96.02 ± 1.19	96.78 ± 0.99
	Weighted Sum	92.74 ± 2.01	96.35 ± 1.00	97.06 ± 0.81
	Hybrid	99.29 ± 0.21	99.65 ± 0.10	99.71 ± 0.08
MIT-BIH	Concatenation	91.51 ± 0.79	86.93 ± 1.10	97.42 ± 0.27
	Sum	91.89 ± 0.47	87.50 ± 0.87	97.55 ± 0.15
	Weighted Sum	91.56 ± 0.72	86.70 ± 1.13	97.44 ± 0.24
	Hybrid	94.63 ± 0.29	91.28 ± 0.54	98.37 ± 0.09

The best fusion method is the late proposed method for the three datasets.

Results MLHC 2022

Dataset	Fusion Type	MCC	F1-Score	Accuracy
HITS	Concatenation	84.96 ± 2.54	86.37 ± 2.11	90.62 ± 1.65
	Sum	89.04 ± 1.98	90.23 ± 1.71	93.16 ± 1.29
	Weighted Sum	86.31 ± 2.80	87.73 ± 2.32	91.31 ± 1.92
	Hybrid	89.33 ± 2.77	91.15 ± 1.97	93.39 ± 1.74
PTB	Concatenation	92.91 ± 2.61	96.42 ± 1.33	97.11 ± 1.05
	Sum	92.12 ± 2.33	96.02 ± 1.19	96.78 ± 0.99
	Weighted Sum	92.74 ± 2.01	96.35 ± 1.00	97.06 ± 0.81
	Hybrid	99.29 ± 0.21	99.65 ± 0.10	99.71 ± 0.08
MIT-BIH	Concatenation	91.51 ± 0.79	86.93 ± 1.10	97.42 ± 0.27
	Sum	91.89 ± 0.47	87.50 ± 0.87	97.55 ± 0.15
	Weighted Sum	91.56 ± 0.72	86.70 ± 1.13	97.44 ± 0.24
	Hybrid	94.63 ± 0.29	91.28 ± 0.54	98.37 ± 0.09

For the HITS dataset: the intermediate sum fusion method achieve similar performances as the late hybrid fusion method

Results MLHC 2022

Dataset	Fusion Type	MCC	F1-Score	Accuracy
HITS	Concatenation	84.96 ± 2.54	86.37 ± 2.11	90.62 ± 1.65
	Sum	89.04 ± 1.98	90.23 ± 1.71	93.16 ± 1.29
	Weighted Sum	86.31 ± 2.80	87.73 ± 2.32	91.31 ± 1.92
	Hybrid	89.33 ± 2.77	91.15 ± 1.97	93.39 ± 1.74
PTB	Concatenation	92.91 ± 2.61	96.42 ± 1.33	97.11 ± 1.05
	Sum	92.12 ± 2.33	96.02 ± 1.19	96.78 ± 0.99
	Weighted Sum	92.74 ± 2.01	96.35 ± 1.00	97.06 ± 0.81
	Hybrid	99.29 ± 0.21	99.65 ± 0.10	99.71 ± 0.08
MIT-BIH	Concatenation	91.51 ± 0.79	86.93 ± 1.10	97.42 ± 0.27
	Sum	91.89 ± 0.47	87.50 ± 0.87	97.55 ± 0.15
	Weighted Sum	91.56 ± 0.72	86.70 ± 1.13	97.44 ± 0.24
	Hybrid	94.63 ± 0.29	91.28 ± 0.54	98.37 ± 0.09

- The other fusion methods have similar performances for the three datasets.
- Worst performances than the best single feature model of experiment 1.

Results MLHC 2022

Results MLHC 2022

Attention weights for the HITS dataset

Results MLHC 2022

Class	Spectrogram	Raw Signal
Artifacts	0.46 ± 0.29	0.54 ± 0.29
Gaseous Emboli	0.65 ± 0.17	0.35 ± 0.17
Solid Emboli	0.71 ± 0.15	0.29 ± 0.15

Attention weights for the HITS dataset

Results MLHC 2022

Class	Spectrogram	Raw Signal
Artifacts	0.46 ± 0.29	0.54 ± 0.29
Gaseous Emboli	0.65 ± 0.17	0.35 ± 0.17
Solid Emboli	0.71 ± 0.15	0.29 ± 0.15

Attention weights for the HITS dataset

Attention weights for the PTB dataset

Results MLHC 2022

Class	Spectrogram	Raw Signal
Artifacts	0.46 ± 0.29	0.54 ± 0.29
Gaseous Emboli	0.65 ± 0.17	0.35 ± 0.17
Solid Emboli	0.71 ± 0.15	0.29 ± 0.15

Attention weights for the HITS dataset

Class	Spectrogram	Raw Signal
Normal	0.49 ± 0.12	0.51 ± 0.12
Abnormal	0.18 ± 0.10	0.82 ± 0.10

Attention weights for the PTB dataset

Results MLHC 2022

Class	Spectrogram	Raw Signal
Artifacts	0.46 ± 0.29	0.54 ± 0.29
Gaseous Emboli	0.65 ± 0.17	0.35 ± 0.17
Solid Emboli	0.71 ± 0.15	0.29 ± 0.15

Attention weights for the HITS dataset

Class	Spectrogram	Raw Signal
Normal	0.49 ± 0.12	0.51 ± 0.12
Abnormal	0.18 ± 0.10	0.82 ± 0.10

Attention weights for the PTB dataset

Attention weights for the MIT-BIH dataset

Results MLHC 2022

Class	Spectrogram	Raw Signal
Artifacts	0.46 ± 0.29	0.54 ± 0.29
Gaseous Emboli	0.65 ± 0.17	0.35 ± 0.17
Solid Emboli	0.71 ± 0.15	0.29 ± 0.15

Attention weights for the HITS dataset

Class	Spectrogram	Raw Signal
Normal	0.49 ± 0.12	0.51 ± 0.12
Abnormal	0.18 ± 0.10	0.82 ± 0.10

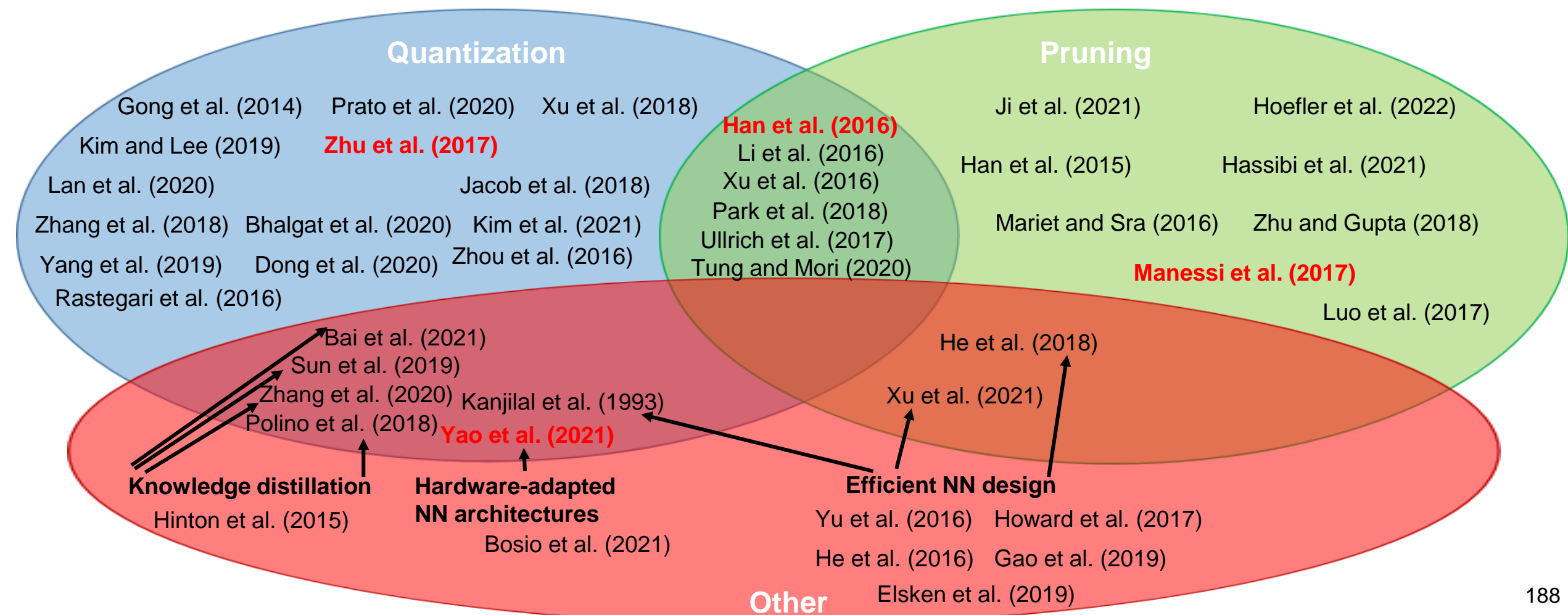
Attention weights for the PTB dataset

Class	Spectrogram	Raw Signal
N	0.48 ± 0.01	0.52 ± 0.01
S	0.50 ± 0.01	0.50 ± 0.01
V	0.50 ± 0.01	0.50 ± 0.01
F	0.49 ± 0.02	0.51 ± 0.02
Q	0.50 ± 0.003	0.50 ± 0.003

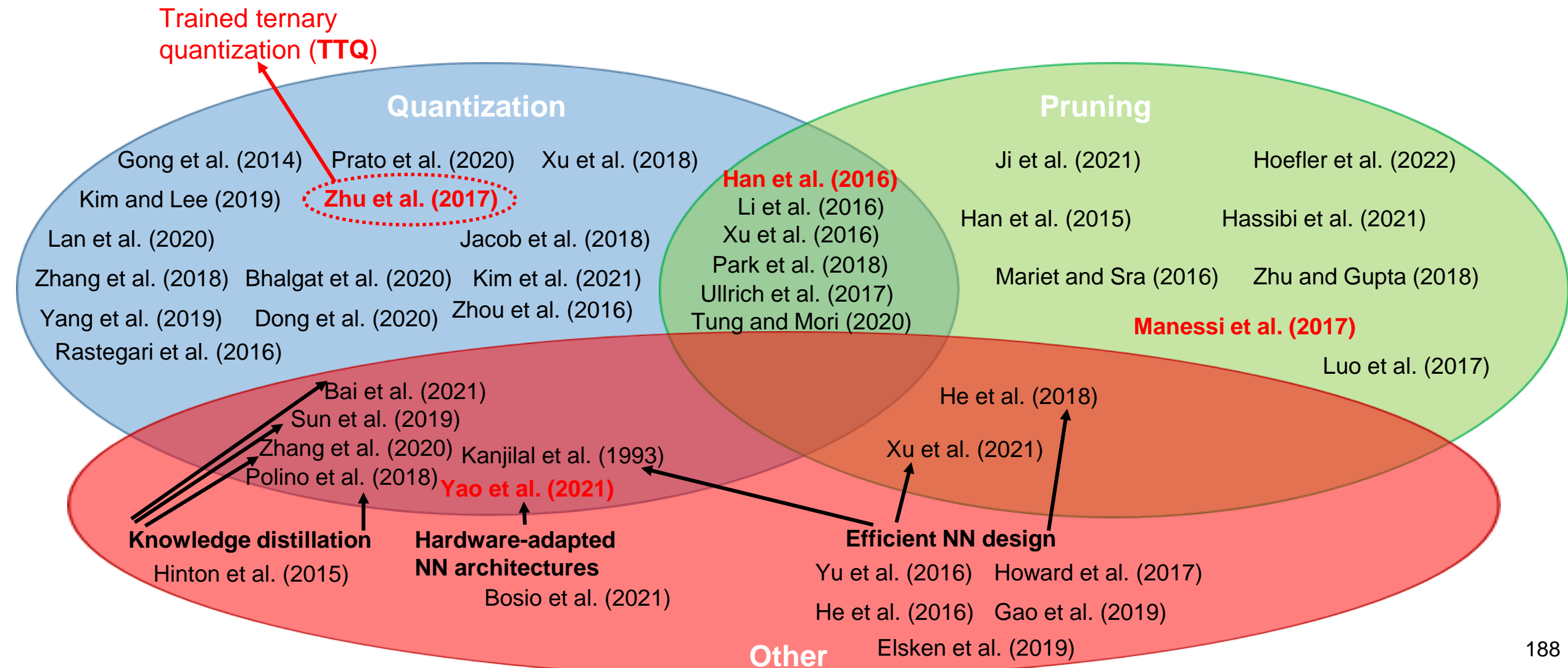
Attention weights for the MIT-BIH dataset

Contribution 3 : Model compression based on extreme quantization

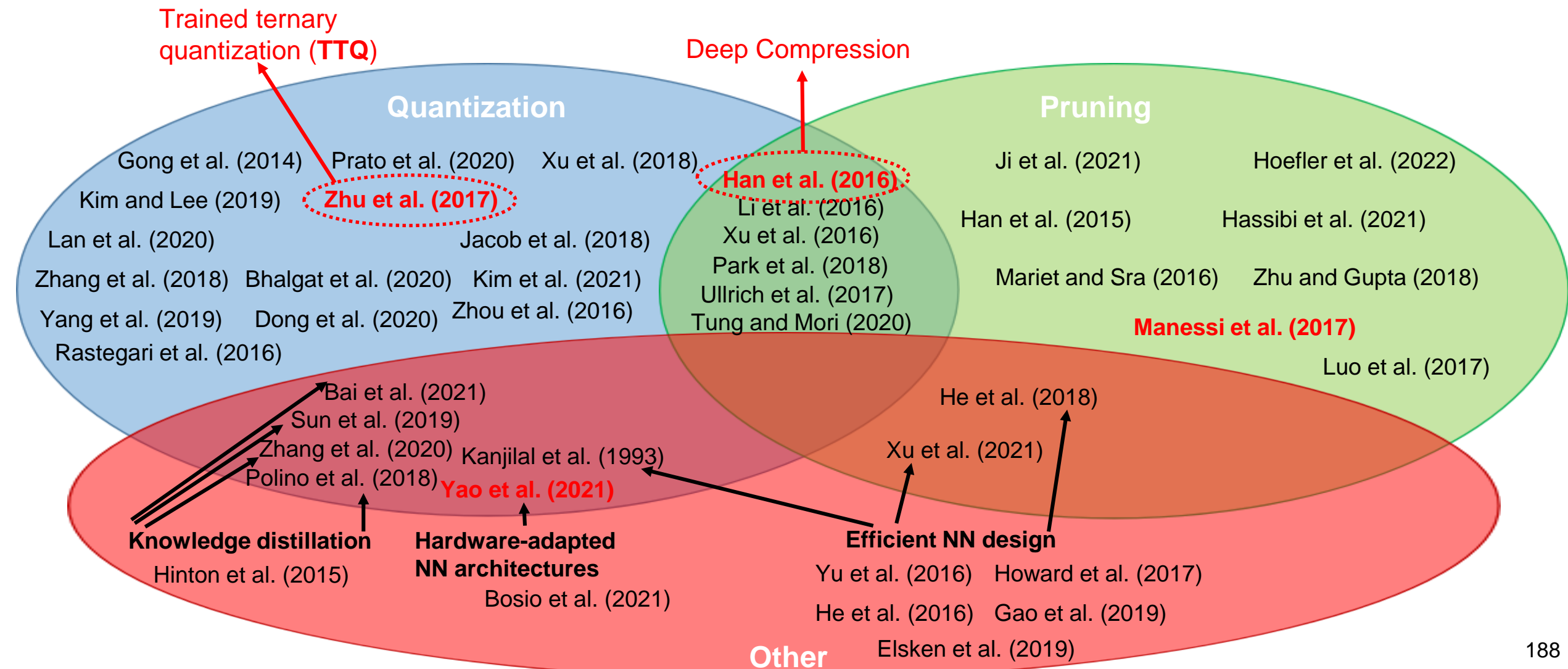
General Overview



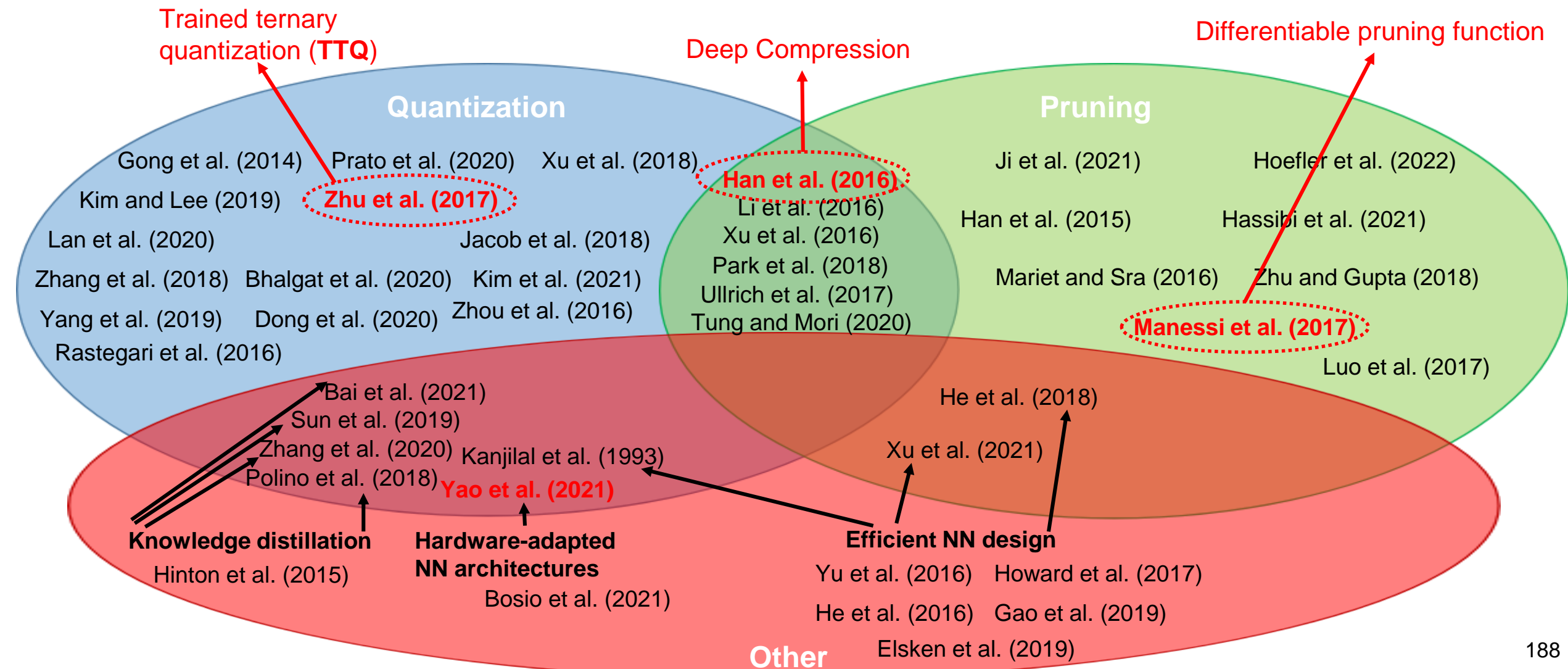
General Overview



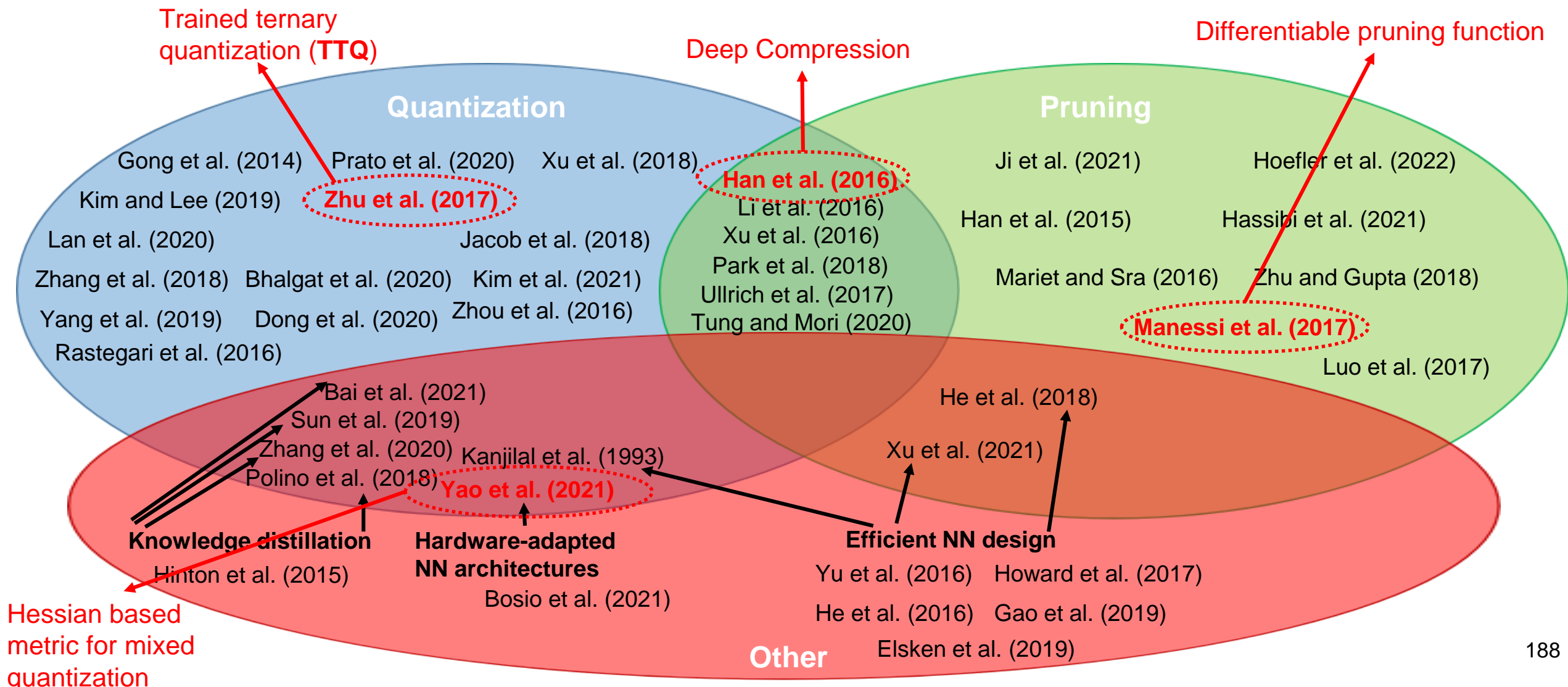
General Overview



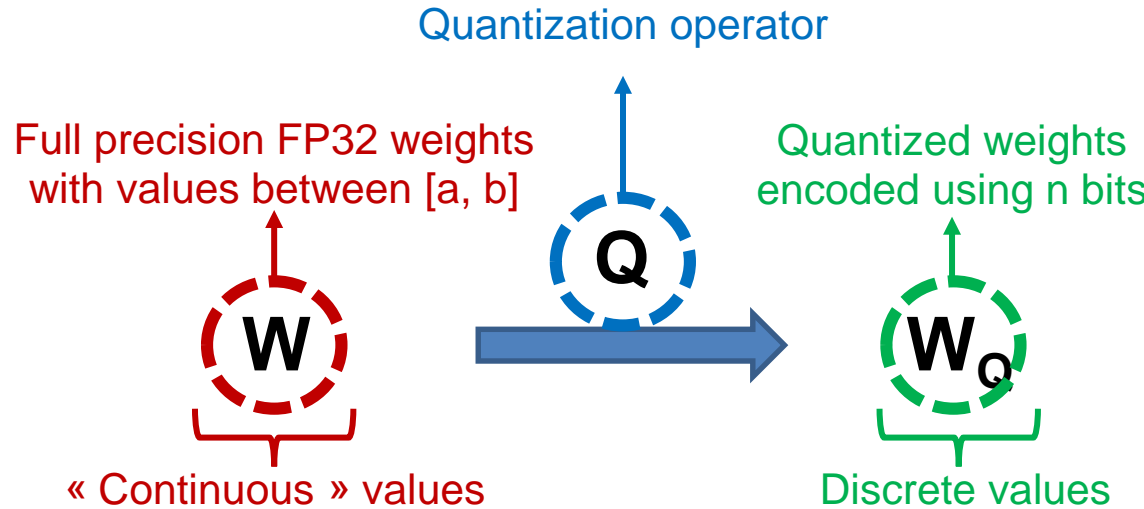
General Overview



General Overview

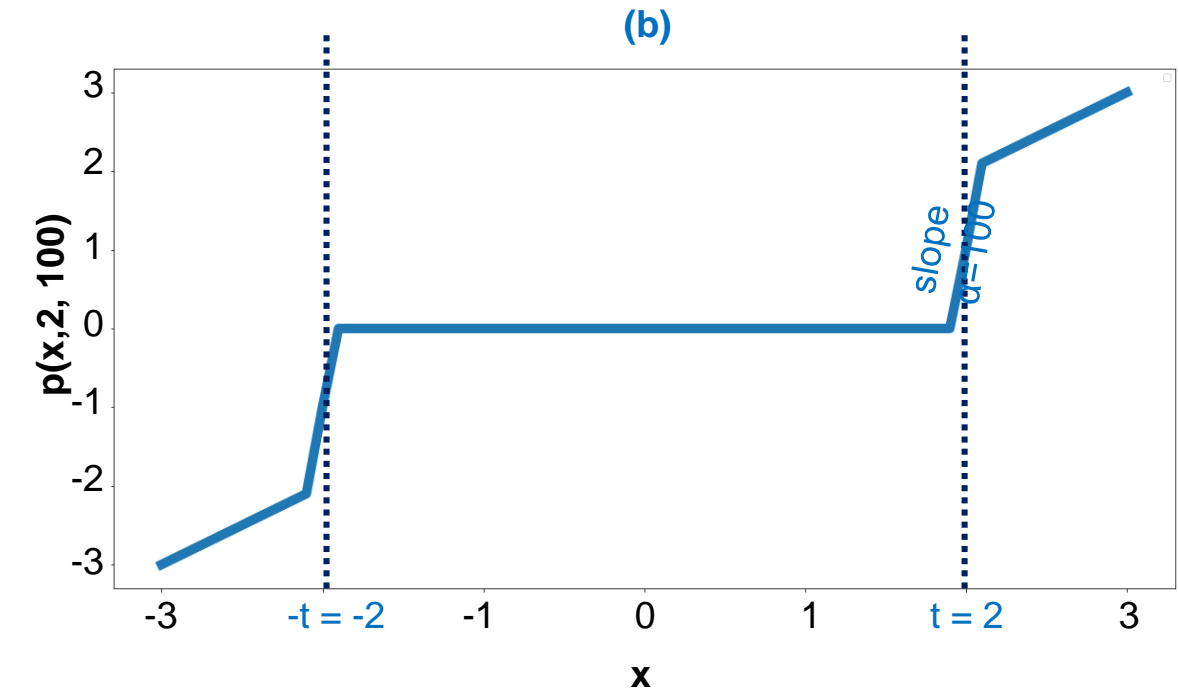
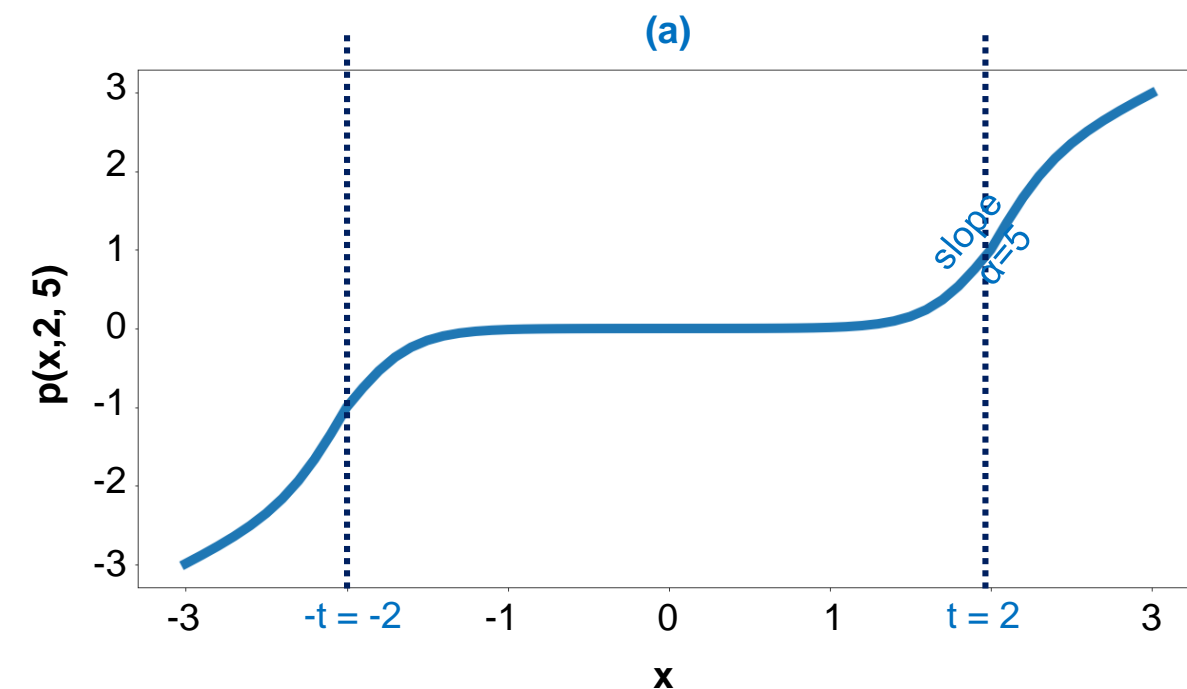


Quantization principle



- **Clipping range** : interval [a, b] where the values of **W** live.
- **Calibration** : step of clipping range search.
- **Scaling factor S** : Number of partitions of the clipping range to use.

Differentiable pruning function



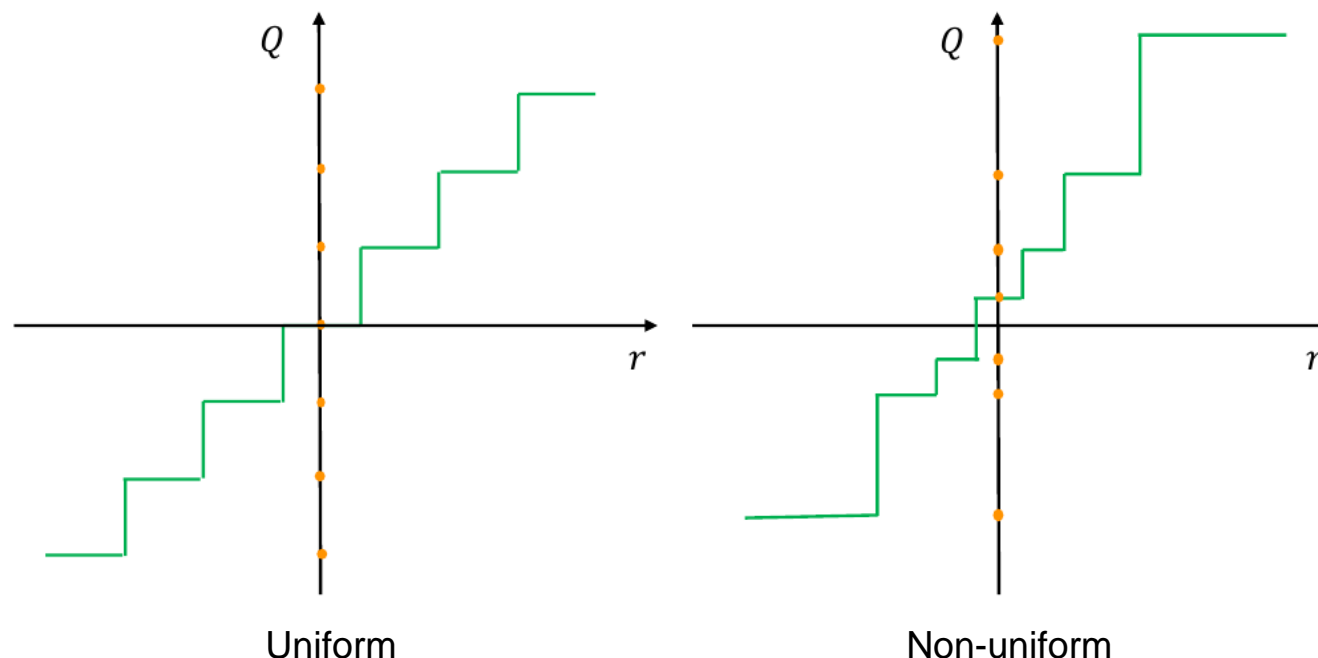
$$\forall x, t, \alpha \in \mathbb{R}, p(x; t, \alpha) = [ReLU(x - t) + t \times \sigma(\alpha \times (x - t))] + [-ReLU(-x - t) - t \times \sigma(\alpha \times (-x - t))]$$

Figure – Differentiable pruning function (Manessi et al. 2017)

Quantization

Uniform vs non-uniform :

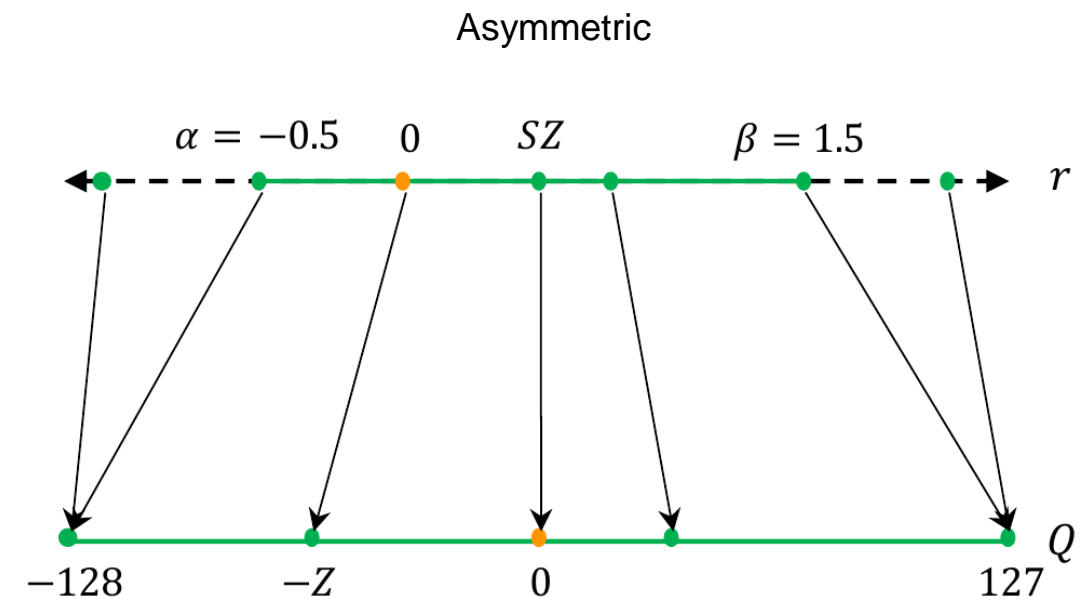
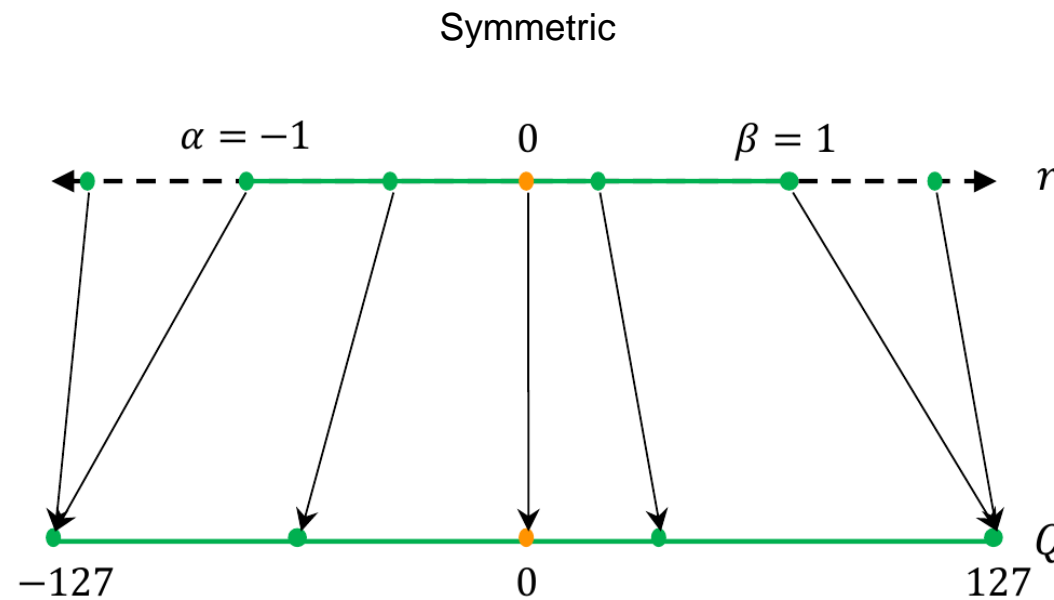
- + Easier to deploy
- Worst classification performances



- + Higher classification performances
- More difficult to deploy

Quantization

Symmetric vs asymmetric :



- + Easier to implement
- + Reduce computational cost
- Not adapted to imbalanced weights/activations
- Worst classification performances

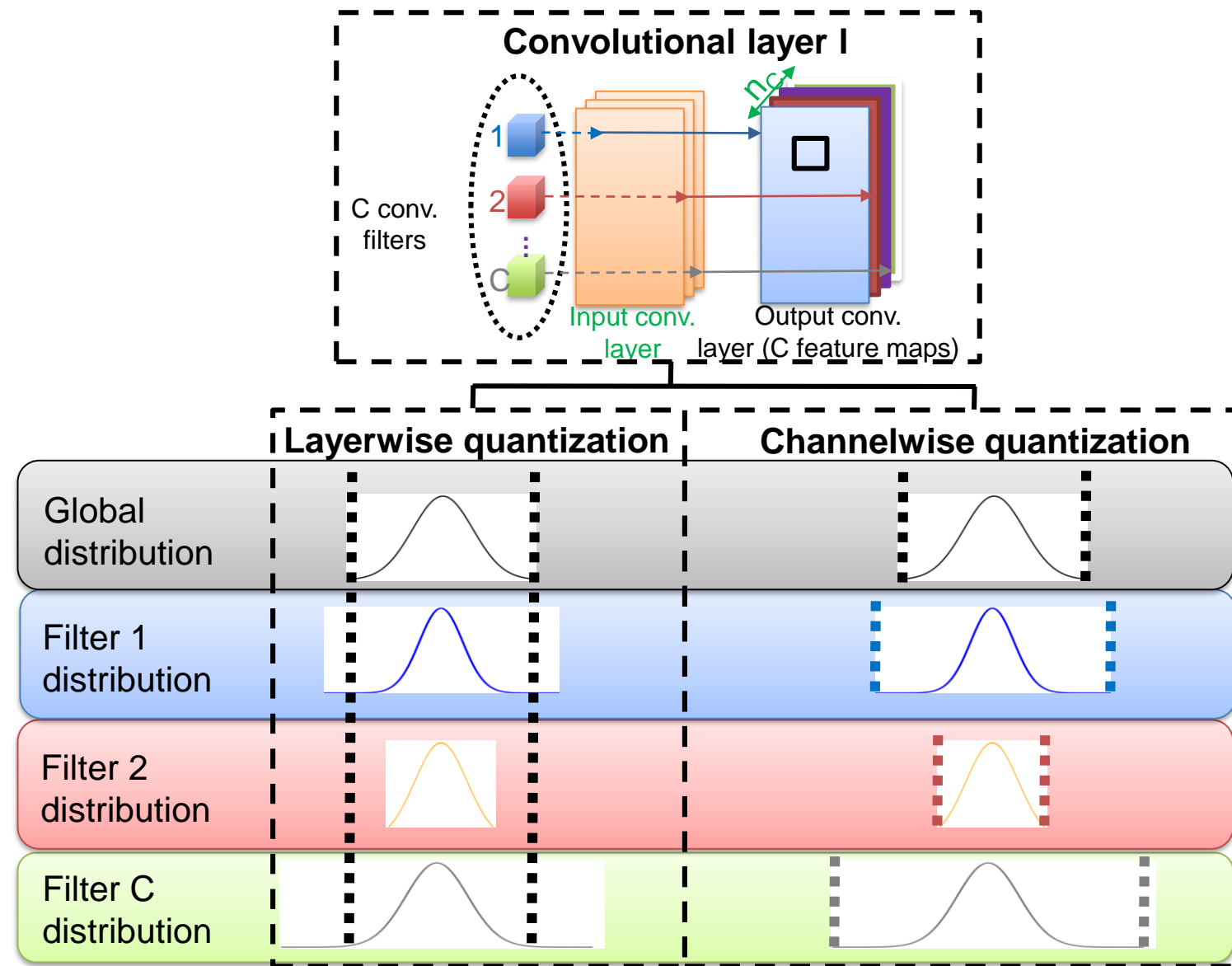
- + Better classification performances
- + Adapted for imbalanced weights/activations
- More difficult to implement
- More computationally expensive

Quantization

Static vs dynamic (w.r.t. clipping range) :

Static	Dynamic
Clipping range pre-computed before inference	Clipping range computed dynamically during inference
+ Less computation resources	+ Higher performances
- Lower performances	- Computationally expensive
==> Most commonly used	

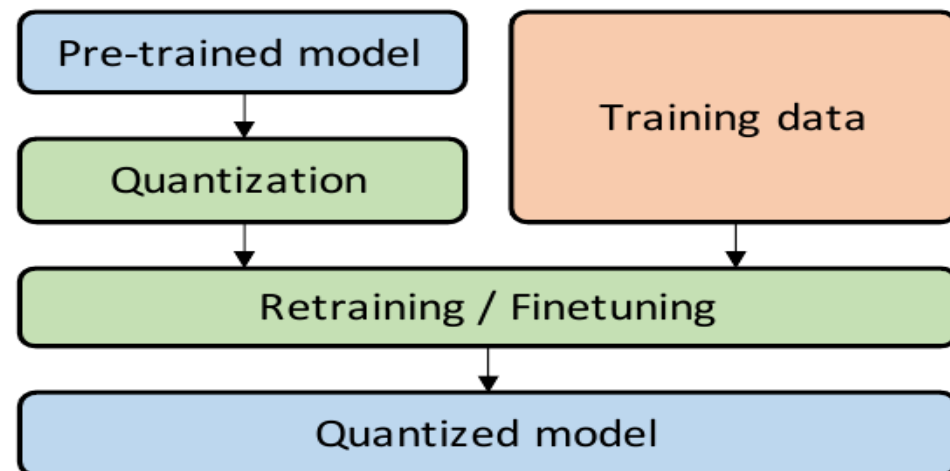
Quantization granularities



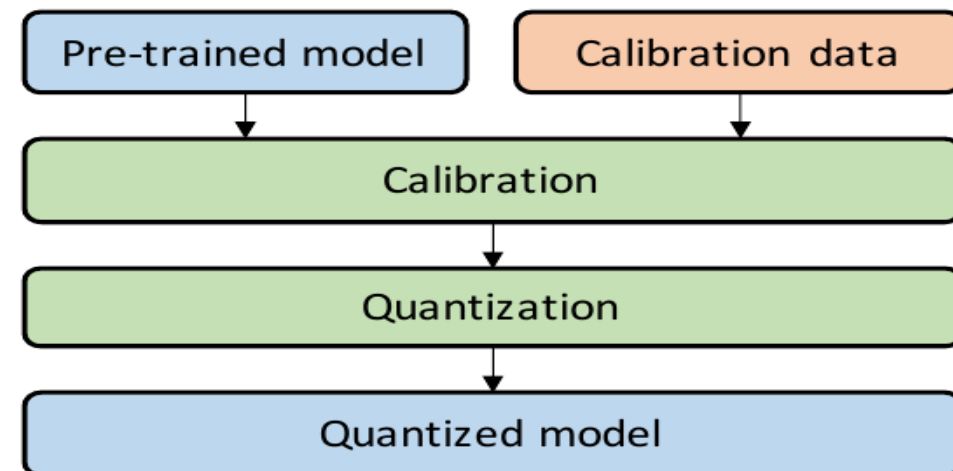
Quantization

QAT vs PTQ vs ZSQ :

Quantized Aware Training (QAT)



Post-Training Quantization



- + Higher classification performances
- ~ Be careful with gradient computation
- Expensive during training

- + Does not modify the training procedure
- Lower classification performances

Types of quantization approaches (Gholami et al. 2021)

- QAT vs PTQ vs ZSQ :
 - Zero-Shot Quantization:
 - No need of training, validation or testing data.
 - Good when we do not have access to the original training data.
 - Can be mixed with QAT and PTQ:
 - No data + fine-tuning ==> ZSQ + PTQ.
 - Correcting biases introduced in the quantized weights.
 - No data + fine-tuning ==> ZSQ + QAT
 - Ex.: use of synthetic data.

Quantization

Stochastic vs deterministic :

Stochastic

$$Q(W) = \begin{cases} W_Q \text{ with probability } p \\ W_{Q'} \text{ with probability } 1-p \end{cases}$$

Deterministic

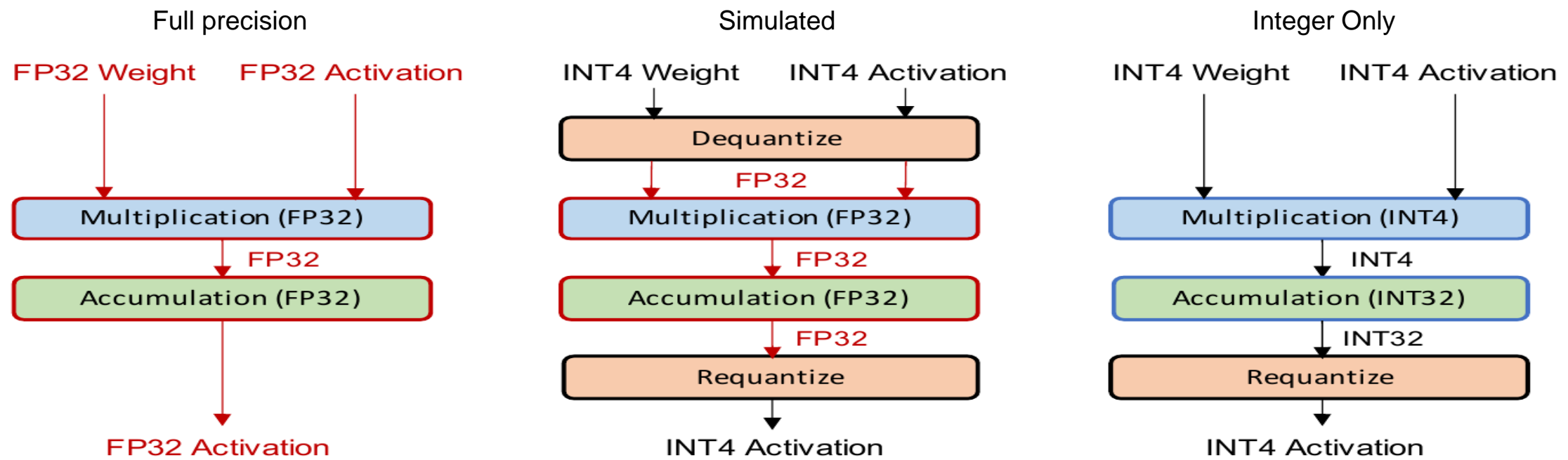
$$Q(W) = w_Q$$

- + Higher classification performances
- Choice of the stochastic strategy
- Overhead due to the generation of random numbers

- + Less computationally expensive
- + “Easier” to optimize
- Lower classification performances

Quantization

Simulated vs Integer-only :



Simulated :

- + Better classification performances
- Does not benefit from low-precision logic

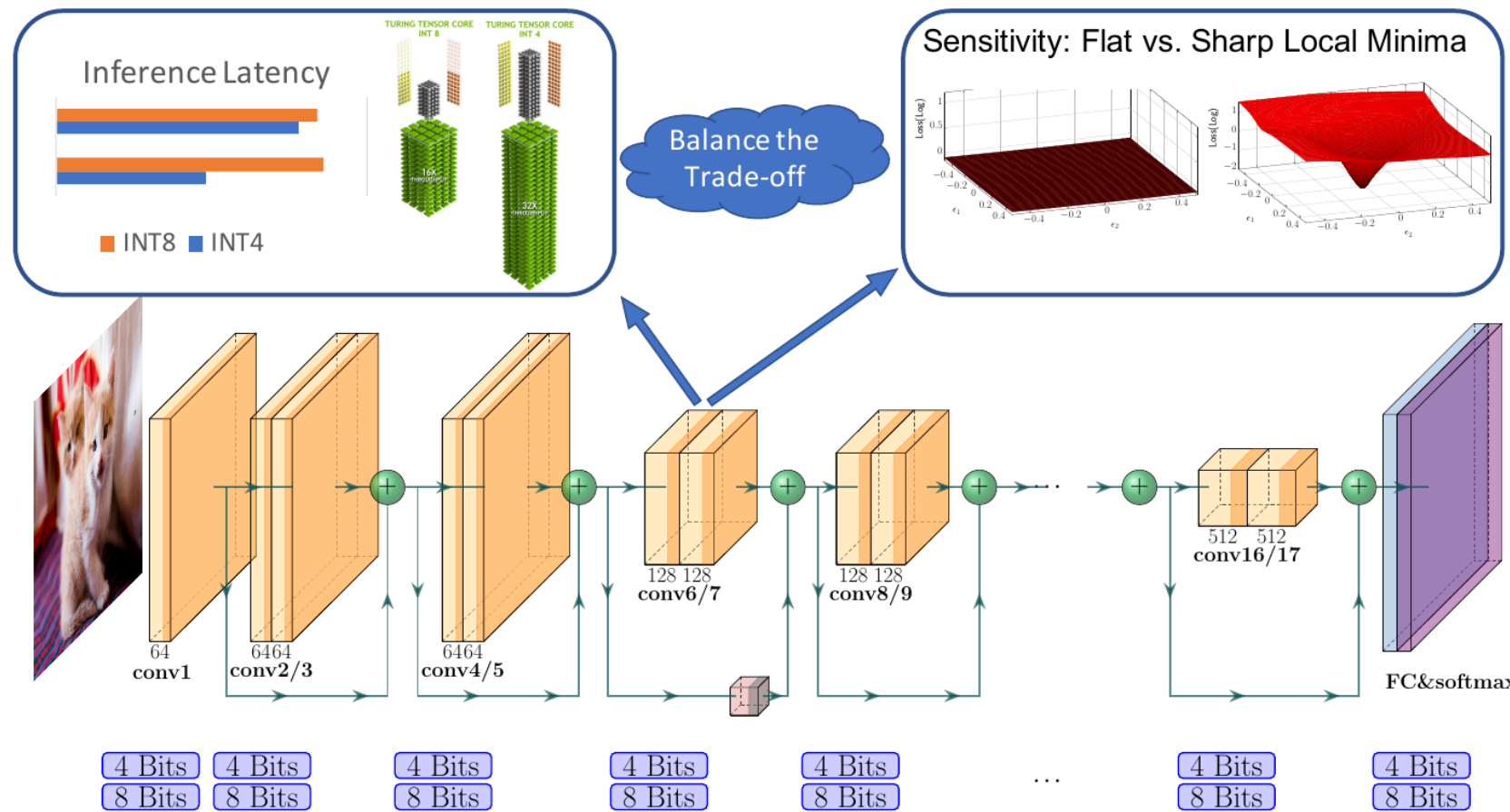
Integer-only :

- + Benefits from low-precision logic
- Lower classification performances
- Most works are limited to ReLU activations

Quantization

Mixed precision :

- Reinforcement learning approaches.
- NAS approaches.
- Regularization approaches.
- Hessian approaches.



HAWQ

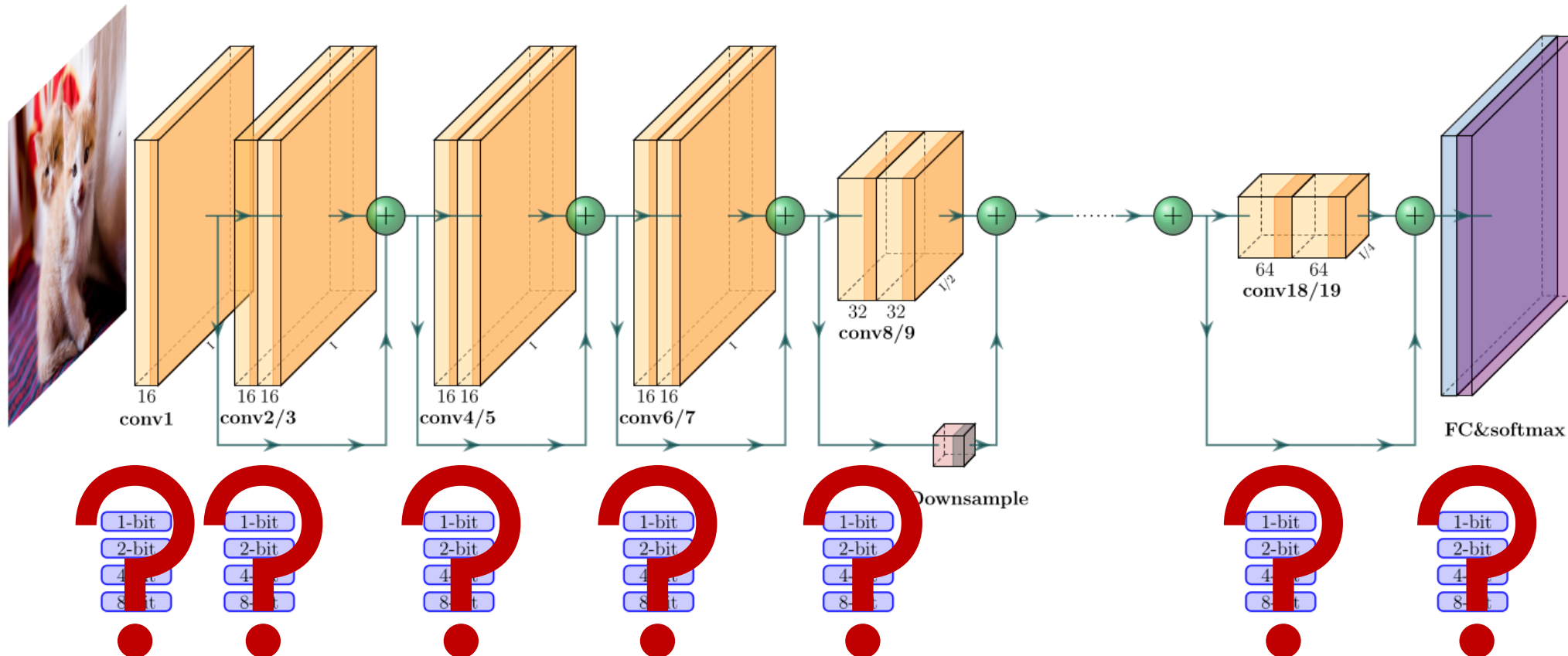


Figure – Hessian aware trace weighted quantization (HAWQ) for mixed quantization (**Dong et al. 2020**)

HAWQ

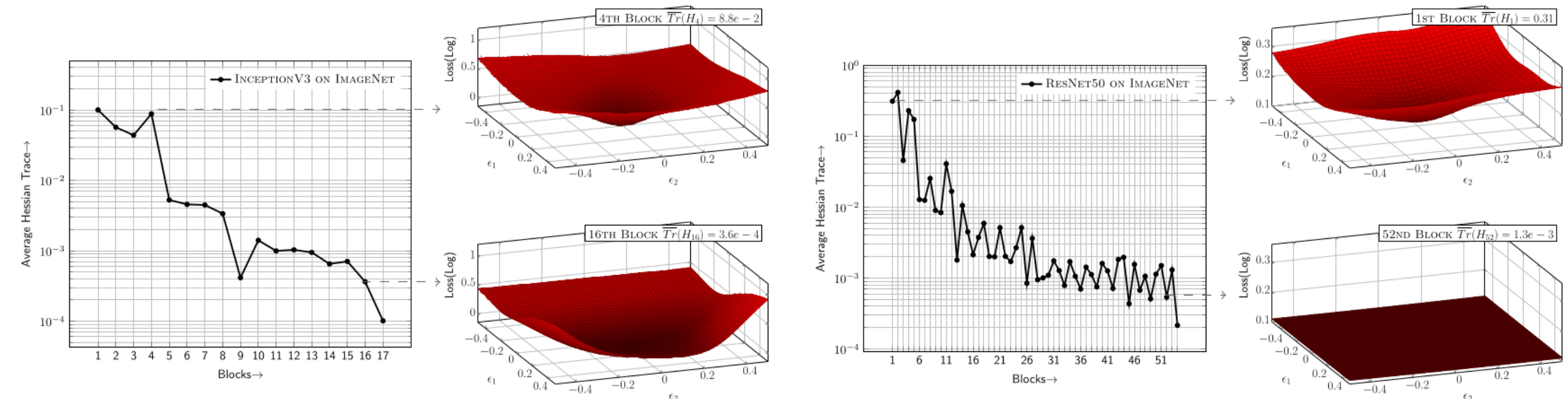
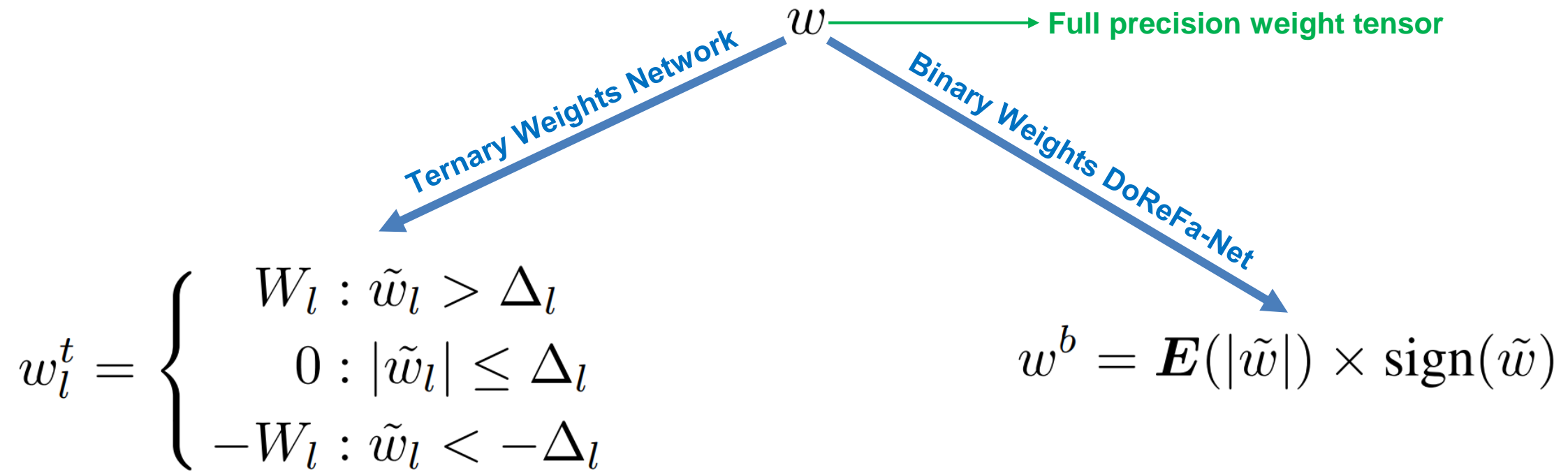


Figure – Hessian aware trace weighted quantization (HAWQ) for mixed quantization (**Dong et al. 2020**)

Ternary Weight Networks and DoReFa-Net



$$\Delta_l = 0.7 \times E(|\tilde{w}_l|)$$

$$W_l = \underset{i \in \{i|\tilde{w}_l(i)| > \Delta\}}{E} (|\tilde{w}_l(i)|)$$

Compression evaluation metrics

Sparsity-based metric

$$SRQW(\mathcal{M}_{FP}, \mathcal{M}_C) = \frac{nqw(\mathcal{M}_C)}{nqw(\mathcal{M}_{FP})}$$

Diagram illustrating the components of the Sparsity-based metric:

- A green dashed circle encloses \mathcal{M}_{FP} and \mathcal{M}_C .
- An arrow labeled "Full precision model" points to \mathcal{M}_{FP} .
- An arrow labeled "Quantized model" points to \mathcal{M}_C .
- An arrow labeled "Function counting the number of quantized weights having a value of 0" points to the numerator $nqw(\mathcal{M}_C)$.
- An arrow labeled "Function counting the number of weights that can be quantized" points to the denominator $nqw(\mathcal{M}_{FP})$.

Compression-based metrics

$$CR(\mathcal{M}_{FP}, \mathcal{M}_Q) = \frac{nbits(\mathcal{M}_Q)}{nbits(\mathcal{M}_{FP})} ; CR_G(\mathcal{M}_{FP}, \mathcal{M}_Q) = 1 - CR(\mathcal{M}_{FP}, \mathcal{M}_Q)$$

Diagram illustrating the components of the Compression-based metric:

- A green dashed circle encloses \mathcal{M}_Q and \mathcal{M}_{FP} .
- An arrow labeled "Function counting the number of bits necessary to store the weights (using COO sparse storage format)" points to the numerator $nbits(\mathcal{M}_Q)$.

Energy consumption evaluation metrics

Energy of mult-adds

$$EC_{MA}(\mathcal{M}) = N_{MA} \times 3.7 \times 10^{-12}$$

Number of nonzero mult-adds

Order of magnitude of the energy cost of a 32-bit multiplication (Horowitz et al. 2014)

Energy consumption evaluation metrics

Energy of data transfers

$$EC_{DT}(\mathcal{M}) = 10^{-9} \times \sum_{i=1}^p \left(\lceil \frac{nnzw(L_i) \times B_i}{32} \rceil + N_{SF}^i \right)$$

Order of magnitude of data transfers to memory from Molka et al. (2010)

Number of layers in the model

Current layer

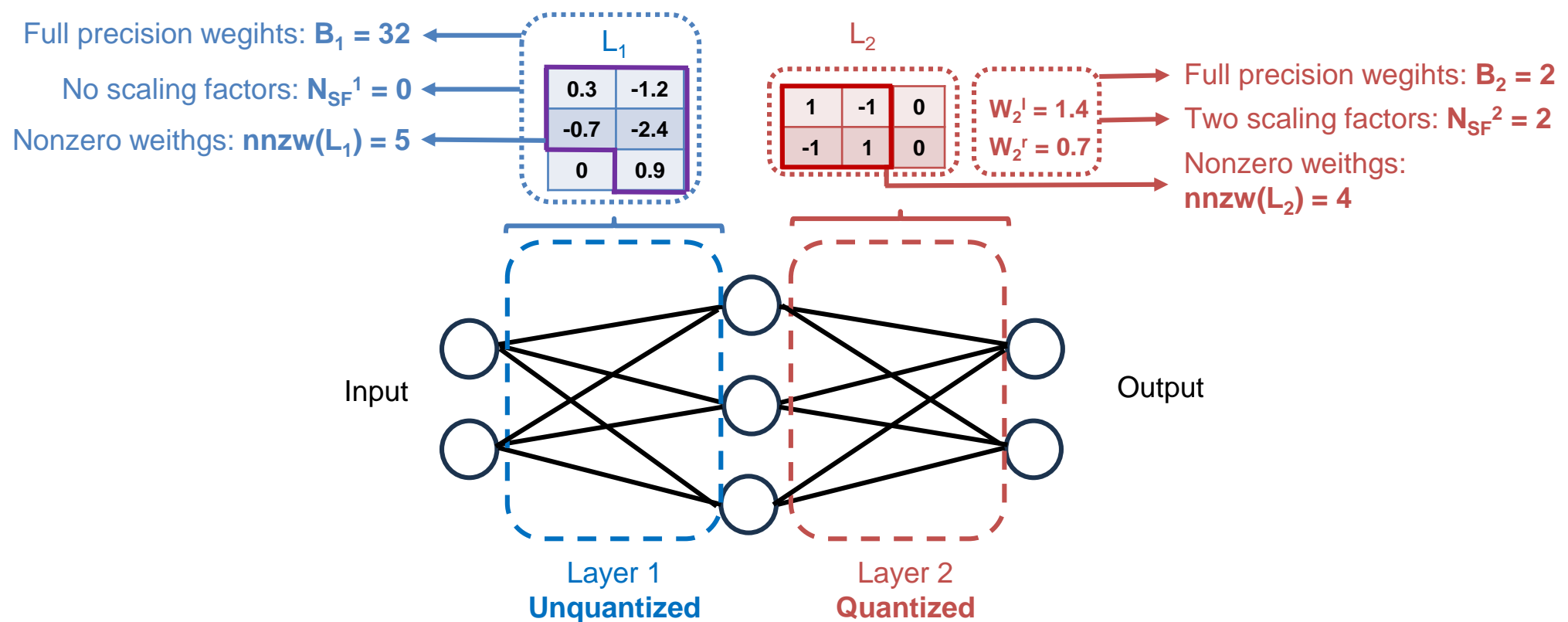
Number of bits necessary to encode the weights of the layer

Number of scaling factors

Function counting the number of nonzero weights

Energy consumption evaluation metrics

Energy of data transfers



$$\begin{aligned}
 EC_{DT}(\mathcal{M}) &= 10^{-9} \times \left(\left\lceil \frac{nnzw(L_1) \times B_1}{32} \right\rceil + N_{SF}^1 \right) + \left(\left\lceil \frac{nnzw(L_2) \times B_2}{32} \right\rceil + N_{SF}^2 \right) \\
 &= 10^{-9} \times \left[\left(\left\lceil \frac{5 \times 32}{32} \right\rceil + 0 \right) + \left(\left\lceil \frac{4 \times 2}{32} \right\rceil + 2 \right) \right] \\
 &= 10^{-9} \times [(5 + 0) + (1 + 2)] = 8 \times 10^{-9} \text{ J}
 \end{aligned}$$

Energy consumption evaluation metrics

Total energy

$$EC_T(\mathcal{M}) = EC_{MA}(\mathcal{M}) + EC_{DT}(\mathcal{M})$$

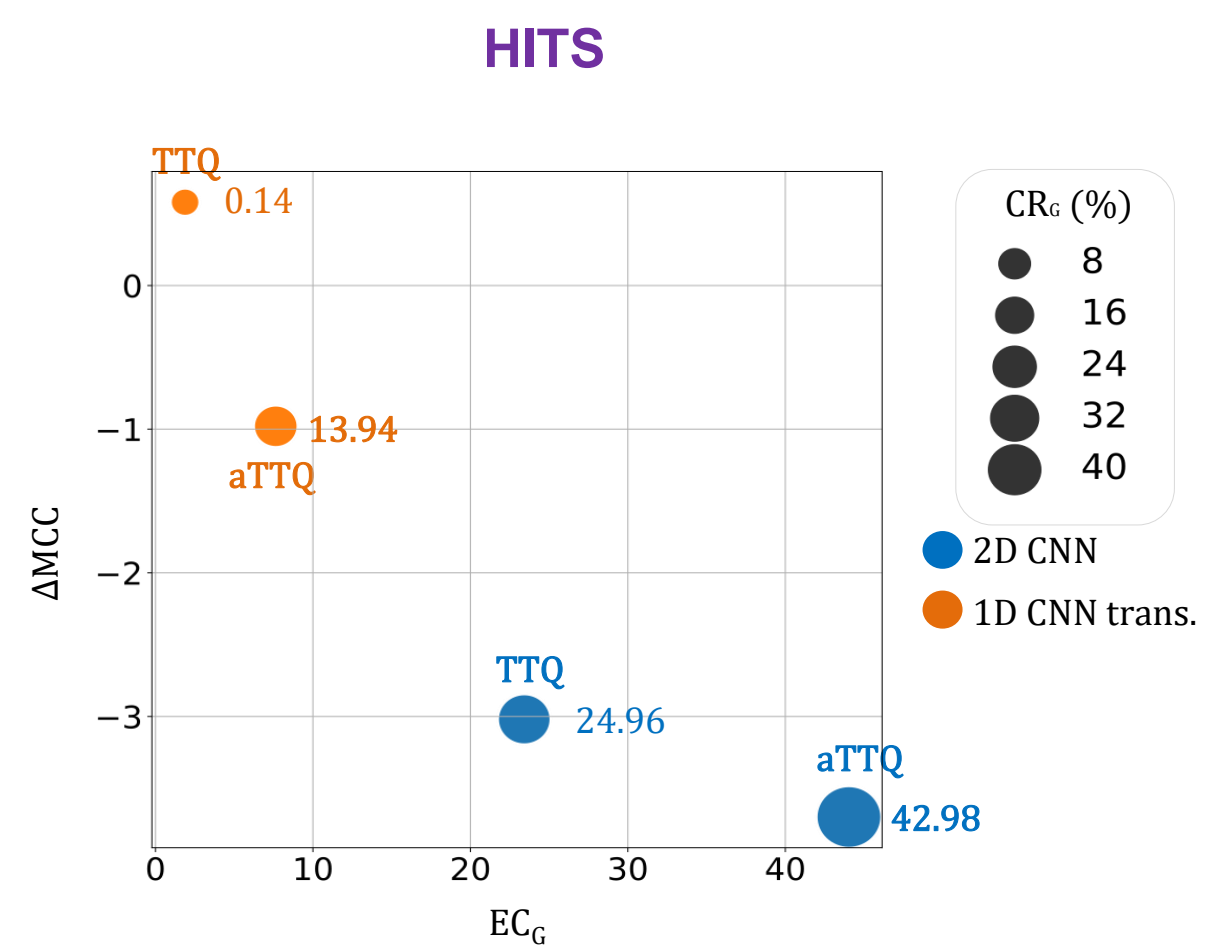
↑
Takes into account sparsity
↓
Takes into account sparsity AND reduced precision

$$EC_G^T(\mathcal{M}_{FP}, \mathcal{M}_C) = \frac{|EC_T(\mathcal{M}_{FP}) - EC_T(\mathcal{M}_C)|}{EC_T(\mathcal{M}_{FP})}$$

→ Takes into account sparsity
 → The higher the better

Experiment: SOTA comparison

HITS



ESR

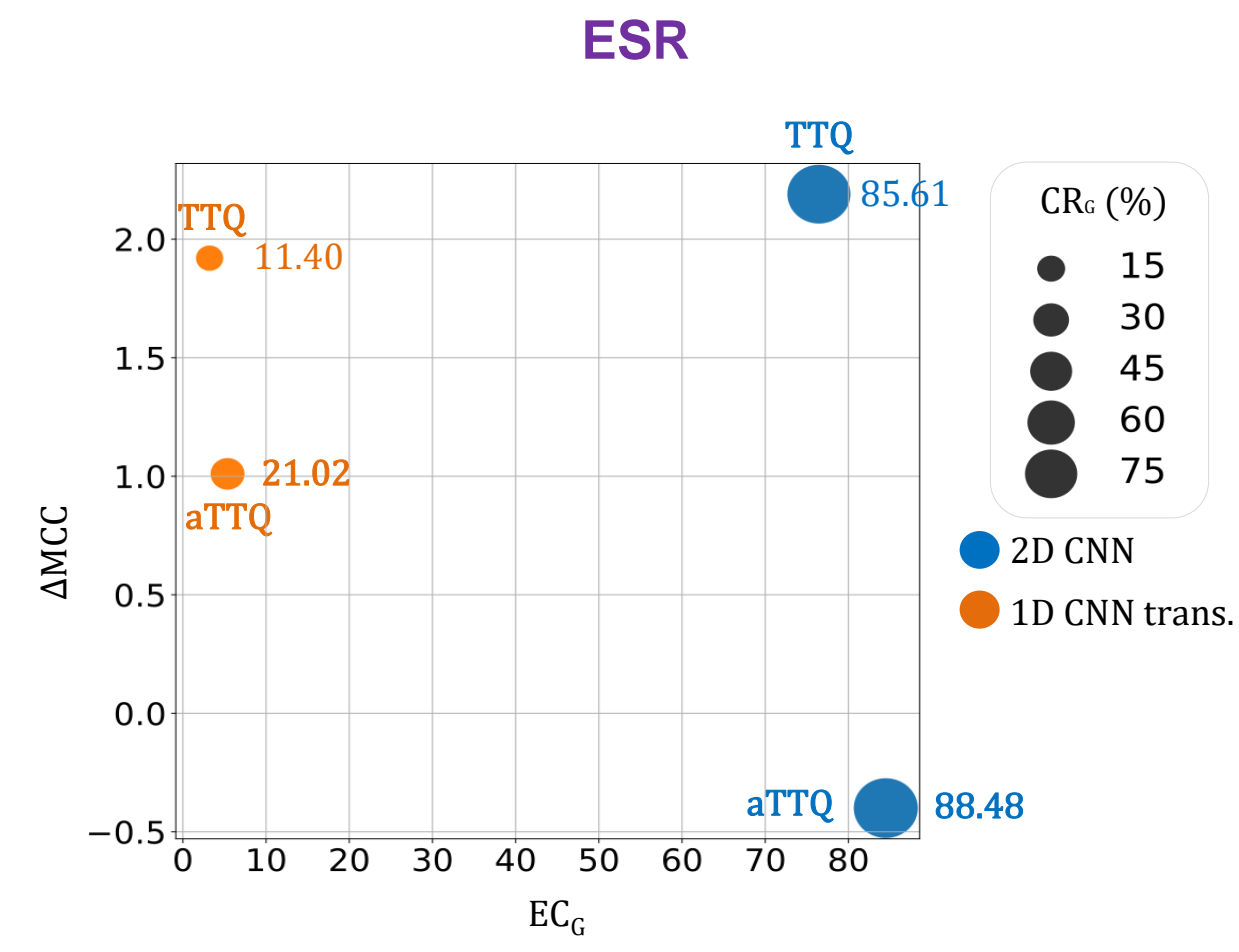
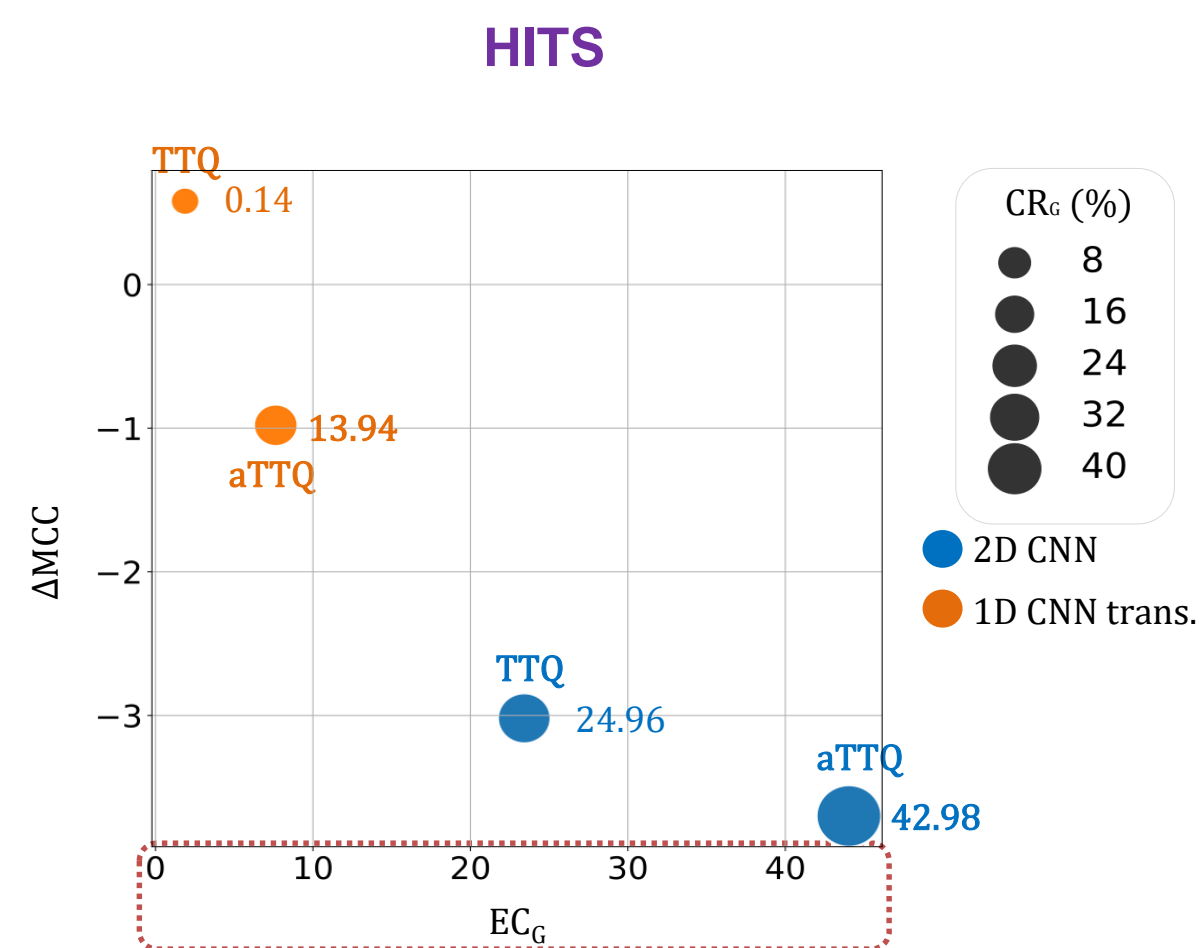


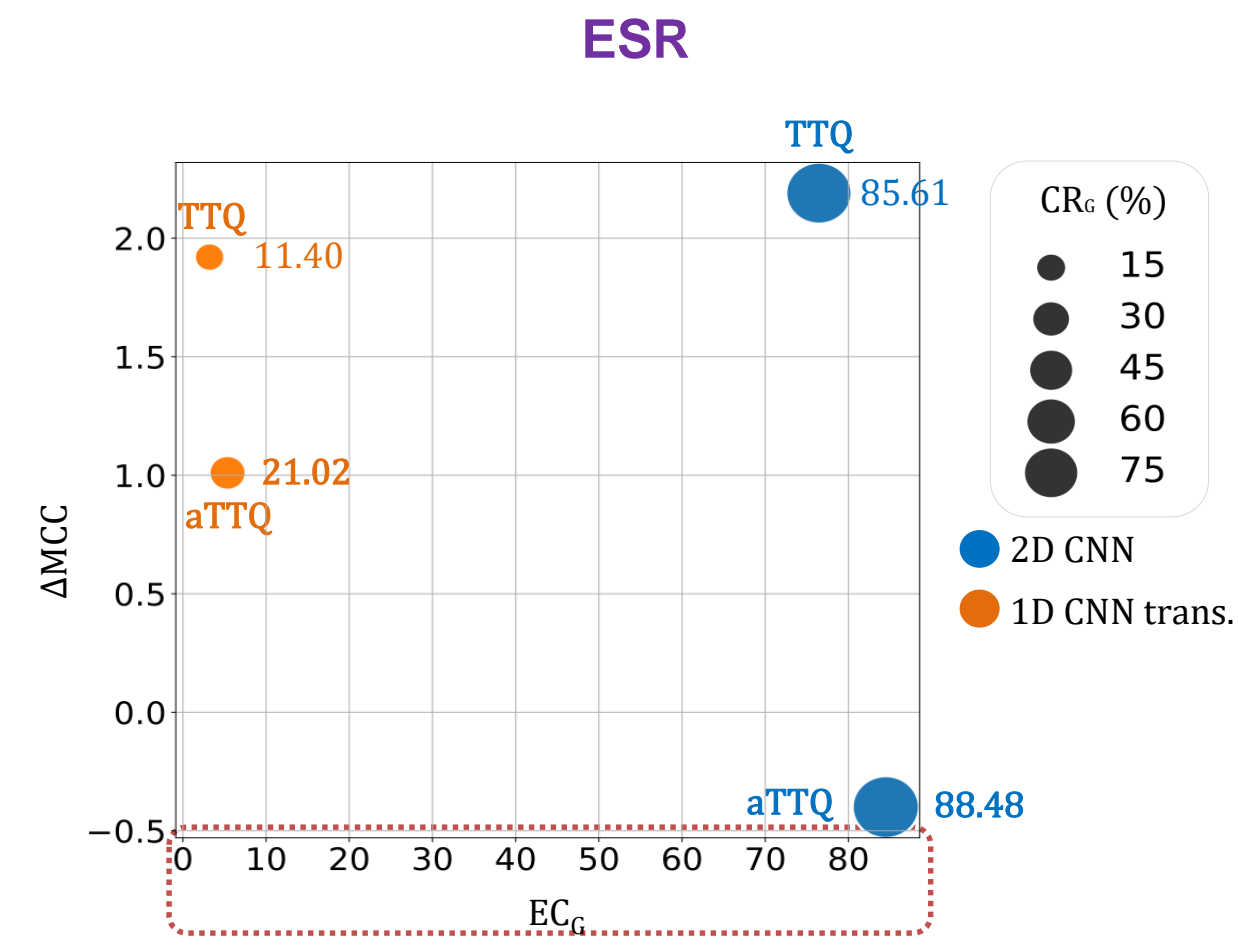
Figure – Comparison of aTTQ with FP and TTQ

Experiment: SOTA comparison

HITS



ESR

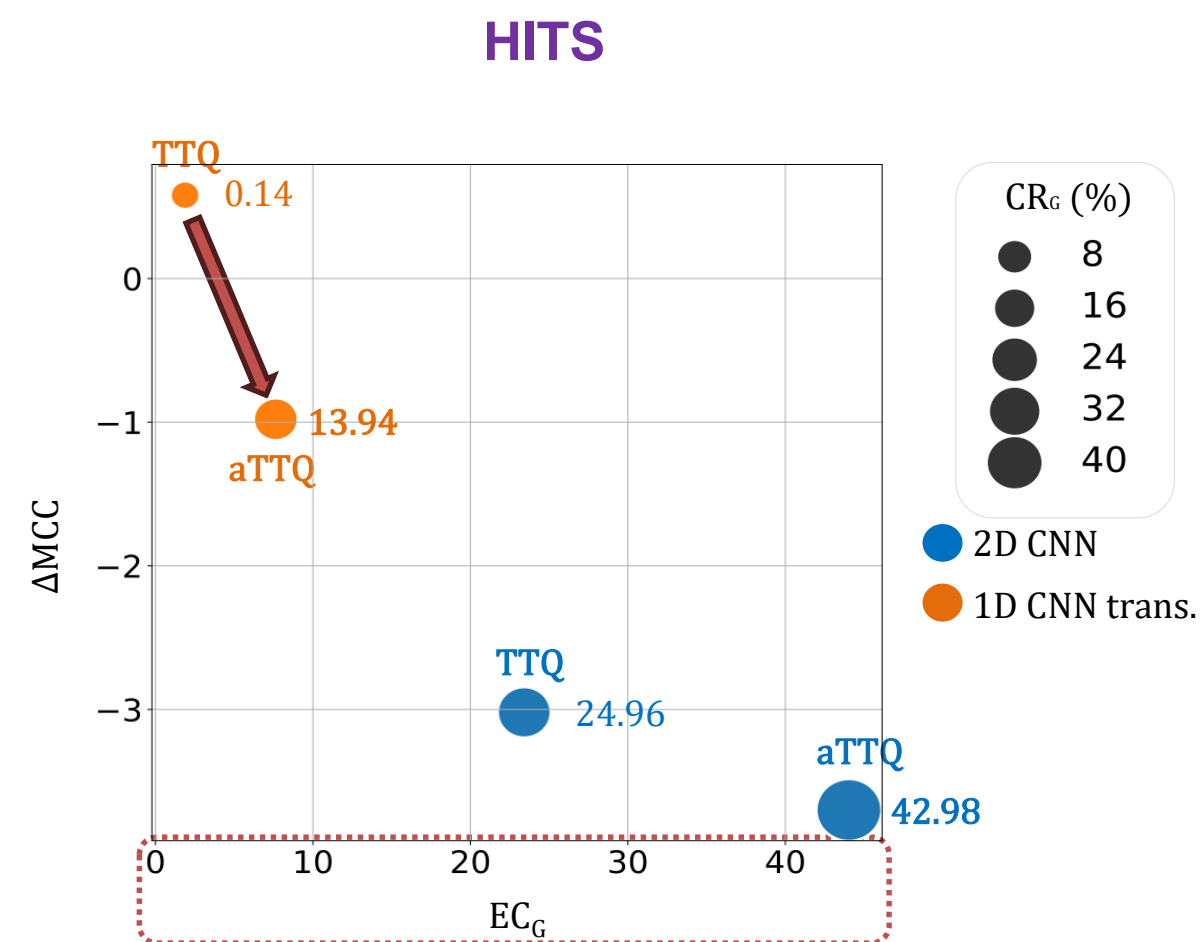


→ aTTQ always have higher energy consumption gains compared to TTQ.

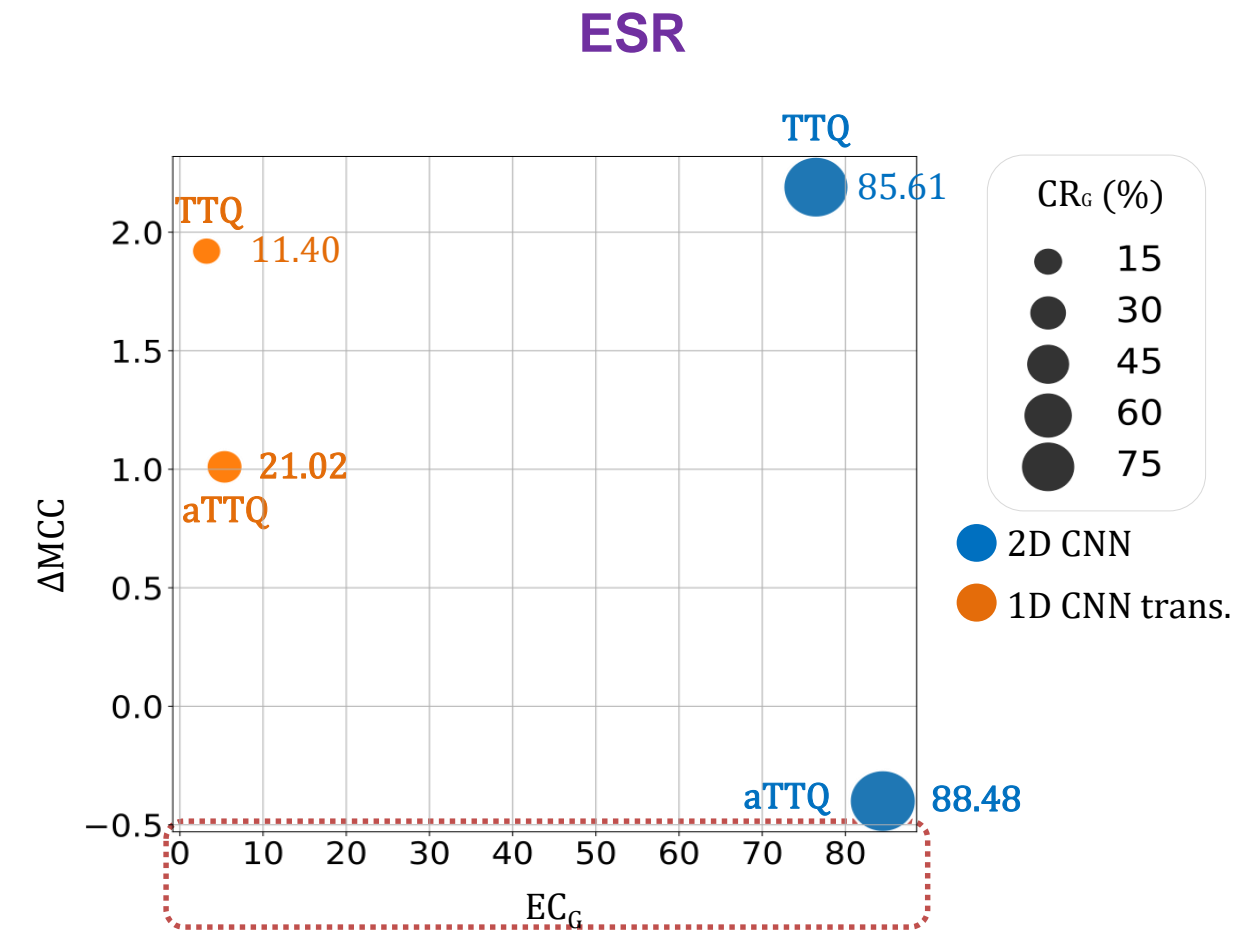
Figure – Comparison of aTTQ with FP and TTQ

Experiment: SOTA comparison

HITS



ESR

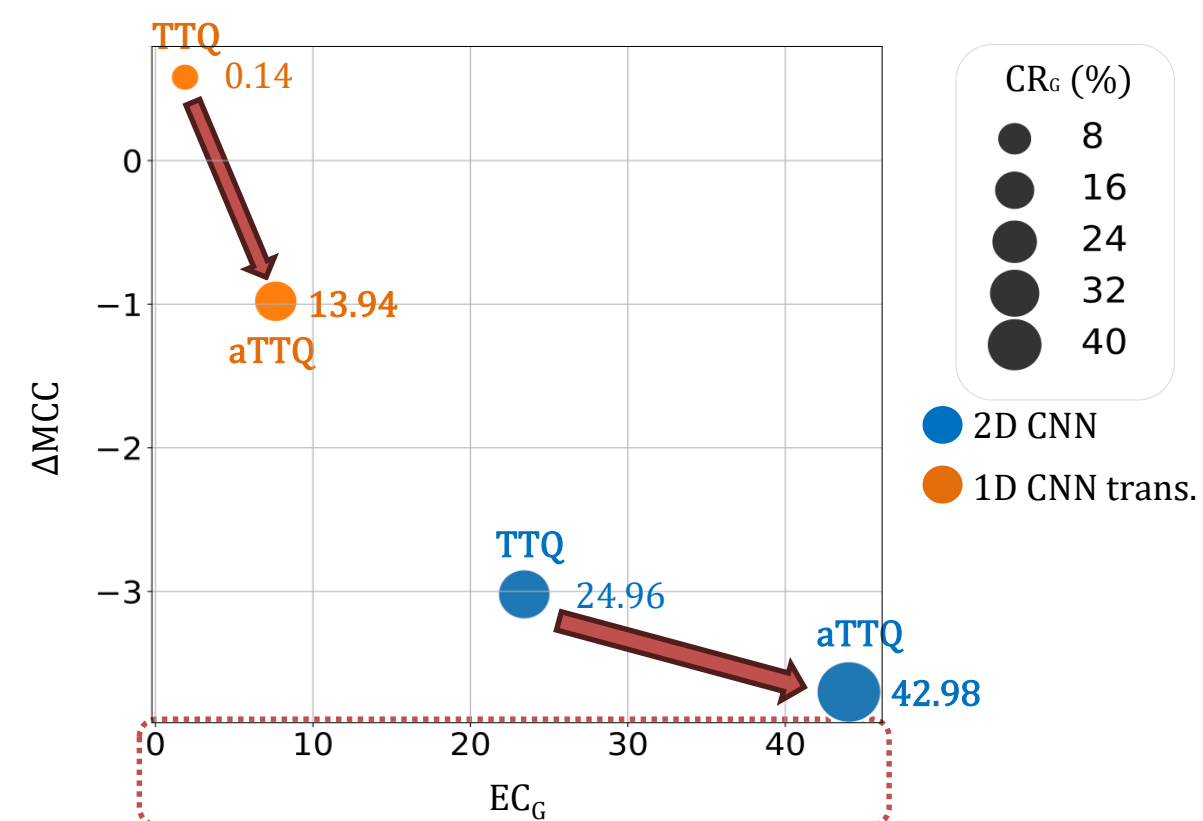


→ aTTQ always have higher energy consumption gains compared to TTQ.

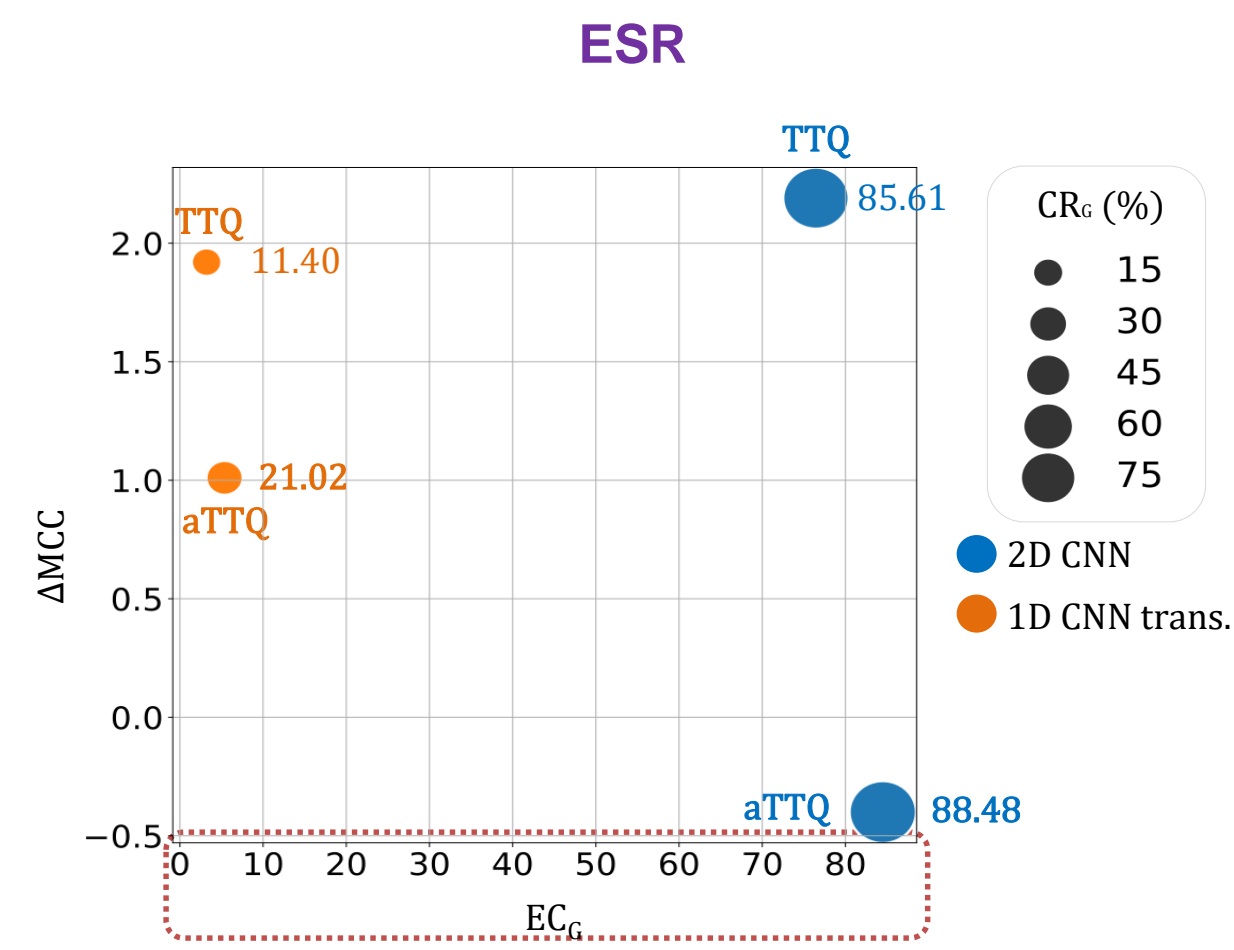
Figure – Comparison of aTTQ with FP and TTQ

Experiment: SOTA comparison

HITS



ESR

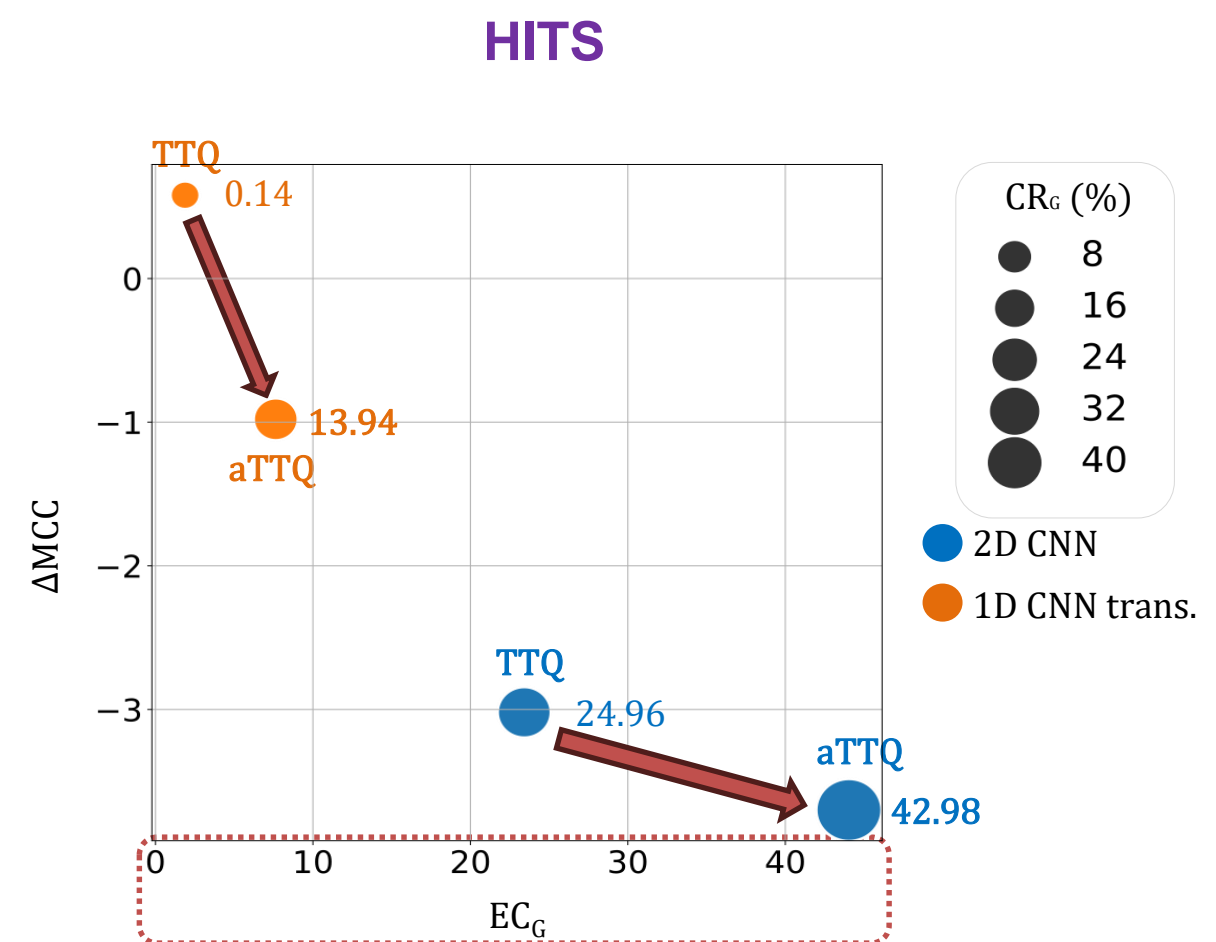


→ aTTQ always have higher energy consumption gains compared to TTQ.

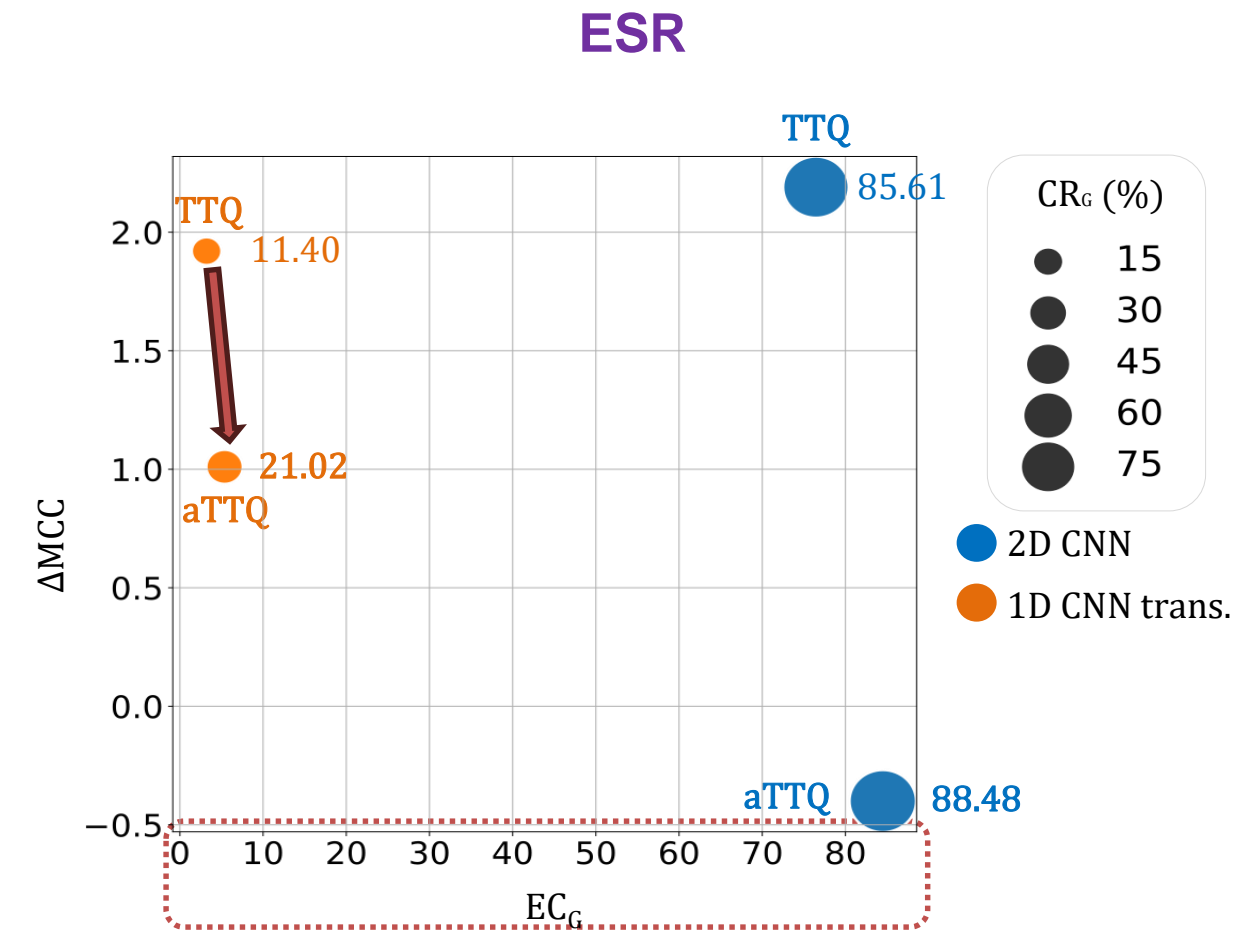
Figure – Comparison of aTTQ with FP and TTQ

Experiment: SOTA comparison

HITS



ESR

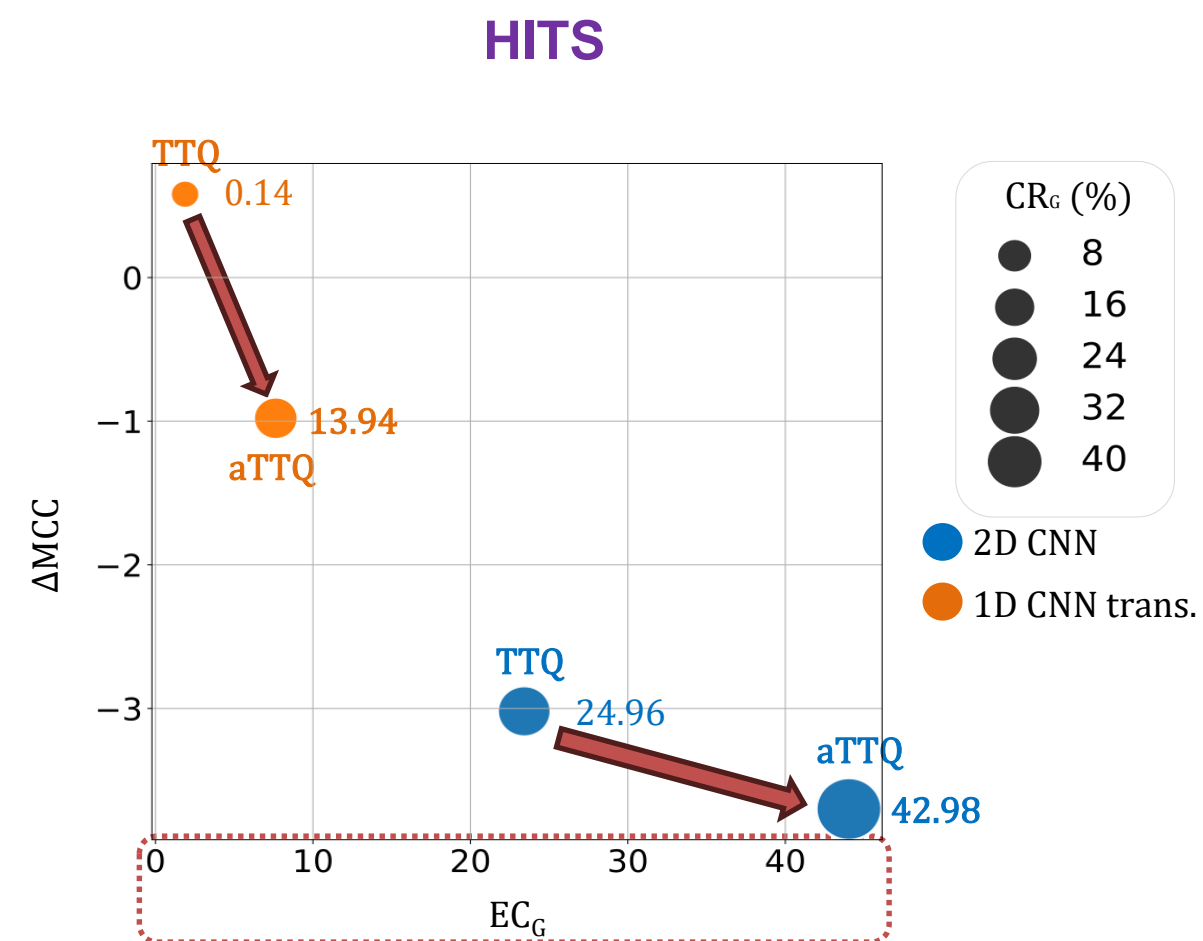


→ aTTQ always have higher energy consumption gains compared to TTQ.

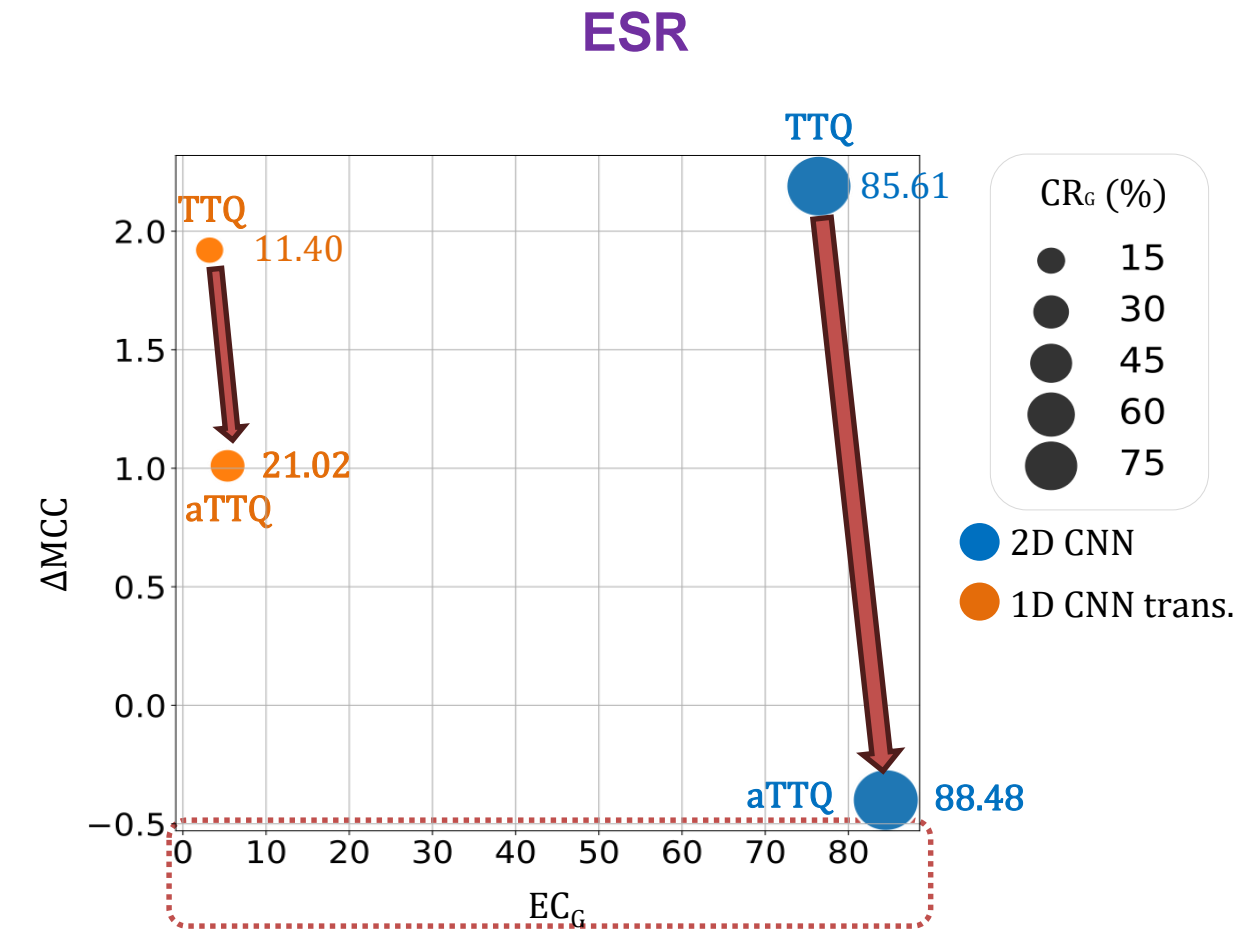
Figure – Comparison of aTTQ with FP and TTQ

Experiment: SOTA comparison

HITS



ESR

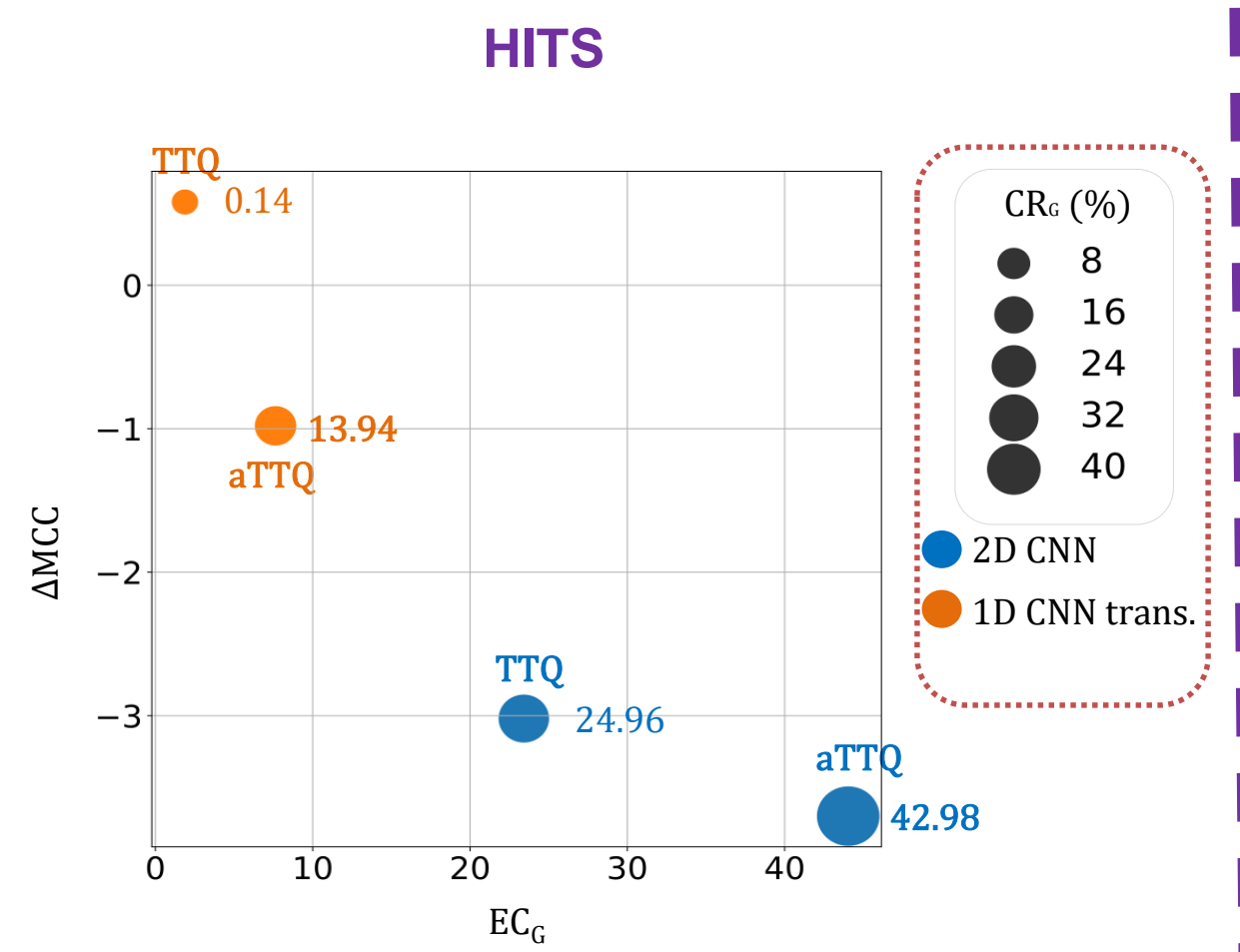


→ aTTQ always have higher energy consumption gains compared to TTQ.

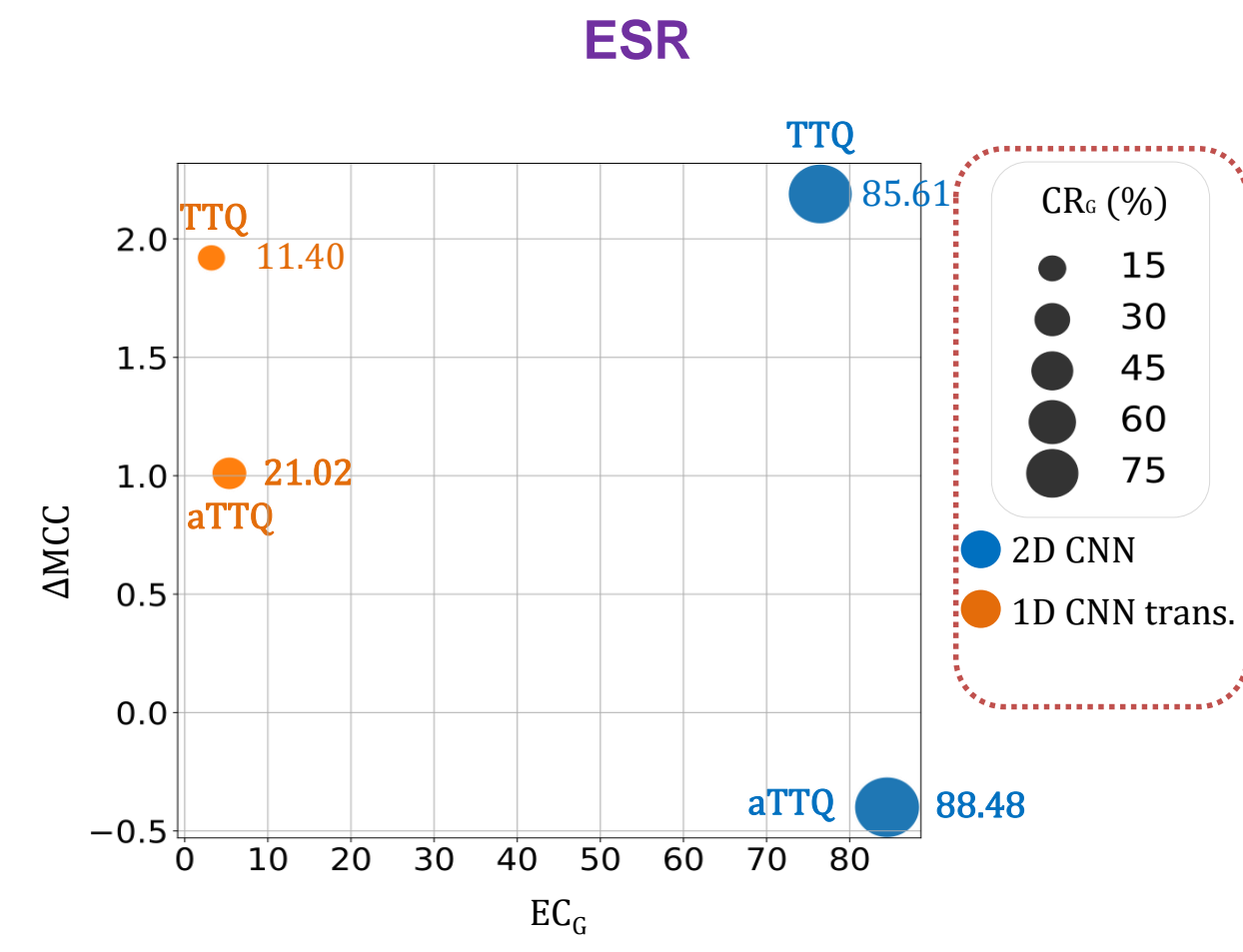
Figure – Comparison of aTTQ with FP and TTQ

Experiment: SOTA comparison

HITS



ESR



→ aTTQ always achieves higher sparsity rates compared to TTQ.

Figure – Comparison of aTTQ with FP and TTQ

Experiment: SOTA comparison

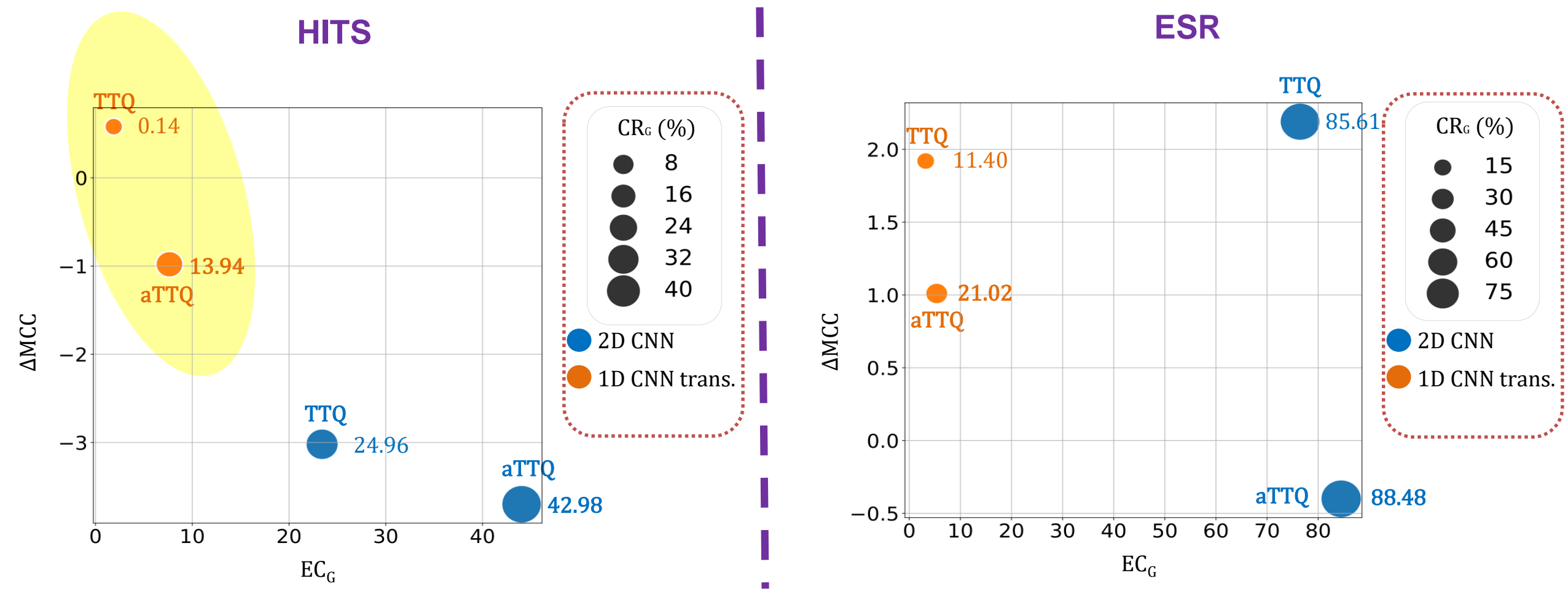


Figure – Comparison of aTTQ with FP and TTQ

Experiment: SOTA comparison

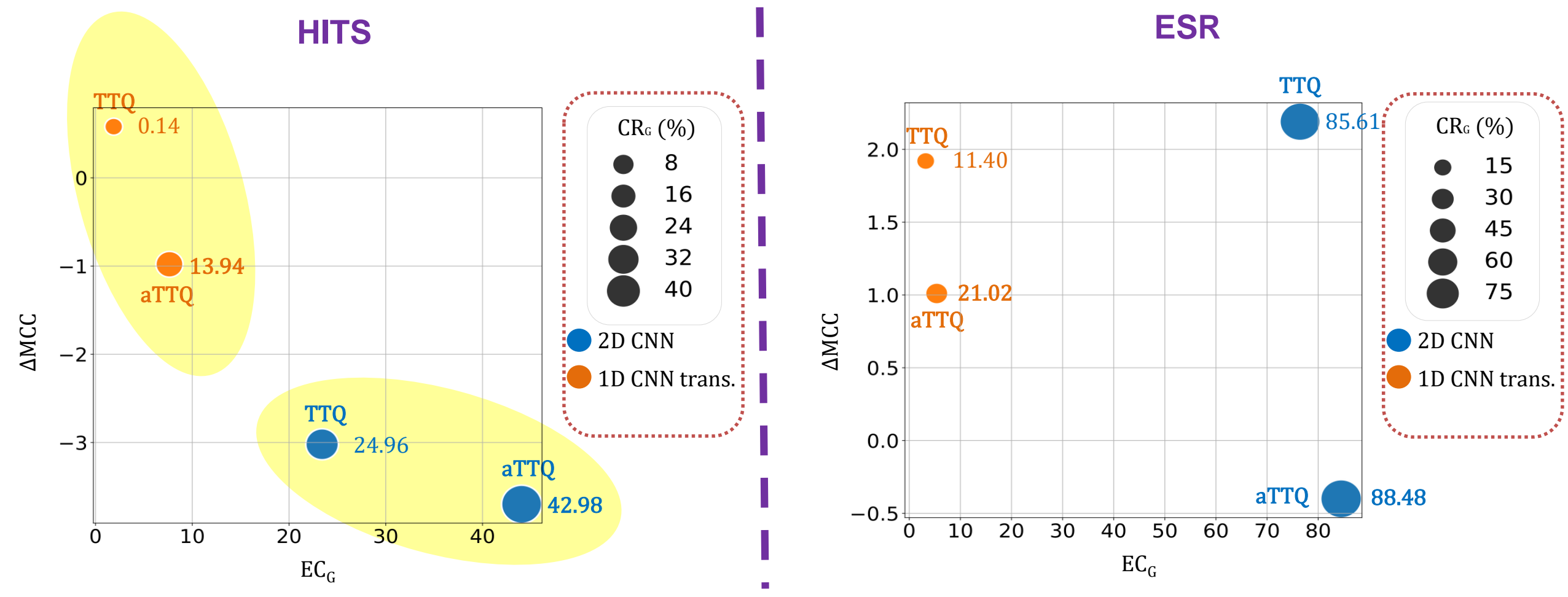
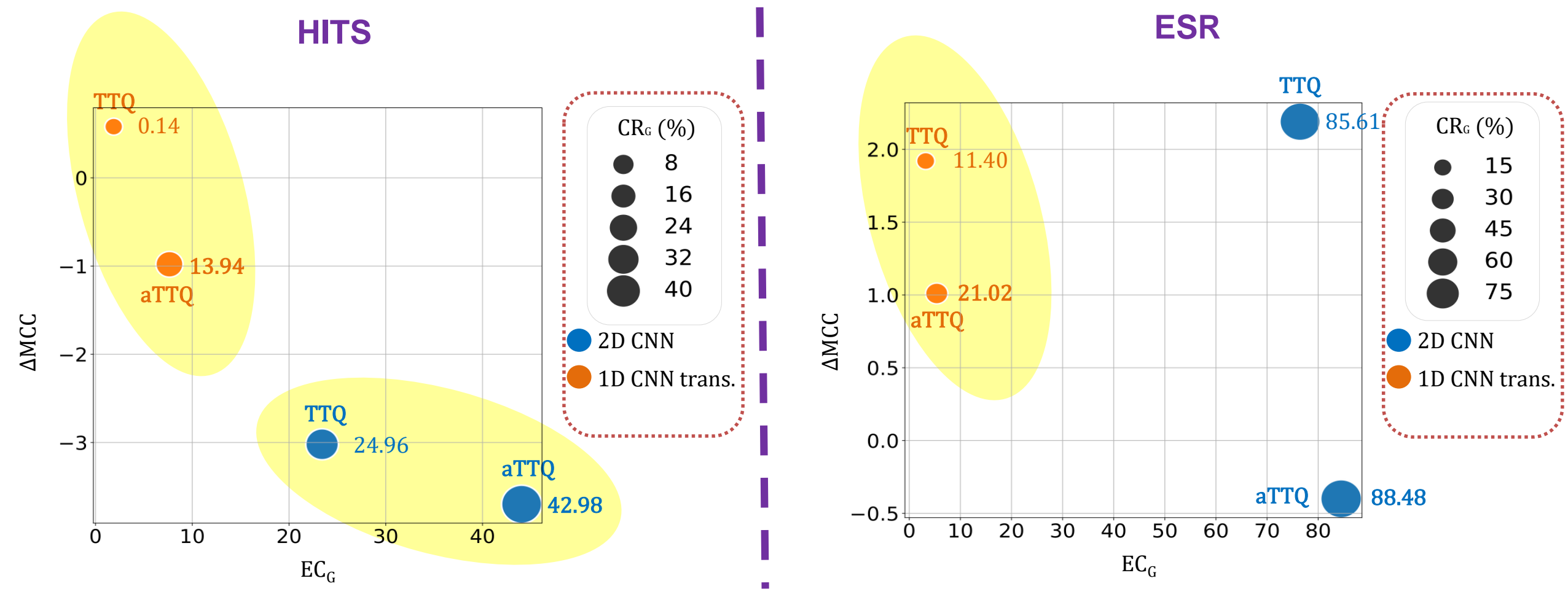


Figure – Comparison of aTTQ with FP and TTQ

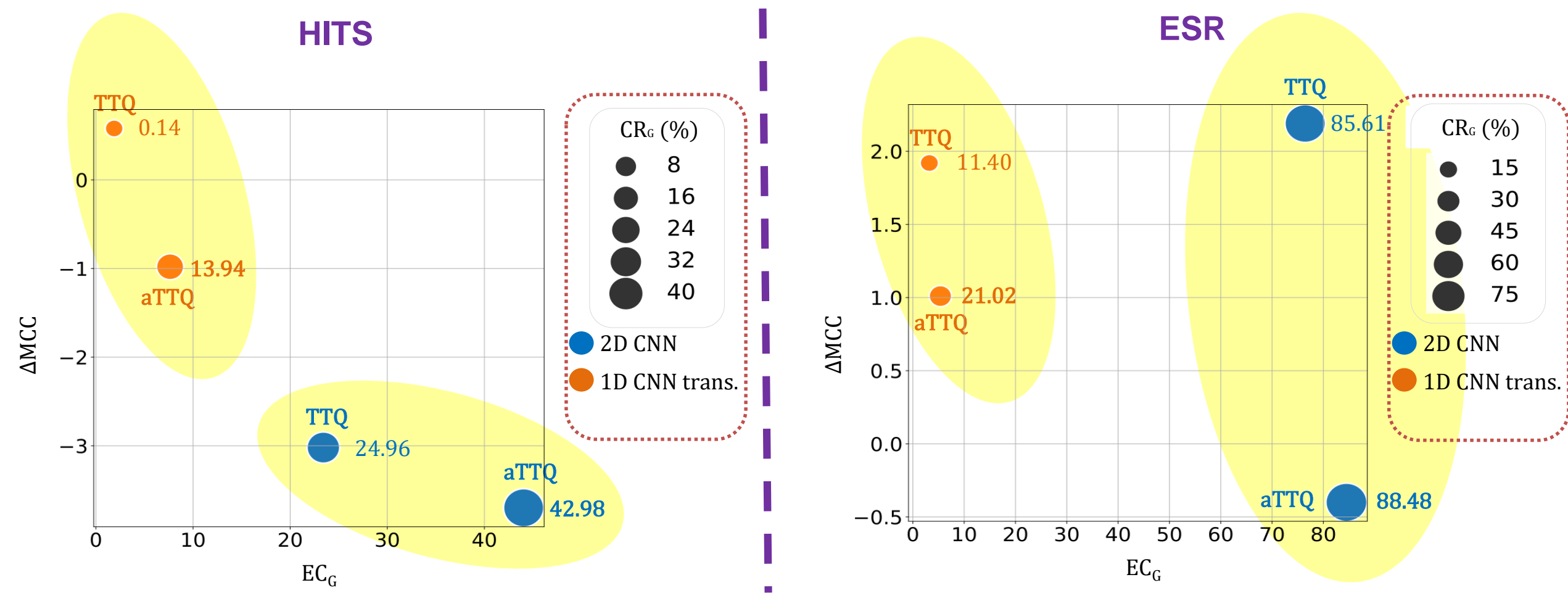
Experiment: SOTA comparison



→ aTTQ always achieves higher sparsity rates compared to TTQ.

Figure – Comparison of aTTQ with FP and TTQ

Experiment: SOTA comparison

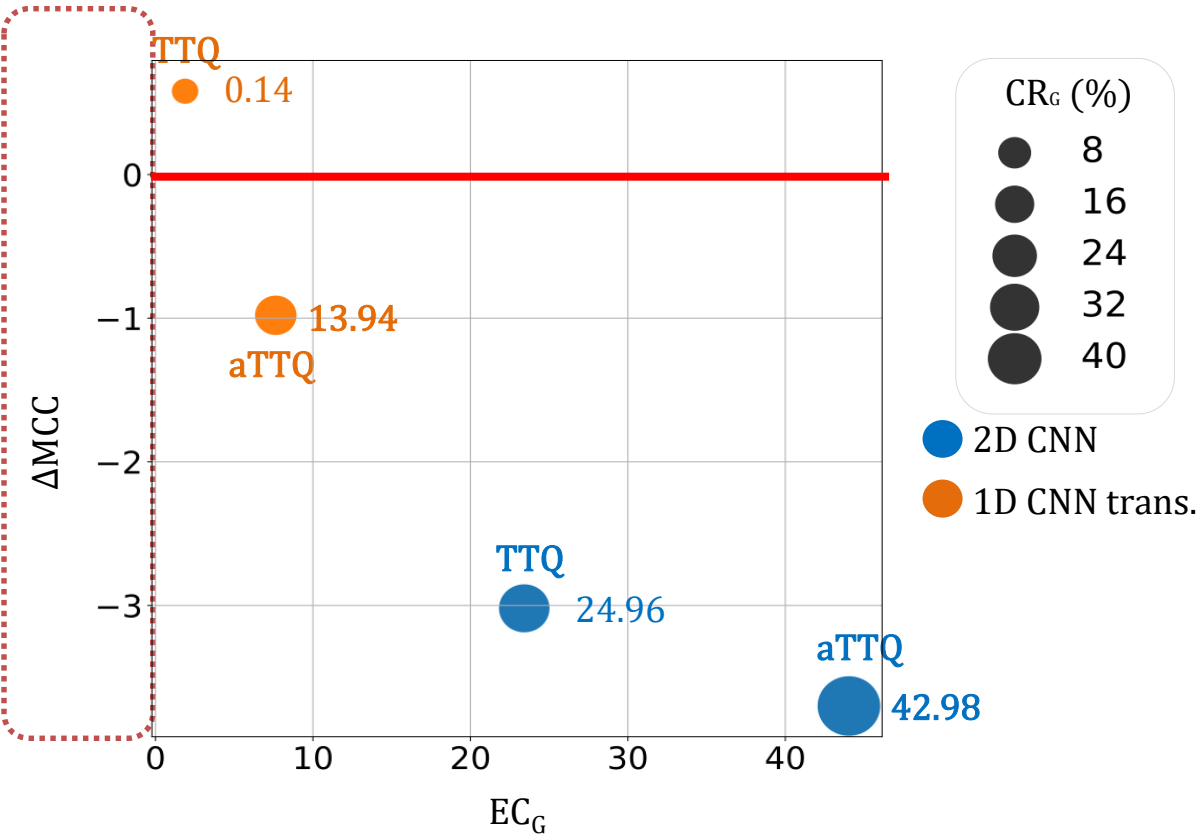


→ aTTQ always achieves higher sparsity rates compared to TTQ.

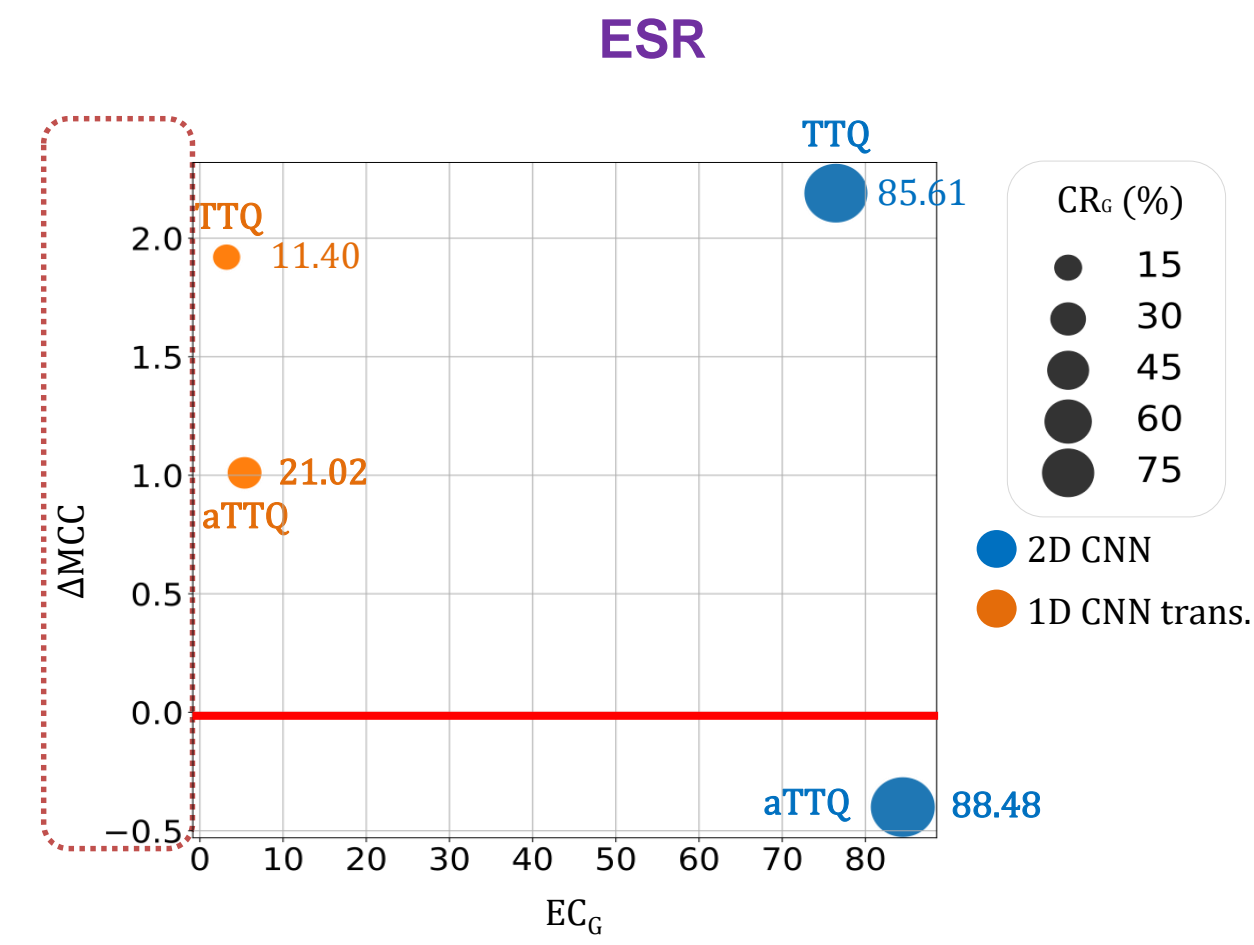
Figure – Comparison of aTTQ with FP and TTQ

Experiment: SOTA comparison

HITS



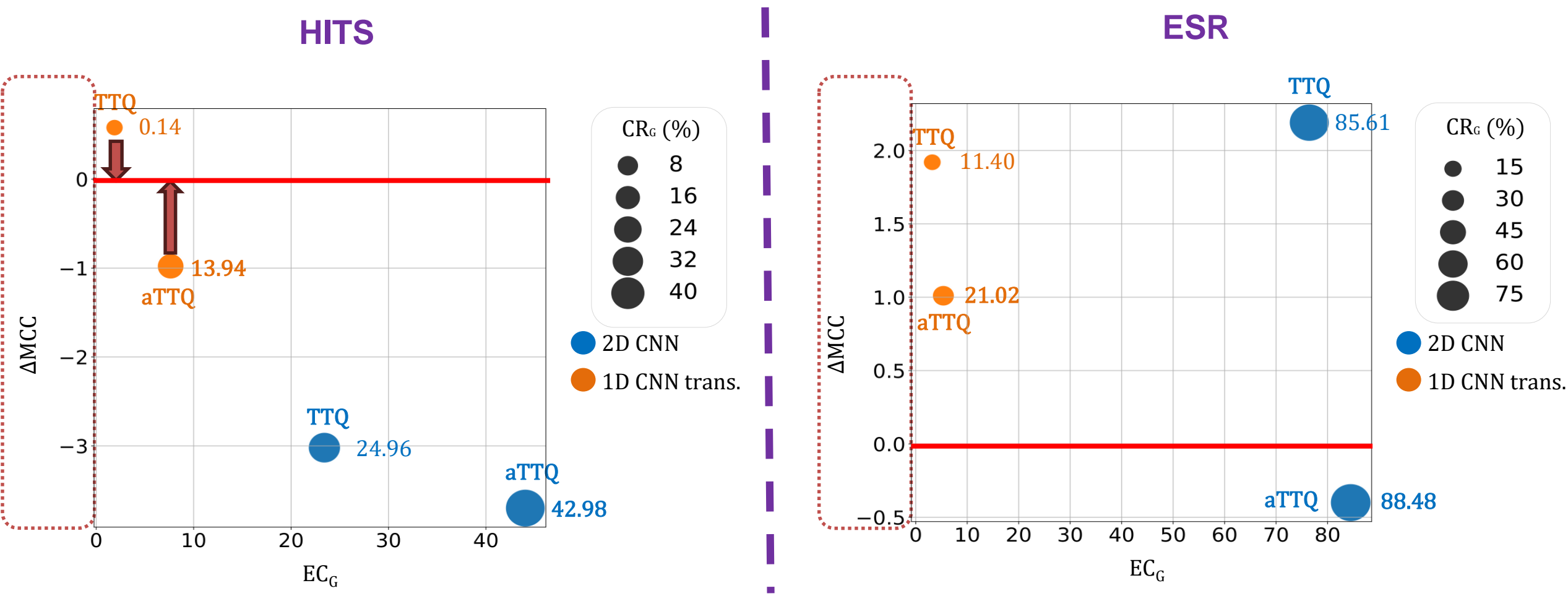
ESR



Both aTTQ and TTQ perform similarly than the FP model in terms of classification

Figure – Comparison of aTTQ with FP and TTQ

Experiment: SOTA comparison

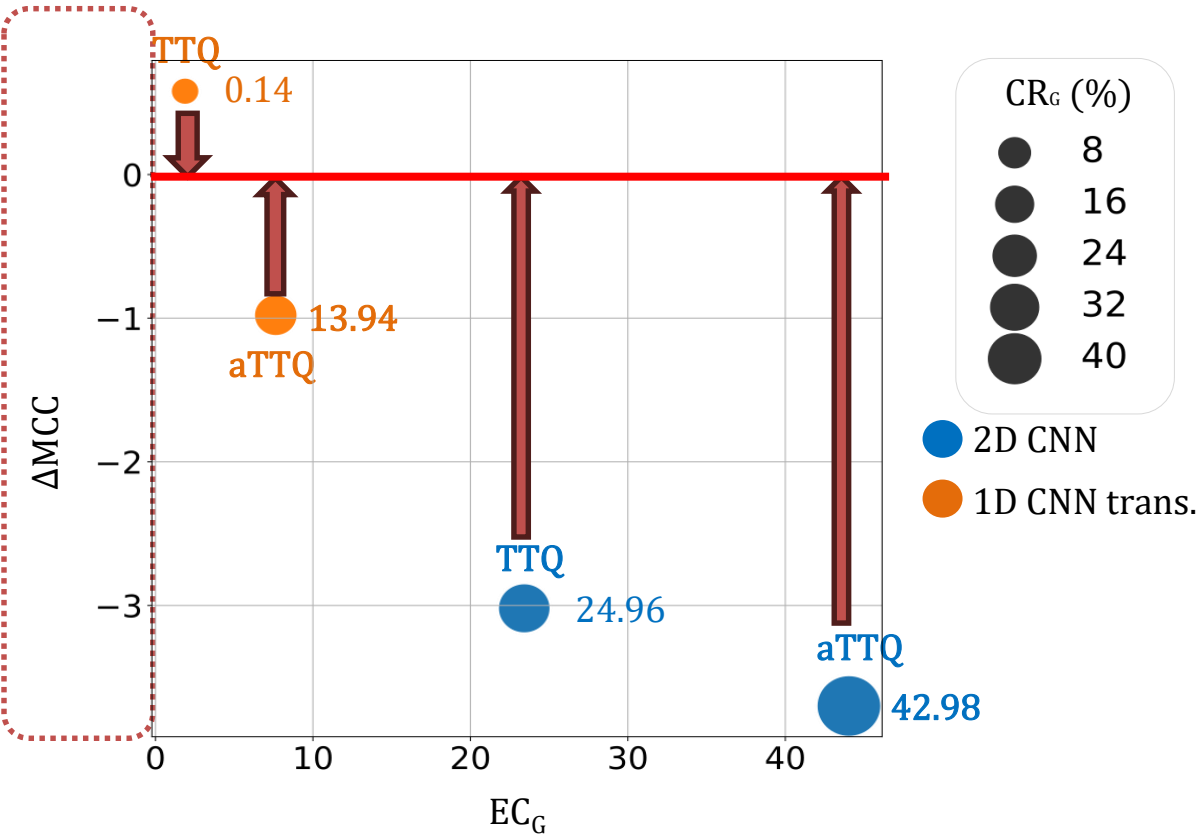


Both aTTQ and TTQ perform similarly than the FP model in terms of classification

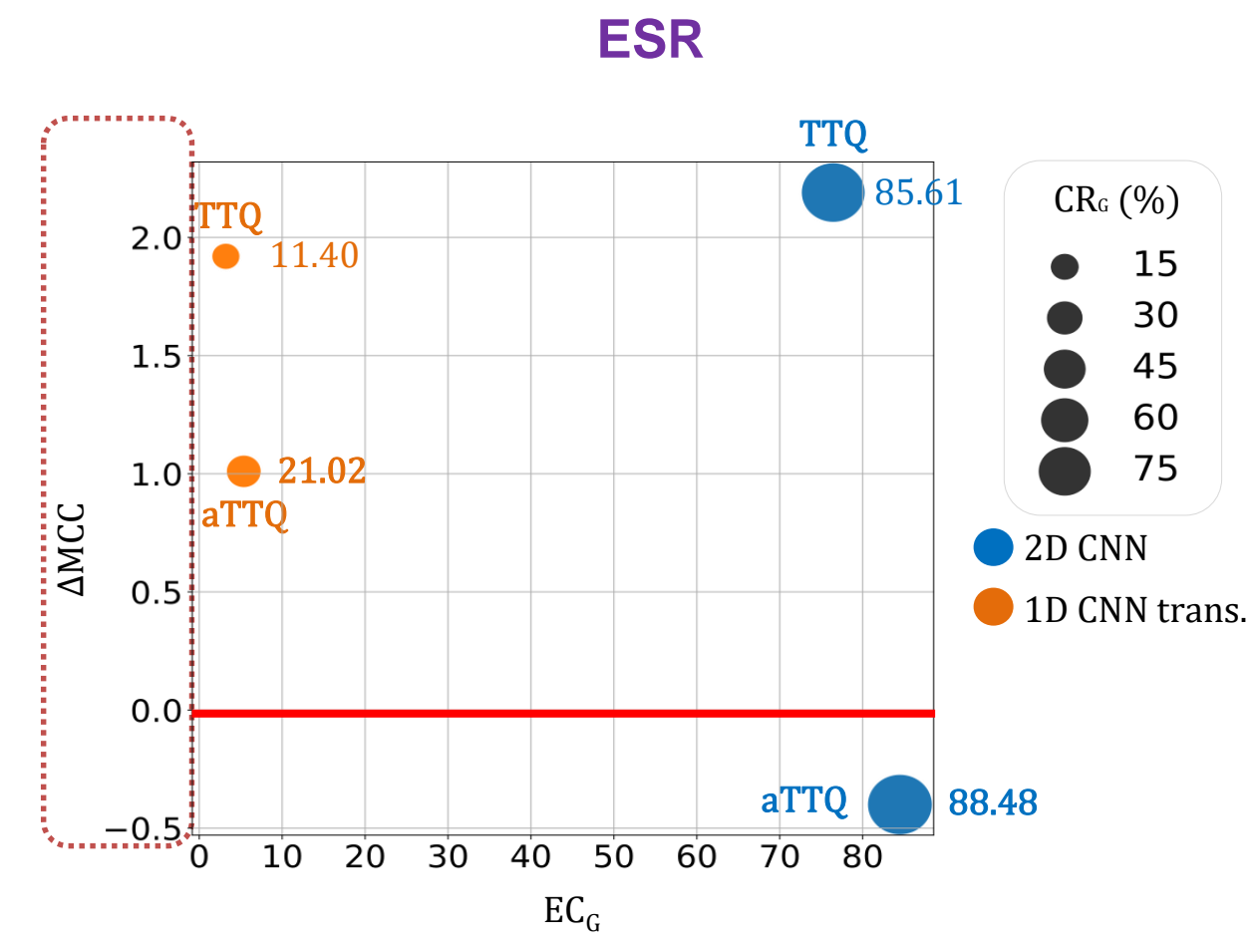
Figure – Comparison of aTTQ with FP and TTQ

Experiment: SOTA comparison

HITS



ESR

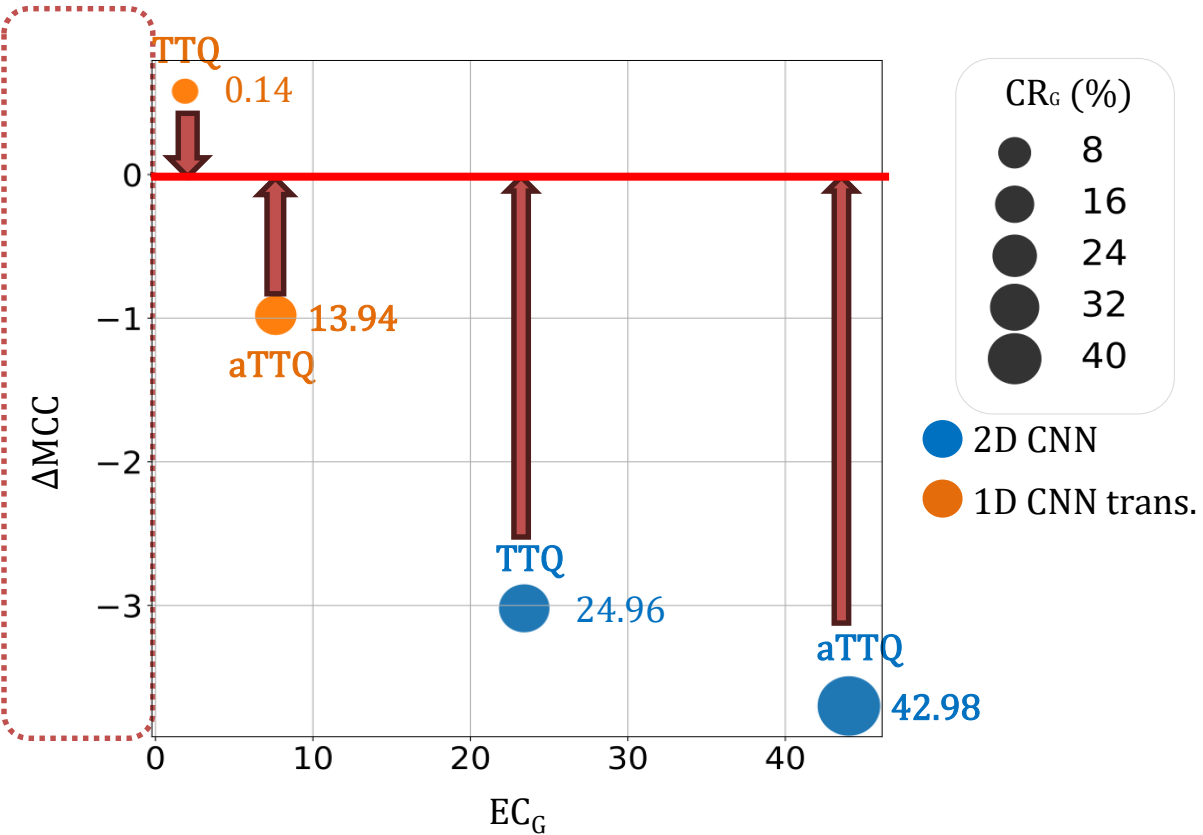


Both aTTQ and TTQ perform similarly than the FP model in terms of classification

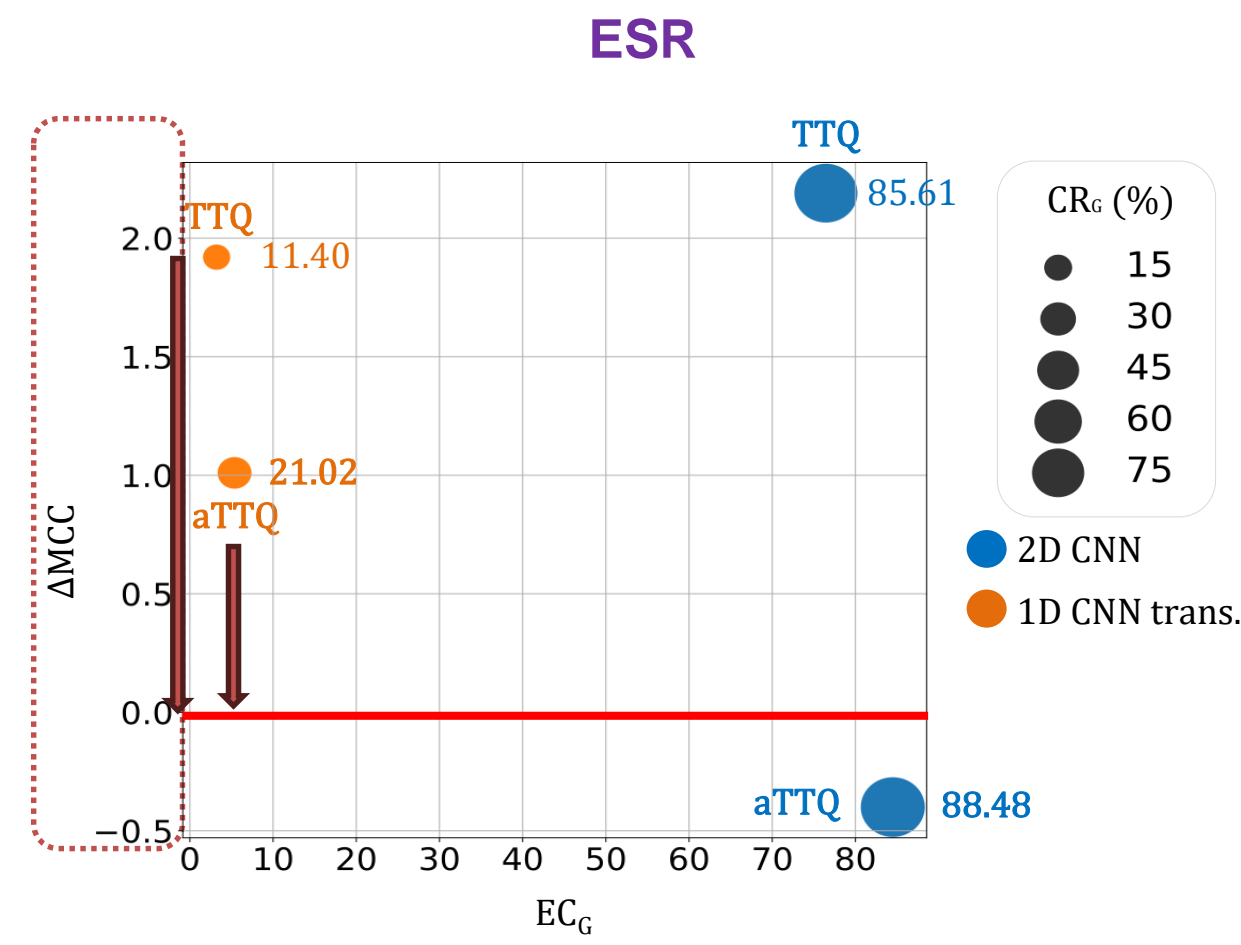
Figure – Comparison of aTTQ with FP and TTQ

Experiment: SOTA comparison

HITS



ESR

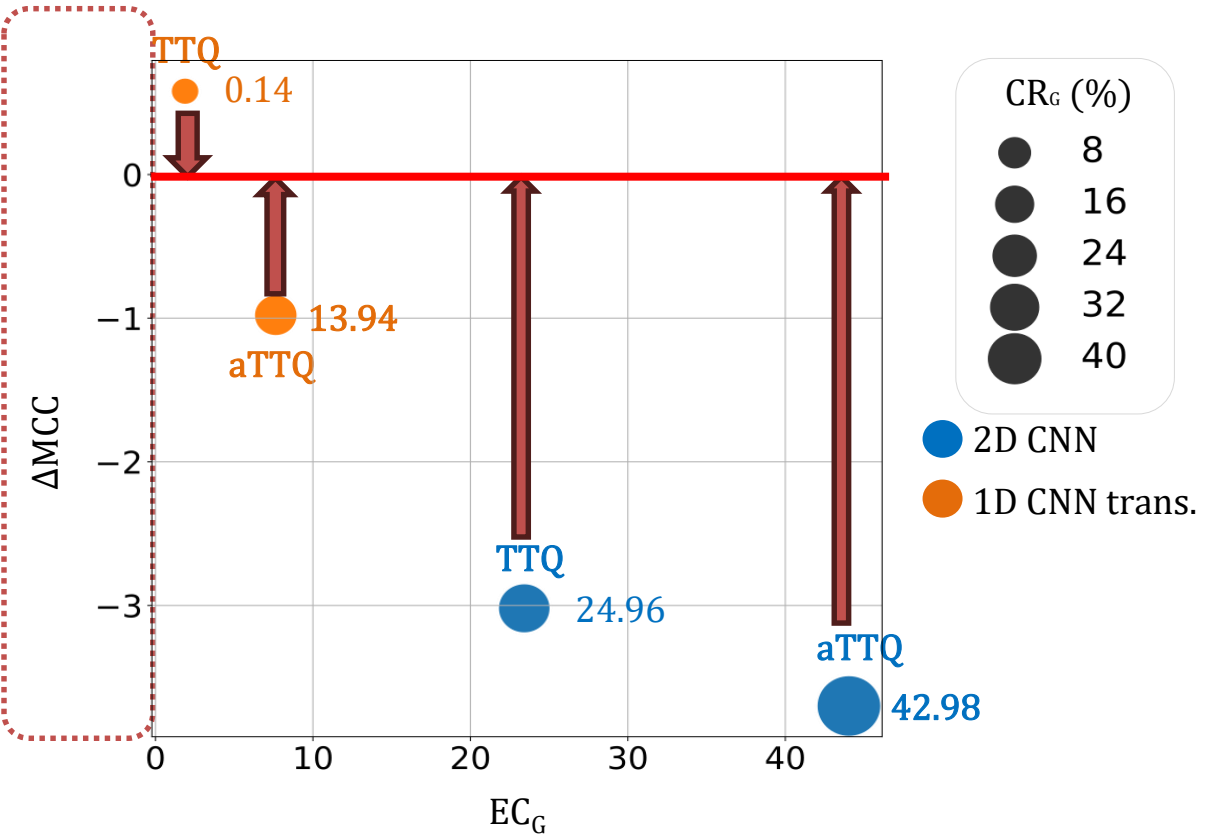


Both aTTQ and TTQ perform similarly than the FP model in terms of classification

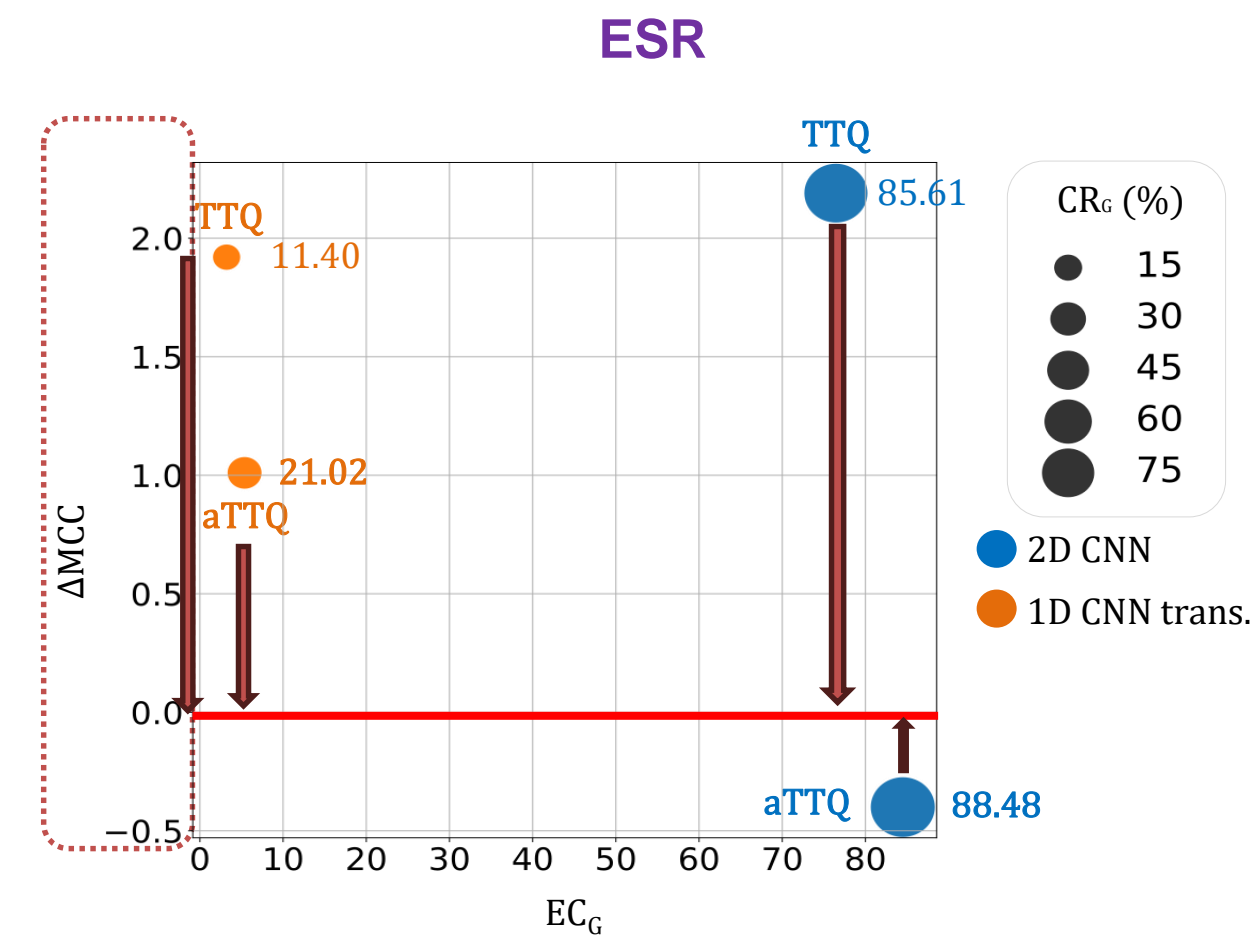
Figure – Comparison of aTTQ with FP and TTQ

Experiment: SOTA comparison

HITS



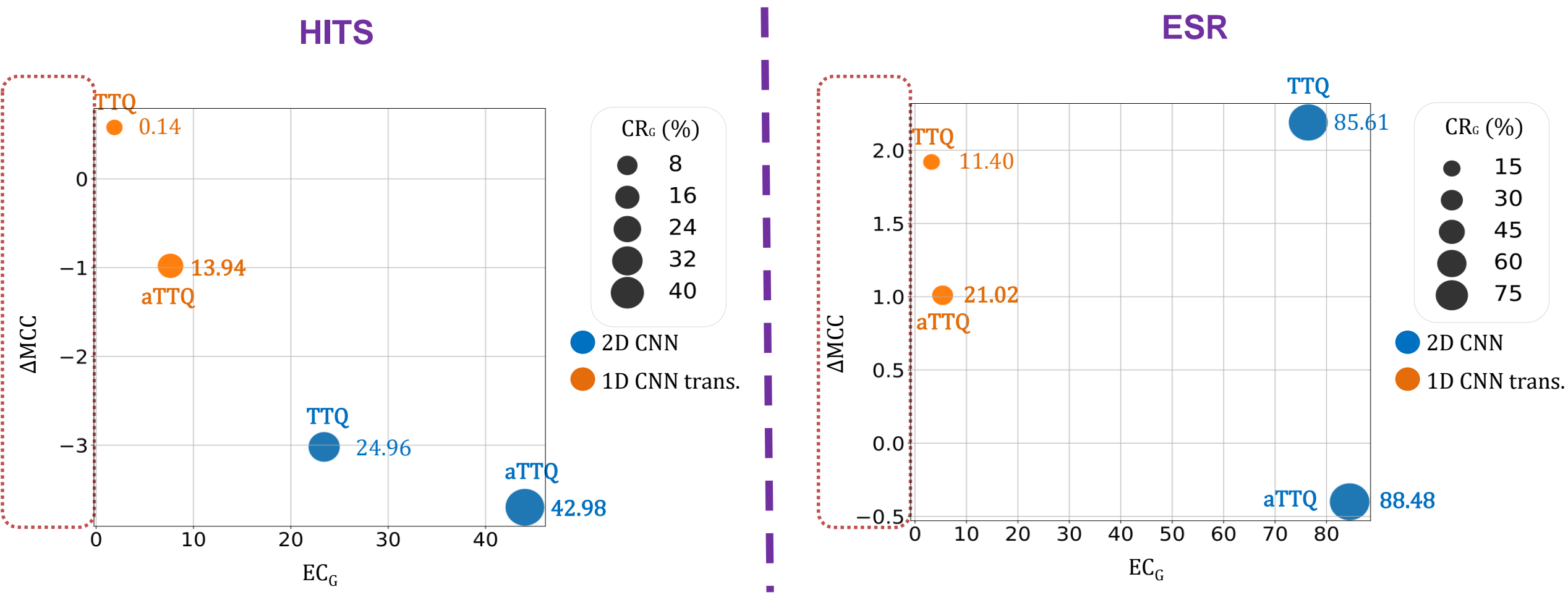
ESR



Both aTTQ and TTQ perform similarly than the FP model in terms of classification

Figure – Comparison of aTTQ with FP and TTQ

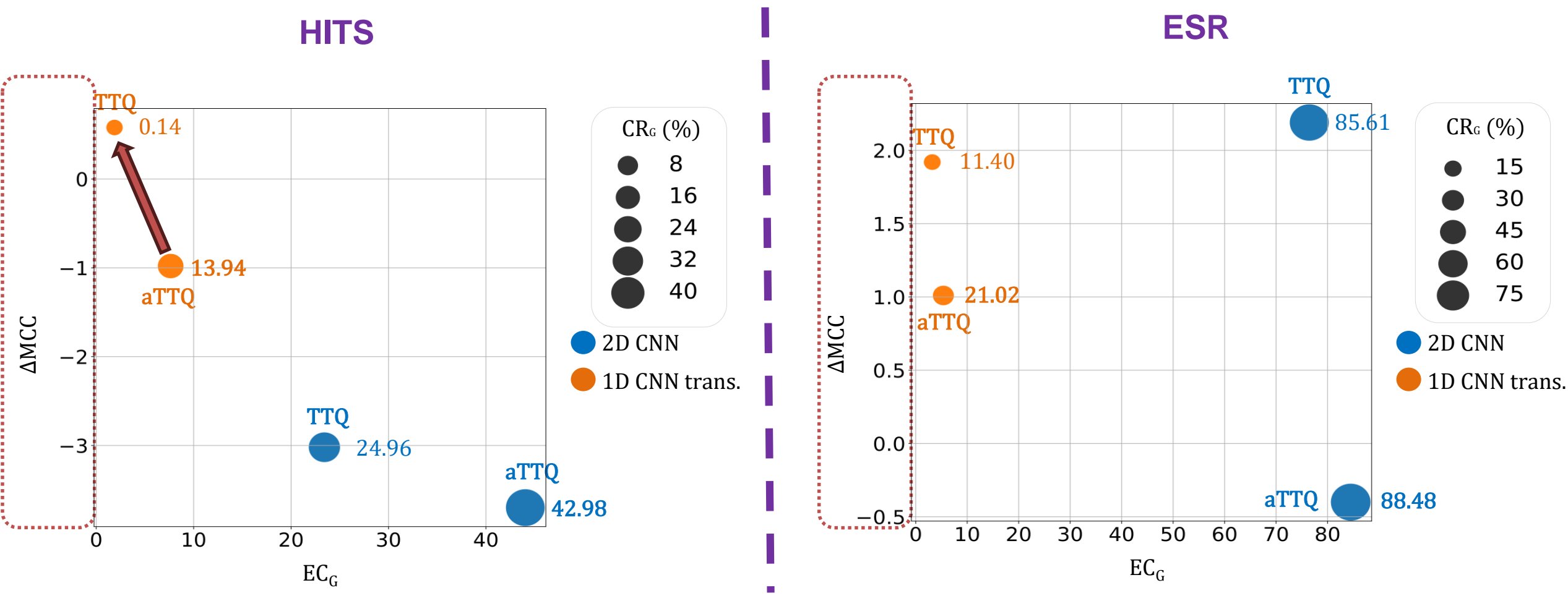
Experiment: SOTA comparison



→ TTQ tend to have slightly higher classification performances than aTTQ

Figure – Comparison of aTTQ with FP and TTQ

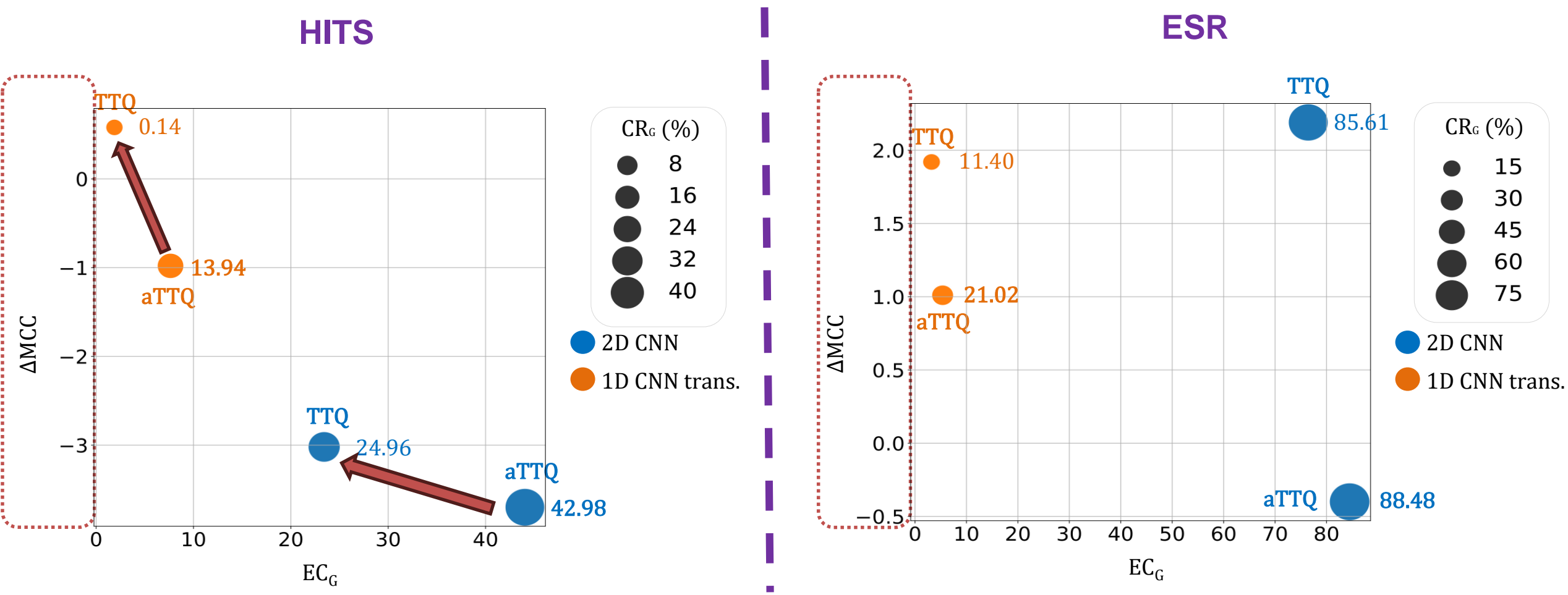
Experiment: SOTA comparison



→ TTQ tend to have slightly higher classification performances than aTTQ

Figure – Comparison of aTTQ with FP and TTQ

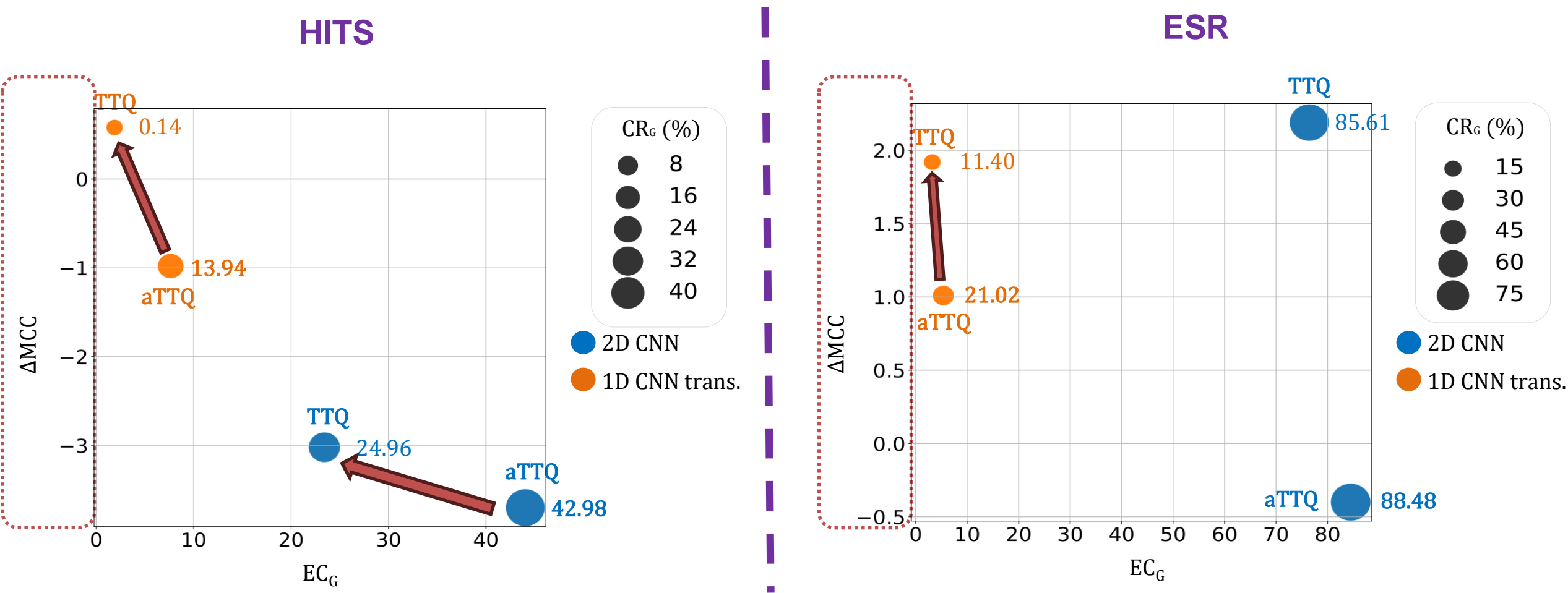
Experiment: SOTA comparison



→ TTQ tend to have slightly higher classification performances than aTTQ

Figure – Comparison of aTTQ with FP and TTQ

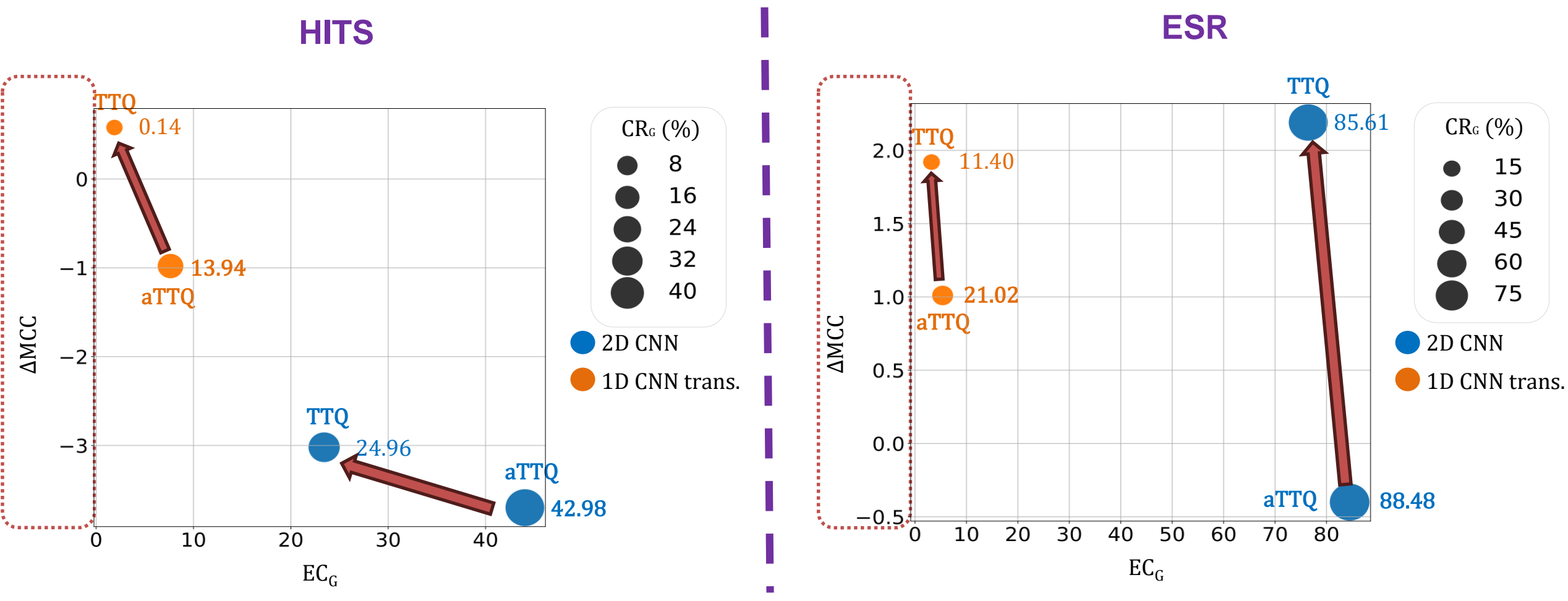
Experiment: SOTA comparison



→ TTQ tend to have slightly higher classification performances than aTTQ

Figure – Comparison of aTTQ with FP and TTQ

Experiment: SOTA comparison



→ TTQ tend to have slightly higher classification performances than aTTQ

Figure – Comparison of aTTQ with FP and TTQ

Experiment: SOTA comparison

Dataset	Model	Quant. method	$CR_G^T \uparrow$	$CR_G^Q \uparrow$	$SRQW \uparrow$	$EC_G^T \uparrow$	$MCC \uparrow$	$\Delta MCC \uparrow$
HITS	2D CNN	FP	-	-	-	-	89.84 ± 3.09	-
		DoReFa [21]	89.18 ± 0	96.87 ± 0	-	3.54 ± 0	85.05 ± 5.96	-4.79
		TTQ [16]	24.96 ± 2.25	27.12 ± 2.44	28.96 ± 2.12	23.42 ± 1.30	86.82 ± 2.29	-3.02
		aTTQ	42.98 ± 0.23	46.69 ± 0.25	45.95 ± 0.21	44.04 ± 0.19	86.14 ± 3.37	-3.70
	1D CNN-trans.	FP	-	-	-	-	82.64 ± 1.77	-
		DoReFa [21]	14.50 ± 0	96.87 ± 0	-	0.37 ± 0.03	84.07 ± 3.11	+1.43
		TTQ [16]	0.14 ± 0.04	0.91 ± 0.27	6.75 ± 0.26	1.88 ± 0.03	83.22 ± 2.36	+0.58
		aTTQ	13.94 ± 0.02	93.17 ± 0.16	93.53 ± 0.15	7.64 ± 0.11	81.66 ± 4.17	-0.98
ESR	2D CNN	FP	-	-	-	-	92.81 ± 3.53	-
		DoReFa [21]	96.40 ± 0	96.87 ± 0	-	29.90 ± 0	94.12 ± 0.87	+1.31
		TTQ [16]	85.61 ± 1.37	86.03 ± 1.37	86.59 ± 1.29	76.45 ± 1.13	95.00 ± 1.11	+2.19
		aTTQ	88.48 ± 0.44	88.91 ± 0.45	89.30 ± 0.42	84.49 ± 0.33	92.41 ± 2.22	-0.40
	1D CNN-trans.	FP	-	-	-	-	94.33 ± 1.51	-
		DoReFa [21]	23.46 ± 0	96.86 ± 0	-	0.90 ± 0	96.79 ± 0.55	+2.46
		TTQ [16]	11.40 ± 2.61	47.07 ± 10.79	50.22 ± 10.16	3.21 ± 0.66	96.25 ± 0.79	+1.92
		aTTQ	21.02 ± 0.15	86.78 ± 0.63	87.59 ± 0.59	5.37 ± 0.04	95.34 ± 0.79	+1.01
MNIST	2D MNIST CNN	FP	-	-	-	-	94.39 ± 0.46	-
		DoReFa [21]	51.67 ± 0	96.84 ± 0	-	3.28 ± 0	87.03 ± 7.14	-7.36
		TTQ [16]	13.86 ± 2.33	25.97 ± 4.37	30.40 ± 4.12	2.58 ± 0.35	92.09 ± 0.89	-2.30
		aTTQ	28.98 ± 1.26	54.32 ± 2.36	57.08 ± 2.22	4.97 ± 0.22	93.62 ± 0.96	-0.77

Table – Comparison of aTTQ with other quantization methods

Experiment: influence of normalization

Objective:

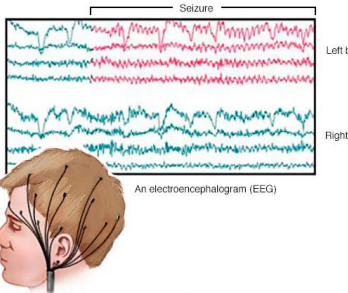
- Study the influence of normalization on aTTQ.

Datasets:



HITS:

- TCD Data.
- 1 545 samples.
- Three classes.
- Sampling frequency: 4385 Hz.



ESR:

- EEG Data.
- 11 500 samples.
- Two classes.
- Sampling frequency: 174 Hz.

```
0 0 0 0 0 0 0 0 0 0 0 0 0 0 0 0 0 0 0 0 0 0 0 0 0 0 0
1 1 1 1 1 1 1 1 1 1 1 1 1 1 1 1 1 1 1 1 1 1 1 1 1 1 1
2 2 2 2 2 2 2 2 2 2 2 2 2 2 2 2 2 2 2 2 2 2 2 2 2 2 2
3 3 3 3 3 3 3 3 3 3 3 3 3 3 3 3 3 3 3 3 3 3 3 3 3 3 3
4 4 4 4 4 4 4 4 4 4 4 4 4 4 4 4 4 4 4 4 4 4 4 4 4 4 4
5 5 5 5 5 5 5 5 5 5 5 5 5 5 5 5 5 5 5 5 5 5 5 5 5 5 5
6 6 6 6 6 6 6 6 6 6 6 6 6 6 6 6 6 6 6 6 6 6 6 6 6 6 6
7 7 7 7 7 7 7 7 7 7 7 7 7 7 7 7 7 7 7 7 7 7 7 7 7 7 7
8 8 8 8 8 8 8 8 8 8 8 8 8 8 8 8 8 8 8 8 8 8 8 8 8 8 8
9 9 9 9 9 9 9 9 9 9 9 9 9 9 9 9 9 9 9 9 9 9 9 9 9 9 9
```

MNIST subset:

- 28x28 images.
- 20 000 samples.
- Ten classes.

Metrics:

- Mathews Correlation Coefficient (MCC).
- CR_G .

Models:

- 2D CNN.
- 1D CNN-transformer.

Loss function:

- Cross entropy (CE)

Experiment: influence of normalization

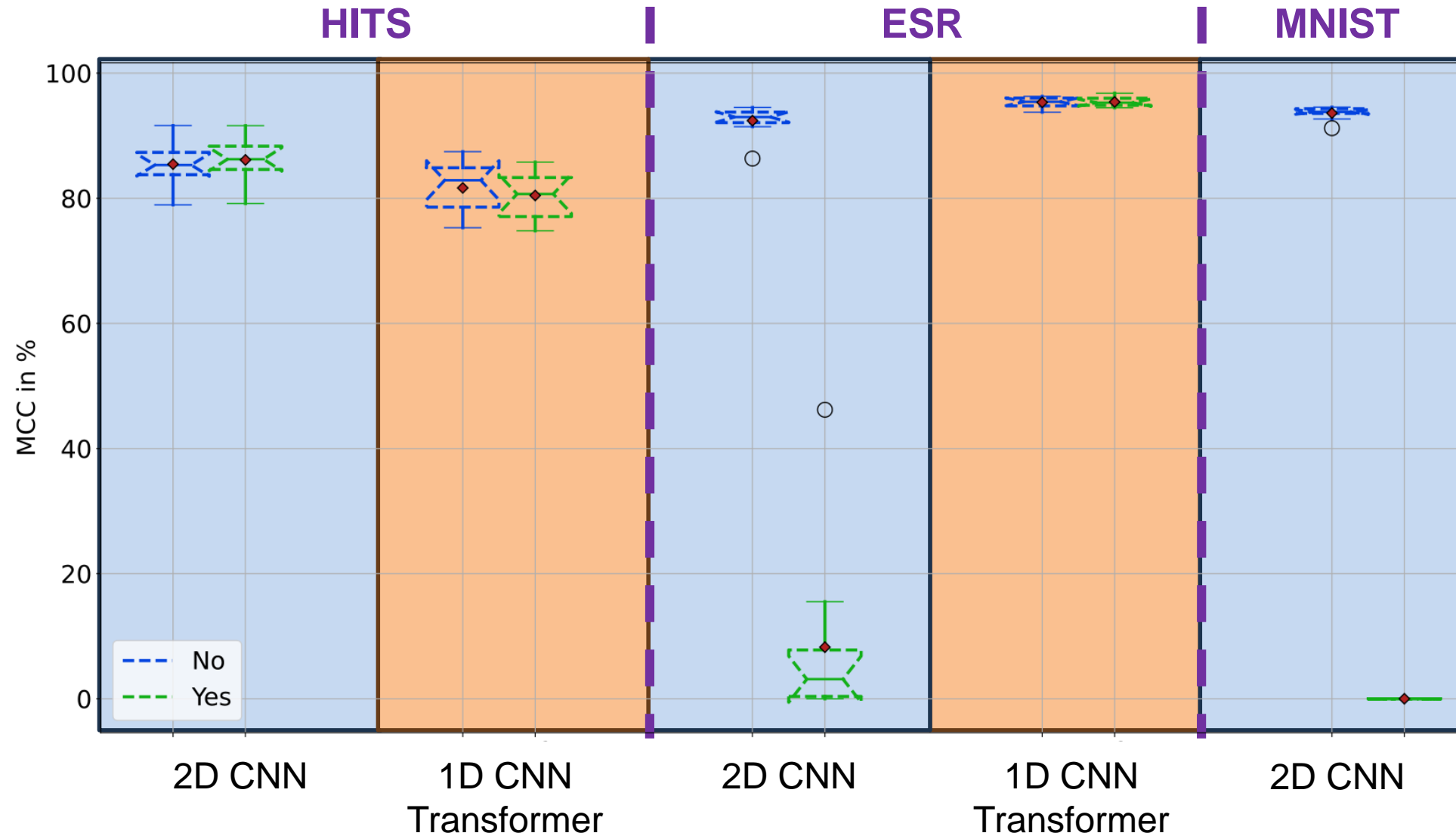


Figure – Influence of normalization on aTTQ from the **classification** perspective

Experiment: influence of normalization

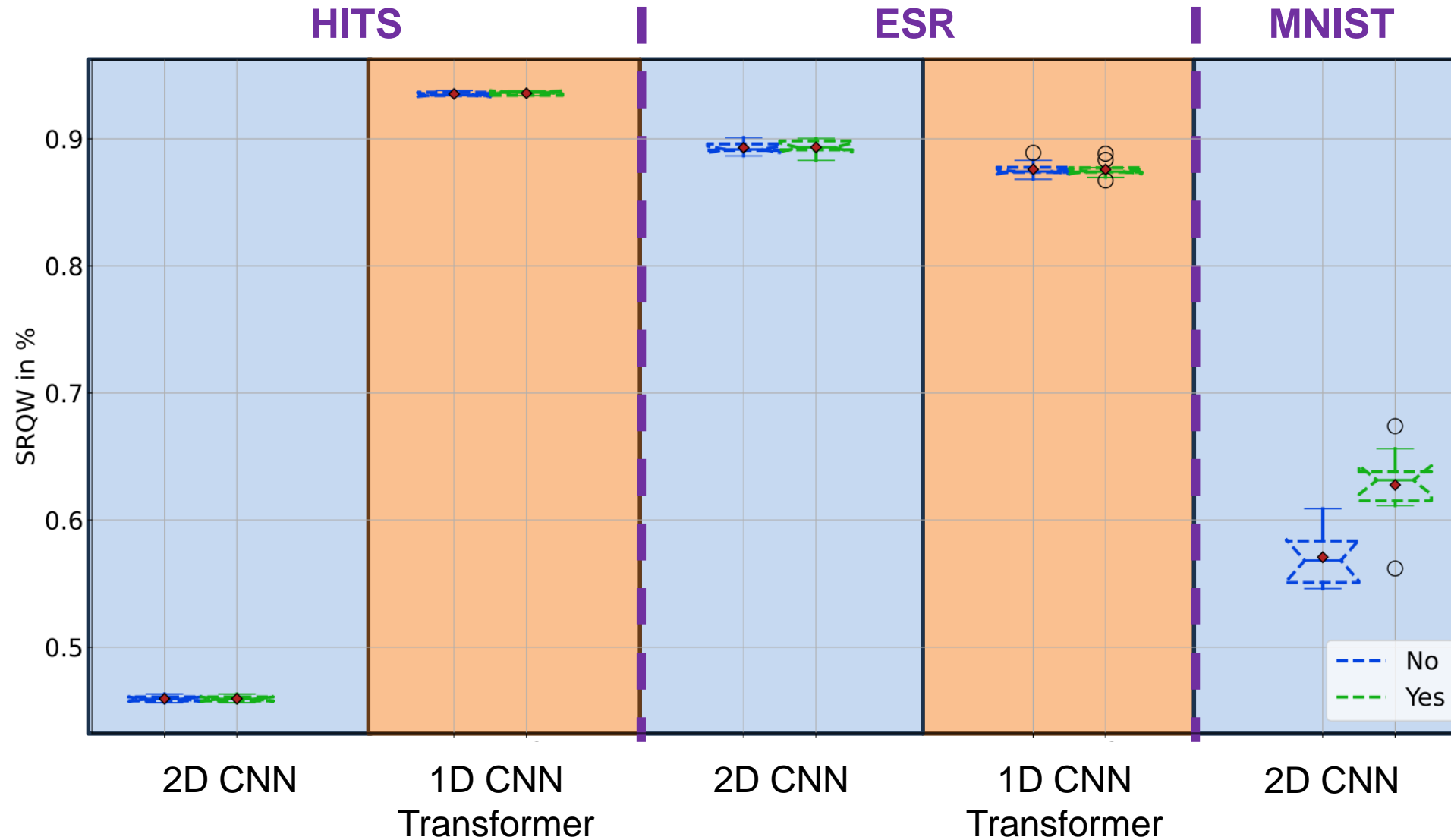


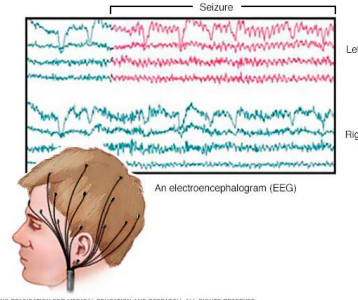
Figure – Influence of normalization on aTTQ from the **sparsity/compression** perspective

Experiment: influence of t_{\min} and t_{\max}

Objective:

- Study the influence of our trade-off parametrization t_{\min} and t_{\max} .

Dataset:



ESR:

- EEG Data.
- 11 500 samples.
- Two classes.
- Sampling frequency: 174 Hz.

Metrics:

- Matthews correlation coefficient (MCC).
- Sparsity rate of the quantized weights (SRQW).

Model:

- 1D CNN-transformer.

Loss function:

- Cross entropy (CE)

ESR
1D CNN-
transformer

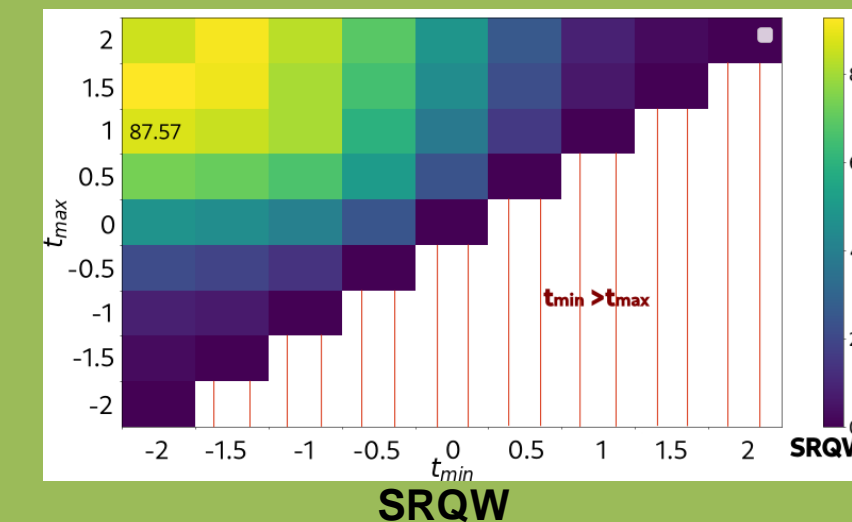
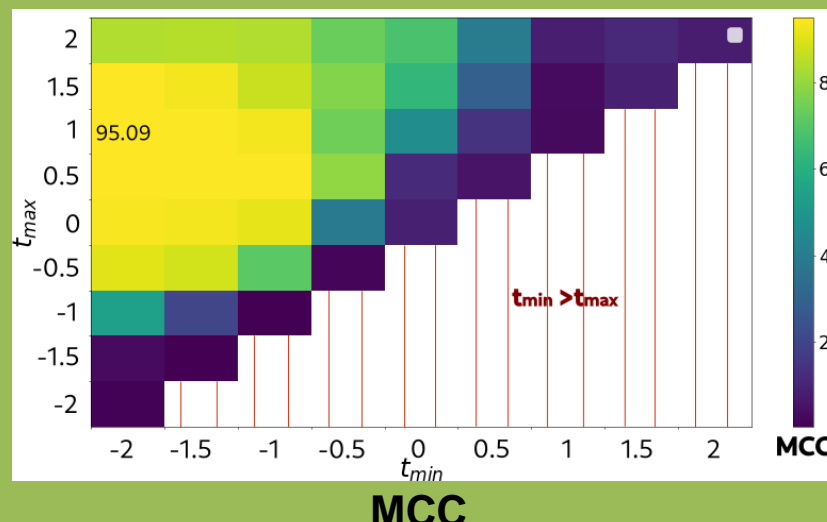


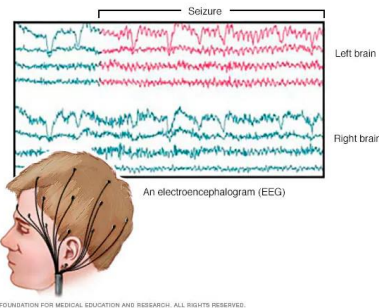
Figure – SMCC and SRQW for different values of t_{\min} and t_{\max} .

Experiment: influence of t_{\min} and t_{\max}

Objective:

- Study the influence of our trade-off parametrization t_{\min} and t_{\max} .

Datasets:



ESR:

- EEG Data.
- 11 500 samples.
- Two classes.
- Sampling frequency: 174 Hz.

Metrics:

- Mathews Correlation Coefficient (MCC).
- CR_G .

Models:

- 2D CNN.
- 1D CNN-transformer.

Loss function:

- Cross entropy (CE)

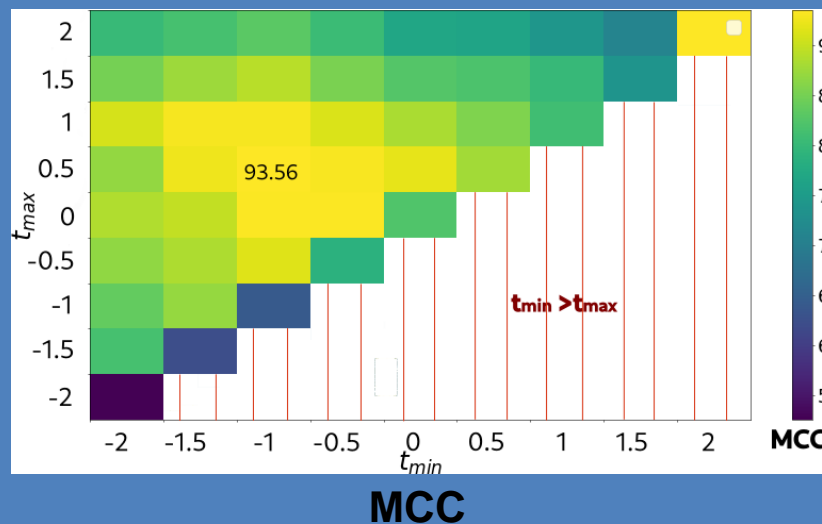
0	0	0	0	0	0	0	0	0	0	0	0	0	0	0	0	0
1	1	1	1	1	1	1	1	1	1	1	1	1	1	1	1	1
2	2	2	2	2	2	2	2	2	2	2	2	2	2	2	2	2
3	3	3	3	3	3	3	3	3	3	3	3	3	3	3	3	3
4	4	4	4	4	4	4	4	4	4	4	4	4	4	4	4	4
5	5	5	5	5	5	5	5	5	5	5	5	5	5	5	5	5
6	6	6	6	6	6	6	6	6	6	6	6	6	6	6	6	6
7	7	7	7	7	7	7	7	7	7	7	7	7	7	7	7	7
8	8	8	8	8	8	8	8	8	8	8	8	8	8	8	8	8
9	9	9	9	9	9	9	9	9	9	9	9	9	9	9	9	9

MNIST subset:

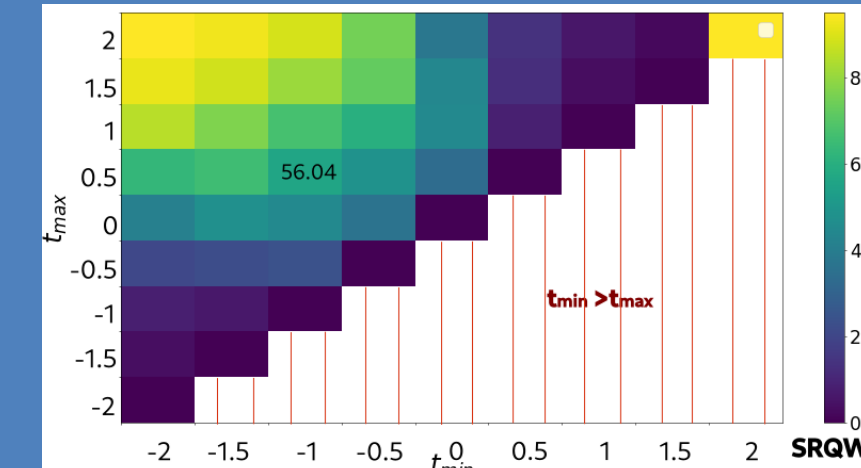
- 28x28 images.
- 20 000 samples.
- Ten classes.

Experiment: influence of t_{\min} and t_{\max}

MNIST
2D CNN

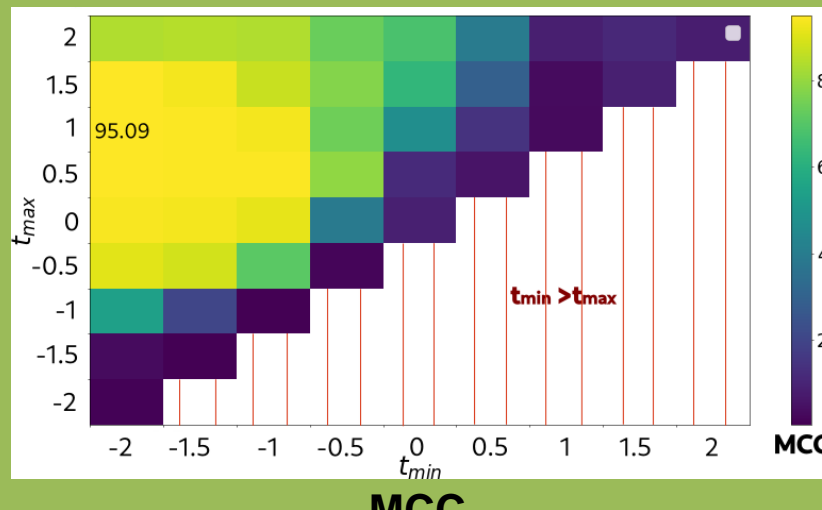


MCC

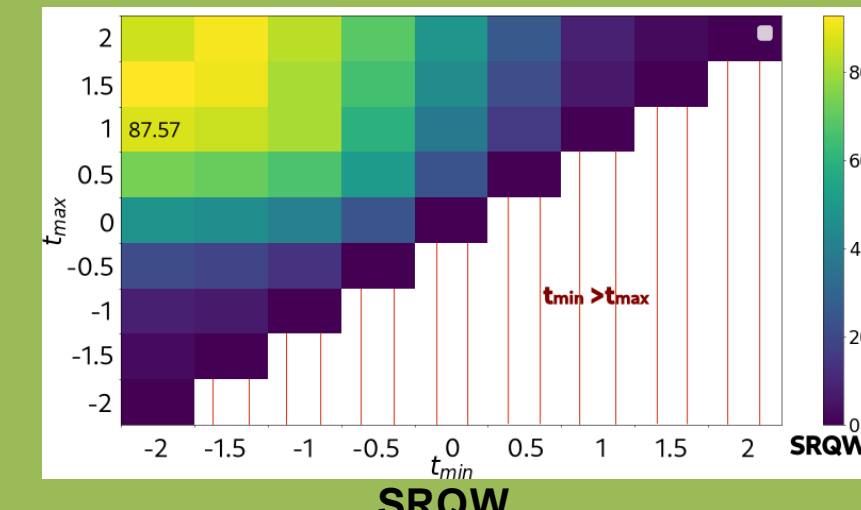


SRQW

ESR
1D CNN-
transformer



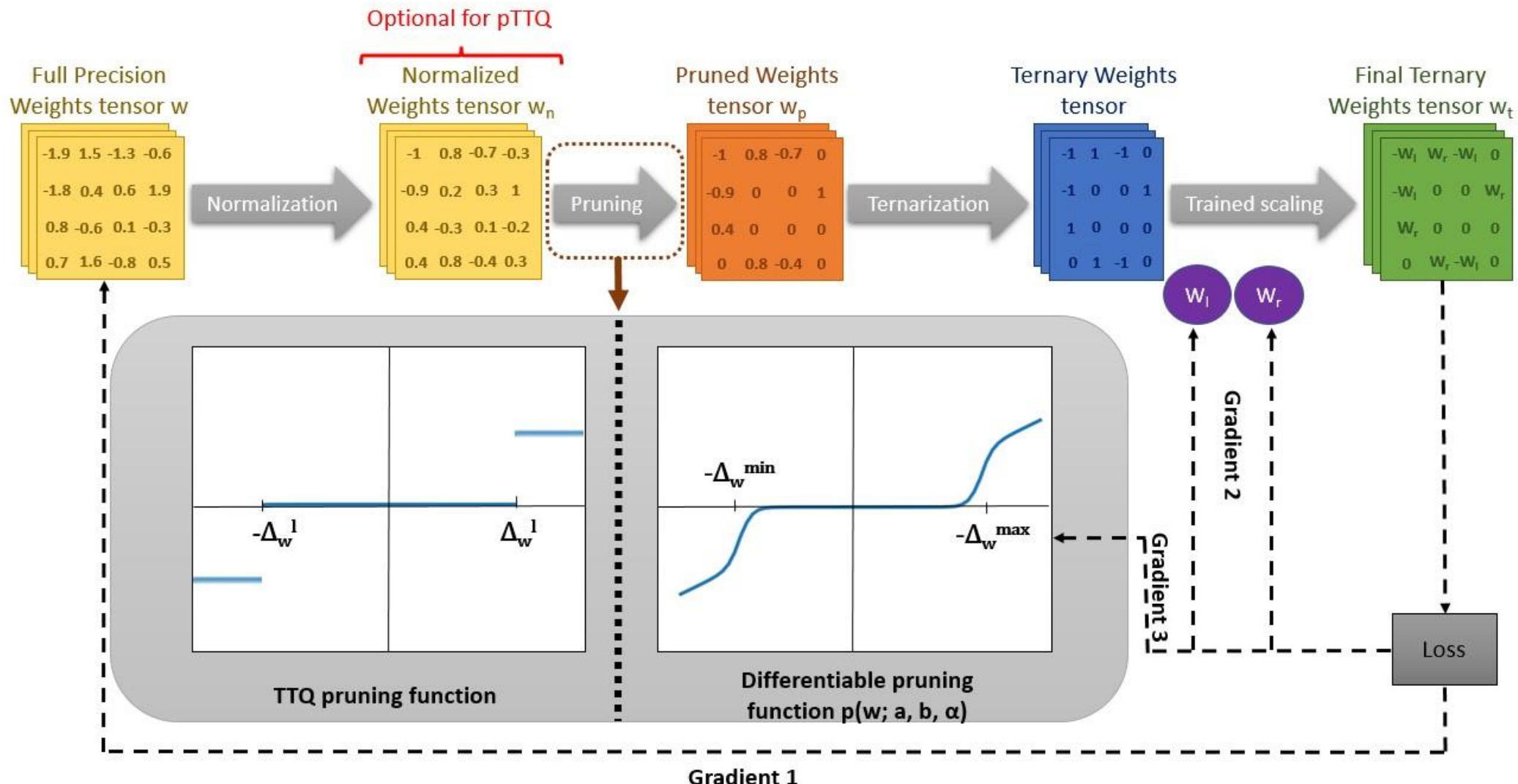
MCC



SRQW

Figure – SMCC and SRQW for different values of t_{\min} and t_{\max} .

Pruned trained ternary quantization (pTTQ)



Pruned trained ternary quantization (pTTQ)

Pruning function:

$$p(w; t_{min}, t_{max}, \alpha) = \text{ReLU}(w - \Delta_w(t_{max})) + \Delta_w(t_{max}) * S(\alpha \times (w - \Delta_w(t_{max})))$$

$$- \text{ReLU}(-w - \Delta_w(t_{min})) - \Delta_w(t_{min}) * S(\alpha \times (-w - \Delta_w(t_{min})))$$

$$\Delta_w : t \rightarrow \mu_w + t \times \sigma_w$$

Mean

Standard deviation

Slope of thresholding

Sigmoid function

Pruned trained ternary quantization (pTTQ)

Gradients:

Heaviside
function

$$\frac{\partial p}{\partial t_{min}}(w; t_{min}, t_{max}, \alpha) = \sigma_w \times H(-w - \Delta_w^{min}) - \sigma_w \times S(\alpha \times (-w - \Delta_w^{min})) + \sigma_w \times \alpha \times \Delta_w^{min} \times S(\alpha \times (-w - \Delta_w^{min})) \times (1 - S(-w - \Delta_w^{min}))$$

$$\frac{\partial p}{\partial t_{min}}(w; t_{min}, t_{max}, \alpha) = -\sigma_w \times H(w - \Delta_w^{max}) + \sigma_w \times S(\alpha \times (w - \Delta_w^{max})) - \sigma_w \times \alpha \times \Delta_w^{max} \times S(\alpha \times (w - \Delta_w^{max})) \times (1 - S(w - \Delta_w^{max}))$$

Pruned trained ternary quantization (pTTQ)

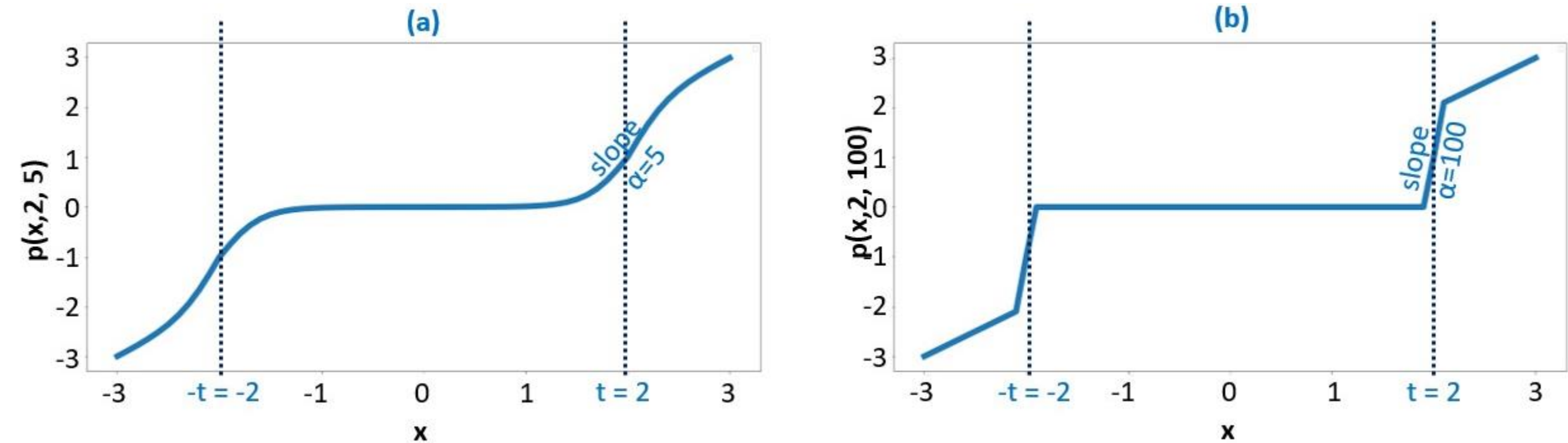


Figure – Examples of pruning functions for different thresholds and values of α

Pruned trained ternary quantization (pTTQ)

Dataset	Model	Quant. method	$CR_G^T \uparrow$	$CR_G^Q \uparrow$	$SRQW$	$EC_G^T \uparrow$	MCC \uparrow	Δ MCC \uparrow
HITS	2D CNN	FP	-	-	-	-	89.84 ± 3.09	-
		DoReFa [33]	89.18 ± 0	96.87 ± 0	-	3.54 ± 0	85.05 ± 5.96	-4.79
		TTQ [13]	24.96 ± 2.25	27.12 ± 2.44	28.96 ± 2.12	23.42 ± 1.30	86.82 ± 2.29	-3.02
		pTTQ	75.54 ± 3.39	82.06 ± 3.69	83.12 ± 3.47	75.53 ± 1.53	89.33 ± 4.45	-0.55
	1D CNN-trans.	FP	-	-	-	-	82.64 ± 1.77	-
		DoReFa [33]	14.50 ± 0	96.87 ± 0	-	0.37 ± 0.03	84.07 ± 3.11	+1.43
		TTQ [13]	0.14 ± 0.04	0.91 ± 0.27	6.75 ± 0.26	1.88 ± 0.03	83.22 ± 2.36	+0.58
		pTTQ	8.37 ± 0.05	55.89 ± 0.34	58.50 ± 0.32	2.01 ± 0.05	85.12 ± 1.94	+2.48
ESR	2D CNN	FP	-	-	-	-	92.81 ± 3.53	-
		DoReFa [33]	96.40 ± 0	96.87 ± 0	-	29.90 ± 0	94.12 ± 0.87	+1.31
		TTQ [13]	85.61 ± 1.37	86.03 ± 1.37	86.59 ± 1.29	76.45 ± 1.13	95.00 ± 1.11	+2.19
		pTTQ	93.35 ± 0.96	93.80 ± 0.96	94.17 ± 0.91	90.32 ± 0.69	92.23 ± 2.32	-0.58
	1D CNN-trans.	FP	-	-	-	-	94.33 ± 1.51	-
		DoReFa [33]	23.46 ± 0	96.86 ± 0	-	0.90 ± 0	96.79 ± 0.55	+2.46
		TTQ [13]	11.40 ± 2.61	47.07 ± 10.79	50.22 ± 10.16	3.21 ± 0.66	96.25 ± 0.79	+1.92
		pTTQ	23.86 ± 0.04	98.54 ± 0.16	98.67 ± 0.15	6.04 ± 0.01	96.35 ± 0.95	+2.02
MNIST	2D MNIST CNN	-	-	-	-	-	94.39 ± 0.46	-
		DoReFa [33]	51.67 ± 0	96.84 ± 0	-	3.28 ± 0	87.03 ± 7.14	-7.36
		TTQ [13]	13.86 ± 2.33	25.97 ± 4.37	30.40 ± 4.12	2.58 ± 0.35	92.09 ± 0.89	-2.30
		pTTQ	33.92 ± 1.02	63.58 ± 1.92	65.79 ± 1.80	6.10 ± 0.15	91.01 ± 0.61	-3.38

Table – Comparison of pTTQ with other state-of-the-art methods

Experiment: pTTQ SOTA comparison

Dataset	Model	Quant. method	$CR_G^T \uparrow$	$CR_G^Q \uparrow$	$SRQW$	$EC_G^T \uparrow$	$MCC \uparrow$	$\Delta MCC \uparrow$
HITS	2D CNN	FP	-	-	-	-	89.84 ± 3.09	-
		DoReFa [33]	89.18 ± 0	96.87 ± 0	-	3.67 ± 0	85.05 ± 5.96	-4.79
		TTQ [13]	24.96 ± 2.25	27.12 ± 2.44	28.96 ± 2.12	23.13 ± 1.27	86.82 ± 2.29	-3.02
		pTTQ	75.54 ± 3.39	82.06 ± 3.69	83.12 ± 3.47	75.26 ± 1.61	89.33 ± 4.45	-0.55
	1D CNN-trans.	FP	-	-	-	-	82.64 ± 1.77	-
		DoReFa [33]	14.50 ± 0	96.87 ± 0	-	0.32 ± 0.03	84.07 ± 3.11	+1.43
		TTQ [13]	0.14 ± 0.04	0.91 ± 0.27	6.75 ± 0.26	1.86 ± 0.03	83.22 ± 2.36	+0.58
		pTTQ	8.37 ± 0.05	55.89 ± 0.34	58.50 ± 0.32	1.82 ± 0.04	85.12 ± 1.94	+2.48
ESR	2D CNN	FP	-	-	-	-	92.81 ± 3.53	-
		DoReFa [33]	96.40 ± 0	96.87 ± 0	-	42.65 ± 0	94.12 ± 0.87	+1.31
		TTQ [13]	85.61 ± 1.37	86.03 ± 1.37	86.59 ± 1.29	72.01 ± 1.08	95.00 ± 1.11	+2.19
		pTTQ	93.35 ± 0.96	93.80 ± 0.96	94.17 ± 0.91	88.68 ± 0.60	92.23 ± 2.32	-0.58
	1D CNN-trans.	FP	-	-	-	-	94.33 ± 1.51	-
		DoReFa [33]	23.46 ± 0	96.86 ± 0	-	0.91 ± 3.69	96.79 ± 0.55	+2.46
		TTQ [13]	11.40 ± 2.61	47.07 ± 10.79	50.22 ± 10.16	2.79 ± 0.57	96.25 ± 0.79	+1.92
		pTTQ	23.86 ± 0.04	98.54 ± 0.16	98.67 ± 0.15	5.21 ± 0.01	96.35 ± 0.95	+2.02
MNIST	2D MNIST CNN	-	-	-	-	-	94.39 ± 0.46	-
		DoReFa [33]	51.67 ± 0	96.84 ± 0	-	3.39 ± 6.94	87.03 ± 7.14	-7.36
		TTQ [13]	13.86 ± 2.33	25.97 ± 4.37	30.40 ± 4.12	1.65 ± 0.16	92.09 ± 0.89	-2.30
		pTTQ	33.92 ± 1.02	63.58 ± 1.92	65.79 ± 1.80	4.10 ± 0.10	91.01 ± 0.61	-3.38

Table – Comparison of pTTQ with other quantization methods

Conclusion et perspectives

Conclusion

Dataset creation and annotation



- Semi-supervised data annotation
- Soft labelling (annotation)

Novel methodology for **semi-automatic data annotation** based on local-quality metrics.

Selection strategy of the best **projection** obtained by a dimensionality reduction technique.

Use robust loss functions to improve the classification performances of a **classifier trained** on a **noisy** semi-automatic labeled **dataset**.

Conclusion

Multiple representations



- Different models with different inputs
- Multi-feature models

Novel **hybrid CNN-transformer** models, **exploiting** the **complementarity** between the **temporal** and **spectral characteristics** of a medical signal.

Guided and regularized intermediate fusion approach, improving generalization while handling **imbalanced** datasets and **label-noise**.

Late-fusion mechanisms, based on **learnable** and **interpretable attention weights**.

Conclusion

Resource hungry models



- Lite models
- Model compression
- (Soft labelling training)

→ **Novel ternarization heuristic**, based on the weights' statistics.

→ **Direct asymmetric pruning** before ternarization, allowing a **better trade-off** between compression, energy, and classification.

→ **Asymmetric parametrization** of the sparsity rate, controlling the abovementioned **trade-off**.

Perspectives

Dataset creation and annotation



- Semi-supervised data annotation
- Soft labelling (annotation)

More complex encoding models (VAE, GANs, diffusion models, ...)

Stronger regularization (DEC, contrastive learning, more complex projection metrics, ...)

Active learning by proposing to human experts the most difficult samples

Perspectives

Multiple representations



- Different models with different inputs
- Multi-feature models

Test other types of models (LSTM, ViT, ResNet, ...) and datasets (medical and non-medical)

Use other representations of the raw signal (cochleagram, binary encodings, chromagram, ...)

Use other types of regularization (contrastive learning with weak supervision, link constraints, ...)

Perspectives

Resource hungry models



- Lite models
- Model compression
- (Soft labelling training)

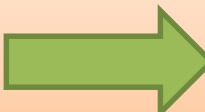
Differentiable pruning function, with asymmetric learnable parameters

Mixed quantization to completely quantize the models with different precisions

Hardware implementation to take advantage of the compressed models

Perspectives

Soft labelling



- Capture expert uncertainty
- Noise robustness

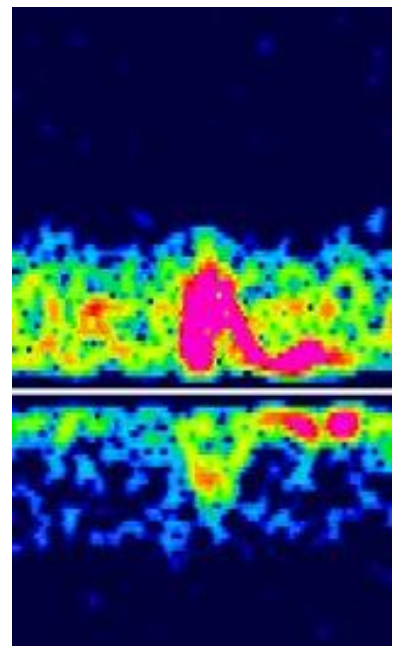
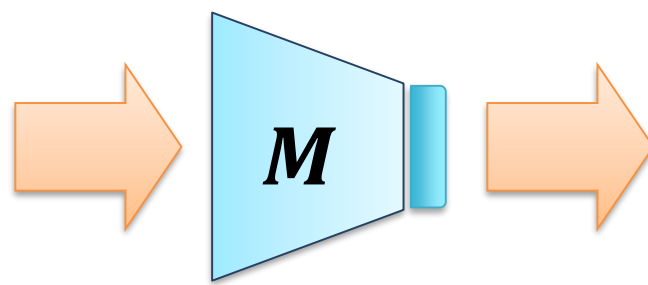
Take advantage of soft annotations using soft-labels loss functions (soft CE, Jensen-Shannon divergence, ...), to capture the human expert uncertainty,

New loss functions robust against soft-label noise (geometric mean Jensen-Shannon divergence).

Semi-automatic soft label annotation evaluation.

Soft labels

Working with soft labels (vs hard labels)

Sample X 

Deep model

Soft prediction

$$M(X)_S = \begin{pmatrix} y_s^{Art} \\ y_s^{GE} \\ y_s^{SE} \end{pmatrix} = \begin{pmatrix} 0.1 \\ 0.3 \\ 0.6 \end{pmatrix}$$

conversion to
hard prediction
→ highest score

$$M(X)_H = \begin{pmatrix} 0 \\ 0 \\ 1 \end{pmatrix}$$

Soft labels

Loss functions

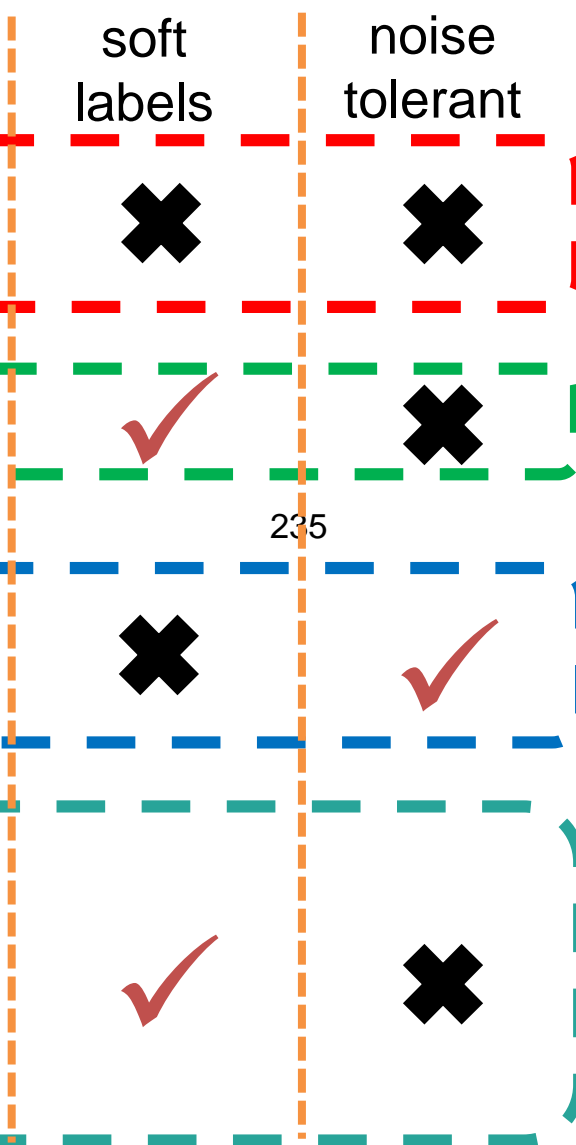
$$\left\{ \begin{array}{l} L_{CE}(y_H, M(X)_H) = H(y_H, M(X)_H) \\ \text{cross-entropy (baseline)} \end{array} \right.$$

$$\left\{ \begin{array}{l} L_{SoftCE}(y_S, M(X)_S) = H(y_S, M(X)_S) \end{array} \right.$$

$$\left\{ \begin{array}{l} L_{SymCE}(y_H, M(X)_H) \\ = \alpha \times H(y_H, M(X)_H) + \beta \times H(M(X)_H, y_H) \end{array} \right.$$

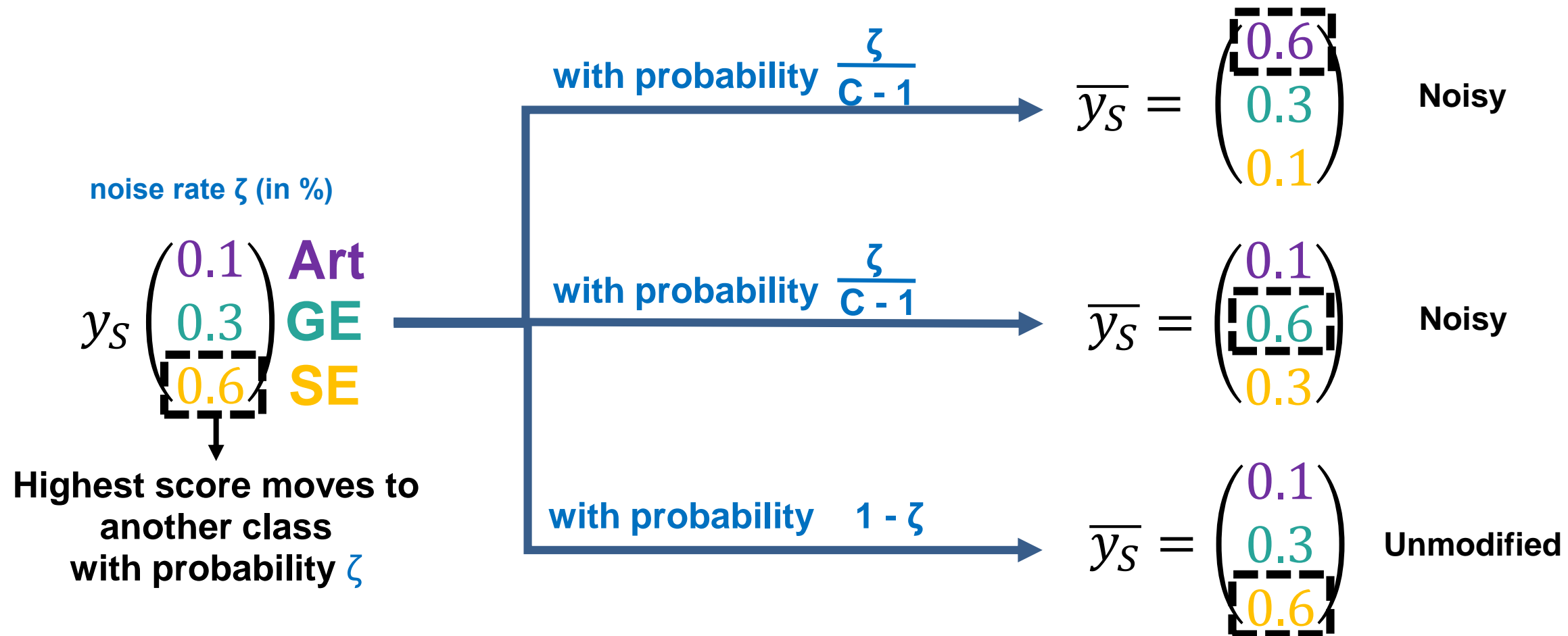
$$\left\{ \begin{array}{l} L_{JSD}(y_S, M(X)_S) = \frac{1}{2} \times (KL(y_S, m_S) + KL(M(X)_S, m_S)) \end{array} \right.$$

$$\text{with } m_S = \frac{1}{2} \times (y_S + M(X)_S)$$



Soft labels

Adding symmetric noise to soft labels



Soft labels

Adding symmetric noise to soft labels

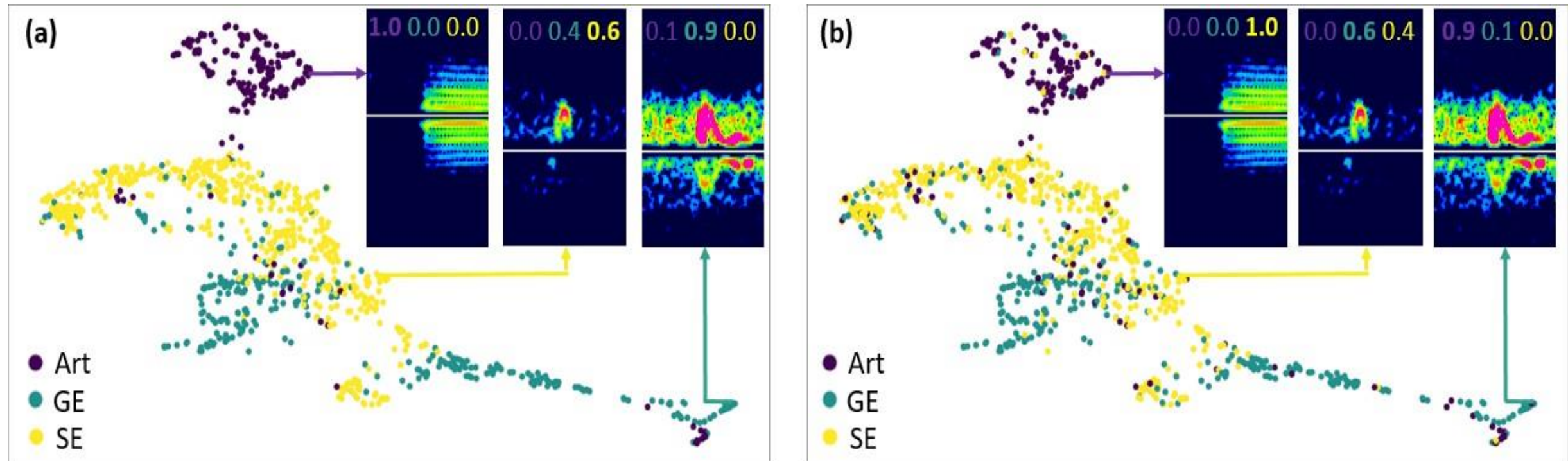
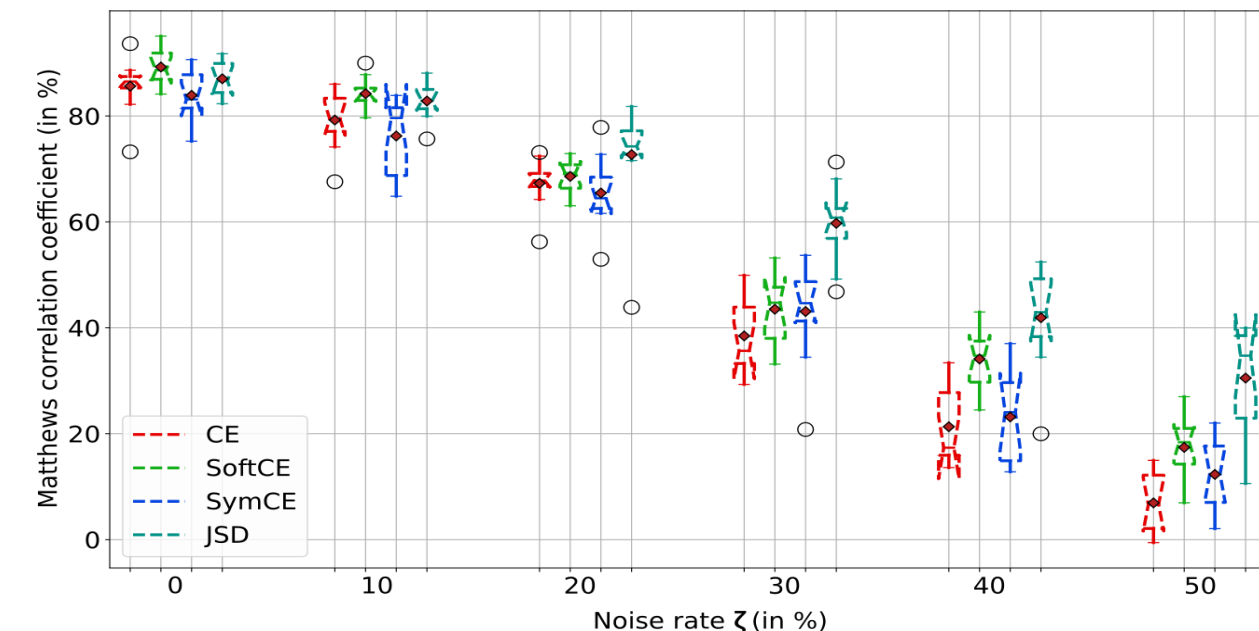


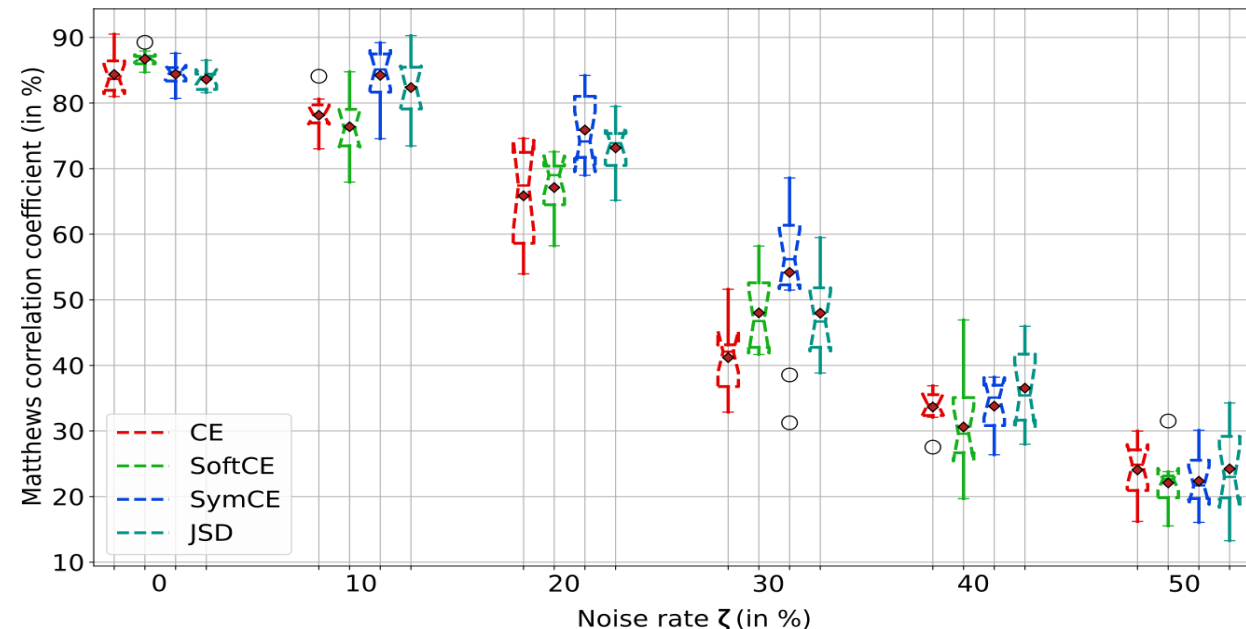
Figure - (a) HITS dataset without noise, **(b)** HITS dataset with 10% of symmetric noise in the soft labels.

Soft labels

Soft labels noise resistance



(a) 2D time-frequency CNN

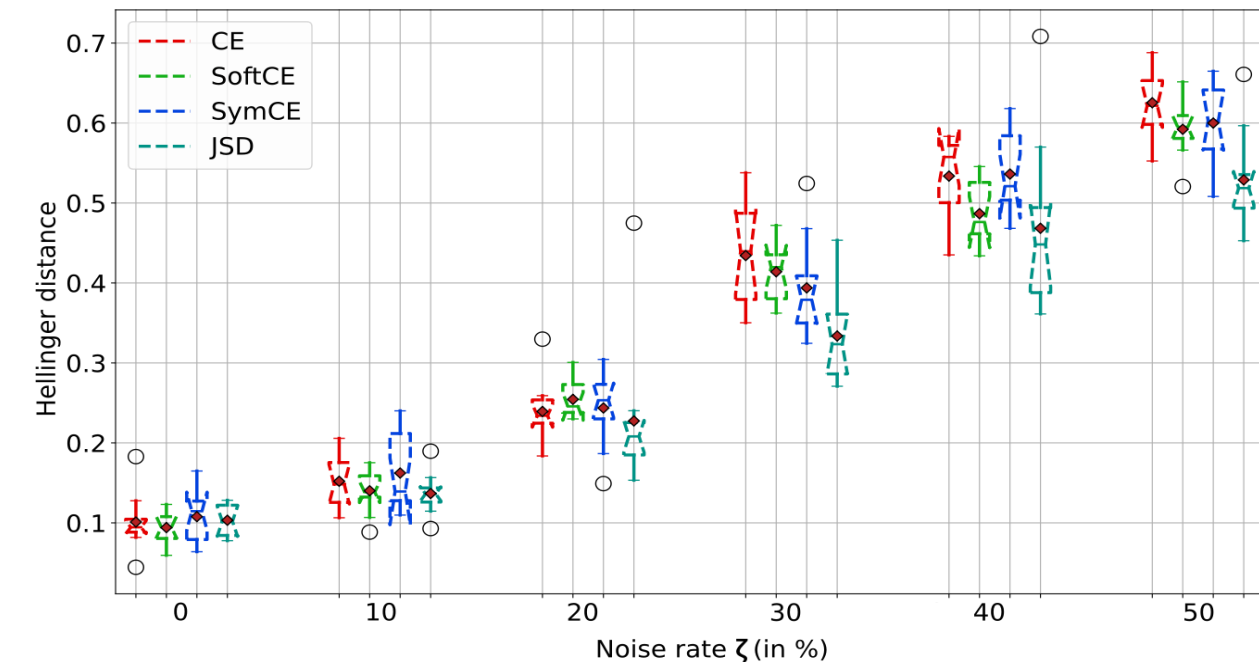


(b) Doppler signal 1D CNN-transformer

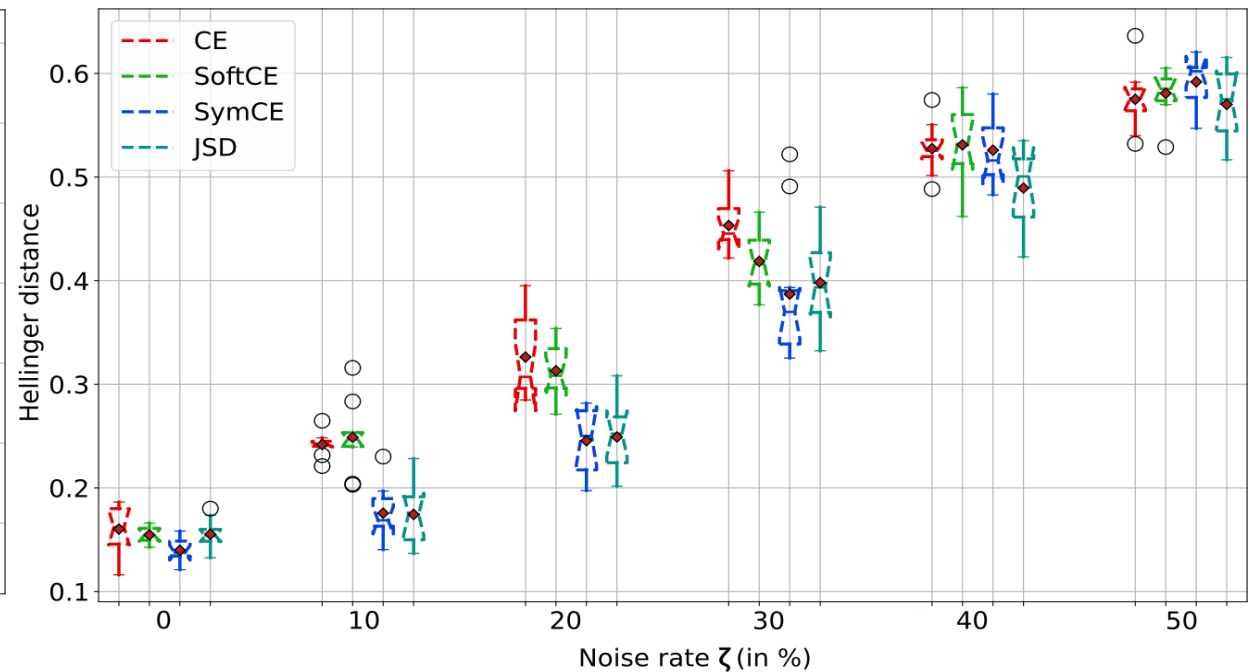
Figure - Classification performance of two types of models trained using the presented soft and hard label loss function

Soft labels

Uncertainty capturing



(a) 2D time-frequency CNN



(b) Doppler signal 1D CNN-transformer

Figure - Uncertainty capturing evaluation of two types of models trained using the presented soft and hard label loss function

Soft labels

Geometric Mean Jensen-Shannon Divergence (GEO JSD)

$$JSR(P||Q) = \alpha (1 - \alpha) [\beta(H(P, P) - H(Q, P)) + \underbrace{\gamma(H(Q, Q) - H(P, Q))}_{\text{Robustesse au bruit prouvée théoriquement}}$$

Robustesse au bruit
prouvée théoriquement

Soft labels

Résultats préliminaires GEO JSD

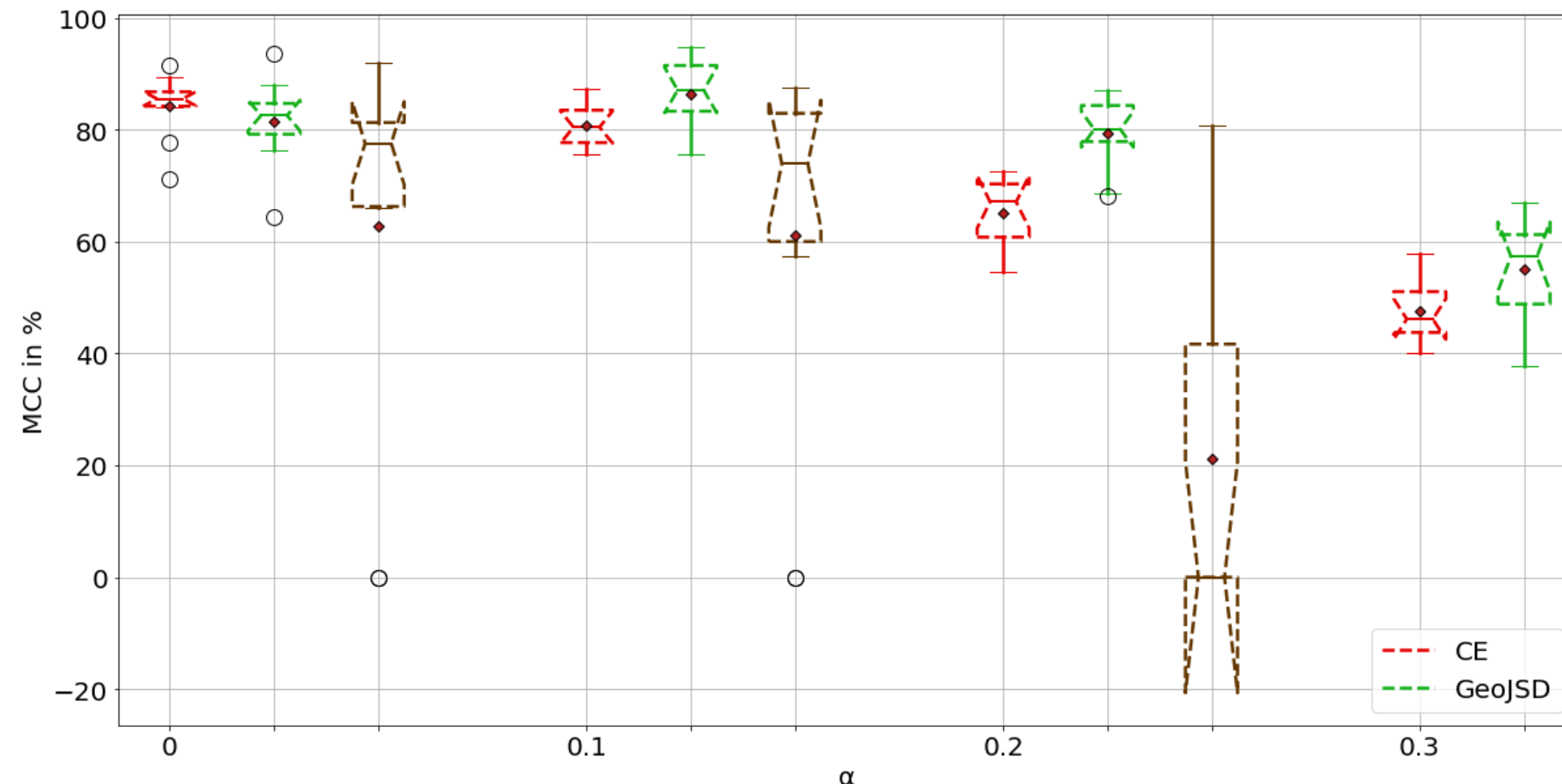


Figure – Résultats HITS-small

Soft labels

Résultats préliminaires GEO JSD

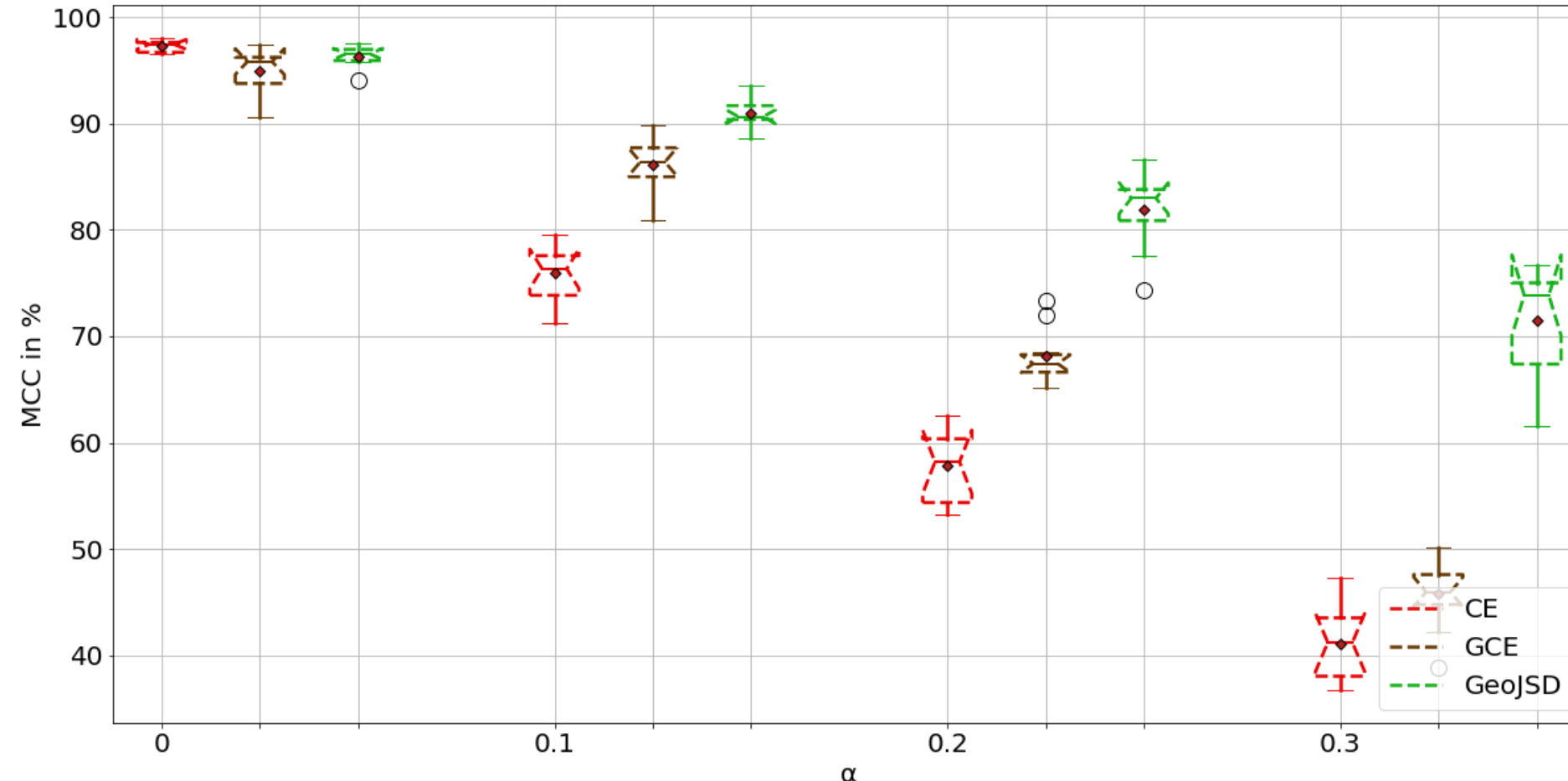


Figure – Résultats PTB

Mathews Correlation Coefficient (Binary classification)

$$MCC = \frac{TP \times TN - FP \times FN}{\sqrt{(TP + FP)(TP + FN)(TN + FP)(TN + FN)}}$$



$$MCC = 0 \Leftrightarrow TP \times TN = FP \times FN$$



Random classifier !

Statistical tests for comparison

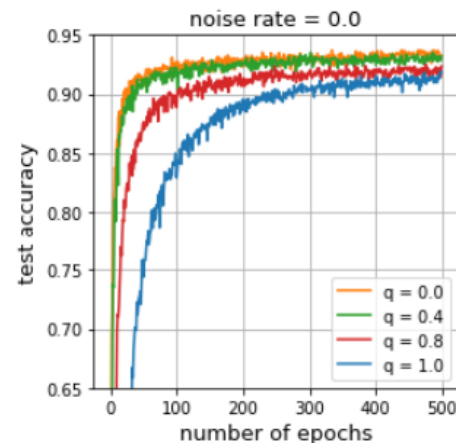
- Important hypothesis for several statistical tests → **Independence of observations.**
 - For k-fold cross-validation:
 - One sample belongs to the training dataset $k-1$ times
 - For repeated holdout:
 - The training and testing datasets are fixed during repetitions.
- **Solutions**
 - Create different datasets, one per repetition → Not yet possible for the HITS.
 - Reduces training and testing samples per dataset.
 - 5x2 cross-validation → Difficult to do it subject-wise.
 - Other tests without independence hypothesis ?



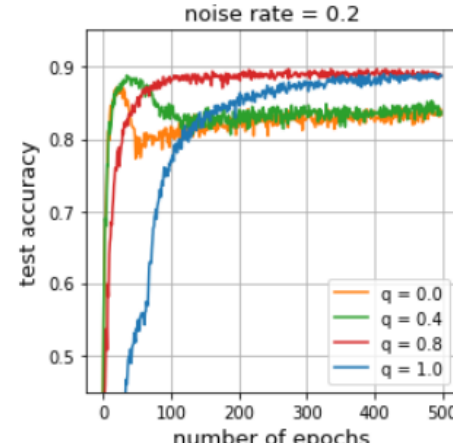
The mean estimates are not independent !



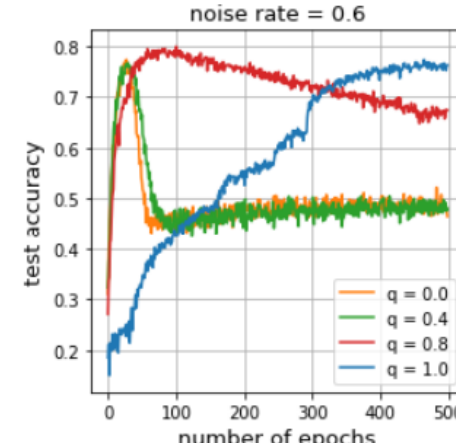
Choice of q hyperparameter for GCE



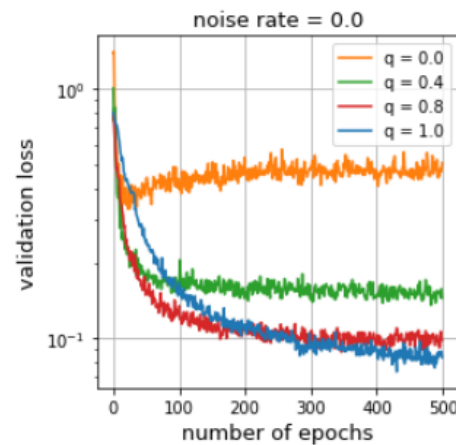
(a)



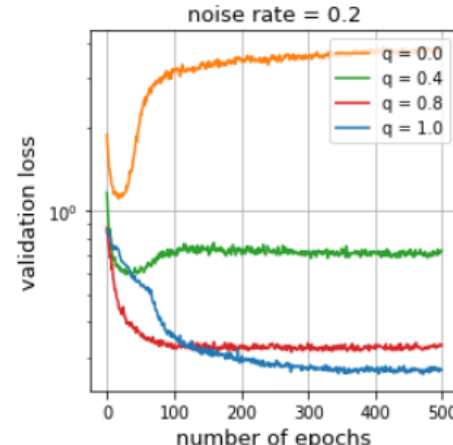
(b)



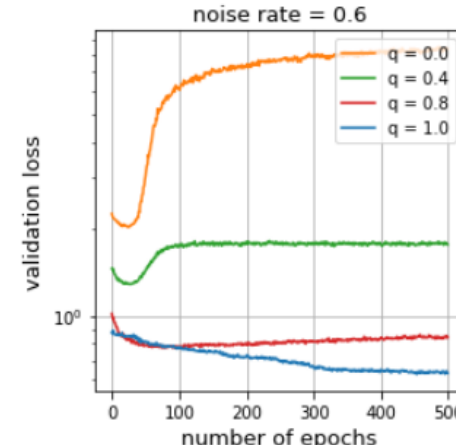
(c)



(d)



(e)



(f)

Figure – Test accuracy and validation GCE, for different values of q, on the XXX dataset (Zhang et Sabuncu 2018)

Automatic annotation vs Manual annotation

Split	No. patients	Total	SE	GE	Art.
Train	39	1541	456	610	6 198
Test	12	139	39	47	53

Table – HITS-small-I dataset.

Model	MCC
2D CNN	87.09 ± 4.31
1D CNN-trans.	79.17 ± 6.64
MIF-GR	91.89 ± 2.64

Split	No. patients	Total	SE	GE	Art.
Train	40	7 264	456	610	6 198
Test	11	1 421	240	392	789

Table – HITS-sada dataset.

Model	MCC
2D CNN	84.03 ± 1.20
1D CNN-trans.	85.74 ± 1.16
MIF-GR	87.35 ± 0.85

Table – Multi-feature GDCE compared to single feature models on a noisy semi-automatically labeled dataset **HITS-small-I**.

Table – Multi-feature GDCE compared to single feature models on a noisy semi-automatically labeled dataset **HITS-sada**.



Not the same test sets between experiments, so results are not directly comparable.



Test set of HITS-sada is harder.

Choice of the pruning parameters aTTQ

- **Choice of t_{min} and t_{max} is critical.**
 - **Bad choice:**
 - Poor classification performances.
 - Poor compression/energy performances
 - **→ It happens also for other methods** such as TTQ or TWN !
 - **Careful choice:**
 - **Great compression/energy/classification trade-off.**
- **Solutions**
 - Pruned trained ternary quantization with learnable threshold parameters !
 - Bayesian hyperparameter searching.
 - Larger study to understand influence of t_{min} and t_{max} .

Industrial application and impact on patient care

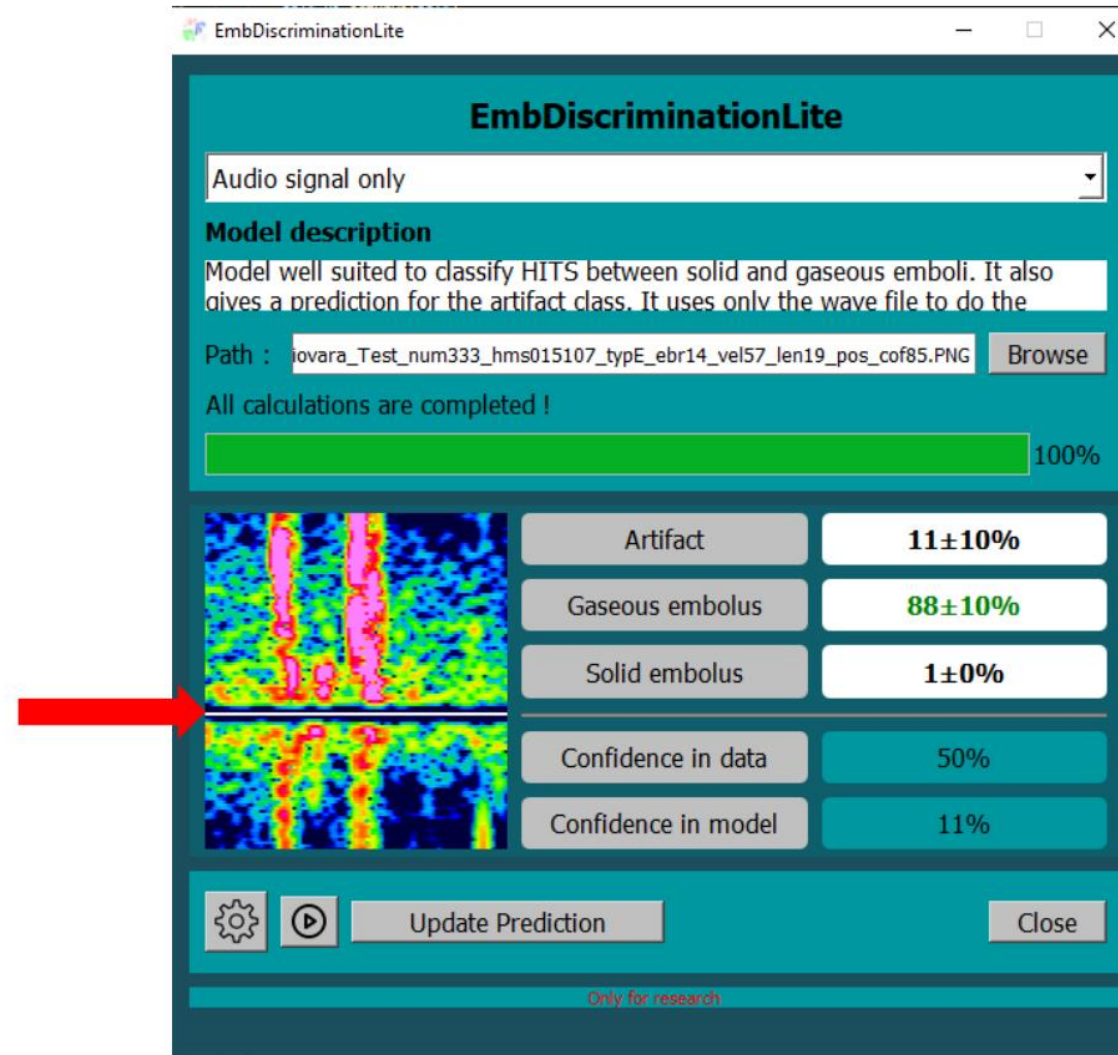
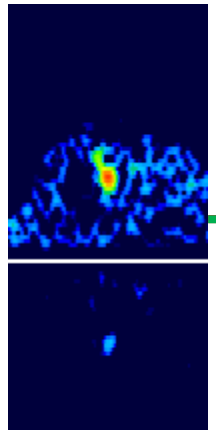


Figure – EmbDiscriminationLite application, deep learning classification module for ADMS for Atys Medical

Industrial application and impact on patient care

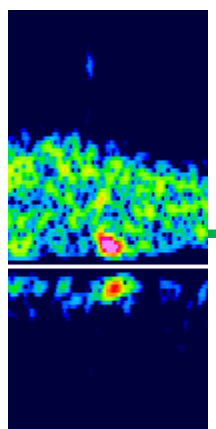
Solid embolus



Good diagnosis → Adapted treatment → Stroke prevention

Bad diagnosis → No treatment needed → Stroke risk

Artifact



Good diagnosis → No treatment needed

Bad diagnosis → Wrong treatment → Risk of complications

Model compression comparison with other SOTA method

Dataset	Model	Quant. method	$CR_G^T \uparrow$	$CR_G^Q \uparrow$	$SRQW$	$ECT_G^T \uparrow$	$MCC \uparrow$	$\Delta MCC \uparrow$
HITS	2D CNN	FP	-	-	-	-	89.84 ± 3.09	-
		DoReFa	89.18 ± 0	96.87 ± 0	-	3.54 ± 0	85.05 ± 5.96	-4.79
		TTQ	24.96 ± 2.25	27.12 ± 2.44	28.96 ± 2.12	23.42 ± 1.30	86.82 ± 2.29	-3.02
		aTTQ	42.98 ± 0.23	46.69 ± 0.25	45.95 ± 0.21	44.04 ± 0.19	86.14 ± 3.37	-3.70
		pTTQ	75.54 ± 3.39	82.06 ± 3.69	83.12 ± 3.47	75.53 ± 1.53	89.33 ± 4.45	-0.55
	1D CNN-trans.	FP	-	-	-	-	82.64 ± 1.77	-
		DoReFa	14.50 ± 0	96.87 ± 0	-	0.37 ± 0.03	84.07 ± 3.11	+1.43
		TTQ	0.14 ± 0.04	0.91 ± 0.27	6.75 ± 0.26	1.88 ± 0.03	83.22 ± 2.36	+0.58
		aTTQ	13.94 ± 0.02	93.17 ± 0.16	93.53 ± 0.15	7.64 ± 0.11	81.66 ± 4.17	-0.98
		pTTQ	8.37 ± 0.05	55.89 ± 0.34	58.50 ± 0.32	2.01 ± 0.05	85.12 ± 1.94	+2.48
ESR	2D CNN	FP	-	-	-	-	92.81 ± 3.53	-
		DoReFa	96.40 ± 0	96.87 ± 0	-	29.90 ± 0	94.12 ± 0.87	+1.31
		TTQ	85.61 ± 1.37	86.03 ± 1.37	86.59 ± 1.29	76.45 ± 1.13	95.00 ± 1.11	+2.19
		aTTQ	88.48 ± 0.44	88.91 ± 0.45	89.30 ± 0.42	84.49 ± 0.33	92.41 ± 2.22	-0.40
		pTTQ	93.35 ± 0.96	93.80 ± 0.96	94.17 ± 0.91	90.32 ± 0.69	92.23 ± 2.32	-0.58
	1D CNN-trans.	FP	-	-	-	-	94.33 ± 1.51	-
		DoReFa	23.46 ± 0	96.86 ± 0	-	0.90 ± 0	96.79 ± 0.55	+2.46
		TTQ	11.40 ± 2.61	47.07 ± 10.79	50.22 ± 10.16	3.21 ± 0.66	96.25 ± 0.79	+1.92
		aTTQ	21.02 ± 0.15	86.78 ± 0.63	87.59 ± 0.59	5.37 ± 0.04	95.34 ± 0.79	+1.01
		pTTQ	23.86 ± 0.04	98.54 ± 0.16	98.67 ± 0.15	6.04 ± 0.01	96.35 ± 0.95	+2.02
MNIST	2D MNIST CNN	-	-	-	-	-	94.39 ± 0.46	-
		DoReFa	51.67 ± 0	96.84 ± 0	-	3.28 ± 0	87.03 ± 7.14	-7.36
		TTQ	13.86 ± 2.33	25.97 ± 4.37	30.40 ± 4.12	2.58 ± 0.35	92.09 ± 0.89	-2.30
		aTTQ	28.98 ± 1.26	54.32 ± 2.36	57.08 ± 2.22	4.97 ± 0.22	93.62 ± 0.96	-0.77
		pTTQ	33.92 ± 1.02	63.58 ± 1.92	65.79 ± 1.80	6.10 ± 0.15	91.01 ± 0.61	-3.38

Table – Comparison of aTTQ with other state-of-the-art methods

Difficulty of measuring energy consumption on real CPU/GPU

- **Energy consumption depends on**
 - Used hardware and the model.
 - Operations implementations.
 - Optimization of the trained models.
- **What is implemented ?**
 - Some sparse operations in PyTorch (Beta version).
 - Simulated quantization → All operations are treated as 32 bits operations.
- **Current codes do not allow efficient operations on common hardware**
 - Specialized hardware is needed for further improvements.



**Simulation
(difficult)**